BONE AND CARTILAGE DISEASES – THE ROLE AND POTENTIAL OF NATURAL PRODUCTS

EDITED BY: Longhuo Wu, Qian Chen, Daohua Xu and Walter Luyten
PUBLISHED IN: Frontiers in Pharmacology

frontiers Research Topics

Frontiers eBook Copyright Statement

The copyright in the text of individual articles in this eBook is the property of their respective authors or their respective institutions or funders. The copyright in graphics and images within each article may be subject to copyright of other parties. In both cases this is subject to a license granted to Frontiers.

The compilation of articles constituting this eBook is the property of Frontiers.

Each article within this eBook, and the eBook itself, are published under the most recent version of the Creative Commons CC-BY licence. The version current at the date of publication of this eBook is CC-BY 4.0. If the CC-BY licence is updated, the licence granted by Frontiers is automatically updated to the new version.

When exercising any right under the CC-BY licence, Frontiers must be attributed as the original publisher of the article or eBook, as applicable.

Authors have the responsibility of ensuring that any graphics or other materials which are the property of others may be included in the CC-BY licence, but this should be checked before relying on the CC-BY licence to reproduce those materials. Any copyright notices relating to those materials must be complied with.

Copyright and source acknowledgement notices may not be removed and must be displayed in any copy, derivative work or partial copy which includes the elements in question.

All copyright, and all rights therein, are protected by national and international copyright laws. The above represents a summary only. For further information please read Frontiers' Conditions for Website Use and Copyright Statement, and the applicable CC-BY licence.

ISSN 1664-8714
ISBN 978-2-83250-046-0
DOI 10.3389/978-2-83250-046-0

About Frontiers

Frontiers is more than just an open-access publisher of scholarly articles: it is a pioneering approach to the world of academia, radically improving the way scholarly research is managed. The grand vision of Frontiers is a world where all people have an equal opportunity to seek, share and generate knowledge. Frontiers provides immediate and permanent online open access to all its publications, but this alone is not enough to realize our grand goals.

Frontiers Journal Series

The Frontiers Journal Series is a multi-tier and interdisciplinary set of open-access, online journals, promising a paradigm shift from the current review, selection and dissemination processes in academic publishing. All Frontiers journals are driven by researchers for researchers; therefore, they constitute a service to the scholarly community. At the same time, the Frontiers Journal Series operates on a revolutionary invention, the tiered publishing system, initially addressing specific communities of scholars, and gradually climbing up to broader public understanding, thus serving the interests of the lay society, too.

Dedication to Quality

Each Frontiers article is a landmark of the highest quality, thanks to genuinely collaborative interactions between authors and review editors, who include some of the world's best academicians. Research must be certified by peers before entering a stream of knowledge that may eventually reach the public - and shape society; therefore, Frontiers only applies the most rigorous and unbiased reviews.
Frontiers revolutionizes research publishing by freely delivering the most outstanding research, evaluated with no bias from both the academic and social point of view. By applying the most advanced information technologies, Frontiers is catapulting scholarly publishing into a new generation.

What are Frontiers Research Topics?

Frontiers Research Topics are very popular trademarks of the Frontiers Journals Series: they are collections of at least ten articles, all centered on a particular subject. With their unique mix of varied contributions from Original Research to Review Articles, Frontiers Research Topics unify the most influential researchers, the latest key findings and historical advances in a hot research area! Find out more on how to host your own Frontiers Research Topic or contribute to one as an author by contacting the Frontiers Editorial Office: frontiersin.org/about/contact

BONE AND CARTILAGE DISEASES – THE ROLE AND POTENTIAL OF NATURAL PRODUCTS

Topic Editors:
Longhuo Wu, Gannan Medical University, China
Qian Chen, Brown University, United States
Daohua Xu, Guangdong Medical University, China
Walter Luyten, KU Leuven, Belgium

Citation: Wu, L., Chen, Q., Xu, D., Luyten, W., eds. (2022). Bone and Cartilage Diseases – The Role and Potential of Natural Products. Lausanne: Frontiers Media SA. doi: 10.3389/978-2-83250-046-0

Table of Contents

05 ***Editorial: Bone and Cartilage Diseases—The Role and Potential of Natural Products***
Daohua Xu, Longhuo Wu and Qian Chen

08 ***Xanthohumol Inhibited Mechanical Stimulation-Induced Articular ECM Degradation by Mediating lncRNA GAS5/miR-27a Axis***
Tiansheng Zheng, Qingluo Zhou, Jishang Huang, Jinliang Lai, Guanglin Ji and Dechao Kong

19 ***Suppression of Dendritic Cell Maturation by Kefir Peptides Alleviates Collagen-Induced Arthritis in Mice***
Chien-Fu Chen, Hsin-Pei Li, Ya-Hsuan Chao, Min-Yu Tu, Chih-Ching Yen, Ying-Wei Lan, Shang-Hsun Yang, Kowit-Yu Chong, Chi-Chien Lin and Chuan-Mu Chen

33 ***Serum Amyloid A Correlates With the Osteonecrosis of Femoral Head by Affecting Bone Metabolism***
Xiaoyuan Peng, Yiyang Ma, Qiyang Wang, Yanchun Gao, Guangyi Li, Chenyi Jiang, Yun Gao and Yong Feng

45 ***Research Progress of the Role of Anthocyanins on Bone Regeneration***
Wei Mao, Guowei Huang, Huan Chen, Liangliang Xu, Shengnan Qin and Aiguo Li

55 ***Jintiange Capsules Ameliorate Osteoarthritis by Modulating Subchondral Bone Remodeling and Protecting Cartilage Against Degradation***
Chenyang Zhuang, Zixiang Wang, Weisin Chen, Hanquan Wang, Bo Tian and Hong Lin

67 ***The Therapeutic Effect of Huo Xue Tong Luo Capsules in Association Research Circulation Osseous (ARCO) Stage II Osteonecrosis of the Femoral Head: A Clinical Study With an Average Follow-up Period of 7.95 Years***
Xiao-Ming He, Min-Cong He, Peng Yang, Qing-Wen Zhang, Zhen-Qiu Chen, Wei He and Qiu-Shi Wei

79 ***Corrigendum: The Therapeutic Effect of Huo Xue Tong Luo Capsules in Association Research Circulation Osseous (ARCO) Stage II Osteonecrosis of the Femoral Head: A Clinical Study With an Average Follow-up Period of 7.95 Years***
Xiao-Ming He, Min-Cong He, Peng Yang, Qing-Wen Zhang, Zhen-Qiu Chen, Wei He and Qiu-Shi Wei

80 ***A Traditional Chinese Medicine Plant Extract Prevents Alcohol-Induced Osteopenia***
Dongyang Qian, Hui Zhou, Pan Fan, Tao Yu, Anish Patel, Morgan O'Brien, Zhe Wang, Shiguang Lu, Guoqiang Tong, Yimin Shan, Lei Wang, Yuan Gao, Yuan Xiong, Lily Zhang, Xin Wang, Yuancai Liu and Shuanhu Zhou

95 ***Phytochemicals Mediate Autophagy Against Osteoarthritis by Maintaining Cartilage Homeostasis***
Zheng Tian, Xinan Zhang and Mingli Sun

114 *Effects of* Sparganii Rhizoma *on Osteoclast Formation and Osteoblast Differentiation and on an OVX-Induced Bone Loss Model*
Sungyub Lee, Minsun Kim, Sooyeon Hong, Eom Ji Kim, Jae-Hyun Kim, Youngjoo Sohn and Hyuk-Sang Jung

137 *The Effects of Crocin on Bone and Cartilage Diseases*
Shayan Vafaei, Xuming Wu, Jiajie Tu and Seyed Noureddin Nematollahi-mahani

148 *Botanical Drug Extracts Combined With Biomaterial Carriers for Osteoarthritis Cartilage Degeneration Treatment: A Review of 10 Years of Research*
Panyun Mu, Jie Feng, Yimei Hu, Feng Xiong, Xu Ma and Linling Tian

171 *Eucommia, Cuscuta, and Drynaria Extracts Ameliorate Glucocorticoid-Induced Osteoporosis by Inhibiting Osteoclastogenesis Through PI3K/Akt Pathway*
Junwen Han, Li Li, Chen Zhang, Qianqian Huang, Shanglong Wang, Wenyu Li, Jiancheng Zong, Lijie Li, Zhen Zhao, Zengliang Zhang, Zimin Liu, Qi Wang and Yuanyuan Shi

189 *Mogrol Attenuates Osteoclast Formation and Bone Resorption by Inhibiting the TRAF6/MAPK/NF-κB Signaling Pathway* In vitro *and Protects Against Osteoporosis in Postmenopausal Mice*
Yongjie Chen, Linlin Zhang, Zongguang Li, Zuoxing Wu, Xixi Lin, Na Li, Rong Shen, Guojun Wei, Naichun Yu, Fengqing Gong, Gang Rui, Ren Xu and Guangrong Ji

203 *Identification of Polysaccharides From* Dipsacus asperoides *and Their Effects on Osteoblast Proliferation and Differentiation in a High-Glucose Environment*
Duoduo Xu, Jia Liu, Wei Zheng, Qipin Gao, Yang Gao and Xiangyang Leng

213 *Ginsenoside Compound K Enhances Fracture Healing* via *Promoting Osteogenesis and Angiogenesis*
Lingli Ding, Song Gu, Bingyu Zhou, Min Wang, Yage Zhang, Siluo Wu, Hong Zou, Guoping Zhao, Zhao Gao and Liangliang Xu

223 *The Role of Flavonoids in the Osteogenic Differentiation of Mesenchymal Stem Cells*
Jinli Zhang, Zhihe Liu, Yang Luo, Xiaojian Li, Guowei Huang, Huan Chen, Aiguo Li and Shengnan Qin

235 *Traditional Chinese Medicine as a Promising Strategy for the Treatment of Alzheimer's Disease Complicated With Osteoporosis*
Weifan Xu, Yiping Jiang, Nani Wang, Huanhuan Bai, Shengyan Xu, Tianshuang Xia and Hailiang Xin

frontiers | Frontiers in Pharmacology

EDITORIAL
published: 26 May 2022
doi: 10.3389/fphar.2022.938303

Editorial: Bone and Cartilage Diseases—The Role and Potential of Natural Products

Daohua Xu[1]*, *Longhuo Wu*[2] and *Qian Chen*[3]

[1]Guangdong Key Laboratory for Research and Development of Natural Drugs, School of Pharmacy, Guangdong Medical University, Dongguan, China, [2]College of Pharmacy, Gannan Medical University, Ganzhou, China, [3]Department of Orthopaedics, Warren Alpert Medical School of Brown University/Rhode Island Hospital, Providence, United States

Keywords: bone, cartilage, osteoporosis, osteoarthritis, medicinal plants

Editorial on the Research Topic

Bone and Cartilage Diseases—The Role and Potential of Natural Products

Traditional medicinal plants and nutraceuticals are often used in the therapeutic management of bone and cartilage diseases, and the secondary metabolites are the main agents responsible for their pharmacological activities. The metabolites provide a great resource for developing new potential drugs.

The pathological mechanisms of bone and cartilage diseases, such as osteoporosis and osteoarthritis, are orchestrated by dysregulated signaling pathways, which disrupt homeostasis by induction of catabolic factors as well as down-regulation of anabolic factors. A large number of studies reveal that many signaling pathways, such as NF-κB pathway, MAPK pathway, TLR pathway, Wnt/β-catenin, TGF-β, and Notch pathways, have been involved in regulating the development of bone and cartilage diseases, and the key factors in these pathways might be potential targets for new drugs development. Thus, understanding the underlying molecular mechanisms offers an avenue for researchers to explore the potential interaction between secondary metabolites and bone and cartilage diseases. The research topic entitled "Bone and Cartilage Diseases—The Role and Potential of Natural Products" included 10 original research, 5 review and 1 clinical trial.

OSTEOPOROSIS

Osteoporosis is a common metabolic bone disease, including bone loss due to postmenopausal, senile, and secondary osteoporosis. Although there are many therapeutic drugs available for osteoporosis treatment including bisphosphonates, calcitonin, and parathyroid hormone, the long-term use of these drugs may produce inherent side effects. It is imperative to search for alternative natural compounds (Wang et al., 2017).

Han et al. showed that E.C.D. extracts, consisting of *Eucommia ulmoides* Oliv., *Cuscuta chinensis* Lam, *Davallia trichomanoides* Blume, decreased the loss of urinal calcium and phosphorus and the expression of RANKL and C-terminal telopeptides of type l collagen (CTX) in rat serum. In addition, E.C.D. extracts increased the levels of serum calcium, phosphorus, and osteoprotegerin in experimental glucocorticoid-induced osteoporosis (GIO) rats. E.C.D. extracts also improved bone density, structural integrity, and biomechanical function in experimental GIO rats. The mechanisms of E.C.D. extracts against osteoporosis may be associated with the inhibition of osteoclast differentiation through PI3K/Akt pathway.

OPEN ACCESS

Edited and reviewed by:
Michael Heinrich,
University College London,
United Kingdom

***Correspondence:**
Daohua Xu
daohuax108@163.com

Specialty section:
This article was submitted to Ethnopharmacology, a section of the journal Frontiers in Pharmacology

Received: *07 May 2022*
Accepted: *13 May 2022*
Published: *26 May 2022*

Citation:
Xu D, Wu L and Chen Q (2022) Editorial: Bone and Cartilage Diseases—The Role and Potential of Natural Products. Front. Pharmacol. 13:938303. doi: 10.3389/fphar.2022.938303

The study by Lee et al. showed that *Sparganii Rhizoma* protected against bone loss in ovariectomy rats. *Sparganii Rhizoma* inhibited osteoclast differentiation and bone resorption by down-regulating the activity of NF-κB and MAPK pathways. *Sparganii Rhizoma* also stimulated osteoblast differentiation by increasing the expression of bone morphogenetic protein 2 (BMP-2)/SMAD pathway. Mogrol treatment reduced the bone loss in ovariectomy mice and inhibited the differentiation of osteoclasts by mediating NF-κB and MAPK signaling pathways. It suggested that Mogrol might be a promising compound for preventing or treating osteoporosis (Chen et al.).

The traditional Chinese medicine herbal extracts (Jing extracts) includes *Astragalus mongholicus* Bunge, *Cistanche deserticola* Y.C.Ma, *Dioscorea polystachya* Turcz., *Lycium barbarum* L., *Epimedium brevicornu* Maxim, *Cinnamomum cassia* (L.) J. Presl, *Syzygium aromaticum* Merr. and L.M.Perry, *Angelica sinensis* (Oliv.) Diels, and *Curculigo orchioides* Gaertn. The original research by Qian et al. showed that the Jing extracts alleviated alcohol-induced bone loss by micro-CT analysis of the proximal tibia of male mice. The Jing extracts prevented chronic excessive alcohol consumption-induced osteopenia in male mice.

Diabetic osteoporosis is a disorder of bone metabolism, which is caused by long-term exposure to high glucose and impairment of osteoblast function. Xu et al. showed DAI-1 was a polysaccharide extracted from *Dipsacus asperoides*, which could reverse the inhibition of MC3T3-E1 cell proliferation and differentiation by high levels of glucose. The mechanism is through mediating the activity of BMP-2/Smad/Runx2 signaling pathway.

Anthocyanins are a class of naturally water-soluble flavonoid compounds obtained from colored plants. Mao et al. reviewed the effects of anthocyanins on bone regeneration and their molecular mechanisms. This review showed that anthocyanins promoted osteogenesis by the BMP2 pathway, Wnt/β-catenin pathway, and FGF pathway. In addition, anthocyanins inhibited osteoclastogenesis by the MAPK pathway, NF-κB pathway, and Ca^{2+} pathway.

Bone marrow mesenchymal stem cells (MSCs) are multipotent, which may have the rapeutic potential for bone related diseases. Zhang et al. reviewed the roles of flavonoids in the osteogenic differentiation of MSCs. Flavonoids promoted proliferation and osteogenic differentiation of MSCs and regulated the microenvironment in damaged bone. Combination of MSCs with flavonoids may be a promising alternative to stem cell therapy alone.

FRACTURE

Bone is one of the organs with regenerative ability. Fracture repair usually restores a damaged bone to its pre-injury state. However, approximately 10% of fractures do not heal properly (Einhorn and Gerstenfeld, 2015). It is important to develop drugs for fracture healing. Ginsenoside compound K improved fracture repair in rat open femoral fracture model (Ding et al.). Mechanically, Ginsenoside compound K promoted osteogenic differentiation of bone marrow mesenchymal stem cells through activating Wnt/β-catenin signaling pathway. In addition, Ginsenoside compound K increased the tube formation capacity of human umbilical vein endothelial cells (HUVECs) and angiogenesis during fracture healing.

OSTEONECROSIS OF FEMORAL HEAD

Osteonecrosis of femoral head (ONFH), a progressive hip joint disorder, is associated with impaired blood supply to the femoral head. The pathogenesis mechanism of ONFH is not fully elucidated (Rezus et al., 2021). Peng et al. found that serum amyloid A (SAA), an acute phase lipophilic protein, increased significantly in the serum of ONFH patients. SAA inhibited osteogenic differentiation and promoted the adipogenic differentiation of MSCs. *In vivo* results showed that SAA reduced new bone formation. Thus, SAA is a vital protein in the physiological process of ONFH and may be a potential therapeutic target. Huo Xue Tong Luo (HXTL) capsule is composed of seven herbs, including Cajan leaf, *Angelica sinensis* (Oliv.) Diels, *Paeonia lactiflora* Pall, *Ligusticum striatum* DC, *Prunus persica* (L.) Batsch, *Carthamus tinctorius* L, and *Rehmannia glutinosa* (Gaertn.) DC. A clinical study by Peng et al. showed that HXTL capsules improved hip function and delayed progression to femoral head collapse in ONFH of Association Research Circulation Osseous (ARCO) stage II. HXTL capsule was effective and ideally used when the anterior and lateral portions of the femoral head were not affected.

OSTEOARTHRITIS

Osteoarthritis (OA) is a progressive arthrosis disease characterized by subchondral bone damage, synovitis, and articular cartilage degradation. More than 10% of people under the age of 60 worldwide suffers from OA (Runhaar et al., 2015). In this research topic, three reviews and two original studies focused on OA. Phytochemicals for OA treatment were reviewed by Tian et al., who demonstrated that many phytochemicals exhibited therapeutic effects against OA by mediating relevant autophagy-related pathways. Another review by Mu et al. summarized the roles of botanical drug extracts (BDEs) combining with biomaterial carriers to treat OA in recent 10 years. BDEs, containing flavonoids, polyphenols, alkaloids, and saponins, improved joint functions, promoted repair of damaged cartilage, and delayed progression of OA. The combination of BDEs with biomaterial carriers can relieve OA symptoms and delay the progression of OA. Vafaei et al. reviewed the effects of crocin on bone and cartilage diseases. Specifically, crocin has therapeutic potentials on OA, rheumatoid arthritis, and osteoporosis. Crocin reduced oxidative stress and inflammatory responses, promoted the osteogenic differentiation of MSCs, and suppressed osteoclast functions.

Zhuang et al. demonstrated that Jintiange capsule, a traditional medicine composed of various animal bones, organic compounds, and polysaccharides, reduced the subchondral

bone remodeling and cartilage degeneration in OA mouse models. The mechanism of Jintiange capsule in the treatment of OA is related to its inhibition of osteoclast activation and chondrocyte apoptosis. The extracellular matrix (ECM) is an important constituent of cartilage (Rahmati et al., 2017). Zheng et al. showed that xanthohumol is a naturally occurring prenylflavonoid derived from hops and beer and inhibited the mechanical stimulation-induced ECM degradation by mediating the GAS5/miR-27a signaling pathway in OA chondrocytes.

RHEUMATOID ARTHRITIS

Rheumatoid arthritis (RA) is an autoimmune disease characterized by joint inflammation, followed by cartilage destruction and bone erosion (Jang et al., 2022). The study by Chen et al. demonstrated that kefir peptides alleviated collagen-induced arthritis in the mouse models by inhibiting dendritic cells maturation and inflammatory cytokine release. The kefir peptides may be potential for the clinical use in RA patients.

CONCLUSION

In conclusion, the research topic comprising a collection of 16 articles presents the roles of many natural products for treatment of bone and cartilage diseases. The natural products have shown great prospects for the development of new drugs, which may become new and/or alternative treatment for bone and cartilage diseases. However, randomized, controlled, and double-blind clinical trials of natural products for the treatment of bone and cartilage diseases are needed. Since the roles of natural products could be multi-component and multi-targeted, modern analytical methods in genomics, proteomics, and metabolomics should be applied to unravel their mechanisms of action in treatment of bone and cartilage diseases in the future.

AUTHOR CONTRIBUTIONS

DX drafted the editorial. LW and QC provided critical comments and revised the manuscript.

REFERENCES

Einhorn, T. A., and Gerstenfeld, L. C. (2015). Fracture Healing: Mechanisms and Interventions. *Nat. Rev. Rheumatol.* 11, 45–54. doi:10.1038/nrrheum.2014.164

Jang, S., Kwon, E.-J., and Lee, J. J. (2022). Rheumatoid Arthritis: Pathogenic Roles of Diverse Immune Cells. *Int. J. Mol. Sci.* 23, 905. doi:10.3390/ijms23020905

Rahmati, M., Nalesso, G., Mobasheri, A., and Mozafari, M. (2017). Aging and Osteoarthritis: Central Role of the Extracellular Matrix. *Ageing Res. Rev.* 40, 20–30. doi:10.1016/j.arr.2017.07.004

Rezus, E., Tamba, B. I., Badescu, M. C., Popescu, D., Bratoiu, I., and Rezus, C. (2021). Osteonecrosis of the Femoral Head in Patients with Hypercoagulability-From Pathophysiology to Therapeutic Implications. *Int. J. Mol. Sci.* 22, 6801. doi:10.3390/ijms22136801

Runhaar, J., van Middelkoop, M., Reijman, M., Willemsen, S., Oei, E. H., Vroegindeweij, D., et al. (2015). Prevention of Knee Osteoarthritis in Overweight Females: The First Preventive Randomized Controlled Trial in Osteoarthritis. *Am. J. Med.* 128, 888–e4. doi:10.1016/j.amjmed.2015.03.006

Wang, T., Liu, Q., Tjhioe, W., Zhao, J., Lu, A., Zhang, G., et al. (2017). Therapeutic Potential and Outlook of Alternative Medicine for Osteoporosis. *Curr. Drug Targets* 18, 1051–1068. doi:10.2174/1389450118666170321105425

Conflict of Interest: The authors declare that the research was conducted in the absence of any commercial or financial relationships that could be construed as a potential conflict of interest.

Publisher's Note: All claims expressed in this article are solely those of the authors and do not necessarily represent those of their affiliated organizations, or those of the publisher, the editors and the reviewers. Any product that may be evaluated in this article, or claim that may be made by its manufacturer, is not guaranteed or endorsed by the publisher.

Copyright © 2022 Xu, Wu and Chen. This is an open-access article distributed under the terms of the Creative Commons Attribution License (CC BY). The use, distribution or reproduction in other forums is permitted, provided the original author(s) and the copyright owner(s) are credited and that the original publication in this journal is cited, in accordance with accepted academic practice. No use, distribution or reproduction is permitted which does not comply with these terms.

frontiers in Pharmacology

ORIGINAL RESEARCH
published: 10 September 2021
doi: 10.3389/fphar.2021.737552

Xanthohumol Inhibited Mechanical Stimulation-Induced Articular ECM Degradation by Mediating lncRNA GAS5/miR-27a Axis

Tiansheng Zheng[1], *Qingluo Zhou*[1], *Jishang Huang*[1], *Jinliang Lai*[2], *Guanglin Ji*[1]* and *Dechao Kong*[3]*

[1]Department of Orthopedics, The First Affiliated Hospital of Gannan Medical University, Ganzhou, China, [2]Department of Emergency, The First Affiliated Hospital of Gannan Medical University, Ganzhou, China, [3]Department of Trauma Center, Shanghai General Hospital, Shanghai Jiao Tong University School of Medicine, Shanghai, China

Osteoarthritis (OA) is histopathologically marked by extracellular matrix (ECM) degradation in joint cartilage. Abnormal mechanical stimulation on joint cartilage may result in ECM degeneration and OA development. Matrix metalloproteinase 13 (MMP-13) is one of the catabolic enzymes contributing to the degradation of ECM, and it has become the potential biomarker for the therapeutic management of OA. Xanthohumol (XH), a naturally occurring prenylflavonoid derived from hops and beer, shows the protective activity against OA development. However, the potential mechanisms still need great effort. In this article, mechanical stimulation could significantly increase the expression of MMP-13 and lncRNA GAS5 (GAS5) and promoting ECM degradation. These could be effectively reversed by XH administration. Suppressed expression GAS5 ameliorated mechanical stimulation-induced MMP-13 expression. MiR-27a was predicted and verified as a target of GAS5, and overexpression of miR-27a down regulated the expression of MMP-13. Collectively, XH exhibited protective effects against mechanical stimulation-induced ECM degradation by mediating the GAS5/miR-27a signaling pathway in OA chondrocytes.

Keywords: osteoarthritis, extracellular matrix, mmp-13, xanthohumol, Gas5, miR-27a

OPEN ACCESS

Edited by:
Galina Sud'ina,
Lomonosov Moscow State University, Russia

Reviewed by:
Patrizia Zaramella,
Università degli Studi di Padova, Italy
Yusei Ohshima,
University of Fukui, Japan

***Correspondence:**
Guanglin Ji
jiguanglingygk@163.com
Dechao Kong
441502564@qq.com

Specialty section:
This article was submitted to Inflammation Pharmacology, a section of the journal Frontiers in Pharmacology

Received: *08 July 2021*
Accepted: *27 August 2021*
Published: *10 September 2021*

Citation:
Zheng T, Zhou Q, Huang J, Lai J, Ji G and Kong D (2021) Xanthohumol Inhibited Mechanical Stimulation-Induced Articular ECM Degradation by Mediating lncRNA GAS5/miR-27a Axis. Front. Pharmacol. 12:737552. doi: 10.3389/fphar.2021.737552

INTRODUCTION

Osteoarthritis (OA) is histopathologically marked by progressive degradation of extracellular matrix (ECM) in joint articular cartilage. Mechanical stimulation, implicated in articular cartilage development and maintenance, is dynamic, and it is supposed to support the synthesis of extracellular matrix (ECM) under normal mechanical loading and inhibit the production of ECM under persistent improper loading (Fang et al., 2021). Many studies have reported that exercise affects the physiological actions of a joint in a mechanical intensity-dependent manner. Moderate intensity of exercise plays a critical role in the prevention and therapeutic management of OA, whereas excessive intensity is assumed to induce or exaggerate OA development (Ni et al., 2013; Song et al., 2021). The chondrocyte is the unique cell type in the articular cartilage, and the biochemical activities of chondrocytes responding to mechanical stimulation might affect the biological components and functions of ECM. Excessive mechanical stimulation has been demonstrated to be associated with increased chondrocytes apoptosis in OA cartilage (Yang

et al., 2020). However, the relationship between mechanical stimulation and ECM degradation is still under investigation.

Long noncoding RNA (lncRNA), more than 200 nucleotides, usually cannot be translated into proteins due to lack of an open reading frame (Andrey and Duboule, 2014). Many dysregulated lncRNAs have been involved in the pathological changes of OA, including ECM degradation (He et al., 2021). LncRNA H19 has been demonstrated to ameliorate the mechanical force-induced cartilage degeneration in developmental dysplasia of the hip by mediating miR-485/Dusp5 axis, as indicated by increased expression of COL2A1 and aggrecan and decreased expression of MMP3 and ADAMTS5 in intermittent cyclic mechanical stress (ICMS)-induced chondrocytes (Wang et al., 2020). LncRNA MSR has been reported to be enhanced in response to mechanical stress in chondrocytes. Up regulation of lncRNA MSR facilitates pathological development and leads to cartilage degradation (Liu et al., 2016). Growth arrest specificity 5 (GAS5) is involved in the pathological mediation of OA. Increased expression of GAS5 was observed in human OA cartilage tissues. Forced expression of GAS5 increases the apoptosis rate and inhibits the proliferative activity by sponging miR-137 in chondrocytes (Gao et al., 2020). In contrast, silencing GAS5 expression results in decreased apoptosis and enhanced proliferation in OA chondrocytes (Ji et al., 2020). However, the roles of GAS5 in mechanical stimulation-dependent OA are still unclear.

Xanthohumol (XH) is a naturally occurring prenyl-flavonoid extracted from hops and beer. It has been shown that XH effectively prevents the over-production of hyaluronan, protecting against the early development of OA (Stracke et al., 2011). Specifically, XH can activate NRF2/HO-1 and inhibit NF-κB pathways, reducing cisplatin-induced nephrotoxicity (Li et al., 2018). Our previous study showed that XH could protect OA chondrocytes against IL-1β-induced inflammation and ECM degradation by activating NRF2/HO-1 and inhibiting NF-κB pathways (Zhang et al., 2021). However, the effects of XH on mechanical stimulation-induced OA chondrocytes are still unclear.

MATERIALS AND METHODS

General

This project (GMU201809038) was approved scientifically by the Institutional Animal Care and Use Committee of the First Affiliated Hospital of Gannan Medical University and carried out under the guideline of Animal Care and Use.

Duplication of Mice Osteoarthritis Models by Forced Running

Eight-week-old male C57BL/6 mice were obtained from the Animal Center of Gannan Medical University (Ganzhou, China). Mice were divided into four groups: 1) the negative control group (non-running), 2) the model group (running), 3) the low-dose group (running + treatment with XH (purity≧98%, dissolved in 0.5% carboxymethyl cellulose (CMC) by intragastric administration) at the dose of 30 mg/kg/d (Miranda et al., 2016)), and 4) the high-dose group (running + XH (60 mg/kg/d (Miranda et al., 2016))). Mice were subjected to forced running on a treadmill. The running protocols (Yamagishi et al., 2018) were designed with minor modifications. Simply, mice were forced to run at the speed of 30 m/min for 30 min/day on 5 days/week. The running distance by each mouse was 36 km after 8 weeks. The knee joints were collected and kept in a −80°C refrigerator for gross observation, histochemical examination, and immunohistochemical evaluation.

Cell Isolation and Culture

The articular cartilage from the terminal femur and upper tibia in the knee joints was collected under sterile conditions. The cartilage was then cut into small pieces and digested with pancreatic enzyme (0.25%) and collagenase II (0.2%) at 37°C for 4 h. The collected cells were cultured in DMEM (low glucose) supplemented with 10% FBS and penicillin/streptomycin in an incubator with 5% CO_2 at 37°C. The second or third generation of the isolated chondrocytes was used for the following experiments.

Cyclic Mechanical Stimulation Application

Cells (1×10^5 cells/well) cultured on the 6-well BioFlex plates coated with collagen type I (Flexcell Int. Co., Hillsborough, NC, United States) at 80% confluence were transferred to a computer-controlled Flexcell Tension System (FX-4000) (Flexcell) with 20% surface elongation at a frequency of 6 cycles/min. Cells were harvested after 24 h (Xu et al., 2019).

Cell Viability Assays

The chondrocytes viability was determined using the CCK-8 kit. Simply, cells (5,000 cells/well) were grown in 96-well plates for 24 h. CCK-8 solution (10 μL) was added carefully and co-incubated at 37°C for 4 h. The 450 nm wavelength for absorbance was used for detection using a microplate system.

Cell Transfection

The shRNAs GAS5 (5′-ACTTGCCTGGACCAGCTTAAT-3′) and a scrambled shRNA control (sh-NC: 5′-GCCCACTTA CACTTGAGCA-3′) were obtained from GeneChem (Shanghai, China). They were inserted into pGPH1/Neo and then transfected into chondrocytes using lipofectamine 3000 (Invitrogen), according to the procedures of the manufacturer's instructions. Neomycin was used to select the stable transfectants.

MiR-27a mimics (5′-CCACCAUCGGUUUAGCGUAUG-3′), miR-27a inhibitors (5′-GGUUUACCUUCCCGGGAC AAU-3′), and microRNA negative controls (miR-NC: 5′-GUG AGGACCACCUGUCUCAUU-3′) were purchased from RiboBio (Guangzhou, China). Chondrocytes at the confluence of 60% (1×10^5 cells/well) were conducted for transfection using lipofectamine 3000, after they were cultured for 1 day in the 6-well plates. The designed concentrations of miR-27a mimics, miR-27a inhibitors, and miR-NC in the final transfection system were all 50 nM.

Immunofluorescence

For *in situ* assays, the samples were fixed with 4% paraformaldehyde at room temperature for 48 h. Decalcification was conducted in the solution consisting of EDTA and ammonium hydroxide for 1 week. Paraffin-embedded 5-μm sections of tissues were deparaffinized in xylene and hydrated in a decreasing series of ethanol solutions. The sections were probed with the primary MMP-13 antibody in a humidified chamber at 4°C overnight and secondary horseradish peroxidase (HRP)-conjugated antibodies at room temperature for 1 h. A confocal laser scanning microscope was employed and the fluorescence intensity was detected by using ImageJ.

Chondrocytes were grown and fixed with 4% paraformaldehyde on glass coverslips. Triton X-100 (0.1%) was employed to infiltrate cell and nuclear membranes. Cells were blocked by 5% bovine serum albumin (BSA) (protease-free) and then co-incubated with the primary antibody at 4°C overnight. After that, the secondary goat anti-rabbit IgG antibody was co-incubated for 1 h at room temperature. Subsequently, the medium containing DAPI was used. A confocal laser scanning microscope was employed and the fluorescence intensity was detected by using ImageJ.

qRT-PCR

Cartilage tissues were collected, minced, and homogenized in Trizol reagent (Invitrogen; Thermo Fisher Scientific, Inc.), according to the manufacturer's instructions. Specifically, cartilage was homogenized in 1 ml of TRIzol reagent per 50 mg of tissue. The resultant samples in TRIzol were then mixed thoroughly with 0.2 ml chloroform (Sigma), spun down and the upper fraction was harvested. The fraction was mixed with the same volume of isopropanol, and centrifuged at 10,000 × g for 10 min at 4°C. The pellet was washed with 0.8 ml of 75% ethanol, and dissolved in RNase-free water (Ambion, Thermo Fisher Scientific, United States). All steps were performed under RNase-free conditions. The total amount of the collected RNA was evaluated based on optical density at 260 nm, with its purity determined using the 260/280 nm absorption ratio (NanoDrop 2000 spectrophotometer, Thermo-Fischer Scientific, Waltham, MA, United States).

RNA (2 μg) was reverse transcribed to cDNA using M-MLV. Quantitative PCR assays were conducted on Power SYBRs Green PCR Master Mix (Applied Biosystems, CA, United States) to detect the expression of GAS5 and MMP-13. The expression of miR-27a was detected using the Taqman MicroRNA Reverse Transcription Kit and Taqman Universal Master Mix II kit (Applied Biosystems). GAPDH and U6 were used as the internal reference for mRNA and miRNA, respectively. All the primers were obtained from Biomics. The listed primer sequences are showed as follows: GAS5 forward: 5′-CTTGCCTGGACCAGCTTAAT-3′, reverse: 5′-CAAGCC GACTCTCCATACCT-3'; MMP-13 forward: 5′-CAAGGCTGG TTACCCAACAG-3′, reverse: 5′-CACCTGGGACAACTGGAA TC-3'; GAPDH forward: 5′-AGGTGAAGGTAGGAGTCAACG-3′, reverse: 5′-AGGGGTCACTGATGGCAACA-3'; miR-27a forward: 5′-TTCACAGTGGCTAAGTTCCGC-3′, reverse: 5′-CTCTACAGCTATATTGCCAGCCAC-3'; U6 forward: 5′-CTC GCTTCAGCAGCACA-3′, reverse: 5′-AACGCTGCACGAATT TGCGT-3'. Fold changes by using $2^{-\triangle\triangle CT}$ method were indicated for the expression of miRNA and mRNA.

Western Blot Assays

The total proteins in cells were extracted and the protein concentrations were determined by BCA protein assay kit (Beyotime). 30 μg of the total proteins were applied to 10% SDS-PAGE and then transferred onto PVDF membranes. After being blocked in TBS containing 5% non-fat milk for 1 h, the membranes were co-incubated with the primary antibodies at 4°C overnight against MMP-13 (1:1,000 dilutions, Cell signaling technology, Cat. no.69926), Col2a1 (1:1,000 dilutions, Sigma, Cat. no.SAB4500366), and GAPDH (1:1,000 dilutions, Cell signaling technology, Cat. no.5174), and then with the secondary antibody conjugated with peroxidase (1:2000 dilutions, Sigma-Aldrich, Cat. no. AP510). Protein bands were detected using the enhanced chemiluminescence detection system.

Dual-Luciferase Reporter Assay

The predicted system StarBase v2.0 was used for screening the potential miRNA targets of GAS5. The recombinant luciferase plasmids were constructed by cloning the sequences of wild-type (WT) GAS5 into the pGL-3 luciferase basic vector. In addition, the mutant-type with its mutant binding sites for miR-27a was also constructed as MUT-GAS5. Each constructed plasmid was transfected into chondrocytes with miR-27a mimics/miR-NC using lipofectamine 3000. Following incubation for 48 h at 37°C, the activities of firefly and Renilla luciferase were detected using the Glomax 96 luminometer. Firefly luciferase reporter was quantitatively normalized to Renilla luciferase activity.

RIP Assays

This assay was used for investigating the direct interaction between GAS5 and miR-27a by employing Magna RNA immunoprecipitation kit (Millipore). Chondrocytes (about 2×10^7 cells) were lysed and then co-incubated with magnetic beads, which were previously coated with antibodies against Argonaute2 (Ago2, Cell Signaling Technology, Cat. no.2897). Anti-IgG was used as the negative control. The RNA expression was detected by qRT-PCR. Finally, the levels of GAS5 and miR-27a in anti-IgG and anti-Ago2 groups were compared.

Statistical Analysis

All experiments were performed three independent times and data are expressed as the mean ± standard deviation. SPSS 20.0 software was used for statistical analysis. One-way ANOVA and Tukey's post hoc test were used to analyze the differences between multiple groups. $p < 0.05$ was indicated a significant difference statistically.

RESULTS

XH Protected Against Mechanical Stimulation-Induced Extracellular Matrix Degradation in Mice

To explore the roles of XH on mechanical stimulation-induced OA, a forced running protocol was designed. After 8-weeks running and treatment with XH (Low, 30 mg/kg/d; High, 60 mg/kg/d) by oral administration, the mice were sacrificed. As

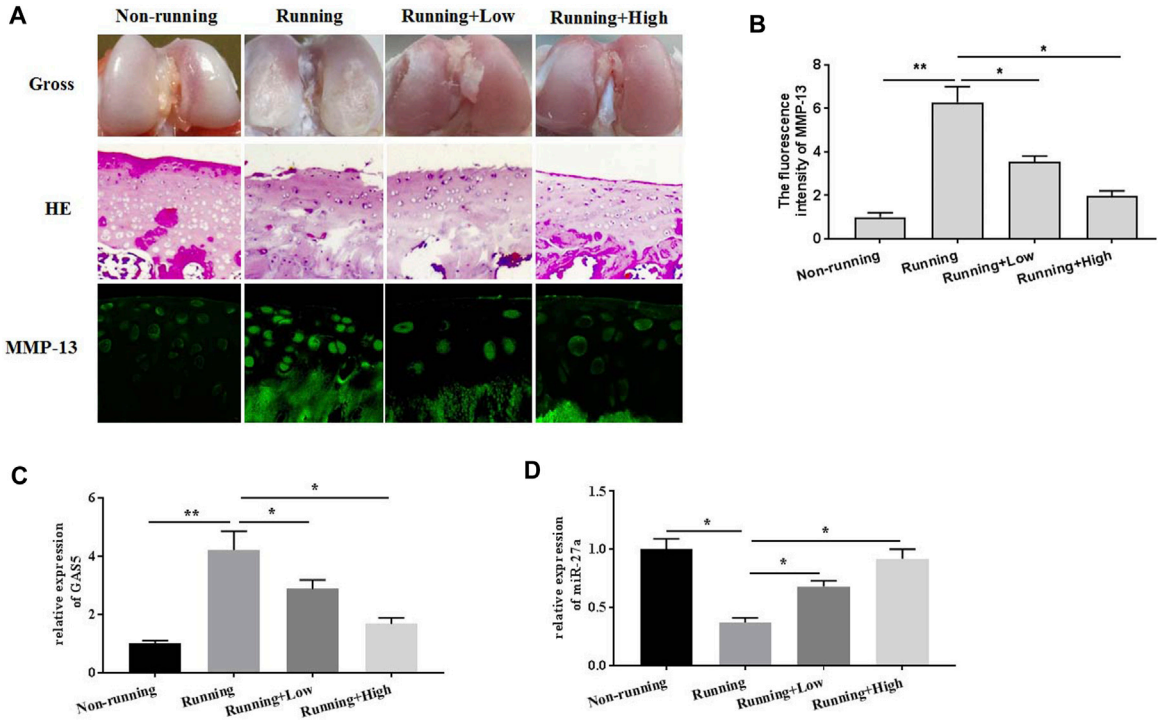

FIGURE 1 | The effects of XH on mechanical stimulation-induced OA cartilage in mice were investigated. **(A)** The gross observation, histochemical examination, and immunofluorescence activity of MMP-13 were indicated (magnification×40). **(B)** The calculation of fluorescence activity of MMP-13. The expression of GAS5 **(C)** and miR-27a **(D)** in the knee joint cartilages were detected by qRT-PCR. *$p < 0.05$ and **$p < 0.01$. Low, the group treated with XH (30 mg/kg/d); High, the group treated with XH (60 mg/kg/d).

results showed in **Figure 1A**, no obvious tissue damages were observed in the non-running (negative control) group in gross observation and HE staining. In contrast, the erosion on the rough surface in the cartilage of the running group was significantly showed. The immunofluorescence activity of MMP-13 (**Figure 1A-B**) in the running group was also dramatically increased, compared with that in the non-running group. Interestingly, administration of XH orally could effectively protect articular cartilage against mechanical stimulation-induced damage, as shown by smoother cartilage surface and thicker cartilage. In addition, XH also significantly decreased the immunofluorescence activity of MMP-13. These suggested that XH exhibited protective activity against mechanical stimulation-induced damage in mice. The expression of GAS5 (**Figure 1C**) and miR-27a (**Figure 1D**) were also determined. The results had shown that mechanical stimulation upregulated GAS5 expression but downregulated miR-27a expression. XH could reverse the effects of mechanical stimulation on cartilage.

XH Ameliorated Mechanical Stimulation-Induced MMP-13 and GAS5 Expression

The cell viability assays indicated that mechanical stimulation (20% surface elongation at a frequency of 6 cycles/min) could decrease chondrocytes viability (**Figure 2A**). XH protected chondrocytes and increased viability. The immunofluorescence assays (**Figures 2B,C**) also indicated that XH significantly decreased the intensity of MMP-13, compared with that in the running group. Mechanical stimulation increased the mRNA (**Figure 2D**) and protein (**Figures 2E,F**) expression of MMP-13 and decreased the expression of Col2a1 (**Figures 2E,G**). In addition, mechanical stimulation up regulated GAS5 expression (**Figure 2H**) but down regulated miR-27a expression (**Figure 2I**) in cultured chondrocytes. These effects could be ameliorated by XH administration.

Suppressed Expression of GAS5 Attenuated Mechanical Stimulation-Induced MMP-13 Expression

To explore the roles of GAS5 in mechanical stimulation-treated chondrocytes, suppressed expression of GAS5 was conducted by transfection of shRNA-GAS5. The expression of GAS5 was detected by qRT-PCR for identification of successful transfection (**Figure 3A**). Transfection of shRNA-GAS5 significantly increased the cell viability (**Figure 3B**), compared with non-transfection. In addition, suppressed expression of GAS5 enhanced the expression of miR-27a (**Figure 3C**),

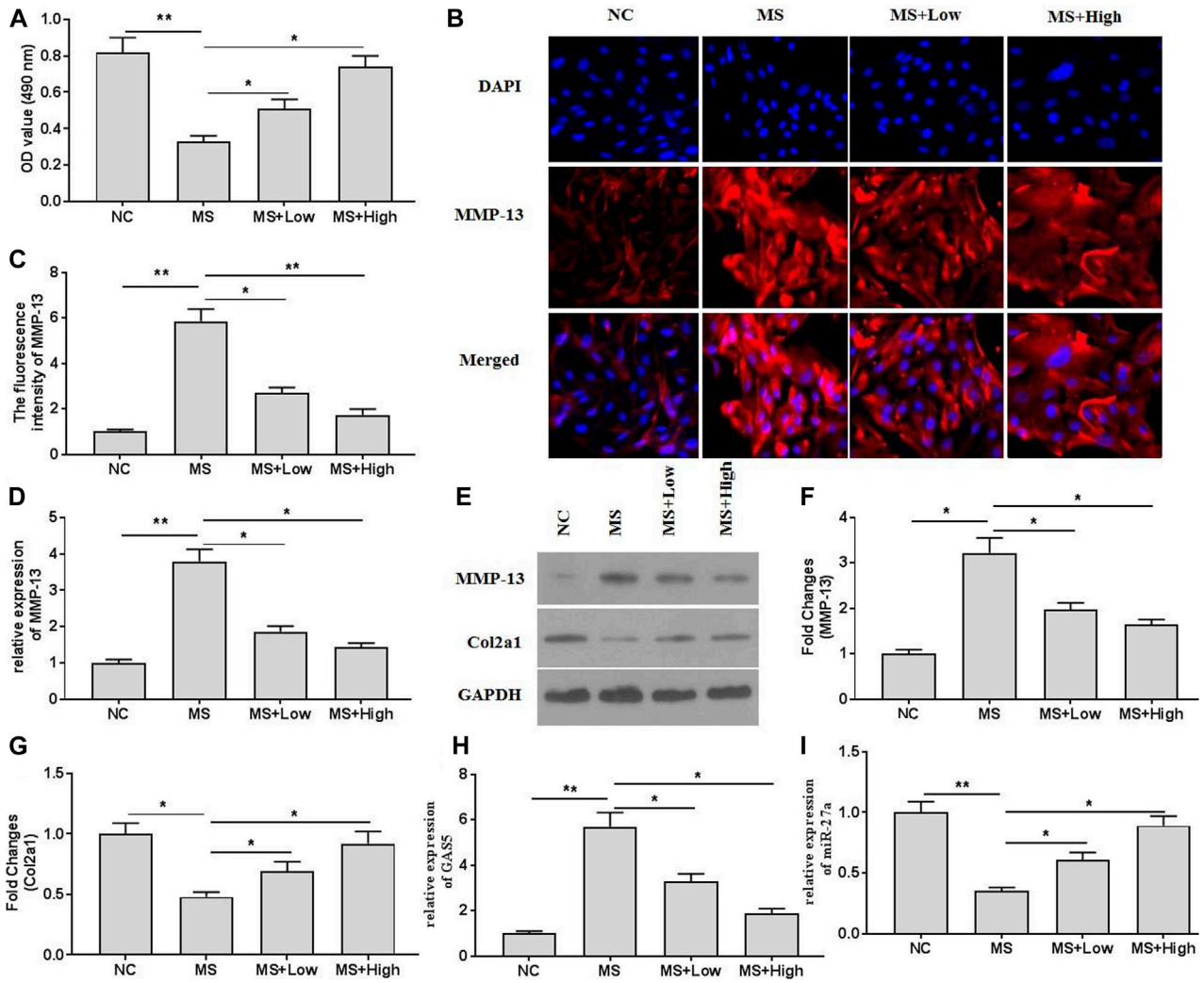

FIGURE 2 | The effects of XH on mechanical stimulation-induced MMP-13 and GAS5/miR-27a expression in chondrocytes were investigated. **(A)** The cell viability was determined by CCK-8 assays. **(B)** The immunofluorescence intensity of MMP-13 in mechanical stimulation-treated chondrocytes was detected. **(C)** The calculation of fluorescence activity of MMP-13. The mRNA **(D)** expression of MMP-13 was determined by qRT-PCR, and the protein expression of MMP-13 **(E-F)** and Col2a1 **(E**, and **G)** were determined by western blotting assays. The expression of GAS5 **(H)** and miR-27a **(I)** was detected by qRT-PCR. $^{*}p < 0.05$ and $^{**}p < 0.01$. NC, negative control; MS, mechanical stimulation; Low, XH (5 μM); High, XH (20 μM).

attenuated the expression of MMP-13 (**Figures 3D–F,H,I**), and promoted the expression of Col2a1 (**Figures 3E,G**).

GAS5 Interacted With miR-27a

To further investigate the possible mechanisms of GAS5 in mediating mechanical stimulation-induced OA development, the potential miRNAs that bind to GAS5 were explored by the predicting software Starbase2.0. It was predicted that miR-27a could be a potential target of GAS5 (**Figure 4A**). The dual-luciferase reporter assays showed that the luciferase activity in the reporter containing the WT-GAS5 decreased by more than 60%. In contrast, no significant differences were observed in the relative luciferase activities between the NC reporter and the reporter containing the MUT-GAS5 (**Figure 4B**). In addition, RIP assays demonstrated that GAS5 could physically interact with miR-27a (**Figure 4C**). Taken together, miR-27a could be a potential target of GAS5.

Overexpression of miR-27a Attenuated Mechanical Stimulation-Induced MMP-13 Expression

To investigate the roles of miR-27a in mediating mechanical stimulation-induced chondrocytes, miR-27a mimics were transfected into chondrocytes. The expression of miR-27a was detected by qRT-PCR for identification of successful transfection (**Figure 5A**). It has been reported that MMP-13 was a direct target of miR-27a (Zhang et al., 2020). MiR-27a-mimics transfection effectively decreased the expression of GAS5 (**Figure 5B**) and MMP-13 (**Figures 5C–E**, **G-H**) and increased

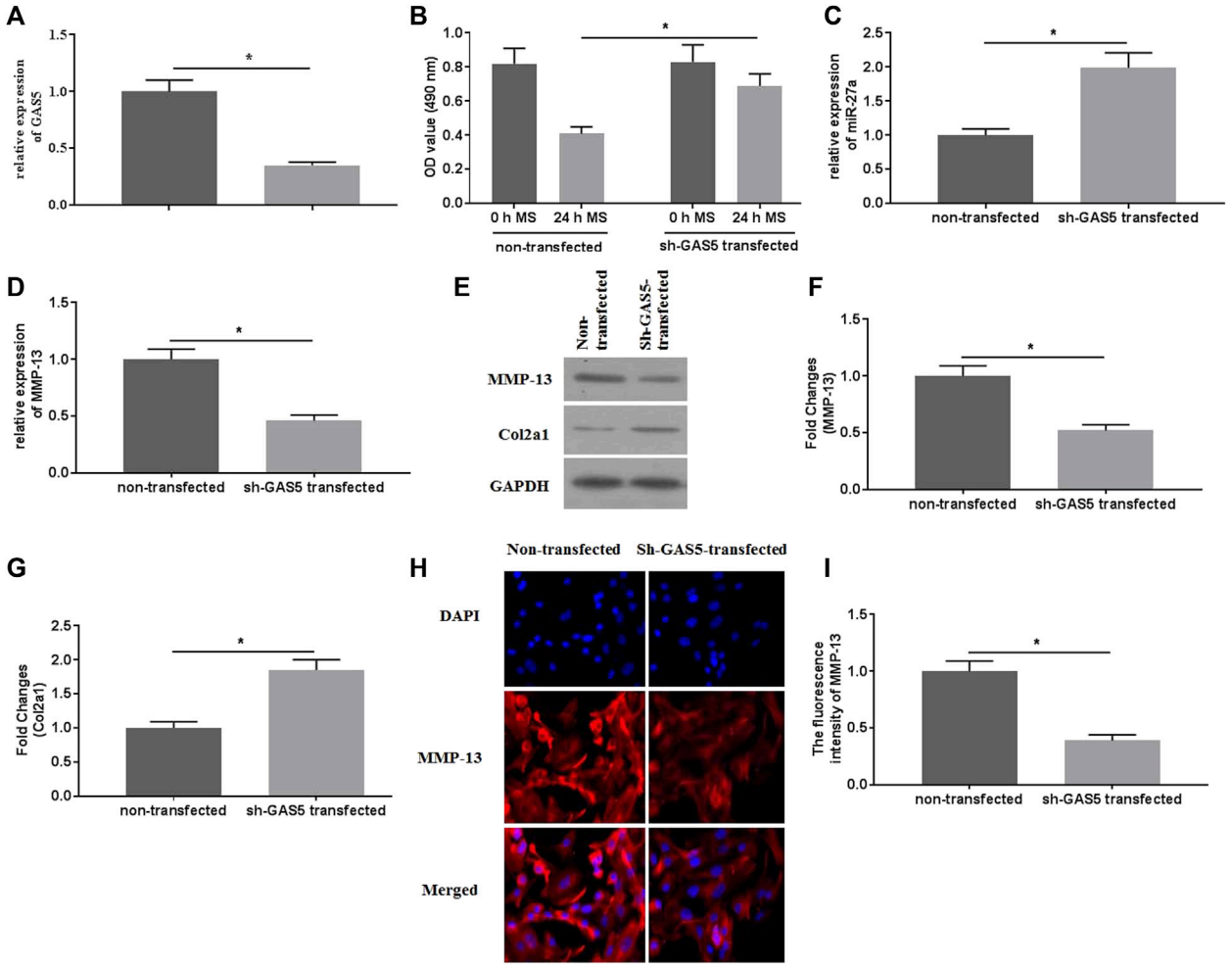

FIGURE 3 | The effects of suppressed GAS5 expression on mechanical stimulation-induced MMP-13 expression were investigated. **(A)** The expression of GAS5 was detected by qRT-PCR in sh-GAS5-transfected chondrocytes. **(B)** The cell viability was determined by CCK-8 assays. **(C)** The expression of miR-27a was determined by qRT-PCR. The mRNA **(D)** expression of MMP-13 was determined by qRT-PCR, and the protein expression of MMP-13 **(E-F)** and Col2a1 **(E** and **G)** were detected bywestern blotting assays. **(H)** The immunofluorescence intensity of MMP-13 was detected. **(I)** The calculation of fluorescence activity of MMP-13. $^{*}p < 0.05$ and $^{**}p < 0.01$.

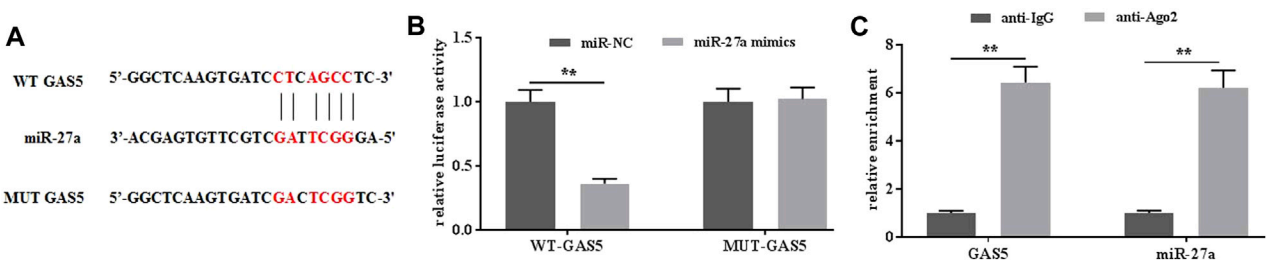

FIGURE 4 | GAS interacted with miR-27a. **(A)** The potential interaction between GAS5 and miR-27a was predicted by Starbase2.0 software. **(B)** The relative luciferase activity was determined in chondrocytes co-transfected with both WT/MUT-GAS5 and miR-27a mimics/miR-NC. **(C)** The interaction between GAS5 and miR-27a was confirmed by RIP assays. $^{**}p < 0.01$.

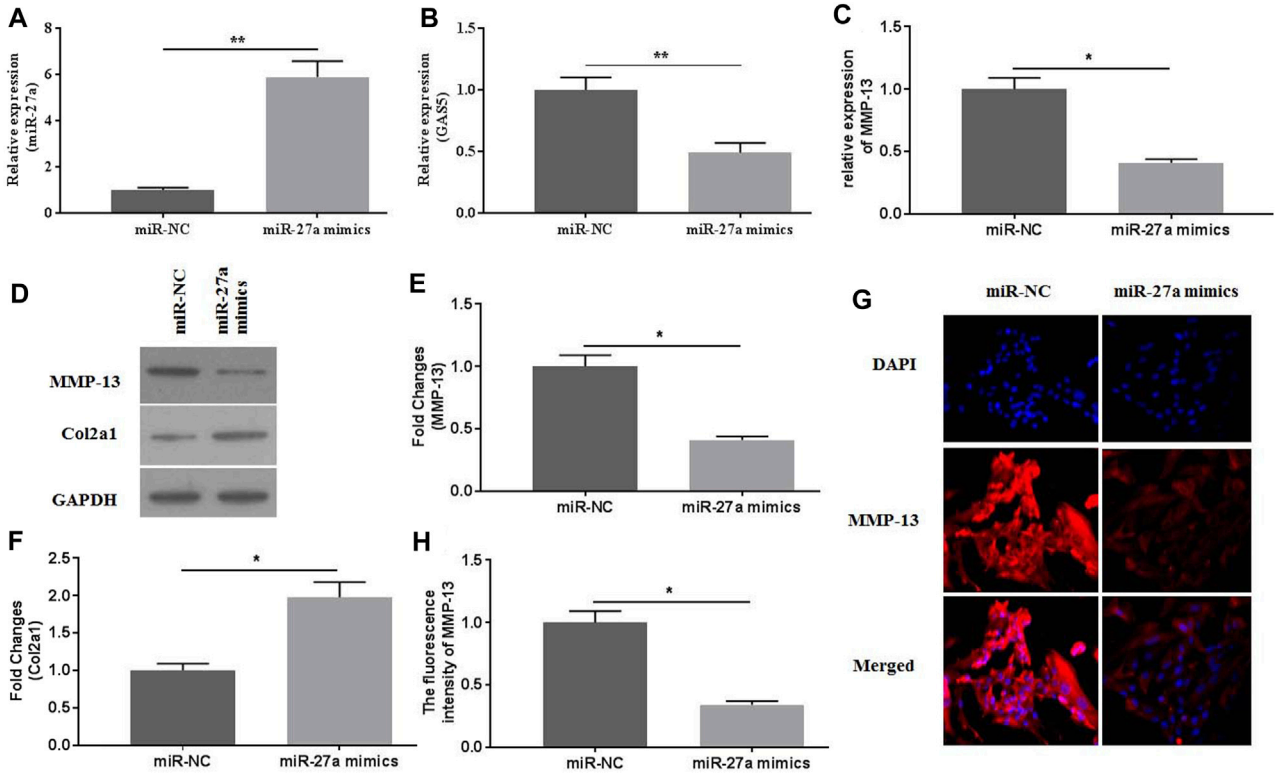

FIGURE 5 | The effects of miR-27a mimic-transfection on mechanical stimulation-induced MMP-13 expression were investigated. The expression of miR-27a **(A)** and GAS5 **(B)** was determined by qRT-PCR in miR-27a mimic-transfected chondrocytes. The mRNA **(C)** expression of MMP-13 was determined by qRT-PCR, and the protein expression of MMP-13 **(D-E)** and Col2a1 **(D** and **F)** were determined by western botting assays. **(G)** The immunofluorescence intensity of MMP-13 was detected. **(H)** The calculation of fluorescence activity of MMP-13. *$p < 0.05$ and **$p < 0.01$.

the expression of Col2a1 (**Figures 5D,F**). Collectively, mechanical stimulation induced the expression of MMP-13 by mediating the activity GAS5/miR-27a signaling pathway.

XH Protected Chondrocytes Against Mechanical Stimulation-Induced Damages by Mediating GAS5/miR-27a Signaling Pathway

To investigate whether XH exhibited protective activity against mechanical stimulation-induced damages, miR-27a inhibitors were transfected. The expression of miR-27a was determined by qRT-PCR for identification of successful transfection (**Figure 6A**). MiR-27a inhibitors transfection abrogated the increased cell viability by XH (**Figure 6B**). Suppressed expression of miR-27a could reverse the inhibitory effects of XH on MMP-13 and Col2a1 expression, as showed by no significant difference in fluorescence activity (**Figures 6C,D**) of MMP-13, increased expression of MMP-13 (**Figures 6E–G**), and decreased expression of Col2a1 (**Figures 6F,H**). In addition, Suppressed expression of miR-27a up regulated the expression of GAS5 (**Figure 6I**). Collectively, XH exhibited protective activity against mechanical stimulation-induced MMP-13 by mediating GAS5/miR-27a signaling pathway in chondrocytes.

DISCUSSION

Abnormal mechanical stimulation associated with obesity, trauma, and joint instability has been demonstrated to change joint loading and be closely related to chondrocytes apoptosis and cartilage degeneration (Guilak, 2011). However, the underlying mechanism of mechanical stimulation in mediating cartilage degeneration is still unclear. It is necessary to explore the roles of mechanical stimulation in OA pathological development. In this article, we found that XH significantly protected against mechanical stimulation-ECM degradation in forced running mice models. *In vitro*, isolated chondrocytes were stimulated with 20% surface elongation at a frequency of 6 cycles/min. XH exhibited protective activity against MMP-13 expression, which could be enhanced by GAS5. Suppressed expression of GAS5 attenuated mechanical stimulation-induced MMP-13 expression. MiR-27a could interact with GAS5, and overexpression of miR-27a significantly decreased the expression of MMP-13. Collectively, XH protected against mechanical stimulation-induced cartilage damages by mediating GAS5/miR-27a signaling pathway.

Articular cartilage is a deficiency of regenerative capacity when subjected to acute or long-term abnormal mechanical stimulation. Under such circumstances, articular cartilage is susceptible to develop degenerative lesions and OA pathology (Fang et al., 2021). Many factors have been demonstrated to contribute to mechanical stimulation-mediated OA development, but their precise roles

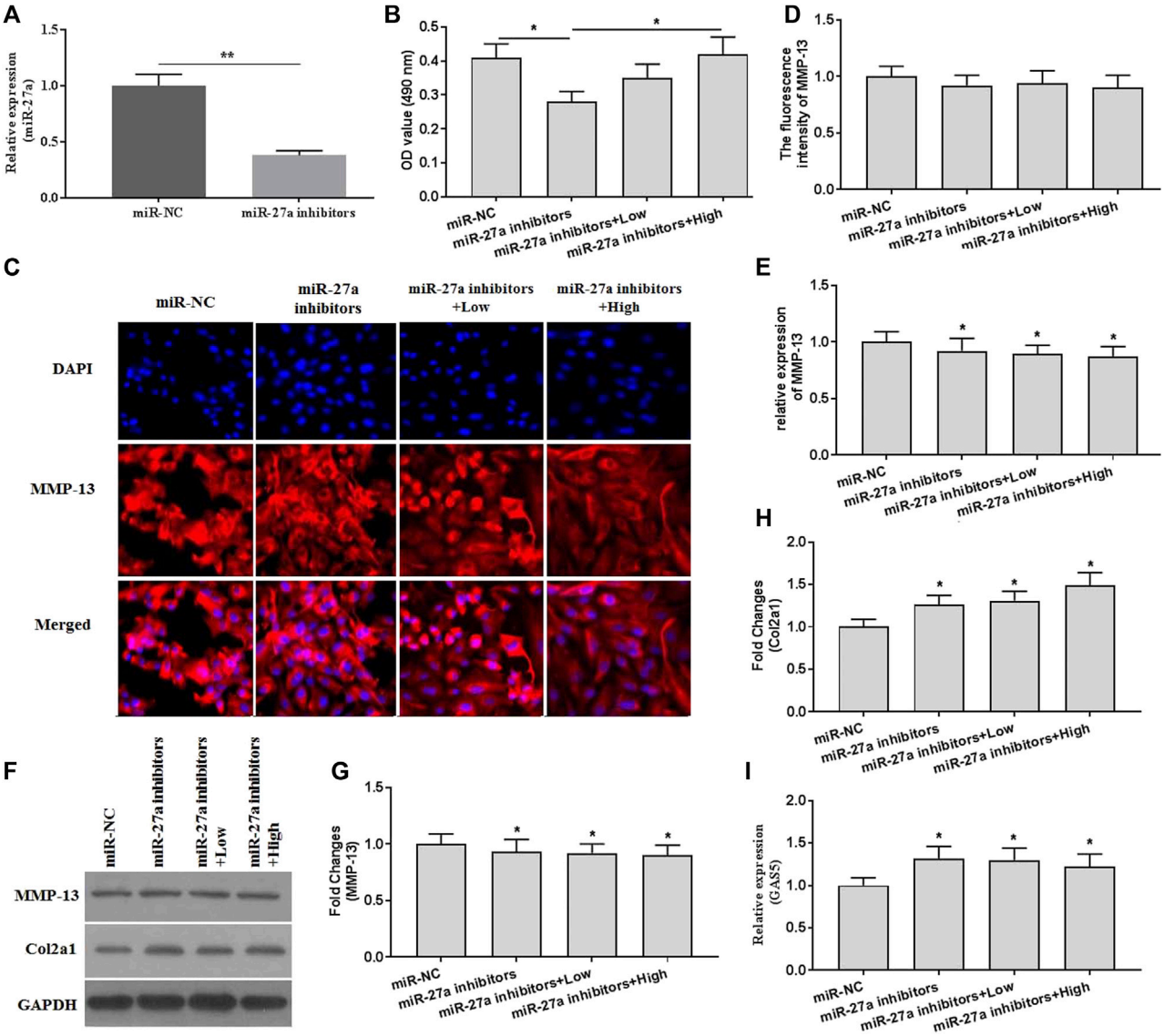

FIGURE 6 | The effects of XH on the expression of MMP-13 in miR-27a inhibitor-transfected chondrocytes with mechanical stimulation were investigated. **(A)** The expression of miR-27a was determined by qRT-PCR in miR-27a inhibitor-transfected chondrocytes. **(B)** The cell viability was determined by CCK-8 assays after mechanical stimulation for 24 h. **(C)** The immunofluorescence intensity of MMP-13 was determined. **(D)** The calculation of fluorescence activity of MMP-13. The mRNA **(E)** expression of MMP-13 was determined by qRT-PCR, and the protein expression of MMP-13 **(F-G)** and Col2a1 **(F** and **H)** were determined by western blotting assays. **(I)** The expression of GAS5 was determined by qRT-PCR in miR-27a inhibitor-transfected chondrocytes. $^{*}p < 0.05$ and $^{**}p < 0.01$. NC, negative control; Low, XH (5 μM); High, XH (20 μM).

need to be further elucidated. NF-κB- and MAPK-mediated inflammatory responses are significantly enhanced by overloading (Choi et al., 2019). Wnt/β-catenin signaling is also activated by overloading, leading to up regulation of MMPs activity and degradation of ECM (Pérez-García et al., 2019). Transforming growth factor-β (TGF-β) maintains functions of articular cartilage by transducing Smad2/3 signals, thereby promoting collagen (Col2a1) and fibronectin synthesis and inhibiting ECM degradation induced by overloading (Madej et al., 2016). Mechanical loading also causes differential expression of miRNAs (Kwak et al., 2020) and lncRNAs (He et al., 2021), which regulate the activities of MMPs and the progress of OA development.

Many studies have demonstrated that bulk RNA sequencing and single-cell sequencing data have been used for the analysis in the pathological development of OA (Li et al., 2021). LncRNA LINC00917 and CTD-2246P4.1 have been reported to regulate angiogenesis in OA cartilage by mediating SPHK1 (Chen et al., 2015), which is associated with angiogenesis and promotes the survival of endothelial cells, the processes of cartilage degradation, and the development of OA (Minashima et al., 2014). Increased expression of lncRNA PVT1 in diabetic OA cartilage has been associated with Mankin score and reduced expression of type II collagen by negatively interacting with miR-146a, increasing the productions of inflammatory cytokines, and activating the

TGFβ/SMAD4 signaling pathway. LncRNA GAS5 expression is up regulated in OA cartilage tissues. Silence of GAS5 increases the autophagy ability and decreases the apoptosis rate by sponging miR-144 (Ji et al., 2021). Similarly, our study also demonstrated that GAS5 expression was significantly increased by mechanical stimulation *in vivo* and *in vitro*. Suppressed expression of GAS5 effectively ameliorated the expression of MMP-13, which plays a critical role in ECM degradation and OA development.

MicroRNAs suppress genes expression post-transcriptionally. Dysregulation of microRNAs in OA has been reported (Shvedova and Kobayashi, 2020). MiR-29 acts across the development and progression of OA by negatively regulating Smad, NF-κB, and canonical Wnt signaling pathways (Le et al., 2016). MiR-34a/miR-146a/miR-181a has been considered as the potential mediator in mediating the hydrostatic pressure effects on oxidative stress in osteoarthritic chondrocytes. Silencing expression of miR-34a/miR-146a/miR-181a significantly down regulates the expression of MMP-13 and ADAMTS-5 and up regulates the expression of Col2a1, mediating the effects of hydrostatic pressure on chondrocytes apoptosis (Cheleschi et al., 2020). In our study, miR-27a expression was significantly decreased in mechanical stimulation-treated chondrocytes. MMP-13 was a direct target of miR-27a (Zhang et al., 2020), and miR-27a was a direct target of GAS5. Overexpression of miR-27a greatly decreased the expression of MMP-13 and GAS5 and increased the expression of Col2a1. Suppressed expression of miR-27a exhibited reverse effects. In another study, it showed that GAS5 also exaggerates the pathological development of OA by interacting with miR-137 (Gao et al., 2020). Both miR-27a and miR-137 are the downstream factors of GAS5. However, the direct relationship between miR-27a and miR-137 has not been reported. A study showed that miR-137 can ameliorate the cell damages induced by H2O2 (Wang et al., 2021). Consistently, miR-137 is also reported to decrease inflammation, oxidative stress, neuronal injury, and cognitive impairment in mice with ischemic stroke (Tian et al., 2020). Similarly, a study reports that miR-27a mimics can suppress oxygen glucose deprivation (OGD)-induced oxidative injury in HT22 cells (Li et al., 2021). Both miR-137 and miR-27a exhibits protective activities against oxidative stress. However, their relationships needs to be further elucidated.

Recently, natural products have been intensively studied for developing new potential drugs. Harpagoside, isolated from Harpagophytum procumbens, has been demonstrated to protect OA cartilage against degradation by inhibiting the expression of MMP-13 and pro-inflammatory cytokines (Haseeb et al., 2017). Morroniside is a natural compound from Cornus officinalis. It has been reported that morroniside protects against ECM degradation and OA development by decreasing the expression of MMP-3/-13 in the destabilization of the medial meniscus-induced mouse OA models (Park et al., 2021). Alpinetin, a natural flavonoid compound, can effectively reduce TNFα-induced MMP-13 and ADAMTS-5 expression and protect against cartilage destruction in rat OA chondrocytes (Gao et al., 2020). XH has been shown various biological activities, including anti-inflammation, anti-oxidation, anti-proliferation, and anti-angiogenesis (Harikumar et al., 2009; Krajka-Kuźniak et al., 2020). Our previous study shows that XH inhibits the production of inflammatory cytokines by activating the NRF2/HO-1 signaling pathway, protecting OA chondrocytes (Zhang et al., 2021). In this study, XH exhibited inhibitory activity against ECM degradation by mediating GAS5/miR-27a signaling pathway *in vivo* and *in vitro*.

Interestingly, how XH mediated GAS5/miR-27a signaling pathway is still unclear. The biological activity of XH has been demonstrated by activating the NRF2/HO-1 signaling, and whether NRF2/HO-1 signaling is involved in the mechanism of XH in mediating the GAS5/miR-27a pathway still needed to be elucidated. GAS5 has been reported to enhance oxidative stress in melanoma cells (Xu et al., 2020), macrophages (Zhang et al., 2021), and rats with cerebral ischemic stroke (Wu et al., 2021). MiR-27a expression can be activated by NRF2/HO-1 signaling in DSS-induced colitis mouse model (Dun et al., 2021). It is plausible that activation of NRF2/HO-1 signaling might suppress the expression of GAS5/miR-27a axis, which should be confirmed in chondrocytes. And this might be involved in the pharmacological activity of XH in protecting against OA development.

There are limitations to this study. CMC is often used as a good cosolvent to improve the bioavailability of natural products. Recently, CMC has been demonstrated to reduce post-prandial plasma glucose levels (Miehle et al., 2021). No control group with CMC administration was designed, and this made the possibility to confuse the biological activity of XH alone or combined with CMC. It needed more efforts to elucidate the possible roles of CMC in the biological activity of XH *in vivo*.

CONCLUSION

XH protected against mechanical stimulation-induced ECM degradation in OA chondrocytes by mediating the GAS5/miR-27a/MMP-13 signaling pathway.

DATA AVAILABILITY STATEMENT

The original contributions presented in the study are included in the article/supplementary material, further inquiries can be directed to the corresponding authors.

ETHICS STATEMENT

The animal study was reviewed and approved by the Institutional Animal Care and Use Committee of the First Affiliated Hospital of Gannan Medical University.

AUTHOR CONTRIBUTIONS

GJ and DK provided the idea of this paper. TZ, QZ, JH, and JL conducted the experiments and revised and finalized the paper. All authors approved the final paper.

FUNDING

This study was financially supported by Team Construction Projects from Gannan Medical University (TS202002).

REFERENCES

Andrey, G., and Duboule, D. (2014). SnapShot: Hox Gene Regulation. *Cell* 156 (4), 856–e1. e851. doi:10.1016/j.cell.2014.01.060

Cheleschi, S., Barbarino, M., Gallo, I., Tenti, S., Bottaro, M., Frati, E., et al. (2020). Hydrostatic Pressure Regulates Oxidative Stress through microRNA in Human Osteoarthritic Chondrocytes. *Int. J. Mol. Sci.* 21 (10). doi:10.3390/ijms21103653

Chen, Y., Ni, H., Zhao, Y., Chen, K., Li, M., Li, C., et al. (2015). Potential Role of lncRNAs in Contributing to Pathogenesis of Intervertebral Disc Degeneration Based on Microarray Data. *Med. Sci. Monit.* 21, 3449–3458. doi:10.12659/msm.894638

Choi, M. C., Jo, J., Park, J., Kang, H. K., and Park, Y. (2019). NF-κB Signaling Pathways in Osteoarthritic Cartilage Destruction. *Cells* 8 (7). doi:10.3390/cells8070734

Dun Su, S., Wang, X., Ma, Y., Hao, J., Jinshen Wang, W., Yongqu Lu, L., et al. (2021). Nrf2-induced miR-23a-27a-24-2 Cluster Modulates Damage Repair of Intestinal Mucosa by Targeting the Bach1/HO-1 axis in Inflammatory Bowel Diseases. *Free Radic. Biol. Med.* 163, 1–9. doi:10.1016/j.freeradbiomed.2020.11.006

Fang, T., Zhou, X., Jin, M., Nie, J., and Li, X. (2021). Molecular Mechanisms of Mechanical Load-Induced Osteoarthritis. *Int. Orthop.* 45 (5), 1125–1136. doi:10.1007/s00264-021-04938-1

Gao, S. T., Yu, Y. M., Wan, L. P., Liu, Z. M., and Lin, J. X. (2020a). LncRNA GAS5 Induces Chondrocyte Apoptosis by Down-Regulating miR-137. *Eur. Rev. Med. Pharmacol. Sci.* 24 (21), 10984–10991. doi:10.26355/eurrev_202011_23582

Gao, Y., Wang, S., He, L., Wang, C., and Yang, L. (2020b). Alpinetin Protects Chondrocytes and Exhibits Anti-inflammatory Effects via the NF-Kb/ERK Pathway for Alleviating Osteoarthritis. *Inflammation* 43 (5), 1742–1750. doi:10.1007/s10753-020-01248-3

Guilak, F. (2011). Biomechanical Factors in Osteoarthritis. *Best Pract. Res. Clin. Rheumatol.* 25 (6), 815–823. doi:10.1016/j.berh.2011.11.013

Harikumar, K. B., Kunnumakkara, A. B., Ahn, K. S., Anand, P., Krishnan, S., Guha, S., et al. (2009). Modification of the Cysteine Residues in IkappaBalpha Kinase and NF-kappaB (P65) by Xanthohumol Leads to Suppression of NF-kappaB-Regulated Gene Products and Potentiation of Apoptosis in Leukemia Cells. *Blood* 113 (9), 2003–2013. doi:10.1182/blood-2008-04-151944

Haseeb, A., Ansari, M. Y., and Haqqi, T. M. (2017). Harpagoside Suppresses IL-6 Expression in Primary Human Osteoarthritis Chondrocytes. *J. Orthop. Res.* 35 (2), 311–320. doi:10.1002/jor.23262

He, C. P., Jiang, X. C., Chen, C., Zhang, H. B., Cao, W. D., Wu, Q., et al. (2021). The Function of lncRNAs in the Pathogenesis of Osteoarthritis. *Bone Jt. Res* 10 (2), 122–133. doi:10.1302/2046-3758.102.Bjr-2020-0228.R1

Ji, Q., Qiao, X., Liu, Y., Wang, D., and Yan, J. (2020). Silencing of Long-chain N-on-coding RNA GAS5 in O-steoarthritic C-hondrocytes I-s M-ediated by T-argeting the miR-34a/Bcl-2 axis. *Mol. Med. Rep.* 21 (3), 1310–1319. doi:10.3892/mmr.2019.10900

Ji, Q., Qiao, X., Liu, Y., and Wang, D. (2021). Expression of Long-Chain Noncoding RNA GAS5 in Osteoarthritis and its Effect on Apoptosis and Autophagy of Osteoarthritis Chondrocytes. *Histol. Histopathol*, 18312. doi:10.14670/hh-18-312

Krajka-Kuźniak, V., Cykowiak, M., Szaefer, H., Kleszcz, R., and Baer-Dubowska, W. (2020). Combination of Xanthohumol and Phenethyl Isothiocyanate Inhibits NF-Kb and Activates Nrf2 in Pancreatic Cancer Cells. *Toxicol. Vitro* 65, 104799. doi:10.1016/j.tiv.2020.104799

Kwak, Y. H., Kwak, D. K., Kim, N. Y., Kim, Y. J., Lim, J. S., and Yoo, J. H. (2020). Significant Changes in Synovial Fluid microRNAs after High Tibial Osteotomy in Medial Compartmental Knee Osteoarthritis: Identification of Potential Prognostic Biomarkers. *PLoS One* 15 (1), e0227596. doi:10.1371/journal.pone.0227596

Le, L. T., Swingler, T. E., Crowe, N., Vincent, T. L., Barter, M. J., Donell, S. T., et al. (2016). The microRNA-29 Family in Cartilage Homeostasis and Osteoarthritis. *J. Mol. Med. (Berl)* 94 (5), 583–596. doi:10.1007/s00109-015-1374-z

Li, F., Yao, Y., Huang, H., Hao, H., and Ying, M. (2018). Xanthohumol Attenuates Cisplatin-Induced Nephrotoxicity through Inhibiting NF-Kb and Activating Nrf2 Signaling Pathways. *Int. Immunopharmacol* 61, 277–282. doi:10.1016/j.intimp.2018.05.017

Li, W., Zhu, Q., Xu, X., and Hu, X. (2021a). MiR-27a-3p Suppresses Cerebral Ischemia-Reperfusion Injury by Targeting FOXO1. *Aging (Albany NY)* 13 (8), 11727–11737. doi:10.18632/aging.202866

Li, X., Liao, Z., Deng, Z., Chen, N., and Zhao, L. (2021b). Combining Bulk and Single-Cell RNA-Sequencing Data to Reveal Gene Expression Pattern of Chondrocytes in the Osteoarthritic Knee. *Bioengineered* 12 (1), 997–1007. doi:10.1080/21655979.2021.1903207

Liu, Q., Hu, X., Zhang, X., Dai, L., Duan, X., Zhou, C., et al. (2016). The TMSB4 Pseudogene LncRNA Functions as a Competing Endogenous RNA to Promote Cartilage Degradation in Human Osteoarthritis. *Mol. Ther.* 24 (10), 1726–1733. doi:10.1038/mt.2016.151

Madej, W., Buma, P., and van der Kraan, P. (2016). Inflammatory Conditions Partly Impair the Mechanically Mediated Activation of Smad2/3 Signaling in Articular Cartilage. *Arthritis Res. Ther.* 18, 146. doi:10.1186/s13075-016-1038-6

Miehle, E., Bader-Mittermaier, S., Schweiggert-Weisz, U., Hauner, H., and Eisner, P. (2021). Effect of Physicochemical Properties of Carboxymethyl Cellulose on Diffusion of Glucose. *Nutrients* 13 (5). doi:10.3390/nu13051398

Minashima, T., Campbell, K. A., Hadley, S. R., Zhang, Y., and Kirsch, T. (2014). The Role of ANK Interactions with MYBBP1a and SPHK1 in Catabolic Events of Articular Chondrocytes. *Osteoarthritis Cartilage* 22 (6), 852–861. doi:10.1016/j.joca.2014.04.008

Miranda, C. L., Elias, V. D., Hay, J. J., Choi, J., Reed, R. L., and Stevens, J. F. (2016). Xanthohumol Improves Dysfunctional Glucose and Lipid Metabolism in Diet-Induced Obese C57BL/6J Mice. *Arch. Biochem. Biophys.* 599, 22–30. doi:10.1016/j.abb.2016.03.008

Ni, G. X., Liu, S. Y., Lei, L., Li, Z., Zhou, Y. Z., and Zhan, L. Q. (2013). Intensity-dependent Effect of Treadmill Running on Knee Articular Cartilage in a Rat Model. *Biomed. Res. Int.* 2013, 172392. doi:10.1155/2013/172392

Park, E., Lee, C. G., Han, S. J., Yun, S. H., Hwang, S., Jeon, H., et al. (2021). Antiosteoarthritic Effect of Morroniside in Chondrocyte Inflammation and Destabilization of Medial Meniscus-Induced Mouse Model. *Ijms* 22 (6), 2987. doi:10.3390/ijms22062987

Pérez-García, S., Carrión, M., Villanueva-Romero, R., Hermida-Gómez, T., Fernández-Moreno, M., Mellado, M., et al. (2019). Wnt and RUNX2 Mediate Cartilage Breakdown by Osteoarthritis Synovial Fibroblast-Derived ADAMTS-7 and -12. *J. Cel Mol Med* 23 (6), 3974–3983. doi:10.1111/jcmm.14283

Shvedova, M., and Kobayashi, T. (2020). MicroRNAs in Cartilage Development and Dysplasia. *Bone* 140, 115564. doi:10.1016/j.bone.2020.115564

Song, C. X., Liu, S. Y., Zhu, W. T., Xu, S. Y., and Ni, G. X. (2021). Excessive Mechanical Stretch-mediated O-steoblasts P-romote the C-atabolism and A-poptosis of C-hondrocytes via the Wnt/β-catenin S-ignaling P-athway. *Mol. Med. Rep.* 24 (2). doi:10.3892/mmr.2021.12232

Stracke, D., Schulz, T., and Prehm, P. (2011). Inhibitors of Hyaluronan export from Hops Prevent Osteoarthritic Reactions. *Mol. Nutr. Food Res.* 55 (3), 485–494. doi:10.1002/mnfr.201000210

Tian, R., Wu, B., Fu, C., and Guo, K. (2020). miR-137 Prevents Inflammatory Response, Oxidative Stress, Neuronal Injury and Cognitive Impairment via Blockade of Src-Mediated MAPK Signaling Pathway in Ischemic Stroke. *Aging (Albany NY)* 12 (11), 10873–10895. doi:10.18632/aging.103301

Wang, C. L., Zuo, B., Li, D., Zhu, J. F., Xiao, F., Zhang, X. L., et al. (2020). The Long Noncoding RNA H19 Attenuates Force-Driven Cartilage Degeneration via miR-483-5p/Dusp5. *Biochem. Biophys. Res. Commun.* 529 (2), 210–217. doi:10.1016/j.bbrc.2020.05.180

Wang, L., Tian, Y., Cao, Y., Ma, Q., and Zhao, S. (2021). MiR-137 Promotes Cell Growth and Inhibits Extracellular Matrix Protein Expression in H2O2-Induced Human Trabecular Meshwork Cells by Targeting Src. *Neurosci. Lett.* 755, 135902. doi:10.1016/j.neulet.2021.135902

Wu, R., Yun, Q., Zhang, J., and Bao, J. (2021). Long Non-coding RNA GAS5 Retards Neural Functional Recovery in Cerebral Ischemic Stroke through Modulation of the microRNA-455-5p/PTEN axis. *Brain Res. Bull.* 167, 80–88. doi:10.1016/j.brainresbull.2020.12.002

Xu, B., Xing, R., Huang, Z., Yin, S., Li, X., Zhang, L., et al. (2019). Excessive Mechanical Stress Induces Chondrocyte Apoptosis through TRPV4 in an Anterior Cruciate Ligament-Transected Rat Osteoarthritis Model. *Life Sci.* 228, 158–166. doi:10.1016/j.lfs.2019.05.003

Xu, W., Yan, Z., Hu, F., Wei, W., Yang, C., and Sun, Z. (2020). Long Non-coding RNA GAS5 Accelerates Oxidative Stress in Melanoma Cells by Rescuing EZH2-

Mediated CDKN1C Downregulation. *Cancer Cel Int* 20, 116. doi:10.1186/s12935-020-01167-1

Yamagishi, K., Tsukamoto, I., Nakamura, F., Hashimoto, K., Ohtani, K., and Akagi, M. (2018). Activation of the Renin-Angiotensin System in Mice Aggravates Mechanical Loading-Induced Knee Osteoarthritis. *Eur. J. Histochem.* 62 (3). doi:10.4081/ejh.2018.2930

Yang, H., Wen, Y., Zhang, M., Liu, Q., Zhang, H., Zhang, J., et al. (2020). MTORC1 Coordinates the Autophagy and Apoptosis Signaling in Articular Chondrocytes in Osteoarthritic Temporomandibular Joint. *Autophagy* 16 (2), 271–288. doi:10.1080/15548627.2019.1606647

Zhang, M., Zhang, R., Zheng, T., Chen, Z., Ji, G., Peng, F., et al. (2021a). Xanthohumol Attenuated Inflammation and ECM Degradation by Mediating HO-1/C/EBPβ Pathway in Osteoarthritis Chondrocytes. *Front. Pharmacol.* 12, 680585. doi:10.3389/fphar.2021.680585

Zhang, Q. C., Hu, S. Q., Hu, A. N., Zhang, T. W., Jiang, L. B., and Li, X. L. (2020). Autophagy-activated Nucleus Pulposus Cells Deliver Exosomal miR-27a to Prevent Extracellular Matrix Degradation by Targeting MMP-13. *J. Orthop. Res.* 39, 1921–1932. doi:10.1002/jor.24880

Zhang, Y., Lu, X., Yang, M., Shangguan, J., and Yin, Y. (2021b). GAS5 Knockdown Suppresses Inflammation and Oxidative Stress Induced by Oxidized Low-Density Lipoprotein in Macrophages by Sponging miR-135a. *Mol. Cel Biochem* 476 (2), 949–957. doi:10.1007/s11010-020-03962-w

Conflict of Interest: The authors declare that the research was conducted in the absence of any commercial or financial relationships that could be construed as a potential conflict of interest.

Publisher's Note: All claims expressed in this article are solely those of the authors and do not necessarily represent those of their affiliated organizations, or those of the publisher, the editors and the reviewers. Any product that may be evaluated in this article, or claim that may be made by its manufacturer, is not guaranteed or endorsed by the publisher.

Copyright © 2021 Zheng, Zhou, Huang, Lai, Ji and Kong. This is an open-access article distributed under the terms of the Creative Commons Attribution License (CC BY). The use, distribution or reproduction in other forums is permitted, provided the original author(s) and the copyright owner(s) are credited and that the original publication in this journal is cited, in accordance with accepted academic practice. No use, distribution or reproduction is permitted which does not comply with these terms.

frontiers in Pharmacology

ORIGINAL RESEARCH
published: 05 October 2021
doi: 10.3389/fphar.2021.721594

Suppression of Dendritic Cell Maturation by Kefir Peptides Alleviates Collagen-Induced Arthritis in Mice

Chien-Fu Chen[1,2], Hsin-Pei Li[1], Ya-Hsuan Chao[3], Min-Yu Tu[4,5,6], Chih-Ching Yen[1,7], Ying-Wei Lan[1], Shang-Hsun Yang[8], Kowit-Yu Chong[9,10], Chi-Chien Lin[3]* and Chuan-Mu Chen[1,11]**

[1]Department of Life Sciences, and Ph.D. Program in Translational Medicine, College of Life Sciences, National Chung Hsing University, Taichung, Taiwan, [2]Department of Orthopedic Surgery, Taichung Armed Forces General Hospital, Taichung, Taiwan, [3]Institute of Biomedical Sciences, National Chung Hsing University, Taichung, Taiwan, [4]Kaohsiung Armed Forces General Hospital Gangshan Branch, Kaohsiung, Taiwan, [5]Department of Health Business Administration, Meiho University, Pingtung, Taiwan, [6]Institute of Medical Science and Technology, National Sun Yat-Sen University, Kaohsiung, Taiwan, [7]Department of Internal Medicine, China Medical University Hospital, and College of Health Care, China Medical University, Taichung, Taiwan, [8]Department of Physiology, and Institute of Basic Medical Sciences, College of Medicine, National Cheng Kung University, Tainan, Taiwan, [9]Department of Medical Biotechnology and Laboratory Science and Graduate Institute of Biomedical Sciences, Division of Biotechnology, College of Medicine, Chang Gung University, Taoyuan, Taiwan, [10]Hyperbaric Oxygen Medical Research Lab, Bone and Joint Research Center, and Department of Laboratory Medicine, Chang Gung Memorial Hospital, Taoyuan, Taiwan, [11]The iEGG and Animal Biotechnology Center, and the Rong Hsing Research Center for Translational Medicine, National Chung Hsing University, Taichung, Taiwan

OPEN ACCESS

Edited by:
Qian Chen,
Warren Alpert Medical School of Brown University, United States

Reviewed by:
Olin Liang,
Brown University, United States
Ju-Pi Li,
Chung Shan Medical University, Taiwan

***Correspondence:**
Chuan-Mu Chen
chchen1@dragon.nchu.edu.tw
Chi-Chien Lin
lincc@dragon.nchu.edu.tw
Kowit-Yu Chong
kchong@mail.cgu.edu.tw

Specialty section:
This article was submitted to Ethnopharmacology, a section of the journal Frontiers in Pharmacology

Received: 28 June 2021
Accepted: 17 September 2021
Published: 05 October 2021

Citation:
Chen C-F, Li H-P, Chao Y-H, Tu M-Y, Yen C-C, Lan Y-W, Yang S-H, Chong K-Y, Lin C and Chen C-M (2021) Suppression of Dendritic Cell Maturation by Kefir Peptides Alleviates Collagen-Induced Arthritis in Mice. Front. Pharmacol. 12:721594. doi: 10.3389/fphar.2021.721594

Arthritis is a disorder that is characterized by joint inflammation and other symptoms. Rheumatoid arthritis (RA), an autoimmune disease, is one of the most common arthritis in worldwide. Inflammation of the synovium is the main factor that triggers bone erosion in the joints in RA, but the pathogenesis of RA is not clearly understood. Kefir grain-fermented products have been demonstrated to enhance immune function and exhibit immune-modulating bioactivities. This study aims to explore the role of kefir peptides (KPs) on the regulation of dendritic cell, which are found in RA synovial fluid, and the protection effects of KPs on mice with collagen-induced arthritis (CIA). Immature mouse bone marrow-derived dendritic cells (BMDCs) were treated with KPs (2.2 and 4.4 mg/ml) and then exposed to lipopolysaccharide (LPS) to study the immune regulation function of KPs in dendritic cells. Mice with CIA (n = 5 per group) were orally administrated KPs (3.75 and 7.5 mg/day/kg) for 21 days and therapeutic effect of KPs on mice with arthritis were assessed. In this study, we found that KPs could inhibit surface molecule expression, reduce inflammatory cytokine release, and repress NF-κB and MAPK signaling in LPS-stimulated mouse BMDCs. In addition, a high dose of KPs (7.5 mg/kg) significantly alleviated arthritis symptoms, decreased inflammatory cytokine expression, suppressed splenic DC maturation and decrease the percentage of Th1 and Th17 in the spleens on mice with CIA. Our findings demonstrated that KPs ameliorate CIA in mice through the mechanism of suppressing DC maturation and inflammatory cytokine releases.

Keywords: kefir peptides, rheumatoid arthritis, collagen-induced arthritis, bone marrow-derived dendritic cells, CD4$^+$ T cells

INTRODUCTION

Arthritis is a chronic disorder that involves joint inflammation, and the related symptoms generally include joint pain and stiffness. Two of the most common types of arthritis are osteoarthritis (OA) and rheumatoid arthritis (RA) (Kidd et al., 2007). OA is a painful condition caused by gradually mechanical wear and tear on joints, whereas RA is an autoimmune disease arising from an abnormal immune response in which patient's own immune system attacks the joints (Parekh et al., 1985). The pathogenesis of RA is not clearly understood but may involve genomic variations, gene transcription, protein translation and posttranslational modifications (Song and Lin, 2017). The erosion of cartilage and bone is a classical feature of RA. One of the major factors that triggers cartilage and bone erosion in joints during RA progression is inflammation of the synovium (Chabaud et al., 2000; Won et al., 2011).

Previous studies demonstrated the importance of activated T cells in RA pathogenesis. The collagen-induced arthritis (CIA) animal model demonstrated the involvement of activated pro-inflammatory Th1 and Th17 cells, as well as suppressed Treg cells may be involved in the pathogenesis of RA (Sarkar et al., 2010). In addition, dendritic cells (DCs), also known as sensory cells, are antigen-presenting cells (APCs) that display antigen complexes in the context of major histocompatibility complexes (MHCs) on the cell surfaces to induce immune responses (Kambayashi and Laufer, 2014). DCs are derived from bone marrow stem cells (BMSC) and found in an immature state in the blood. DCs mainly function to process antigens, upregulate costimulatory molecule expressions and migrate to lymph nodes that polarize naïve T-cell differentiation into, such as Th1, Th2 or Th17 effector cells to enhance immunity against foreign antigens and tolerance to self-antigens during activation. DCs also secrete many important cytokines to adjust immune responses (Blanco et al., 2008; Chang et al., 2014). However, both immature and mature DCs have been found to accumulate in the synovial joint tissues in RA patients (Pettit et al., 2000; Lebre et al., 2008).

The excessive production of pro-inflammatory cytokines or chemokines and the continuous presentation of autoantigens by DCs in the CIA mice are considered to be the important factors leading to the pathogenesis and progression of arthritis (Leung et al., 2002). Therefore, inhibiting the up-regulation of DCs is a potential strategy to regulate immune-mediated rheumatic diseases (Khan et al., 2009; Benham et al., 2015; Ahmed and Bae, 2016). Recent researches seeking to inhibit the maturation of DCs in RA has attracted great attention to the development and exploration of RA drugs. For example, gold sodium thiomalate and leflunomide derivatives have recently been shown to affect the maturation and differentiation of DCs, and may reduce the progression of RA (Wang et al., 2002; Kirsch et al., 2005; Zeyda et al., 2005).

Kefir is produced from milk proteins by a microbial community derived from fermented kefir grains (Tu et al., 2015). The health benefits of kefir products have mostly been elucidated; these benefits include improved gastrointestinal flora, increased immune modulatory, antithrombotic, antimicrobial and calcium absorption bioactivities (Chen et al., 2020). Our previous studies demonstrated that treatment with KPs decreased $PM_{4.0}$-induced reactive oxygen species (ROS) generation, significantly reduced p-NF-κB, NLRP3, caspase-1, IL-1β, IL-4, IL-6, and TNF-α expression and also increased SOD antioxidant activity in an NF-κB-Luc$^{+/+}$ transgenic mouse model (Chen et al., 2019).

In this study, we focused on the investigation of crucial role of KPs in the regulation of immune function in BMDCs *in vitro*, and in a mouse model of CIA *in vivo*, which is the most commonly utilized model for autoimmune RA.

MATERIALS AND METHODS

Ethics Statement

The animal experiments were approved by the Institutional Animal Care and Use Committee of National Chung Hsing University, Taiwan (IACUC no. 109-106) and were carried out in compliance with institutional guidelines.

Animals

Female DBA/1 mouse strain (aged 6–8 weeks) was obtained from the Jackson Laboratory (Bar Harbor, ME, United States), and OT-II TCR transgenic mice were kindly provided by Prof. Ching-Liang Chu (National Taiwan University, Taipei, Taiwan). All the mice were housed under controlled conditions with ad *libitum* supply of chow and water in a specific pathogen-free (SPF) animal facility.

Preparation of KPs

Kefir starter grains purchased from Phermpep Co. (Taichung, Taiwan) were inoculated in sterilized fresh milk and incubated at 20°C for overnight to activate the grains. The grains were retrieved with a fine-mesh sieve, reinoculated into sterilized milk protein broth and incubated at the condition as previously described (Shi et al., 2018; Tu et al., 2020). The total peptide content in the KPs powder, calculated as the triglycine equivalent, was 23.1 g/100 g.

Preparation of Bone Marrow-Derived DCs

BMDCs were isolated from mouse bone marrow cells as previously described (Chen et al., 2016; Yang et al., 2020). Briefly, the bone marrow cells were flushed from the tibiae and femurs of female DBA/1 or OT-II mice, and the cells were cultured in RPMI-1640 medium (Thermo Fisher Scientific, Waltham, MA, United States). On days 2, 4 and 6 of culture, the nonadherent cells were gently removed, and replaced with fresh medium supplemented with GM-CSF (20 ng/ml) and IL-4 (10 ng/ml). The loosely adherent cells were harvested on day 7 and considered immature BMDCs.

Flow Cytometry Analysis of Surface Maker Expression by BMDCs and Splenic DCs

For detection of BMDC differentiation *in vitro*, the 1:1000 dilution of anti-CD11c antibody was utilized to detect the expression of CD11c marker via an Accuri five flow cytometer

following 2.2 or 4.4 mg/ml of KPs were added to the culture media. Fresh KPs were supplemented each time whenever the medium was changed. BMDCs with the density of 1×10^6 cells/well were pretreated with KPs (2.2 or 4.4 mg/ml) for 1 h and then stimulated by LPS (100 ng/ml) for 24 h. After treatment, the cells were stained at 4°C for 30 min with a FITC-labeled mouse anti-CD11c antibody, PE-labeled anti-CD40, CD80 and CD86 antibodies or isotype-matched control antibody, and the cells were subsequently analyzed by an Accuri five flow cytometer (BD Biosciences, Franklin Lakes, NJ, United States). The mean fluorescence intensity (MFI) of surface markers, CD40, CD80 and CD86, were calculated by Accuri C6 software (BD Biosciences) after gating based on forward scatter (FSC) and $CD11c^+$ expression. Splenocytes were prepared from the spleen on day 42, and a single cell suspension was obtained. The cellular markers expressed by the splenocytes were also analyzed by the Accuri five flow cytometer after gating based on FSC and $CD11c^+$ expression to identify splenic dendritic cells.

CCK-8 Cell Viability Assay

The viability of BMDCs was determined by a CCK-8 colorimetric assay accordingly (Sigma-Aldrich, St. Louis, MO, United States). Briefly, BMDCs (5×10^4 cells/well) were plated on 96-well plates, incubated in the presence or absence of KPs (2.2 or 4.4 mg/ml) for 1 h, and stimulated with LPS (100 ng/ml) for 24 h. After treatment, CCK-8 solution (10 μl) was added to the test wells and incubated for 4 h. Then, the O.D. absorbance was detected at a wavelength of 450 nm.

Lactate Dehydrogenase Assay

Cellular toxicity was examined based on LDH release from cells into the culture medium using an LDH assay kit (Cayman Chemical Co., Ann Arbor, MI, United States). The amount of LDH was measured at a wavelength of 450 nm with a microplate reader (Tecan, Durham, NC, United States).

Cytokine Measurement *in vitro*

BMDCs (5×10^4 cells/well) were incubated in the presence or absence of KPs (4.4 mg/ml) for 1 h, and stimulated with 100 ng/ml LPS, 20 μg/ml zymosan, 20 μg/ml lipoteichoic acid, 250 μg/ml polyinosine polycytidylic acid, 500 ng/ml flagellin, 20 ng/ml Pam2Cys-Ser-Lys4, or 200 nM CpG oligodeoxynucleotides-1826 for 24 h. The cytokine levels of IL-6, IL-12p70, IL-23 and TNF-α were quantified in cell-free supernatants using mouse ELISA kits (Thermo Fisher Scientific).

OVA-specific T Cell Activation

BMDCs were purified from OT-II mice with magnetic beads conjugated to anti-CD11c mAb (Miltenyi Biotec, Auburn, CA, United States) and were pulsed with 2 μg/ml OVAP2 (Echo Chemical Co., Taichung, Taiwan) and incubated with LPS (100 ng/ml), KPs (4.4 mg/ml), or LPS + KPs for 18 h. After incubation, the BMDCs (5×10^5) were cocultured with OVAP2-specific $CD4^+$ T cells that were negatively enriched from the spleens of OT-II mice at cellular ratios of 1:5 ($CD11c^+$ DC:$CD4^+$ T cell) for 72 h ^{3}H-labeled thymidine (1 μCi/well) was added for the last 18 h (Tian et al., 2020). The cells were collected, and the ^{3}H-thymidine incorporation was quantified by liquid scintillation counting (Beckman, Boulevard Brea, CA, United States).

Western Blotting Analysis

Purified BMDCs were pretreated with or without KPs (2.2 or 4.4 mg/ml) for 1 h and further incubated for 6 h with 100 ng/ml LPS before being harvested. The protein blots were incubated overnight at 4°C with primary antibodies against p38, phospho-p38 (Thr180/Tyr182), p42/44 (137F5), phospho-p42/44 (Thr202/Tyr204, 20G11), JNK, phospho-JNK (81E11), or GAPDH. The appropriate horseradish peroxidase (HRP)-labeled secondary antibodies (Jackson ImmunoResearch, West Grove, PA, United States) were used. The bands were developed with enhanced chemiluminescence (ECL) detection kit reagent (GE Healthcare Life Sciences). All the band densities were quantified by densitometric analysis using ImageJ 1.47 software (NIH, Bethesda, MD, United States) and normalized to the expression of GAPDH in each lane (Tung et al., 2020).

Nuclear Extract Preparation and NF-κB/p65 Activity Assay

BMDCs were pretreated with or without KPs (4.4 mg/ml) for 1 h and further cultured for 6 h with LPS (100 ng/ml) before being harvested. A NE-PER extraction system (Thermo Fisher Scientific) was used to prepare the nuclear extracts. To detect nuclear NF-κB/p65 binding, a total of 20 μg nuclear extract was used in a Trans-AM NF-κB ELISA kit (Active Motif North America, Carlsbad, CA, United States).

Th1 and Th17 Cell Differentiation *in vitro*

Purified $CD4^+$ T cells were obtained from the spleens of naïve DBA/1 mice and stimulated with 1 μg/ml plate-coated anti-CD3 (clone 2C11) and 1 μg/ml soluble-form anti-CD28 (clone PV1.17) under Th1-polarizing conditions [5 ng/ml IL-2, 10 ng/ml IL-12 and 2 μg/ml anti-IL-4 antibody (Biolegend, San Diego, CA, United States)] or Th17-polarizing conditions (20 ng/ml IL-6, 2.5 ng/ml TGF-β, 10 μg/ml anti-IFN-γ and 10 μg/ml anti-IL-4), and the cells treated with or without KPs (4.4 mg/ml) starting at the beginning of the induction. The cells were collected on day 4 of KPs treatment, and intracellular cytokine analysis was performed.

Induction of CIA and KPs Treatment

Induction of arthritis was achieved using an established method (Brand et al., 2007). Briefly, CIA was induced by a single subcutaneous injection of 100 μg bovine type II collagen (CII; Morwell Diagnostic, Zurich, Switzerland) emulsified with equal Freund's complete adjuvant (Difco Laboratories, Franklin Lakes, NJ, United States) into the base of the tail. On day 21, all the mice were boosted with an injection of 100 μg CII emulsified in Freund's incomplete adjuvant (Difco Laboratories). After the CII induction of arthritis, the mice were randomly distributed into four groups as follows: 1) no immunization (normal; n = 5); 2) CIA control (n = 5); 3) CIA treated with a high dose of KPs (7.5 mg/day/kg body weight (BW), n = 5); and 4) CIA treated

with a low dose of KPs (3.75 mg/day/kg BW, n = 5). The different doses of KPs were suspended in 10 ml ddH_2O and orally administered at the same volume of 0.2 ml per mouse every day for 3 weeks.

Clinical Assessment of Arthritis

The arthritis score for clinical assessment was evaluated in each paw and recorded every 3 days using a scoring system as previously described (Yue et al., 2017). After booster immunization, the mouse paws were assessed using a 0–4 points scale based on increasing levels of paw swelling, erythema, edema and joint rigidity. The arthritis score for each mouse was the sum of the severity of all four paws (maximum 16 points for each mouse).

Histological Evaluation

After the mice was sacrificed (on day 42), the right hind limbs were harvested and fixed in 10% formalin. The sections were stained with hematoxylin and eosin (H&E) and observed under light microscopy at a magnification of 100 × (Lan et al., 2019; Chen et al., 2020). Histological changes were scored in the parameters as previously described (Wasserman, 2011): 1) cell infiltration, 2) synovial hyperplasia and 3) cartilage destruction. Scores of 0–3 were assigned on the following criteria: 0, no changes; 1, mild changes; 2, moderate changes; and 3, severe changes.

Cytokine Measurement in Paw Tissues

Frozen paw tissues (100 mg) were homogenized in RIPA lysis buffer (1 ml) containing a protease inhibitor cocktail (Pierce, Rockford, IL, United States), and the protein concentration was calculated with a bicinchoninic acid (BCA) assay kit (Thermo Fisher Scientific). The levels of the cytokines, IFN-γ, IL-6, IL-10, IL-17A, and TNF-α, were measured using murine ELISA kits (eBioscience Inc., San Diego, CA, United States) (Yen et al., 2020).

Analysis of Anti-Collagen Type II (CII) IgG Antibodies

Blood samples were collected on day 42. The anti-CII IgG antibody titers were analyzed with commercially available kits and anti-mouse CII IgG TMB (2036T; Chondrex, Redmond, WA, United States) according to the manufacturer's instructions.

Spleen Cell Proliferation and Cytokine Production in Response to Collagen II

Splenocytes (2×10^6 cells/ml) were cultured in 200 µl of medium containing fetal calf serum (10%), gentamicin (50 µg/ml), glutamine (2 mM), and 2-mercaptoethanol (50 µM). The splenocytes were stimulated with 20 µg/ml mouse CII for 72 h ^{3}H-labeled thymidine incorporation was quantified to assess the cellular proliferation. The numbers of $CD4^+IFN\text{-}\gamma^+$ Th1 cells and $CD4^+IL\text{-}17A^+$ Th17 cells were analyzed to assess intracellular cytokine levels.

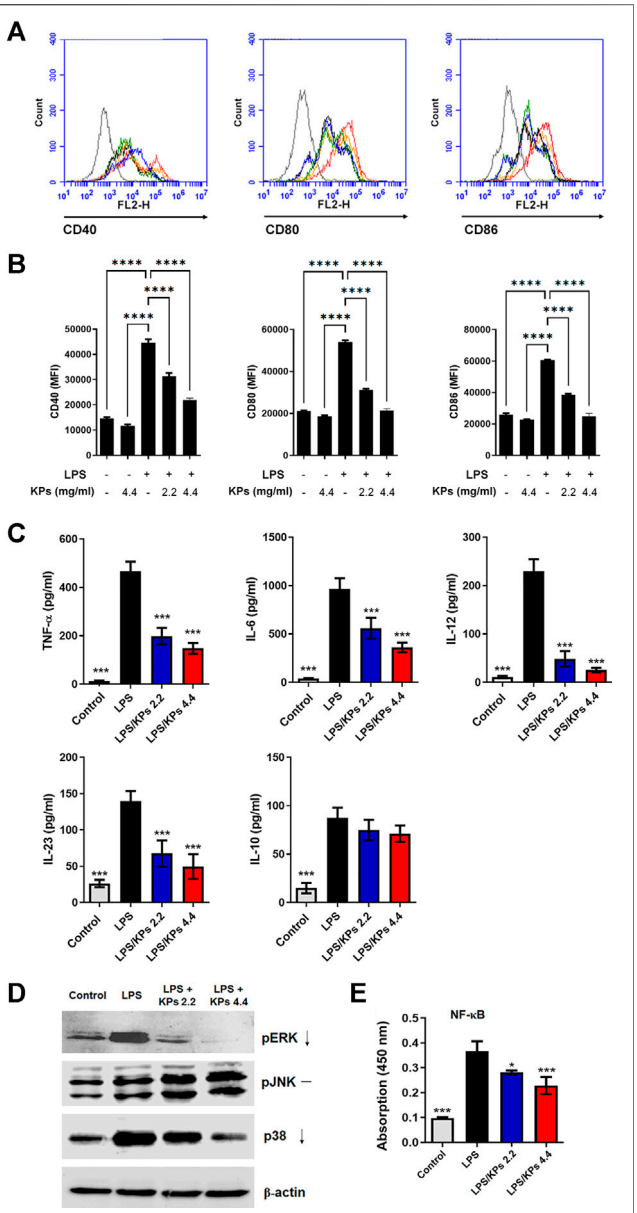

FIGURE 1 | Effect of KPs on the expression of immunomodulatory cell surface markers, the cytokine release, MAPK phosphorylation and NF-κB translocation in LPS-treated mouse BMDCs. Immature murine BMDCs were stimulated with LPS (100 ng/ml) in the presence or absence of KPs (2.2 mg/ml and 4.4 mg/ml) for 24 h. **(A)** Representative histogram graphs of the mean fluorescence intensity (MFI) of costimulatory molecules CD40, CD80 and CD86 on $CD11c^+$ DC cells examined by flow cytometry. **(B)** MFI values presented as the mean ± SEM from three independent experiments (n = 3). ****$p < 0.0001$, as determined by one-way ANOVA test. **(C)** Cell-free supernatants were collected, and cytokine production was measured by ELISA. The concentrations are presented as the mean ± SEM (n = 3). **(D)** Immature BMDCs were stimulated with LPS (100 ng/ml) with or without KPs (2.2 mg/ml and 4.4 mg/ml) and lysed at 6 h after treatment. The levels of phosphorylated pERK, pJNK and p38 MAPK in whole cell lysates were analyzed by Western blotting. Representative images from one of three independent experiments are shown. **(E)** The concentration of NF-κB/p65 in nuclear extracts was measured using a Trans^{AM} assay. The values are presented as the mean ± SEM (n = 3). *$p < 0.05$; ***$p < 0.001$ vs the LPS alone control group, as determined by one-way ANOVA with Dunnett's test.

Statistical Analysis

All the data are presented as the mean ± SEM. One-way or two-way ANOVA followed by Dunnett's multiple comparison test was used to compare multiple experimental groups with GraphPad Prism v5.0 (La Jolla, CA, United States). A $p \leq 0.05$ was considered statistically significant.

RESULTS

KPs Inhibit Surface Costimulatory Molecules in LPS-Stimulated Mouse BMDCs

Immature mouse BMDCs were treated with KPs (2.2 and 4.4 mg/ml) and then exposed to LPS which is a bacterial product known to induce DC maturation. The LPS-stimulated mouse BMDCs significantly increased the expression levels of the surface costimulatory molecules, CD40, CD80 and CD86, while KPs treatment reduced the expression of these molecules in a dose-dependent manner (**Figures 1A,B**, and also **Supplementary Figure S1**). Data showed that KP-treated alone at the high concentration (4.4 mg/ml) did not cause a notable change in immature mice BMDCs compared to vehicle control. Furthermore, these effects did not occur due to cytotoxicity because we used LDH and CCK-8 (**Supplementary Figure S2A, B**, respectively) assays to confirm that the cell viability in the KPs-treated groups was not significantly different from that in the water-treated control group.

KPs Suppress Cytokine Release From LPS-Stimulated Mouse BMDCs

As shown in **Figure 1C**, KPs-pretreated mouse BMDCs secreted lower concentrations of proinflammatory cytokines, including TNF-α, a Th1-specific cytokine (IL-12) and Th17-specific cytokines (IL-6 and IL-23), following LPS stimulation. However, KPs did not significantly affect the anti-inflammatory cytokine IL-10 expression in LPS-stimulated BMDCs. Moreover, we stimulated BMDCs with other TLR ligands, including zymosan, lipoteichoic acid, synthetic diacylated lipoprotein Pam2Cys-Ser-Lys4, peptidoglycan (TLR1, 2, or six ligands), polyinosine polycytidylic acid (TLR3 ligand), flagellin (TLR5 ligand), and synthetic CpG oligodeoxynucleotides (TLR9 ligand). Results showed that KPs (4.4 mg/ml) significantly reduced TNF-α expression level in response to all these ligands (**Supplementary Figure S3**).

KPs Suppress NF-κB and MAPK Pathways in LPS-Stimulated BMDCs

To discover the molecular mechanisms underlying the inhibitory effect of KPs, we determined the effect of KPs on MAPK and NF-κB activation in LPS-stimulated BMDCs. As shown in **Figure 1D**, the levels of phosphorylated MAPKs, namely, ERK, p38, and JNK, were significantly increased in the LPS-stimulated BMDC group relative to the control BMDC group. In contrast, the phospho-ERK and p38 levels were greatly decreased in the KPs treatment group (also shown in **Supplementary Figure S4** for the original blots). Furthermore, we used Trans^{AM} assays to measure the concentrations of NF-κB/p65 in nuclear extracts. The nuclear translocation of NF-κB/p65 was significantly increased in BMDCs after stimulation with LPS. However, pretreatment with KPs significantly reduced this effect in a dose-dependent manner (**Figure 1E**).

KPs Inhibit the Ability of Mouse BMDCs to Trigger CD4$^+$ T Cell Proliferation and Th1/Th17 Cytokine Production in Mixed Cell Culture Reactions

To elucidate the relevance of the KPs-mediated suppression of DC functions to immune responses, we analyzed the effects of KPs in a coculture system that induced ovalbumin (OVA)-specific CD4$^+$ T cells from OT-II transgenic mice and BMDCs treated under different conditions. The proliferation results in **Figure 2A** showed that coculture with LPS-stimulated BMDCs effectively increased proliferative responses, while LPS-stimulated DCs were pretreated with KPs, a reduced amount of [^{3}H] uptake was observed. In addition, the ELISA results revealed decreased Th1 (IFN-γ) and Th17 (IL-17A) cytokine production in the cocultures that included KPs-treated BMDCs (**Figure 2B**).

KPs Do Not Directly Affect Th1 and Th17 Cell-Lineage Differentiation

We next extended to elucidate whether KPs could directly affect T cell lineage differentiation. As shown in **Figures 2C,D**, the administration of KPs to mouse naïve CD4$^+$ T cells cultured under Th1- or Th17-polarizing conditions did not significantly affect the numbers of IFN-γ- and IL-17A-producing cells.

KPs Alleviate the Symptoms of CIA in DBA/1 Mice

In the typical arthritic animal model, CIA mice, the excessive production of pro-inflammatory cytokines or chemokines and continuous presentation of autoantigens by DCs are regarded as contributing factors to the pathogenesis and progression of murine arthritis (Leung et al., 2002). Based on the *in vitro* finding that KPs sufficiently suppressed BMDCs maturation and function, we further investigate the immunosuppressive properties of KPs in the murine CIA model. Although KP cannot effectively reduce the incidence of CIA arthritis (**Figure 3A**), but the administration of a high dose of KPs (7.5 mg/kg), starting at day 1 after the second immunization, significantly ameliorated the severity of CIA, which was characterized by paw swelling, erythema and joint rigidity (**Figures 3B,C**). In addition, H&E staining was performed to evaluate the histopathological changes in the joints (**Figure 3D**). KPs administration significantly reduced synovial tissue inflammatory infiltration, hyperplasia, and cartilage erosion in the knee joints in a dose-dependent manner (**Figure 3E**).

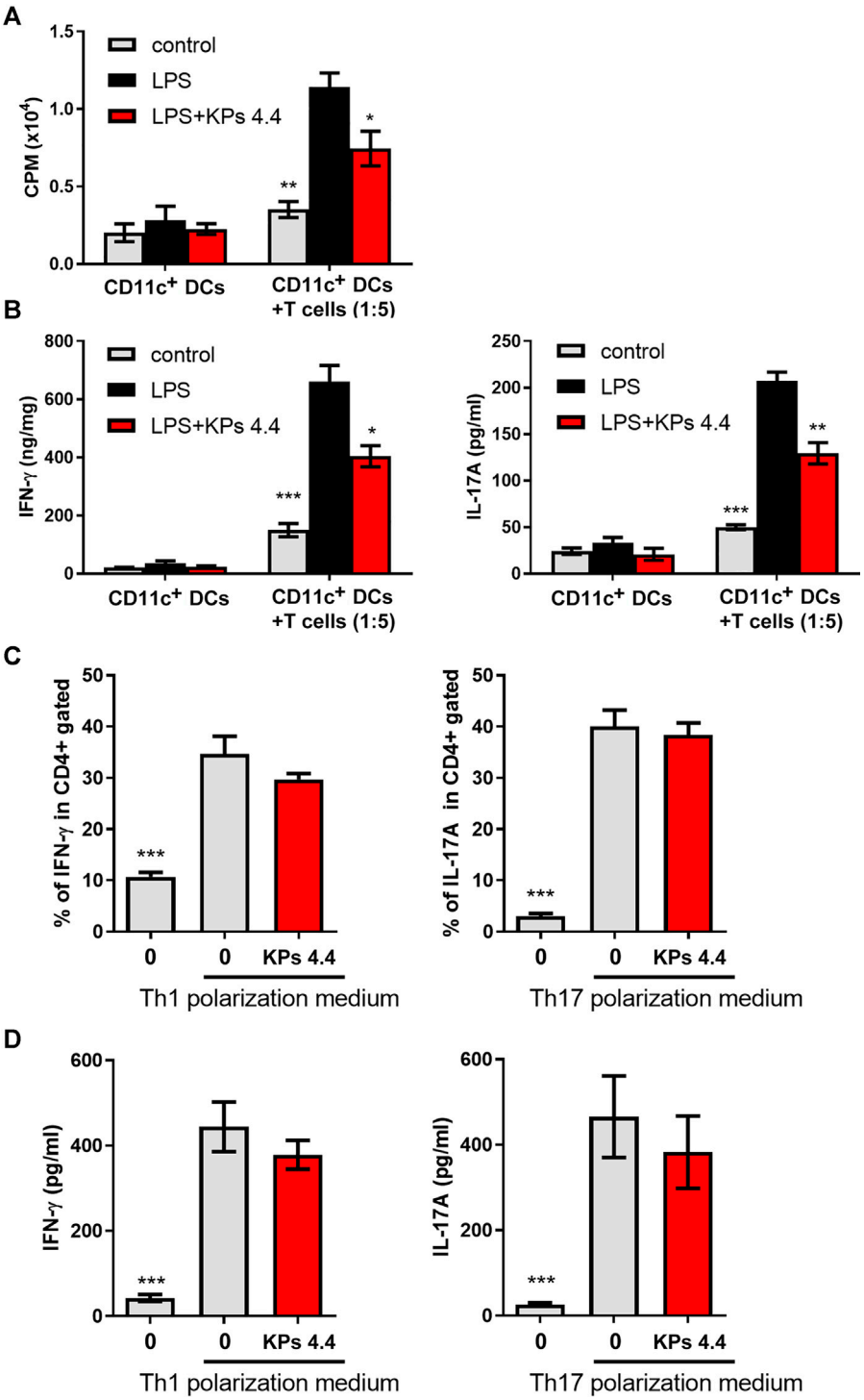

FIGURE 2 | Effects of KPs on $CD4^+$ T cells proliferation, LPS-stimulated BMDC cytokine production *in vitro*, and Th1 and Th17 differentiation *in vitro*. **(A)** OT-II-specific $CD4^+$ T cells were cocultured with BMDCs in the presence of OVA and LPS. KPs were added at a concentration of 4.4 mg/ml at the beginning of the induction. After 3 days of culture, the changes in T cell proliferation via the ^{3}H-TdR incorporation assay were quantified in counts per minute (CPM) by liquid scintillation counting. **(B)** The levels of IFN-γ and IL1-7A in the supernatants of the cocultures. The values are presented as the mean ± SEM (n = 3). $^*p < 0.05$; $^{**}p < 0.01$; $^{***}p < 0.001$ vs the LPS alone group, as determined by one-way ANOVA with Dunnett's test. **(C)** Naïve $CD4^+$ T cells were cultured in Th1- or Th17-polarizing conditioned medium. KPs were added at a concentration of 4.4 mg/ml at the beginning of induction. Bar graphs showing the percentages of $CD4^+$ T cells expressing IFN-γ and IL-17A, as determined by flow cytometry. **(D)** The levels of IFN-γ and IL-17A produced under Th1- or Th17-polarizing conditions were examined with ELISA kits. The data are expressed as the mean ± SEM (n = 3). $^{***}p < 0.001$ compared to the LPS-stimulated group without KPs treatment, as determined by one-way ANOVA with Dunnett's test.

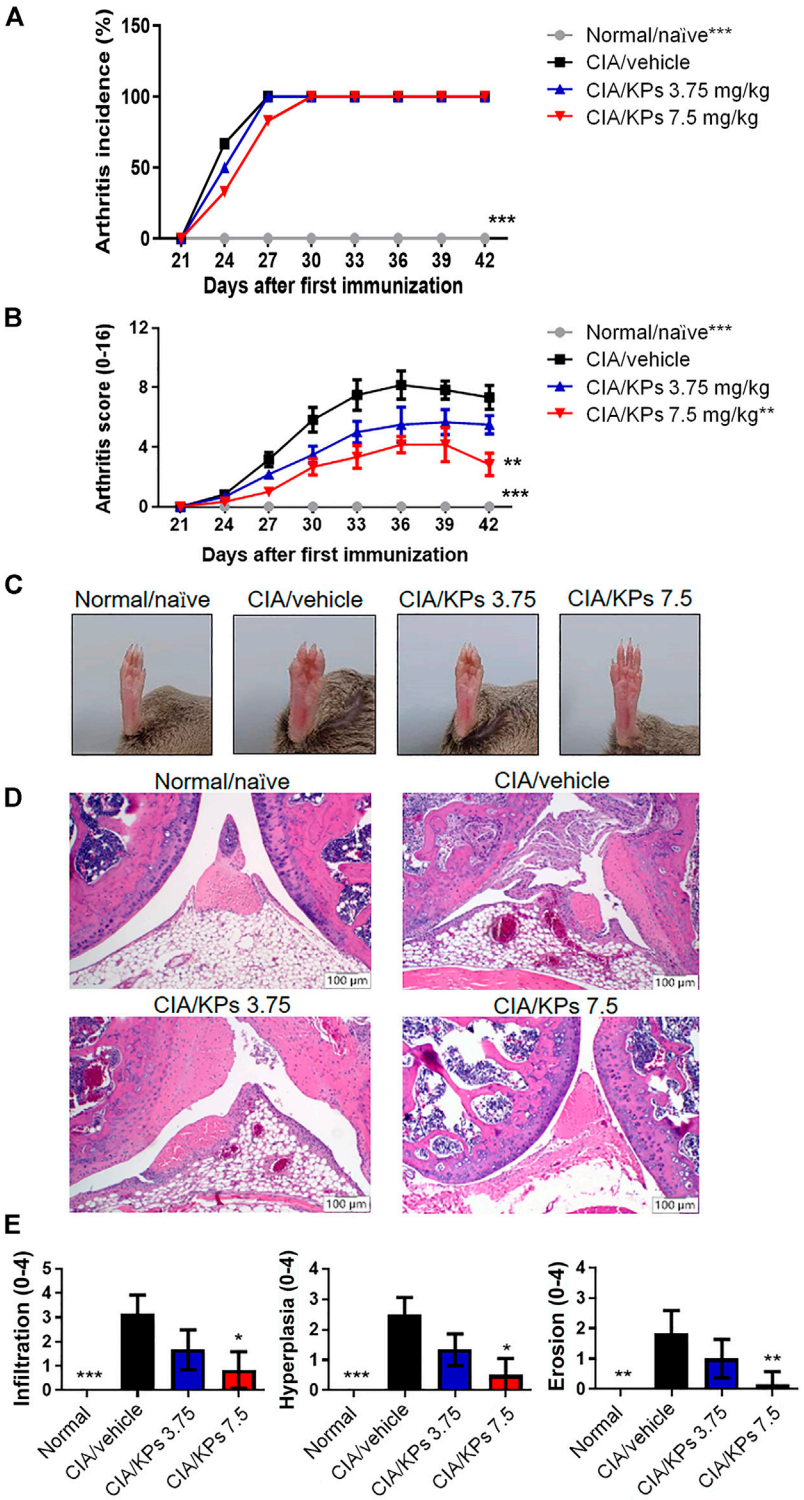

FIGURE 3 | Effects of KPs on type II CIA severity. The arthritis incidence **(A)** and arthritis score **(B)** were observed every 3 days after type II collagen (CII) booster immunization (day 21). **(C)** The whole view of the severity of arthritis in the right legs of the mice. Characterization of paw swelling, erythema, edema, and joint rigidity in groups subjected to different treatment. **(D)** Representative photographs of histopathological examination by H&E staining (100× magnification) on day 42. **(E)** Pathogenic scores of CIA were determined. The data are presented as the mean ± SEM (n = 5). $^{*}p < 0.05$; $^{**}p < 0.01$; $^{***}p < 0.001$ vs the CIA/vehicle control group, as determined by two-way ANOVA (**A**, **B**) or one-way ANOVA with Dunnett's test **(E)**.

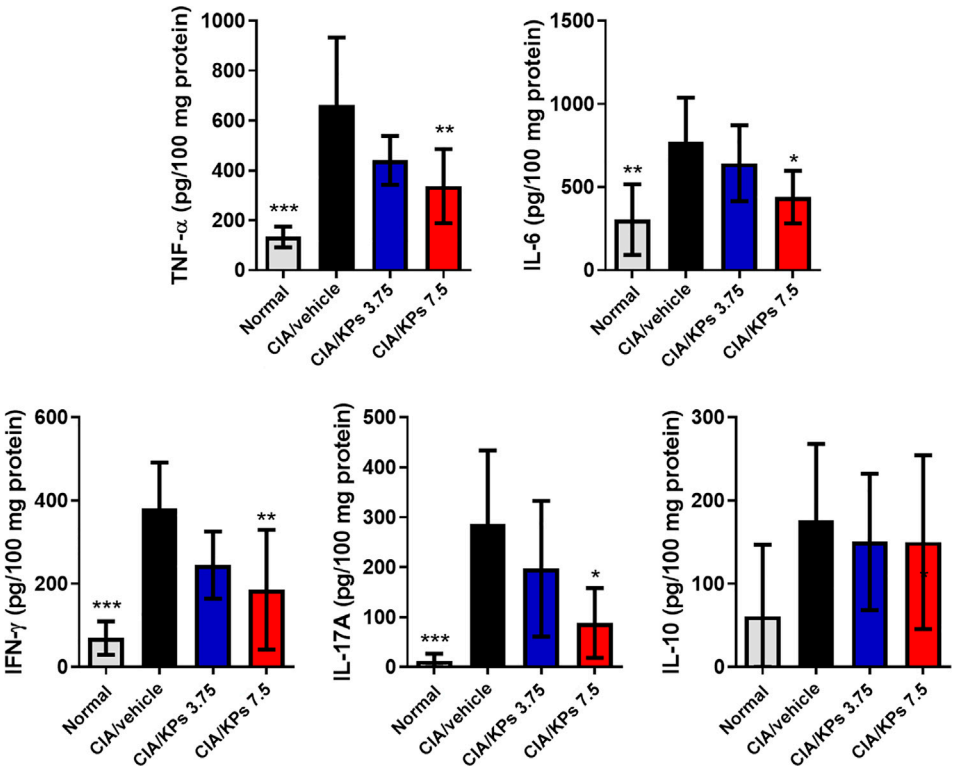

FIGURE 4 | Effects of KPs on proinflammtory cytokine expression in the paws of CIA mice. The paw tissue homogenates were obtained on day 42. The cytokines TNF-α, IL-6, IFN-γ, IL-17A, and IL-10 were measured by ELISA. The data are presented as the mean ± SEM (n = 5). $^{*}p < 0.05$; $^{**}p < 0.01$; $^{***}p < 0.001$ vs the CIA/vehicle control group, as determined by one-way ANOVA with Dunnett's test.

KPs Decrease the Production of Inflammatory Cytokines in the Paws of Mice With CIA

The ELISA results revealed remarkable expression of the inflammatory cytokines, including TNF-α, IL-6, IFN-γ and IL-17A, in the paws of CIA/vehicle control mice (**Figure 4**). In contrast, the expression levels of these cytokines were significantly reduced after KPs treatment, especially after treatment with the high dose of KPs (7.5 mg/kg). On the contrary, the anti-inflammatory cytokine, IL-10, showed no significant changes regardless of KPs dose (**Figure 4**).

KPs Suppress Collagen-specific Immune Responses in Mice With CIA

We further estimated the anti-type II collagen antibody (anti-CII IgG) titers in cultures of serum and spleen cells that proliferated in response to CII. The results showed that suppression of the anti-CII IgG antibody titer in the KPs-treated CIA groups (**Figure 5A**). In addition, the results in **Figure 5B** revealed that CII significantly increased the spleen cell proliferation in the CIA/vehicle group compared to the normal control group ($p < 0.001$). Nevertheless, KPs oral administration significantly decreased the CII-induced spleen cell proliferation in the CIA mouse groups in a dose-dependent manner (**Figure 5B**).

KPs Decrease the Ratio of Th1 and Th17 Cells in the Spleen Tissues of Mice With CIA

Subsequently, we assessed the $CD4^+$ T cell subset profiles in the lymphocytes from the spleens of mice with CIA subjected to different treatments. Compared with that in the naïve mouse group, the ratio of splenic $CD4^+IFN\text{-}\gamma^+$ Th1 cells (**Figure 5C**) and $CD4^+IL\text{-}17A^+$ Th17 cells (**Figure 5D**) in the CIA/vehicle control group was significantly higher, and the percentages of Th1 and Th17 cells were significantly decreased in groups of mice with CIA treated with the high dose of KPs ($p < 0.001$).

KPs Suppress Splenic DC Maturation in Mice With CIA

To understand whether KPs can also affect the maturation of dendritic cells in the CIA model, we further analyzed the expression of the costimulatory molecules, including CD40, CD80 and CD86, in splenic dendritic cells using flow cytometry (**Supplementary Figures S5, 6**). Results showed that despite the elevation in surface marker expression, high-dose KPs (7.5 mg/kg/day) treatment was sufficient to suppress the expression of the costimulatory molecules, CD40 (**Figure 6A**), CD80 (**Figure 6B**) and CD86 (**Figure 6C**), by the splenic DCs of mice with CIA.

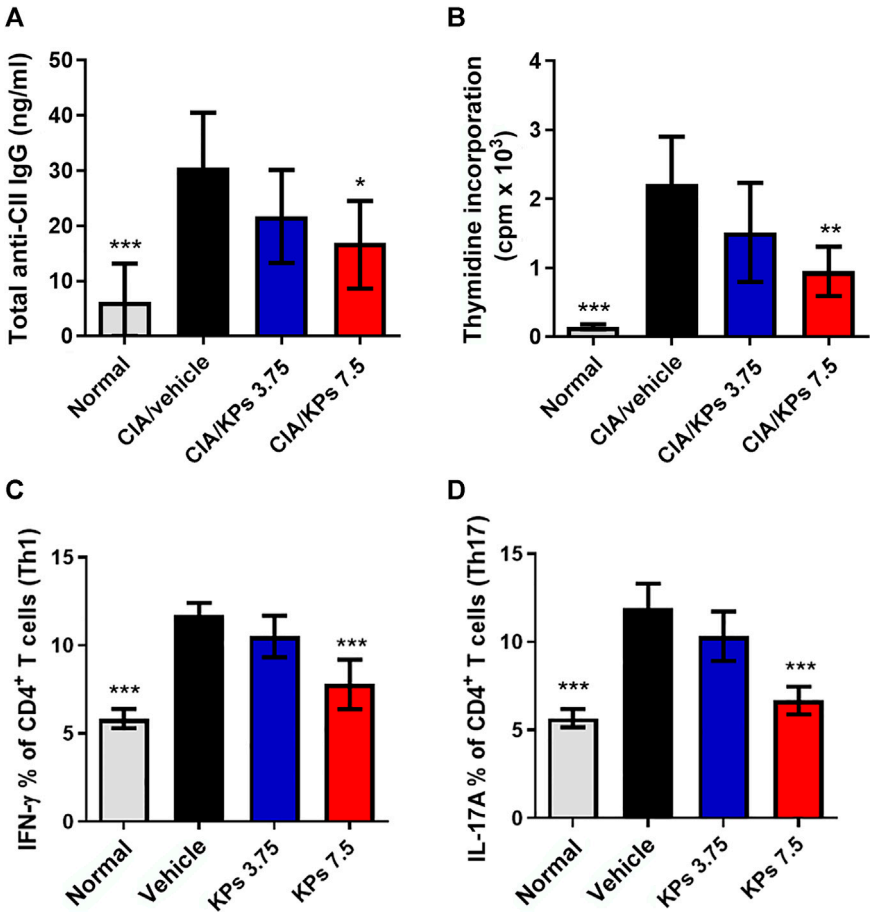

FIGURE 5 | Effect of KPs on CII-specific immune responses in serum and the $CD4^+$ T cell subset profiles in the spleens of CIA mice. **(A)** Sera were collected by orbital sinus venipuncture at day 42 after primary immunization to estimate anti-type II collagen (IgG) antibody levels by ELISA. **(B)** Splenocytes were harvested at day 42. Cultures were pulsed with ^{3}H-thymidine (1 μCi/well) and the incorporation of radioactivity was quantified in counts per minute (cpm) by liquid scintillation counting after 18 h of incubation. Intracellular flow cytometry analysis of cells collected from the spleens of the mice in different groups on day 42 after immunization. Flow cytometry analysis of Th1 and Th17 cells. The cells were gated on the $CD4^+$ population. Bar graph of the quantification of $CD4^+$ T cell subsets, Th1 **(C)** and Th17 **(D)**, plotted from three independent experiments. The data are expressed as the mean ± SEM (n = 5). $^*p < 0.05$; $^{**}p < 0.01$; $^{***}p < 0.001$ vs the CIA/vehicle control group, as determined by one-way ANOVA with Dunnett's test.

The Effect of KPs on BMDC Differentiation

Given there was only a small amount of DCs can be retrieved from peripheral blood, synovial tissues, and spleens in mice, we performed an *in vitro* study to elucidate whether DC differentiation was affected by KPs (**Figure 7**). To this end, we isolated myeloid cells from CIA murine bone marrow-derived cells and added KPs (2.2 or 4.4 mg/ml) into the culture medium to incubate and investigate the proportions of $CD11c^+$ cells within the myeloid cells (**Figure 7A**). Compared with the DMSO control, the percentage of $CD11c^+$ cells were significantly reduced at high doses of KP (4.4 mg/ml), but not at low dose of KP (2.2 mg/ml) (**Figure 7B**), suggesting that the effect of KPs on DC *in vivo* is still mainly in its effect of inhibiting maturation.

DISCUSSION

RA is an autoimmune disorder that usually occurs with age and affects the hands and feet (Tian et al., 2020). Although the pathogenesis of RA is still not fully understood, substantial insight into the cellular and molecular mechanisms involved in RA pathogenesis has been obtained in the past decade (Wasserman, 2011; Yue et al., 2017). Bone and cartilage erosions are the major feature of RA (Lee and Weinblatt, 2001). Moreover, the main factor that triggers bone and cartilage erosions in the joints during RA is inflammation of the synovium (Marok et al., 1996; Ideguchi et al., 2006; Schett and Gravallese, 2012; Kim et al., 2015; Komatsu and Takayanagi, 2018). Dendritic cells (DCs) are sensory cells and antigen-presenting cells (APCs) that have been found in RA synovial fluid (Thomas et al., 1999). In this study, we first established an *in vitro* DC inflammation model by stimulating mouse BMDCs with LPS, and we demonstrated that KPs can inhibit DC surface costimulatory molecule expression, reduce inflammatory cytokine release, and repress MAPK and NF-κB signaling. In a mouse model of CIA, we further observed that KPs can alleviate the symptoms of arthritis, decrease the production of

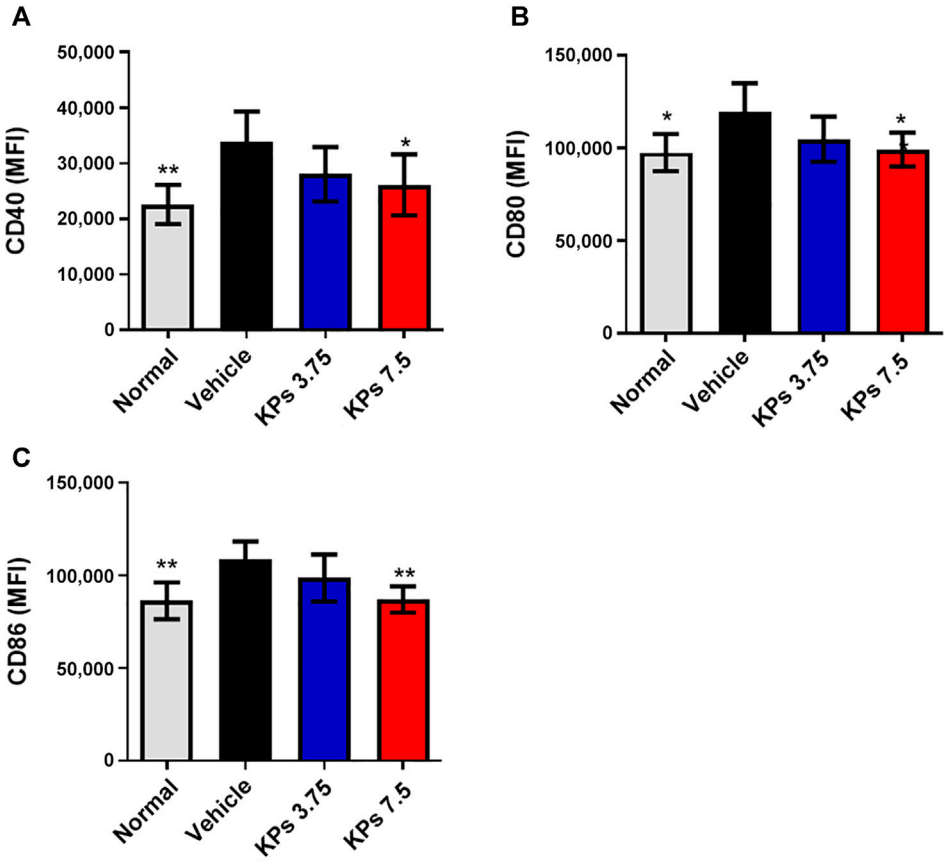

FIGURE 6 | Effect of KPs on splenic DC maturation in mice with CIA. Flow cytometry analysis of cells collected from the spleens of the mice in different groups on day 42 after immunization. MFI of CD40 **(A)**, CD80 **(B)**, and CD86 **(C)** on CD11c$^+$ DC cells was examined by flow cytometry. Bar graphs show the quantified data from three independent experiments. The values are presented as the mean ± SEM (n = 5). $^*p < 0.05$; $^{**}p < 0.01$; $^{***}p < 0.001$ vs the CIA/vehicle control group, as determined by one-way ANOVA with Dunnett's test.

inflammatory cytokines and suppress the maturation of splenic DCs.

The expression of the costimulatory molecules, including CD40, CD80 and CD86, is significantly increased in LPS-stimulated mouse BMDCs (Jones et al., 2010). We provided evidence that KPs treatment reduced the expression of these molecules in mBMDCs treated with LPS in a dose-dependent manner. In addition, LPS-primed mBMDCs were induced to secrete high-level cytokines, including TNF-α, a Th1-specific cytokine (IL-12), and Th17-specific cytokines (IL-6 and IL-23) (Siegemund et al., 2007). We demonstrated that KPs-pretreated mouse BMDCs secrete low concentrations of proinflammatory cytokines following LPS stimulation. Vinderola et al. (2005) showed that administration of kefir induces Th2 cytokine production to regulate the Th1 response in BALB/c mice. Two hundred milliliters of kefir were administered to 18 healthy subjects every day for 6 weeks to increase the polarization of the immune response toward a Th1-type phenotype and reduce the allergic reactions caused by the Th2-type response (Adiloğlu et al., 2013). In addition, a kefir product can activate the surface marker expression of human DC costimulatory molecules (CD80, CD86 and HLADR) and increase the release of cytokines (IL-1β, IL-6, IL-10 and TNF-α) (Ghoneum et al., 2015). However, our *in vitro* and *in vivo* experimental results showed that KPs inhibited the LPS-stimulated expression of BMDC costimulatory molecules and TNF-α, a Th1-specific cytokine (IL-12) and Th17-specific cytokines (IL-6 and IL-23). Therefore, we speculated that our KPs exert an inhibitory effect on DC maturation and cytokine production.

LPS treatment polarized CD4$^+$ T cells and generated Th1 (IFN-γ) and Th17 (IL-17A) cytokine responses in previous studies (Jiang et al., 2002; McAleer and Vella, 2008; Fermin Lee et al., 2013). We analyzed the effects of KPs in a coculture system that included OVA-specific CD4$^+$ T cells from OT-II transgenic mice and BMDCs subjected to different treatments. The results revealed that the proliferative responses were significantly reduced in LPS-stimulated DCs after KPs pretreatment. The results also showed decreased Th1 (IFN-γ) and Th17 (IL-17A) cytokine production in BMDC cocultures that had been treated with KPs.

Mounting evidence showed that several signaling pathway activation are involved in the DC maturation process (Neves et al., 2009). Especially the MAPK and NF-κB activation appeared to be extremely relevant to the process of LPS-induced BMDC

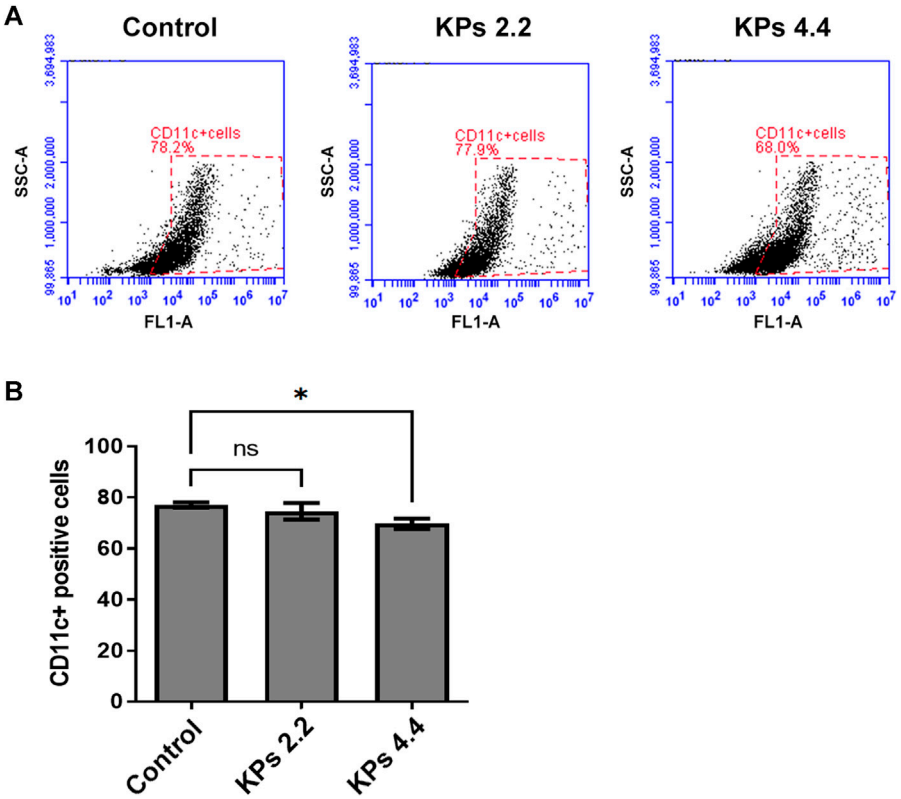

FIGURE 7 | Effect of KPs on differentiation of CD11c$^+$ BMDCs. **(A)** Flow cytometry analysis of the bivariate graphs of BMDCs of CIA mice cultured with the indicated concentration of KPs followed by evaluation of CD11c$^+$ expressions. **(B)** The mean ± SD of the experimental triplicates are presented in the bar graph. Experiments were repeated three times independently. ***p < 0.001 vs 0.1% DMSO-treated mock group, as determined by a one-way ANOVA with Dunnett's test.

maturation (An et al., 2002; Kim et al., 2005). In our study, we showed a similar result that three MAPKs (pERK, p-p38 and pJNK) and NF-κB signaling pathways were activated in LPS-induced DC (**Figure 1**). Kefir and its biological activities exerted anti-inflammatory and antioxidant effects through inhibiting p-p38 and p-NF-κB in several animal diseased model (Chen et al., 2020; Chen et al., 2019; Wang et al., 2012; Azizi et al., 2021) and exhibited antidepressant and antitumor effects through inactivation of p-ERK signaling pathway (Azizi et al., 2021; Chen et al., 2021). As anticipated, we showed a similar result as previous studies described, the levels of p-ERK and p-p38, and NF-κB/p65 nuclear translocation were significantly decreased under both doses of KPs treatment (**Figure 1**). However, inconsistent result was found in the level of p-JNK, which showed no significant change but slightly increased in KPs treatment when compared to LPS group. The results similar to the finding of Kim et al. (2021) showed that JNK phosphorylation increased in kefir-treated drug resistant cancer cells. Because the JNK signaling played a minor and distinct pathway from the p38, ERK, and NF-κB cascades in the LPS-induced DC maturation process (Nakahara et al., 2004). KPs still showed strong inhibitory effects on DC maturation and inflammatory cytokine releases in our study.

DCs have been found in RA synovial fluid, extensively expressing costimulatory molecules while performing their functions to polarize T cells toward Th1, Th2 or Th17 phenotypes. Therefore, DCs appear to play a crucial role in joint inflammation. In a typical arthritic animal model, CIA mice, the excessive production of pro-inflammatory cytokines or chemokines as well as continuous presentation of autoantigens by DCs are regarded as pathogenic factors, leading to the progression of murine arthritis. According to these findings, we investigated the role of KPs in the regulation of immune function in the CIA mouse model, which is used to study RA (Williams, 2004). We found that KPs treatment could suppress BMDC maturation and function; furthermore, KPs treatment for 3 weeks could also alleviate the symptoms of synovial tissue inflammatory infiltration, hyperplasia, and cartilage destruction in the knee joints of DBA/1 mice with CIA. Additionally, the ELISA results showed that the obvious expression of inflammatory cytokines, such as IFN-γ, IL-6, IL-17A and TNF-α, in the CIA/vehicle mice group was significantly reduced following high-dose KPs treatment (7.5 mg/kg/day). Therefore, KPs exert anti-inflammatory and immunomodulatory effects to prevent DC overreaction and mass accumulation in the synovial tissue of CIA mice.

Previous studies have revealed that berberine, an isoquinoline alkaloid, can be used to improve various autoimmune diseases by suppressing CII-specific immune responses in mice with CIA (Hu et al., 2011) or by suppressing Th17 cell responses via inducing cortistatin in the gut of rats with CIA (Yue et al., 2017). Accordingly, we further evaluated the production of anti-CII

IgG antibodies and spleen cell proliferation responses in KPs-treated mice with CIA. We demonstrated that KPs treatment suppressed the anti-CII IgG antibody titers and spleen cell proliferation responses in mice with CIA. Similarly, the $CD4^+$ T cell subset profiles in splenic lymphocytes were assessed. The ratios of Th1 and Th17 cells were also significantly decreased after oral administration of KPs in mice with CIA. It is well known that imbalanced Th17 cell production contributes to the progression of RA and CIA. Increased Th17 cell numbers were easily found in both the synovial fluid and peripheral blood of RA patients (Noack and Miossec, 2014). Our data demonstrated that KPs treatment is effective in lessening the ongoing severity of CIA in mice, and this effect involves the attenuation of the systemic Th17 cell response. In CII-treated spleen cells, KPs reduced the Th1 ($CD4^+$IFN-γ) and Th17 ($CD4^+$IL-17A) cell percentages in a dose-dependent manner. In our *in vitro* experiments, KPs inhibited the expression of costimulatory molecules in LPS-stimulated BMDCs. In an *in vivo* animal experiment, we also found that KPs inhibited the surface expression of CD40, CD80 and CD86 on splenic DCs in mice with CIA, which was consistent with a previous report (Jung et al., 2007). The abovementioned experimental results showed that KPs can inhibit the CII-specific T cell response. Based on the flow cytometry analysis, KPs treatment was sufficient to decrease the expression levels of these costimulatory molecules in an *in vivo* CIA mouse model and an *in vitro* LPS-induced BMDC cell model.

CONCLUSION

In this study, these results demonstrated that KPs treatment can regulate immune functions to decrease inflammatory cytokine release, $CD4^+$ T cell proliferation and Th1/Th17 cytokine production, to suppress splenic DC maturation and to alleviate all the symptoms of collagen type II-induced arthritis in the mouse model. Therefore, KPs treatment provide a novel perspective for investigating immune function in DCs and highlight the potential of KPs for the clinical use in RA patients.

DATA AVAILABILITY STATEMENT

The original contributions presented in the study are included in the article/**Supplementary Material**, further inquiries can be directed to the corresponding authors.

ETHICS STATEMENT

The animal study was reviewed and approved by The animal experiments were approved by the Institutional Animal Care and Use Committee of National Chung Hsing University, Taiwan (IACUC no. 109-106) and were carried out in compliance with institutional guidelines.

AUTHOR CONTRIBUTIONS

Conceptualization, C-FC, H-PL, C-CL, K-YC and C-MC; methodology, Y-HC, M-YT and C-CL; software, C-CL; validation, Y-WL, C-CL, K-YC and C-MC; formal analysis, C-CY and M-YT; investigation, C-FC, H-PL and Y-HC; resources, S-HY and C-MC; data curation, Y-WL, M-YT, S-HY and C-MC; writing original draft preparation, C-FC and C-CL; writing review and editing, K-YC and C-MC; visualization, C-CY and S-HY; supervision, C-MC; project administration, H-PL; funding acquisition, K-YC and C-MC. All authors have read and agreed to the published version of the manuscript.

FUNDING

This work was supported in part by grants MOST-108-2313-B-005-039-MY3 and MOST-108-2314-B-182-052-MY3 from the Ministry of Science and Technology of Taiwan and also supported by the Higher Education Sprout Project from the Ministry of Education (MOE-110-S-0023-A) in Taiwan.

ACKNOWLEDGMENTS

We thank our colleague, Gary Ro-Lin Chang, in the Molecular Embryology and DNA Methylation Laboratory, National Chung Hsing University, for his help with discussions and technical issues.

SUPPLEMENTARY MATERIAL

The Supplementary Material for this article can be found online at: https://www.frontiersin.org/articles/10.3389/fphar.2021.721594/full#supplementary-material

REFERENCES

Adiloğlu, A. K., Gönülateş, N., Işler, M., and Senol, A. (2013). [The Effect of Kefir Consumption on Human Immune System: a Cytokine Study]. *Mikrobiyol. Bul.* 47, 273–281. doi:10.5578/mb.4709

Ahmed, M. S., and Bae, Y. S. (2016). Dendritic Cell-Based Immunotherapy for Rheumatoid Arthritis: from Bench to Bedside. *Immune Netw.* 16, 44–51. doi:10.4110/in.2016.16.1.44

An, H., Yu, Y., Zhang, M., Xu, H., Qi, R., Yan, X., et al. (2002). Involvement of ERK, P38 and NF-kappaB Signal Transduction in Regulation of TLR2, TLR4 and TLR9 Gene Expression Induced by Lipopolysaccharide in Mouse Dendritic Cells. *Immunology* 106, 38–45. doi:10.1046/j.1365-2567.2002.01401.x

Azizi, N. F., Kumar, M. R., Yeap, S. K., Abdullah, J. O., Khalid, M., Omar, A. R., et al. (2021). Kefir and its Biological Activities. *Foods* 10, 1210. doi:10.3390/foods10061210

Benham, H., Nel, H. J., Law, S. C., Mehdi, A. M., Street, S., Ramnoruth, N., et al. (2015). Citrullinated Peptide Dendritic Cell Immunotherapy in HLA Risk Genotype-Positive Rheumatoid Arthritis Patients. *Sci. Transl. Med.* 7, 290ra87. doi:10.1126/scitranslmed.aaa9301

Blanco, P., Palucka, A. K., Pascual, V., and Banchereau, J. (2008). Dendritic Cells and Cytokines in Human Inflammatory and Autoimmune Diseases. *Cytokine Growth Factor. Rev.* 19, 41–52. doi:10.1016/j.cytogfr.2007.10.004

Brand, D. D., Latham, K. A., and Rosloniec, E. F. (2007). Collagen-induced Arthritis. *Nat. Protoc.* 2, 1269–1275. doi:10.1038/nprot.2007.173

Chabaud, M., Garnero, P., Dayer, J. M., Guerne, P. A., Fossiez, F., and Miossec, P. (2000). Contribution of Interleukin 17 to Synovium Matrix Destruction in Rheumatoid Arthritis. *Cytokine* 12, 1092–1099. doi:10.1006/cyto.2000.0681

Chang, S. Y., Ko, H. J., and Kweon, M. N. (2014). Mucosal Dendritic Cells Shape Mucosal Immunity. *Exp. Mol. Med.* 46, e84. doi:10.1038/emm.2014.16

Chen, H. L., Hung, K. F., Yen, C. C., Laio, C. H., Wang, J. L., Lan, Y. W., et al. (2019). Kefir Peptides Alleviate Particulate Matter. *Sci. Rep.* 9, 11529. doi:10.1038/s41598-019-47872-4

Chen, H. L., Lan, Y. W., Tu, M. Y., Tung, Y. T., Chan, M. N., Wu, H. S., et al. (2021). Kefir Peptides Exhibit Antidepressant-like Activity in Mice through the BDNF/TrkB Pathway. *J. Dairy Sci.* 104, 6415–6430. doi:10.3168/jds.2020-19222

Chen, H. L., Tsai, T. C., Tsai, Y. C., Liao, J. W., Yen, C. C., and Chen, C. M. (2016). Kefir Peptides Prevent High-Fructose Corn Syrup-Induced Non-alcoholic Fatty Liver Disease in a Murine Model by Modulation of Inflammation and the JAK2 Signaling Pathway. *Nutr. Diabetes* 6, e237. doi:10.1038/nutd.2016.49

Chen, Y. H., Chen, H. L., Fan, H. C., Tung, Y. T., Kuo, C. W., Tu, M. Y., et al. (2020). Anti-inflammatory, Antioxidant, and Antifibrotic Effects of Kefir Peptides on Salt-Induced Renal Vascular Damage and Dysfunction in Aged Stroke-Prone Spontaneously Hypertensive Rats. *Antioxidants (Basel)* 9, 790. doi:10.3390/antiox9090790

Fermin Lee, A., Chen, H. Y., Wan, L., Wu, S. Y., Yu, J. S., Huang, A. C., et al. (2013). Galectin-3 Modulates Th17 Responses by Regulating Dendritic Cell Cytokines. *Am. J. Pathol.* 183, 1209–1222. doi:10.1016/j.ajpath.2013.06.017

Ghoneum, M., Felo, N., Agrawal, S., and Agrawal, A. (2015). A Novel Kefir Product (PFT) Activates Dendritic Cells to Induce CD4+T and CD8+T Cell Responses *In Vitro*. *Int. J. Immunopathol. Pharmacol.* 28, 488–496. doi:10.1177/0394632015599447

Hu, Z., Jiao, Q., Ding, J., Liu, F., Liu, R., Shan, L., et al. (2011). Berberine Induces Dendritic Cell Apoptosis and Has Therapeutic Potential for Rheumatoid Arthritis. *Arthritis Rheum.* 63, 949–959. doi:10.1002/art.30202

Ideguchi, H., Ohno, S., Hattori, H., Senuma, A., and Ishigatsubo, Y. (2006). Bone Erosions in Rheumatoid Arthritis Can Be Repaired through Reduction in Disease Activity with Conventional Disease-Modifying Antirheumatic Drugs. *Arthritis Res. Ther.* 8, R76. doi:10.1186/ar1943

Jiang, H. R., Muckersie, E., Robertson, M., Xu, H., Liversidge, J., and Forrester, J. V. (2002). Secretion of Interleukin-10 or Interleukin-12 by LPS-Activated Dendritic Cells Is Critically Dependent on Time of Stimulus Relative to Initiation of Purified DC Culture. *J. Leukoc. Biol.* 72, 978–985.

Jones, L. A., Kreem, S., Shweash, M., Paul, A., Alexander, J., and Roberts, C. W. (2010). Differential Modulation of TLR3- and TLR4-Mediated Dendritic Cell Maturation and Function by Progesterone. *J. Immunol.* 185, 4525–4534. doi:10.4049/jimmunol.0901155

Jung, Y. O., Min, S. Y., Cho, M. L., Park, M. J., Jeon, J. Y., Lee, J. S., et al. (2007). CD8alpha+ Dendritic Cells Enhance the Antigen-specific CD4+ T-Cell Response and Accelerate Development of Collagen-Induced Arthritis. *Immunol. Lett.* 111, 76–83. doi:10.1016/j.imlet.2007.05.005

Kambayashi, T., and Laufer, T. M. (2014). Atypical MHC Class II-Expressing Antigen-Presenting Cells: Can Anything Replace a Dendritic Cell. *Nat. Rev. Immunol.* 14, 719–730. doi:10.1038/nri3754

Khan, S., Greenberg, J. D., and Bhardwaj, N. (2009). Dendritic Cells as Targets for Therapy in Rheumatoid Arthritis. *Nat. Rev. Rheumatol.* 5, 566–571. doi:10.1038/nrrheum.2009.185

Kidd, B. L., Langford, R. M., and Wodehouse, T. (2007). Arthritis and Pain. Current Approaches in the Treatment of Arthritic Pain. *Arthritis Res. Ther.* 9, 214. doi:10.1186/ar2147

Kim, D. H., Jeong, C. H., Cheng, W. N., Kwon, H. C., Kim, D.-H., Seo, K.-H., et al. (2021). Effects of Kefir on Doxorubicin-Induced Multidrug Resistance in Human Colorectal Cancer Cells. *J. Funct. Foods* 78, 104371. doi:10.1016/j.jff.2021.104371

Kim, G. Y., Kim, K. H., Lee, S. H., Yoon, M. S., Lee, H. J., Moon, D. O., et al. (2005). Curcumin Inhibits Immunostimulatory Function of Dendritic Cells: MAPKs and Translocation of NF-Kappa B as Potential Targets. *J. Immunol.* 174, 8116–8124. doi:10.4049/jimmunol.174.12.8116

Kim, K. W., Kim, H. R., Kim, B. M., Cho, M. L., and Lee, S. H. (2015). Th17 Cytokines Regulate Osteoclastogenesis in Rheumatoid Arthritis. *Am. J. Pathol.* 185, 3011–3024. doi:10.1016/j.ajpath.2015.07.017

Kirsch, B. M., Zeyda, M., Stuhlmeier, K., Grisar, J., Smolen, J. S., Watschinger, B., et al. (2005). The Active Metabolite of Leflunomide, A77 1726, Interferes with Dendritic Cell Function. *Arthritis Res. Ther.* 7, R694–R703. doi:10.1186/ar1727

Komatsu, N., and Takayanagi, H. (2018). Immune-bone Interplay in the Structural Damage in Rheumatoid Arthritis. *Clin. Exp. Immunol.* 194, 1–8. doi:10.1111/cei.13188

Lan, Y. W., Yang, J. C., Yen, C. C., Huang, T. T., Chen, Y. C., Chen, H. L., et al. (2019). Predifferentiated Amniotic Fluid Mesenchymal Stem Cells Enhance Lung Alveolar Epithelium Regeneration and Reverse Elastase-Induced Pulmonary Emphysema. *Stem Cel Res. Ther.* 10, 163. doi:10.1186/s13287-019-1282-1

Lebre, M. C., Jongbloed, S. L., Tas, S. W., Smeets, T. J., McInnes, I. B., and Tak, P. P. (2008). Rheumatoid Arthritis Synovium Contains Two Subsets of CD83-DC-LAMP- Dendritic Cells with Distinct Cytokine Profiles. *Am. J. Pathol.* 172, 940–950. doi:10.2353/ajpath.2008.070703

Lee, D. M., and Weinblatt, M. E. (2001). Rheumatoid Arthritis. *Lancet* 358, 903–911. doi:10.1016/S0140-6736(01)06075-5

Leung, B. P., Conacher, M., Hunter, D., McInnes, I. B., Liew, F. Y., and Brewer, J. M. (2002). A Novel Dendritic Cell-Induced Model of Erosive Inflammatory Arthritis: Distinct Roles for Dendritic Cells in T Cell Activation and Induction of Local Inflammation. *J. Immunol.* 169, 7071–7077. doi:10.4049/jimmunol.169.12.7071

Marok, R., Winyard, P. G., Coumbe, A., Kus, M. L., Gaffney, K., Blades, S., et al. (1996). Activation of the Transcription Factor Nuclear Factor-kappaB in Human Inflamed Synovial Tissue. *Arthritis Rheum.* 39, 583–591. doi:10.1002/art.1780390407

McAleer, J. P., and Vella, A. T. (2008). Understanding How Lipopolysaccharide Impacts CD4 T-Cell Immunity. *Crit. Rev. Immunol.* 28, 281–299. doi:10.1615/critrevimmunol.v28.i4.20

Nakahara, T., Uchi, H., Urabe, K., Chen, Q., Furue, M., and Moroi, Y. (2004). Role of C-Jun N-Terminal Kinase on Lipopolysaccharide Induced Maturation of Human Monocyte-Derived Dendritic Cells. *Int. Immunol.* 16, 1701–1709. doi:10.1093/intimm/dxh171

Neves, B. M., Cruz, M. T., Francisco, V., Garcia-Rodriguez, C., Silvestre, R., Cordeiro-da-Silva, A., et al. (2009). Differential Roles of PI3-Kinase, MAPKs and NF-kappaB on the Manipulation of Dendritic Cell T(h)1/T(h)2 Cytokine/chemokine Polarizing Profile. *Mol. Immunol.* 46, 2481–2492. doi:10.1016/j.molimm.2009.05.021

Noack, M., and Miossec, P. (2014). Th17 and Regulatory T Cell Balance in Autoimmune and Inflammatory Diseases. *Autoimmun. Rev.* 13, 668–677. doi:10.1016/j.autrev.2013.12.004

Parekh, R. B., Dwek, R. A., Sutton, B. J., Fernandes, D. L., Leung, A., Stanworth, D., et al. (1985). Association of Rheumatoid Arthritis and Primary Osteoarthritis with Changes in the Glycosylation Pattern of Total Serum IgG. *Nature* 316, 452–457. doi:10.1038/316452a0

Pettit, A. R., MacDonald, K. P., O'Sullivan, B., and Thomas, R. (2000). Differentiated Dendritic Cells Expressing Nuclear RelB Are Predominantly Located in Rheumatoid Synovial Tissue Perivascular Mononuclear Cell Aggregates. *Arthritis Rheum.* 43, 791–800. doi:10.1002/1529-0131(200004)43:4<791:AID-ANR9>3.0.CO;2-E

Sarkar, S., Cooney, L. A., and Fox, D. A. (2010). The Role of T Helper Type 17 Cells in Inflammatory Arthritis. *Clin. Exp. Immunol.* 159, 225–237. doi:10.1111/j.1365-2249.2009.04016.x

Schett, G., and Gravallese, E. (2012). Bone Erosion in Rheumatoid Arthritis: Mechanisms, Diagnosis and Treatment. *Nat. Rev. Rheumatol.* 8, 656–664. doi:10.1038/nrrheum.2012.153

Shi, X., Chen, H., Li, Y., Huang, J., and He, Y. (2018). Effects of Kefir Grains on Fermentation and Bioactivity of Goat Milk. *Acta Univ. Cibin. Ser. E Food Technol.* 22, 43–50. doi:10.2478/aucft-2018-0005

Siegemund, S., Schütze, N., Freudenberg, M. A., Lutz, M. B., Straubinger, R. K., and Alber, G. (2007). Production of IL-12, IL-23 and IL-27p28 by Bone Marrow-Derived Conventional Dendritic Cells rather Than Macrophages after LPS/TLR4-dependent Induction by Salmonella Enteritidis. *Immunobiology* 212, 739–750. doi:10.1016/j.imbio.2007.09.004

Song, X., and Lin, Q. (2017). Genomics, Transcriptomics and Proteomics to Elucidate the Pathogenesis of Rheumatoid Arthritis. *Rheumatol. Int.* 37, 1257–1265. doi:10.1007/s00296-017-3732-3

Thomas, R., MacDonald, K. P., Pettit, A. R., Cavanagh, L. L., Padmanabha, J., and Zehntner, S. (1999). Dendritic Cells and the Pathogenesis of Rheumatoid Arthritis. *J. Leukoc. Biol.* 66, 286–292. doi:10.1002/jlb.66.2.286

Tian, F., Jiang, P., Wu, M., Xing, Y., Liu, L., Dai, X., et al. (2020). A Novel Methodology of the Myeloid-Derived Suppressor Cells (MDSCs) Generation with Splenic Stroma Feeder Cells. *Exp. Cel Res.* 394, 112119. doi:10.1016/j.yexcr.2020.112119

Tu, M. Y., Chen, H. L., Tung, Y. T., Kao, C. C., Hu, F. C., and Chen, C. M. (2015). Short-term Effects of Kefir-Fermented Milk Consumption on Bone mineral Density and Bone Metabolism in a Randomized Clinical Trial of Osteoporotic Patients. *PLoS ONE* 10, e0144231. doi:10.1371/journal.pone.0144231

Tu, M. Y., Han, K. Y., Chang, G. R., Lai, G. D., Chang, K. Y., Chen, C. F., et al. (2020). Kefir Peptides Prevent Estrogen Deficiency-Induced Bone Loss and Modulate the Structure of the Gut Microbiota in Ovariectomized Mice. *Nutrients* 12, 3432. doi:10.3390/nu12113432

Tung, M. C., Lan, Y. W., Li, H. H., Chen, H. L., Chen, S. Y., Chen, Y. H., et al. (2020). Kefir Peptides Alleviate High-Fat Diet-Induced Atherosclerosis by Attenuating Macrophage Accumulation and Oxidative Stress in ApoE Knockout Mice. *Sci. Rep.* 10, 8802. doi:10.1038/s41598-020-65782-8

Vinderola, C. G., Duarte, J., Thangavel, D., Perdigón, G., Farnworth, E., and Matar, C. (2005). Immunomodulating Capacity of Kefir. *J. Dairy Res.* 72, 195–202. doi:10.1017/s0022029905000828

Wang, H. F., Tseng, C. Y., Chang, M. H., Lin, J. A., Tsai, F. J., Tsai, C. H., et al. (2012). Anti-inflammatory Effects of Probiotic Lactobacillus Paracasi on Ventricles of BALB/C Mice Treated with Ovalbumin. *Chin. J. Physiol.* 55, 37–46. doi:10.4077/CJP.2012.AMM107

Wang, Z. Y., Morinobu, A., Kawano, S., Saegusa, J., Wang, B., and Kumagai, S. (2002). Gold Sodium Thiomalate Suppresses the Differentiation and Function of Human Dendritic Cells from Peripheral Blood Monocytes. *Clin. Exp. Rheumatol.* 20, 683–688.

Wasserman, A. M. (2011). Diagnosis and Management of Rheumatoid Arthritis. *Am. Fam. Physician* 84, 1245–1252.

Williams, R. O. (2004). Collagen-induced Arthritis as a Model for Rheumatoid Arthritis. *Methods Mol. Med.* 98, 207–216. doi:10.1385/1-59259-771-8:207

Won, H. Y., Lee, J. A., Park, Z. S., Song, J. S., Kim, H. Y., Jang, S. M., et al. (2011). Prominent Bone Loss Mediated by RANKL and IL-17 Produced by CD4+ T Cells in TallyHo/JngJ Mice. *PLoS One* 6, e18168. doi:10.1371/journal.pone.0018168

Yang, R., Gao, H., Chen, L., Fang, N., Chen, H., Song, G., et al. (2020). Effect of Peripheral Blood-Derived Mesenchymal Stem Cells on Macrophage Polarization and Th17/Treg Balance *In Vitro*. *Regen. Ther.* 14, 275–283. doi:10.1016/j.reth.2020.03.008

Yen, C. C., Chang, W. H., Tung, M. C., Chen, H. L., Liu, H. C., Liao, C. H., et al. (2020). Lactoferrin Protects Hyperoxia-Induced Lung and Kidney Systemic Inflammation in an *In Vivo* Imaging Model of NF-κB/Luciferase Transgenic Mice. *Mol. Imaging Biol.* 22, 526–538. doi:10.1007/s11307-019-01390-x

Yue, M., Xia, Y., Shi, C., Guan, C., Li, Y., Liu, R., et al. (2017). Berberine Ameliorates Collagen-Induced Arthritis in Rats by Suppressing Th17 Cell Responses via Inducing Cortistatin in the Gut. *FEBS J.* 284, 2786–2801. doi:10.1111/febs.14147

Zeyda, M., Kirsch, B. M., Geyeregger, R., Stuhlmeier, K. M., Zlabinger, G. J., Hörl, W. H., et al. (2005). Inhibition of Human Dendritic Cell Maturation and Function by the Novel Immunosuppressant FK778. *Transplantation* 80, 1105–1111. doi:10.1097/01.tp.0000178301.19732.a1

Conflict of Interest: The authors declare that the research was conducted in the absence of any commercial or financial relationships that could be construed as a potential conflict of interest.

Publisher's Note: All claims expressed in this article are solely those of the authors and do not necessarily represent those of their affiliated organizations, or those of the publisher, the editors and the reviewers. Any product that may be evaluated in this article, or claim that may be made by its manufacturer, is not guaranteed or endorsed by the publisher.

Copyright © 2021 Chen, Li, Chao, Tu, Yen, Lan, Yang, Chong, Lin and Chen. This is an open-access article distributed under the terms of the Creative Commons Attribution License (CC BY). The use, distribution or reproduction in other forums is permitted, provided the original author(s) and the copyright owner(s) are credited and that the original publication in this journal is cited, in accordance with accepted academic practice. No use, distribution or reproduction is permitted which does not comply with these terms.

frontiers in Pharmacology

ORIGINAL RESEARCH
published: 18 October 2021
doi: 10.3389/fphar.2021.767243

Serum Amyloid A Correlates With the Osteonecrosis of Femoral Head by Affecting Bone Metabolism

Xiaoyuan Peng†, Yiyang Ma†, Qiyang Wang, Yanchun Gao, Guangyi Li, Chenyi Jiang, Yun Gao and Yong Feng**

Department of Orthopedic Surgery, Shanghai Jiao Tong University Affiliated Sixth People's Hospital, Shanghai, China

Osteonecrosis of femoral head (ONFH) is a progressive hip joint disease without disease-modifying treatment. Lacking understanding of the pathophysiological process of ONFH has become the humper to develop therapeutic approach. Serum amyloid A (SAA) is an acute phase lipophilic protein during inflammation and we found that SAA is increased for the first time in the serum of ONFH patients through proteomic studies and quantitatively verified by ELISA. Treating rBMSCs with SAA inhibited the osteogenic differentiation *via* Wnt/β-catenin signaling pathway deactivation and enhanced the adipogenic differentiation *via* MAPK/PPARγ signaling pathway activation. Finally, bilateral critical-sized calvarial-defect rat model which received SAA treated rBMSCs demonstrated reduction of bone formation when compared to untreated rBMSCs implantation control. Hence, SAA is a vital protein in the physiological process of ONFH and can act as a potential therapeutic target to treat ONFH.

Keywords: serum amyloid a, osteonecrosis of femoral head, proteomics, wnt/β-catenin signaling pathway, MAPK/PPARγ signaling pathway

OPEN ACCESS

Edited by:
Longhuo Wu,
Gannan Medical University, China

Reviewed by:
Yiqin Zhou,
Second Military Medical University, China
Denghui Xie,
Southern Medical University, China

****Correspondence:***
Yun Gao
terminatoryun@hotmail.com
Yong Feng
fengyongxsh@gmail.com

†These authors have contributed equally to this work and share first authorship

Specialty section:
This article was submitted to Ethnopharmacology, a section of the journal Frontiers in Pharmacology

Received: *30 August 2021*
Accepted: *27 September 2021*
Published: *18 October 2021*

Citation:
Peng X, Ma Y, Wang Q, Gao Y, Li G, Jiang C, Gao Y and Feng Y (2021) Serum Amyloid A Correlates With the Osteonecrosis of Femoral Head by Affecting Bone Metabolism. Front. Pharmacol. 12:767243. doi: 10.3389/fphar.2021.767243

INTRODUCTION

Osteonecrosis of femoral head (ONFH) is a progressive hip joint disorder without consensus of effective treatment, ultimately leading to total hip replacement (Mont et al., 2006). The pathogenesis of ONFH is perplexing and needs further investigation (Hines et al., 2021). Use of steroid, overuse of alcohol and trauma of femoral neck or head are the three well known risk factors for ONFH. Previous study has indicated that the pathogenesis of ONFH is related to the severe degradation of the bone tissue (Weinstein et al., 2000), promoted differentiation of bone mesenchymal stem cells (BMSCs) to adipocytes and hypertrophy of the adipocyte through increasing intracellular lipid synthesis (Peckett et al., 2011). The increase of marrow fat cell induces intra-osseous hypertension in the proximal femur. Venous sinusoids are compressed due to the intra-osseous hypertension and then intravascular coagulation occurs. Arterial blood flow is blocked and eventually results in ischemia in the femoral head (Yoon et al., 2020). However, the specific underlying molecular mechanism of aberrant bone metabolic balance has not been completely elucidated.

Serum amyloid A (SAA) is a family of acute phase response proteins which is coded by various genes, which exhibit high degrees of allelic variation and mammalian homology (Uhlar et al., 1994; Lloyd-Price et al., 2019). Apart from high levels of SAA found in the liver (Strnad et al., 2017), the protein has been found to be expressed in monocytes/macrophages (Meek et al., 1992), chondrocytes (Zerega et al., 2004) and adipocytes (Han et al., 2020). Meanwhile, SAA is thought as a crucial marker of inflammation and a precursor protein of amyloidosis involved in cellular cholesterol homeostasis,

promotion of signalling cascades, and modulation of intercellular calcium levels (Artl et al., 2000; Baranova et al., 2005; Husebekk et al., 2010). Previous study has indicated that SAA is a lipid soluble protein, of which the 95% surface has lipophilic receptors, especially for high density lipoprotein (HDL) (Frame and Gursky, 2017). In particular, SAA is involved with cholesterol metabolism in both physiologic and inflammatory conditions (Sack, 2018). Clearly, the intimate relationship among SAA/HDL/cholesterol has implicated SAA in the pathogenesis of various diseases, such as rheumatoid arthritis (Mun et al., 2021), atherosclerosis (Webb, 2021), alcoholic liver cirrhosis (Kim et al., 2014) and insulin resistance (Li et al., 2021). Mechanistically, SAA participates in the processes of the above diseases by binding with HDL, promoting adipogenic differentiation and promoting the proliferation of preadipocytes. In this study, we aimed to explore the role of SAA in bone metabolism to deepen the research on the pathophysiologic mechanism of ONFH.

In an effort to better understand those mechanisms underlying ONFH, proteomics has emerged as a well-defined strategy which, through in-depth characterization of the whole tissues, sera, and biofluid proteome, has provided substantial data in terms of potential protein biomarkers associated with the mechanism pathways and prognosis of disease (Pan et al., 2005; Veenstra et al., 2005; Zapico Muñiz et al., 2005). In this study, the serum proteome technology was exploited to assess the differentiate expression levels of serum proteins between ONFH patients and healthy controls. Based on the results of proteomics, SAA was hypothesised to exhibit a correlation with ONFH, and this assumption was confirmed with ELISA. The influence of SAA on the osteogenic and adipogenic differentiation of BMSCs was determined to confirm the link between SAA and ONFH. Combined with the results of *in vitro* experiments, the effect of SAA on bone metabolism had also been verified *in vivo* experiments. This work will provide us with the in-depth knowledge of SAA-induced bone metabolism disorder and ONFH pathogenesis.

MATERIAL AND METHODS

Proteomics Analysis

Patients

For proteome analysis, the steroid-induced ONFH group comprised 11 patients who received corticosteroid medication. These patients were diagnosed with ONFH from magnetic resonance imaging (MRI) findings and were not treated for ONFH. A set of 11 healthy volunteers matched with sex and age was included as the control group. The clinical features and demographic information of the steroid-induced ONFH group and the control group were summarized in **Supplementary Material**. For ELISA, 20 patients with steroid-induced ONFH, 20 with alcohol-induced ONFH, 20 with trauma-induced ONFH, and 20 healthy volunteers were enrolled. All the patients and volunteers participating in the ELISA study did not have underlying factors other than ONFH that might cause the elevation of SAA. The clinical features and demographic information of the patients and volunteers were summarized in **Supplementary Material**. All procedures performed in this study involving human participants were in accordance with the ethical standards of the institutional and/or national research committee and with the 1964 Declaration of Helsinki and its later amendments or comparable ethical standards. Informed consent was obtained from all individual participants included in the study.

Preparation of Serum Samples

A total of 5 ml of peripheral venous blood was withdrawn from patients and healthy volunteers. The blood samples were coagulated at 37°C for 15 min and centrifuged at 2,000 × g for 15 min. The supernatant was collected and stored at −80°C.

Elimination of Highly Abundant Proteins and Quantification

The serum samples were thawed and attenuated at 37°C. The attenuated serum samples were percolated with filter membranes (0.22 μm pore size). The 14 most abundant proteins were depleted from the plasma using the multiple affinity removal column system (MARS, Agilent Technologies spin columns, United States) according to the manufacturer's protocol. The depleted sample was buffer exchanged with 50 mm ammonium bicarbonate using Vivaspin concentrator (5,000 molecular weight cut-off, Sartorius Group, Germany). The proteins from the processed serum samples were quantified using a protein assay reagent kit (Bio-Rad Laboratories Inc, Hercules, CA, United States) and stored at −80°C.

Two-Dimensional Gel Electrophoresis

The serum samples were subjected to two-dimensional gel electrophoresis. Briefly, 100 μg of each serum sample was loaded onto an immobilized pH gradient (IPG) strip (GE Amersham, United Kingdom) with pH variation from 3 to 10. The first dimensional isoelectric focusing was implemented as follows: 30 V for 12 h, 500 V for 1 h, 1,000 V for 1 h, 8,000 V for 8 h, and 500 V for 4 h using Ettan IPGphor Isoelectric Focusing System (GE Amersham, United Kingdom). The proteins after iso-electrophoresis were separated with second dimensional sodium dodecyl sulphate polyacrylamide gel electrophoresis (SDS-PAGE) using Hofer SE 600 (GE Amersham, United Kingdom). The second-dimension gel electrophoresis was performed on the 12.5% SDS-polyacrylamide slab gels at 15 mA for 30 min and 30 mA until the trace of bromophenol blue was 0.5 cm away from the bottom of the gel.

Silver Staining

The silver staining of the gels after electrophoresis was performed according to the modified silver-staining protocol with the Silver Stain PlusOne kit (GE Amersham, United Kingdom). The gels were fixed with 50% methanol and 5% ethyl alcohol for 1 h, sensitized with sensitizing solution comprising 0.2% sodium thiosulphate, 30% methanol, and 68 g/L sodium acetate for 5 min, washed thrice with distilled water for 5 min, incubated with 0.25% silver nitrate for 20 min, and rinsed thrice with distilled water for 1 min. The gels were developed with 0.04% formaldehyde and 2% sodium carbonate by vigorous shaking and the reaction was terminated with 5% acetic acid till the coloration was moderate.

Gel Imaging

The silver-stained gels were scanned with UMax Powerlook 2110XL (GE Amersham, United Kingdom) and the spot patterns of the gel images were matched using Image Master 2D system (Amersham Biosciences). The densities of all the matched spots were standardized with the total protein amount in the gel.

Destaining and Trypsin Digestion

Different groups of spots were excised from the gel and rinsed with de-ionised water. The washed gommures were destained with 50 µl of a solution containing 30 mmol/L potassium ferricyanide ($K_3Fe(CN)_6$) and 100 mmol/L of sodium thiosulfate ($Na_2S_2O_3$) at a ratio of 1:1. After lyophilization, digestion was performed with 5 µL of trypsin (Promega, United States) at 37°C for 20 h. The enzymatic hydrolysate was subsequently extracted, and the residual was treated with 100 µl of 60% acetonitrile (ACN) and 0.1% trifluoroacetic acid (TFA). The samples were ultrasonically washed for 15 min and the cleaned solution obtained was merged with the enzymatic hydrolysate. The collected fluid was desalted with ZipTip (Millipore, United States) and freeze dried.

Matrix-Assisted Laser Desorption Ionisation Time-Of-Flight Mass Spectrometry

The dried samples were dissolved in 2 µl of 20% acetonitrile and treated with supersaturated *a*-cyano-4-hydroxycinnamic acid (CHCA) matrix solution. The solvent composed of 0.5% TFA and 50% ACN. All the samples were analyzed on 4800 Plus MALDI TOF/TOFTM Analyzer (Applied Biosystems, United States) at a scan range of 800–4,000 Da with UV light at 355 nm using Nd:YAG laser. The data were searched using the International Protein Index human protein database with Mascot search engine.

ELISA

The serum levels of the identified protein, SAA, were determined with ELISA performed using the human SAA ELISA Kit (Anogen, Canada) according to the manufacturer's instructions. The patients and volunteers were enrolled in the study and the serum samples were obtained as mentioned before.

Vitro Experiment

Isolation and Cultivation of rBMSCs

RBMSCs were obtained from Sprague-Dawley male rats. Briefly, the marrow from the femur and tibia of male rats was flushed under aseptic conditions. For the isolation of rBMSCs, the cell suspension was sifted with a 400-mesh filter. The filtered cell suspension was centrifuged for 5 min at 4°C. The floating fraction was discarded, and the enriched cells were treated with an erythrocyte lysis buffer. rBMSCs were suspended and transferred into culture flasks and cultured with α-Modified Eagle Medium (α-MEM, HyClone, United States), supplemented with 10% foetal bovine serum (FBS, Gibco, United States) and 1/100 penicillin-streptomycin (Gibco). The cells were maintained in a humidified atmosphere containing 5% CO_2 at 37°C, and the culture medium was replaced every 2 days. After three to five passages, rBMSCs were used for subsequent experiments. For osteogenic differentiation, rBMSCs were incubated in culture medium supplemented with 10^{-2} M β-sodium glycerophosphate, 50 µg/ml of L-ascorbic acid, and 10^{-7} M dexamethasone for 14 days. For adipogenic differentiation, the cells were incubated with an adipogenic induction culture medium (Cyagen, China) for 2 wk.

Cell Counting Kit-8 (CCK-8) Assay

Direct cell counting was performed to compare the proliferative rate of rBMSCs untreated or treated with SAA (PeproTech, United States). A total of 1×10^{-4} rBMSCs were seeded in a 96-well plate and treated as the group information mentioned before. The toxicity and proliferation of cells were detected with CCK-8 kit (Beyotime, China). At each time point (Day 1, 3, and 7), the proliferative rate of rBMSCs was assessed according to the manufacturer's instructions.

Bromo-4-chloro-3-indolyl-phosphate (BCIP)/Nitro Blue Tetrazolium (NBT) Staining

To visualise the alkaline phosphatase (ALP) activity, the BCIP/NBT staining was used. rBMSCs were seeded into a 24-well plate at 1×10^{-5} cells per well. Different groups of rBMSCs were cultured in osteogenic induction culture medium for 7 days. The culture medium was renewed every 2 days. Following treatment, the cells were washed with phosphate-buffered saline (PBS) and fixed with 4% paraformaldehyde for 20 min at room temperature. The fixed cells were re-washed thrice with PBS and treated with BCIP/NBT solution (Beyotime, China) in the dark for 1 h at room temperature. Images were observed and acquired using a microscope (Leica, Germany) and digital camera (Canon, Japan). The ALP activity in the cellular fraction was measured using a microplate test kit (Nanjing Jiancheng Biotechnology Co Ltd Jiangsu, China) following the manufacturer's instructions, and the absorbance at 520 nm was measured using a microplate reader.

Alizarin Red Staining

Alizarin red staining is widely used to evaluate the osteogenic differentiation of cells based on the detection of calcium deposition in the extracellular matrix that serves as a marker of early osteogenesis. After co-cultivation with osteogenic induction medium and SAA for 14 days, different groups of rBMSCs were fixed with 4% paraformaldehyde for 20 min and washed thrice with PBS at 37°C. The cells were stained with alizarin red solution (Cyagen, China) for 30 min, and images of general view were captured with digital camera under 10× using microscope. To quantify mineralization, the calcium deposition was desorbed with 10% cetylpyridinium chloride (Sigma-Aldrich), after which the solution was collected, and the OD was measured at 570 nm.

Oil Red O Staining

Oil red O staining was performed after 14 days of treatment with adipogenic induction culture medium (Cyagen, China) to evaluate the adipogenic differentiation of various groups of rBMSCs. The cells were fixed with 4% paraformaldehyde for

20 min, rinsed thrice with PBS, and stained with Oil red O solution comprising PBS and 0.5% oil red O stock solution. The neutral lipids were stained red and served as the biomarker of adipogenesis. Microscope was used to capture images of the stained cells under 10× magnification. After the observation, isopropanol was used to release the stain, and the degree of adipogenesis was detected by measuring at 540 nm.

Western Blot Analysis

The rBMSCs were plated in a six-well plate and cultured until they reached 90% confluency. The cells were induced with osteogenesis or adipogenesis culture medium and incubated in the presence of 150 mg/L of SAA for 7 days. The proteins were subsequently collected after treatment with the combination of cell lysis buffer, phosphatase inhibitor, proteinase inhibitor, their concentration was determined with bicinchoninic acid protein assay kit (Cell Signalling Technology, Shanghai, China). Equal amounts of proteins (20 μg) were separated on SDS-PAGE gels by electrophoresis and transferred onto polyvinylidene difluoride (PVDF) membranes. The membranes were blocked with a blocking buffer for 1 h and incubated with the corresponding primary antibody at room temperature. After washing thrice with TBST, the membranes were incubated with horseradish peroxidase (HRP)-conjugated polyclonal goat antibodies, *ß*-actin or glyceraldehyde 3-phosphate dehydrogenase (GAPDH) were used as internal references. Extracellular signal-regulated kinase (ERK)-1/2, phospho-ERK1/2, glycogen synthase kinase 3 beta (GSK3β) and phospho-GSK3βantibodies were purchased from Cell Signalling Technology (Shanghai, China), while *ß*-catenin antibodies were obtained from Abcam (United Kingdom). Peroxisome proliferator-activated receptor gamma (PPARγ) and GAPDH antibodies were supplied by Servicebio (Wuhan, China).

Real-Time Reverse-Transcription Polymerase Chain Reaction (RT-PCR)

The mRNA expression of osteogenic differentiation-related genes (*ALP*, *OCN*, *Runx2*, and *COL-1*) and adipogenic differentiation-related genes (*aP2*, *Adipoq*, and *PPARγ*) was assessed with real-time RT-PCR. After 7 days of incubation in an appropriate induction medium and stimulation with various concentrations of SAA, the total RNA was extracted from cells using EZ-press RNA purification Kit (EZ Bioscience, China) and reverse transcribed to generate complementary DNA using 4× Reverse Transcription Master Mix (EZ Bioscience, China). The forward and reverse primers (BioTNT, China) for cDNAs were designed as indicated in **Table 1**. A total of 10 μl of mixture comprising 1 μl of cDNA, 0.3 μl of forward primer, 0.3 μl of reverse primer, 5 μl of qPCR SuperMix (BioTNT, China), and 3.4 μl of distillation-distillation H_2O was loaded to each well of a 384-well plate and real-time RT-PCR was performed on 7900HT Fast Real-Time PCR System (Thermo Fisher Scientific, United States). The thermal cycle for RT-PCR was as followed: 95°C for 30 s; 40 cycles at 95°C for 10 s and at 60°C for 30 s. The expression of mRNAs was calculated by the $2^{-\triangle\triangle Ct}$ method and the expression of target gene was normalised to that of *ß*-actin.

Vivo Experiment

Bilateral Critical-Sized Calvarial-Defect Model

To test the ability of SAA affecting bone metabolism *in vivo*, fifteen 12-wk-old male SpragueeDawley rats (body weight: 250–300 g) were obtained from the experimental animal centre at the Hospital, China. Prior to surgery, rats were anesthetized by pentobarbital sodium through intraperitoneal injection. The rats' heads were stabilized with a stereotactic frame to prevent movement during surgical procedures. The surgical areas were shaved, and the skin was disinfected with 75% ethanol. A 1.5–2 cm length mid-sagittal skin incision was created on scalp, and two 5°mm-diameter, critical size, circular bone defects were created with electric trephine drill (Nouvag AG; Goldach, Switzerland) with a low-speed handpiece under continuous saline irrigation to both parietal bones bilaterally symmetrical by the reference of the bregma point and sagittal suture. ShakeGel™ 3D hydrogel (Biomaterials United States, VA, United States) was used as the scaffold to load rBMSCs. Cells were mixed into the hydrogel following the manufacturer's protocol, and the cell/hydrogel composites were then applied to the calvarial bone defects in rats. For groups implanted with rBMSCs treated with SAA, the cells were precultured with 150 mg/L SAA for 5 days before being mixed with the hydrogel. To ensure that the cells were exposed to SAA *in vivo*, SAA was added to the mixed hydrogel composites at a final concentration of 150 mg/L. All the animals were permitted access to food and water freely and daily observe for potential complications or abnormal behaviour. All experimental procedures were approved by the Animal Research Committee of the Hospital.

Micro-CT Scanning Analysis

Twelve-weeks after bilateral critical-sized calvarial-defect model establishment, all the rats were euthanized. The craniums of rats were scanned by a microCT scanner (Bruker, Germany) and the 2-D images were analysed by CTAn software (Bruker, Germany). For the craniums, the parameters of the new bone volume/total volume (BV/TV), bone mineral density (BMD) and Trabecular thickness (TbTh) of the bone defect area were recorded and collected for analysis.

Immunofluorescence Staining

Polychrome sequential fluorescent labelling was conducted to observe the rate of new bone formation and mineralization. The rats were intraperitoneally injected fluorochromes under anaesthesia as follow, 25 mg/kg tetracycline, (Sigma, United States), week 2; 30 mg/kg alizarin red, (Sigma, United States), week 4; 20 mg/kg calcein, (Sigma, United States), week 6. The defected calvarias were collected at week 12 and dehydrated by gradient alcohol. The undecalcified specimens were embedded in poly-methyl-methacrylate and sectioned to 150 μm thick in the orientation of the sagittal surface. Then fluorescent signals were observed using a confocal microscope (Leica, Germany).

Histological Analysis

The craniums from afformentioned rat model were sectioned coronally through the central area of the defect at a thickness of 5 μm with a microtome (Leica, Hamburg, Germany). Next,

TABLE 1 | List of forward and reverse primers used for RT-PCR.

Primer	Forward	Reverse
Alp	5′-CGT TGA CTG TGG TTA CTG CTG-3′	5′-CTT CTT GTC CGT GTC GCT-3′
OCN	5′-CAG ACA AGT CCC ACA CAG CA-3′	5′-CCA GCA GAG TGA GCA GAG AGA-3′
COL-1	5′-TGT GCG ATG GCG TGC TAT-3′	5′-CCT ATG ACT TCT GCG TCT GGT G-3′
Runx2	5′-ATC ATT CAG TGA CAC CAC CAG-3′	5′-GTA GGG GCT AAA GGC AAA AG-3′
PPARγ	5′-CCT CTC TGT GAT GGA TGA CCA-3′	5′-ACA TCC CGT TCA CAA GAG CT-3′
aP2	5′-TGA AAC TGA CGA TCA CAC AGG-3′	5′-ACA GAA CTC ACT GGG ACC TGG-3′
Adipoq	5′-ATG ATA CCA ACT GAC TGC CAC T-3′	5′-TTG CTT ACT TTG AGG GTT CTG A-3′
β-actin	5′-CCT CTA TGC CAA CAC AGT-3′	5′-AGC CAC CAA TCC ACA CAG-3′

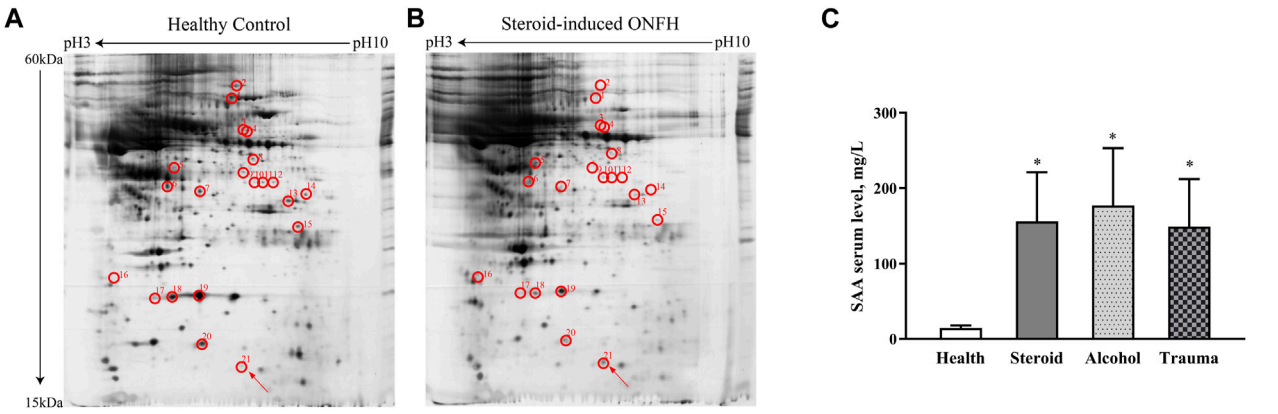

FIGURE 1 | A pair of representative two-dimensional gel electrophoresis gels from the sera of 11 healthy controls **(A)** and 11 patients with steroid-induced ONFH **(B)**. The circled spots that showed identified, significant and consistent differences between two groups. SAA protein was pointed out by arrows **(C)** SAA serum level in patients with steroid-, alcohol-, and trauma-ONFH and healthy volunteers, *$p < 0.05$ compared with healthy volunteers.

Masson staining, Safranine solid green staining and HE staining were performed to evaluate new bone formation according to the standard procedures.

Statistical Analysis

SPSS 22.0 was used to analyse the data, which were expressed as the mean ± standard deviation (SD). Comparisons between different groups were assessed with one-way analysis of variance (ANOVA). Fisher's LSD test was used for each comparison. A value of $p < 0.05$ was considered statistically significant. Detailed statistical data are reported in **Supplementary Material**.

RESULTS

Overexpression and Quantitative Validation of SAA in Patients With ONFH

Protein profiles from the sera of 11 patients with steroid-induced ONFH and 11 healthy volunteers were analysed with two-dimensional gel electrophoresis and silver staining. We observed 21 prominent protein spots that differed between the two groups. Three of these proteins were upregulated and the rest 18 proteins were downregulated in patients with steroid-induced ONFH (**Figures 1A,B**). The spots determined in the steroid-induced ONFH and health control groups were replicable. As shown in **Table 2**, the spot no. 21 corresponding to an upregulated protein in patients with steroid-induced ONFH was identified as SAA. Thus, SAA was identified as elevated in the serum of patients with ONFH. The serum level of SAA was quantitatively validated by ELISA and was found to be increased in the patients with steroid-, alcohol-, and trauma-induced ONFH as compared with the health controls (**Figure 1C**). Based on the results of the ELISA study, however, no significant difference was observed among the three ONFH groups. Based on the results of the ELISA study, the final concentration of SAA used in the following experiments was decided as 150 mg/L.

SAA Inhibits the Osteogenic Differentiation of rBMSCs *in vitro*

The proliferation and differentiation of BMSC plays an important role in the pathophysiological process of ONFH. Thus, to examine the effect of SAA on the proliferative rate of rBMSCs, CCK-8 assay was performed at day 1, 3, and 7. The comparison of the absorbance at 450 nm wavelength revealed the ability of 150 mg/L SAA to induce rBMSCs proliferation. After

TABLE 2 | Proteins with significant changes in the sera of patients with steroid-induced ONFH as compared with healthy controls.

Spot no	PI	MW	Protein score	Accession No	Protein name
1	6.67	86,847	424	IPI00921523	CFB Isoform 1 of Complement factor B (Fragment)
2	6.41	109,332.8	71	IPI00879709	C6 Complement component C6 precursor
4	6.55	52,384.6	87	IPI00022488	HPX Hemopexin
5	8.48	31,673	582	IPI00431645	HPR 31 kDa protein
6	6.13	38,940.5	693	IPI00478493	HPR haptoglobin isoform 2 preproproteins
7	6.13	38,940.5	439	IPI00478493	HPR haptoglobin isoform 2 preproproteins
8	6.32	41,816.7	164	IPI00479708	IGHM Full-length Cdna clone CS0DD006YL02 of Neuroblastoma of Homo sapiens
9	7.38	38,766.4	140	IPI00011264	CFHR1 Complement factor H-related protein 1
10	7.38	38,766.4	232	IPI00011264	CFHR1 Complement factor H-related protein 1
11	7.38	38,766.4	326	IPI00011264	CFHR1 Complement factor H-related protein 1
13	6.89	194,170.1	78	IPI00418163	C4B complement C4-B preproprotein
14	5.64	71,474.7	404	IPI00019568	F2 Prothrombin (Fragment)
15	4.86	78,174.4	242	IPI00017696	C1S Complement C1s subcomponent
17	6.13	45,860.8	237	IPI00641737	HPR Haptoglobin
18	6.13	45,860.8	268	IPI00641737	HPR Haptoglobin
19	6.13	45,860.8	227	IPI00641737	HPR Haptoglobin
20	6.13	38,940.5	467	IPI00478493	HPR haptoglobin isoform 2 preproproteins
21	6.28	13,580.5	292	IPI00552578	serum amyloid A protein 1 and 2

incubation with SAA, rBMSCs showed higher proliferation than those from control group and the proliferative rate of the rBMSCs exposed to 150 mg/L SAA was obviously enhanced at 7 days (**Figure 2A**). BCIP/NBT staining was performed to evaluate the effect of SAA on osteogenic differentiation of rBMSCs. As shown in **Figures 2B,C**, the bluish colouration of rBMSCs cultured with SAA was sparse as compared with the cells cultured without SAA. In agreement with the result of BCIP/NBT staining, rBMSCs treated with SAA revealed minor mineralisation than that observed with rBMSCs cultured without SAA, suggestive of the ability of SAA to suppress osteogenic differentiation (**Figures 2D,E**).

The mechanism underlying the inhibitory effect of SAA was further excavated. ETC-159 was added as inhibitor of the Wnt signalling pathway and BML-284 was added as activator of Wnt signalling pathway. According to **Figures 2B–E**, there is little difference in the inhibition of osteogenic differentiation between rBMSCs treated with SAA and ETC-159. However, when BML-284 was added as antagonist of SAA's osteogenic inhibition, the osteogenic differentiation of rBMSCs returned to normal. Further evidence was provided by Western blot analysis, on the basis of **Figures 2F,G**, a decrease in the phosphorylation level of GSK3β was founded and downregulated the expression of β-catenin owing to the addition of SAA, consistent with the results of rBMSCs added with ETC-159. While rBMSCs were co-cultured with SAA and BML-284, the protein expression of Wnt signalling pathway was not significantly different from that of control group. Real-time RT-PCR was performed to monitor the expression of osteogenesis-related genes. The expression of *ALP*, *Runx2*, *OCN*, and *COL-1* was downregulated among the groups treated with SAA than control group. Furthermore, no difference was found between group added with SAA and ETC-159, or between group added with SAA + BML-284 and control group (**Figures 2H–K**).

SAA Promotes the Adipogenic Differentiation of rBMSCs *in vitro*

Because adipocyte is found proliferated in ONFH, we further investigated whether SAA had other effects on the differentiation of rBMSCs. Oil red O staining was used to detect the effect of SAA on adipogenic differentiation of rBMSCs. As the results showed in **Figures 3A,B**, the number of red stained lipid droplets was significantly higher in the rBMSCs treated with SAA than in those from control group. To further test if MAPK/PPARγ pathway is affected by SAA, bosutinib (SKI-606) was used as the inhibitor of Erk phosphorylation and T0070907 as a potent selective PPARγ inhibitor was used to antagonize the adipogenic effect of SAA on rBMSCs. In accordance with **Figures 3A,B** SAA and SKI-606 had the same ability to promote adipogenic differentiation of rBMSCs. However, the ability was antagonized by T0070907.

Erk1/2, one of the mitogen-activated protein kinase (MAPK) family member, is known to play an important role in adipogenesis. As shown in **Figures 3C,D** the phosphorylation level of ERK1/2 reduced following treatment with SAA or SKI-606 or SAA + T0070907. However, the expression of downstream PPARγ was not up-regulated by SAA due to T0070907. The expression of *aP2*, *PPARγ*, and *Adipoq* was analysed in rBMSCs subjected to adipogenic induction and SAA treatment with real-time RT-PCR. As shown in **Figures 3E–G**, the expression of these biomarkers was significantly upregulated following stimulation with SAA or SKI-606, which attributed to the inhibitory of *p*-Erk1/2. Nevertheless, T0070907 antagonized SAA's up-regulation of PPARγ downstream genes' expression by inhibiting PPARγ expression.

SAA Reduces New Bone Formation *in vivo*

Lastly, the effect of SAA on bone metabolism was tested by in a bilateral critical-sized calvarial defect rat model. In short, the pre-treated rBMSCs was implanted into the critical sized, circular bone defects by using ShakeGel™ 3D hydrogel as scaffold to detect their

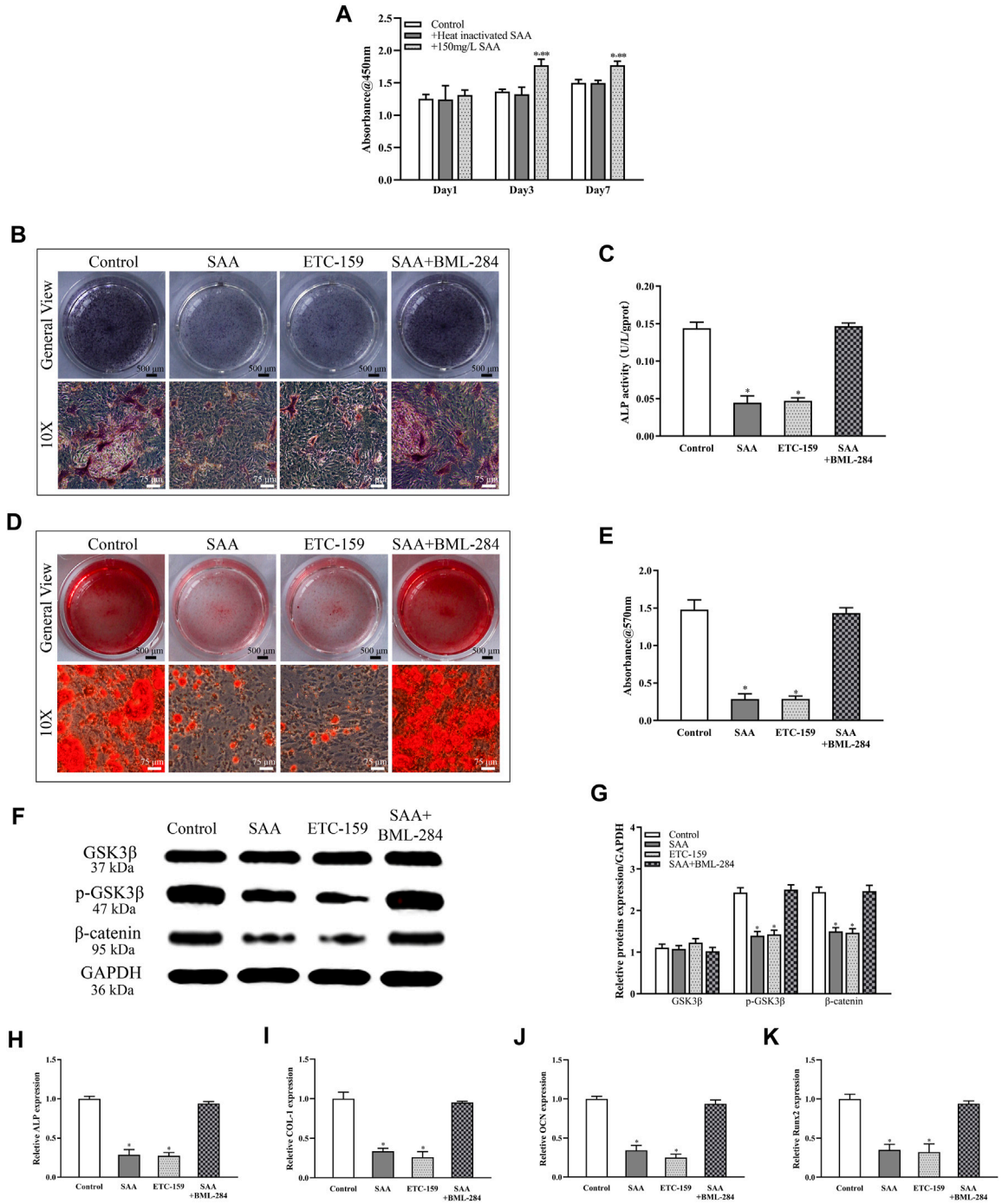

FIGURE 2 | (A) CCK-8 **(B)** NBT/BCIP staining **(C)** ALP activity assays **(D)** Alizarin red staining **(E)** Calcium deposition was determined by measuring optical density **(F)** The stable cell lines were subjected to western blot analysis for the detection of the expression of GSK3β, *p*-GSK3β, and *β*-catenin following normalization to GAPDH level **(G)** The intensity of relative proteins. The mRNA expression of **(H)** ALP **(I)** COL-1 **(J)** OCN(K) Runx2. **p* < 0.05 compared with control group, ***p* < 0.05 compared with group added with heat-inactivated SAA. All experiments were performed in triplicates.

osteogenic ability *in vivo*. 12 wk after the operation, the new bone formation in the defect area of the craniums was assessed by MicroCT scanning. As **Figure 4A** shown, the 3D reconstruction and coronal images rarely exhibited newly formed bone in the control group. Contrarily, the rBMSCs group showed an increase in bone formation. Besides, the rBMSCs treated with SAA group showed little evidence of new bone formation, which was almost indistinguishable from the control group. The trend was quantitively

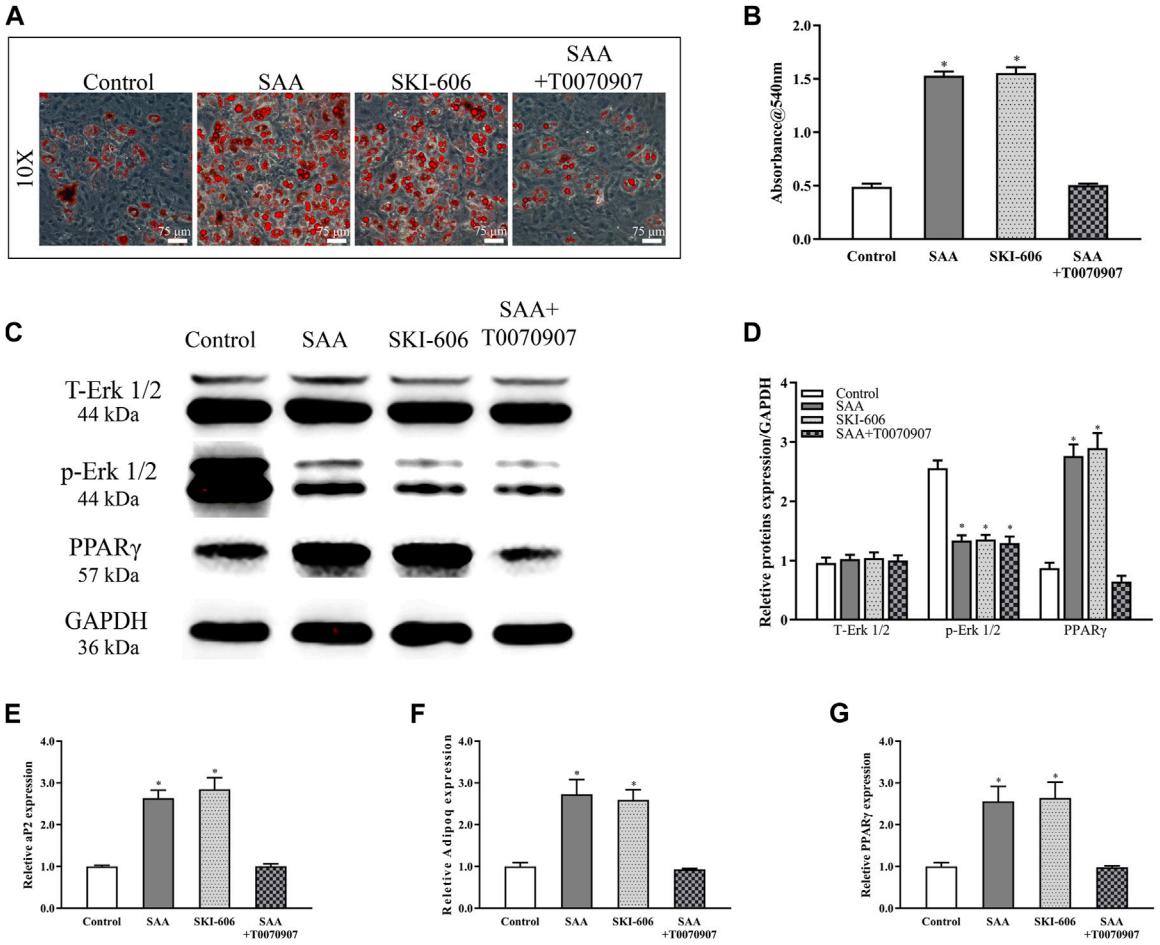

FIGURE 3 | (A) Oil red O staining **(B)** Lipid droplet was determined by measuring optical density **(C)** The stable cell lines were subjected to western blot analysis for the detection of the expression of T-ERK1/2, *p*-ERK1/2, and PPARγ after normalization to GAPDH expression **(D)** The intensity of relative proteins. The mRNA expression of **(D)** aP2 **(E)** Adipoq and **(F)** PPARγ. *$p < 0.05$ compared with control group. All experiments were performed in triplicates.

verified by BMD (**Figure 4B**) and BV/TV (**Figure 4C**) increased. The fluorescence signalling of tetracycline, alizarin red and calcein indicated the loci of new bone formation and mineralization. The formation of new bone in different time periods can be detected by fluorescence labelling injected at different time points. In accordance with **Figures 4D,E**, the fluorescence intensity of rBMSCs group was significantly stronger than the control group or rBMSCs + SAA group. Consistent with the above findings, the histological results of Masson, Safranin solid green and HE staining (**Figure 4F**) indicated that rBMSCs group showed increased mineralized bone tissues within the defect areas. However, after treating with SAA, rBMSCs lost their ability to promote new bone formation, which totally pointed that SAA reduced new bone formation *in vivo*.

DISCUSSION

Tracing the history of ONFH, research of its pathogenesis has been ongoing since the disease was described by Jean Cruveilhier, a French anatomist and pathologist but keeps incompletely understood (Dubois and Cozen, 1960). However, there is one agreement that local ischemia due to compromised blood flow is the final common pathway in the pathogenesis of ONFH (Hines et al., 2021). Most well-known risk factors and associated conditions of ONFH eventually leads to a kind of intra-osseous compartment syndrome inside the femoral head due to an ischemic cascade: *1*) overgrowth of marrow adipocyte *2*) intra-osseous hypertension; *3*) vascular compression and intravascular hypercoagulability; *4*) bone marrow necrosis and osteocyte death and *5*) fibrovascular reparation around the necrotic zone (Yoon et al., 2020). Therefore, finding the factors that cause the affected differentiation of BMSCs is potential key to further research.

Proteomics analysis, in which total protein in tissue are identified and quantified directly, has shown to be a valuable way to elucidate the molecular basis of disease etiology and pathogenesis. ONFH (Chen et al., 2015a). Previous studies have focused on the change of protein in bone tissue and cartilage (Zeng et al., 2019; Song et al., 2021). Admittedly, there have been many proteomic studies on various

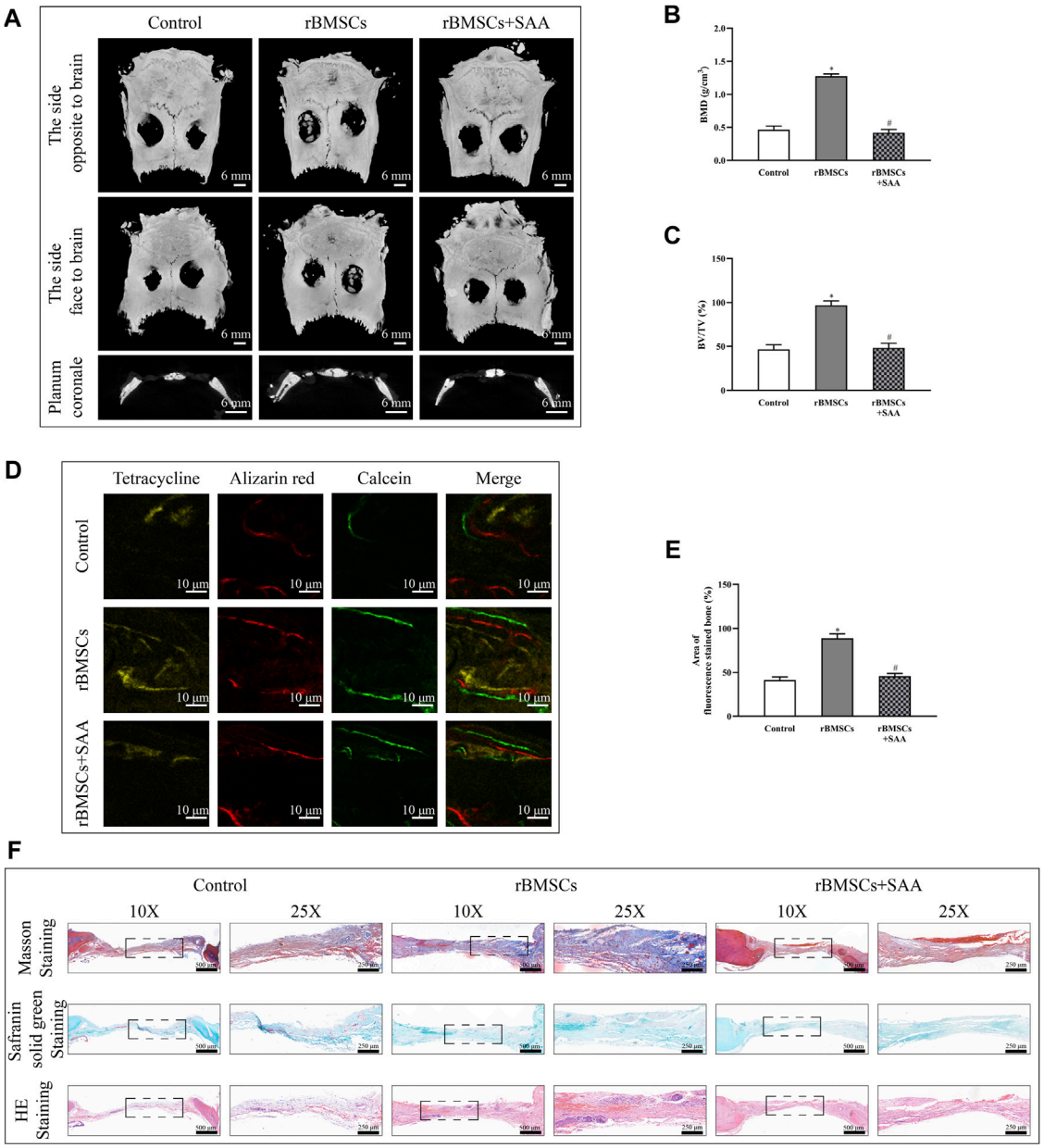

FIGURE 4 | (A) MicroCT 3D reconstruction and coronal images of the defect area at 8 weeks after operation in each group. MicroCT analyses of bone mineral density (BMD) **(B)** and bone volume/total volume (BV/TV) **(C,D)** Representative image of fluorescence assay for tetracycline, alizarin red and calcein **(E)** Statistical evaluation of fluorochrome area **(F)** Histological evaluation of the defect area by Masson, Safranin solid green and HE staining. *$p < 0.05$ compared with control group. #$p < 0.05$ compared with the rBMSCs group. All experiments were performed in triplicates.

pathological tissues of ONFH. In previous studies, tissue sources have tended to be local bone or cartilage rather than serum samples taken from peripheral blood. However, the risk factors of ONFH, excluding trauma, tend to be systemic rather than local. Hence, the proteomic research to investigate the expression of mutated proteins in the sera of patients with ONFH is indispensable. In the present study, proteomic analysis was performed to evaluate the systemic changes in the expression levels of proteins. To improve the reproducibility, sensitivity, and objectivity of the research, the sample selection criteria were strictly followed, and the highly abundant proteins were removed to avoid masking of the proteins expressed in low levels. Accordingly, 21 proteins were found to exhibit variable expression patterns in patients with steroid-induced ONFH as compared with healthy volunteers. Although 18 of these proteins were identified, we focused specifically on SSA, which showed upregulated expression in the serum of patients with steroid-induced ONFH as compared with normal subjects.

SAA is present in the blood of healthy individuals at low levels (20–50 mg/L), but its expression increases to about 1,000-fold within 24 h from the onset of acute phase response (APR), which includes a series of physiologic changes as a consequence of infection, inflammation, trauma, or other events (Gabay and Kushner, 1999; Yoo and Desiderio, 2003; Kushner, 1982). There are two possible explanations for the phenomenon we found above. Firstly, there is mutual similarity between the risk factors of ONFH and the factors leading to the increase of SAA. No matter alcohol, hormone or trauma can cause the increase of SAA expression (Knesek et al., 2010; Kim et al., 2014; Li et al., 2021), which was verified by ELISA. The causes may be related to liver damage caused by heavy drinking, abnormal lipid metabolism caused by alcohol and corticosteroids, and APR caused by acute trauma. Secondly, the necrosis of bone marrow and osteocytes, absorption of necrotic area, and synovial inflammation may cause focal inflammation occurred during ONFH resulted in the upregulation of SAA expression (Chen et al., 2015b; O'Hara et al., 2010).

Adipogenesis and osteogenesis of BMSCs were shown as significant factors affecting the process of osteonecrosis. The inhibition of osteogenic differentiation followed by increased lipid generation resulted in a decrease in bone formation. Moreover, blood circulation in femoral head was impaired following accumulation of the fatty tissue, eventually resulting in ONFH (Cui et al., 2006). The influence of SAA on bone metabolism was investigated here to explore its role in maintaining the balance between osteogenesis and adipogenesis of BMSCs. SAA exhibited the capability of promoting proliferation, curbing osteogenesis, and facilitating adipogenesis.

The Wnt/β-catenin signalling pathway is considered as a mediator of osteogenic differentiation (Chen et al., 2012; Luo et al., 2015). The decrease in β-catenin expression, which is in line with GSK3β phosphorylation, results in the inhibition of ALP activity and mineralisation (Ni et al., 2010). The inhibitory effect of SAA on osteogenesis was initially assessed using BCIP/NBT and alizarin red staining. The molecular mechanism underlying the inhibitory effect of SAA was investigated; the addition of SAA resulted in the downregulation of the phosphorylation of GSK3β, which repressed the expression of β-catenin in the downstream signalling pathway. The expression of *ALP*, *Runx2*, *OCN*, and *COL-1*, the biomarkers of osteogenic differentiation (Lee et al., 2009; Heo et al., 2010; Satija et al., 2013), was simultaneously downregulated following treatment with SAA proteins, as observed with PCR results. For adipogenic differentiation, the conversion of BMSCs to preadipocytes that differentiate into adipocytes is triggered by the enforced expression of PPARγ, which is regulated by the MAPK/PPARγ signalling pathways (Kang et al., 2007; Gierloff et al., 2014). Scilicet, the decreased phosphorylation Erk1/2 upregulated the expression of PPARγ and facilitated the adipogenic differentiation, as demonstrated in the present study. The expression of adipogenesis-related genes, not only *PPARγ* but also *aP2* and *Adipoq* (Lee et al., 2009; Muruganandan et al., 2009; Tokuzawa et al., 2010), was detected and confirmed the positive effects of SAA on the adipogenic differentiation of rBMSCs. The two pathways worked together to break the balance of bone metabolism of which the effect was reflected in a markable reduction of bone formation *in vivo*.

In this study, we first started from serum samples of ONFH patients and verified by proteomics and ELISA experiments that SAA was significantly increased in the serum of ONFH patients. Then, SAA was found to inhibit osteogenic differentiation and promote adipogenic differentiation of BMSCs *in vitro*. Further studies on the molecular mechanism of this phenomenon by Western Blot and PCR showed that SAA could inhibit Wnt/β-catenin signalling pathway and activate downstream PPARγ of MAPK signalling pathway. Finally, we verified *in vivo* that SAA can cause abnormal bone metabolism of BMSC and reduce bone formation (**Figure 5**). Hence, SAA is a vital protein in the physiological process of ONFH and can act as a potential therapeutic target to treat ONFH.

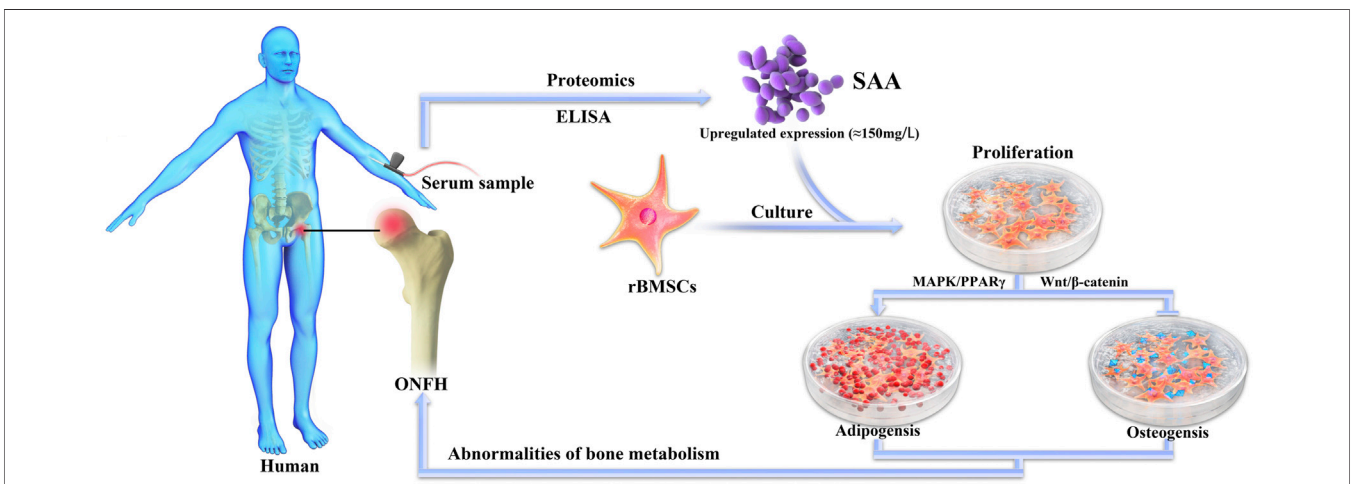

FIGURE 5 | A graphical summary of the whole study.

DATA AVAILABILITY STATEMENT

The datasets presented in this study can be found in online repositories. The names of the repository/repositories and accession number(s) can be found in the articles/**Supplementary Material**.

ETHICS STATEMENT

The animal study was reviewed and approved by Animal Research Committee of the Sixth People's Hospital of Shanghai Jiao Tong University.

AUTHOR CONTRIBUTIONS

XP, YM, and YF designed and conducted the experiments. XP, YM, and YG drafted the manuscript. XP, GL, and YF collected and analyzed the samples of proteomics. QW and YG assisted to vitro experiments. YM assisted to construct animal models. CJ assisted in statistical analysis. XP, QW, YG, and YF conceived, designed, and revised the articles. All authors have reviewed the articles.

FUNDING

This work was supported by the National Natural Science Foundation of China (81371959), Joint Project of Major Diseases of Shanghai Health System (2004ZYJB0301) and Program of Shanghai Jiao Tong University (YG2021QN98).

ACKNOWLEDGMENTS

The mass spectrometry proteomics data have been deposited to the ProteomeXchange Consortium *via* the PRIDE (Mont et al., 2006) partner repository with the dataset identifier PXD028318.

SUPPLEMENTARY MATERIAL

The Supplementary Material for this article can be found online at: https://www.frontiersin.org/articles/10.3389/fphar.2021.767243/full#supplementary-material

REFERENCES

Artl, A., Marsche, G., Lestavel, S., Sattler, W., and Malle, E. (2000). Role of Serum Amyloid A during Metabolism of Acute-phase HDL by Macrophages. *Arterioscler Thromb. Vasc. Biol.* 20, 763–772. doi:10.1161/01.atv.20.3.763

Baranova, I. N., Vishnyakova, T. G., Bocharov, A. V., Kurlander, R., Chen, Z., Kimelman, M. L., et al. (2005). Serum Amyloid A Binding to CLA-1 (CD36 and LIMPII Analogous-1) Mediates Serum Amyloid A Protein-Induced Activation of ERK1/2 and P38 Mitogen-Activated Protein Kinases. *J. Biol. Chem.* 280, 8031–8040. doi:10.1074/jbc.M405009200

Chen, B., Li, X. D., Liu, D. X., Wang, H., Xie, P., Liu, Z. Y., et al. (2012). Canonical Wnt Signaling Is Required for Panax Notoginseng Saponin-Mediated Attenuation of the RANKL/OPG Ratio in Bone Marrow Stromal Cells During Osteogenic Differentiation. *Phytomedicine* 19, 1029–1034. doi:10.1016/j.phymed.2012.06.002

Chen, W. H., Chen, S. B., Cheng, L. M., Gao, P., Guo, W. S., He, W., et al. (2015). Guideline for Diagnostic and Treatment of Osteonecrosis of the Femoral Head. *Orthop. Surg.* 7, 200–207. doi:10.1111/os.12193

Chen, Y., Zeng, C., Zeng, H., Zhang, R., Ye, Z., Xing, B., et al. (2015). Comparative Serum Proteome Expression of the Steroid-Induced Femoral Head Osteonecrosis in Adults. *Exp. Ther. Med.* 9, 77–83. doi:10.3892/etm.2014.2069

Cui, Q., Wang, Y., Saleh, K. J., Wang, G. J., and Balian, G. (2006). Alcohol-induced Adipogenesis in a Cloned Bone-Marrow Stem Cell. *J. Bone Jt. Surg Am* 88, 148–154. doi:10.2106/JBJS.F.00534

Dubois, E. L., and Cozen, L. (1960). Avascular (Aseptic) Bone Necrosis Associated with Systemic Lupus Erythematosus. *Jama* 174, 966–971. doi:10.1001/jama.1960.03030080028005

Frame, N. M., and Gursky, O. (2017). Structure of Serum Amyloid A Suggests a Mechanism for Selective Lipoprotein Binding and Functions: SAA as a Hub in Macromolecular Interaction Networks. *Amyloid* 24, 13–14. doi:10.1080/13506129.2016.1270930

Gabay, C., and Kushner, I. (1999). Acute-phase Proteins and Other Systemic Responses to Inflammation. *N. Engl. J. Med.* 340, 448–454. doi:10.1056/NEJM199902113400607

Gierloff, M., Petersen, L., Oberg, H. H., Quabius, E. S., Wiltfang, J., Açil, Y., et al. (2014). Adipogenic Differentiation Potential of Rat Adipose Tissue-Derived Subpopulations of Stromal Cells. *J. Plast. Reconstr. Aesthet. Surg.* 67, 1427–1435. doi:10.1016/j.bjps.2014.05.042

Han, C. Y., Kang, I., Harten, I. A., Gebe, J. A., Chan, C. K., Omer, M., et al. (2020). Adipocyte-Derived Versican and Macrophage-Derived Biglycan Control Adipose Tissue Inflammation in Obesity. *Cell Rep* 31, 107818. doi:10.1016/j.celrep.2020.107818

Heo, J. S., Lee, S. Y., and Lee, J. C. (2010). Wnt/β-catenin Signaling Enhances Osteoblastogenic Differentiation from Human Periodontal Ligament Fibroblasts. *Mol. Cell* 30, 449–454. doi:10.1007/s10059-010-0139-3

Hines, J. T., Jo, W. L., Cui, Q. J., Mont, M. A., Koo, K. H., Cheng, E. Y., et al. (2021). Osteonecrosis of the Femoral Head: An Updated Review of ARCO on Pathogenesis, Staging and Treatment. *J. Korean Med. Sci.* 36, e177. doi:10.3346/jkms.2021.36.e177

Husebekk, A., Skogen, B., Husby, G., and Marhaug, G. (2010). Transformation of Amyloid Precursor SAA to Protein AA and Incorporation in Amyloid Fibrils In Vivo. *Scand. J. Immunol.* 21, 283–287. doi:10.1111/j.1365-3083.1985.tb01431.x

Kang, S., Bennett, C. N., Gerin, I., Rapp, L. A., Hankenson, K. D., and Macdougald, O. A. (2007). WNT Signaling Stimulates Osteoblastogenesis of Mesenchymal Precursors by Suppressing c/EBPα and PPARγ. *J. Biol. Chem.* 282 (2007), 14515–14524.

Kim, S. R., Kondo, F., Otono, Y., Imoto, S., Ando, K., Hirakawa, M., et al. (2014). Serum Amyloid A and C-Reactive Protein Positive Nodule in Alcoholic Liver Cirrhosis, Hard to Make Definite Diagnosis. *Hepatol. Res.* 44, 584–590. doi:10.1111/hepr.12145

Knesek, M. J., Litinas, E., Adiguzel, C., Hopkinson, W., Hoppensteadt, D., Lassen, M., et al. (2010). Inflammatory Biomarker Profiling in Elderly Patients with Acute Hip Fracture Treated with Heparins. *Clin. Appl. Thromb. Hemost.* 16, 42–50. doi:10.1177/1076029609351876

Kushner, I. (1982). The Phenomenon of the Acute Phase Response *. *Ann. New York Acad. Sci.* 389, 39–48. doi:10.1111/j.1749-6632.1982.tb22124.x

Lee, H. J., Koh, J. M., Hwang, J. Y., Choi, K. Y., Lee, S. H., Park, E. K., et al. (2009). Association of a RUNX2 Promoter Polymorphism with Bone Mineral Density in Postmenopausal Korean Women. *Calcif Tissue Int.* 84, 439–445. doi:10.1007/s00223-009-9246-6

Li, D., Xie, P., Zhao, S., Zhao, J., Yao, Y., Zhao, Y., et al. (2021). Hepatocytes Derived Increased SAA1 Promotes Intrahepatic Platelet Aggregation and Aggravates Liver Inflammation in NAFLD. *Biochem. Biophysical Res. Commun.* 555, 54–60. doi:10.1016/j.bbrc.2021.02.124

Lloyd-Price, J., Arze, C., Ananthakrishnan, A. N., Schirmer, M., Avila-Pacheco, J., Poon, T. W., et al. (2019). Multi-omics of the Gut Microbial Ecosystem in Inflammatory Bowel Diseases. *Nature* 569, 655–662. doi:10.1038/s41586-019-1237-9

Luo, Z., Liu, M., Sun, L., and Rui, F. (2015). Icariin Recovers the Osteogenic Differentiation and Bone Formation of Bone Marrow Stromal Cells from a Rat Model of Estrogen Deficiency-Induced Osteoporosis. *Mol. Med. Rep.* 12, 382–388. doi:10.3892/mmr.2015.3369

Meek, R. L., Eriksen, N., and Benditt, E. P. (1992). Murine Serum Amyloid A3 Is a High Density Apolipoprotein and Is Secreted by Macrophages. *Proc. Natl. Acad. Sci. U S A.* 89, 7949–7952. doi:10.1073/pnas.89.17.7949

Mont, M. A., Jones, L. C., Hungerford, D. S., Jones, L. C., and Lieberman, J. R. (2006). Nontraumatic Osteonecrosis of the Femoral Head. *The J. Bone Jt. Surgery-American Volume* 88, 1117–1132. doi:10.2106/00004623-200605000-00025

Mun, S., Lee, J., Park, M., Shin, J., Lim, M. K., and Kang, H. G. (2021). Serum Biomarker Panel for the Diagnosis of Rheumatoid Arthritis. *Arthritis Res. Ther.* 23. doi:10.1186/s13075-020-02405-7

Muruganandan, S., Roman, A. A., Sinal, C. J., and Sciences, M. L. (2009). Adipocyte Differentiation of Bone Marrow-Derived Mesenchymal Stem Cells: Cross Talk with the Osteoblastogenic Program. *Cell Mol Life Sci* 66, 236–253. doi:10.1007/s00018-008-8429-z

Ni, T., Song, W. X., Luo, J., Luo, X., Jin, C., Sharff, K. A., et al. (2010). BMP-9-induced Osteogenic Differentiation of Mesenchymal Progenitors Requires Functional Canonical Wnt/β-catenin Signalling. *J. Cell Mol. Med.* 13, 2448–2464.

O'Hara, R., Murphy, E. P., Whitehead, A. S., Fitzgerald, O., and Bresnihan, B. (2010). Local Expression of the Serum Amyloid A and Formyl Peptide Receptor-like 1 Genes in Synovial Tissue Is Associated with Matrix Metalloproteinase Production in Patients with Inflammatory Arthritis. *Arthritis Rheum.* 50, 1788–1799. doi:10.1002/art.20301

Pan, S., Zhang, H., Rush, J., Eng, J., Zhang, N., Patterson, D., et al. (2005). High Throughput Proteome Screening for Biomarker Detection. *Mol. Cel Proteomics* 4, 182–190. doi:10.1074/mcp.M400161-MCP200

Peckett, A. J., Wright, D. C., and Riddell, M. C. (2011). The Effects of Glucocorticoids on Adipose Tissue Lipid Metabolism. *Metabolism* 60, 1500–1510. doi:10.1016/j.metabol.2011.06.012

Sack, G. H. (2018). Serum Amyloid A - A Review. *Mol. Med.* 24, 46. doi:10.1186/s10020-018-0047-0

Satija, N. K., Sharma, D., Afrin, F., Tripathi, R. P., and Gangenahalli, G. (2013). High Throughput Transcriptome Profiling of Lithium Stimulated Human Mesenchymal Stem Cells Reveals Priming towards Osteoblastic Lineage. *Plos One* 8, e55769. doi:10.1371/journal.pone.0055769

Song, J., Wu, J., Poulet, B., Liang, J., Bai, C., Dang, X., et al. (2021). Proteomics Analysis of Hip Articular Cartilage Identifies Differentially Expressed Proteins Associated with Osteonecrosis of the Femoral Head. *Osteoarthritis and Cartilage* 29, 1081–1092. doi:10.1016/j.joca.2021.04.005

Strnad, P., Tacke, F., Koch, A., and Trautwein, C. (2017). Liver - Guardian, Modifier and Target of Sepsis. *Nat. Rev. Gastroenterol. Hepatol.* 14, 55–66. doi:10.1038/nrgastro.2016.168

Tokuzawa, Y., Yagi, K., Yamashita, Y., Nakachi, Y., Nikaido, I., Bono, H., et al. (2010). Id4, a New Candidate Gene for Senile Osteoporosis, Acts as a Molecular Switch Promoting Osteoblast Differentiation. *Plos Genet.* 6, e1001019. doi:10.1371/journal.pgen.1001019

Uhlar, C. M., Burgess, C. J., Sharp, P. M., and Whitehead, A. S. (1994). Evolution of the Serum Amyloid A (SAA) Protein Superfamily. *Genomics* 19, 228–235. doi:10.1006/geno.1994.1052

Veenstra, T. D., Conrads, T. P., Hood, B. L., Avellino, A. M., Ellenbogen, R. G., and Morrison, R. S. (2005). Biomarkers: Mining the Biofluid Proteome. *Mol. Cel Proteomics* 4, 409–418. doi:10.1074/mcp.M500006-MCP200

Webb, N. R. (2021). High-Density Lipoproteins and Serum Amyloid A (SAA). *Curr. Atheroscler. Rep.* 23, 7. doi:10.1007/s11883-020-00901-4

Weinstein, R. S., Nicholas, R. W., and Manolagas, S. C. (2000). Apoptosis of Osteocytes in Glucocorticoid-Induced Osteonecrosis of the Hip. *J. Clin. Endocrinol. Metab.* 85, 2907–2912. doi:10.1210/jcem.85.8.6714

Yoo, J. Y., and Desiderio, S. (2003). Innate and Acquired Immunity Intersect in a Global View of the Acute-phase Response. *Proc. Natl. Acad. Sci. U S A.* 100, 1157–1162. doi:10.1073/pnas.0336385100

Yoon, B. H., Mont, M. A., Koo, K. H., Chen, C. H., Cheng, E. Y., Cui, Q., et al. (2020). The 2019 Revised Version of Association Research Circulation Osseous Staging System of Osteonecrosis of the Femoral Head. *J. Arthroplasty* 35, 933–940. doi:10.1016/j.arth.2019.11.029

Zapico Muñiz, E., Mora Brugés, J., and Blanco Vaca, F. (2005). Early Cancer Diagnosis through Proteomics of Serum: Fiction or Fact. *Med. Clin.* 124, 181–185. doi:10.1157/13071481

Zeng, P., Chen, J., Li, J., Qin, G., He, K., Du, M., et al. (2019). A Study on Differential Proteomics in Traumatic Osteonecrosis of the Femoral Head. *Orthop. J. China* 27, 453–458. doi:10.3977/j.issn.1005-8478.2019.05.15

Zerega, B., Pagano, A., Pianezzi, A., Ulivi, V., Camardella, L., Cancedda, R., et al. (2004). Expression of Serum Amyloid A in Chondrocytes and Myoblasts Differentiation and Inflammation: Possible Role in Cholesterol Homeostasis. *Matrix Biol.* 23, 35–46. doi:10.1016/j.matbio.2004.02.002

Conflict of Interest: The authors declare that the research was conducted in the absence of any commercial or financial relationships that could be construed as a potential conflict of interest.

Publisher's Note: All claims expressed in this article are solely those of the authors and do not necessarily represent those of their affiliated organizations, or those of the publisher, the editors and the reviewers. Any product that may be evaluated in this article, or claim that may be made by its manufacturer, is not guaranteed or endorsed by the publisher.

Copyright © 2021 Peng, Ma, Wang, Gao, Li, Jiang, Gao and Feng. This is an open-access article distributed under the terms of the Creative Commons Attribution License (CC BY). The use, distribution or reproduction in other forums is permitted, provided the original author(s) and the copyright owner(s) are credited and that the original publication in this journal is cited, in accordance with accepted academic practice. No use, distribution or reproduction is permitted which does not comply with these terms.

frontiers in Pharmacology

REVIEW
published: 29 October 2021
doi: 10.3389/fphar.2021.773660

Research Progress of the Role of Anthocyanins on Bone Regeneration

Wei Mao[1,2], Guowei Huang[1], Huan Chen[1], Liangliang Xu[3], Shengnan Qin[1]* and Aiguo Li[1]**

[1]Department of Orthopedics, Guangzhou Institute of Traumatic Surgery, Guangzhou Red Cross Hospital, Medical College, Jinan University, Guangzhou, China, [2]Department of Clinical Medicine, Guizhou Medical University, Guiyang, China, [3]Lingnan Medical Research Center, The First Affiliated Hospital of Guangzhou University of Chinese Medicine, Guangzhou University of Chinese Medicine, Guangzhou, China*

Bone regeneration in osteoporosis and fragility fractures which are highly associated with age remains a great challenge in the orthopedic field, even though the bone is subjected to a continuous process of remodeling which persists throughout lifelong. Regulation of osteoblast and osteoclast differentiation is recognized as effective therapeutic targets to accelerate bone regeneration in osteopenic conditions. Anthocyanins (ACNs), a class of naturally occurring compounds obtained from colored plants, have received increasing attention recently because of their well-documented biological effects, such as antioxidant, anti-inflammation, and anti-apoptosis in chronic diseases, like osteoporosis. Here, we summarized the detailed research progress on ACNs on bone regeneration and their molecular mechanisms on promoting osteoblast differentiation as well as inhibiting osteoclast formation and differentiation to explore their promising therapeutic application in repressing bone loss and helping fragility fracture healing. Better understanding the role and mechanisms of ACNs on bone regeneration is helpful for the prevention or treatment of osteoporosis and also for the exploration of new bone regenerative medicine.

Keywords: anthocyanins, fracture, bone regeneration, osteogenesis, osteoclastogenesis

OPEN ACCESS

Edited by:
Daohua Xu,
Guangdong Medical University, China

Reviewed by:
Longhuo Wu,
Gannan Medical University, China
Long Zhang,
Xi'an Jiaotong University, China

****Correspondence:***
Aiguo Li
liaiguo7161@163.com
Shengnan Qin
qinqinsn@163.com
Liangliang Xu
xull-2016@gzucm.edu.cn

Specialty section:
This article was submitted to Integrative and Regenerative Pharmacology, a section of the journal Frontiers in Pharmacology

Received: *13 September 2021*
Accepted: *14 October 2021*
Published: *29 October 2021*

Citation:
Mao W, Huang G, Chen H, Xu L, Qin S and Li A (2021) Research Progress of the Role of Anthocyanins on Bone Regeneration. Front. Pharmacol. 12:773660. doi: 10.3389/fphar.2021.773660

INTRODUCTION

Osteoporosis is a condition that bones become weak and brittle, so brittle that a fall or a cough can cause a fracture which is often called fragility fracture. Fragility fractures commonly occur in the hip, wrist, or spine, and hip fracture is associated with significant mortality and morbidity. Osteoporosis is closely related to aging. According to the first report on the prevalence of osteoporosis in China issued by the National Health Commission in 2018, 32% of people aged over 65 suffer from osteoporosis. More seriously, 46.4% of individuals aged over 50 were in the condition of low bone mass, suggesting they were at a high risk of becoming osteoporosis (Wang et al., 2021).

The process of bone maintenance is regulated by bone-forming osteoblasts and bone-resorbing osteoclasts. Bone is highlighted by its unique ability to regenerate throughout adulthood, restoring to a fully functional, pre-injury state (Salhotra et al., 2020). For osteoporosis and fragility fractures, the dysregulation of bone biology in the setting of bone repair is "lack of bone". The excessive bone resorption guided by osteoclasts and/or the impaired capability of bone formation regulated by osteoblasts attributes the bone loss.

Recently, an emphasis has been placed on the relationship between diet and disease, and pieces of evidence have also emerged from clinical trials demonstrating that a dietary pattern, rich in anthocyanins (ACNs), is related to the reduced risk for chronic diseases, such as cancers,

TABLE1 | Therapies to promote bone regeneration.

Treatment strategies	Treatments	Treatment principle	Advantages	Disadvantages
Bone transplantation	Autogenous bone transplantation Fillingham and Jacobs (2016)	The transfer of cancellous or cortical bone from one part of the body to another	1. Abundant living cells	1. Less available bone source
			2. Low Immunogenicity	2. Poor osteogenesis of donor tissue leads to failure
			3. Low risk of virus transmission	—
			4. Success rate of 80–90%	—
	Allograft bone transplantation Gómez-Barrena et al. (2015)	Obtained from another person	Suitable substitute for autogenous bone	Prolonged operation time and pain
Stem cell therapy	Bone mesenchymal stem cells (BMSCs) Casati et al. (2019)	Interact with a variety of growth factors to promote differentiation of osteoblasts	Wide application	1. Low accessibility 2. Lack of standardized isolation 3. Poor long-term stability
	HUC-MSCs (L et al., 2019)	Indirectly promotes bone formation by promoting angiogenesis	1. Wide sources 2. Low risk of infection 3. Less immunogenicity	Low application in bone regeneration
	PCs Casati et al. (2019)	Periosteum-derived cells (PDCs) were implanted into the defect using scaffolds	1. Strong bone regeneration ability	1. Bionics research is still in its infancy
			2. Be widely used in the treatment of bone nonunion	2. Material selection need to be improved
Drug treatments	rhBMP Nishimura et al. (2008)	1. Promote the differentiation of MSCs into osteogenic and chondrogenic lineages	3. Promote bone regeneration and accelerate healing	1. Expensive treatment
		2. Promote chondrocyte hypertrophy differentiation		2. The spread of rhBMP can lead to ectopic bone formation
		3. Promote callus remodeling		3. Natural bone resorption
		—		4. Soft tissue swelling
		—		5. Dissolve the bone
	PTH James et al. (2016)	1. Promote proliferation	1. Reduce the risk of fractures	High dose injection of PTH induce catabolic reaction leads to fracture healing and repairing
		2. Delay chondrocyte hypertrophy	2. Promote callus formation	
		—	3. Reduce healing time	
Physical adjuvant therapy Padilla et al., (2016), Bhavsar et al., (2020)	Low intensity pulsed ultrasound	Accelerate the repair of fracture injury through external stimulation	Promote angiogenesis and remodeling in callus	Poor healing results in many cases

obesity, diabetes, and cardiovascular disease (Khoo and Azlan, 2017; D'cunha et al., 2018). ACNs are a class of naturally occurring compounds and show their positive influences on health owing to their antioxidant, anti-inflammatory, and anti-apoptotic potential in various chronic diseases, especially age-related diseases (Aqil et al., 2012; Huang et al., 2018; Speer et al., 2020). Increasing evidence from experimental, and clinical studies showed the consumption of ACNs rich foods played a role in protecting bone loss and helping the healing of fractures (Hardcastle et al., 2011; Mcnaughton et al., 2011).

CLINICAL THERAPIES OF PROMOTING BONE REGENERATION

Clinical strategies used in promoting bone regeneration mainly include bone transplantation, stem cell therapy, physical adjuvant therapy, and local injection of growth factors. These approaches and their current advantages and disadvantages are summarized in **Table1**.

Autogenous, allograft, and bone grafted substitutes are widely used in the treatment of posttraumatic conditions such as fracture, delayed union, and nonunion (Baldwin et al., 2019). Available in abundant living cells and various growth factors that facilitate the osteogenic differentiation of stem/progenitor cells, the autogenous bone graft is regarded as the gold standard (Gómez-Barrena et al., 2015; Baldwin et al., 2019). Nevertheless, problems like the limited quantity of bone available for harvest make autograft a less-than-ideal option for individuals with osteoporosis (Fillingham and Jacobs, 2016). Allograft and bone graft substitutes provide viable alternatives due to their convenience, abundance, and lack of procurement-related patient morbidity (Baldwin et al., 2019).

Stem cells, including bone mesenchymal stem cells (BMSCs), Human umbilical cord mesenchymal stem cells (HUC-MSCs), and periosteal cells (PCs), owing to their multipotency, anti-inflammatory, and immune-modulatory properties, have been applied in bone repair. BMSCs are the most commonly used stem cells in the field of bone regeneration (L et al., 2019). Endogenous BMSC activation or exogenous BMSCs are utilized for the repair of long bone and vertebrae fractures due to osteoporosis or trauma (Gómez-Barrena et al., 2019). HUC-MSCs Indirectly increased bone formation by promoting angiogenesis, but it is relatively rare for their use on bone regeneration (Li et al., 2016).

TABLE 2 | The basic information of six major anthocyanins.

Anthocyanin	Formula	CAS number	Sources	Biological effects	Molecular structure
Delphinidin	$C_{15}H_{11}ClO_7$	528-53-0	Berries and red wine	Antioxidant; Anti-inflammatory	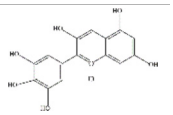
Petunidin	C16H13O7	1,429-30-7	Purple potato and black goji	Antioxidant	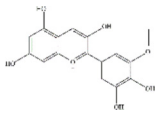
Malvidin	$C_{17}H_{15}ClO_7$	643-84-5	Blueberries	Apoptosis-inducing; Antioxidant; Anti-tumorogenesis	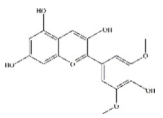
Cyanidin	C15H11O6	13,306-05-3	Cherries	Antioxidant; Anti-angiogenic; Antiviral	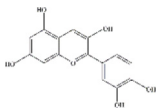
Peonidin	C16H13O6	134-01-0	Berries	Antioxidant; Apoptosis-inducing	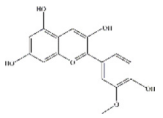
Pelargonidin	C15H11O5	7,690-51-9	Stawberries	Antioxidant	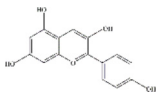

PCs were widely used in the treatment of bone nonunion and especially used as a source of cells for tissue engineering of bone or cartilage (Li et al., 2016; Duchamp De Lageneste et al., 2018). For stem cell therapy, scaffolds or biomaterials are normally needed to improve their efficacy and stability.

Recombinant human bone morphogenetic protein (rhBMP) is the only osteoinductive growth factor as a bone graft substitute applied in the clinical setting (James et al., 2016). BMP-2 could improve the impaired fusion capacity for some patients, thereby decreasing the prevalence of repeated surgical re-entry, trauma, complications, and additional medical cost (Cahill et al., 2011). However, considering that the delivery of rhBMP often exceeds the physiological dose, this not only leads to the high cost of treatment, but also results in the spread of rhBMP that can lead to adverse effects such as heterotopic bone formation, natural bone resorption, soft tissue swelling, and bone lysis (James et al., 2016). Parathyroid hormone (PTH) provides anabolic therapy for osteoporosis clinically as it has been documented to increase bone mineral density and to reduce the rate of fractures in patients with osteoporosis and also improve fragility fracture-healing (Goltzman, 2018). Systemic injections of parathyroid hormone (PTH) also promoted the proliferation of chondrocytes and osteoblasts (Peichl et al., 2011). However, continuous high-dose injection of PTH could induce a catabolic reaction, which is not conducive to fracture healing and repair (Wojda and Donahue, 2018). In addition, consideration must be given to the instability and variability of growth factors after being injected.

Electrical stimulation (EStim) has been proven to promote bone healing in experimental settings and has been used clinically for many years. Low intensity pulsed ultrasound is the most widespread and studied technique which could accelerate fracture repair in some cases. However, it has not become a mainstream clinical treatment due to the great variation in methods reported, and the inconsistent results associated with this treatment approach (Padilla et al., 2016; Bhavsar et al., 2020).

By now, clinical treatment options for bone regeneration are relatively limited, so it is necessary to develop and improve drugs that are more effective, more economic, and have fewer side effects.

ANTHOCYANINS AND THEIR BIOLOGICAL EFFECTS ON CHRONIC DISEASES

ACNs are a class of water-soluble natural pigments that are prominent in colored plants and belong to flavonoid compounds. More than 635 ACNs have been identified based on the number and location of hydroxyl and methoxy groups (Wu and Prior, 2005; Mulabagal and Calderón, 2012; Sehitoglu et al., 2014; Wallace and Giusti, 2015; Smeriglio et al., 2016; Cerletti et al., 2017; Khoo and Azlan, 2017; Li et al., 2017). Different ACNs may exhibit different bioactive chemical

TABLE 3 | The roles of anthocyanin in bone regeneration.

Anthocyanin	Functions	*In vitro*	*In vivo*	
—	—	—	Animal model	Micro-CT
Delphinidin	1. Stimulate bone formation	1. BMP2, Runx2, Osx, OCN ↑	OVX rat	1. BV/TV↑ 2. Tb.Th↑ 3. Tb.N↑
	—	—		
	2. Inhibit bone resorption	2. NF-κB, c-Fos, NFATc1↓ MMP9, CTSK, DC-stamp↓		4. Tb.Sp↓ 5. ES/BS↓
	—	—		6. N.Oc/BS↓
Delphinidin-3-rutinoside	Enhance osteoblast proliferation	CoL1, OCN, ALP↑	—	—
Petunidin	1. Suppress bone resorption	1. >5 μg/ml c-Fos, NFATc1↓ MMP9, CTSK, DC-stamp↓	Osteopenic mouse model	1. BV/TV↑ 2. Tb.Th↑ 3. Tb.N↑
	—	—		4. Tb.Sp↓
	2. Accelerate osteogenesis	2. >16 μg/ml BMP2, OCN↑		5. Oc.S/BS —
Malvidin	Stimulate bone formation	BMP2, Runx2↑	—	—
			—	—
Cyanidin Chloride	Protect against bone loss	1. NF-κB↓ 2. IκB-α↑ 3. ERK↓ 4. NFATc1, c-Fos↑	OVX-induced osteoporosis mouse model	1. BV/TV↑ 2. OcS/BS↑ 3. N.Oc/BS↑ —
Cyanidin-3-glucoside	1. Enhance osteoblast proliferation	1. OCN, ALP, Runx2↑	—	—
		—		
	2. Inhibit bone resorption	2. c-Fos, NFATc1↓ CTSK, OSCAR, Tm7sf4, Atp6v0d↓		

structures due to their specificity. They are derived from the flesh, skin, roots of many colored fruits and vegetables. Anthocyanins, particularly glucosides and galactosides of cyanidin, peonidin, delphinidin, petunidin, Pelargonidin, and malvidin are responsible for the final color of the berries (Millar et al., 2017), and the information of these six major ACNs is summarized in **Table 2**.

ACNs are well documented for their antioxidant, anti-inflammatory, and anti-apoptotic effects on human health (Henriques et al., 2020; Kozłowska and Dzierżanowski, 2021; Liu et al., 2021; Pérez-Torres et al., 2021; Vega-Galvez et al., 2021). ACNs could be rapidly absorbed in the stomach and detected in the blood and urine (Fang, 2014; Tian et al., 2019), so these pigments are recognized as one of the leading nutraceuticals for prolonging health benefits through the attenuation of chronic, non-communicable diseases, including cancers, obesity, diabetes, cardiovascular diseases, and neurodegenerative diseases.

ACNs have the potential anti-tumor effects for their anti-carcinogenic activities in the initial stage of tumorigenesis, the cancer formation stage, and the cancer development stage (Lin et al., 2017). Delphinidin strongly inhibited cell transformation and migration during tumorigenesis of various cancers (Yun et al., 2009; Ozbay and Nahta, 2011), and it significantly inhibited proliferation and induced apoptosis in osteosarcoma (OS) cell lines (Kang et al., 2018). In addition, delphinidin also showed its promise as a potential chemotherapeutic agent by blocking the development and progression of tumors by inducing apoptotic cell death of osteosarcoma cells (Lee et al., 2018).

ACNs also showed their biological effects on anti-inflammation and anti-oxidative stress (Lee et al., 2017; Samarpita et al., 2020; Tsuda et al., 2000; Choi et al., 2010; Jakesevic et al., 2011; Mane et al., 2011; Kim et al., 2013; Fintini et al., 2020; Casati et al., 2019). With the increase of age, low-grade inflammation and the production of reactive oxygen species (ROS) increased which were involved in the imbalance of bone homeostasis (Domazetovic et al., 2017). Cyanidin could be used for rheumatoid arthritis (RA) treatment as Interleukin 17A/IL-17 receptor A (IL-17/17RA) signaling targeted therapy and could alleviate clinical symptoms, synovial growth, immune cell infiltration, and bone erosion in adjuvant-induced arthritis (AA) rats (Samarpita et al., 2020; Samarpita and Rasool, 2021). Anthocyanins could reduce oxidative stress *in vivo* and *in vitro* (Ali et al., 2018; Ullah et al., 2019; Chen et al., 2020). Delphinidin repressed pathological cardiac hypertrophy by modulating oxidative stress through the AMPK/NADPH oxidase (NOX)/mitogen-activated protein kinase (MAPK) signaling pathway (Chen et al., 2020). The significant increase in the intracellular ROS levels induced by tert-butyl hydroperoxide was prevented by Delphinidin-3-rutinoside treatment (Casati et al., 2019).

However, there are controversial reports of the role of delphinidin on apoptosis. Delphinidin enhanced β2m-/Thy1+ bone marrow-derived hepatocyte stem cells (BDHSCs) survival by inhibiting transforming growth factor-β1 (TGF-β1)-induced apoptosis via PI3K/AKT signaling pathway (Chen et al., 2019), but it induced apoptosis of human osteosarcoma cells with compromising the cellular protective mechanisms (Lee et al., 2018). Therefore, the role of ACNs on apoptosis needs to be

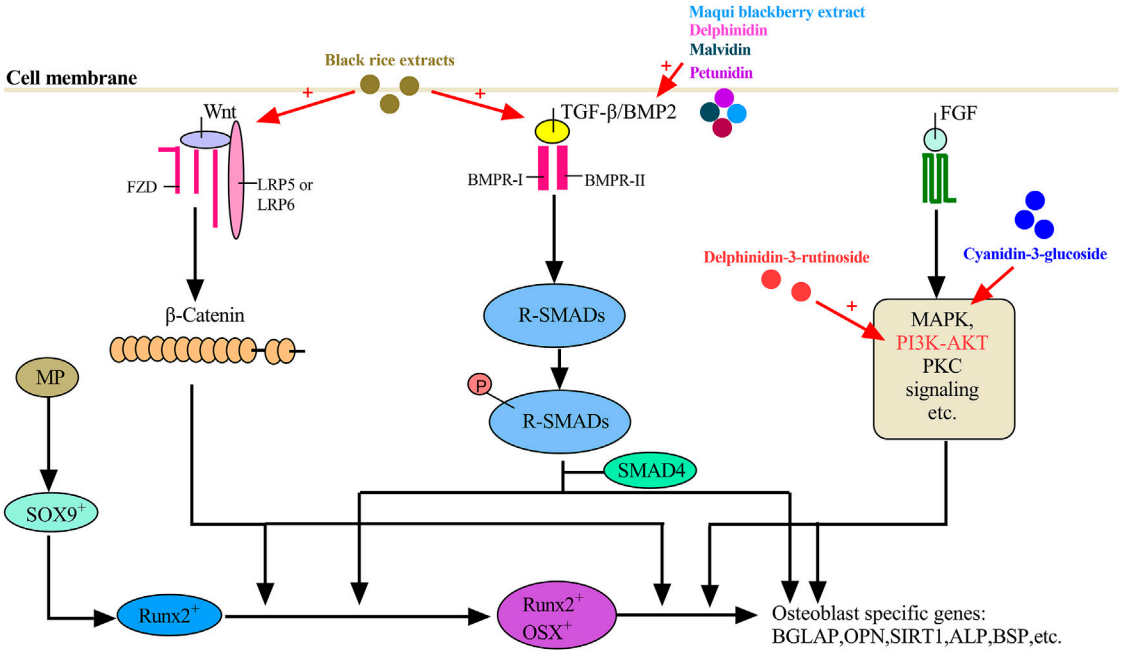

FIGURE 1 | A proposed working model for the promotion of anthocyanins on osteogenesis.

explored in the future to better understand the effects of ACNs on apoptosis.

ROLE OF ANTHOCYANINS ON BONE REGENERATION

Increasing evidence has demonstrated the beneficial role of ACNs on bone health (Zheng et al., 2016; Melough et al., 2017; Shimizu et al., 2018; Speer et al., 2020). Many ACNs could promote the differentiation of mesenchymal stem cells into osteoblasts and/or inhibit osteoclastogenesis (Park et al., 2015; Dou et al., 2016; Sakaki et al., 2018; Nagaoka et al., 2019a; Nagaoka et al., 2019b; Casati et al., 2019; Saulite et al., 2019; Domazetovic et al., 2020; Hu et al., 2021; Imangali et al., 2021; Karunarathne et al., 2021). In this review, the effects of different ACNs on bone regeneration were described in detail respectively as below and summarized in **Table 3**.

The molecular mechanisms of ACNs underline bone regeneration have also been explored. For osteogenesis, as shown in **Figure 1**, there are three major pathways involved, including the BMP2 pathway, WNT-β catenin pathway, and FGF pathway. The pathways involved in the differentiation of the osteoblast lineage normally function in a coordinated manner. For example, BMP2 promotes osteoblast differentiation by targeting Runx2 downstream (Salhotra et al., 2020). As shown in **Figure 1**, the role of Delphinidin-3-rutinoside and Cyanidin-3-glucoside on osteoblast differentiation is mainly by activating the fibroblast growth factor (FGF) pathway, while the mechanisms of other ACNs, including delphinidin, malvidin, and petunidin as well as black rice extracts and maqui blackberry extracts, which also accelerating osteogenesis *in vitro*, are not yet explored. The transcription factors Sox9, Runx2, and Osterix (Osx) are three major components that commit stem/progenitor cells to osteoprogenitor cells, and most of ACNs which could promote osteogenesis upregulated the gene expressions of these transcription factors, at least one of them, as well as osteoblastic markers, such as type 1 collagen (Col1), osteopontin (OPN), osteocalcin (OCN), and alkaline phosphatase (ALP).

The mechanisms of most ACNs on osteoclast differentiation were investigated. For osteoclastogenesis, as shown in **Figure 2**, the c-Fos pathway, NF-κB pathway, JNK pathway, Ca^{2+} pathway, and ROS pathway are four major pathways in osteoclastogenesis. These pathways also interact with each other to be functional. Three subfamilies (P38, ERK1/2, and JNK) of mitogen-activated protein kinases (MAPKs) also play an important role in RANK signal-mediated osteoclast generation (Zhai et al., 2014). The nuclear factor of activated T-cells 1(NFATc1) is a major transcription factor and a key target gene of most of the pathways that regulate osteoclastic differentiation. As shown in **Figure 2**, the regulation of ACNs which suppressed osteoclast formation and differentiation is through more than one of these pathways. For example, CC could regulate osteoclastogenesis by repressing the expression of ERK1/2, IKBα, and NFATc1, indicating it is involved in several key pathways. Furthermore, most of ACNs downregulated the expression of NFATc1, indicating that they might be involved in several pathways. Most of ACNs that inhibit osteoclastogenesis downregulated the gene expressions of osteoclast specific markers such as Tartrate-resistance acid phosphatase (TRAP), cathepsin K (CTSK), matrix metalloproteinase (MMP9), and dendritic cell-specific transmembrane proteins (DC-stamp). These substances can enhance the bone resorption activity of osteoclasts, decompose bone matrix proteins and inhibit matrix mineralization.

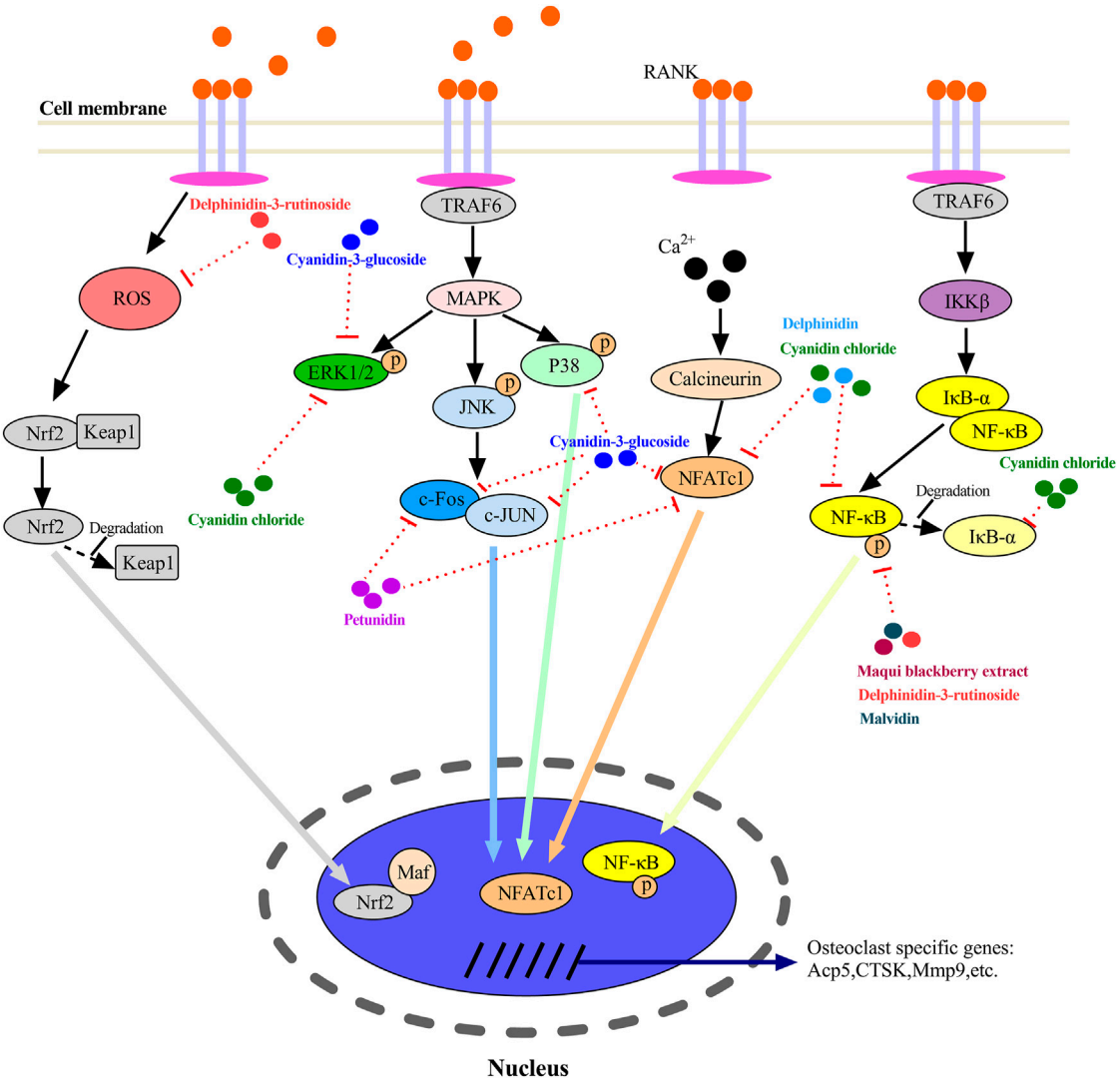

FIGURE 2 | A proposed working model for the inhibition of anthocyanins on osteoclastogenesis.

Delphinidin

Delphinidin [2-(3,4,5-trihydroxyphenyl) chromenylium-3,5,7-triol], a flavonoid compound rich in berries, represents its role in the protection against bone loss by regulating osteoblasts and osteoclasts (Moriwaki et al., 2014; Nagaoka et al., 2019a; Nagaoka et al., 2019b; Imangali et al., 2021). Maqui blackberry extract (MBE), rich in delphinidin, prevented bone loss in osteopenic conditions by not only inhibiting bone resorption by suppressing the NF-κB pathway but also promoting bone formation by enhancing mineralized nodule formation and upregulating osteoblastic genes including BMP-2, Runx2, Osx, and OCN (Nagaoka et al., 2019a) (**Figure 1**). Osx is another transcript factor and triggers differentiation of immature osteoblasts to mature osteoblasts and eventually into osteocytes (Sinha and Zhou, 2013). Delphinidin could markedly inhibit the osteoclastic differentiation and prevented bone loss in both RANKL-induced osteoporosis model mice and OVX model mice by suppressing the activities of NF-κB, c-Fos, and NFATc1 (Moriwaki et al., 2014).

Delphinidin-3-rutinoside (D3R) is a simpler delphinidin derivative than nasunin (Azuma et al., 2008). D3R protected mouse embryo osteoblast precursor cells (MC3T3-E1) from oxidative damage, and promoted the osteoblastic differentiation of MC3T3-E1 by the PI3K/AKT pathway and increased Col1α1, ALP, and OCN gene expressions after D3R treatment (**Figure 1**), suggesting the potential utility of dietary D3R supplement to prevent osteoblast dysfunction in age-related osteoporosis (Casati et al., 2019). D3R also exerted their anti-inflammatory effects in LPS-induced osteoclastogenesis partly by inhibiting nuclear translocation of NF-κB (**Figure 2**), indicating its potential in suppressing bone resorption (Lee et al., 2014).

Petunidin

Petunidin, a B-ring 5'-O-methylated derivative of delphinidin, also showed its protection against bone loss and multi-faced function on bone cells. Daily oral administration of petunidin (7.5 mg/kg/day) could prevent bone mass loss in RANKL-induced osteopenic mice *in vivo* (Nagaoka et al., 2019b). *In vitro*, petunidin (>5 μg/ml) significantly suppressed osteoclastic differentiation by downregulating c-Fos, NFATc1, MMP9, CTSK, and DC-stamp mRNA expression in pre-osteoclasts (Nagaoka et al., 2019b) (**Figure 2**). Conversely, petunidin (>16 μg/ml) stimulated mineralized matrix formation and gene expression of BMP2 and OCN, specific osteoblastic markers, of pre-osteoblasts (Nagaoka et al., 2019b) (**Figure 1**).

Malvidin

Malvidin is one of the primary plant pigments mainly existing in fruit skins and abundant in blueberries. Blueberries, consist of malvidin (16%), exerted their anti-inflammatory effects in macrophages by inhibiting nuclear translocation of NF-κB (Lee et al., 2014). Reports on the role of malvidin on bone regeneration are rare by now, but it still showed promising application in promoting bone formation. Malvidin induced a significantly higher accumulation of calcium deposits in MSCs comparing to untreated MSCs, as well as upregulated the osteocyte-specific gene BMP-2 and Runx-2 expression and induced BMP-2 secretion (Saulite et al., 2019) (**Figure 1**).

Cyanidin

Cyanidin is an anthocyanin widely distributed in cherries. Cyanidin Chloride (CC) and Cyanidin-3-glucoside (C3G) are two cyanidins that are able to regulate bone homeostasis.

Kinds of literatures on the role of CC in regulating osteoclastogenesis are controversial. Cheng et al. (2018) found that CC inhibited osteoclast formation, hydroxyapatite resorption, and RANKL-induced signal pathways *in vitro* and protected against OVX-induced bone loss *in vivo*, indicating its therapeutic potential for osteolytic diseases. CC inhibited RANKL-induced NF-κB activation, suppresses the degradation of IκB-α, and attenuates the phosphorylation of extracellular signal-regulated kinases (ERK). In addition, CC abrogated RANKL-induced calcium oscillations, the activation of nuclear factor of activated T cells calcineurin-dependent 1 (NFATc1), and the expression of c-Fos (**Figure 2**). However, Dou et al. (2016) suggested that CC had a dual role in the differentiation of osteoclasts. Only a high dosage of cyanidin (>10 μg/ml) suppressed osteoclastogenesis and osteoclast fusion whereas a low dosage (<1 μg/ml) showed an opposite impact.

C3G has also played a role in bone regeneration by regulating osteoblast and osteoclast differentiation. C3G could improve the proliferation of osteoblasts, and upregulate the expression of osteogenic genes, including OCN, ALP, and Runx2 (Park et al., 2015; Kim et al., 2019; Hu et al., 2021). C3G mainly activated the ERK1/2 pathway to regulate the expression of OCN, enhancing the maturation of osteoblasts and promoting bone nodule formation (Cheng et al., 2018) (**Figure 1**). C3G has also shown promise in inhibiting bone resorption by regulating osteoclastic differentiation. C3G-rich blackberries treatment at the level of 5% (w/w) may modestly reduce OVX-induced bone loss evident by improved tibial, vertebral, and femoral BMD values, and tibial bone microstructural parameters (Kaume et al., 2015). C3G significantly reduced the expression of osteoclastic differentiation markers including CTSK, Osteoclast-associated receptor (OSCAR), transmembrane 7 superfamily member (Tm7sf4) and ATPase, H+ transporting, lysosomal 38kda, V0 subunit d2 (Atp6v0d2), and significantly inhibited the nuclear translocation of c-Fos and NFATc1 (Park et al., 2015) (**Figure 2**). Furthermore, C3G considerably reduced the induction of extracellular signal-regulated kinase, c-Jun N-terminal kinase, and p38 mitogen-activated kinases activation, which were major pathways regulated by RANKL in osteoclast precursor cells (**Figure 2**). In the process of osteoclast formation induced by RANKL, NF-κB and ERK/MAPK were activated by RANKL, while C3G attenuated the induction of RANKL in cultured cells *in vitro*, suggesting that C3G could inhibit the generation of osteoclasts (Aqil et al., 2012) (**Figure 2**).

CONCLUSION

In recent years, increasing studies have shown that anthocyanins display their beneficial role on bone formation, including upregulating the osteoblastic genes, promoting the proliferation of osteoblasts and enhancing the mineral nodule formation. Also, they play an important role in inhibiting osteoclastogenesis, able to protect against bone mass loss in osteopenic conditions. Nevertheless, reports of these pigments as therapeutic applications on bone homeostasis, especially on fracture healing, are limited and role of these pigments on bone homeostasis need to be further explored.

PERSPECTIVE OF ANTHOCYANINS

As a class of natural compounds, ACNs are rich in dietary sources, and their use in the prevention and treatment of adverse health events deserves attention. ACNs are a safe and inexpensive way to prevent diseases with minimal side effects. In the light of the molecular mechanisms, it is possible to find new targets for treating bone-related diseases such as fragility fractures in the future, and provide a new perspective for therapies. Most studies have been conducted *in vitro* or in animal models, while ACNs have rarely been studied in humans. In the future randomized controlled trials are needed to determine the role and mechanism of ACNs in human bone health. Further studies on the preventive dose of ACNs for bone health should standardize the amount of anthocyanin-rich fruits and vegetables consumed by humans. In addition, in order to better apply anthocyanin in orthopedic clinics, it is necessary to further study the role of anthocyanin in bone health, including dose, administration mode, toxicity, and side effects, etc. More importantly, Random Clinical Trial is needed to establish the role and mechanism of anthocyanin.

AUTHOR CONTRIBUTIONS

WM, GH, and HC write the manuscript; LX, SQ, and AL revised the manuscript.

REFERENCES

Ali, T., Kim, T., Rehman, S. U., Khan, M. S., Amin, F. U., Khan, M., et al. (2018). Natural Dietary Supplementation of Anthocyanins via PI3K/Akt/Nrf2/HO-1 Pathways Mitigate Oxidative Stress, Neurodegeneration, and Memory Impairment in a Mouse Model of Alzheimer's Disease. *Mol. Neurobiol.* 55, 6076–6093. doi:10.1007/s12035-017-0798-6

Aqil, F., Gupta, A., Munagala, R., Jeyabalan, J., Kausar, H., Sharma, R. J., et al. (2012). Antioxidant and Antiproliferative Activities of Anthocyanin/ellagitannin-Enriched Extracts from Syzygium Cumini L. (Jamun, the Indian Blackberry). *Nutr. Cancer* 64, 428–438. doi:10.1080/01635581.2012.657766

Azuma, K., Ohyama, A., Ippoushi, K., Ichiyanagi, T., Takeuchi, A., Saito, T., et al. (2008). Structures and Antioxidant Activity of Anthocyanins in many Accessions of Eggplant and its Related Species. *J. Agric. Food Chem.* 56, 10154–10159. doi:10.1021/jf801322m

Baldwin, P., Li, D. J., Auston, D. A., Mir, H. S., Yoon, R. S., and Koval, K. J. (2019). Autograft, Allograft, and Bone Graft Substitutes: Clinical Evidence and Indications for Use in the Setting of Orthopaedic Trauma Surgery. *J. Orthop. Trauma* 33, 203–213. doi:10.1097/BOT.0000000000001420

Bhavsar, M. B., Han, Z., Decoster, T., Leppik, L., Costa Oliveira, K. M., and Barker, J. H. (2020). Electrical Stimulation-Based Bone Fracture Treatment, if it Works So Well Why Do Not More Surgeons Use it?. *Eur. J. Trauma Emerg. Surg.* 46, 245–264. doi:10.1007/s00068-019-01127-z

Cahill, K. S., Chi, J. H., Groff, M. W., Mcguire, K., Afendulis, C. C., and Claus, E. B. (2011). Outcomes for Single-Level Lumbar Fusion: the Role of Bone Morphogenetic Protein. *Spine (Phila Pa 1976)* 36, 2354–2362. doi:10.1097/BRS.0b013e31820bc9e5

Casati, L., Pagani, F., Fibiani, M., Lo Scalzo, R., and Sibilia, V. (2019). Potential of Delphinidin-3-Rutinoside Extracted from Solanum Melongena L. As Promoter of Osteoblastic MC3T3-E1 Function and Antagonist of Oxidative Damage. *Eur. J. Nutr.* 58, 1019–1032. doi:10.1007/s00394-018-1618-0

Cerletti, C., De Curtis, A., Bracone, F., Digesù, C., Morganti, A. G., Iacoviello, L., et al. (2017). Dietary Anthocyanins and Health: Data from FLORA and ATHENA EU Projects. *Br. J. Clin. Pharmacol.* 83, 103–106. doi:10.1111/bcp.12943

Chen, J., Li, H. Y., Wang, D., and Guo, X. Z. (2019). Delphinidin Protects β2m-/Thy1+ Bone Marrow-Derived Hepatocyte Stem Cells against TGF-B1-Induced Oxidative Stress and Apoptosis through the PI3K/Akt Pathway *In Vitro*. *Chem. Biol. Interact* 297, 109–118. doi:10.1016/j.cbi.2018.10.019

Chen, Y., Ge, Z., Huang, S., Zhou, L., Zhai, C., Chen, Y., et al. (2020). Delphinidin Attenuates Pathological Cardiac Hypertrophy via the AMPK/NOX/MAPK Signaling Pathway. *Aging (Albany NY)* 12, 5362–5383. doi:10.18632/aging.102956

Cheng, J., Zhou, L., Liu, Q., Tickner, J., Tan, Z., Li, X., et al. (2018). Cyanidin Chloride Inhibits Ovariectomy-Induced Osteoporosis by Suppressing RANKL-Mediated Osteoclastogenesis and Associated Signaling Pathways. *J. Cel Physiol* 233, 2502–2512. doi:10.1002/jcp.26126

Choi, M. J., Kim, B. K., Park, K. Y., Yokozawa, T., Song, Y. O., and Cho, E. J. (2010). Anti-aging Effects of Cyanidin under a Stress-Induced Premature Senescence Cellular System. *Biol. Pharm. Bull.* 33, 421–426. doi:10.1248/bpb.33.421

D'cunha, N. M., Georgousopoulou, E. N., Dadigamuwage, L., Kellett, J., Panagiotakos, D. B., Thomas, J., et al. (2018). Effect of Long-Term Nutraceutical and Dietary Supplement Use on Cognition in the Elderly: a 10-year Systematic Review of Randomised Controlled Trials. *Br. J. Nutr.* 119, 280–298. doi:10.1017/S0007114517003452

Domazetovic, V., Marcucci, G., Falsetti, I., Bilia, A. R., Vincenzini, M. T., Brandi, M. L., et al. (2020). Blueberry Juice Antioxidants Protect Osteogenic Activity against Oxidative Stress and Improve Long-Term Activation of the Mineralization Process in Human Osteoblast-like SaOS-2 Cells: Involvement of SIRT1. *Antioxidants (Basel)* 9, 125, doi:10.3390/antiox9020125

Domazetovic, V., Marcucci, G., Iantomasi, T., Brandi, M. L., and Vincenzini, M. T. (2017). Oxidative Stress in Bone Remodeling: Role of Antioxidants. *Clin. Cases Miner Bone Metab.* 14, 209–216. doi:10.11138/ccmbm/2017.14.1.209

Dou, C., Li, J., Kang, F., Cao, Z., Yang, X., Jiang, H., et al. (2016). Dual Effect of Cyanidin on RANKL-Induced Differentiation and Fusion of Osteoclasts. *J. Cel Physiol* 231, 558–567. doi:10.1002/jcp.24916

Duchamp De Lageneste, O., Julien, A., Abou-Khalil, R., Frangi, G., Carvalho, C., Cagnard, N., et al. (2018). Periosteum Contains Skeletal Stem Cells with High Bone Regenerative Potential Controlled by Periostin. *Nat. Commun.* 9, 773. doi:10.1038/s41467-018-03124-z

Fang, J. (2014). Bioavailability of Anthocyanins. *Drug Metab. Rev.* 46, 508–520. doi:10.3109/03602532.2014.978080

Fillingham, Y., and Jacobs, J. (2016). Bone Grafts and Their Substitutes. *Bone Jt. J* 98-b, 6–9. doi:10.1302/0301-620X.98B.36350

Fintini, D., Cianfarani, S., Cofini, M., Andreoletti, A., Ubertini, G. M., Cappa, M., et al. (2020). The Bones of Children with Obesity. *Front. Endocrinol. (Lausanne)* 11, 200. doi:10.3389/fendo.2020.00200

Goltzman, D., Mannstadt, M., and Marcocci, C. (2018). Physiology of the Calcium-Parathyroid Hormone-Vitamin D Axis. *Front. Horm. Res.* 50, 1–13. doi:10.1159/000486060

Gómez-Barrena, E., Rosset, P., Gebhard, F., Hernigou, P., Baldini, N., Rouard, H., et al. (2019). Feasibility and Safety of Treating Non-unions in Tibia, Femur and Humerus with Autologous, Expanded, Bone Marrow-Derived Mesenchymal Stromal Cells Associated with Biphasic Calcium Phosphate Biomaterials in a Multicentric, Non-comparative Trial. *Biomaterials* 196, 100–108. doi:10.1016/j.biomaterials.2018.03.033

Gómez-Barrena, E., Rosset, P., Lozano, D., Stanovici, J., Ermthaller, C., and Gerbhard, F. (2015). Bone Fracture Healing: Cell Therapy in Delayed Unions and Nonunions. *Bone* 70, 93–101. doi:10.1016/j.bone.2014.07.033

Hardcastle, A. C., Aucott, L., Fraser, W. D., Reid, D. M., and Macdonald, H. M. (2011). Dietary Patterns, Bone Resorption and Bone mineral Density in Early post-menopausal Scottish Women. *Eur. J. Clin. Nutr.* 65, 378–385. doi:10.1038/ejcn.2010.264

Henriques, J. F., Serra, D., Dinis, T. C. P., and Almeida, L. M. (2020). The Anti-neuroinflammatory Role of Anthocyanins and Their Metabolites for the Prevention and Treatment of Brain Disorders. *Int. J. Mol. Sci.* 21, 653. doi:10.3390/ijms21228653

Hu, B., Chen, L., Chen, Y., Zhang, Z., Wang, X., and Zhou, B. (2021). Cyanidin-3-glucoside Regulates Osteoblast Differentiation via the ERK1/2 Signaling Pathway. *ACS Omega* 6, 4759–4766. doi:10.1021/acsomega.0c05603

Huang, W., Yan, Z., and Li, D. (2018). Antioxidant and Anti-inflammatory Effects of Blueberry Anthocyanins on High Glucose-Induced Human Retinal Capillary Endothelial Cells. *Oxid. Med. Cell Longev.* 2018, 1862462.

Imangali, N., Phan, Q. T., Mahady, G., and Winkler, C. (2021). The Dietary Anthocyanin Delphinidin Prevents Bone Resorption by Inhibiting Rankl-Induced Differentiation of Osteoclasts in a Medaka (*Oryzias latipes*) Model of Osteoporosis. *J. Fish. Biol.* 98, 1018–1030. doi:10.1111/jfb.14317

Jakesevic, M., Aaby, K., Borge, G. I., Jeppsson, B., Ahrné, S., and Molin, G. (2011). Antioxidative protection of Dietary Bilberry, Chokeberry and Lactobacillus Plantarum HEAL19 in Mice Subjected to Intestinal Oxidative Stress by Ischemia-Reperfusion. *BMC Complement. Altern. Med.* 11, 8. doi:10.1186/1472-6882-11-8

James, A. W., Lachaud, G., Shen, J., Asatrian, G., Nguyen, V., Zhang, X., et al. (2016). A Review of the Clinical Side Effects of Bone Morphogenetic Protein-2. *Tissue Eng. Part. B Rev.* 22, 284–297. doi:10.1089/ten.TEB.2015.0357

Kang, H. M., Park, B. S., Kang, H. K., Park, H. R., Yu, S. B., and Kim, I. R. (2018). Delphinidin Induces Apoptosis and Inhibits Epithelial-To-Mesenchymal Transition via the ERK/p38 MAPK-Signaling Pathway in Human Osteosarcoma Cell Lines. *Environ. Toxicol.* 33, 640–649. doi:10.1002/tox.22548

Karunarathne, W. A. H. M., Molagoda, I. M. N., Lee, K. T., Choi, Y. H., Jin, C. Y., and Kim, G. Y. (2021). Anthocyanin-enriched Polyphenols from Hibiscus Syriacus L. (Malvaceae) Exert Anti-osteoporosis Effects by Inhibiting GSK-3β and Subsequently Activating β-catenin. *Phytomedicine* 91, 153721. doi:10.1016/j.phymed.2021.153721

Kaume, L., Gilbert, W., Smith, B. J., and Devareddy, L. (2015). Cyanidin 3-O-β-D-Glucoside Improves Bone Indices. *J. Med. Food* 18, 690–697. doi:10.1089/jmf.2014.0029

Khoo, H. E., Azlan, A., Tang, S. T., and Lim, S. M. (2017). Anthocyanidins and Anthocyanins: Colored Pigments as Food, Pharmaceutical Ingredients, and the Potential Health Benefits. *Food Nutr. Res.* 61, 1361779. doi:10.1080/16546628.2017.1361779

Kim, B., Ku, C. S., Pham, T. X., Park, Y., Martin, D. A., Xie, L., et al. (2013). Aronia Melanocarpa (Chokeberry) Polyphenol-Rich Extract Improves Antioxidant

Function and Reduces Total Plasma Cholesterol in Apolipoprotein E Knockout Mice. *Nutr. Res.* 33, 406–413. doi:10.1016/j.nutres.2013.03.001

Kim, J. M., Yang, Y. S., Park, K. H., Oh, H., Greenblatt, M. B., and Shim, J. H. (2019). The ERK MAPK Pathway Is Essential for Skeletal Development and Homeostasis. *Int. J. Mol. Sci.* 20, 1803. doi:10.3390/ijms20081803

Kozłowska, A., and Dzierżanowski, T. (2021). Targeting Inflammation by Anthocyanins as the Novel Therapeutic Potential for Chronic Diseases: An Update. *Molecules* 26. doi:10.3390/molecules26144380

Lee, D. Y., Park, Y. J., Hwang, S. C., Kim, K. D., Moon, D. K., and Kim, D. H. (2018). Cytotoxic Effects of Delphinidin in Human Osteosarcoma Cells. *Acta Orthop. Traumatol. Turc* 52, 58–64. doi:10.1016/j.aott.2017.11.011

Lee, S. G., Kim, B., Yang, Y., Pham, T. X., Park, Y. K., Manatou, J., et al. (2014). Berry Anthocyanins Suppress the Expression and Secretion of Proinflammatory Mediators in Macrophages by Inhibiting Nuclear Translocation of NF-Kb Independent of NRF2-Mediated Mechanism. *J. Nutr. Biochem.* 25, 404–411. doi:10.1016/j.jnutbio.2013.12.001

Lee, Y. M., Yoon, Y., Yoon, H., Park, H. M., Song, S., and Yeum, K. J. (2017). Dietary Anthocyanins against Obesity and Inflammation. *Nutrients* 9, 1089. doi:10.3390/nu9101089

Li, D., Wang, P., Luo, Y., Zhao, M., and Chen, F. (2017). Health Benefits of Anthocyanins and Molecular Mechanisms: Update from Recent Decade. *Crit. Rev. Food Sci. Nutr.* 57, 1729–1741. doi:10.1080/10408398.2015.1030064

Li, N., Song, J., Zhu, G., Li, X., Liu, L., Shi, X., et al. (2016). Periosteum Tissue Engineering-A Review. *Biomater. Sci.* 4, 1554–1561. doi:10.1039/c6bm00481d

Lin, B. W., Gong, C. C., Song, H. F., and Cui, Y. Y. (2017). Effects of Anthocyanins on the Prevention and Treatment of Cancer. *Br. J. Pharmacol.* 174, 1226–1243. doi:10.1111/bph.13627

Liu, J., Zhou, H., Song, L., Yang, Z., Qiu, M., Wang, J., et al. (2021). Anthocyanins: Promising Natural Products with Diverse Pharmacological Activities. *Molecules* 26, 3807. doi:10.3390/molecules26133807

Mane, C., Loonis, M., Juhel, C., Dufour, C., and Malien-Aubert, C. (2011). Food Grade Lingonberry Extract: Polyphenolic Composition and *In Vivo* Protective Effect against Oxidative Stress. *J. Agric. Food Chem.* 59, 3330–3339. doi:10.1021/jf103965b

Mcnaughton, S. A., Wattanapenpaiboon, N., Wark, J. D., and Nowson, C. A. (2011). An Energy-Dense, Nutrient-Poor Dietary Pattern Is Inversely Associated with Bone Health in Women. *J. Nutr.* 141, 1516–1523. doi:10.3945/jn.111.138271

Melough, M. M., Sun, X., and Chun, O. K. (2017). The Role of AOPP in Age-Related Bone Loss and the Potential Benefits of Berry Anthocyanins. *Nutrients* 9, 789. doi:10.3390/nu9070789

Millar, C. L., Duclos, Q., and Blesso, C. N. (2017). Effects of Dietary Flavonoids on Reverse Cholesterol Transport, HDL Metabolism, and HDL Function. *Adv. Nutr.* 8, 226–239. doi:10.3945/an.116.014050

Moriwaki, S., Suzuki, K., Muramatsu, M., Nomura, A., Inoue, F., Into, T., et al. (2014). Delphinidin, One of the Major Anthocyanidins, Prevents Bone Loss through the Inhibition of Excessive Osteoclastogenesis in Osteoporosis Model Mice. *PLoS One* 9, e97177. doi:10.1371/journal.pone.0097177

Mulabagal, V., and Calderón, A. I. (2012). Liquid Chromatography/mass Spectrometry Based Fingerprinting Analysis and Mass Profiling of Euterpe Oleracea (Açaí) Dietary Supplement Raw Materials. *Food Chem.* 134, 1156–1164. doi:10.1016/j.foodchem.2012.02.123

Nagaoka, M., Maeda, T., Moriwaki, S., Nomura, A., Kato, Y., Niida, S., et al. (2019b). Petunidin, a B-Ring 5'-O-Methylated Derivative of Delphinidin, Stimulates Osteoblastogenesis and Reduces sRANKL-Induced Bone Loss. *Int. J. Mol. Sci.* 20, 795. doi:10.3390/ijms20112795

Nagaoka, M., Maeda, T., Chatani, M., Handa, K., Yamakawa, T., Kiyohara, S., et al. (2019a). A Delphinidin-Enriched Maqui Berry Extract Improves Bone Metabolism and Protects against Bone Loss in Osteopenic Mouse Models. *Antioxidants (Basel)* 8, 386. doi:10.3390/antiox8090386

Nishimura, R., Hata, K., Ikeda, F., Ichida, F., Shimoyama, A., Matsubara, T., et al. (2008). Signal Transduction and Transcriptional Regulation during Mesenchymal Cell Differentiation. *J. Bone Miner Metab.* 26, 203–212. doi:10.1007/s00774-007-0824-2

Ozbay, T., and Nahta, R. (2011). Delphinidin Inhibits HER2 and Erk1/2 Signaling and Suppresses Growth of HER2-Overexpressing and Triple Negative Breast Cancer Cell Lines. *Breast Cancer (Auckl)* 5, 143–154. doi:10.4137/BCBCR.S7156

Padilla, F., Puts, R., Vico, L., Guignandon, A., and Raum, K. (2016). Stimulation of Bone Repair with Ultrasound. *Adv. Exp. Med. Biol.* 880, 385–427. doi:10.1007/978-3-319-22536-4_21

Park, K. H., Gu, D. R., So, H. S., Kim, K. J., and Lee, S. H. (2015). Dual Role of Cyanidin-3-Glucoside on the Differentiation of Bone Cells. *J. Dent Res.* 94, 1676–1683. doi:10.1177/0022034515604620

Peichl, P., Holzer, L. A., Maier, R., and Holzer, G. (2011). Parathyroid Hormone 1-84 Accelerates Fracture-Healing in Pubic Bones of Elderly Osteoporotic Women. *J. Bone Jt. Surg Am* 93, 1583–1587. doi:10.2106/JBJS.J.01379

Pérez-Torres, I., Castrejón-Téllez, V., Soto, M. E., Rubio-Ruiz, M. E., Manzano-Pech, L., and Guarner-Lans, V. (2021). Oxidative Stress, Plant Natural Antioxidants, and Obesity. *Int. J. Mol. Sci.* 22. doi:10.3390/ijms22041786

Sakaki, J., Melough, M., Lee, S. G., Kalinowski, J., Koo, S. I., Lee, S. K., et al. (2018). Blackcurrant Supplementation Improves Trabecular Bone Mass in Young but Not Aged Mice. *Nutrients* 10, 1671. doi:10.3390/nu10111671

Salhotra, A., Shah, H. N., Levi, B., and Longaker, M. T. (2020). Mechanisms of Bone Development and Repair. *Nat. Rev. Mol. Cel Biol* 21, 696–711. doi:10.1038/s41580-020-00279-w

Samarpita, S., Ganesan, R., and Rasool, M. (2020). Cyanidin Prevents the Hyperproliferative Potential of Fibroblast-like Synoviocytes and Disease Progression via Targeting IL-17A Cytokine Signalling in Rheumatoid Arthritis. *Toxicol. Appl. Pharmacol.* 391, 114917. doi:10.1016/j.taap.2020.114917

Samarpita, S., and Rasool, M. (2021). Cyanidin Attenuates IL-17A Cytokine Signaling Mediated Monocyte Migration and Differentiation into Mature Osteoclasts in Rheumatoid Arthritis. *Cytokine* 142, 155502. doi:10.1016/j.cyto.2021.155502

Saulite, L., Jekabsons, K., Klavins, M., Muceniece, R., and Riekstina, U. (2019). Effects of Malvidin, Cyanidin and Delphinidin on Human Adipose Mesenchymal Stem Cell Differentiation into Adipocytes, Chondrocytes and Osteocytes. *Phytomedicine* 53, 86–95. doi:10.1016/j.phymed.2018.09.029

Sehitoglu, M. H., Farooqi, A. A., Qureshi, M. Z., Butt, G., and Aras, A. (2014). Anthocyanins: Targeting of Signaling Networks in Cancer Cells. *Asian Pac. J. Cancer Prev.* 15, 2379–2381. doi:10.7314/apjcp.2014.15.5.2379

Shimizu, S., Matsushita, H., Morii, Y., Ohyama, Y., Morita, N., Tachibana, R., et al. (2018). Effect of Anthocyanin-Rich Bilberry Extract on Bone Metabolism in Ovariectomized Rats. *Biomed. Rep.* 8, 198–204. doi:10.3892/br.2017.1029

Sinha, K. M., and Zhou, X. (2013). Genetic and Molecular Control of Osterix in Skeletal Formation. *J. Cel Biochem* 114, 975–984. doi:10.1002/jcb.24439

Smeriglio, A., Barreca, D., Bellocco, E., and Trombetta, D. (2016). Chemistry, Pharmacology and Health Benefits of Anthocyanins. *Phytother Res.* 30, 1265–1286. doi:10.1002/ptr.5642

Speer, H., D'cunha, N. M., Alexopoulos, N. I., Mckune, A. J., and Naumovski, N. (2020). Anthocyanins and Human Health-A Focus on Oxidative Stress, Inflammation and Disease. *Antioxidants (Basel)* 9, 366. doi:10.3390/antiox9050366

Tian, L., Tan, Y., Chen, G., Wang, G., Sun, J., Ou, S., et al. (2019). Metabolism of Anthocyanins and Consequent Effects on the Gut Microbiota. *Crit. Rev. Food Sci. Nutr.* 59, 982–991. doi:10.1080/10408398.2018.1533517

Tsuda, T., Horio, F., and Osawa, T. (2000). The Role of Anthocyanins as an Antioxidant under Oxidative Stress in Rats. *Biofactors* 13, 133–139. doi:10.1002/biof.5520130122

Ullah, R., Khan, M., Shah, S. A., Saeed, K., and Kim, M. O. (2019). Natural Antioxidant Anthocyanins-A Hidden Therapeutic Candidate in Metabolic Disorders with Major Focus in Neurodegeneration. *Nutrients* 11, 1195. doi:10.3390/nu11061195

Vega-Galvez, A., Rodríguez, A., and Stucken, K. (2021). Antioxidant, Functional Properties and Health-Promoting Potential of Native South American Berries: a Review. *J. Sci. Food Agric.* 101, 364–378. doi:10.1002/jsfa.10621

Wallace, T. C., and Giusti, M. M. (2015). Anthocyanins. *Adv. Nutr.* 6, 620–622. doi:10.3945/an.115.009233

Wang, L., Yu, W., Yin, X., Cui, L., Tang, S., Jiang, N., et al. (2021). Prevalence of Osteoporosis and Fracture in China. *JAMA Netw. Open* 4, e2121106. doi:10.1001/jamanetworkopen.2021.21106

Wojda, S. J., and Donahue, S. W. (2018). Parathyroid Hormone for Bone Regeneration. *J. Orthop. Res.* 36, 2586–2594. doi:10.1002/jor.24075

Wu, X., and Prior, R. L. (2005). Identification and Characterization of Anthocyanins by High-Performance Liquid Chromatography-Electrospray Ionization-Tandem Mass Spectrometry in Common Foods in the United States: Vegetables, Nuts, and Grains. *J. Agric. Food Chem.* 53, 3101–3113. doi:10.1021/jf0478861

Yun, J. M., Afaq, F., Khan, N., and Mukhtar, H. (2009). Delphinidin, an Anthocyanidin in Pigmented Fruits and Vegetables, Induces Apoptosis and Cell Cycle Arrest in Human colon Cancer HCT116 Cells. *Mol. Carcinog* 48, 260–270. doi:10.1002/mc.20477

Zhai, Z. J., Li, H. W., Liu, G. W., Qu, X. H., Tian, B., Yan, W., et al. (2014). Andrographolide Suppresses RANKL-Induced Osteoclastogenesis *In Vitro* and Prevents Inflammatory Bone Loss *In Vivo*. *Br. J. Pharmacol.* 171, 663–675. doi:10.1111/bph.12463

Zheng, X., Mun, S., Lee, S. G., Vance, T. M., Hubert, P., Koo, S. I., et al. (2016). Anthocyanin-Rich Blackcurrant Extract Attenuates Ovariectomy-Induced Bone Loss in Mice. *J. Med. Food* 19, 390–397. doi:10.1089/jmf.2015.0148

Conflict of Interest: The authors declare that the research was conducted in the absence of any commercial or financial relationships that could be construed as a potential conflict of interest.

Publisher's Note: All claims expressed in this article are solely those of the authors and do not necessarily represent those of their affiliated organizations, or those of the publisher, the editors and the reviewers. Any product that may be evaluated in this article, or claim that may be made by its manufacturer, is not guaranteed or endorsed by the publisher.

Copyright © 2021 Mao, Huang, Chen, Xu, Qin and Li. This is an open-access article distributed under the terms of the Creative Commons Attribution License (CC BY). The use, distribution or reproduction in other forums is permitted, provided the original author(s) and the copyright owner(s) are credited and that the original publication in this journal is cited, in accordance with accepted academic practice. No use, distribution or reproduction is permitted which does not comply with these terms.

frontiers in Pharmacology

ORIGINAL RESEARCH
published: 11 November 2021
doi: 10.3389/fphar.2021.762543

Jintiange Capsules Ameliorate Osteoarthritis by Modulating Subchondral Bone Remodeling and Protecting Cartilage Against Degradation

Chenyang Zhuang[1†], *Zixiang Wang*[1†], *Weisin Chen*[1], *Hanquan Wang*[1], *Bo Tian*[1*] and *Hong Lin*[1,2*]

[1]Department of Orthopedics, Zhongshan Hospital, Fudan University, Shanghai, China, [2]Department of Orthopedics, Shanghai Geriatric Medical Centre, Fudan University, Shanghai, China

OPEN ACCESS

Edited by:
Longhuo Wu,
Gannan Medical University, China

Reviewed by:
Lipeng Wang,
Shanghai University, China
Yueqi Chen,
Army Medical University, China

***Correspondence:**
Bo Tian
poetian@163.com
Hong Lin
lin.hong1@zs-hospital.sh.cn

[†]These authors have contributed equally to this work

Specialty section:
This article was submitted to Ethnopharmacology, a section of the journal Frontiers in Pharmacology

Received: 24 August 2021
Accepted: 25 October 2021
Published: 11 November 2021

Citation:
Zhuang C, Wang Z, Chen W, Wang H, Tian B and Lin H (2021) Jintiange Capsules Ameliorate Osteoarthritis by Modulating Subchondral Bone Remodeling and Protecting Cartilage Against Degradation. Front. Pharmacol. 12:762543. doi: 10.3389/fphar.2021.762543

Osteoarthritis (OA) is the most prevalent joint disease worldwide, making it a major cause of pain and disability. Identified as a chronic and progressive disease, effective treatment at the early stages of OA has become critical to its management. Jintiange (Jtg) capsules are a traditional Chinese medicine produced from multiple organic components of various animal bones and routinely used to treat osteoporosis in China. However, the effect of Jtg on subchondral bone and cartilage degeneration in OA remains unknown. The purpose of the present study was to investigate the biomolecular role and underlying mechanisms of Jtg in OA progression. Herein, we found that Jtg inhibited receptor activator of nuclear factor-κB ligand (RANKL)-induced osteoclast formation and it functions through the NF-κB signaling pathway. Jtg also inhibited chondrocyte apoptosis via reducing the reactive oxygen species concentration in these cells. Moreover, *in vivo* evaluation revealed that Jtg significantly attenuates subchondral bone remodeling and cartilage destruction in anterior cruciate ligament transection (ACLT) mouse models. Taken together, our data demonstrate that Jtg inhibits osteoclast differentiation in subchondral bone and chondrocyte apoptosis in cartilage, supporting its potential therapeutic value for treating OA.

Keywords: Jintiange capsule, osteoarthritis, subchondral bone, cartilage, osteoclast, chondrocyte

INTRODUCTION

Osteoarthritis (OA), the most common chronic and degenerative joint disease globally, greatly threatens the quality of life of millions of people, especially the elderly. OA affects approximately 10% of men and 18% of women aged >60 years (Bijlsma et al., 2011; Litwic et al., 2013). Pain, joint stiffness or deformity, and even disability at the end stages are commonly reported in studies from around the world as typical symptoms of OA (Hochberg et al., 2013; Riegger and Brenner, 2020). However, existing pharmacotherapies focus on pain relief with no effective disease-modifying effects. Joint replacement surgery is routinely performed to improve joint function for end-stage OA patients, but the economic cost and complications associated with this type of intervention should not be ignored (Arden et al., 2021). Hence, there is a growing need to investigate and identify effective early-stage OA treatment schemes targeting underlying pathogenesis.

OA is primarily characterized by the degradation of the articular cartilage and the remodeling of the subchondral bone, which indicate aberrant activity in the chondrocytes and osteoclasts, respectively (Hunter and Bierma-Zeinstra, 2019). Chondrocytes, which account for 1–5% of the total cartilage volume, are unique cells specifically responsible for the physiological function and composition of the cartilage (Glyn-Jones et al., 2015). Patients with OA exhibit increased chondrocyte apoptosis, which is closely associated with the degradation of extracellular matrix components such as type II collagen and aggrecan. Increasing compelling evidence indicates that chondrocytes undergo apoptosis and induce cartilage destruction in response to various stimuli including mechanical, inflammatory, and metabolic factors and was, until recently, considered the primary pathogenic driver of OA (Lepetsos and Papavassiliou, 2016; Bolduc et al., 2019). However, experimental animal studies have shown that OA is not the inevitable result of scarification in the articular cartilage, suggesting that more specialized mechanisms are involved in OA associated cartilage degradation (Meachim, 1964; Meachim et al., 1965). There is increasing evidence that bone changes in the subchondral bone occur earlier than cartilage destruction in early-stage OA, and alterations in the subchondral bone are likely to be early mediators of OA progression (Goldring, 2009; Goldring and Goldring, 2010). The subchondral bone is a vital support of the articular cartilage, indicating that it has distinct effects on the stress dispersion and conformation of joints; these effects are significantly suppressed in OA joints. Tensile and shear stresses as well as other mechanical overload are exacerbated in subchondral bone plates with lower density and stiffness, further exposing articular cartilage to abnormal mechanical and biochemical effects. In early-stage OA, hyperactivity in the osteoclasts and increasing subchondral bone remodeling were the driving forces behind the bone loss in and thinning of the subchondral bone plate, which induced the catabolism of the articular cartilage. Recently, researchers have suggested that many factors may dysregulate homeostasis of both subchondral bone and cartilage microenvironments *via* the activation of certain signaling pathways. It has been demonstrated that aberrant activation of transforming growth factor *ß* (TGF-β) through osteoclastogenesis in subchondral bone in response to abnormal mechanical loading in onset of OA induces apoptosis of chondrocytes, thereby blocking extracellular matrix integrity in cartilage (Hu et al., 2020). This means that interventions designed to target osteoclastogenesis in subchondral bone are expected to be the most effective approaches to designing novel therapeutics for early-stage OA.

Non-steroidal anti-inflammatory drugs (NSAIDs) are the first-line treatment for OA and demonstrate significant pain-relieving effects, but these effects are accompanied by many safety concerns, including increased risks for gastrointestinal and cardiovascular adverse events. In addition, NSAIDs demonstrate clinically relevant reduction in symptoms without disease-modifying effects. It is hoped that traditional Chinese medicine-based approaches may have the potential and flexibility to help develop novel combination therapies for treating OA (Kong and Wen, 2019; Tang, 2019; Wu et al., 2019). Many theories of traditional Chinese medicine provide anecdotal evidence that bones from certain animals such as tigers, cattle and horses can inhibit bone resorption and remodeling (Ma et al., 2011; Suntornsaratoon et al., 2018). Artificial tiger bone powder, also called Jintiange (Jtg) capsules, is mixed in a pre-determined ratio with calcium, collagen, bone morphogenetic protein, bone growth factors, polypeptides, amino acids, and polysaccharides and used to treat bone-related conditions. Jtg is known for having similar medical effects to real tiger bone and has been reported to have distinct effects on osteoporosis in many experimental animal and clinical studies (Sun et al., 2019). However, the effects of Jtg on articular cartilage and subchondral bone and its underlying mechanisms remain elusive.

This study aimed to determine the effects of Jtg on receptor activator of nuclear factor-κB ligand (RANKL)-induced osteoclastogenesis and chondrocyte apoptosis, which mimic the two typical cellular dysfunctions of OA *in vitro*. Our results are expected to provide some translational value in developing a novel treatment strategy incorporating elements from traditional Chinese medicine for early-stage OA treatment.

MATERIALS AND METHODS

Media and Reagents

Jtg (Purity > 95%) was obtained from Ginwa (Xi'an, China), and dissolved in Dimethyl sulfoxide (DMSO) (Sigma-Aldrich, Milwaukee, WI, United States). α-minimum essential medium (α-MEM) and Dulbecco's minimum essential medium (DMEM) were purchased from Hyclone (Logan, UT, United States). Fetal bovine serum, insulin-transferrin-selenite (Livshits et al., 2010) and penicillin/streptomycin were purchased from Gibco (New York, NY, United States). Receptor activator of nuclear factor-κB ligand (RANKL) and macrophage colony stimulating factor (M-CSF) were obtained from R&D Systems (Minneapolis, MN, United States). H_2O_2 solution, the TUNEL apoptosis detection kit, cell counting kit-8 assay, DCFH-DA probe and RIPA lysis buffer were obtained from Beyotime Biotechnology (Shanghai, China). Antibodies against nuclear factor-kappa B (NF-κB) and mitogen-activated protein kinase (MAPK) were purchased from Cell Signaling Technology (Danvers, MA, United States). Rhodamine-conjugated phalloidin, 4′,6-diamidino-2-phenylindole (DAPI) and TRIzol reagent were obtained from Invitrogen (Carlsbad, CA, United States).

Cell Culture

Primary bone marrow stromal cells (BMSCs) were isolated from 6-week-old, female C57BL/6 mice by flushing their femurs and tibias with α-MEM (adding 10% FBS, 1% penicillin and streptomycin). After supplementing the medium with macrophage colony stimulating factor (M-CSF, 30 ng/ml) and incubating in a humidified atmosphere of 5% CO2 at 37°C, primary bone marrow macrophages (BMMs) were obtained. The murine chondroprogenitor cell line ATDC5 purchased from the National Collection of Authenticated Cell Cultures (Shanghai, China) were cultured in DMEM (adding 10% FBS, 1% penicillin and streptomycin). ATDC5 is a well-established

culture model *in vitro*, which has been commonly used for chondrogenic differentiation in the previous studies (Yao and Wang, 2013). To induce differentiation of the cells into chondrocyte-like cells, the medium containing DMEM and 5% FBS was supplemented with 1% ITS and the medium was changed every 2 days until the culture reached 80% confluence.

Cell Viability Assay

The cytotoxic effects of Jtg on BMMs and ATDC5 cells were evaluated with a cell counting kit-8 assay (CCK-8) following the manufacturer's instruction. BMMs were seeded in 96-well plates at a density of 1×10^4 cells/well in triplicate, and co-cultured in 100 μL complete α-MEM medium with 30 ng/mL M-CSF and different concentrations of Jtg (0, 1.25, 2.5, 5, 10, 20, 40 mg/L) for 24 h. Similarly, ATDC5 cells were cultured with different concentrations of Jtg (0, 1.25, 2.5, 5, 10, 20, 40 mg/L) for 24 h. After washing with PBS for three times, 10 μL CCK-8 buffer was added to each well and incubated at 37°C for additional 2 h. Then, the absorbance was measured at a wavelength of 450 nm and quantitated as the percentage compared with the untreated control group with a microplate reader (Bio-Tech, CA, United States).

Osteoclastogenesis and Bone Resorption Pit Assay

To further differentiate osteoclasts, the BMMs obtained as mentioned above were seeded in a 96-well plate with 6×10^3 cells per well and treated with complete α-MEM medium containing 30 ng/mL M-CSF, 50 ng/ml RANKL and different concentrations of Jtg (0, 5, 10 mg/L). After changing the medium every other day for 5 days, cells were fixed with 4% paraformaldehyde for 20 min and stained for TRAP activity. TRAP-positive osteoclasts with no less than 3 nuclei were scored under a microscope. To perform the bone resorption pit assay, BMMs were seeded on the bovine bone slices in a 96-well plate and treated with α-MEM medium containing 30 ng/mL M-CSF, 50 ng/ml RANKL, and different concentrations of Jtg (0, 5, 10 mg/L). After changing the medium every other day for 5 days, the slides were washed with PBS and further treated with mechanical agitation and sonication to completely remove the cells. Bone resorption pits were observed using scanning electron microscopy (HITACHI-S520; Hitachi, Tokyo, Japan) and quantified using ImageJ software (National Institutes of Health, Bethesda, MD, United States).

Immunofluorescence Staining of F-Actin Ring

BMMs were seeded in 35 mm glass bottom microwell dishes at the concentration of 6×10^3 cells per well and cultured with α-MEM medium containing 30 ng/mL M-CSF, 50 ng/ml RANKL, with or without Jtg. After formation of mature osteoclasts, cells were fixed with 4% paraformaldehyde for 20 min and subsequently permeabilized with 0.1% Triton X-100 for 5 min. Fixed cells were stained with rhodamine-conjugated phalloidin for 1.5 h. The cells were then mounted on slides, and the nuclei were stained with 4′,6-diamidino-2-phenylindole (DAPI) for 5 min and were observed with confocal fluorescence microscopy (FV3000, Olympus, Tokyo, Japan).

Measurement of ROS in ATDC5 Cells

ROS level was assessed with a DCFH-DA probe in ATDC5 cells, according to the manufacturer's instructions. ATDC5 cells were cultured with or without various concentrations of Jtg (0, 5, 10 mg/L) and 200 μM H_2O_2 for 24 h based on the previous study (Zhou et al., 2019). After incubated with 10 μM DCFH-DA in the dark for 20 min at 37°C, the cells were washed three times with PBS. The fluorescence microscopy was then used to detect and count ROS-positive cells. Meanwhile, the cytometry analysis was further used to determine the ROS-positive cells stained by the DCFH-DA probe using a flow cytometer (BD Cytometer System, CA, United States).

Quantitative Real-Time Polymerase Chain Reaction

Quantitative PCR was used to quantify the specific genes expression of osteoclastogenesis and ATDC5 cell apoptosis. BMMs were seeded in 6-well plates at a density of 1×10^5 cells per well and cultured in complete α-MEM containing 30 ng/mL M-CSF and 50 ng/ml RANKL. The BMMs were treated with 10 mg/L Jtg for 0–5 days. ATDC5 cells were seeded in 6-well plates at a density of 1×10^5 cells per well and treated with complete DMEM supplemented with 200 μM H_2O_2 and different concentrations of Jtg (0, 2.5, 5, 10 mg/L) for 24 h. Total RNA was extracted using TRIzol reagent. cDNA synthesis was performed with a reverse transcription reagent (Applied Biosystems, Foster, CA, United States) and followed with the transcription-PCR using real-time PCR (ABI 7500; Applied Biosystems, Foster City, CA). The mouse primer sequences of Cathepsin K (CTSK), TRAP, c-Fos, NFATc1, GAPDH, Bcl-2, Bcl-xL and Bak were listed in **Table 1**.

Western Blot

BMMs were seeded in 6-well plates at a density of 6×10^5 cells/well and cultured with 50 ng/ml RANKL in the presence or absence of 10 mg/L Jtg in complete α-MEM for 0, 5, 10, or 60 min. ATDC5 cells were seeded in 6-well plates at a density of 6×10^5 cells/well and cultured with or without 10 mg/L Jtg and 200 μM H_2O_2 in complete DMEM. The total protein was extracted from BMMs and ATDC5 cells using RIPA lysis buffer according to the manufacturer's instructions. The protein concentrations were quantitated and analyzed using a BCA protein assay kit (Thermo Pierce, Rockford, IL, United States). 30 μg of total protein were separated by 10% sodium dodecyl sulfate-polyacrylamide gel electrophoresis (SDS-PAGE) and transferred onto PVDF membranes (Millipore Corp, Billerica, MA). After being blocked by 5% skimmed milk, the membranes were incubated with primary antibodies at 4°C overnight. Furthermore, the membranes were incubated with horseradish peroxidase-conjugated secondary antibody diluted in the blocking buffer at room temperature for 1 h. Finally, the blots were visualized using Image-quant LAS 4000 Analyzer (GE Healthcare, Silverwater, NSW, Australia).

TABLE 1 | Sequences of both the forward and reverse primers of mRNAs in RT-PCR.

Gene	Forward (5′-3′)	Reverse (3′-5′)
CTSK	CTTCCAATACGTGCAGCAGA	TCTTCAGGGCTTTCTCGTTC
TRAP	CTGGAGTGCACGATGCCA GCGACA	TCCGTGCTCGGCGATGGA CCAGA
c-Fos	CCAGTCAAGAGCATCAGCAA	AAGTAGTGCAGCCCGGAGTA
NFATc1	CCGTTGCTTCCAGAAAATAACA	TGTGGGATGTGAACTCGGAA
GAPDH	ACCCAGAAGACTGTGGATGG	CACATTGGGGGTAGGAACAC
Bcl-2	ATGCCTTTGTGGAACTAT ATGGC	GGTATGCACCCAGAGTGATGC
Bcl-xL	TGCGTGGAAAGCGTAGACAA	ATTCAGGTAAGTGGCCAT CCAA
Bak	CCCAGGACACAGAGGAGGTTT	GCCTCCTGTTCCTGCTGATG

P65 Nuclear Translocation Staining

BMMs were seeded in 6-well plates at a density of 6×10^5 cells/well and cultured with 50 ng/ml RANKL in the presence or absence of 10 mg/L Jtg in complete α-MEM. Then the cells were fixed with 4% paraformaldehyde for 15 min, washed with 0.2% Triton X-100 in PBS for 5 min, blocked with 1% BSA in PBS, and incubated with monoclonal anti-P65 antibody followed by biotinylated goat anti-mouse IgG antibody as the secondary antibody. The cells were further stained with DAPI for 5 min and observed using a confocal fluorescence microscopy.

Cell Apoptosis Measurement

An Annexin V-FITC/PI apoptosis kit was used to determine the rate of ATDC5 cells apoptosis. ATDC5 cells were seeded in 6-well plate and cultured with or without 200 μM H_2O_2 and various concentrations of Jtg for 24 h, followed by re-suspended in 500 μL binding buffer and stained with annexin V-FITC/PI staining. Then, the sample was tested and analyzed using the flow cytometer. The results are represented as the percentage of apoptotic cells.

TUNEL Staining

To evaluate the alterations associated with ATDC5 cell apoptosis, TdT-UTP nick end labeling (TUNEL) staining was conducted using the one step TUNEL fluorescence kit according to the manufacturer's instructions. After treated with or without 200 μM H_2O_2 and 5 or 10 mg/L Jtg for 24 h, the cells were permeabilized with 0.1% Triton X-100 for 2 min and stained with TUNEL mixture for 1 h according to the manufacturer's instructions. The cells were further stained with DAPI for 5 min and observed using a confocal fluorescence microscopy. The cells with green fluorescence were defined as apoptotic cells.

ACLT-Induced OA Mouse Model

ACLT model was established in 10-week-old C57BL/6J male mice purchased from the Animal Center of Zhongshan Hospital, Fudan University (Shanghai, China). After approved by the Animal Ethical Committee of Zhongshan Hospital, Fudan University (2019-065), the model is produced by complete transection of anterior cruciate ligament after direct visualization of it. A sham operation was conducted by only opening the joint capsule and visualizing the anterior cruciate ligament without transection. Mice were randomly divided into four groups as follows: Sham; ACLT; ACLT + Jtg (low dose); ACLT + Jtg (high dose); (n = 12 per group). The ACLT + Jtg group received Jtg (10 mg/kg and 30 mg/kg for low and high dose, respectively) dissolved in 0.9% normal saline (NS) by intragastric administration every other day. Mice in the sham group and ACLT group were administered an equivalent volume of NS. To prevent infection, each mouse was administered penicillin every day during the first 3 days after surgery. Six mice in each group were sacrificed 2 weeks after surgery and another 24 mice were euthanized 4 weeks post operation, and tibia and femur bones were collected for further micro-CT scanning and histological observation.

Micro-CT Scanning

After fixed in 4% paraformaldehyde, specimens were scanned using micro-CT (QuantumGX; PerkinElmer, Waltham, MA, United States). The subchondral bone was evaluated using three-dimensional structural parameters including bone mineral density (BMD), bone volume fraction (BV/TV), trabecular pattern factor (Tb. PF), and subchondral bone plate thickness (SBP. Th), were analyzed.

Histological Examination

Knee joint samples were all sectioned on a microtome at a thickness of 5 μm after decalcified in 10% EDTA and embedded in paraffin. Then hematoxylin and eosin (H&E), Safranin O and TRAP staining were performed. Osteoarthritis Research Society International (OARSI) scoring system was used to assess the progression of OA according to the previous study. Immunohistochemical staining of aggrecan, MMP-13, TGF-β, Caspase-3, and TUNEL were further performed and analyzed.

Statistical Analysis

All the experiments were performed at least three times, and the data are presented as the mean ± SD. Statistical analysis was performed using one-way analysis of variance (ANOVA). A $p < 0.05$ was considered significant.

RESULTS

Jtg Inhibits RANKL-Induced Osteoclastogenesis in BMMs

The composition of Jtg was analyzed with HPLC (**Supplementary Figure S1**). We first evaluated the cytotoxic effects of different Jtg concentrations on BMMs using a CCK-8 assay. BMMs remained viable when treated with Jtg at concentrations ranging from 1.25 to 40 mg/L, and the BMMs were also incubated with M-CSF (30 ng/ml) and RANKL (50 ng/ml) to induce osteoclast differentiation. Notably, the Jtg treatment of these cells exhibited a dose-dependent inhibition of TRAP-positive mature osteoclasts (**Figures 1A,D,E**). Then we seeded BMMs on bovine cortical bone slices and stimulated them with RANKL and different Jtg concentrations (0, 5, and 10 mg/L) to assess the bone resorption capacity of these osteoclasts. Consequently, we observed a significant increase in bone resorption following RANKL stimulation, but this resorption was ameliorated in a dose-dependent manner when treated with Jtg (**Figures 1B,F**). In addition, evaluations of the F-actin ring, reflecting the

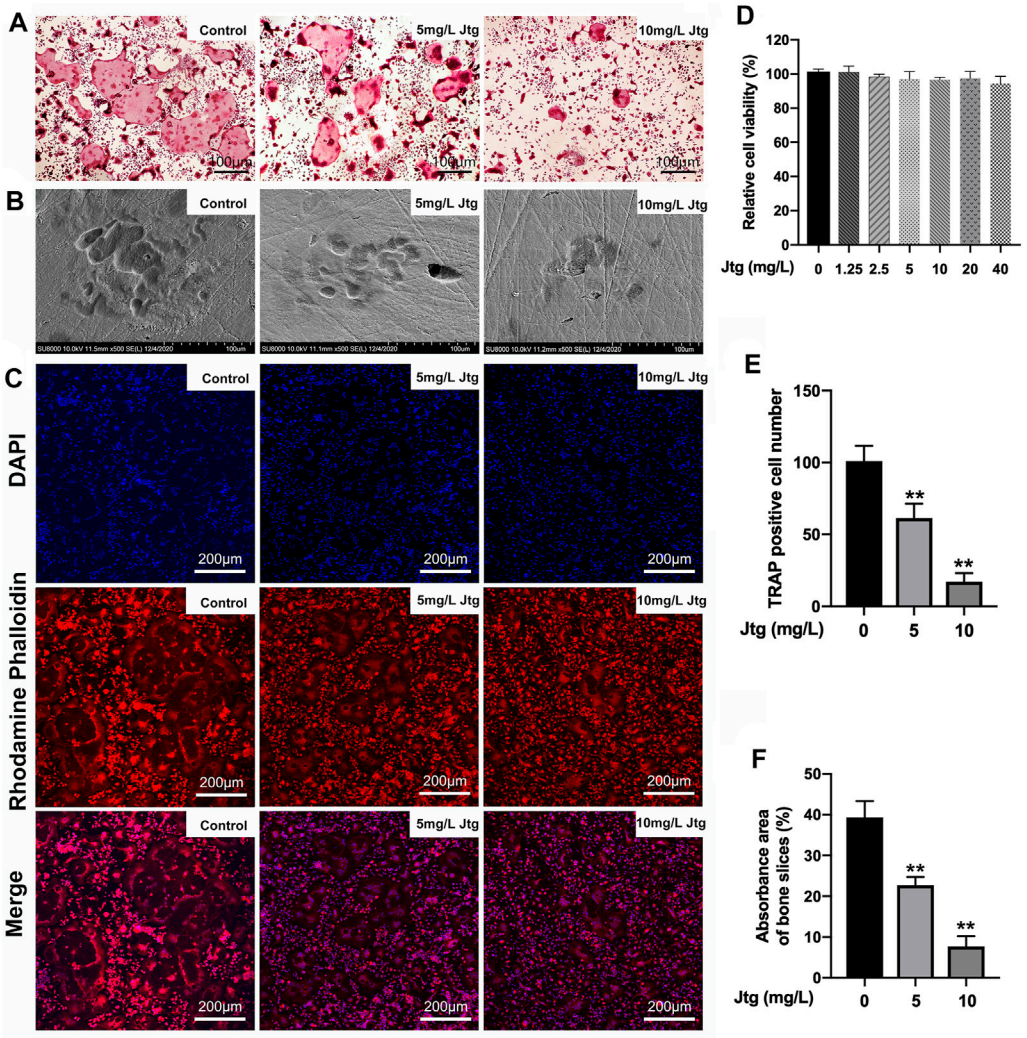

FIGURE 1 | Jtg prevents receptor activator of nuclear factor-kappa B ligand (RANKL)-induced osteoclastogenesis *in vitro*. **(A)** Tartrate-resistant acid phosphatase (TRAP) staining of osteoclasts treated with different concentrations of Jtg. **(B)** Representative SEM images of bone resorption pits. **(C)** Representative images of actin rings formation were observed with confocal microscopy. **(D)** BMMs were treated with various concentrations of Jtg for 24 h and cell survival was measured using a CCK-8 assay. **(E)** The number of TRAP-positive cells (containing three or more nuclei) were determined. **(F)** The total areas of resorption pits were measured. *Compared with the control group (**$p < 0.01$).

cytoskeletal structure of the osteoclasts, revealed that this structure increased in size in response to RANKL and decreased in both size and number following treatment with Jtg (**Figure 1C**). These findings indicate that Jtg treatment effectively inhibits osteoclast differentiation and function *in vitro*.

Jtg Inhibits NF-κB Signaling in RANKL Activated BMMs

We then determined the mechanisms by which Jtg treatment affects RANKL-induced osteoclastogenesis. To this end, we investigated changes in several key RANKL-signaling pathways, including the NF-κB and MAPK signaling pathways, in response to Jtg treatment using western blot. The phosphorylation of IκBa and the nuclear translocation of NF-κB (p65) are used to evaluate the activation of the NF-κB signaling pathway in BMMs. Western blot (**Figures 2A,B**, **Supplementary Figure S2**) revealed that the phosphorylation of both IκBα and p65 were significantly increased in response to RANKL. However, these effects were significantly inhibited following treatment with Jtg. Moreover, p65 nuclear translocation staining demonstrated that p65 was mostly located in the nuclear of BMMs in the control group after RANKL pretreatment while the translocation was decreased significantly in the cells cultured with Jtg (**Figure 2C**). These results indicated that Jtg attenuated osteoclast formation by blocking osteoclastogenesis-related NF-κB signaling. Many studies have demonstrated that the MAPK pathway is also closely associated with osteoclast differentiation. Thus, we also evaluated the interactions between Jtg and RANKL-induced MAPK signaling in an effort to further refine the underlying

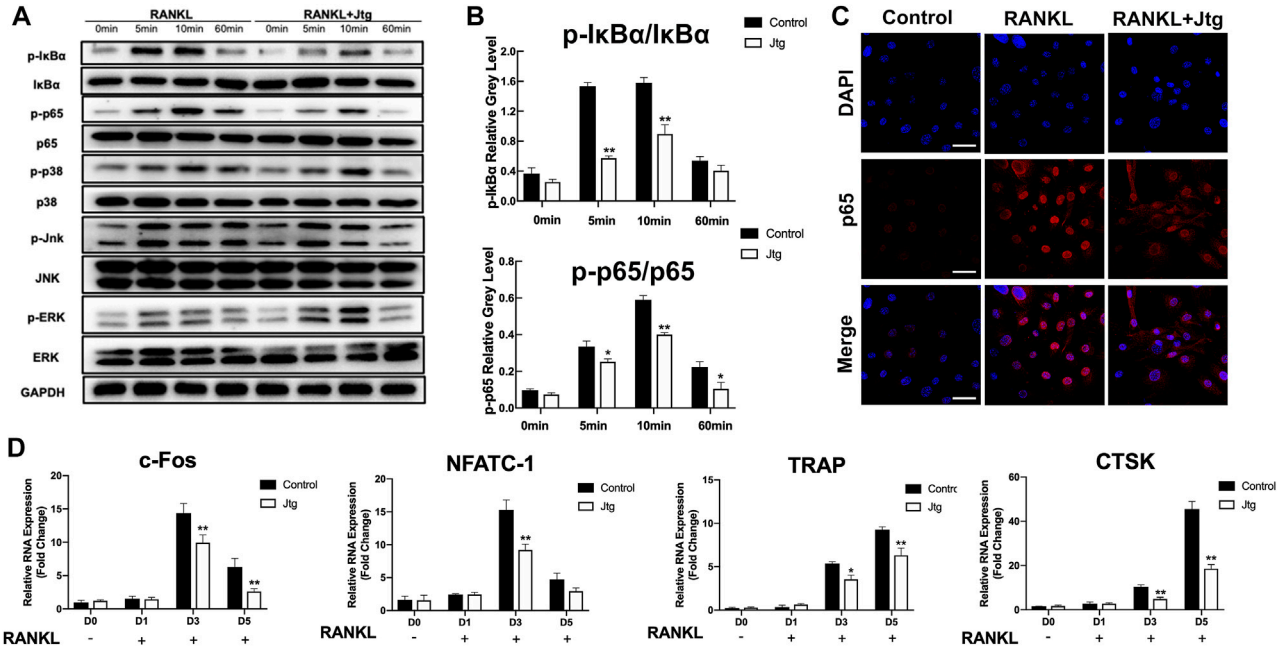

FIGURE 2 | Jtg inhibits RANKL-induced osteoclast-specific gene expression and NF-κB signaling pathway without affecting MAPK pathway. **(A)** Western blot assay was performed to analyze the expression of osteoclastogenesis-related transcription factors in the NF-κB and MAPK signaling pathways including IκBα, p65, p38, ERK, and JNK. **(B)** The band intensities corresponding to p-IκBα/IκBα and p-p65/p65. **(C)** Immunofluorescence staining was performed to analyze the nuclear translocation of p65 upon RANKL stimulation in BMMs, scale bar, 50 μm. **(D)** The expression of osteoclast-specific mRNA, including c-FOS, NFATc1, TRAP, and cathepsin K (CTSK) was analyzed using RT-PCR. The mRNA-expression levels were normalized relative to the expression of GAPDH mRNA. *Compared with the control group (*$p < 0.05$; **$p < 0.01$).

mechanisms of JTG treatment. However, Jtg treatment had no significant impact of the phosphorylation of p38, ERK and JNK, indicating that MAPK signaling pathway was not the mechanism mediating the effects of Jtg on osteoclastogenesis (**Figure 2A**, **Supplementary Figure S3**).

Jtg Suppresses Osteoclast-Specific Gene Expression

We then used RT-PCR to examine the effects of Jtg on the transcription of several genes associated with osteoclastogenesis and bone resorption. BMMs were stimulated with RANKL (50 ng/ml) and then treated with 10 mg/L Jtg for 5 days and then subjected to RT-PCR. Osteoclastogenic genes, including c-FOS, NFATc1, TRAP and CTSK, were significantly upregulated by RANKL and markedly suppressed following Jtg treatment (**Figure 2D**), suggesting that Jtg treatment counteracts the RANKL-induced upregulation of osteoclast-specific gene expression.

Jtg Prevents ATDC5 Cells From Undergoing ROS-Induced Apoptosis

The immunofluorescence staining and flow cytometry were used to evaluate cellular ROS generation under several conditions. These evaluations revealed significant increases in ROS levels in H_2O_2 (200 μM) treated ATDC5 cells (**Figures 3A–C**), as previously described. In contrast, Jtg treatment reduced the accumulation of ROS in H_2O_2-treated ATDC5 cells. Flow cytometry analysis was then used to determine the apoptotic status of these cells revealing that exposure to H_2O_2 (200 μM) significantly increased apoptosis in ATDC5 cells Additionally, Jtg treatment could inhibit this apoptosis in a dose-dependent manner (**Figures 3D,E**). These results were further confirmed by TUNEL staining, which identified significantly more TUNEL positive apoptotic cells in the H_2O_2-treated group than in the Jtg-treated group (**Figures 3F,G**). These findings strongly suggest that Jtg inhibits chondrocyte apoptosis by preventing ROS accumulation.

Jtg Blocks ROS-Induced ATDC5 Cells Apoptosis by Regulating the Expression of Key Apoptosis-Related Genes

Western blot and RT-PCR were used to determine the underlying mechanism involved in Jtg's antiapoptotic effect in these cells. The anti-apoptotic genes Bcl-2 and Bcl-xL were downregulated, whereas the pro-apoptotic genes Bax and Bak were significantly upregulated after H_2O_2 stimulation. However, Jtg reversed these effects in all four apoptosis-related genes (**Figure 3J**). This was validated by the western blot assays that recorded similar findings for the expression of apoptosis-related proteins, including Cleaved Caspase-3, Bax and Bcl-2 (**Figures 3H,I**). Taken together, these results suggest that Jtg treatment alleviates

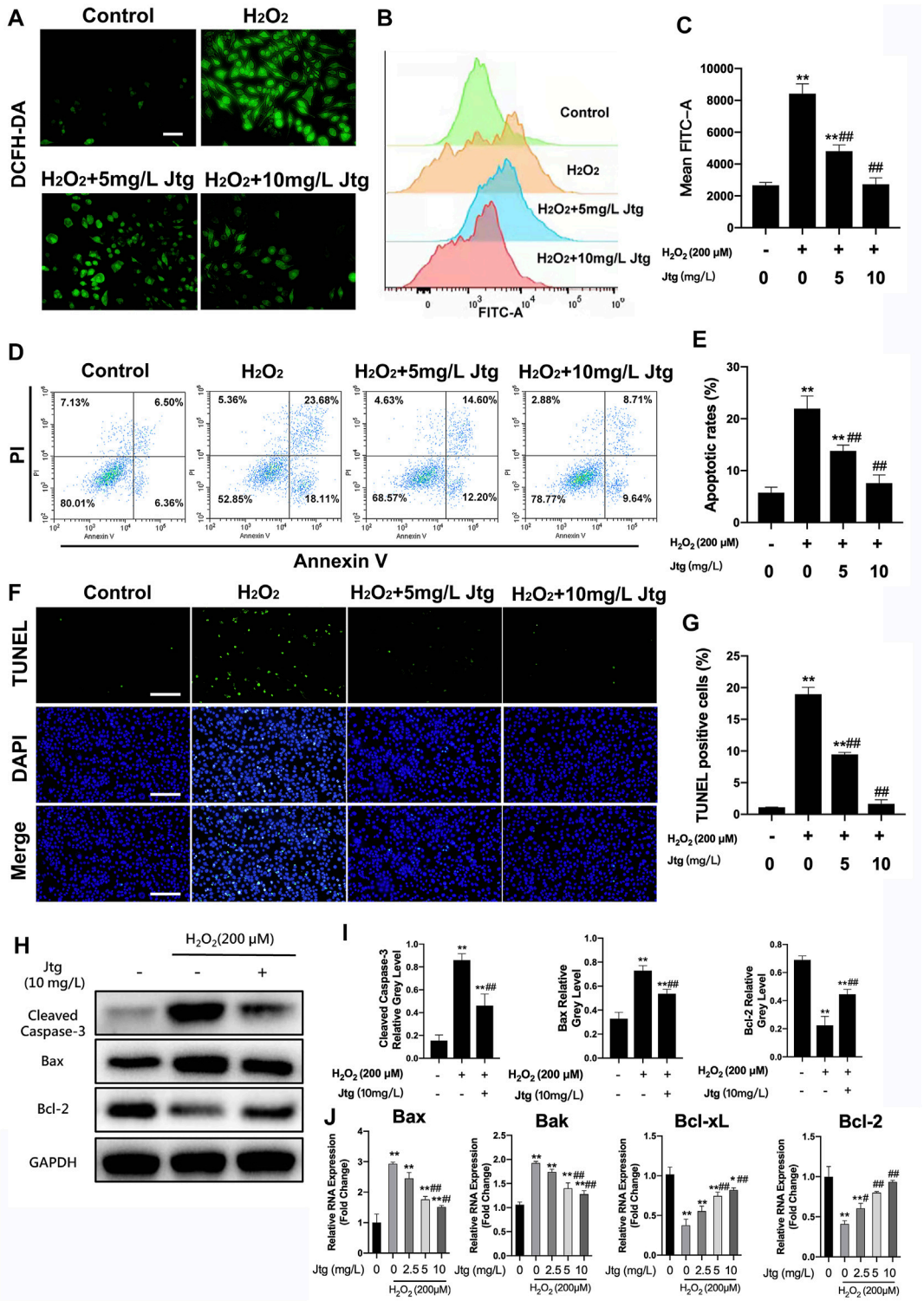

FIGURE 3 | Jtg ameliorates reactive oxygen species (ROS)-induced ATDC5 cell apoptosis. **(A)** The production of intracellular ROS detected by DCFH-DA probe, scale bar, 50 μm. **(B)** ROS positive cells were detected by flow cytometry and **(C)** demonstrated as mean FITC-A level. **(D)** Cell apoptosis assessed using flow cytometry and **(E)** statistical analysis. **(F)** Detection of apoptotic cells by TUNEL and DAPI staining assay, scale bar, 200 μm and **(G)** statistical analysis. **(H, I)** Western blot assay was performed to analyze the expression of apoptosis-related proteins, including Cleaved Caspase-3, Bax and Bcl-2. **(J)** The expression of apoptosis-related mRNA, including Bcl-2 and Bcl-xL (anti-apoptotic) and Bax and Bak (pro-apoptotic), was analyzed using RT-PCR. *Compared with the control group and #compared with the H_2O_2 without Jtg group ($^{*}p < 0.05$, $^{\#}p < 0.05$; $^{**}p < 0.01$, $^{\#\#}p < 0.01$).

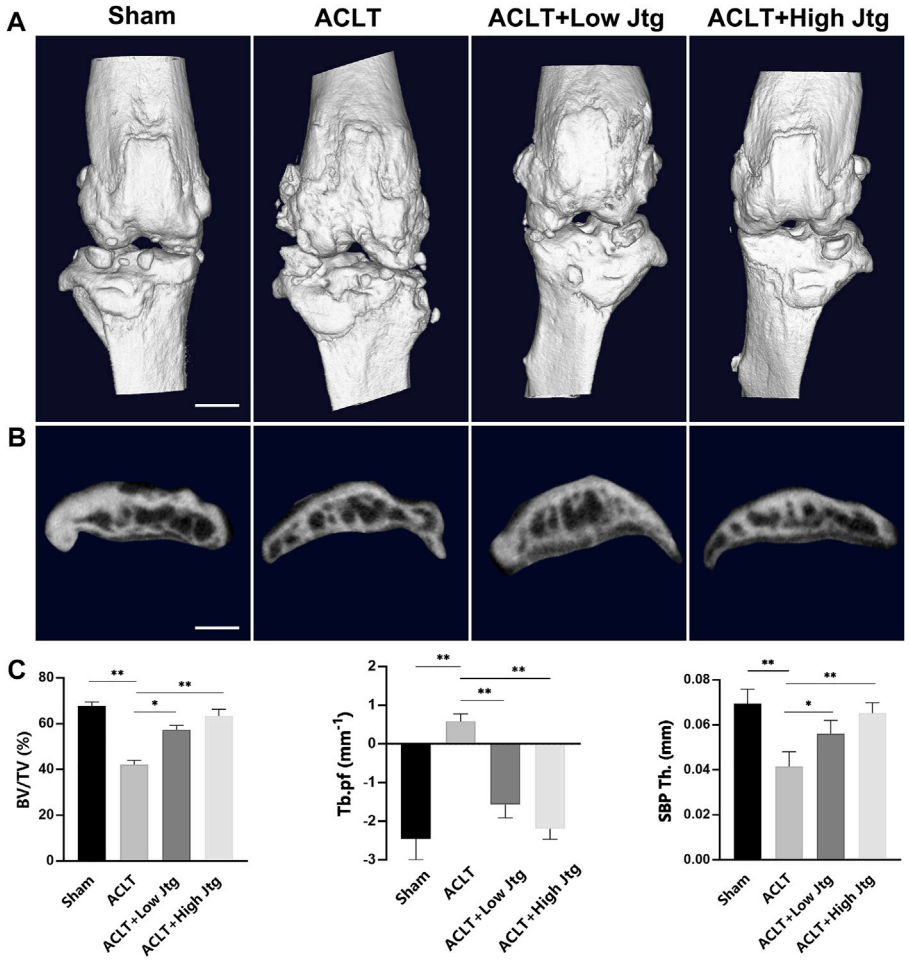

FIGURE 4 | Jtg relieves abnormal subchondral bone remodeling in a mouse anterior cruciate ligament transection (ACLT) model *in vivo*. **(A)** 3D micro-CT images of frontal views of the knee joints at 4 weeks after the sham operation or the ACLT operation. **(B)** 3D micro-CT images of sagittal views of subchondral bone medial compartment after sham operation or ACLT surgery, scale bar, 1 mm. **(C)** Quantitative micro-CT analysis of tibial subchondral bone of bone volume fraction (BV/TV), trabecular pattern factor (Tb.pf), and subchondral bone plate thickness (SBP Th). *Compared with the ACLT group (*$p < 0.05$; **$p < 0.01$).

ROS-induced ATDC5 apoptosis via its regulation of the expression of various apoptosis-related genes.

Jtg Sustains Coupled Subchondral Bone Remodeling *in vivo*

Given the positive outcomes in the *in vitro* assays we then explored the effects of Jtg on OA progression *in vivo* using an ACLT mouse model, one of the most common OA animal models. Micro-CT showed that ACLT injury induces significant subchondral bone resorption and osteophyte formation (**Figures 4A,B**). Both BV/TV and SBP Th. were significantly reduced in the ACLT group when compared with the Sham group, indicating the distinct influence of ACLT on subchondral bone mineralization and resorption. These animals also showed higher Tb. PF. Nevertheless, Jtg treatment restored these parameters and sustained coupled bone remodeling in a dose-dependent manner (**Figure 4C**).

Jtg Inhibits Early-Stage Osteoclastogenesis and Articular Cartilage Degeneration *in vivo*

Safranin O/Fast Green and H&E staining were combined with the OARSI score to evaluate ACLT induced cartilage degeneration in our model. ACLT surgery significantly reduced proteoglycan and destroyed articular cartilage over a 4-week period when compared to the sham treatment control (**Figures 5A,B,F**). Moreover, these animals experienced early hyperactivity of the osteoclasts as shown by increased TRAP staining in the ACLT group at 2 weeks post-operation when no significant deterioration in the cartilage could be detected (**Figures 5C,G**, **Supplementary Figure S4**). However, the severity of the OA in ACLT mice was relieved following treatment with Jtg, which significantly reduced both the number of lesions and the OARSI score. We also evaluated the degree of proteoglycan and matrix degradation in these animals using immunohistochemistry against both Aggrecan and MMP-13 (**Figures 5D,E**). These evaluations revealed that Jtg treatment reduced the level of matrix-degrading collagenases, including

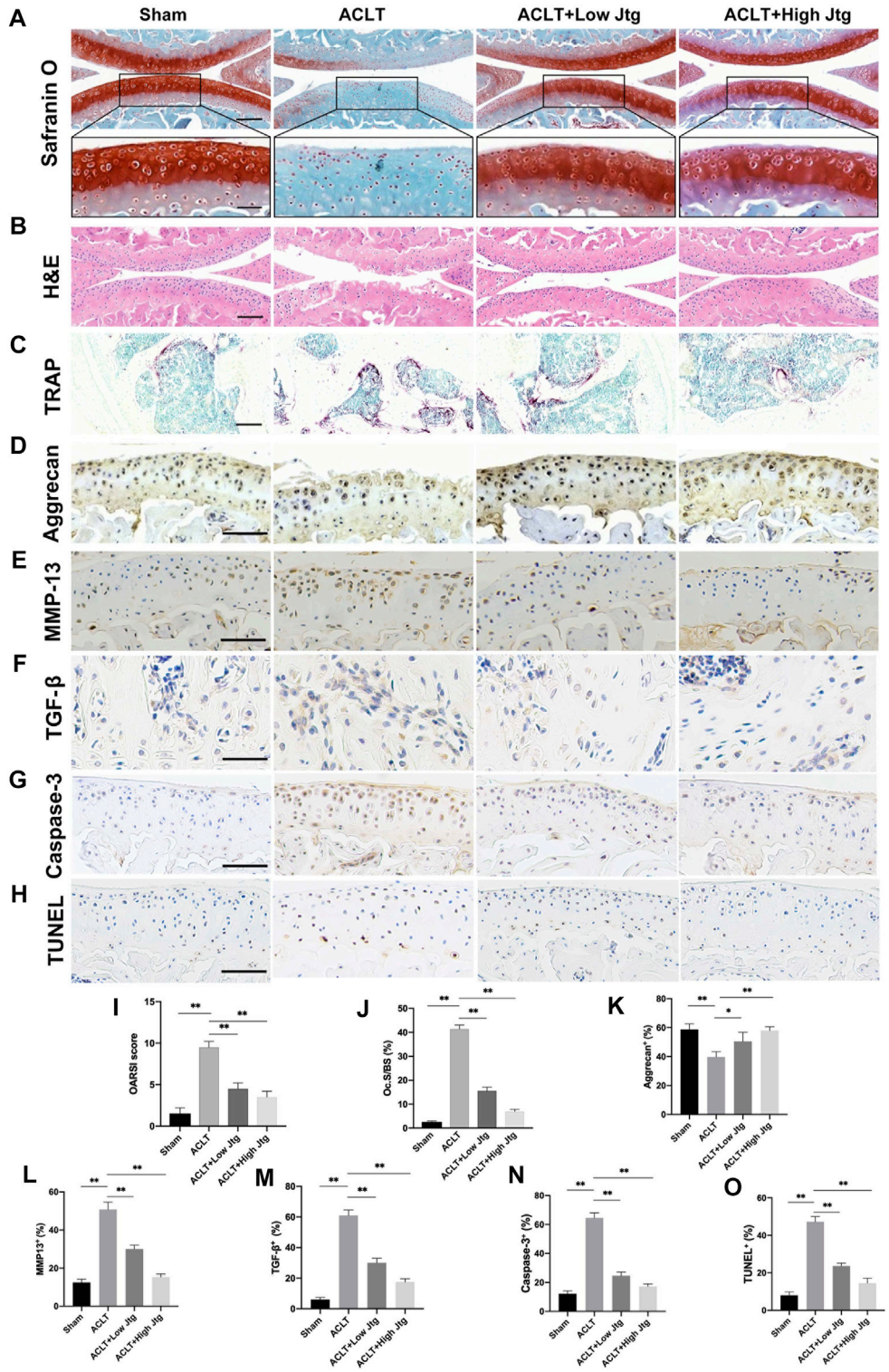

FIGURE 5 | Histological analysis of Jtg treatment in a mouse anterior cruciate ligament transection (ACLT) model *in vivo*. **(A)** Safranin O staining, scale bar, 200 μm (top panels); 100 μm (bottom panels). **(B)** HE staining, scale bar, 200 μm. **(C)** Tartrate-resistant acid phosphatase (TRAP) staining, scale bar, 200 μm. **(D–H)** Immunohistochemical staining of aggrecan, MMP-13, TGF-β, Caspase-3 and TUNEL expression, scale bar, 100 μm. **(I)** Osteoarthritis Research Society International (OARSI) score indicate cartilage degeneration at 4 weeks after the ACLT operation. **(J)** Quantitative analysis of osteoclast surface per millimeter bone perimeter (Oc.s/BS) indicate subchondral bone remodeling at 2 weeks after the ACLT operation. **(K–O)** The quantitative analysis of positive cells of aggrecan, MMP-13, TGF-β, Caspase-3, and TUNEL in each group. *Compared with the ACLT group (*$p < 0.05$; **$p < 0.01$).

MMP-13, in these samples while markedly increasing the level of Aggrecan (**Figures 5H,I**). Moreover, we observed highly expressed TGF-β through osteoclastogenesis in subchondral bone in ACLT mice was decreased by Jtg (**Figures 5F,M**). Caspase-3 and TUNEL staining demonstrated that Jtg mitigated chondrocyte apoptosis in degenerated cartilage in ACLT mice (**Figures 5G,H,N,O**). These findings indicate that Jtg relieves cartilage degradation and even early-stage OA while inhibiting subchondral bone resorption.

DISCUSSION

Traditional Chinese medicine is widely used to treat many chronic orthopedic diseases including osteoporosis, rheumatic arthritis, and OA, and it is known for its higher effectiveness and fewer side effects (Zhang et al., 2010; Lin et al., 2017; Wang et al., 2020). Jtg, a traditional medicine composed of various animal bones and organic compounds such as collagen and polysaccharides, has demonstrated outstanding efficacy in treating osteoporosis in various animal and clinical trials and is recommended for the treatment of osteoporosis in China. In addition, increasing evidence suggests that Jtg therapies may reduce bone loss and accelerate bone formation (Sun et al., 2019; Zhao et al., 2019; Zhao et al., 2021). When we combined this with the basic findings of several previous studies, we hypothesized that Jtg might also play a critical role in the treatment of another chronic orthopedic disease, OA.

Although originally thought to be restricted to the cartilage, OA is now recognized as a heterogeneous disease that affects various structures in the joint using a wide range of underlying mechanisms (Loeser et al., 2016). Osteochondral junctions play a pivotal role in the loadbearing and metabolism of the joint. As the important structure within the osteochondral junction, the subchondral bone undergoes extensive remodeling and changes all of which have been detected in early-stage OA prior to cartilage degradation by hybrid SPECT-CT, indicating its significant role in both the onset and progression of OA (Hügle and Geurts, 2017). Moreover, MRI revealed that more bone marrow lesions occur in the osteochondral junctions of OA patients which is likely a result of the increased remodeling of the subchondral bone in these joints and acts as a predictor of cartilage degeneration (Maas et al., 2015). Furthermore, accumulating evidence have shown that subchondral bone mainly undergoes a spatiotemporal uncoupled remodeling process which is notably characterized by macrophage infiltration and osteoclast activation in early-stage OA and concomitant increased osteoblast activity leading to spatial remineralization and osteosclerosis in end-stage disease (Yu et al., 2016; Jiang et al., 2021). In this study, we also attached great importance to the effects of Jtg on osteoclasts in early-stage OA. Given the close physical association between overlying cartilage and subchondral bone, the osteoclast-chondrocyte crosstalk in bone-cartilage microenvironment is a promising therapeutic target to restrain OA. Increasing evidence indicates that TGF-β plays a crucial role in osteoclast-chondrocyte crosstalk in onset of OA. Zhang et al. found that overexpression of TGF-β from osteoclasts in subchondral bone in response to altered mechanical loadings induced chondrocyte apoptosis and cartilage degeneration (Zhang et al., 2018). Moreover, Zhen et al. demonstrated that knockout of the TGF–β receptor and inhibition of TGF-β activity relieved osteoarthritis in ACLT mice (Zhen et al., 2013). Consistently, we observed aberrant TGF-β level was decreased by Jtg treatment in the subchondral bone in ACLT mice and alleviated chondrocyte apoptosis significantly, suggesting the pivotal role of Jtg in the regulation of osteoclast-chondrocyte crosstalk in OA.

Moreover, we also detected aberrant subchondral bone remodeling including decreased BV/TV and SBP Th, and increased Tb, PF, and TRAP-positive osteoclasts in early-stage OA which occurs before cartilage degradation, cementing the importance of subchondral bone remodeling in early-stage OA. Osteoclast hyperactivity is considered as the major hallmark of bone resorption. Specific interactions between RANKL and its receptor RANK play a crucial role in osteoclast formation and activation (Boyce and Xing, 2008). Meanwhile, downstream signaling transcription factors, such as NF-κB and MAPKs (p38, ERK, and JNK) are activated to further initiate osteoclastogenesis and bone resorption. Thus, any agent capable of blocking the expression of osteoclast-associated genes and signaling pathways or inhibiting RANKL/RANK interactions is likely to exert significant therapeutic effects on OA. Here, we found that Jtg suppressed RANKL-induced osteoclastogenesis in a dose-dependent manner and blocked the NF-κB signaling pathway by downregulating osteoclast-specific gene expression. This suggests that Jtg alleviates subchondral bone remodeling through the inhibition of osteoclast differentiation and activation.

As the most important constituent of cartilage, extracellular matrix components provide the tensile strength and compressive resilience facilitating the basic functionality of the joint (Rahmati et al., 2017). Increasing evidence suggests that extracellular matrix components including type II collagen and aggrecan are significantly reduced in the cartilage of OA patients. Chondrocytes, the only cells that populate avascular extracellular matrix components are responsible for this change in OA cartilage (Riegger and Brenner, 2020). As chemical byproducts of the mitochondrial electron transport chain, ROS are known to act as primary intermediates for many signaling pathways including cellular apoptosis (Zhang et al., 2016). A low-oxygen-tension environment helps to maintain the collagen turnover rate mediated by chondrocytes under physiological conditions. Oxidant-induced chondrocyte apoptosis, which is induced in response to excessive ROS generation, is known to be a crucial event in OA (Arra et al., 2020). Our findings suggest that Jtg treatment inhibits H_2O_2-induced chondrocyte apoptosis *in vitro*. We also showed that Jtg treatment reduced the expression level of matrix-degrading enzymes and increased the expression level of matrix proteins. Furthermore, both the Safranin O/Fast Green staining and H&E staining revealed similar outcomes *in vivo*. Thus, we also show that Jtg treatment can protect cartilage against degeneration through its inhibition of chondrocyte apoptosis.

There are several potential limitations in our study. First, the primary cells used in this study were obtained from mice instead

of humans, so it is necessary to use human cells in future studies to make our results more reliable. And we just studied the potential effects of Jtg on the NF-κB and MAPK pathway, we should also detect other mediators and signaling pathways involved in the pharmacologic mechanism of Jtg in future studies.

In summary, this study demonstrates, for the first time, that Jtg treatment effectively inhibits osteoclast differentiation and activation by inhibiting NF-κB signaling cascades and ROS-induced chondrocyte apoptosis. These dual effects eventually ameliorate the subchondral bone remodeling and cartilage degeneration associated with OA in ACTL mouse models. Taken together, these results suggest that Jtg is a potential alternative therapeutic agent for attenuating early-stage OA.

DATA AVAILABILITY STATEMENT

The original contributions presented in the study are included in the article/**Supplementary Material**, further inquiries can be directed to the corresponding authors.

ETHICS STATEMENT

The animal study was reviewed and approved by the Animal Ethical Committee of Zhongshan Hospital, Fudan University (2019-065).

AUTHOR CONTRIBUTIONS

CZ and ZW designed the research and wrote the manuscript. CZ, ZW, WC, and HW performed the experiments and analyzed the data. BT and HL revised the manuscript and guided the research.

FUNDING

This study was supported by the Natural Science Foundation of Shanghai (21ZR1455800), the Non-profit Central research Institute Fund of Chinese academy of Medical sciences (2020-JKCS-013), the Research Start-up Fund of Fudan University(267) and the Shanghai Sailing Program (18YF1404400).

ACKNOWLEDGMENTS

The authors appreciate all participants of this study for their selfless participation and dedication. We would like to thank Editage (www.editage.cn) for English language editing.

SUPPLEMENTARY MATERIAL

The Supplementary Material for this article can be found online at: https://www.frontiersin.org/articles/10.3389/fphar.2021.762543/full#supplementary-material

REFERENCES

Arden, N. K., Perry, T. A., Bannuru, R. R., Bruyère, O., Cooper, C., Haugen, I. K., et al. (2021). Non-surgical Management of Knee Osteoarthritis: Comparison of ESCEO and OARSI 2019 Guidelines. *Nat. Rev. Rheumatol.* 17 (1), 59–66. doi:10.1038/s41584-020-00523-9

Arra, M., Swarnkar, G., Ke, K., Otero, J. E., Ying, J., Duan, X., et al. (2020). LDHA-mediated ROS Generation in Chondrocytes Is a Potential Therapeutic Target for Osteoarthritis. *Nat. Commun.* 11 (1), 3427. doi:10.1038/s41467-020-17242-0

Bijlsma, J. W., Berenbaum, F., and Lafeber, F. P. (2011). Osteoarthritis: an Update with Relevance for Clinical Practice. *Lancet* 377 (9783), 2115–2126. doi:10.1016/s0140-6736(11)60243-2

Bolduc, J. A., Collins, J. A., and Loeser, R. F. (2019). Reactive Oxygen Species, Aging and Articular Cartilage Homeostasis. *Free Radic. Biol. Med.* 132, 73–82. doi:10.1016/j.freeradbiomed.2018.08.038

Boyce, B. F., and Xing, L. (2008). Functions of RANKL/RANK/OPG in Bone Modeling and Remodeling. *Arch. Biochem. Biophys.* 473 (2), 139–146. doi:10.1016/j.abb.2008.03.018

Glyn-Jones, S., Palmer, A. J., Agricola, R., Price, A. J., Vincent, T. L., Weinans, H., et al. (2015). Osteoarthritis. *Lancet* 386 (9991), 376–387. doi:10.1016/s0140-6736(14)60802-3

Goldring, M. B., and Goldring, S. R. (2010). Articular Cartilage and Subchondral Bone in the Pathogenesis of Osteoarthritis. *Ann. N. Y Acad. Sci.* 1192, 230–237. doi:10.1111/j.1749-6632.2009.05240.x

Goldring, S. R. (2009). Role of Bone in Osteoarthritis Pathogenesis. *Med. Clin. North. Am.* 93 (1), 25–35,xv. doi:10.1016/j.mcna.2008.09.006

Hochberg, M. C., Yerges-Armstrong, L., Yau, M., and Mitchell, B. D. (2013). Genetic Epidemiology of Osteoarthritis: Recent Developments and Future Directions. *Curr. Opin. Rheumatol.* 25 (2), 192–197. doi:10.1097/BOR.0b013e32835cfb8e

Hu, W., Chen, Y., Dou, C., and Dong, S. (2020). Microenvironment in Subchondral Bone: Predominant Regulator for the Treatment of Osteoarthritis. *Ann. Rheum. Dis.* 80 (4), 413–422. doi:10.1136/annrheumdis-2020-218089

Hügle, T., and Geurts, J. (2017). What Drives Osteoarthritis?-Synovial versus Subchondral Bone Pathology. *Rheumatology (Oxford)* 56 (9), 1461–1471. doi:10.1093/rheumatology/kew389

Hunter, D. J., and Bierma-Zeinstra, S. (2019). Osteoarthritis. *Lancet* 393 (10182), 1745–1759. doi:10.1016/s0140-6736(19)30417-9

Jiang, A., Xu, P., Sun, S., Zhao, Z., Tan, Q., Li, W., et al. (2021). Cellular Alterations and Crosstalk in the Osteochondral Joint in Osteoarthritis and Promising Therapeutic Strategies. *Connect. Tissue Res.* 17, 1–11. doi:10.1080/03008207.2020.1870969

Kong, X. Y., and Wen, C. P. (2019). On Research Progress of Western and Chinese Medicine Treatment on Pre-rheumatoid Arthritis. *Chin. J. Integr. Med.* 25 (9), 643–647. doi:10.1007/s11655-019-3223-3

Lepetsos, P., and Papavassiliou, A. G. (2016). ROS/oxidative Stress Signaling in Osteoarthritis. *Biochim. Biophys. Acta* 1862 (4), 576–591. doi:10.1016/j.bbadis.2016.01.003

Lin, J., Zhu, J., Wang, Y., Zhang, N., Gober, H. J., Qiu, X., et al. (2017). Chinese Single Herbs and Active Ingredients for Postmenopausal Osteoporosis: From Preclinical Evidence to Action Mechanism. *Biosci. Trends* 11 (5), 496–506. doi:10.5582/bst.2017.01216

Litwic, A., Edwards, M. H., Dennison, E. M., and Cooper, C. (2013). Epidemiology and burden of Osteoarthritis. *Br. Med. Bull.* 105, 185–199. doi:10.1093/bmb/lds038

Livshits, G., Ermakov, S., Popham, M., Macgregor, A. J., Sambrook, P. N., Spector, T. D., et al. (2010). Evidence that Bone mineral Density Plays a Role in Degenerative Disc Disease: the UK Twin Spine Study. *Ann. Rheum. Dis.* 69 (12), 2102–2106. doi:10.1136/ard.2010.131441

Loeser, R. F., Collins, J. A., and Diekman, B. O. (2016). Ageing and the Pathogenesis of Osteoarthritis. *Nat. Rev. Rheumatol.* 12 (7), 412–420. doi:10.1038/nrrheum.2016.65

Ma, D., Zhu, W., Liang, X., Long, Z., Wang, N., Zhang, W., et al. (2011). Effects of Enzymatic Bone Powder on Calcium Absorption and Bone Density in Rats. *Wei Sheng Yan Jiu* 40 (4), 492–494. doi:10.19813/j.cnki.weishengyanjiu.2011.04.024

Maas, O., Joseph, G. B., Sommer, G., Wild, D., and Kretzschmar, M. (2015). Association between Cartilage Degeneration and Subchondral Bone Remodeling in Patients with Knee Osteoarthritis Comparing MRI and (99m)Tc-DPD-SPECT/CT. *Osteoarthritis Cartilage* 23 (10), 1713–1720. doi:10.1016/j.joca.2015.05.014

Meachim, G., Ghadially, F. N., and Collins, D. H. (1965). Regressive Changes in the Superficial Layer of Human Articular Cartilage. *Ann. Rheum. Dis.* 24 (1), 23–30. doi:10.1136/ard.24.1.23

Meachim, G. (1964). Sulphate Metabolism of Articular Cartilage after Surgical Interference with the Joint. *Ann. Rheum. Dis.* 23 (5), 372–380. doi:10.1136/ard.23.5.372

Rahmati, M., Nalesso, G., Mobasheri, A., and Mozafari, M. (2017). Aging and Osteoarthritis: Central Role of the Extracellular Matrix. *Ageing Res. Rev.* 40, 20–30. doi:10.1016/j.arr.2017.07.004

Riegger, J., and Brenner, R. E. (2020). Pathomechanisms of Posttraumatic Osteoarthritis: Chondrocyte Behavior and Fate in a Precarious Environment. *Int. J. Mol. Sci.* 21 (5), 1560. doi:10.3390/ijms21051560

Sun, J., Yang, X. G., and Hu, Y. C. (2019). Efficacy of Jintiange Capsules in the Treatment of Osteoporosis: A Network Meta-Analysis. *Orthop. Surg.* 11 (2), 176–186. doi:10.1111/os.12439

Suntornsaratoon, P., Charoenphandhu, N., and Krishnamra, N. (2018). Fortified Tuna Bone Powder Supplementation Increases Bone mineral Density of Lactating Rats and Their Offspring. *J. Sci. Food Agric.* 98 (5), 2027–2034. doi:10.1002/jsfa.8688

Tang, C. H. (2019). Research of Pathogenesis and Novel Therapeutics in Arthritis. *Int. J. Mol. Sci.* 20 (7), 1646. doi:10.3390/ijms20071646

Wang, M., Liu, L., Zhang, C. S., Liao, Z., Jing, X., Fishers, M., et al. (2020). Mechanism of Traditional Chinese Medicine in Treating Knee Osteoarthritis. *J. Pain Res.* 13, 1421–1429. doi:10.2147/jpr.S247827

Wu, Y. R., Kuang, G. Y., Lu, F. G., Wang, H. X., Lu, M., and Zhou, Q. (2019). Pathological Relationship between Intestinal Flora and Osteoarthritis and Intervention Mechanism of Chinese Medicine. *Chin. J. Integr. Med.* 25 (9), 716–720. doi:10.1007/s11655-019-3224-2

Yao, Y., and Wang, Y. (2013). ATDC5: an Excellent *In Vitro* Model Cell Line for Skeletal Development. *J. Cel Biochem.* 114 (6), 1223–1229. doi:10.1002/jcb.24467

Yu, D., Xu, J., Liu, F., Wang, X., Mao, Y., and Zhu, Z. (2016). Subchondral Bone Changes and the Impacts on Joint Pain and Articular Cartilage Degeneration in Osteoarthritis. *Clin. Exp. Rheumatol.* 34 (5), 929–934.

Zhang, P., Li, J., Han, Y., Yu, X. W., and Qin, L. (2010). Traditional Chinese Medicine in the Treatment of Rheumatoid Arthritis: a General Review. *Rheumatol. Int.* 30 (6), 713–718. doi:10.1007/s00296-010-1370-0

Zhang, J., Wang, X., Vikash, V., Ye, Q., Wu, D., Liu, Y., et al. (2016). ROS and ROS-Mediated Cellular Signaling. *Oxid Med. Cel Longev* 2016, 4350965. doi:10.1155/2016/4350965

Zhang, R. K., Li, G. W., Zeng, C., Lin, C. X., Huang, L. S., Huang, G. X., et al. (2018). Mechanical Stress Contributes to Osteoarthritis Development through the Activation of Transforming Growth Factor Beta 1 (TGF-β1). *Bone Jt. Res.* 7 (11), 587–594. doi:10.1302/2046-3758.711.BJR-2018-0057.R1

Zhao, Y. R., Wei, X., Jiang, J. J., Zhang, Y. L., Wang, S. Q., and Xie, Y. M. (2019). Systemic Review of Jintiange Capsules in Treatment of Postmenopausal Osteoporosis. *Zhongguo Zhong Yao Za Zhi* 44 (1), 186–192. doi:10.19540/j.cnki.cjcmm.20180709.007

Zhao, J., Zeng, L., Wu, M., Huang, H., Liang, G., Yang, W., et al. (2021). Efficacy of Chinese Patent Medicine for Primary Osteoporosis: A Network Meta-Analysis. *Complement. Ther. Clin. Pract.* 44, 101419. doi:10.1016/j.ctcp.2021.101419

Zhen, G., Wen, C., Jia, X., Li, Y., Crane, J. L., Mears, S. C., et al. (2013). Inhibition of TGF-β Signaling in Mesenchymal Stem Cells of Subchondral Bone Attenuates Osteoarthritis. *Nat. Med.* 19 (6), 704–712. doi:10.1038/nm.3143

Zhou, F., Mei, J., Yuan, K., Han, X., Qiao, H., and Tang, T. (2019). Isorhamnetin Attenuates Osteoarthritis by Inhibiting Osteoclastogenesis and Protecting Chondrocytes through Modulating Reactive Oxygen Species Homeostasis. *J. Cel Mol Med.* 23 (6), 4395–4407. doi:10.1111/jcmm.14333

Conflict of Interest: The authors declare that the research was conducted in the absence of any commercial or financial relationships that could be construed as a potential conflict of interest.

Publisher's Note: All claims expressed in this article are solely those of the authors and do not necessarily represent those of their affiliated organizations, or those of the publisher, the editors and the reviewers. Any product that may be evaluated in this article, or claim that may be made by its manufacturer, is not guaranteed or endorsed by the publisher.

Copyright © 2021 Zhuang, Wang, Chen, Wang, Tian and Lin. This is an open-access article distributed under the terms of the Creative Commons Attribution License (CC BY). The use, distribution or reproduction in other forums is permitted, provided the original author(s) and the copyright owner(s) are credited and that the original publication in this journal is cited, in accordance with accepted academic practice. No use, distribution or reproduction is permitted which does not comply with these terms.

frontiers in Pharmacology

CLINICAL TRIAL
published: 23 November 2021
doi: 10.3389/fphar.2021.773758

The Therapeutic Effect of Huo Xue Tong Luo Capsules in Association Research Circulation Osseous (ARCO) Stage II Osteonecrosis of the Femoral Head: A Clinical Study With an Average Follow-up Period of 7.95 Years

Xiao-Ming He[1,2†], Min-Cong He[1,2†], Peng Yang[1,2], Qing-Wen Zhang[1,2], Zhen-Qiu Chen[3], Wei He[1,2] and Qiu-Shi Wei[1,2*]*

[1]Guangdong Research Institute for Orthopedics and Traumatology of Chinese Medicine, Guangzhou, China, [2]Joint Center, The Third Affiliated Hospital of Guangzhou University of Chinese Medicine, Guangzhou, China, [3]The Third Orthopaedic Region, The First Affiliated Hospital of Guangzhou University of Chinese Medicine, Guangzhou, China

Background: Huo Xue Tong Luo (HXTL) capsules are an oral preparation that could relieve pain and ameliorate osteonecrosis in patients with asymptomatic osteonecrosis of femoral head (ONFH). We wanted to verify whether it could be a treatment option for ARCO stage II ONFH.

Methods: A total of 44 patients (66 hips) with ARCO stage II ONFH were recruited from June 1996 to October 2013 (clinical trial registry number: ChiCTR-RPC-15006,290). HXTL capsules were given under a specific protocol, and the endpoint was set as femoral head collapse. The clinical indicators [including visual analog scale (VAS) and Harris Hip Score (HHS)] and radiological indicators [including Tonnis classification, ARCO stage, Japanese Investigation Committee (JIC) classification, lateral preserved angle (LPA), anterior preserved angle (APA), and combined preserved angle (CPA)] before and after treatment were compared. Kaplan–Meier survival analysis and Cox regression analysis were used to identify the risk factors associated with femoral head collapse.

Result: Twenty-six males and 18 females with an average age of 38.3 ± 2.8 were followed for an average of 7.95 years. Forty-six of the 66 (69.7%) hips had no progression in pain or collapse, and patients exhibited a higher HHS ($p < 0.05$) after therapy. Twenty of the 66 (30.3%) hips progressed in Tonnis classification and ARCO stage, but only one of the 66 (1.5%) hips required total hip arthroplasty (THA). The Kaplan–Meier survivorship curve suggested that the survival rates were 96.97% at 5 years, 69.15% at 10 years, and 40.33% at 15 years. Patients with type A necrotic lesions on anteroposterior (AP) and frog-leg lateral (FLL) radiographs revealed 100% survival rates. Multivariate Cox regression analysis revealed that patients with an LPA ≤ 60.9 exhibited a 3.87 times higher risk of collapse of the femoral head [95% confidence interval (CI), 1.241–5.673] than did those patients with an LPA>60.9.

OPEN ACCESS

Edited by:
Daohua Xu,
Guangdong Medical University, China

Reviewed by:
Weiheng Chen,
Beijing University of Chinese Medicine, China
Zhang Peng,
Shenzhen Institutes of Advanced Technology (CAS), China
Yajun Yang,
Guangdong Medical University, China

***Correspondence:**
Wei He
hw13802516062@163.com
Qiu-Shi Wei
weiqshi@126.com

[†]These authors have contributed equally to this work and share first authorship

Specialty section:
This article was submitted to Ethnopharmacology, a section of the journal Frontiers in Pharmacology

Received: 10 September 2021
Accepted: 01 November 2021
Published: 23 November 2021

Citation:
He X-M, He M-C, Yang P, Zhang Q-W, Chen Z-Q, He W and Wei Q-S (2021) The Therapeutic Effect of Huo Xue Tong Luo Capsules in Association Research Circulation Osseous (ARCO) Stage II Osteonecrosis of the Femoral Head: A Clinical Study With an Average Follow-up Period of 7.95 Years. Front. Pharmacol. 12:773758. doi: 10.3389/fphar.2021.773758

Conclusion: HXTL capsules could be a treatment option for ARCO stage II ONFH, resulting in improved hip function and delayed progression to femoral head collapse, especially when the anterior and lateral portions of the femoral head were not affected. However, an LPA of less than 60.9° may be a risk factor for collapse of the femoral head.

Clinical Trial Registration: http://www.chictr.org.cn/showproj.aspx?proj=10829, identifier ChiCTR-OPC-15007030

Keywords: osteonecrosis of femoral head, ARCO stage II, therapeutic effect, risk factor, huo xue tong luo capsules

INTRODUCTION

Osteonecrosis of femoral head (ONFH) commonly occurs in young and middle-aged adults and is associated with impaired blood supply to the femoral head secondary to the use of glucocorticoids or other factors (Cohen-Rosenblum and Cui, 2019). The literature reports that there are approximately 20 million patients with femoral head necrosis worldwide, and the number of ONFH patients in China is approximately five to seven million, increasing at a rate of 100,000–200,000 per year (Cui et al., 2016). "Necrosis–repair–collapse–osteoarthritis" is the natural pathological process that is followed by most patients with ONFH (Chen et al., 2020). There are a variety of hip preservation methods for the treatment of ONFH before collapse occurs (Mont et al., 2015). Even if there are widespread necrotic lesions, it is possible to prevent collapse. However, once collapse occurs, the treatment options are limited (Wei QS. et al., 2019; Chen et al., 2020). Studies show that Chinese herbal medicine has the potential to improve the blood flow to the necrotic femoral head, which is critical for the preservation of the hip (Wang et al., 2011; Jiang et al., 2015; Yu et al., 2016; Zhang et al., 2018). Huo Xue Tong Luo (HXTL) capsules, containing seven vasoactive herbal compounds, have been shown to delay joint collapse in patients with asymptomatic ONFH (Wei QS. et al., 2019). Because the active ingredients in HXTL capsules have been proven to promote angiogenesis, they have great potential in the treatment of ONFH (Hong et al., 2019).

Patients with ONFH tend to be young and active, and they generally have a higher rate of revision after total hip arthroplasty (THA)) which means that they are likely to have higher medical costs and experience greater physical and mental stress (Ancelin et al., 2016; Moerman et al., 2018; Kuijpers et al., 2019; Boontanapibul et al., 2020). Especially in China, due to the great social and economic pressures on young people, not all patients with ONFH can afford THA, and conservative treatment is a relatively acceptable option for them. Therefore, it is necessary to find new methods to delay the need for, or even avoid, THA (Sodhi et al., 2020). In an *in vitro* experiment examining femoral head samples, we found that the RNA level of myocardial infarction-associated transcript (Miat) in necrotic tissue was much higher than that in normal tissue and that silencing endogenous lncRNA-Miat could promote the osteogenesis of rat bone marrow mesenchymal stem cells (rBMSCs). PCR and ChIP assays showed that HXTL capsules promoted osteogenesis in rBMSCs, significantly increasing the presence of H3K27me3 and decreasing the presence of H3K4me3 in the promoter regions of Miat, demonstrating that HXTL capsules inhibited Miat expression through histone modifications. This indicates that HXTL capsules can promote osteogenesis to ameliorate ONFH by inhibiting the transcriptional expression of Miat (Fang et al., 2019). In a previous clinical trial, we used HXTL capsules to treat asymptomatic ONFH patients, and the results showed that HXTL capsules can significantly relieve pain in patients who become symptomatic and suppress necrosis progression toward femoral head collapse in the short to mid term (Wei QS. et al., 2019). Hence, we designed this clinical study to assess the therapeutic effect of HXTL capsules and reveal the risk factors related to the collapse of the femoral head to further determine whether HXTL can be an optimal treatment for ARCO stage II ONFH.

MATERIALS AND METHODS

Inclusion and Exclusion Criteria for the Clinical Study Participants

The inclusion criteria were as follows: 1) patients with ARCO stage II ONFH diagnosed by physical examination, magnetic resonance imaging (MRI), and X-ray imaging (Yoon et al., 2020) and 2) patients who had not previously received systemic treatment. The exclusion criteria were as follows: 1) patients who were allergic to HXTL capsules; 2) patients who had undergone previous hip surgery or hip injection; 3) patients with a history of hip, femoral head, or femoral neck trauma; 4) patients with severe congenital malformation of the hip joint; 5) patients with severe bone metabolic disease; 6) patients with any diseases that could affect the hip joint, including rheumatoid arthritis, ankylosing spondylitis, joint tuberculosis, and pyogenic arthritis; and 7) patients with Type C2 necrosis lesions according to the JIC classification criteria [for which surgery is often required (Kuroda et al., 2019; Yoon et al., 2020)].

Treatment

HXTL capsules are a vasoactive herbal preparation (institutional approval number: Z20071224) that improves the blood supply to the femoral head, promoting tissue regeneration and removing obstruction. It has been used in the clinical treatment of ONFH for more than 20 years and is made up of seven herbs, including Cajan leaf, *Angelica sinensis* (Oliv.) Diels, *Paeonia lactiflora* Pall, *Ligusticum striatum* DC, *Prunus persica* (L.) Batsch, *Carthamus tinctorius* L, and *Rehmannia glutinosa* (Gaertn.) DC (Wei QS. et al., 2019). According to the theory of traditional Chinese medicine, "obstruction leads to pain" and blood stasis can lead to local blood blockage, which is one of the causes of pain in patients with ONFH. The function of HXTL capsules is to promote qi and blood

circulation, which can reduce the state of obstruction in the femoral head and thus relieve pain. Our treatment protocol was as follows: in addition to taking HXTL capsules orally three times a day (6 g/day), patients were also required to follow personalized restricted weight-bearing protocols. After bilateral hip X-ray examination in the AP and FLL positions, we assessed the location of the necrosis and bone repair, from which we developed a restricted load-bearing regimen. Asymptomatic patients with necrotic lesions not located in the weight-bearing area were allowed to walk using the normal weight-bearing areas, and regular examinations were conducted. Patients with pain and necrosis lesions that involved the weight-bearing area were advised to walk with crutches until their pain was relieved and the bone repair was complete. During follow-up, if the patient developed progressively increasing pain, it was recommended that he or she visit the hospital for further examination to determine whether the femoral head had collapsed. Disease progression has reached its endpoint when the femoral head collapses. If the femoral head did not collapse, then the patient was instructed to reduce activity and strictly follow our treatment protocol. During follow-up, all patients adjusted their treatment regimens according to the state of their bone repair. The flowchart is shown in **Figure 1**.

Clinical and Radiological Evaluations

We used the VAS and Harris Hip Score (HHS) as clinical efficacy indices to evaluate clinical function before and after treatment (Reed and Van Nostran, 2014; Hoeksma et al., 2003). The radiological evaluation included Tonnis classification, ARCO stage, JIC classification, LPA, APA, and CPA. Tonnis classification directly reflects the actual situation of hip osteoarthritis: Grade 0 means that there are no signs of osteoarthritis in hip; Grade 1 indicates slight narrowing of the joint space, slight lipping at the joint margin, and slight sclerosis of hip joint (the femoral head or acetabulum); Grade 2 indicates that small bony cysts are present on the femoral head or acetabulum, further narrowing the joint space, and that moderate flattening of the femoral head is present; Grade 3 indicates that severe deformity of the femoral head is present, with large cysts and severe narrowing of the joint space (Kovalenko et al., 2018). In the 2001 JIC classification, a type A necrotic lesion involves the medial one-third or less of the weight-bearing portion of the femoral head; a type B lesion indicates a necrotic lesion occupying the medial two-thirds or less of the weight-bearing portion; a type C lesion occupies more than the medial two-thirds of the weight-bearing portion; and type C lesions are further divided into C1 (necrotic lesions that do not extend laterally to the acetabular edge) and C2 (necrotic lesion that extends laterally to the acetabular edge) (Sugano et al., 2002). Because type C2 ONFH warrants surgery, only patients with type C1 were included in this study, and type C in this article refers only to type C1 (Kuroda et al., 2019). In addition, according to the results from our previous study, JIC classification on FLL radiographs is of clinical significance (Wei QS. et al., 2019; Wei et al., 2018). Therefore, we focused on the location of the necrotic lesions on both AP and FLL X-rays of the hip joint (**Figure 2**). For the AP X-rays, patients were positioned supine on the X-ray table, with both legs abducted in a neutral position so that their two feet were shoulder width apart. For the FLL X-rays, patients were positioned supine on the X-ray table, and the bilateral hips were flexed 30°. The thigh was abducted and externally rotated while ensuring that the feet contacted each other at the level of the ipsilateral knee. The X-ray beam was directed anterior to posterior and centered on the femoral head, while the plane of the pelvis was parallel to the plane of the table (**Figure 3**) (Wei et al., 2019b). Furthermore, to investigate the correlation between collapse and integrity of the anterior and lateral portion of the femoral head, the LPA (the larger the LPA, the smaller the necrotic lesion on the lateral portion of the femoral head) (**Figure 4A, C**), APA (the greater the APA, the smaller the necrotic lesion on the anterior portion of femoral head) (**Figure 4B, D**), and CPA (equal to the sum of LPA and APA; the larger the CPA, the smaller the necrotic lesion on the anterior and lateral portions of the femoral head) of the ONFH patients with and without collapse were measured and compared.

All patients were assessed clinically and radiologically every 3 months for the first 2 years, and annually thereafter, until the time of femoral head collapse. Each assessment was performed by two orthopedic surgeons specializing in ONFH. If the results were inconsistent, they were reviewed by two other, more senior, orthopedic surgeons with more experience, until the results were consistent.

Statistical Analysis

Measurement data are expressed as the mean ± standard deviation. We used SPSS (version 24.0.0, SPSS Inc., Chicago, IL, USA) to analyze the data. A p value of less than 0.05 was considered statistically significant. We performed ROC curve analysis to explore the sensitivity and specificity of LPA, APA, and CPA in predicting femoral head collapse. Kaplan–Meier survival analysis and Cox regression analysis were used to identify the survival rate and the risk factors associated with collapse (including the location of necrosis in AP and FFL views, Tonnis classification, VAS, HHS, LPA, APA, and CPA).

RESULTS

A total of 44 patients with ARCO stage II ONFH were enrolled from June 1996 to October 2013, including 26 men and 18 women with an average age of 38.3 ± 2.8 years (range, 19–63 years). A total of 66 affected hips were included: 22 patients had bilateral ONFH, and 22 had unilateral ONFH. Thirty-seven patients had steroid-induced ONFH (SONFH), 20 patients had alcohol-associated ONFH (AONFH), and nine patients were diagnosed with idiopathic ONFH (IONFH) without obvious cause. According to the JIC classification criteria revised in 2019, there were 23 hips with type A, 25 hips with type B, and 18 hips with type C necrotic lesions in AP radiographs, and there were 19 hips with type A, 26 hips with type B, and 21 hips with type C necrotic lesions in FLL radiographs.

In terms of the clinical efficacy of this study, 46 of the 66 hips (69.7%) had no progression in pain (**Figure 5A**), while there was also no significant difference in the degree of pain before and after treatment (**Figure 5B**). In terms of the radiological efficacy, 46 of

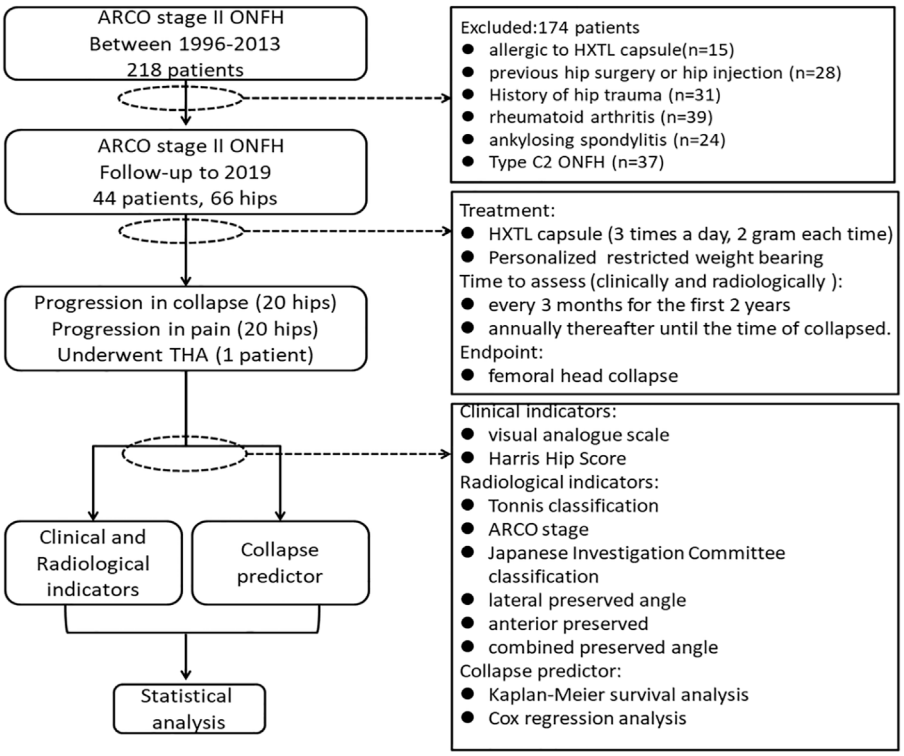

FIGURE 1 | Flowchart of the study.

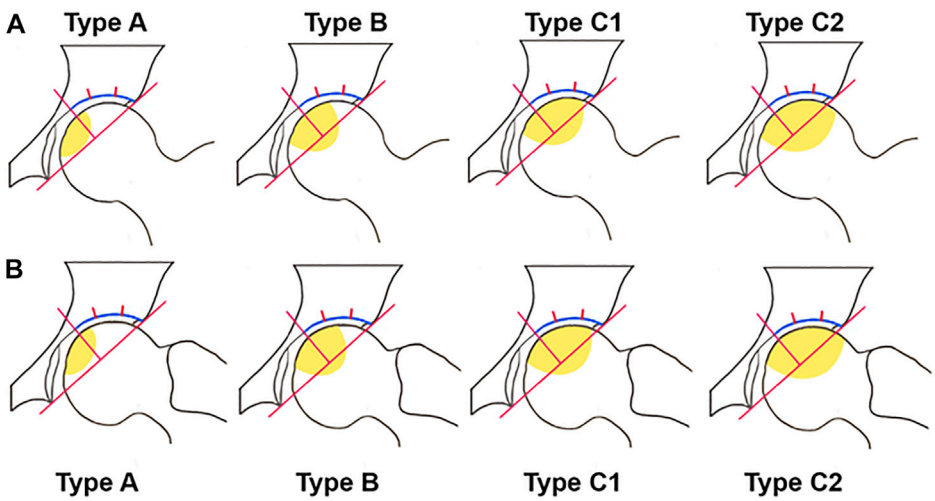

FIGURE 2 | JIC classification. **(A)** JIC classification in AP view. **(B)** JIC classification in FLL view. Type A: necrotic lesion involved the medial one-third or less of the weight-bearing portion; Type B: necrotic lesion occupies the medial two-thirds or less of the weight-bearing portion; Type C1: necrotic lesion occupies more than the medial two-thirds of the weight-bearing portion but does not extend laterally to the acetabular edge; Type C2: necrotic lesion occupies more than the medial two-thirds of the weight-bearing portion and extends laterally to the acetabular edge (Sugano et al., 2002; Wei et al., 2018; Wei QS. et al., 2019).

the 66 femoral heads (69.7%) showed no progression toward collapse (**Figure 5C**). Ten of the 20 cases with collapsed femoral heads showed no worsening of pain or hip function, while 10 of the 20 experienced pain progression and increasing hip dysfunction (**Figure 5D**). Nine patients progressed to Tonnis grade 1 from Tonnis grade 0. Two patients progressed to Tonnis grade 2 from Tonnis grade 0, and eight patients progressed to Tonnis grade 2 from Tonnis grade 1. One patient had progressed to Tonnis grade 3 from Tonnis grade 2 and underwent THA (**Figure 5E**). At the end of follow-up, 17 patients had progressed

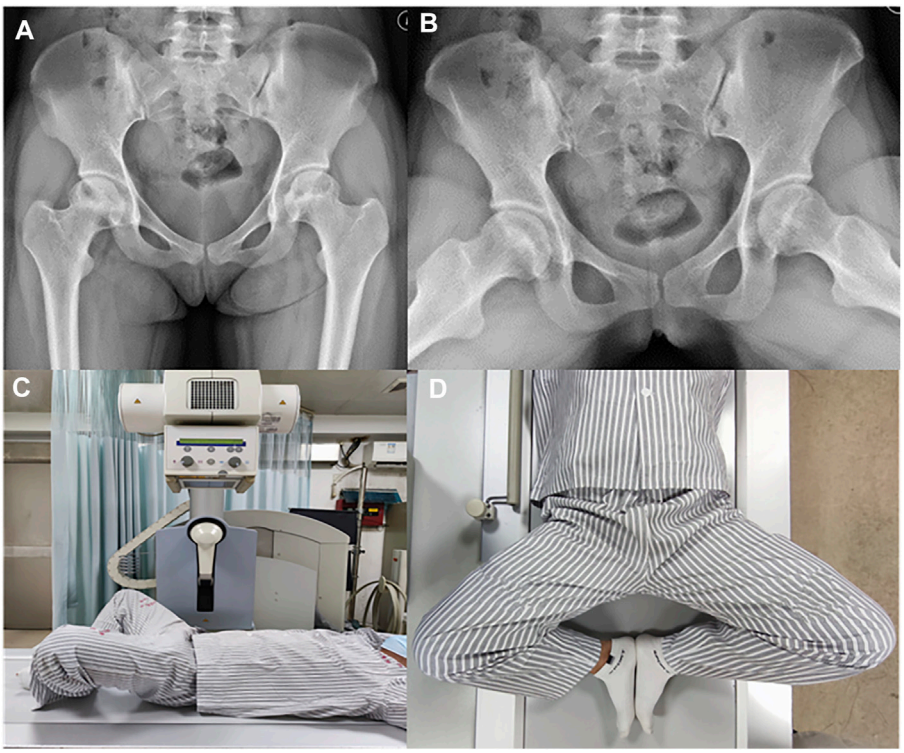

FIGURE 3 | Radiological assessment **(A)** AP view of hip joint. Patients were positioned supine on the x-ray table and bilateral legs abducted in neutral position so that the distance between the two feet is equal to shoulder width. **(B)** FLL view of hip joint. **(C)** For the FLL x-rays, patients were positioned supine on the x-ray table and the bilateral hips were flexed at a degree of 30°. **(D)** For the FLL x-rays, the thigh was abducted and externally rotated while ensuring that the feet contacted close to each other at the level of ipsilateral knee. The x-ray beam was directed anterior to posterior and centered on the femoral head while the plane of the pelvis was parallel to the plane of the table (Wei QS. et al., 2019).

to ARCO stage III, three patients developed ARCO stage IV, and one of them underwent THA (**Figure 5F**).

The condition of the ARCO stage II ONFH patients treated with HXTL capsules was analyzed according to the etiology and location/extent of their necrotic lesions (**Table 1**). The survival rates of femoral heads with JIC type A in AP and FLL radiographs was 100% (**Table 1**). The survival rates were 96.97% at 5 years, 69.15% at 10 years, and 40.33% at 15 years with the endpoint set as collapse of the femoral head (**Figure 6A**). There were no differences ($p > 0.05$) among etiologies (**Figure 6B**). The log-rank test showed longer durations ($p < 0.001$) of survival for femoral heads with type A or type B necrotic lesions in both AP and FLL radiographs than for femoral heads with type C necrotic lesions (**Figure 6C, D**).

We compared various parameters between patients with collapsed femoral heads and those without collapsed femoral heads (**Table 2**). There were no differences ($p > 0.05$) in age, sex, follow-up period, etiology, or extent of necrotic lesions, while there were significant differences ($p < 0.05$) in the location of necrotic lesions (in AP and FLL radiographs), Tonnis classification, LPA, APA, CPA, HHS, and VAS. None of the patients with JIC type A (in AP or FLL radiographs) had femoral head collapse. Patients with intact femoral heads exhibited higher values of LPA, APA, and CPA than did patients with collapsed femoral heads. The HHS of patients with intact femoral heads was significantly higher than that of patients with collapsed femoral heads, while the VAS of patients with intact femoral heads was lower than that of patients with collapsed femoral heads (**Table 2**).

Moreover, all LPA, APA, or CPA values in ONFH patients without collapsed femoral heads were significantly greater than those in patients with collapsed femoral head ($p < 0.001$) (**Figure 7A**). ROC curves were used to analyze the sensitivity and specificity of each angle for predicting collapse. The ROC curve analysis showed LPA (AUC = 0.96, 95% CI: 0.87–0.99, $p < 0.001$, cutoff value = 60.9°, sensitivity = 100%, specificity = 95.65%) (**Figure 7B**), APA (AUC = 0.95, 95% CI: 0.86–0.98, $p < 0.001$, cutoff value = 62.21°, sensitivity = 100%, specificity = 86.96%) (**Figure 7C**), and CPA (AUC = 0.93, 95% CI: 0.84–0.97, $p < 0.001$, cutoff value = 121.11°, sensitivity = 100%, specificity = 84.78%) (**Figure 7D**) had high sensitivity and specificity in predicting collapse among those patients who received HXTL capsule treatment.

Univariate Cox regression analysis revealed that patients with different JIC classifications in AP and FLL views, LPA, APA, CPA, VAS, and HHS were at different ($p < 0.05$) risks for collapse (**Table 3**). The multivariate Cox regression analysis revealed that LPA was an independent factor associated with femoral head collapse, and patients with LPA ≤ 60.9° exhibited a 3.87 times higher risk for collapse of the femoral head [95% confidence interval (CI), 1.241–5.673] than those with LPA >60.9°.

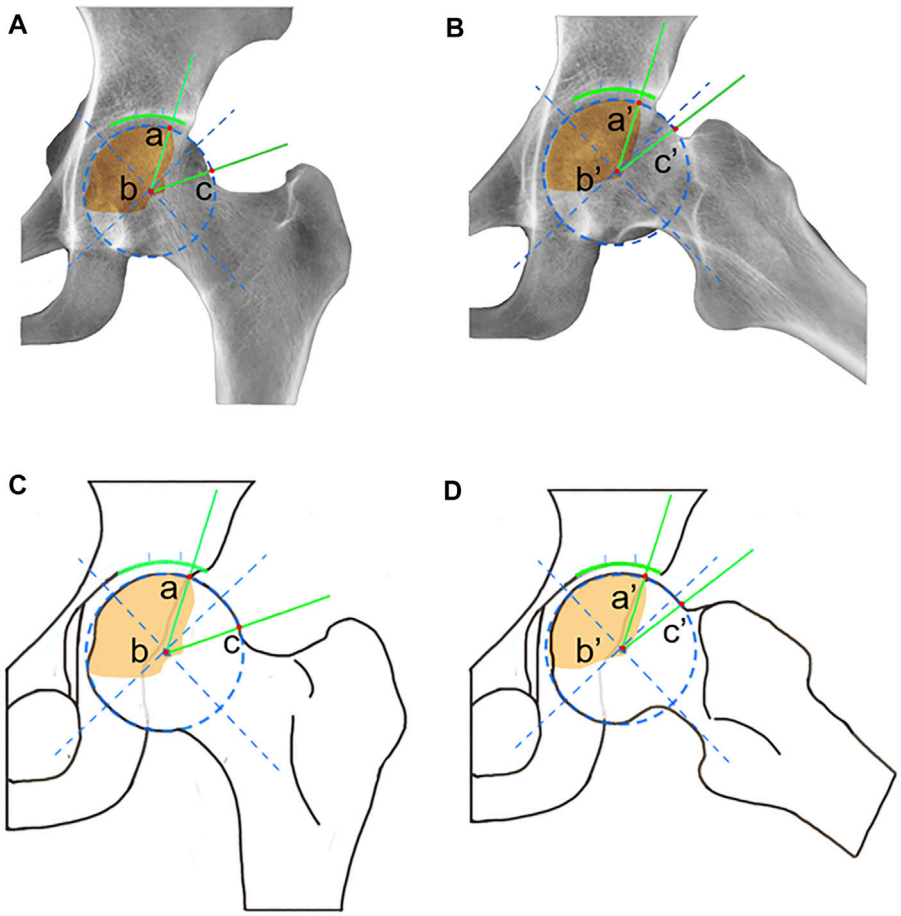

FIGURE 4 | Schematic diagram of LPA, APA, and CPA. **(A)** For LPA measured in AP radiographs, point a is the intersection of necrotic area and the edge of the femoral head, point b is the center of the femoral head, and point c is the junction of the femoral head and the femoral neck. The unit of LPA is degrees, and the LPA ranges from 0 to 180°. **(B)** For APA measured in FLL radiographs, point a′ is the intersection of the necrotic area and the edge of the femoral head, point b′ is the center of the femoral head, and point c′ is the junction of the femoral head and the femoral neck. The unit of APA is degrees, and the APA ranges from 0 to 180°. CPA equal to the sum of LPA and APA.

DISCUSSION

In this study, we found that treatment with HXTL capsules not only improved hip function in patients with ARCO stage II ONFH but also prevented 69.7% of hips from progressing to pain and collapse. Patients with type A necrotic lesions in AP and FLL radiographs showed 100% survival rates. LPA less than 60.9° may be a risk factor for collapse of the femoral head with HXTL capsule treatment. Currently, pharmacological agents for ARCO stage II patients remain controversial, and rigorous studies are still needed to provide guidance for a treatment algorithm. Lai et al. demonstrated that bisphosphonates could decrease the rates of disease progression and the need for arthroplasty in hips (Lai et al., 2005), but the results were less favorable when bisphosphonates were combined with other modalities (Carli et al., 2014). Statins were reported to lower bone pressure and ameliorate osteonecrosis (Kang et al., 2010). Ajmal et al. found that, among 2,881 patients who received organ transplantation and underwent long-term high-dose steroid use, there was no statistically significant difference in the occurrence of ONFH between the 127 patients who took statins compared with the 201 patients who did not take statins (Ajmal et al., 2009). The therapeutic effect of bisphosphonates or statins on patients with ARCO stage II ONFH is still unclear, and more rigorous studies are needed to confirm this hypothesis. Our previous study showed that HXTL capsules can relieve hip pain and prevent joint collapse in patients with asymptomatic ONFH (Wei QS. et al., 2019). It is necessary to further determine whether HXTL can be used as an optional treatment for ARCO stage II ONFH.

In our study, 69.7% of patients experienced no aggravation in pain or progression toward femoral head collapse after oral treatment with HXTL capsules. In terms of the clinical efficacy index, patients did not show significant progress ($p > 0.05$) in VAS, but they had a significant increase ($p < 0.05$) in HHS after treatment. The increase in HHS reflects the improvement of hip function, suggesting that HXTL capsules can improve hip

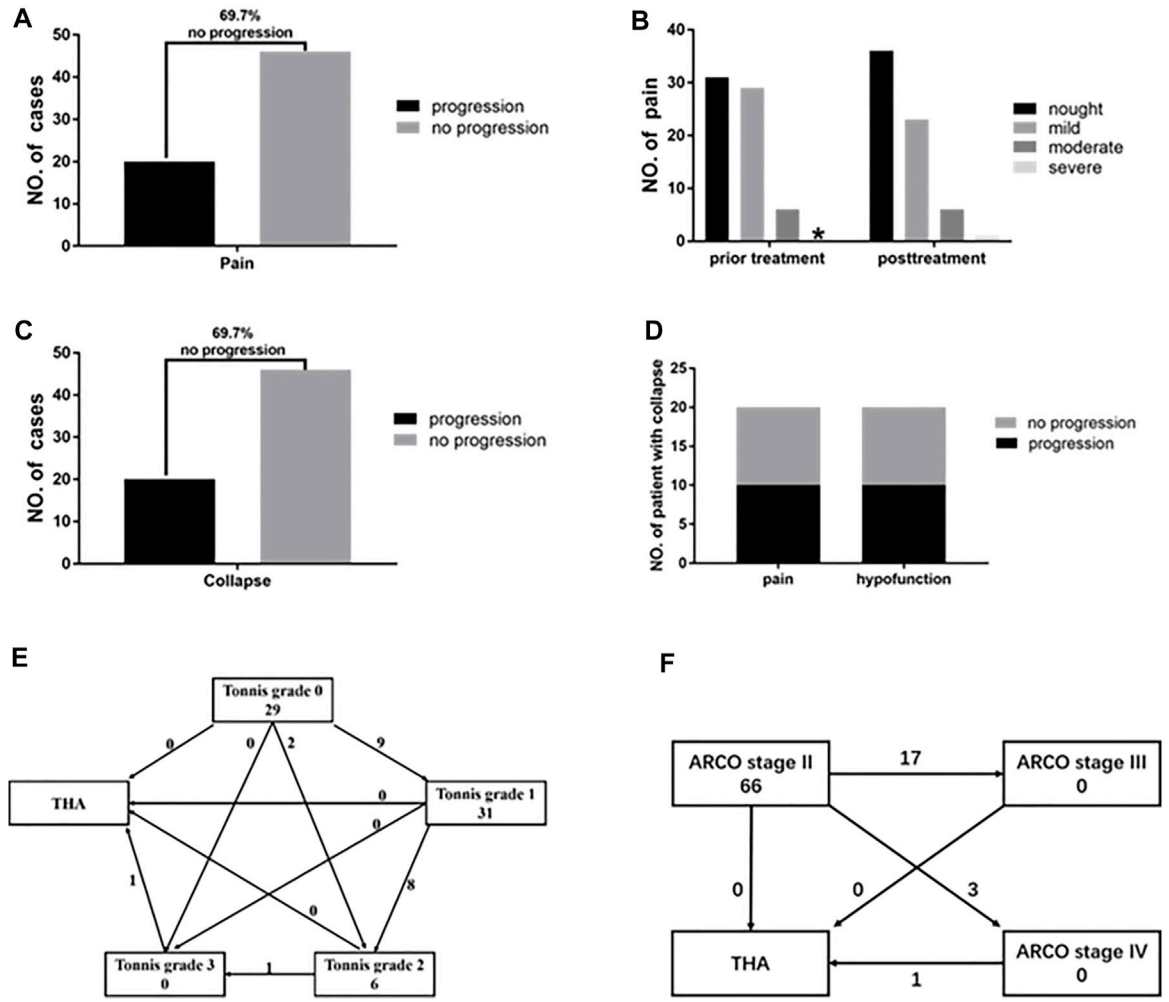

FIGURE 5 | ARCO stage II ONFH patients after average 7.95 years of follow-up. **(A)** After taking HXTL capsule there were 69.7% of patients showed no progress in pain. **(B)** The degree of pain before and after taking HXTL capsule exhibited no significant difference. Nought means VAS is 0, mild means VAS from 1 to 3, moderate means VAS from 4 to 6, and severe means VAS from 7 to 10.* means the number is 0. **(C)** After taking the HXTL capsule, there were 69.7% of patients that showed no progress in collapse. **(D)** Among the 20 femoral heads that collapsed, 10 of them had no progression in pain and hypofunction (50%), and 10 of them experienced pain progression and hip dysfunction (50%). **(E)** Changes in Tonnis classification before and after treatment. **(F)** Changes in the ARCO stage of the patients after treatment.

function in patients with ARCO stage II ONFH (Hoeksma et al., 2003). From a radiological perspective, 20 of the 66 (30.3%) hips progressed to osteoarthritis and necrosis, but 10 hips with collapse showed no further deterioration in pain or function, indicating that the changes in clinical function in the treatment of ARCO stage II with HXTL capsules are not completely consistent with the radiological changes. Although some patients progressed in radiographic appearances, they showed no deterioration in hip function. The core of the treatment for ONFH is to promote the repair of necrosis and delay or avoid the collapse of the femoral head (Zhao et al., 2020; Mont et al., 2020). A systematic literature review described the progression of 394 of 664 (59%) untreated asymptomatic hips to symptoms or collapse (Mont et al., 2010). Hernigou et al. stated that 77% (93 of 121) of untreated asymptomatic ONFH collapsed and that all 23 (100%) Steinberg stage II patients experienced femoral head collapse at an average of 11 months following the onset of pain (Hernigou et al., 2006). A prospective, randomized, open-label, multicenter study found that zoledronate did not prevent collapse of the femoral head or reduce the need for THA, while the collapse rate among Steinberg stage II patients treated with zoledronate was 57.7% (15 of 26) (Lee et al., 2015). In summary, the efficacy of HXTL capsules in patients with ARCO stage II ONFH appears to be acceptable.

Kaplan–Meier survival analysis was used to analyze the factors that may affect femoral head collapse. The results suggested that patients with different JIC classifications on FLL or AP radiographs have different risks for collapse. Patients with type A necrotic lesions on AP and FLL radiographs had 100% survival rates. This result shows that the location of necrosis is the key factor affecting collapse when using HXTL capsules. The lateral portion of the femoral head is the key site affecting the prognosis

TABLE 1 | Fate of ARCO stage II ONFH patients according to the etiology and location/extent of necrotic lesion.

Variables	Hips	Progress in pain	Progress in collapse
Total hips	66	20 (30.3%)	20 (30.3%)
Etiology			
AONFH	20 (30.3%)	2 (10.0%)	7 (35.0%)
SONFH	37 (56.1%)	15 (40.5%)	9 (56.1%)
IONFH	9 (13.6%)	3 (33.3%)	4 (13.6%)
Location			
AP			
Type A	23 (34.8%)	7 (30.4%)	0 (0)
Type B	25 (37.8%)	5 (20.1%)	3 (12.0%)
Type C	18 (27.2%)	8 (44.4%)	17 (94.4%)
FLL			
Type A	19 (28.8%)	4 (21.1%)	0 (0)
Type B	26 (39.4%)	7 (26.9%)	4 (15.4%)
Type C	21 (3.8%)	9 (42.9%)	16 (90.5%)
Extent[a]			
Small	19 (28.8%)	4 (20.0%)	1 (5.0%)
Medium	30 (45.5%)	6 (30.0%)	5 (25.0%)
Large	17 (25.8%)	10 (50.0%)	14 (70.0%)

[a]*Small = the extent of necrosis less than 15%, medium = the extent of necrosis between 15 and 30%, large = the extent of necrosis greater than 30% (Sugano et al., 2002).*

if necrosis involves the lateral portion, and there is an increased risk of conservative treatment failure (Sugano et al., 2002; Ha et al., 2006; Gao et al., 2018; Liu et al., 2020). Combined with our results, it can be concluded that the survival rate of ARCO stage II patients treated with HXTL capsules is relatively high when necrosis does not involve the anterior or lateral portion of the femoral head. We found that the LPA, APA, and CPA of patients with collapsed femoral heads were significantly lower than those of patients without collapsed femoral heads. All three indicators had high sensitivity and specificity in predicting femoral head collapse (**Figures 8A,B**). According to the JIC classification and the measurement methods of LPA, APA, and CPA, we considered that these three indicators can be used as references to evaluate whether the weight-bearing area of the femoral head is involved. Although we have given the cutoff values in this paper, more studies are needed to determine whether they can be generalized to all patients with ONFH. Combined with the results of this study and the relevant literature about femoral head collapse, we performed Cox regression analysis for the factors potentially affecting collapse (Zalavras and Lieberman, 2014; Mont et al., 2020). The results suggested that LPA was an independent factor associated with collapse. Patients with an LPA ≤ 60.9° exhibited a 3.87 times higher risk of femoral head collapse [95% CI, 1.241–5.673] than those with an LPA>60.9°. Considering the sensitivity and specificity of LPA for predicting collapse, we believe that LPA can be used as an indicator to predict collapse because it can better reflect whether necrotic lesions affect the lateral portion of the femoral head, which is consistent with the study from Kuroda et al. (Kuroda et al., 2019). In summary, when the necrotic lesion did not involve the anterior or lateral portion of the femoral head, the success rate of using HXTL capsules in the treatment of ARCO stage II ONFH was relatively satisfactory.

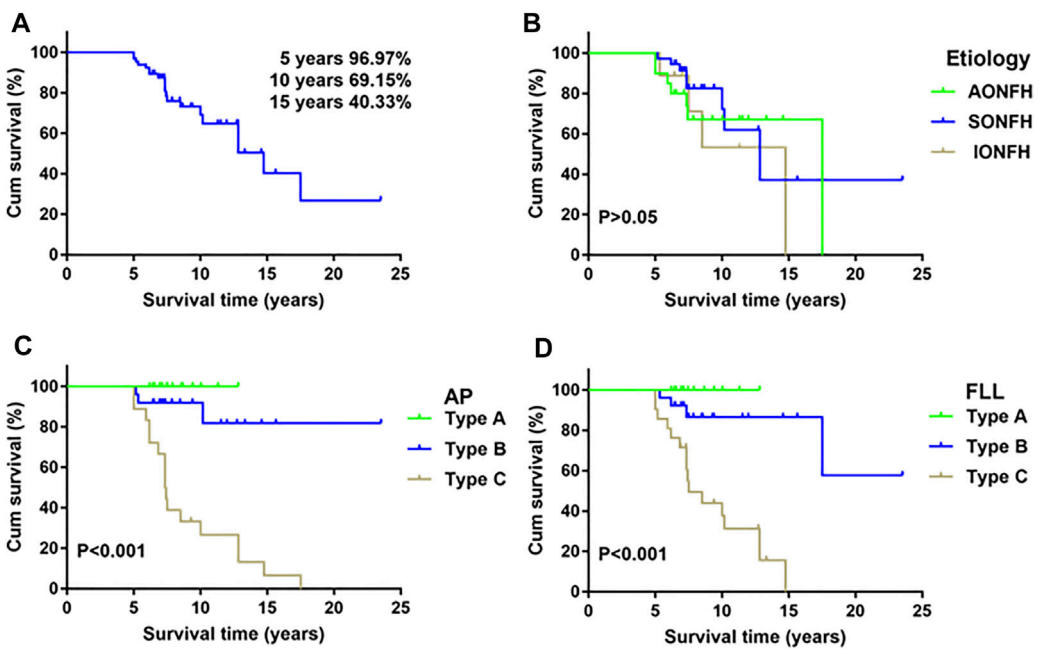

FIGURE 6 | Kaplan–Meier survivorship curve. **(A)** The cumulative rates of survival (with 95% confidence intervals) are 96.97% at 5 years, 69.15% at 10 years, and 40.33% at 15 years with collapse of the femoral head as the endpoint. **(B)** Survival rates according to etiology. There were no differences ($p = 0.56$, log-rank test) in survival among etiology. **(C)** The log-rank test showed longer durations ($p < 0.001$) of survival for femoral heads with type A or type B necrotic lesions both in AP radiographs than for femoral heads with type C necrotic lesions. **(D)** The log-rank test showed longer durations ($p < 0.001$) of survival for femoral heads with type A or type B necrotic lesions both in FLL radiographs than for femoral heads with type C necrotic lesions.

TABLE 2 | Relationship between various parameters and final state of femoral head in ARCO stage II ONFH patients.

Variables	No collapsed	Collapsed	*p*
Number of hips: 66	46 (69.7%)	20 (30.3%)	-
Age (years)	35.2 ± 8.9	41.1 ± 12.7	0.069
Females: males (no.)	12:17	6:9	0.930
Follow-up period (years)	9.28 ± 3.88	8.45 ± 3.51	0.412
Etiology (alcohol: steroid: idiopathic) (no.)	13:28:5	7:9:4	0.430
Location in AP (Type A: B: C) (no.)	23:22:1	0:3:17	0.000
Location in FLL (Type A: B: C) (no.)	19:22:5	0:4:16	0.000
Extent (S: M: L) (no.)	3:25:18	1:5:14	0.066
Tonnis classification (Grade 0:1:2:3) (no.)	17:29:0:0	5:9:5:1	0.002
LPA (degree)	66.88 ± 6.75	57.48 ± 3.47	0.000
APA (degree)	66.00 ± 3.65	59.20 ± 4.52	0.000
CPA (degree)	132.88 ± 8.99	116.68 ± 7.54	0.000
HHS (point)	81.36 ± 3.06	73.45 ± 4.66	0.000
VAS (point)	0.61 ± 0.85	2.4 ± 1.66	0.000

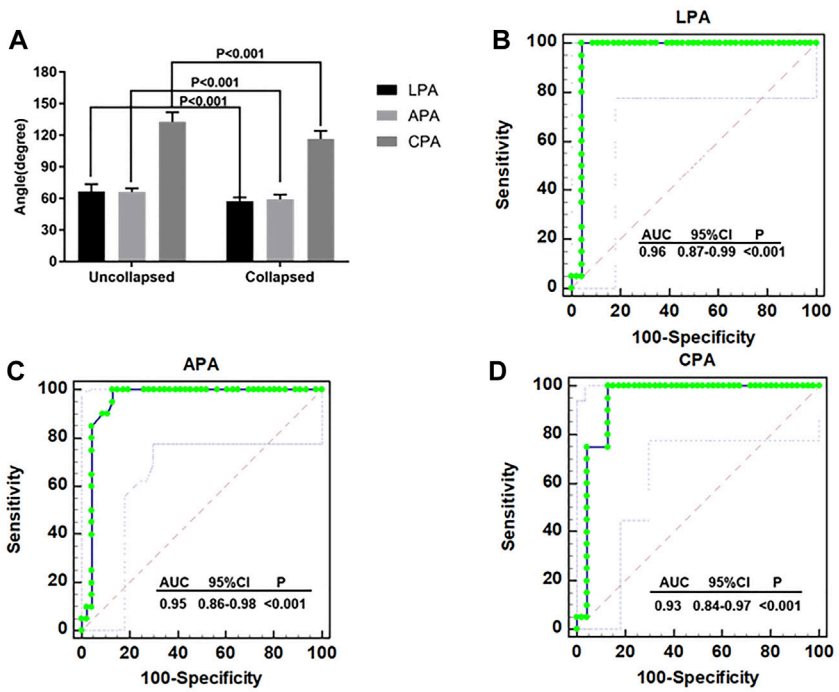

FIGURE 7 | ROC curve analysis **(A)** The LPA, APA, and CPA of patients without collapse were significantly higher than patients with collapse ($p < 0.001$). **(B)** ROC curve analysis for the LPA in terms of predicting collapse (AUC = 0.96, 95% CI 0.87–0.99, $p < 0.001$, cutoff value = 60.9°, sensitivity = 100%, specificity = 95.65%). **(C)** ROC curve analysis for the APA in terms of predicting collapse (AUC = 0.95, 95% CI 0.86–0.98, $p < 0.001$, cutoff value = 62.21°, sensitivity = 100%, specificity = 86.96%). **(D)** ROC curve analysis for the CPA in terms of predicting collapse (AUC = 0.93, 95% CI 0.84–0.97, $p < 0.001$, cutoff value = 121.11°, sensitivity = 100%, specificity = 84.78%).

From the perspective of modern evidence-based Chinese medicine, ischemia is the pathological state of blood stasis syndrome, which is a main feature in the pathological process of ONFH. Scholars have applied vasoactive agents to improve the revascularization of the femoral head and promote the repair of necrotic bone. Kong et al. reported that the ethyl acetate fraction of Huo Gu formula (a Chinese medicine compound that activates blood circulation) could promote the repair of necrotic bone (Kong et al., 2017). Jiang et al. found that tetramethylpyrazine can enhance vascularization and prevent osteonecrosis in rats (Jiang et al., 2015). The reparative effect of vasoactive agents on osteonecrosis can be useful and important in the treatment of ONFH. We have found that HXTL capsules can promote the repair of the femoral head (Wei QS. et al., 2019; Fang et al., 2019). In this study, we further confirmed that HXTL capsules could improve hip function in patients with ARCO

TABLE 3 | Univariate Cox regression analysis of the risk factors associated with collapse.

Variables	*p*	B	HR	95% CI
Location				
AP	0.03			
Type C	—		—	—
Type B	0.938	−13.079	—	—
Type A	0.001	−2.147	0.117	0.034–0.400
FLL	**0.007**			
Type C	—		—	—
Type B	0.939	−12.702	—	—
Type A	0.002	−1.994	0.136	0.039–0.472
Tonnis classification	**0.185**			
Grade 0	—		—	—
Grade 1	0.405	0.455	—	—
Grade 2	0.066	1.094	—	—
LPA (degree)				
>60.9	—		—	—
≤60.9	**0.014**	5.209	182.976	2.915–11,484.47
APA (degree)				
>62.21	—		—	—
≤62.21	**0.013**	4.894	133.434	2.765–6,438.96
CPA (degree)				
>121.11	—		—	—
≤121.11	**0.014**	5.209	182.97	2.915–11,484.47
VAS (point)	**0.001**			
0	—		—	—
1–3	0.048	1.186	3.275	1.013–10.587
4–6	0.000	2.452	11.608	3.133–43.011
HHS (point)	**0.007**			
80–89	—			
70–79	0.002	3.343	28.294	3.261–245.513
<70	0.002	3.216	24.935	3.262–190.605

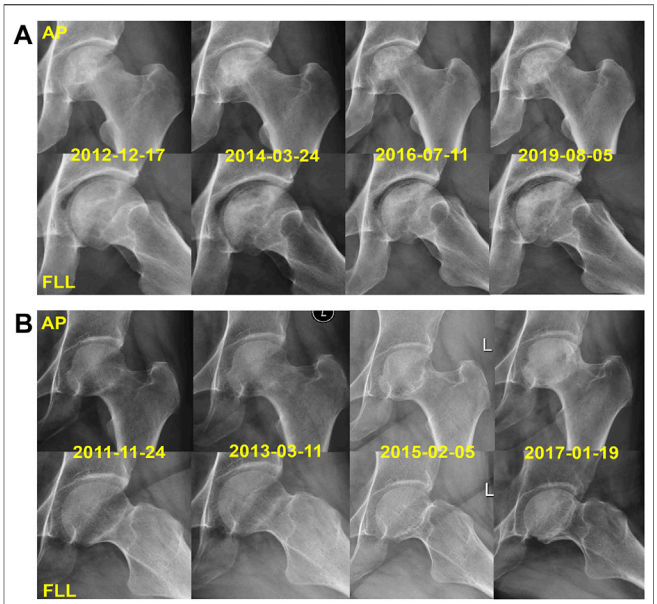

FIGURE 8 | Two representative cases with JIC type C1 lesions. **(A)** X-rays of the left hip joint of a 42-year-old male with AONFH had a pretreatment LPA of 65° and APA of 67°; there was no collapse of the femoral head in the follow-up of 7.04 years. **(B)** X-rays of the left hip joint of a 38-year-old female with SONFH had a pretreatment LPA of 57.17° and APA of 59.31°; she has a femoral head collapse in 5.08 years of follow-up.

stage II ONFH. In addition, we also discussed the indications for the use of HXTL capsules in the treatment of ARCO stage II ONFH. The results of this study show that HXTL capsules are effective and ideally used when neither the anterior nor the lateral portions of the femoral head are affected. In addition, LPA, APA, and CPA can be used as indicators to evaluate the anterior and lateral femoral head, which is helpful in assessing the therapeutic effect of HXTL capsules more accurately; the LPA is especially useful. Based on the above results, we will further explore the indications for HXTL capsules in the treatment of ONFH in the future.

Limitations

First, because of the long duration of this study, it was not easy to find a matching control group. Second, although we have discussed the importance of the anterior and lateral portions of the femoral head for conservative management by LPA, APA, and CPA, whether or not they are suitable for all types of patients with ONFH needs further study. Third, the study subjects were all outpatients, and inconsistent compliance and other factors could not be excluded during the follow-up; for example, incorrect restrictive weight bearing and intense exercise or an irregular lifestyle may have influenced the study results. Moreover, the collapse rate reported in this study may be underestimated since we excluded ARCO stage II patients with JIC Type C2 lesions. Our team will carry out more studies in the future to confirm the effect of HXTL capsules on type C2 patients.

CONCLUSION

In conclusion, HXTL capsules, a vasoactive herbal formula that could improve hip function and delay the progression of femoral head collapse, is an option for patients with ARCO stage II ONFH, especially when the anterior and lateral portions of the femoral head remain intact. LPA >60.9° is a risk factor for collapse of the femoral head in ARCO stage II ONFH patients treated with HXTL capsules. Multicenter prospective studies with long-term follow-up are necessary to elucidate the potential benefits of HXTL capsule treatment in ARCO stage II ONFH.

DATA AVAILABILITY STATEMENT

The original contributions presented in the study are included in the article/supplementary material; further inquiries can be directed to the corresponding authors.

ETHICS STATEMENT

The studies involving human participants were reviewed and approved by the Guangdong Research Institute for Orthopedics and Traumatology of Chinese Medicine. The patients/

participants provided their written informed consent to participate in this study.

AUTHOR CONTRIBUTIONS

X-MH and M-CH contributed equally to the study as co-first authors. X-MH carried out the experiments and data analysis and drafted and critically revised the manuscript. M-CH critically revised the manuscript. PY revised the manuscript and provided technical assistance in preparing the manuscript. Z-QC carried out the statistical analysis. Q-WZ supervised the project and critically revised the manuscript for important intellectual content. WH and Q-SW| contributed equally to the study design, clinical studies, and critically revised the manuscript for important intellectual content as corresponding author.

FUNDING

This study was supported by grants from the project of the National Natural Science Foundation of China (grant number 81873327, 82004392 and 81573996), the Double First-class Discipline Construction Project of Guangzhou University of Chinese Medicine (grant number Z2015002), the major project of "Double First-class" and High-level University Discipline Collaborative Innovation Team of Guangzhou University of Chinese Medicine (grant number 2021XK05), the cultivated project of "Double First-class" and High-level University Discipline Collaborative Innovation Team of Guangzhou University of Chinese Medicine (grant number 2021XK41 and 2021XK46) and the Foundation of Guangdong Educational Committee for Youth Scientists (grant number 2019KQNCX017).

REFERENCES

Ajmal, M., Matas, A. J., Kuskowski, M., and Cheng, E. Y. (2009). Does Statin Usage Reduce the Risk of Corticosteroid-Related Osteonecrosis in Renal Transplant Population? *Orthop. Clin. North. Am.* 40 (2), 235–239. doi:10.1016/j.ocl.2009.01.004

Ancelin, D., Reina, N., Cavaignac, E., Delclaux, S., and Chiron, P. (2016). Total Hip Arthroplasty Survival in Femoral Head Avascular Necrosis versus Primary Hip Osteoarthritis: Case-Control Study with a Mean 10-year Follow-Up after Anatomical Cementless Metal-On-Metal 28-mm Replacement. *Orthop. Traumatol. Surg. Res.* 102 (8), 1029–1034. doi:10.1016/j.otsr.2016.08.021

Boontanapibul, K., Steere, J. T., Amanatullah, D. F., Huddleston, J. I., Maloney, W. J., and Goodman, S. B. (2020). Diagnosis of Osteonecrosis of the Femoral Head: Too Little, Too Late, and Independent of Etiology. *J. Arthroplasty.* 35 (9), 2342–2349. doi:10.1016/j.arth.2020.04.092

Carli, A., Albers, A., Séguin, C., and Harvey, E. J. (2014). The Medical and Surgical Treatment of ARCO Stage-I and II Osteonecrosis of the Femoral Head: A Critical Analysis Review. *JBJS Rev.* 2 (2), 1. doi:10.2106/JBJS.RVW.M.00066

Chen, L., Hong, G., Hong, Z., Lin, T., Chen, Z., Zhang, Q., et al. (2020). Optimizing Indications of Impacting Bone Allograft Transplantation in Osteonecrosis of the Femoral Head. *Bone Jt. J* 102-B (7), 838–844. doi:10.1302/0301-620X.102B7.BJJ-2019-1101.R2

Cohen-Rosenblum, A., and Cui, Q. (2019). Osteonecrosis of the Femoral Head. *Orthop. Clin. North. Am.* 50 (2), 139–149. doi:10.1016/j.ocl.2018.10.001

Cui, L., Zhuang, Q., Lin, J., Jin, J., Zhang, K., Cao, L., et al. (2016). Multicentric Epidemiologic Study on Six Thousand Three Hundred and Ninety Five Cases of Femoral Head Osteonecrosis in China. *Int. Orthop.* 40 (2), 267–276. doi:10.1007/s00264-015-3061-7

Fang, B., Li, Y., Chen, C., Wei, Q., Zheng, J., Liu, Y., et al. (2019). Huo Xue Tong Luo Capsule Ameliorates Osteonecrosis of Femoral Head through Inhibiting lncRNA-Miat. *J. Ethnopharmacol.* 238, 111862. doi:10.1016/j.jep.2019.111862

Gao, F., Han, J., He, Z., and Li, Z. (2018). Radiological Analysis of Cystic Lesion in Osteonecrosis of the Femoral Head. *Int. Orthop.* 42 (7), 1615–1621. doi:10.1007/s00264-018-3958-z

Ha, Y. C., Jung, W. H., Kim, J. R., Seong, N. H., Kim, S. Y., and Koo, K. H. (2006). Prediction of Collapse in Femoral Head Osteonecrosis: a Modified Kerboul Method with Use of Magnetic Resonance Images. *J. Bone Jt. Surg. Am.* 88 (Suppl. 3), 35–40. doi:10.2106/JBJS.F.00535

Hernigou, P., Habibi, A., Bachir, D., and Galacteros, F. (2006). The Natural History of Asymptomatic Osteonecrosis of the Femoral Head in Adults with Sickle Cell Disease. *J. Bone Jt. Surg. Am.* 88 (12), 2565–2572. doi:10.2106/JBJS.E.01455

Hoeksma, H. L., Van Den Ende, C. H., Ronday, H. K., Heering, A., and Breedveld, F. C. (2003). Comparison of the Responsiveness of the Harris Hip Score with Generic Measures for Hip Function in Osteoarthritis of the Hip. *Ann. Rheum. Dis.* 62 (10), 935–938. doi:10.1136/ard.62.10.935

Hong, M., Shi, H., Wang, N., Tan, H. Y., Wang, Q., and Feng, Y. (2019). Dual Effects of Chinese Herbal Medicines on Angiogenesis in Cancer and Ischemic Stroke Treatments: Role of HIF-1 Network. *Front. Pharmacol.* 10, 696. doi:10.3389/fphar.2019.00696

Jiang, Y., Liu, C., Chen, W., Wang, H., Wang, C., and Lin, N. (2015). Tetramethylpyrazine Enhances Vascularization and Prevents Osteonecrosis in Steroid-Treated Rats. *Biomed. Res. Int.* 2015, 315850. doi:10.1155/2015/315850

Kang, P., Gao, H., Pei, F., Shen, B., Yang, J., and Zhou, Z. (2010). Effects of an Anticoagulant and a Lipid-Lowering Agent on the Prevention of Steroid-Induced Osteonecrosis in Rabbits. *Int. J. Exp. Pathol.* 91 (3), 235–243. doi:10.1111/j.1365-2613.2010.00705.x

Kong, X., Li, X., Zhang, C., Zhu, L., Liu, C., Qin, Q., et al. (2017). Ethyl Acetate Fraction of Huogu Formula Inhibits Adipogenic Differentiation of Bone Marrow Stromal Cells via the BMP and Wnt Signaling Pathways. *Int. J. Biol. Sci.* 13 (4), 480–491. doi:10.7150/ijbs.18430

Kovalenko, B., Bremjit, P., and Fernando, N. (2018). Classifications in Brief: Tönnis Classification of Hip Osteoarthritis. *Clin. Orthop. Relat. Res.* 476 (8), 1680–1684. doi:10.1097/01.blo.0000534679.75870.5f

Kuijpers, M. F. L., Hannink, G., Vehmeijer, S. B. W., van Steenbergen, L. N., and Schreurs, B. W. (2019). The Risk of Revision after Total Hip Arthroplasty in Young Patients Depends on Surgical Approach, Femoral Head Size and Bearing Type; an Analysis of 19,682 Operations in the Dutch Arthroplasty Register. *BMC Musculoskelet. Disord.* 20 (1), 385. doi:10.1186/s12891-019-2765-z

Kuroda, Y., Tanaka, T., Miyagawa, T., Kawai, T., Goto, K., Tanaka, S., et al. (2019). Classification of Osteonecrosis of the Femoral Head: Who Should Have Surgery? *Bone Jt. Res* 8 (10), 451–458. doi:10.1302/2046-3758.810.BJR-2019-0022.R1

Lai, K. A., Shen, W. J., Yang, C. Y., Shao, C. J., Hsu, J. T., and Lin, R. M. (2005). The Use of Alendronate to Prevent Early Collapse of the Femoral Head in Patients with Nontraumatic Osteonecrosis. A Randomized Clinical Study. *J. Bone Jt. Surg. Am.* 87 (10), 2155–2159. doi:10.2106/JBJS.D.02959

Lee, Y. K., Ha, Y. C., Cho, Y. J., Suh, K. T., Kim, S. Y., Won, Y. Y., et al. (2015). Does Zoledronate Prevent Femoral Head Collapse from Osteonecrosis? A Prospective, Randomized, Open-Label, Multicenter Study. *J. Bone Jt. Surg Am* 97 (14), 1142–1148. doi:10.2106/JBJS.N.01157

Liu, G. B., Li, R., Lu, Q., Ma, H. Y., Zhang, Y. X., Quan, Q., et al. (2020). Three-dimensional Distribution of Cystic Lesions in Osteonecrosis of the Femoral Head. *J. Orthop. Translat* 22, 109–115. doi:10.1016/j.jot.2019.10.010

Moerman, S., Mathijssen, N. M. C., Tuinebreijer, W. E., Vochteloo, A. J. H., and Nelissen, R. G. H. H. (2018). Hemiarthroplasty and Total Hip Arthroplasty in 30,830 Patients with Hip Fractures: Data from the Dutch Arthroplasty Register on Revision and Risk Factors for Revision. *Acta Orthop.* 89 (5), 509–514. doi:10.1080/17453674.2018.1499069

Mont, M. A., Cherian, J. J., Sierra, R. J., Jones, L. C., and Lieberman, J. R. (2015). Nontraumatic Osteonecrosis of the Femoral Head: Where Do We Stand Today?

A Ten-Year Update. *J. Bone Jt. Surg. Am.* 97 (19), 1604–1627. doi:10.2106/JBJS.O.00071

Mont, M. A., Salem, H. S., Piuzzi, N. S., Goodman, S. B., and Jones, L. C. (2020). Nontraumatic Osteonecrosis of the Femoral Head: Where Do We Stand Today?: A 5-Year Update. *J. Bone Jt. Surg. Am.* 102 (12), 1084–1099. doi:10.2106/JBJS.19.01271

Mont, M. A., Zywiel, M. G., Marker, D. R., Mcgrath, M. S., and Delanois, R. E. (2010). The Natural History of Untreated Asymptomatic Osteonecrosis of the Femoral Head: a Systematic Literature Review. *J. Bone Jt. Surg. Am.* 92 (12), 2165–2170. doi:10.2106/JBJS.I.00575

Reed, M. D., and Van Nostran, W. (2014). Assessing Pain Intensity with the Visual Analog Scale: a Plea for Uniformity. *J. Clin. Pharmacol.* 54 (3), 241–244. doi:10.1002/jcph.250

Sodhi, N., Acuna, A., Etcheson, J., Mohamed, N., Davila, I., Ehiorobo, J. O., et al. (2020). Management of Osteonecrosis of the Femoral Head. *Bone Jt. J* 102-B (7_Suppl. e_B), 122–128. doi:10.1302/0301-620X.102B7.BJJ-2019-1611.R1

Sugano, N., Atsumi, T., Ohzono, K., Kubo, T., Hotokebuchi, T., and Takaoka, K. (2002). The 2001 Revised Criteria for Diagnosis, Classification, and Staging of Idiopathic Osteonecrosis of the Femoral Head. *J. Orthop. Sci.* 7 (5), 601–605. doi:10.1007/s007760200108

Wang, W., Yu, J. N., and Tao, X. J. (2011). Systemic Lupus Erythematosus Complicated with Femoral Head Ischemic Necrosis Treated by Chinese Medicine Therapy for Activating Blood and Dredging Collaterals Method. *Chin. J. Integr. Med.* 17 (2), 105–110. doi:10.1007/s11655-011-0637-y

Wei, Q., Fang, B., Chen, Z., Mincong, H., Chen, X., Yang, F., et al. (2019b). Role of Bone Status in Anterolateral Portion of Femoral Head in the Progression of Osteonecrosis of the Femoral Head. *Zhongguo Zuzhi Gongcheng Yanjiu* 23 (16), 2516–2522. doi:10.3969/j.issn.2095-4344.1148

Wei, Q. S., Hong, G. J., Yuan, Y. J., Chen, Z. Q., Zhang, Q. W., and He, W. (2019a). Huo Xue Tong Luo Capsule, a Vasoactive Herbal Formula Prevents Progression of Asymptomatic Osteonecrosis of Femoral Head: A Prospective Study. *J. Orthop. Translat* 18, 65–73. doi:10.1016/j.jot.2018.11.002

Wei, Q., Zhang, Q., He, W., Chen, Z., Fang, B., Yang, P., et al. (2018). Clinical Significance for New Type of Necrotic Femoral Head Based on X- ray. *Chin. J. Jt.* 12 (6), 845–856. doi:10.3877/cma.j

Yoon, B. H., Mont, M. A., Koo, K. H., Chen, C. H., Cheng, E. Y., Cui, Q., et al. (2020). The 2019 Revised Version of Association Research Circulation Osseous Staging System of Osteonecrosis of the Femoral Head. *J. Arthroplasty.* 35 (4), 933–940. doi:10.1016/j.arth.2019.11.029

Yu, T., Zhang, Z., Xie, L., Ke, X., and Liu, Y. (2016). The Influence of Traditional Chinese Medicine Constitutions on the Potential Repair Capacity after Osteonecrosis of the Femoral Head. *Complement. Ther. Med.* 29, 89–93. doi:10.1016/j.ctim.2016.09.010

Zalavras, C. G., and Lieberman, J. R. (2014). Osteonecrosis of the Femoral Head: Evaluation and Treatment. *J. Am. Acad. Orthop. Surg.* 22 (7), 455–464. doi:10.5435/JAAOS-22-07-455

Zhang, Q., Yang, F., Chen, Y., Wang, H., Chen, D., He, W., et al. (2018). Chinese Herbal Medicine Formulas as Adjuvant Therapy for Osteonecrosis of the Femoral Head: A Systematic Review and Meta-Analysis of Randomized Controlled Trials. *Medicine (Baltimore)* 97 (36), e12196. doi:10.1097/MD.0000000000012196

Zhao, D., Zhang, F., Wang, B., Liu, B., Li, L., Kim, S. Y., et al. (2020). Guidelines for Clinical Diagnosis and Treatment of Osteonecrosis of the Femoral Head in Adults (2019 Version). *J. Orthop. Translat* 21, 100–110. doi:10.1016/j.jot.2019.12.004

Conflict of Interest: The authors declare that the research was conducted in the absence of any commercial or financial relationships that could be construed as a potential conflict of interest.

Publisher's Note: All claims expressed in this article are solely those of the authors and do not necessarily represent those of their affiliated organizations, or those of the publisher, the editors, and the reviewers. Any product that may be evaluated in this article, or claim that may be made by its manufacturer, is not guaranteed or endorsed by the publisher.

Copyright © 2021 He, He, Yang, Zhang, Chen, He and Wei. This is an open-access article distributed under the terms of the Creative Commons Attribution License (CC BY). The use, distribution or reproduction in other forums is permitted, provided the original author(s) and the copyright owner(s) are credited and that the original publication in this journal is cited, in accordance with accepted academic practice. No use, distribution or reproduction is permitted which does not comply with these terms.

frontiers | Frontiers in Pharmacology

CORRECTION
published: 12 April 2022
doi: 10.3389/fphar.2022.896418

Corrigendum: The Therapeutic Effect of Huo Xue Tong Luo Capsules in Association Research Circulation Osseous (ARCO) Stage II Osteonecrosis of the Femoral Head: A Clinical Study With an Average Follow-up Period of 7.95 Years

Xiao-Ming He[1,2†], Min-Cong He[1,2†], Peng Yang[1,2], Qing-Wen Zhang[1,2], Zhen-Qiu Chen[3], Wei He[1,2] and Qiu-Shi Wei[1,2*]*

[1]Guangdong Research Institute for Orthopedics and Traumatology of Chinese Medicine, Guangzhou, China, [2]Joint Center, The Third Affiliated Hospital of Guangzhou University of Chinese Medicine, Guangzhou, China, [3]The Third Orthopaedic Region, The First Affiliated Hospital of Guangzhou University of Chinese Medicine, Guangzhou, China

Keywords: osteonecrosis of femoral head, ARCO stage II, therapeutic effect, risk factor, huo xue tong luo

OPEN ACCESS

Approved by:
Frontiers Editorial Office, Frontiers Media SA, Switzerland

***Correspondence:**
Wei He
hw13802516062@163.com
Qiu-Shi Wei
weiqshi@126.com

†These authors have contributed equally to this work and share first authorship

Specialty section:
This article was submitted to Ethnopharmacology, a section of the journal Frontiers in Pharmacology

Received: *15 March 2022*
Accepted: *16 March 2022*
Published: *12 April 2022*

Citation:
He X-M, He M-C, Yang P, Zhang Q-W, Chen Z-Q, He W and Wei Q-S (2022) Corrigendum: The Therapeutic Effect of Huo Xue Tong Luo Capsules in Association Research Circulation Osseous (ARCO) Stage II Osteonecrosis of the Femoral Head: A Clinical Study With an Average Follow-up Period of 7.95 Years. Front. Pharmacol. 13:896418. doi: 10.3389/fphar.2022.896418

A Corrigendum on

The Therapeutic Effect of Huo Xue Tong Luo Capsules in Association Research Circulation Osseous (ARCO) Stage II Osteonecrosis of the Femoral Head: A Clinical Study With an Average Follow-up Period of 7.95 Years

by He, X.-M., He, M.-C., Yang, P., Zhang, Q.-W., Chen, Z.-Q., He, W., and Wei, Q.-S. (2021). Front. Pharmacol. 12:773758. doi:10.3389/fphar.2021.773758

In the published article, there is an error in the clinical trial registry number and the URL of Clinical Trial Registration. The correct Clinical Trial Registry details are "http://www.chictr.org.cn/showproj.aspx?proj=10829, ChiCTR-OPC-15007030".

The authors apologize for this error and state that this does not change the scientific conclusions of the article in any way. The original article has been updated.

Publisher's Note: All claims expressed in this article are solely those of the authors and do not necessarily represent those of their affiliated organizations, or those of the publisher, the editors and the reviewers. Any product that may be evaluated in this article, or claim that may be made by its manufacturer, is not guaranteed or endorsed by the publisher.

Copyright © 2022 He, He, Yang, Zhang, Chen, He and Wei. This is an open-access article distributed under the terms of the Creative Commons Attribution License (CC BY). The use, distribution or reproduction in other forums is permitted, provided the original author(s) and the copyright owner(s) are credited and that the original publication in this journal is cited, in accordance with accepted academic practice. No use, distribution or reproduction is permitted which does not comply with these terms.

frontiers in Pharmacology

ORIGINAL RESEARCH
published: 15 December 2021
doi: 10.3389/fphar.2021.754088

A Traditional Chinese Medicine Plant Extract Prevents Alcohol-Induced Osteopenia

Dongyang Qian[1,2†], Hui Zhou[3†], Pan Fan[1,4], Tao Yu[1,5], Anish Patel[1], Morgan O'Brien[1], Zhe Wang[3], Shiguang Lu[3], Guoqiang Tong[3], Yimin Shan[3], Lei Wang[3], Yuan Gao[1,6], Yuan Xiong[1,7], Lily Zhang[1], Xin Wang[8], Yuancai Liu[3] and Shuanhu Zhou[1,9]**

[1]Department of Orthopedic Surgery, Brigham and Women's Hospital, Harvard Medical School, Harvard University, Boston, MA, United States, [2]Department of Orthopedics, The First Affiliated Hospital, Guangzhou Medical University, Guangzhou, China, [3]Jing Brand Research Institute, Jing Brand Co., Ltd., Daye, China, [4]Department of Spine Center, Zhongda Hospital, Southeast University Medical School, Nanjing, China, [5]Department of Orthopedic Surgery, Tongji Hospital, School of Medicine, Tongji University, Shanghai, China, [6]Department of Orthopaedics, Qilu Hospital, Shandong University, Jinan, China, [7]Department of Orthopaedics, Union Hospital, Tongji Medical College, Huazhong University of Science and Technology, Wuhan, China, [8]Department of Neurosurgery, Brigham and Women's Hospital, Harvard Medical School, Boston, MA, United States, [9]Harvard Stem Cell Institute, Harvard University, Cambridge, MA, United States

OPEN ACCESS

Edited by:
Daohua Xu,
Guangdong Medical University, China

Reviewed by:
Jun Mao,
Affiliated Hospital of Nanjing University of Chinese Medicine, China
Jinghong Zhang,
Huaqiao University, China
Wei Yang,
Guangdong Pharmaceutical University, China

***Correspondence:**
Shuanhu Zhou
szhou@bwh.harvard.edu
shuanhuzhou@gmail.com
Yuancai Liu
lyc@jingpai.com

[†]These authors have equally contributed to this work

Specialty section:
This article was submitted to Ethnopharmacology, a section of the journal Frontiers in Pharmacology

Received: 05 August 2021
Accepted: 11 November 2021
Published: 15 December 2021

Citation:
Qian D, Zhou H, Fan P, Yu T, Patel A, O'Brien M, Wang Z, Lu S, Tong G, Shan Y, Wang L, Gao Y, Xiong Y, Zhang L, Wang X, Liu Y and Zhou S (2021) A Traditional Chinese Medicine Plant Extract Prevents Alcohol-Induced Osteopenia. Front. Pharmacol. 12:754088. doi: 10.3389/fphar.2021.754088

Traditional Chinese medicine (TCM) has been practiced in the treatment of bone diseases and alcoholism. Chronic excessive alcohol use results in alcohol-induced bone diseases, including osteopenia and osteoporosis, which increases fracture risk, deficient bone repair, and osteonecrosis. This preclinical study investigated the therapeutic effects of TCM herbal extracts in animal models of chronic excessive alcohol consumption-induced osteopenia. TCM herbal extracts (Jing extracts) were prepared from nine Chinese herbal medicines, a combinative herbal formula for antifatigue and immune regulation, including *Astragalus*, *Cistanche deserticola*, *Dioscorea polystachya*, *Lycium barbarum*, *Epimedium*, *Cinnamomum cassia*, *Syzygium aromaticum*, *Angelica sinensis*, and *Curculigo orchioides*. In this study, Balb/c male mice were orally administrated alcohol (3.2 g/kg/day) with/without TCM herbal extracts (0.125 g/kg, 0.25 g/kg, or 0.5 g/kg) by gavage. Our results showed that after 50 days of oral administration, TCM herbal extracts prevented alcohol-induced osteopenia demonstrated by μ-CT bone morphological analysis in young adults and middle-aged/old Balb/c male mice. Biochemical analysis demonstrated that chronic alcohol consumption inhibits bone formation and has a neutral impact on bone resorption, suggesting that TCM herbal extracts (Jing extracts) mitigate the alcohol-induced abnormal bone metabolism in middle-aged/old male mice. Protocatechuic acid, a natural phenolic acid in Jing extracts, mitigates *in vivo* alcohol-induced decline of alkaline phosphatase (ALP) gene expression in the bone marrow of Balb/c male mice and *in vitro* ALP activity in pre-osteoblast MC3T3-E1 cells. Our study suggests that TCM herbal extracts prevent chronic excessive alcohol consumption-induced osteopenia in male mice, implying that

Abbreviations: ALP, Alkaline phosphatase; CTXI, Cross-Linked C-Telopeptide of Type I Collagen; C. BMD, cortical bone mineral density; ELISA, enzyme-linked immunosorbent assay; HPLC, High-performance liquid chromatography; LC/MS, liquid chromatography-mass spectrometry; μ-CT, micro-computed tomography; NMR, nuclear magnetic resonance; OC, osteocalcin; Tb. BMD, trabecular bone mineral density; Tb. BV/TV, tibia trabecular relative bone volume; Tb. Th, trabecular thickness; Tb. Sp, trabecular space; Tb. N, trabecular number; TCM, traditional Chinese medicine.

traditional medicinal plants have the therapeutic potential of preventing alcohol-induced bone diseases.

Keywords: ethnopharmacology, traditional Chinese medicine, alcohol-induced bone diseases, osteoporosis, TCM herbal extracts

INTRODUCTION

Traditional Chinese medicine has treated various diseases, including bone diseases and alcoholism. Osteoporosis is the most common bone disease, representing a significant public health problem worldwide (Cosman et al., 2014; Wright et al., 2014; Langdahl and Andersen, 2018; Compston et al., 2019). There has been considerable progress in understanding postmenopausal and senile osteoporosis; however, knowledge gaps still exist in understanding osteoporosis/osteopenia caused by alcoholism. The effects of alcohol on human health are complex. Although it is debatable about the benefits of moderate drinking, epidemiological studies suggest that light-moderate alcohol consumption benefits the heart and circulatory system, protects against diabetes, and is associated with lower risks for mortality and cancer in older adults (Howard et al., 2004; Karlamangla et al., 2009; Mostofsky et al., 2016; Kunzmann et al., 2018). However, heavy drinking is detrimental to many organs and tissues and is a significant cause of preventable stroke, heart failure, and death (Garaycoechea et al., 2018; GBD, 2018; Wood et al., 2018; USDA and HHS, 2020; NIAAA., 2021). Alcohol has a complex effect on the adult skeleton depending on age, drinking pattern, and alcohol consumption. Light to moderate alcohol consumption is generally reported to be beneficial or have a neutral impact on bone health in old adults, while chronic excessive drinking induces bone mass loss and osteoporosis, which increases fracture risk, deficient bone repair and causes alcohol-induced osteonecrosis (Turner, 2000; Chakkalakal, 2005; Maurel et al., 2012; Sommer et al., 2013; Mikosch 2014; Gaddini et al., 2016).

TCM-based herbal therapies often use alcohol as a delivery medium for centuries; one class of Chinese herbal medicines is Chinese herbal Liqueur (Xia, 2013; Cheung et al., 2021). The alcoholic drinks of herbal extracts are also used for a wide range of medicinal purposes documented in classical pharmacy and ethnobotanical studies in Europe (Egea et al., 2015). The Chinese medicinal or herbal Liqueur, an alcoholic beverage, is commonly produced by soaking precious Chinese medicinal materials (Xia, 2013; Cheung et al., 2021). It became prevalent among Chinese people due to its nourishing and tonic functions or as nutraceuticals. A typical TCM formula has multiple ingredients that synergize in treatment for the symptoms of a disease, which have greater efficacy and safety than a single drug in clinical practices, possibly due to the multiple ingredients synergistic interactions and mutual detoxification (Ung et al., 2007; He et al., 2015; Zhang and Cheng, 2019). The TCM herbal extracts (Jing extracts) used in this study were prepared from a herbal combination formula of nine Chinese herbal medicines, which was used in a famous Chinese Herbal Liqueur, Chinese Jing Liqueur (Liu et al., 2011; Lu et al., 2017; Lu et al., 2018; Shan et al., 2018; Cai et al., 2020; Hu et al., 2021). Preclinical and clinical studies demonstrated that studied herbal formulation has the properties of improving kidney-yang deficiency in rats and relieving main symptoms of patients with Kidney-Yang Deficiency Syndrome, anti-fatigue, and enhancing immunity in humans and animals (Liu et al., 2011; Lu et al., 2017; Lu et al., 2018; Shan et al., 2018; Cai et al., 2020; Hu et al., 2021). The analyses of chemical components by HPLC, LC/MS, and NMR (Liu et al., 2008; Cai et al., 2020; Hu et al., 2021) showed that the extracts of these Chinese herbal medicines (Jing extracts) contain a variety of saponins, flavonoids, active polysaccharides, and other functional factors and nutrients required by the human

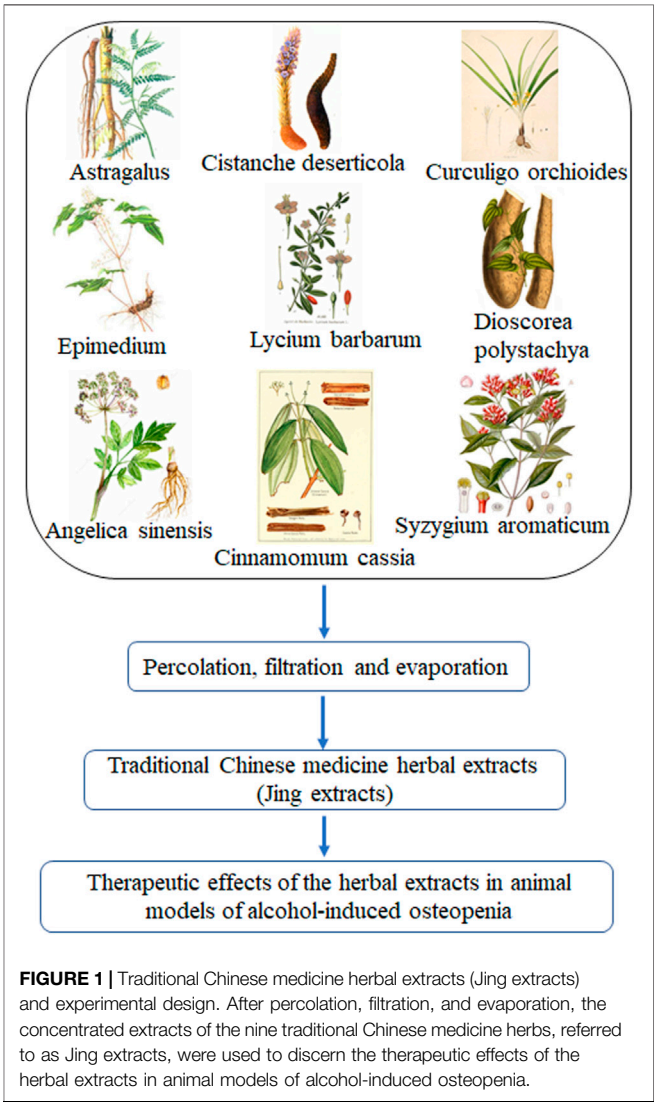

FIGURE 1 | Traditional Chinese medicine herbal extracts (Jing extracts) and experimental design. After percolation, filtration, and evaporation, the concentrated extracts of the nine traditional Chinese medicine herbs, referred to as Jing extracts, were used to discern the therapeutic effects of the herbal extracts in animal models of alcohol-induced osteopenia.

TABLE 1 | The roles of the studied herbs in bone diseases and alcohol use disorder.

Herbs[a]	Roles of herbs in bone diseases	Roles of herbs in alcohol use disorder
Astragalus mongholicus Bunge (*Astragalus*) Chinese: Huang Qi	*Astragalus* with supplemental calcium significantly improved bone mineral density and bone metabolism in ovariectomized rats Kang et al. (2013)	The extracts from *Myristica fragrans*, *Astragalus*, and Poria cocos ameliorated alcohol-induced acute liver toxicity Yimam et al. (2016)
Cistanche deserticola Y. C. Ma (Cistanche deserticola) Chinese: Rou Cong Rong	*Cistanche deserticola* has antiosteoporotic activity in type I osteoporotic rats Zhang et al. (2021) and type II osteoporotic mice Wang et al. (2021)	*Cistanche deserticola* possessed hepatoprotective activity against chronic hepatic injury induced by alcohol Guo et al. (2016)
Dioscorea polystachya Turcz. (*Dioscorea polystachya*, Chinese yam) Chinese: Shan Yao	*Dioscorea spongiosa* prevents glucocorticoid-induced osteoporosis in rats Han et al. (2016) and aging-induced osteoporosis Tikhonova et al. (2015)	*Dioscorea polystachya* extracts have protective effects against alcohol-induced gastric ulcers in mice Byeon et al. (2018)
Lycium barbarum L. (*Lycium barbarum*, Chinese wolfberry or Goji berry) Chinese: Gou Qi	*Lycium barbarum* ameliorates osteoporosis in OVX mice Kim et al. (2017)	*Lycium barbarum* has a hepatoprotective effect against alcohol-induced oxidative damage Wang et al. (2020a)
Epimedium brevicornu Maxim (Epimedium, Herba Epimedii) Chinese: Yin Yang Huo	*Epimedium* reverses bone loss in a rat model of postmenopausal osteoporosis Zhang et al. (2006) and alcohol-induced osteopenia Wu et al. (2018)	Icariin, one of the bioactive compounds in epimedium, may reduce alcohol consumption in bipolar disorder and alcohol use Xiao et al. (2016)
Cinnamomum cassia (L.) J. Presl (*Cinnamomum cassia*, Chinese Cinnamon), Chinese: Rou Gui	*Astragalus membranaceus*, *Cinnamomum cassia*, and *Phellodendron amurense* reverse bone loss in postmenopausal osteoporosis Huh et al. (2015)	Cinnamon extract protects against acute alcohol-induced liver steatosis in mice Kanuri et al. (2009)
Syzygium aromaticum Merr. and L.M.Perry (Syzygium aromaticum, clove) Chinese: Ding Xiang	*Syzygium aromaticum* reverses bone loss in a rat model of postmenopausal osteoporosis Karmakar et al. (2012)	*Syzygium aromaticum* attenuates alcohol-induced gastric injury in rats Jin et al. (2016)
Angelica sinensis (Oliv.) Diels (*Angelica sinensis*, Chinese angelica) Chinese: Dang Gui	*Angelica sinensis* reverses bone loss in a rat model of postmenopausal osteoporosis Lim and Kim, (2014)	*Angelica sinensis* protects against alcoholic liver damage in mice Wang et al. (2020a)
Curculigo orchioides Gaertn. (*Curculigo orchioides*, *Rhizoma curculiginis*, Curculigo Rhizome) Chinese Pinyin: Xian Mao	*Curculigo orchioides* prevents bone loss in ovariectomized rats Cao et al. (2008)	*Curculigo orchioides* extract has antioxidant and hepatoprotective properties in rats Jacob Jesurun and Johan Pandian, (2019)

[a]*The Chinese medicinal plant names referred to The Plant List (http://www.theplantlist.org/), Medicinal Plant Names Services of Royal Botanic Gardens, Kew (https://mpns.science.kew.org/mpns-portal/), or NCBI taxonomy database (https://www.ncbi.nlm.nih.gov/taxonomy).*

body. Although preclinical and clinical data show that saponins, flavonoids, and polysaccharides prevent osteoporosis, the therapeutic effects of Jing extracts on alcohol-induced bone diseases were unknown. In this study, we investigated whether TCM herbal extracts prevent chronic alcohol consumption-induced osteopenia in mice.

MATERIALS AND METHODS

Materials and Experimental Design

The traditional Chinese medicine herbal extracts used in this study is a combinative herbal formula of nine Chinese herbal medicines, including *Astragalus mongholicus* Bunge (*Astragalus*) (10–15% of total herbal medicine weight as described in Liu et al., 2008), *Cistanche deserticola* Y. C. Ma (*Cistanche deserticola*) (10–15%), *Dioscorea polystachya* Turcz. (*Dioscorea polystachya*, Chinese yam) (10–15%), *Lycium barbarum* L. (*Lycium barbarum*, Chinese wolfberry or Goji berry) (10–15%), *Epimedium brevicornu* Maxim (*Epimedium*, Herba Epimedii) (10–15%), *Cinnamomum cassia* (L.) J. Presl (*Cinnamomum cassia*, Chinese Cinnamon) (3–5%), *Syzygium aromaticum* Merr. and L.M.Perry (*Syzygium aromaticum*) (3–5%), *Angelica sinensis* (Oliv.) Diels (*Angelica sinensis*, Chinese angelica) (10–15%), and *Curculigo orchioides* Gaertn. (*Curculigo orchioides*, *Rhizoma curculiginis*) (10–15%) (**Figure 1**; **Supplementary Figure S1**; **Table 1**; **Supplementary Table S1**). This herbal formula was originally designed in late China's Qing Dynasty. After being modified several times by TCM experts in the 1980s, it was approved by China's National Medical Products Administration (Approval # 1997 No. 728) for anti-fatigue and enhancing immunity as the TCM herbal formula in a famous Chinese Herbal Liqueur, Chinese Jing Liqueur (Liu et al., 2011; Lu et al., 2017; Lu et al., 2018; Shan et al., 2018; Cai et al., 2020; Hu et al., 2021). The traditional Chinese medicine herbs were collected by researchers at Jing Brand Research Institute. Voucher specimens (as described in Cai et al., 2020) are deposited at the Herbarium of Jing Brand Research Institute, Daye, Hubei, China. The raw Chinese herbal medicines were washed, dried, and sliced into pieces and superfine pulverization according to the protocols in Chinese Pharmacopoeia. The traditional Chinese medicine herbal extracts (Jing extracts) were prepared with a percolation extraction method with 35% alcohol (50-fold of total herbal medicine weight for 12–15 days) (Liu et al., 2008; Shan et al., 2018; Cai et al., 2020). After percolation, the liquids were separated from insoluble materials with disc centrifuge and membrane separation technology and concentrated via nanofiltration membrane; the concentrated traditional Chinese medicine herbal extracts, referred to as Jing extracts, was obtained for pharmacognostic analysis to discern the effects of Jing extracts on alcohol-induced osteopenia (**Figure 1**). The extracts of these Chinese herbal medicines (Jing extracts) have been characterized by chemical constituent analysis with LC/MS and NMR (Cai et al., 2020; Hu et al., 2021) as well as high-performance liquid chromatogram-gas chromatography fingerprint analysis (Liu et al., 2008) (**Table 2**; **Supplementary Figure S7**).

TABLE 2 | Roles of bioactive compounds in the studied herbs in bone diseases and alcohol use disorder.

Bioactive compounds[a,b]	The herbs contain the compound[c]	Roles of bioactive compounds in bone diseases	Roles of bioactive compounds in alcohol use disorder
Acteoside	*Cistanche deserticola*	Acteoside has a protective effect on OVX-induced bone loss in mice Yang et al. (2019a)	Acteoside ameliorates alcohol-induced hepatic damage Khullar et al. (2019)
Calycosin	*Astragalus Angelica sinensis*	Calycosin has an unusual antiosteoporotic activity in OVX rats Li et al. (2016)	
Daidzin	*Astragalus*	Daidzin is a promising agent in the treatment of osteolytic diseases Wei et al. (2019)	Daidzin is an antidipsotropic agent Keung and Vallee, (1998)
Echinacoside	*Cistanche deserticola*	Echinacoside is especially effective for preventing osteoporosis induced by estrogen deficiency Li et al. (2013)	Echinacoside ameliorates alcohol-induced oxidative stress and hepatic steatosis Tao et al. (2021)
Epimedin A	*Epimedium*	Epimedin A remarkably enhances bone regeneration Liu et al. (2021)	
Eugenol	*Cistanche deserticola Syzygium aromaticum*	*Syzygium aromaticum* extract eugenol reverses bone loss in a rat model of postmenopausal osteoporosis Karmakar et al. (2012)	Eugenol reduced alcohol-induced hepatotoxicity in rats Yildiz and Öztürk, (2020)
Ferulic acid	*Angelica sinensis Lycium barbarum*	Ferulic acid protects against osteoporosis in neonatal rats with glucocorticoid-induced osteoporosis Hou et al. (2019)	Ferulic acid is an anti-hepatotoxic agent on alcohol-induced liver damage Rukkumani et al. (2004)
Hyperoside	*Epimedium*	Hyperoside has potential beneficial effects on bone metabolism in OVX mice Chen et al. (2018)	Hyperoside is one of the polyphenols extracted from a white tea that has preventative effects against alcoholic liver injury Zhou et al. (2019)
Icariside	*Epimedium*	Icariside II might treat dexamethasone-associated osteoporosis/osteonecrosis Liu et al. (2017)	
Icariin	*Epimedium*	Icariin has the potential treatment of postmenopausal osteoporosis Wang et al. (2018)	Icariin may resduce alcohol consumption in people with bipolar disorder and alcholol use Xiao et al. (2016)
Oleanolic acid	*Syzygium aromaticum*	Oleanolic acid significantly increased bone mineral density in OVX mice Cao et al. (2018)	Oleanolic acid protect rats against ethanol-induced liver injury Liu et al. (2014)
Protocatechuic acid	*Angelica sinensis*	Protocatechuic Acid attenuates bone loss in OVX mice Jang et al. (2018)	Protocatechuic acid alleviates alcholic liver injury Fu et al. (2019)
Sagittatoside A and B	*Epimedium*	Sagittatoside A and B might be beneficial for improving postmenopausal osteoporosis Zhao et al. (2016)	
(Z)-Ligustilide	*Angelica sinensis*	Ligustilide promotes bone formation Yang et al. (2019b)	

[a]*Among the 189 compounds by LC/MS and NMR (Cai et al., 2020) and 43 bioactive components by LC/MS (Hu et al., 2021) isolated from the Chinese herbal extracts.*
[b]*The chemical structures of herbal bioactive compounds in* ***Supplementary Figure S7****.*
[c]*Reference to Zeng et al. (2019) and Fai (2009).*

Animal Models of Alcohol-Induced Osteopenia

Two-month-old Balb/c male mice were purchased from Jackson lab (Bar Harbor, ME) as the young adult animal in this study (after 50 experimental periods, the mice were 4-month-old). The middle-aged/old Balb/c male mice (10-month-old) (after 50 experimental periods, the mice were about 12-month-old) were purchased from Envigo (Indianapolis, IN). Mice were provided with standard chow and water *ad libitum*. Animal maintenance and experimental treatments were conducted per the ethical guidelines for animal research established and approved by BWH Institutional Animal Care and Use Committee.

There are several different murine models of alcohol-induced bone loss regarding alcohol administration, including oral alcohol administration by gavage (Iwaniec and Turner, 2013; Martiniakova et al., 2018), alcohol in drinking water (Liu et al., 2016; Okuda et al., 2018), intraperitoneal (i.p.) administration of alcohol by injection (Iwaniec and Turner, 2013), and Liber-DeCarli liquid diet feeding (Dai et al., 2000; Mercer et al., 2012). Although there are advantages and disadvantages among the methods of alcohol administration, oral alcohol administration by gavage in animals is a better model to mimic intermittent drinking in humans. We used the oral alcohol administration by gavage in Balb/c male mice as the murine models of alcohol-induced osteopenia and to study the effects of TCM extracts on alcohol-induced osteopenia. The process of oral alcohol administration by gavage was performed as described in the NIAAA model (Bertola et al., 2013). As shown in **Figure 2**, oral administration of 3.2 g/kg alcohol (0.2 ml of 40% v/v alcohol for a 20 g body weight mouse) by gavage for 50 days was used to study alcohol-induced osteopenia in male Balb/c mice.

Traditional Chinese Medicine Herbal Extracts (Jing Extracts) Administration in Mice

The doses of Jing extracts used in the experimental mice were designed based on the recommended human dose (Liu et al., 2008; Liu et al., 2011; Lu et al., 2017; Lu et al., 2018; Shan et al., 2018) and the human-mouse dose conversion (Wojcikowski and Gobe, 2014; Nair and Jacob S., 2016) (details refer to **Supplementary Material**). Taking into account that the commonly used mouse gavage volume is 10 ml/kg (0.2 ml for a 20 g mouse), we defined the first mouse dose of Chinese herbal extracts (0.2 ml for a 20 g mouse), as the low dose (0.125 g/kg

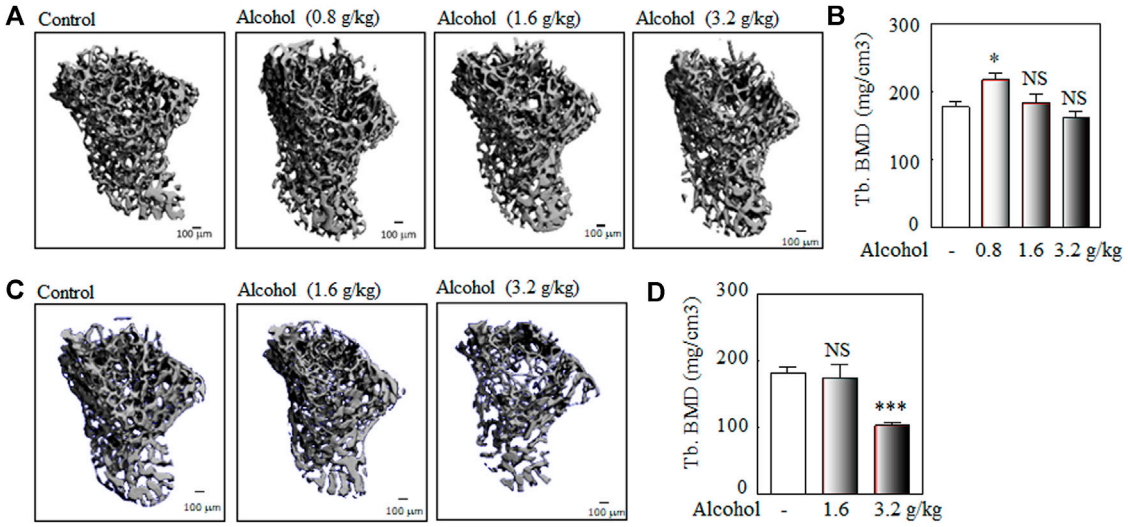

FIGURE 2 | The murine models of alcohol-induced osteopenia: the dose and duration. Balb/c male mice (2-month-old) were used to explore the optimal dose and duration of the oral alcohol administration by gavage for alcohol-induced osteopenia. The young adult Balb/c male mice (2-month-old) were used to analyze the optimal dose (0.8, 1.6 g/kg, and 3.2 g/kg body weight) and duration (once per day at 3–4 PM, 5 days per week for 30 or 50 days) of alcohol-induced osteopenia. **(A)** The representative μ-CT 3-D microstructures of trabecular bone were obtained from male mice with alcohol gavage (Alcohol) or water gavage (Control) for 30 days; bars represent 100 μm. 3-D microstructural properties of the tibia were calculated using software supplied by the manufacturer. **(B)** The quantitative analysis of trabecular bone mineral density (Tb. BMD); the oral alcohol administration of 0.8 g/kg dose of alcohol (n = 4) for 30 days significantly increased BMD in Balb/c adult male mice (alcohol vs. control group, n = 5, $^{*}p < 0.05$, Mann-Whitney test); the 1.6 g/kg (n = 7) and 3.2 g/kg (n = 5) doses of alcohol for 30 days did not induce significant bone loss (alcohol vs. control group, n = 5; NS: not significant, Mann-Whitney test). **(C)** The representative μ-CT 3-D microstructures of trabecular bone were obtained from male mice with alcohol gavage (Alcohol) or water gavage (Control) for 50 days. **(D)** The quantitative analysis of trabecular bone mineral density (Tb. BMD); a lower dose (1.6 g/kg) of alcohol for a longer duration (50 days) did not induce bone loss (alcohol, n = 7, vs. control, n = 18, NS: not significant, Mann-Whitney test); the oral alcohol administration of 3.2 g/kg alcohol for 50 days induced significant bone loss (alcohol, n = 8 vs. control group, n = 18, $^{***}p < 0.001$, t-test).

body weight for a 20 g mouse with 0.2 ml oral administration by gavage of 12.5 g/L of Chinese herbal extracts in 40% v/v alcohol); the second and third doses contained 0.25 g/kg (25 g/L of Chinese herbal extracts in 40% v/v alcohol) and 0.50 g/kg (50 g/L of Chinese herbal extracts in 40% v/v alcohol) of Chinese herbal extracts respectively. We tested the effects of these three doses of Chinese herbal extracts on alcohol-induced bone loss in Balb/c male mice. After 50 days of orally administering 3.2 g/kg of alcohol with/without Chinese herbal extracts by gavage, the mice were sacrificed for bone morphological and biochemical analysis.

Bone Morphological Analysis: μ-CT

Bone morphological analysis of proximal tibia was performed with a μ-CT (μ-CT 35, Scanco Medical, Switzerland) as described (Charles et al., 2012). The scanned region proximal to the growth plate and extending 1.4 mm was selected for trabecular bone analysis (indicated with a box **Supplementary Figure S2**). A second region 0.6 mm in length and centered at the midpoint of the tibia was used to calculate the diaphyseal parameters (shown with a box in **Supplementary Figure S2**). 3-D microstructural properties of bone, e.g., trabecular bone mineral density (Tb. BMD), tibia trabecular relative bone volume (Tb. BV/TV), trabecular thickness (Tb. Th), trabecular space (Tb. Sp), trabecular number (Tb. N), and cortical bone mineral density (C. BMD), were calculated using software supplied by the manufacturer (Scanco Medical, Switzerland).

Bone Morphological Analysis: Histological Analysis

In addition to μ-CT analysis of skeletal parameters, some murine bones were used for histological analysis. The tibia was removed from the attached muscle tissue, fixed with 10% formalin (at least 48 h), decalcified with EDTA, plastic-embedded (JB-4 Kit, Polysciences, Warrington, PA), and sectioned (10 μm); the sections were stained with 0.5% toluidine blue-O, pH 4.0 (Thermo Fisher Scientific, Waltham, MA, United States).

Biochemical Analysis of Alcohol-Induced Bone Loss

The blood was taken 6 h after fasting on the second day of the last gavage, left for 30–60 min after blood collection, centrifuged at 1,500 g for 15 min, and the serum was separated and kept at −80 C until the biochemical analysis for biomarkers of bone formation, e.g., osteocalcin (OC), and bone resorption, e.g., Type I collagen carboxy-terminal telopeptide (CTX). The serum levels of osteocalcin, a non-collagenous protein formed by osteoblasts, were detected by using the mouse osteocalcin ELISA kit (MyBioSource, San Diego, CA, United States). Type I collagen is the main organic component of bones. When physiological or pathological bone resorption is increased (such as osteoporosis), the degradation of type I collagen is

also increased, and the content of decomposed fragments in the blood is correspondingly increased. The main molecular fragment of type I collagen degradation products is the CTX. An increase in the serum CTX level indicates an increase in bone resorption. The serum levels of Type I collagen carboxy-terminal telopeptide (CTX) were detected by using Mouse Cross-Linked C-Telopeptide of Type I Collagen (CTXI) ELISA Kit (MyBioSource, San Diego, CA, United States).

RNA Isolation and RT-PCR

Total RNA was isolated from bone marrow or MC3T3-E1 cells with Trizol reagent (Invitrogen). For RT-PCR, 2 μg of total RNA was reverse-transcribed into cDNA with M-MLV reverse transcriptase (Promega, WI), following the manufacturer's instructions. One-twentieth of the cDNA was used in each 50 μl PCR reaction with Promega GoTaq Flexi DNA Polymerase (30–35 cycles of 94°C for 1 min, 55–60°C for 1 min, and 72°C for 2 min). Amplification conditions were optimized to reflect the exponential phase of amplification for each gene. Gene-specific primers were used to amplify ALP, TNF-α, IL-1β, BSP, RUNX2, and BMP2 as shown in **Supplementary Table S2**. PCR products were separated by 2% agarose gel electrophoresis and captured with KODAK Gel Logic 200 Imaging System and KODAK Molecular Imaging Software (Carestream Health, Rochester, NY, United States). The densitometry of inverted ethidium bromide staining PCR bands was quantified by NIH ImageJ. Relative expression levels were calculated by normalizing the densitometric units to GAPDH, the internal control.

Alkaline Phosphatase Enzyme Assay

MC3T3-E1 cells were cultured in quadruplicate in 24-well-plates in a growth medium. Upon confluence, medium was changed to osteoblastogenic medium (phenol red-free α-MEM with 10% FBS-HI, 100 U/ml penicillin, 100 μg/ml streptomycin plus 5 mM β-glycerophosphate and 50 μg/ml ascorbate-2-phosphate) for 6 days. Protein concentrations were quantified using BCA Assay kit, and ALP enzyme activity was measured spectrophotometrically and expressed as μmol/min/g protein (Zhou et al., 2008).

Statistical Analysis

All experiments were performed at a minimum in triplicate; for *in vivo* experiments, a minimum three mice per experimental group per time were performed; for *in vitro* ALP activity, quadruplicate wells per experimental group were performed. All test parameters were quantified as continuous data and used standard statistical tests. The Kolmogorov-Smirnov tool was used to test whether data sets were distributed normally. Group data are presented as mean ± SEM. Unless otherwise indicated, quantitative data were analyzed with a non-parametric Mann-Whitney test or if data allowed, a parametric *t*-test for group comparisons with GraphPad Instat (GraphPad Software, La Jolla, CA, United States). A value of $p < 0.05$ was considered significant.

RESULTS

The Murine Model of Alcohol-Induced Osteopenia: The Optimal Dose and Duration of Oral Alcohol Administration

The young adult Balb/c male mice (2-month-old) were used to explore the doses (0.8, 1.6, and 3.2 g/kg body weight, once per day at 3–4 PM, 5 days per week) and duration (30 and 50 days) of oral alcohol administration for alcohol-induced osteopenia in male mice. Our data showed that Balb/c male mice (2-month-old) were orally administered alcohol by gavage, the 0.8 g/kg dose of alcohol for 30 days significantly increased BMD in Balb/c adult male mice, and the 1.6 g/kg and 3.2 g/kg alcohol did not induce significant bone loss after 30 days gavage (**Figures 2A,B**); a low dose of 1.6 g/kg alcohol did not affect bone mineral density after 50 days gavage (**Figures 2C,D**); after 50 days of oral administered alcohol, 3.2 g/kg of alcohol-induced significant bone loss in Balb/c male mice (about 4-month-old when sacrificed) (**Figures 2C,D**). Thereafter, we used the dose of 3.2 g/kg alcohol and a duration of 50 days for the effects of TCM extracts on alcohol-induced osteopenia.

Chinese Herbal Extracts Prevent Chronic Alcohol Consumption-Induced Osteopenia in Young Adult Male Mice

We used the dose of 3.2 g/kg of alcohol administered by gavage for 50 days, which induced significant bone loss in young adult male Balb/c mice, as shown in **Figure 2**, for the effects of herbal extracts on alcohol-induced osteopenia. To explore the optimal doses of traditional Chinese medicine herbal extracts (Jing extracts) that prevent alcohol-induced osteopenia, Balb/c male mice (2-month-old) were orally administered 3.2 g/kg alcohol by gavage with or without 0.125 g/kg, 0.25 g/kg, or 0.5 g/kg of traditional Chinese medicine herbal extracts (Jing extracts) (as described in **Figure 1**). After 50 days of oral administration of alcohol with/without Chinese herbal extracts by gavage, the mice were sacrificed for bone morphological analysis by μ-CT with the methods described in **Supplementary Figure S2** and **Figure 3**. The 3-D microstructures of trabecular bone (**Figure 3A**) and quantitative analysis of the microstructural properties of the tibia (**Figures 3B–G**), including trabecular bone mineral density (Tb. BMD), trabecular relative bone volume (Tb. BV/TV), trabecular number per mm (Tb. N), and trabecular Structure modulus index (Tb. SMI), showed that the effect of Chinese herbal extracts is dose-dependent in preventing alcohol-induced bone loss in young adult male mice. Our data showed that 3.2 g/kg alcohol induced significant bone loss in young adult male Balb/c mice after 50 days of oral administration by gavage (**Figure 3**); the low, middle, and high doses of Chinese herbal extracts alleviate the chronic alcohol consumption-induced trabecular bone damage; all three doses of Chinese herbal extracts mitigate the alcohol-induced decreases of bone mineral density and relative bone volume or bone volume fraction (**Figures 3B,C**); the Chinese herbal extracts also alleviate alcohol-reduced trabecular number

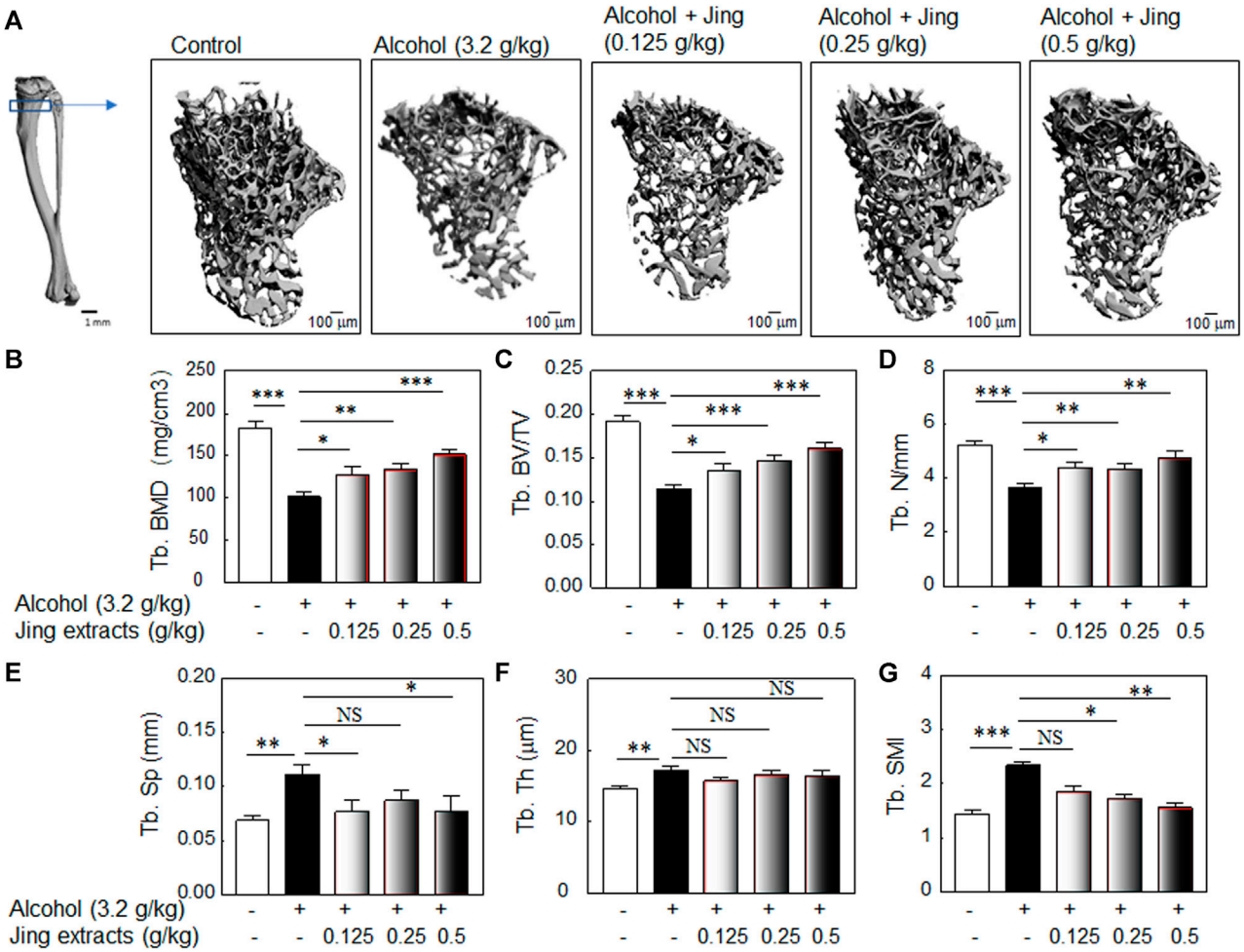

FIGURE 3 | Traditional Chinese medicine herbal extracts (Jing extracts) prevent chronic alcohol consumption-induced osteopenia in young adult male mice. To explore the optimal dose of Jing extracts that prevent alcohol-induced osteopenia in young adult mice, Balb/c male mice (2-month-old) were orally administered 10 ml/kg of 40% alcohol (3.2 g/kg body weight) by gavage for 50 days (gavage once a day, 5 days per week) with or without 0.125 g/kg, 0.25 g/kg or 0.5 g/kg of Jing extracts. **(A)** The representative μ-CT 3-D microstructures of trabecular bone were obtained from male mice with alcohol gavage (Alcohol) ± Jing extracts or without alcohol (Control); bars represent 100 μm. 3-D microstructural properties of the tibia were calculated using software supplied by the manufacturer. **(B)** The quantitative analysis of trabecular bone mineral density (Tb. BMD) (3.2 g/kg of Alcohol, $n = 9$, vs. DDW control, $n = 19$, $^{***}p < 0.001$, *t*-test; Alcohol + 0.125 g/kg of Jing extracts, $n = 4$, vs. Alcohol, $n = 9$, $^{*}p < 0.05$, Mann-Whitney test; Alcohol + 0.25 g/kg of Jing extracts, $n = 11$ vs. Alcohol, $n = 9$, $^{**}p < 0.01$, *t*-test; Alcohol + 0.5 g/kg of Jing extracts, $n = 5$, vs. Alcohol, $n = 9$, $^{***}p < 0.001$, *t*-test). **(C)** The quantitative analysis of tibia trabecular relative bone volume (Tb. BV/TV) ($^{***}p < 0.001$, *t*-test; $^{*}p < 0.05$, Mann-Whitney test). **(D)** The quantitative analysis of tibia trabecular number per mm (Tb. N) ($^{***}p < 0.001$, $^{**}p < 0.01$, *t*-test; $^{*}p < 0.05$, Mann-Whitney test). **(E)** The quantitative analysis of tibia trabecular separation (mm) ($^{**}p < 0.01$, *t*-test; $^{*}p < 0.05$, NS: not significant, Mann-Whitney test). **(F)** The quantitative analysis of trabecular thickness (Tb. Th, μm) ($^{**}p < 0.01$, *t*-test; NS: not significant, Mann-Whitney test). **(G)** The quantitative analysis of tibia trabecular Structure modulus index (Tb. SMI) ($^{***}p < 0.001$, $^{**}p < 0.01$, *t*-test; NS: not significant, Mann-Whitney test).

decrease (**Figure 3D**) and the corresponding increase of trabecular separation (**Figure 3E**), but no effects were observed for trabecular thickness (**Figure 3F**). Although there are controversial in the literature (Salmon et al., 2015), structure model index (SMI), which is widely used to measure rods and plates in trabecular bone, represents the trabecular geometry transitions from being more plate-like (reflected high mechanical stress) to more rod-like (low mechanical stress) as osteoporosis severity increases (Ding et at., 2002; Hildebrand and Rüegsegger, 1997), which inversely correlated with the bone mechanical property (Ding et al., 2002). Our data showed that two doses of 0.25 g/kg and 0.5 g/kg of Chinese herbal medicines significantly mitigate the alcohol-induced damage in the bone mechanical property (**Figure 3G**).

Traditional Chinese Medicine Herbal Extracts (Jing Extracts) Prevent Chronic Alcohol Consumption-Induced Osteopenia in Middle-Aged/Old Male Mice

Prevention of problematic alcohol use is mainly focused on younger adults, while an epidemiological study showed that

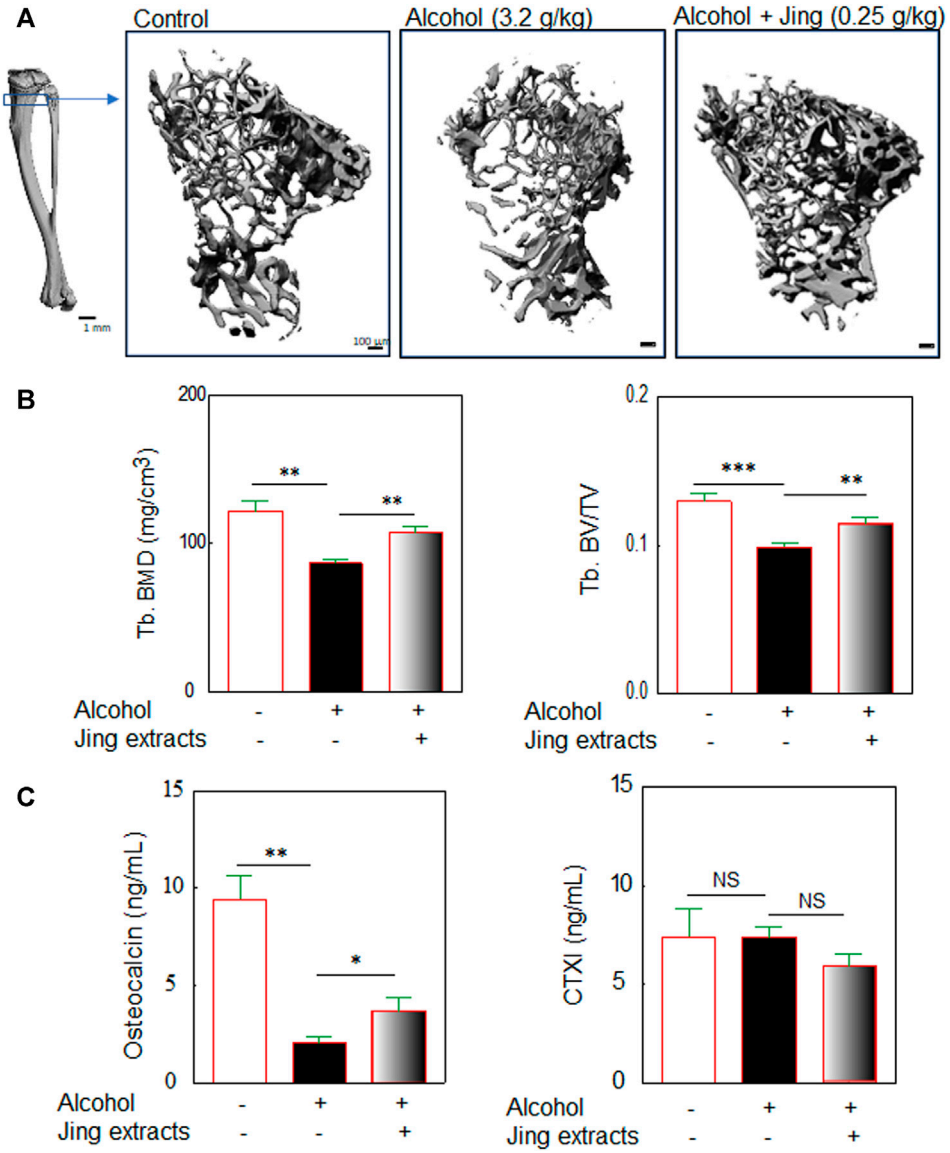

FIGURE 4 | Traditional Chinese medicine herbal extracts (Jing extracts) prevent chronic alcohol consumption-induced osteopenia in middle-aged/old male mice. Balb/c male mice (10-month-old) were orally administered 3.2 g/kg body weight of alcohol by gavage for 50 days (gavage once a day, 5 days per week) with or without 0.25 g/kg of Jing extracts. **(A)** The representative μ-CT 3-D microstructures of trabecular bone were obtained from male mice with alcohol gavage (Alcohol) ± Jing extracts or without alcohol (Control); bars represent 100 μm. 3-D microstructural properties of the tibia were calculated using software supplied by the manufacturer. **(B)** The quantitative analysis of trabecular bone mineral density (Tb. BMD) (3.2 g/kg of Alcohol, n = 8, vs. DDW control, n = 9, $^{**}p < 0.01$; Alcohol + 0.25 g/kg of Jing extracts, n = 9, vs. Alcohol, n = 8, $^{**}p < 0.01$, t-test) and tibia trabecular relative bone volume (Tb. BV/TV) ($^{***}p < 0.001$, $^{**}p < 0.01$, t-test). **(C)** The effects of Jing extracts on biomarkers of bone formation and bone resorption in middle-aged/old Balb/c male mice. Balb/c male mice (10-month-old) were orally administered 3.2 g/kg body weight of alcohol by gavage for 50 days (gavage once a day, 5 days per week) with or without 0.25 g/kg of Jing extracts (about 12-month-old when mice were sacrificed). Biochemical analysis of bone formation biomarker osteocalcin in serum of middle-aged/old mice (alcohol, n = 6, vs. control, n = 9, $^{**}p < 0.01$, t-test; Jing extracts, n = 7, vs. alcohol, n = 6, $^{*}p < 0.05$, Mann-Whitney test) and biochemical analysis of bone resorption biomarker cross-linked C-Telopeptide of Type I Collagen (CTXI) (NS: not significant, t-test).

heavy drinking in middle-aged and older adults is more frequent with a greater impact on function and health (Veerbeek et al., 2019). There are age-related changes in bone structure and strength in Balb/c mice (Willinghamm et al., 2010). To investigate the preventing effects of Jing extracts on chronic alcohol consumption-induced osteopenia, we used 10-month-old Balb/c male mice (about 12 months old after the experiments of chronic alcohol consumption-induced osteopenia), which have a significantly lower bone mineral density than the young adult mice (about 4 months old after the experiments) (**Supplementary Figure S3**), but still have enough trabecular bones, as shown by μ-CT and histological staining, to study the chronic alcohol consumption-induced bone loss and the preventive effects of herbal extracts on osteopenia.

To study the effects of traditional Chinese medicine herbal extracts on chronic alcohol consumption-induced osteopenia in middle-aged mice, Balb/c male mice (10-month-old) were orally administered 3.2 g/kg alcohol by gavage with or without 0.25 g/kg of Chinese herbal extracts (as described in **Figure 1**). After 50 days of oral administration of alcohol by gavage with/without Chinese herbal extracts (the mice were about 12-month-old at the end of the experiments), the mice were sacrificed for bone morphological analysis with μ-CT as the methods described in **Supplementary Figure S2**, including the 3-D microstructures of trabecular bone (**Figure 4A**) and quantitative analysis of the microstructural properties of the tibia, including trabecular bone mineral density (Tb. BMD) (**Figure 4B**) and trabecular relative bone volume (Tb. BV/TV) (**Figure 4B**). Our data showed that alcohol (3.2 g/kg) induced significant bone loss in middle-aged/old male Balb/c mice after 50 days of oral administration by gavage (**Figure 4**); the 0.25 g/kg of Chinese herbal extracts alleviate the chronic alcohol consumption-induced trabecular bone damage, which was demonstrated by Chinese herbal extracts mitigating the alcohol-induced decreases of bone mineral density and relative bone volume or bone volume fraction (**Figure 4B**).

The biochemical analysis for biomarkers of bone formation and bone resorption was performed by using the serum obtained from the middle-aged/old mice. The serum levels of osteocalcin, a bone formation biomarker, were detected with a mouse osteocalcin ELISA kit (MyBioSource, San Diego, CA, United States). An increase in the serum type I collagen carboxy-terminal telopeptide (CTX) level indicates increased bone resorption. The serum levels of Type I collagen carboxy-terminal telopeptide (CTX) were detected by using a Mouse Cross-Linked C-Telopeptide Of Type I Collagen (CTXI) ELISA Kit (MyBioSource, San Diego, CA, United States). Our biochemical analysis (**Figure 4C**) showed that 3.2 g/kg of alcohol significantly reduced serum levels of osteocalcin (**Figure 4C**) but did not reduce serum levels of CTXI (**Figure 4C**) in middle-aged/old Balb/c male mice. Out data suggest that chronic alcohol consumption inhibits bone formation but has no effects on bone resorption, which is consistent with previous reports (summarized in Sampson, 1998), indicated that alcoholic osteoporosis is characterized by decreased bone formation but normal levels of resorption. The Chinese herbal extracts mitigate the alcohol-induced decreases of osteocalcin, a bone formation biomarker (**Figure 4C**), implying that phytomedicines may prevent alcohol-induced osteopenia *via* reducing the alcohol-induced damage in osteoblastogenesis.

Protocatechuic Acid Mitigates Alcohol-Induced Decline of Alkaline Phosphatase

Among the 189 compounds identified by HPLC, LC/MS, and NMR (Cai et al., 2020) and 43 bioactive components identified by LC/MS (Hu et al., 2021) in Jing extracts, after a comprehensive literature review, we identify that Acteoside, Daidzin, Echinacoside, Eugenol, Ferulic acid, Hyperoside, Icariin, Oleanolic acid, and Protocatechuic acid have therapeutic potential for either bone or alcohol-related diseases (**Table 2**). To study the roles of bioactive compounds in the studied herbs in bone diseases, we selected Protocatechuic acid (**Figure 5A**) as a representative bioactive compound in the Jing extracts to test its effects on alkaline phosphatase and other bone metabolic factors in the bone marrow of Balb/c male mice and *in vitro* alkaline phosphatase activity in murine pre-osteoblastic cell line MC3T3-E1 cells.

Balb/c male mice (2-month-old) were orally administered 3.2 g/kg alcohol by gavage with or without 0.25 g/kg of Jing extracts or 50 mg/kg of PCA for 10 days, a time pint that alcohol damaged other organs, e.g., liver (Bertola et al., 2013), but not bones. Our data (**Figures 5B,C**) showed that as the Jing extracts, PCA significantly mitigates alcohol-induced decline of alkaline phosphatase gene expression in the bone marrow of Balb/c male mice. Jing extracts and PCA reduced the alcohol-induced elevated inflammatory factors, e.g., TNF-α and IL-1β in the bone marrow of Balb/c male mice (**Supplementary Figure S6**). To study the effects of PCA on alkaline phosphatase (ALP) activity, murine pre-osteoblastic cell line MC3T3-E1 cells were treated with or without alcohol and/or PCA in an osteogenic medium. Our data (**Figure 5D**) showed that PCA significantly alleviates the inhibitory effects of alcohol on ALP activity in MC3T3-E1 cells.

DISCUSSION

Alcohol is a nonessential diet component, and the overall impact of drinking on bone health, especially at moderate levels, is not well understood (Gaddini et al., 2016). Light to moderate alcohol consumption refers to two drinks or less in a day for men or one drink or less in a day for women per Dietary Guidelines for Americans (USDA and HHS, 2020). Epidemiological studies showed that light to moderate alcohol consumption is generally reported to be beneficial, resulting in higher bone mineral density (BMD) and reduced age-related bone loss, especially in men and postmenopausal women (Felson et al., 1995; Tucker et al., 2009; Sommer et al., 2013). However, heavy alcohol consumption is generally associated with decreased BMD, impaired bone quality, and increased fracture risk (Turner, 2000; Maurel et al., 2012; Mikosch, 2014; Gaddini et al., 2016). Similar to the epidemiological data, our preclinical studies showed that the effects of alcohol on bone health in mice are dose-and time-dependent. Our data showed that oral alcohol administration of a low dose of alcohol (0.8 g/kg body weight) significantly increased BMD in adult male mice (**Figure 2**); a low dose of oral alcohol administration by gavage (1.6 g/kg for 50 days) or higher doses (3.2 g/kg) for a shorter period of gavage time (30 days) have a neutral effect on bone mineral density in young adult Balb/c male mice (**Figure 2**). However, a high dose of alcohol administration (3.2 g/kg) with a longer gavage time (50 days) induces significant bone loss in young adult Balb/c male mice (**Figure 2** and **Figure 3**); thus, we used 3.2 g/kg alcohol dose and the duration of 50 days to study the effects of TCM herbal extracts on alcohol-induced osteopenia.

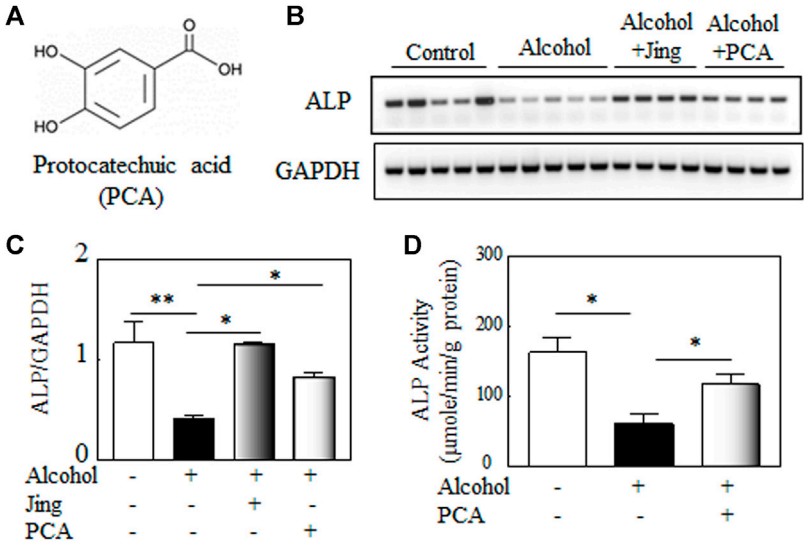

FIGURE 5 | Protocatechuic acid (PCA) mitigates alcohol-induced decline of alkaline phosphatase (ALP). **(A)** The chemical structure of Protocatechuic acid. **(B)** Representative gel electrophoretogram of RT-PCR products shows *ALP* and *GAPDH*, the internal control, gene expression in the bone marrows of Balb/c male mice. **(C)** The quantitative analysis of *ALP* gene expression shows that Jing extracts and PCA mitigate the alcohol-induced decline of ALP gene expression *in vivo* (alcohol, $n = 5$, vs. control, $n = 5$, $^{**}p < 0.01$; alcohol + Jing extracts, $n = 4$, or alcohol + PCA, $n = 4$ vs. alcohol, $^{*}p < 0.05$; Mann-Whitney test). **(D)** The effects of PCA on ALP activity in murine pre-osteoblastic cell line MC3T3-E1 cells. PCA (100 μM) significantly alleviates the inhibitory effects of alcohol (500 mM) on ALP activity *in vitro* (osteogenic control or alcohol + PCA vs. alcohol, $^{*}p < 0.05$; $n = 4$, Mann-Whitney test).

Osteoporosis is the most common bone disease, representing a significant public health problem worldwide (Cosman et al., 2014; Wright et al., 2014; Zhou and Glowacki, 2017; Langdahl and Andersen, 2018; Zhou and Glowacki, 2018; Compston et al., 2019). There has been considerable progress in understanding postmenopausal (Type I) and senile (Type II) osteoporosis, the primary osteoporosis; however, gaps of knowledge still exist in understanding osteoporosis/osteopenia caused by alcoholism, one type of secondary osteoporosis. Alcohol-induced osteopenia/osteoporosis is distinct from primary osteoporosis; particularly, alcohol-induced osteopenia results mainly from decreased bone formation rather than increased bone resorption (Chakkalakal, 2005), which is confirmed in old male mice by our biomarker analysis (**Figure 4C**). Our biochemical study (**Figure 4**) showed that alcohol significantly reduced serum levels of bone formation biomarker osteocalcin but not the serum levels of bone resorption biomarker CTXI in the middle-aged/old Balb/c male mice, suggesting that chronic alcohol consumption inhibits bone formation but has no effects on bone resorption. There is a paucity of studies regarding alcohol-induced osteoporosis therapy (Abukhadir et al., 2013). Although the study found that abstinence can stop bone loss and the lost bone can be partially restored when alcohol abuse ends (Alvisa-Negrín et al., 2009), research indicates that the effects of heavy alcohol use on bone cannot be reversed, even if alcohol consumption is terminated (Sampson, 2002). Additional studies should examine whether alcohol-induced osteoporosis is reversible. Nevertheless, severe osteoporosis, especially alcohol-induced osteoporosis in the elders, needs osteoporotic management.

Due to the nature of alcohol-induced osteopenia resulted mainly from decreased bone formation rather than increased bone resorption (Chakkalakal, 2005 and **Figure 4C**), anabolic treatments for osteoporosis, such as Teriparatide (parathyroid hormone 1–34), Abaloparatide (a parathyroid hormone-related protein analog drug), and Romosozumab (a humanized antibody against sclerostin), may help address these unmet needs. Other anabolic anti-osteoporotic agents, which stimulate bone formation, such as vitamin D and estrogen, should prevent alcohol-induced bone loss and benefit bone loss recovery during alcoholism and abstinence. Our data of oral administration of Vitamin D in Balb/c male mice (**Supplementary Figure S5**) confirmed a preclinical study that Vitamin D supplementation prevents chronic liquid diet alcohol-induced bone loss in female C57BL/6J mice (Mercer et al., 2012), suggesting that our data of oral alcohol administration by gavage are comparable with the data obtained by Lieber-DeCarli liquid diet feeding.

Traditional Chinese medicine (TCM) formulas have a long history of use in the prevention and treatment of osteoporosis, and phytochemicals from TCM formulas offer great potential for the development of novel antiosteoporotic drugs (Zhang et al., 2016; Lin et al., 2017). One of the molecular mechanisms of TCM antiosteoporotic drugs is the potential of promoting osteoblast-mediated bone formation (An et al., 2016), making TCM a good candidate for alcohol-induced osteoporosis therapy. The Xian-Ling-Gu-Bao capsule (XLGB) is an effective traditional Chinese medicine prescription that is used for the prevention and treatment of osteoporosis in China (Wu et al., 2017; Tang et al., 2020; Ding et al., 2021). We used XLGB as the TCM antiosteoporotic medicine control in our experiments and

showed that TCM XLGB might prevent alcohol-induced osteoporosis in young adult and middle-aged/old male mice (**Supplementary Figure S5**). Traditional Chinese medicines for the treatment of osteoporosis and osteoporotic fractures follow the TCM rule of "Kidneys Govern Bones," which uses herbs that medicate bone by improving the functions of the kidney (An et al., 2016; Wang et al., 2016). The Bone-kidney axis is critical for bone health. Kidney dysfunction, e.g., Chronic kidney disease (CKD), results in mineral and bone disorder (CKD-MBD), a systemic condition that links disorders of mineral and bone metabolism to either one or all of the following: abnormalities of calcium, phosphorus, PTH, or vitamin D metabolism, abnormalities in bone turnover, mineralization, volume, linear growth or strength, and extraskeletal calcification (Zhou et al., 2013; Zhou and Glowacki, 2017). In this study, the traditional Chinese medicine herbal extracts or Jing extracts (**Figure 1**) are a combinative herbal prescription of nine Chinese herbal medicines, including *Astragalus*, *Cistanche deserticola*, *Dioscorea polystachya* (Chinese yam), *Lycium barbarum*, *Epimedium*, *Cinnamomum cassia*, *Syzygium aromaticum*, *Angelica sinensis*, and *Curculigo orchioides*. This TCM formula is used in a famous Chinese Herbal Liqueur, Chinese Jing Liqueur (Liu et al., 2011; Lu et al., 2017; Lu et al., 2018; Shan et al., 2018; Cai et al., 2020; Hu et al., 2021). According to TCM theory of "kidney is the origin of the congenital constitution", this empirical formula of the nine TCM herbs was formulated for the purpose of "tonifying kidney." Among the nine TCM herbs, *Cistanche deserticola* and *Epimedium* are used as the herbs to reinforce the kidney-yang, which supplemented by *Dioscorea polystachya* (Chinese yam) and *Lycium barbarum*, etc., to replenish kidney-yin (Liu et al., 2011; Lu et al., 2017; Lu et al., 2018; Shan et al., 2018). Preclinical and clinical studies demonstrated that studied herbal formulation (Jing extracts) has the properties of improving kidney-yang deficiency in rats and relieving main symptoms of patients with Kidney-Yang Deficiency Syndrome, anti-fatigue, and enhancing immunity in humans and animals (Liu et al., 2011; Lu et al., 2017; Lu et al., 2018; Shan et al., 2018; Cai et al., 2020; Hu et al., 2021). The assertion of "kidney governing bones" in "Huangdi Neijing—Yellow Emperor Canon of Internal Medicine" has been confirmed by an increasing body of scientific data (Ju et al., 2014; Wang et al., 2016). Our data showed that the Chinese herbal medicine extracts prevent alcohol-induced osteopenia, as demonstrated by bone morphological and biochemical analysis, in both young adult and middle-aged male mice (**Figures 3**, **4**), which may due to its kidney-tonifying property *via* kidney governing bones. The preventing mechanism of the phytomedicines in Jing extracts on alcohol-induced osteoporosis needs additional study.

The TCM herbs used in this study and the TCM extracts' bioactive compounds have therapeutic potentials for bone diseases (**Tables 1**, **2**). *Astragalus membranaceus* (Kang et al., 2013), *Astragalus membranaceus* and *Cinnamomum cassia* plus *Phellodendron amurense* (Huh et al., 2015), *Epimedium brevicornum* (Zhang et al., 2006) or a combination of *Astragalus membranaceus*, *Angelica sinensis*, and *Epimedium brevicornum* (Xie et al., 2012), *Syzygium aromaticum* (Karmakar et al., 2012) and *Angelica sinensis* (Lim and Kim, 2014) reverse bone loss in a rat model of postmenopausal osteoporosis. *Cistanche deserticola* has antiosteoporotic activity in type I osteoporotic rats (Zhang et al., 2021) and type II osteoporotic mice (Wang et al., 2021), which may result in the stimulation of bone formation (Li et al., 2012). *Dioscorea spongiosa* prevents glucocorticoid-induced osteoporosis in rats (Han et al., 2016) and aging-induced osteoporosis (Tikhonova et al., 2015). *Lycium barbarum* ameliorates osteoporosis in OVX mice (Kim et al., 2017). The analyses of chemical components of the Chinese herbal extracts we used in this study by LC/MS and NMR (Hu et al., 2021; Cai et al., 2020) showed that herbal extracts contain a variety of saponins, flavonoids, active polysaccharides, and other functional factors including amino acids, organic acids, trace elements and other nutrients that are required by the human body. Among the 189 compounds detected by LC/MS and NMR (Cai et al., 2020) and 43 bioactive components detected by LC/MS (Hu et al., 2021) from the Chinese herbal extracts used in this study, Acteoside, Calycosin, Daidzin, Echinacoside, Epimedin, Eugenol, Ferulic acid, Hyperoside, Icariside, Icariin, Oleanolic acid, Protocatechuic acid, Sagittatoside, and Ligustilide, etc. are antiosteoporotic compounds and some of these compounds have the therapeutic potential for alcohol use disorder (**Table 2**; the chemical structures of these bioactive compounds in **Supplementary Figure S7**). For example, icariin represents a class of flavonoids with bone-promoting activity, which could be used as a potential treatment for postmenopausal osteoporosis (Wang et al., 2018). These antiosteoporotic compounds may prevent alcohol-induced osteopenia by acting alone or in a synergistic manner. Nuclear factor erythroid-derived 2-related factor-2 (Nrf2) is a master regulator of oxidative stress and a critical antiosteoporotic factor (Chen et al., 2021). Cai et al. (2020) reported that Chinese herbal extracts activate Nrf2, implying that Nrf2 may be involved in the preventive effects of Chinese herbal extracts (Jing extracts) on alcohol-induced osteoporosis.

The bone marrow is an alcohol sensitive organ (Wahl et al., 2007); hematopoietic cells and bone cells could be extrinsic factors for each other in the bone marrow niche (Zhou, 2015), which makes bone marrow an ideal organ to study the bone metabolic factors, such as ALP and TNF-α, etc. (Wahl et al., 2007; Zhou, 2015). Our data shows that Protocatechuic acid, a natural phenolic acid in Jing extracts, mitigates *in vivo* alcohol-induced decline of Alkaline phosphatase (ALP) gene expression (**Figure 5**) and elevated inflammatory factors (**Supplementary Figure S6**) in the bone marrow of male Balb/c mice. The murine pre-osteoblastic cell line MC3T3-E1 is a widely used in osteoblast biology (Hwang and Horton, 2019). In this study, MC3T3-E1 cells were treated with or without alcohol and/or PCA to study the effects of PCA on alcohol-induced inhibitory on ALP activity *in vitro*. Our data (**Figure 5D**) showed that PCA significantly alleviates the inhibitory effects of alcohol on ALP activity in MC3T3-E1 cells. Protocatechuic acid (PCA) is antioxidant and anti-inflammatory (Kakkar and Bais, 2014). Oxidative stress and inflammation are two common mechanisms involved in alcohol toxicity. PCA may prevent alcohol-induced bone injury via antioxidant and anti-inflammatory pathways. In this study, we used PCA as a representative bioactive compound in the Jing

extracts. A typical TCM or any ethnomedicine formula has multiple ingredients that synergize in treatment for the symptoms of a disease, which have greater efficacy and safety than a single drug in clinical practices, possibly due to the multiple ingredients synergistic interactions and mutual detoxification. The other bioactive compounds, e.g., Acteoside, Daidzin, Echinacoside, Eugenol, Ferulic acid, Hyperoside, Icariin, and Oleanolic acid, etc. (**Table 2**), and their synergizing in treatment for alcohol-induced bone loss need additional investigations.

The TCM herbs used in this study also have therapeutic potentials for alcohol use disorder, especially alcoholic liver damage (**Table 1**). The chemical composition of TCM herbal extracts includes Acteoside, Daidzin, Echinacoside, Eugenol, Ferulic acid, Hyperoside, Icariin, Oleanolic acid, and Protocatechuic acid have therapeutic potential for alcohol-related diseases (**Table 2**). Osteoporosis is a common complication of many types of liver disease (Nakchbandi and van der Merwe, 2009). Alcohol consumption is an independent risk factor for the onset of osteoporosis, which is prevalent in patients with alcoholic liver disease (López-Larramona et al., 2013). The roles of TCM herbal extracts and their bioactive compounds in the alcohol-induced dysfunction of the liver-bone axis need additional study.

CONCLUSION

In summary, our study in pharmacognosy suggests that traditional Chinese medicine herbal extracts prevent chronic excessive alcohol consumption-induced osteopenia in young adult and middle-aged/old male mice, which indicates that TCM might prevent alcohol-induced osteoporosis. Based on our data and previous reports (Liu et al., 2011; Lu et al., 2017; Lu et al., 2018; Cai et al., 2020; Hu et al., 2021), the potential protective mechanism of traditional Chinese medicine herbal extracts in alcohol-induced osteoporosis may involve the kidney-bone axis to prevent alcohol-induced bone loss and the direct antiosteoporotic potential of the bioactive compounds in the Chinese herbal medicines. Protocatechuic acid, a natural phenolic acid in Jing extracts, mitigates *in vivo* and *in vitro* alcohol-induced decline of alkaline phosphatase gene expression and activity. Additional analysis of the bioactive compounds in Chinese herbal medicines may identify antiosteoporotic compounds as drug candidates for preventing or treating alcohol-induced osteopenia/osteoporosis.

DATA AVAILABILITY STATEMENT

The original contributions presented in the study are included in the article/**Supplementary Material**, further inquiries can be directed to the corresponding authors.

ETHICS STATEMENT

The animal study was reviewed and approved by the BWH Institutional Animal Care and Use Committee (IACUC approval Protocol # 2016N000361).

AUTHOR CONTRIBUTIONS

SZ, YL, and XW: Conceptualization, methodology, and supervision. SZ, DQ, and HZ: Writing—Original draft preparation. DQ, HZ, PF, TY, YX, YG, LZ: Investigation, data curation, and formal analysis. YL, HZ, ZW, SL, GT, YS, and LW: Conceptualization, resources, and methodology. AP and MO'B: Writing—Review and editing. SZ, HZ, and YL: Project administration and funding acquisition.

FUNDING

This work was supported by grants from Hubei State Guoqiang Baojianjiu Center for Engineering and Technology Research, Jing Brand Research Institute (SZ and XW).

ACKNOWLEDGMENTS

The authors thank other members of Jing Brand Research Institute for their constructive discussion and suggestions during the design and execution of the experiments as well as their contribution to the extracts of Chinese herbal medicines.

SUPPLEMENTARY MATERIAL

The Supplementary Material for this article can be found online at: https://www.frontiersin.org/articles/10.3389/fphar.2021.754088/full#supplementary-material

REFERENCES

Abukhadir, S. S., Mohamed, N., and Mohamed, N. (2013). Pathogenesis of Alcohol-Induced Osteoporosis and its Treatment: a Review. *Curr. Drug Targets.* 14, 1601–1610. doi:10.2174/13894501113146660231

Alvisa-Negrín, J., González-Reimers, E., Santolaria-Fernández, F., García-Valdecasas-Campelo, E., Valls, M. R., Pelazas-González, R., et al. (2009). Osteopenia in Alcoholics: Effect of Alcohol Abstinence. *Alcohol Alcohol.* 44, 468–475. doi:10.1093/alcalc/agp038

An, J., Yang, H., Zhang, Q., Liu, C., Zhao, J., Zhang, L., et al. (2016). Natural Products for Treatment of Osteoporosis: The Effects and Mechanisms on Promoting Osteoblast-Mediated Bone Formation. *Life Sci.* 147, 46–58. doi:10.1016/j.lfs.2016.01.024

Bertola, A., Mathews, S., Ki, S. H., Wang, H., and Gao, B. (2013). Mouse Model of Chronic and Binge Ethanol Feeding (The NIAAA Model). *Nat. Protoc.* 8, 627–637. doi:10.1038/nprot.2013.032

Byeon, S., Oh, J., Lim, J. S., Lee, J. S., and Kim, J. S. (2018). Protective Effects of *Dioscorea Batatas* Flesh and Peel Extracts Against Ethanol-Induced Gastric Ulcer in Mice. *Nutrients.* 10 (11), 1680. doi:10.3390/nu10111680

Cai, Y.-S., Xu, J., Chen, M., Wang, D., Yang, Y., Manavalan, A., et al. (2020). Compound Analysis of Jing Liqueur and Nrf2 Activation by Jing Liqueur-One of the Most Popular Beverages in China. *Beverages.* 6, 1. doi:10.3390/beverages6010001

Cao, D. P., Zheng, Y. N., Qin, L. P., Han, T., Zhang, H., Rahman, K., et al. (2008). Curculigo Orchioides, a Traditional Chinese Medicinal Plant, Prevents Bone Loss in Ovariectomized Rats. *Maturitas.* 59, 373–380. doi:10.1016/j.maturitas.2008.03.010

Cao, S., Dong, X. L., Ho, M. X., Yu, W. X., Wong, K. C., Yao, X. S., et al. (2018). Oleanolic Acid Exerts Osteoprotective Effects and Modulates Vitamin D Metabolism. *Nutrients.* 10, 247. doi:10.3390/nu10020247

Chakkalakal, D. A. (2005). Alcohol-Induced Bone Loss and Deficient Bone Repair. *Alcohol. Clin. Exp. Res.* 29, 2077–2090. doi:10.1097/01.alc.0000192039.21305.55

Charles, J. F., Coury, F., Sulyanto, R., Sitara, D., Wu, J., Brady, N., et al. (2012). The Collection of NFATc1-Dependent Transcripts in the Osteoclast Includes Numerous Genes Non-Essential to Physiologic Bone Resorption. *Bone.* 51, 902–912. doi:10.1016/j.bone.2012.08.113

Chen, X., Zhu, X., Wei, A., Chen, F., Gao, Q., Lu, K., et al. (2021). Nrf2 Epigenetic Derepression Induced by Running Exercise Protects Against Osteoporosis. *Bone Res.* 9, 15. doi:10.1038/s41413-020-00128-8

Chen, Y., Dai, F., He, Y., Chen, Q., Xia, Q., Cheng, G., et al. (2018). Beneficial Effects of Hyperoside on Bone Metabolism in Ovariectomized Mice. *Biomed. Pharmacother.* 107, 1175–1182. doi:10.1016/j.biopha.2018.08.069

Cheung, H., Doughty, H., Hinsley, A., Hsu, E., Lee, T. M., Milner-Gulland, E. J., et al. (2021). Understanding Traditional Chinese Medicine to Strengthen Conservation Outcomes. *People Nat.* 3, 115–128. doi:10.1002/pan3.10166

Compston, J. E., McClung, M. R., and Leslie, W. D. (2019). Osteoporosis. *The Lancet.* 393, 364–376. doi:10.1016/S0140-6736(18)32112-3

Cosman, F., de Beur, S. J., LeBoff, M. S., Lewiecki, E. M., Tanner, B., Randall, S., et al. (2014). Clinician's Guide to Prevention and Treatment of Osteoporosis. *Osteoporos. Int.* 25, 2359–2381. doi:10.1007/s00198-014-2794-2

Dai, J., Lin, D., Zhang, J., Habib, P., Smith, P., Murtha, J., et al. (2000). Chronic Alcohol Ingestion Induces Osteoclastogenesis and Bone Loss Through IL-6 in Mice. *J. Clin. Invest.* 106, 887–895. doi:10.1172/JCI10483

Ding, M., Odgaard, A., Danielsen, C. C., and Hvid, I. (2002). Mutual Associations Among Microstructural, Physical and Mechanical Properties of Human Cancellous Bone. *J. Bone Jt. Surg Br.* 84, 900–907. doi:10.1302/0301-620x.84b6.11994

Ding, Y., Ma, H., Xu, Y., Yang, F., Li, Y., Shi, F., et al. (2021). Potentiation of Flutamide-Induced Hepatotoxicity in Mice by Xian-Ling-Gu-Bao through Induction of CYP1A2. *J. Ethnopharmacol.* 278, 114299. doi:10.1016/j.jep.2021.114299

Egea, T., Signorini, M. A., Bruschi, P., Rivera, D., Obón, C., Alcaraz, F., et al. (2015). Spirits and Liqueurs in European Traditional Medicine: Their History and Ethnobotany in Tuscany and Bologna (Italy). *J. Ethnopharmacol.* 175, 241–255. doi:10.1016/j.jep.2015.08.053

Fai, Y. M. (2009). A Review of Presence of Oleanolic Acid in Natural Products. *Nat. Prod. Med.* 2, 64–277.

Felson, D. T., Zhang, Y., Hannan, M. T., Kannel, W. B., and Kiel, D. P. (1995). Alcohol Intake and Bone Mineral Density in Elderly Men and Women. The Framingham Study. *Am. J. Epidemiol.* 142, 485–492. doi:10.1093/oxfordjournals.aje.a117664

Fu, R., Zhou, J., Wang, R., Sun, R., Feng, D., Wang, Z., et al. (2019). Protocatechuic Acid-Mediated miR-219a-5p Activation Inhibits the P66shc Oxidant Pathway to Alleviate Alcoholic Liver Injury. *Oxid Med. Cel Longev.* 2019, 3527809. doi:10.1155/2019/3527809

Gaddini, G. W., Turner, R. T., Grant, K. A., and Iwaniec, U. T. (2016). Alcohol: A Simple Nutrient With Complex Actions on Bone in the Adult Skeleton. *Alcohol. Clin. Exp. Res.* 40, 657–671. doi:10.1111/acer.13000

Garaycoechea, J. I., Crossan, G. P., Langevin, F., Mulderrig, L., Louzada, S., Yang, F., et al. (2018). Alcohol and Endogenous Aldehydes Damage Chromosomes and Mutate Stem Cells. *Nature.* 553, 171–177. doi:10.1038/nature25154

GBD 2016 Alcohol Collaborators (2018). Alcohol Use and Burden for 195 Countries and Territories, 1990-2016: a Systematic Analysis for the Global Burden of Disease Study 2016. *Lancet.* 392, 1015–1035. doi:10.1016/S0140-6736(18)31310-2

Guo, Y., Cao, L., Zhao, Q., Zhang, L., Chen, J., Liu, B., et al. (2016). Preliminary Characterizations, Antioxidant and Hepatoprotective Activity of Polysaccharide From Cistanche Deserticola. *Int. J. Biol. Macromol.* 93 (Pt A), 678–685. doi:10.1016/j.ijbiomac.2016.09.039

Han, N., Xu, J., Xu, F., Liu, Z., and Yin, J. (2016). The *In Vivo* Effects of a Fraction From Dioscorea Spongiosa on Glucocorticoid-Induced Osteoporosis. *J. Ethnopharmacol.* 185, 53–59. doi:10.1016/j.jep.2016.03.033

He, B., Lu, C., Wang, M., Zheng, G., Chen, G., Jiang, M., et al. (2015). Drug Discovery in Traditional Chinese Medicine: From Herbal Fufang to Combinatory Drugs. *Sponsored Suppl. Sci.* 350, S74–S76.

Hildebrand, T., and Rüegsegger, P. (1997). Quantification of Bone Microarchitecture With the Structure Model Index. *Comput. Methods Biomech. Biomed. Engin* 1, 15–23. doi:10.1080/01495739708936692

Hou, T., Zhang, L., and Yang, X. (2019). Ferulic Acid, a Natural Polyphenol, Protects Against Osteoporosis by Activating SIRT1 and NF-Kb in Neonatal Rats With Glucocorticoid-Induced Osteoporosis. *Biomed. Pharmacother.* 120, 109205. doi:10.1016/j.biopha.2019.109205

Howard, A. A., Arnsten, J. H., and Gourevitch, M. N. (2004). Effect of Alcohol Consumption on Diabetes Mellitus: a Systematic Review. *Ann. Intern. Med.* 140, 211–219. doi:10.7326/0003-4819-140-6-200403160-00011

Hu, Y., Wang, Z., Xia, F., Yang, W., Liu, Y. C., and Wan, J. B. (2021). Simultaneous Quantification of Bioactive Components in Chinese Herbal Spirits by Ultra-High Performance Liquid Chromatography Coupled to Triple-Quadrupole Mass Spectrometry (UHPLC-QQQ-MS/MS). *Chin. Med.* 16, 26. doi:10.1186/s13020-021-00435-0

Huh, J. E., Kim, S. J., Kang, J. W., Nam, D. W., Choi, D. Y., Park, D. S., et al. (2015). The Standardized BHH10 Extract, a Combination of Astragalus Membranaceus, Cinnamomum Cassia, and Phellodendron Amurense, Reverses Bone Mass and Metabolism in a Rat Model of Postmenopausal Osteoporosis. *Phytother Res.* 29, 30–39. doi:10.1002/ptr.5218

Hwang, P. W., and Horton, J. A. (2019). Variable Osteogenic Performance of MC3T3-E1 Subclones Impacts Their Utility as Models of Osteoblast Biology. *Sci. Rep.* 9, 8299. doi:10.1038/s41598-019-44575-8

Iwaniec, U. T., and Turner, R. T. (2013). Intraperitoneal Injection of Ethanol Results in Drastic Changes in Bone Metabolism Not Observed When Ethanol Is Administered by Oral Gavage. *Alcohol. Clin. Exp. Res.* 37, 1271–1277. doi:10.1111/acer.12105

Jacob Jesurun, R. S., and Johan Pandian, J. (2019). Evaluation of Antioxidant and Hepatoprotective Property of Ethanolic Extract of Curculigoorchioides in Albino Rats. *Int. J. Basic Clin. Pharmacol.* 8, 1685–1692. doi:10.18203/2319-2003.ijbcp20192672

Jang, S. A., Song, H. S., Kwon, J. E., Baek, H. J., Koo, H. J., Sohn, E. H., et al. (2018). Protocatechuic Acid Attenuates Trabecular Bone Loss in Ovariectomized Mice. *Oxid Med. Cel Longev.* 2018, 7280342. doi:10.1155/2018/7280342

Jin, S. E., Lee, M. Y., Shin, I. S., Jeon, W. Y., and Ha, H. (2016). Syzygium Aromaticum Water Extract Attenuates Ethanol Induced Gastric Injury Through Antioxidant Effects in Rats. *Mol. Med. Rep.* 14 (1), 361–366. doi:10.3892/mmr.2016.5269

Ju, D., Liu, M., Zhao, H., and Wang, J. (2014). Mechanisms of "Kidney Governing Bones" Theory in Traditional Chinese Medicine. *Front. Med.* 8, 389–393. doi:10.1007/s11684-014-0362-y

Kakkar, S., and Bais, S. (2014). A Review on Protocatechuic Acid and its Pharmacological Potential. *ISRN Pharmacol.* 2014, 952943. doi:10.1155/2014/952943

Kang, S. C., Kim, H. J., and Kim, M. H. (2013). Effects of Astragalus Membranaceus With Supplemental Calcium on Bone Mineral Density and Bone Metabolism in Calcium-Deficient Ovariectomized Rats. *Biol. Trace Elem. Res.* 151, 68–74. doi:10.1007/s12011-012-9527-1

Kanuri, G., Weber, S., Volynets, V., Spruss, A., Bischoff, S. C., and Bergheim, I. (2009). Cinnamon Extract Protects Against Acute Alcohol-Induced Liver Steatosis in Mice. *J. Nutr.* 139 (3), 482–487. doi:10.3945/jn.108.100495

Karlamangla, A. S., Sarkisian, C. A., Kado, D. M., Dedes, H., Liao, D. H., Kim, S., et al. (2009). Light to Moderate Alcohol Consumption and Disability: Variable Benefits by Health Status. *Am. J. Epidemiol.* 169, 96–104. doi:10.1093/aje/kwn294

Karmakar, S., Choudhury, M., Das, A. S., Maiti, A., Majumdar, S., and Mitra, C. (2012). Clove (Syzygium Aromaticum Linn) Extract Rich in Eugenol and Eugenol Derivatives Shows Bone-Preserving Efficacy. *Nat. Prod. Res.* 26, 500–509. doi:10.1080/14786419.2010.511216

Keung, W. M., and Vallee, B. L. (1998). Kudzu Root: an Ancient Chinese Source of Modern Antidipsotropic Agents. *Phytochemistry.* 47 (4), 499–506. doi:10.1016/s0031-9422(97)00723-1

Khullar, M., Sharma, A., Wani, A., Sharma, N., Sharma, N., Chandan, B. K., et al. (2019). Acteoside Ameliorates Inflammatory Responses Through NFkB

Pathway in Alcohol Induced Hepatic Damage. *Int. Immunopharmacol.* 69, 109–117. doi:10.1016/j.intimp.2019.01.020

Kim, M. H., Lee, J. E., Lee, J. S., and Yang, W. M. (2017). Improvement of Osteoporosis by Lycium Chinense Administration in Ovariectomized Mice. *J. Chin. Med. Assoc.* 80, 222–226. doi:10.1016/j.jcma.2016.11.006

Kunzmann, A. T., Coleman, H. G., Huang, W. Y., and Berndt, S. I. (2018). The Association of Lifetime Alcohol Use With Mortality and Cancer Risk in Older Adults: A Cohort Study. *Plos Med.* 15, e1002585. doi:10.1371/journal.pmed.1002585

Langdahl, B. L., and Andersen, J. D. (2018). Treatment of Osteoporosis: Unmet Needs and Emerging Solutions. *J. Bone Metab.* 25, 133–140. doi:10.11005/jbm.2018.25.3.133

Li, F., Yang, X., Yang, Y., Guo, C., Zhang, C., Yang, Z., et al. (2013). Antiosteoporotic Activity of Echinacoside in Ovariectomized Rats. *Phytomedicine.* 20, 549–557. doi:10.1016/j.phymed.2013.01.001

Li, N., Tu, Y., Shen, Y., Qin, Y., Lei, C., and Liu, X. (2016). Calycosin Attenuates Osteoporosis and Regulates the Expression of OPG/RANKL in Ovariectomized Rats *via* MAPK Signaling. *Pharmazie.* 71, 607–612. doi:10.1691/ph.2016.6627

Li, T. M., Huang, H. C., Su, C. M., Ho, T. Y., Wu, C. M., Chen, W. C., et al. (2012). Cistanche Deserticola Extract Increases Bone Formation in Osteoblasts. *J. Pharm. Pharmacol.* 64, 897–907. doi:10.1111/j.2042-7158.2012.01483.x

Lim, D. W., and Kim, Y. T. (2014). Anti-osteoporotic Effects of Angelica Sinensis (Oliv.) Diels Extract on Ovariectomized Rats and its Oral Toxicity in Rats. *Nutrients.* 6, 4362–4372. doi:10.3390/nu6104362

Lin, J., Zhu, J., Wang, Y., Zhang, N., Gober, H. J., Qiu, X., et al. (2017). Chinese Single Herbs and Active Ingredients for Postmenopausal Osteoporosis: From Preclinical Evidence to Action Mechanism. *Biosci. Trends.* 11, 496–506. doi:10.5582/bst.2017.01216

Liu, J., Wang, X., Liu, R., Liu, Y., Zhang, T., Fu, H., et al. (2014). Oleanolic Acid Co-administration Alleviates Ethanol-Induced Hepatic Injury via Nrf-2 and Ethanol-Metabolizing Modulating in Rats. *Chem. Biol. Interact.* 221, 88–98. doi:10.1016/j.cbi.2014.07.017

Liu, S., Li, B., Li, X., Tu, P., and Bao, Z. (2008). Method for Checking Quality of Chinese Jing Wine by Using Fingerprint Pattern Technology. *China Patent.*, CN100392399C.

Liu, W., Mao, L., Ji, F., Chen, F., Wang, S., and Xie, Y. (2017). Icariside II Activates EGFR-Akt-Nrf2 Signaling and Protects Osteoblasts from Dexamethasone. *Oncotarget.* 8, 2594–2603. doi:10.18632/oncotarget.13732

Liu, Y., Bi, Y., Chai, L., Song, L., Huang, J., Wang, Q., et al. (2021). Development of Epimedin A Complex Drugs for Treating the Osteoporosis. *J. Mater. Sci. Mater. Med.* 32, 17. doi:10.1007/s10856-020-06472-9

Liu, Y., Kou, X., Chen, C., Yu, W., Su, Y., Kim, Y., et al. (2016). Chronic High Dose Alcohol Induces Osteopenia via Activation of mTOR Signaling in Bone Marrow Mesenchymal Stem Cells. *Stem Cells.* 34, 2157–2168. doi:10.1002/stem.2392

Liu, Y., Yang, Y., Feng, S., Lu, S., Shan, Y., Xia, S., et al. (2011). The Effects of China Jing Wine on the Functions of Hypothalamic-Pituitary-Adrenal axis and Immune System in the Shen-Yang Deficiency Model Rats. *Chin. J. Immunol.* 27, 1080–1084.

López-Larramona, G., Lucendo, A. J., and González-Delgado, L. (2013). Alcoholic Liver Disease and Changes in Bone mineral Density. *Rev. Esp Enferm Dig.* 105 (10), 609–621. doi:10.4321/s1130-01082013001000006

Lu, S., Feng, S., LiYin, J. T., Shi, Y., ShiChen, J. Y., and Liu, Y. (2017). The Effects of Chinese JING Liqueur in Relieving the Fatigue of the Patients With Fatigued Sub-Health Status. *West. J. Traditional Chin. Med.* 30, 82–84.

Lu, S., Li, J., Zhang, Y., Wang, L., Yang, Y., Chen, M., et al. (2018). Clinical Observation of Main Symptoms Relief by Chinese Jing Liqueur in Patients With Kidney Yang Deficiency Syndrome. *Chin. Traditional Patent Med.* 40, 562–570. wpr-710214.

Martiniakova, M., Sarocka, A., Babosova, R., Grosskopf, B., Kapusta, E., Goc, Z., et al. (2018). Changes in the Microstructure of Compact and Trabecular Bone Tissues of Mice Subchronically Exposed to Alcohol. *J. Biol. Res. (Thessalon).* 25, 8. doi:10.1186/s40709-018-0079-1

Maurel, D. B., Boisseau, N., Benhamou, C. L., and Jaffre, C. (2012). Alcohol and Bone: Review of Dose Effects and Mechanisms. *Osteoporos. Int.* 23, 1–16. doi:10.1007/s00198-011-1787-7

Mercer, K. E., Wynne, R. A., Lazarenko, O. P., Lumpkin, C. K., Hogue, W. R., Suva, L. J., et al. (2012). Vitamin D Supplementation Protects Against Bone Loss Associated With Chronic Alcohol Administration in Female Mice. *J. Pharmacol. Exp. Ther.* 343, 401–412. doi:10.1124/jpet.112.197038

Mikosch, P. (2014). Alcohol and Bone. *Wien Med. Wochenschr.* 164, 15–24. doi:10.1007/s10354-013-0258-5

Mostofsky, E., Mukamal, K. J., Giovannucci, E. L., Stampfer, M. J., and Rimm, E. B. (2016). Key Findings on Alcohol Consumption and a Variety of Health Outcomes From the Nurses' Health Study. *Am. J. Public Health.* 106, 1586–1591. doi:10.2105/AJPH.2016.303336

Nair, A. B., and Jacob, S. (2016). A Simple Practice Guide for Dose Conversion Between Animals and Human. *J. Basic Clin. Pharm.* 7, 27–31. doi:10.4103/0976-0105.177703

Nakchbandi, I. A., and van der Merwe, S. W. (2009). Current Understanding of Osteoporosis Associated with Liver Disease. *Nat. Rev. Gastroenterol. Hepatol.* 6 (11), 660–670. doi:10.1038/nrgastro.2009.166

NIAAA (2021). Alcohol Facts and Statistics. Available at: https://www.niaaa.nih.gov/publications/brochures-and-fact-sheets/alcohol-facts-and-statistics.

Okuda, T., Naruo, M., Iijima, O., Igarashi, T., Katsuyama, M., Maruyama, M., et al. (2018). The Contribution of Alcohol Dehydrogenase 3 to the Development of Alcoholic Osteoporosis in Mice. *J. Nippon Med. Sch.* 85, 322–329. doi:10.1272/jnms.JNMS.2018_85-52

Rukkumani, R., Aruna, K., Suresh Varma, P., and Padmanabhan Menon, V. (2004). Hepatoprotective Role of Ferulic Acid: a Dose-dependent Study. *J. Med. Food.* 7 (4), 456–461. doi:10.1089/jmf.2004.7.456

Salmon, P. L., Ohlsson, C., Shefelbine, S. J., and Doube, M. (2015). Structure Model Index Does Not Measure Rods and Plates in Trabecular Bone. *Front. Endocrinol. (Lausanne).* 6, 162. doi:10.3389/fendo.2015.00162

Sampson, H. W. (2002). Alcohol and Other Factors Affecting Osteoporosis Risk in Women. *Alcohol. Res. Health.* 26, 292–298.

Sampson, H. W. (1998). Alcohol's Harmful Effects on Bone. *Alcohol. Health Res. World.* 22, 190–194. doi:10.1111/j.1530-0277.1998.tb05912.x

Shan, Y., Zhou, H., Chen, M., Chen, K., Liu, Y., and Wang, L. (2018). Effects of Chinese Jing Liqueur on Fatigue, Immunity, and Sexual Function. *Chin. Traditional Patent Med.* 40, 1600–1603.

Sommer, I., Erkkilä, A. T., Järvinen, R., Mursu, J., Sirola, J., Jurvelin, J. S., et al. (2013). Alcohol Consumption and Bone mineral Density in Elderly Women. *Public Health Nutr.* 16, 704–712. doi:10.1017/S136898001200331X

Tang, X. Y., Dai, Z. Q., Wu, Q. C., Zeng, J. X., Gao, M. X., Xiao, H. H., et al. (2020). Simultaneous Determination of Multiple Components in Rat Plasma and Pharmacokinetic Studies at a Pharmacodynamic Dose of Xian-Ling-Gu-Bao Capsule by UPLC-MS/MS. *J. Pharm. Biomed. Anal.* 177, 112836. doi:10.1016/j.jpba.2019.112836

Tao, Z., Zhang, L., Wu, T., Fang, X., and Zhao, L. (2021). Echinacoside Ameliorates Alcohol-Induced Oxidative Stress and Hepatic Steatosis by Affecting SREBP1c/FASN Pathway via PPARα. *Food Chem. Toxicol.* 148, 111956. doi:10.1016/j.fct.2020.111956

Tikhonova, M. A., Ting, C. H., Kolosova, N. G., Hsu, C. Y., Chen, J. H., Huang, C. W., et al. (2015). Improving Bone Microarchitecture in Aging With Diosgenin Treatment: A Study in Senescence-Accelerated OXYS Rats. *Chin. J. Physiol.* 58, 322–331. doi:10.4077/CJP.2015.BAD325

Tucker, K. L., Jugdaohsingh, R., Powell, J. J., Qiao, N., Hannan, M. T., Sripanyakorn, S., et al. (2009). Effects of Beer, Wine, and Liquor Intakes on Bone mineral Density in Older Men and Women. *Am. J. Clin. Nutr.* 89, 1188–1196. doi:10.3945/ajcn.2008.26765

Turner, R. T. (2000). Skeletal Response to Alcohol. *Alcohol. Clin. Exp. Res.* 24, 1693–1701. doi:10.1111/j.1530-0277.2000.tb01971.x

Ung, C. Y., Li, H., Cao, Z. W., Li, Y. X., and Chen, Y. Z. (2007). Are Herb-Pairs of Traditional Chinese Medicine Distinguishable From Others? Pattern Analysis and Artificial Intelligence Classification Study of Traditionally Defined Herbal Properties. *J. Ethnopharmacol.* 111, 371–377. doi:10.1016/j.jep.2006.11.037

USDA and HHS (2020). U.S. Department of Agriculture and U.S. Department of Health and Human Services. Dietary Guidelines for Americans, 2020-2025. Available at: DietaryGuidelines.gov.

Veerbeek, M. A., Ten Have, M., van Dorsselaer, S. A., Oude Voshaar, R. C., Rhebergen, D., and Willemse, B. M. (2019). Differences in Alcohol Use Between Younger and Older People: Results From a General Population Study. *Drug Alcohol Depend.* 202, 18–23. doi:10.1016/j.drugalcdep.2019.04.023

Wahl, E. C., Aronson, J., Liu, L., Liu, Z., Perrien, D. S., Skinner, R. A., et al. (2007). Chronic Ethanol Exposure Inhibits Distraction Osteogenesis in a Mouse Model: Role of the TNF Signaling axis. *Toxicol. Appl. Pharmacol.* 220, 302–310. doi:10.1016/j.taap.2007.02.011

Wang, F., Tu, P., Zeng, K., and Jiang, Y. (2021). Total Glycosides and Polysaccharides of Cistanche Deserticola Prevent Osteoporosis by Activating Wnt/β-Catenin Signaling Pathway in SAMP6 Mice. *J. Ethnopharmacol.* 271, 113899. doi:10.1016/j.jep.2021.113899

Wang, H., Li, Y., Liu, J., Di, D., Liu, Y., and Wei, J. (2020a). Hepatoprotective Effect of Crude Polysaccharide Isolated From *Lycium Barbarum* L. Against Alcohol-Induced Oxidative Damage Involves Nrf2 Signaling. *Food Sci. Nutr.* 8 (12), 6528–6538. doi:10.1002/fsn3.1942

Wang, K., Xu, J., Liu, Y., Cui, Z., He, Z., Zheng, Z., et al. (2020b). Self-Assembled Angelica Sinensis Polysaccharide Nanoparticles With an Instinctive Liver-Targeting Ability as a Drug Carrier for Acute Alcoholic Liver Damage protection. *Int. J. Pharm.* 577, 118996. doi:10.1016/j.ijpharm.2019.118996

Wang, X. Q., Zou, X. R., and Zhang, Y. C. (2016). From "Kidneys Govern Bones" to Chronic Kidney Disease, Diabetes Mellitus, and Metabolic Bone Disorder: A Crosstalk between Traditional Chinese Medicine and Modern Science. *Evid. Based Complement. Alternat Med.* 2016, 4370263. doi:10.1155/2016/4370263

Wang, Z., Wang, D., Yang, D., Zhen, W., Zhang, J., and Peng, S. (2018). The Effect of Icariin on Bone Metabolism and its Potential Clinical Application. *Osteoporos. Int.* 29, 535–544. doi:10.1007/s00198-017-4255-1

Wei, G., Liang, T., Wei, C., Nong, X., Lu, Q., and Zhao, J. (2019). Daidzin Inhibits RANKL-Induced Osteoclastogenesis *In Vitro* and Prevents LPS-Induced Bone Loss *In Vivo*. *J. Cel Biochem.* 120, 5304–5314. doi:10.1002/jcb.27806

Willinghamm, M. D., Brodt, M. D., Lee, K. L., Stephens, A. L., Ye, J., and Silva, M. J. (2010). Age-Related Changes in Bone Structure and Strength in Female and Male BALB/c Mice. *Calcif Tissue Int.* 86, 470–483. doi:10.1007/s00223-010-9359-y

Wojcikowski, K., and Gobe, G. (2014). Animal Studies on Medicinal Herbs: Predictability, Dose Conversion and Potential Value. *Phytother Res.* 28, 22–27. doi:10.1002/ptr.4966

Wood, A. M., Kaptoge, S., Butterworth, A. S., Willeit, P., Warnakula, S., Bolton, T., et al. (2018). Risk Thresholds for Alcohol Consumption: Combined Analysis of Individual-Participant Data for 599 912 Current Drinkers in 83 Prospective Studies. *Lancet.* 391, 1513–1523. doi:10.1016/S0140-6736(18)30134-X

Wright, N. C., Looker, A. C., Saag, K. G., Curtis, J. R., Delzell, E. S., Randall, S., et al. (2014). The Recent Prevalence of Osteoporosis and Low Bone Mass in the United States Based on Bone Mineral Density at the Femoral Neck or Lumbar Spine. *J. Bone Miner Res.* 29, 2520–2526. doi:10.1002/jbmr.2269

Wu, J. Z., Liu, P. C., Liu, R., and Cai, M. (2018). Icariin Restores Bone Structure and Strength in a Rat Model of Chronic High-Dose Alcohol-Induced Osteopenia. *Cell Physiol Biochem.* 46 (4), 1727–1736. doi:10.1159/000489248

Wu, Z. H., Zhu, X., Xu, C. K., Chen, Y. J., Zhang, L., and Zhang, C. L. (2017). Effect of Xianling Gubao Capsules on Bone Mineral Density in Osteoporosis Patients. *J. Biol. Regul. Homeost Agents.* 31, 359–363.

Xia, X. L. (2013). History of Chinese Medicinal Wine. *Chin. J. Integr. Med.* 19, 549–555. doi:10.1007/s11655-010-0799-7

Xiao, H., Wignall, N., and Brown, E. S. (2016). An Open-Label Pilot Study of Icariin for Co-Morbid Bipolar and Alcohol Use Disorder. *Am. J. Drug Alcohol. Abuse.* 42 (2), 162–167. doi:10.3109/00952990.2015.1114118

Xie, Q. F., Xie, J. H., Dong, T. T., Su, J. Y., Cai, D. K., Chen, J. P., et al. (2012). Effect of a Derived Herbal Recipe from an Ancient Chinese Formula, Danggui Buxue Tang, on Ovariectomized Rats. *J. Ethnopharmacol.* 144, 567–575. doi:10.1016/j.jep.2012.09.041

Yang, F., Lin, Z. W., Huang, T. Y., Chen, T. T., Cui, J., Li, M. Y., et al. (2019a). Ligustilide, a Major Bioactive Component of Angelica Sinensis, Promotes Bone Formation via the GPR30/EGFR Pathway. *Sci. Rep.* 9, 6991. doi:10.1038/s41598-019-43518-7

Yang, L., Zhang, B., Liu, J., Dong, Y., Li, Y., Li, N., et al. (2019b). Protective Effect of Acteoside on Ovariectomy-Induced Bone Loss in Mice. *Int. J. Mol. Sci.* 20, 2974. doi:10.3390/ijms20122974

Yildiz, H., and Öztürk, E. (2020). Histopathological and Biochemical Effects of Eugenol on Alcohol-Treated Rat Liver. *ADYU J. SCI.* 10 (1), 83–99. doi:10.37094/adyujsci.729426

Yimam, M., Jiao, P., Hong, M., and Jia, Q. (2016). A Standardized Composition From Extracts of Myristica Fragrans, Astragalus Membranaceus, and Poria Cocos Protects Liver From Acute Ethanol Insult. *J. Med. Food.* 19 (8), 780–788. doi:10.1089/jmf.2016.0023

Zeng, X., Zhang, P., Wang, Y., Qin, C., Chen, S., He, W., et al. (2019). CMAUP: a Database of Collective Molecular Activities of Useful Plants. *Nucleic Acids Res.* 47 (D1), D1118–D1127. doi:10.1093/nar/gky965

Zhang, B., Yang, L. L., Ding, S. Q., Liu, J. J., Dong, Y. H., Li, Y. T., et al. (2021). Anti-Osteoporotic Activity of an Edible Traditional Chinese Medicine *Cistanche Deserticola* on Bone Metabolism of Ovariectomized Rats Through RANKL/RANK/TRAF6-Mediated Signaling Pathways. *Front. Pharmacol.* 10, 1412. doi:10.3389/fphar.2019.01412

Zhang, G., Qin, L., Hung, W. Y., Shi, Y. Y., Leung, P. C., Yeung, H. Y., et al. (2006). Flavonoids Derived From Herbal Epimedium Brevicornum Maxim Prevent OVX-Induced Osteoporosis in Rats Independent of its Enhancement in Intestinal Calcium Absorption. *Bone.* 38, 818–825. doi:10.1016/j.bone.2005.11.019

Zhang, N. D., Han, T., Huang, B. K., Rahman, K., Jiang, Y. P., Xu, H. T., et al. (2016). Traditional Chinese Medicine Formulas for the Treatment of Osteoporosis: Implication for Antiosteoporotic Drug Discovery. *J. Ethnopharmacol.* 189, 61–80. doi:10.1016/j.jep.2016.05.025

Zhang, Y. W., and Cheng, Y. C. (2019). Challenge and Prospect of Traditional Chinese Medicine in Depression Treatment. *Front. Neurosci.* 13, 190. doi:10.3389/fnins.2019.00190

Zhao, B. J., Wang, J., Song, J., Wang, C. F., Gu, J. F., Yuan, J. R., et al. (2016). Beneficial Effects of a Flavonoid Fraction of Herba Epimedii on Bone Metabolism in Ovariectomized Rats. *Planta Med.* 82, 322–329. doi:10.1055/s-0035-1558294

Zhou, S., and Glowacki, J. (2017). Chronic Kidney Disease and Vitamin D Metabolism in Human Bone Marrow-Derived MSCs. *Ann. N. Y Acad. Sci.* 1402, 43–55. doi:10.1111/nyas.13464

Zhou, S., and Glowacki, J. (2018). Dehydroepiandrosterone and Bone. *Vitam Horm.* 108, 251–271. doi:10.1016/bs.vh.2018.01.005

Zhou, S., Greenberger, J. S., Epperly, M. W., Goff, J. P., Adler, C., Leboff, M. S., et al. (2008). Age-Related Intrinsic Changes in Human Bone-Marrow-Derived Mesenchymal Stem Cells and Their Differentiation to Osteoblasts. *Aging Cell.* 7, 335–343. doi:10.1111/j.1474-9726.2008.00377.x

Zhou, S., Leboff, M. S., Waikar, S. S., and Glowacki, J. (2013). Vitamin D Metabolism and Action in Human Marrow Stromal Cells: Effects of Chronic Kidney Disease. *J. Steroid Biochem. Mol. Biol.* 136, 342–344. doi:10.1016/j.jsbmb.2012.09.009

Zhou, S. (2015). Paracrine Effects of Haematopoietic Cells on Human Mesenchymal Stem Cells. *Sci. Rep.* 5, 10573. doi:10.1038/srep10573

Zhou, Y., Tan, F., Li, C., Li, W., Liao, W., Li, Q., et al. (2019). White Peony (Fermented *Camellia Sinensis*) Polyphenols Help Prevent Alcoholic Liver Injury via Antioxidation. *Antioxidants (Basel).* 8 (11), 524. doi:10.3390/antiox8110524

Conflict of Interest: Authors HZ, ZW, SL, GT, YS, LW, and YL were employed by the company Jing Brand Co., Ltd.

The remaining authors declare that the research was conducted in the absence of any commercial or financial relationships that could be construed as a potential conflict of interest.

Publisher's Note: All claims expressed in this article are solely those of the authors and do not necessarily represent those of their affiliated organizations, or those of the publisher, the editors and the reviewers. Any product that may be evaluated in this article, or claim that may be made by its manufacturer, is not guaranteed or endorsed by the publisher.

Copyright © 2021 Qian, Zhou, Fan, Yu, Patel, O'Brien, Wang, Lu, Tong, Shan, Wang, Gao, Xiong, Zhang, Wang, Liu and Zhou. This is an open-access article distributed under the terms of the Creative Commons Attribution License (CC BY). The use, distribution or reproduction in other forums is permitted, provided the original author(s) and the copyright owner(s) are credited and that the original publication in this journal is cited, in accordance with accepted academic practice. No use, distribution or reproduction is permitted which does not comply with these terms.

frontiers in Pharmacology

REVIEW
published: 20 December 2021
doi: 10.3389/fphar.2021.795058

Phytochemicals Mediate Autophagy Against Osteoarthritis by Maintaining Cartilage Homeostasis

Zheng Tian, Xinan Zhang and Mingli Sun**

School of Kinesiology, Shenyang Sport University, Shenyang, China

Osteoarthritis (OA) is a common degenerative joint disease and is a leading cause of disability and reduced quality of life worldwide. There are currently no clinical treatments that can stop or slow down OA. Drugs have pain-relieving effects, but they do not slow down the course of OA and their long-term use can lead to serious side effects. Therefore, safe and clinically appropriate long-term treatments for OA are urgently needed. Autophagy is an intracellular protective mechanism, and targeting autophagy-related pathways has been found to prevent and treat various diseases. Attenuation of the autophagic pathway has now been found to disrupt cartilage homeostasis and plays an important role in the development of OA. Therefore, modulation of autophagic signaling pathways mediating cartilage homeostasis has been considered as a potential therapeutic option for OA. Phytochemicals are active ingredients from plants that have recently been found to reduce inflammatory factor levels in cartilage as well as attenuate chondrocyte apoptosis by modulating autophagy-related signaling pathways, which are not only widely available but also have the potential to alleviate the symptoms of OA. We reviewed preclinical studies and clinical studies of phytochemicals mediating autophagy to regulate cartilage homeostasis for the treatment of OA. The results suggest that phytochemicals derived from plant extracts can target relevant autophagic pathways as complementary and alternative agents for the treatment of OA if subjected to rigorous clinical trials and pharmacological tests.

Keywords: autophagy, phytochemicals, Osteoarthritis, chondrocytes, inflammation

OPEN ACCESS

Edited by:
Longhuo Wu,
Gannan Medical University, China

Reviewed by:
Md Jamal Uddin,
Ewha Womans University, South Korea
Kok Yong Chin,
National University of Malaysia, Malaysia

****Correspondence:***
Xinan Zhang
zhangxa2725@163.com
Mingli Sun
sun18940103126@163.com

Specialty section:
This article was submitted to Ethnopharmacology, a section of the journal Frontiers in Pharmacology

Received: *14 October 2021*
Accepted: *01 December 2021*
Published: *20 December 2021*

Citation:
Tian Z, Zhang X and Sun M (2021) Phytochemicals Mediate Autophagy Against Osteoarthritis by Maintaining Cartilage Homeostasis. Front. Pharmacol. 12:795058. doi: 10.3389/fphar.2021.795058

1 INTRODUCTION

Osteoarthritis (OA) is a common degenerative joint disease occurring in the elderly population and is the most common cause of pain and disability worldwide. Its pathology is characterized by progressive cartilage degeneration, increased subchondral bone remodeling and bone redundancy formation (Kraus et al., 2015), which poses a great burden to the patient's family and society (Nelson, 2018; Jones et al., 2019). The main pathological features of OA include articular cartilage erosion, synovitis and subchondral bone degeneration (Hunter and Bierma-Zeinstra, 2019), but the exact mechanisms are not known. Available studies suggest that multiple pathological factors such as overloading, trauma, imbalance of inflammatory systems, and impairment of anti-inflammatory pathways are involved in the development and progression of OA, leading to cellular senescence, reduced cell density, abnormal secretory activity, extracellular matrix (ECM) degradation, and impaired articular cartilage development (Goldring and Otero, 2011; Sofat et al., 2011; Doria et al., 2013; Robinson et al., 2016; Li et al., 2017b; Khan et al., 2018; Wang and He, 2018).

Conservative treatment is currently the main treatment for OA and is mainly limited to pain control. Various drugs, such as Nonsteroidal anti-inflammatory drugs (NSAIDs), cyclooxygenase-2 (COX-2) inhibitors, glucosamine, steroids, and hyaluronic acid (Philp et al., 2017) have been used clinically to slow the progression of OA, but they are limited to pain control and do not reverse the effects of OA, and all have significant side effects with long-term use (Bert and Bert, 2014; Cutolo et al., 2015; Hunter and Bierma-Zeinstra, 2019). Joint replacement is the mainstay of treatment for advanced knee OA, and although it is effective, it is expensive and has a limited lifespan (Zhang et al., 2016; Nelson, 2018; Kloppenburg and Berenbaum, 2020). Therefore, there is an urgent need to explore new means of OA treatment.

Autophagy is a self-protective mechanism (Benderdour et al., 2015; Sohn et al., 2017) that relies on autophagosomes and lysosomes to efficiently maintain internal environment homeostasis by removing protein aggregates or unwanted cellular components (Zhi et al., 2018). Under hypoxia, nutritional deficiency, endoplasmic reticulum stress (ERS), or other pathological conditions, autophagy is activated to degrade dysfunctional intracellular components, thereby improving cell survival and function (Li et al., 2019b). Currently, targeting autophagy-related pathways has been shown to be a new approach to treating diseases such as liver diseases and tumors, and has received widespread attention from researchers (Togano et al., 2021; Zhou et al., 2021a). During the development of OA, decreased chondrocyte autophagy leads to impaired cellular function, resulting in joint aging and dysfunction (Netea-Maier et al., 2016), indicating that autophagy plays an important role in the development of OA and is expected to be an important target for OA treatment.

Recently, relevant studies have found that phytochemicals play an important role in disease prevention and treatment by mediating the autophagic pathway (Zhang et al., 2015; Ranjan et al., 2019; Mao et al., 2020). In recent decades, due to the effectiveness of phytochemicals in disease prevention and treatment, botanical drugs and natural products are widely used as complementary and alternative medicines for the treatment of OA to function (Cameron and Chrubasik, 2014) and have received increasing attention in the last decade. Naturally sourced phytochemicals are both widely available and inexpensive, and provide a valuable source of lead compounds or adjuvant components for the development of new drugs against OA. In recent years, many studies (Chin and Pang, 2017; Jiang et al., 2020; Luk et al., 2020) have shown that phytochemicals derived from plants or botanical drugs may play an important role in the prevention or treatment of OA by activating autophagy through different mechanisms. However, there is no comprehensive review article reporting preclinical and clinical studies of phytochemicals improving OA by mediating autophagy-related pathways. Given the important role of autophagy in the progression of OA, we carefully reviewed phytochemicals from different plant sources that may help regulate autophagy-related signaling pathways and can be used to treat OA through improved cartilage. We searched the scientific literature for the last decade systematically using the authoritative internet databases of PubMed, Web of Science, and Embase by combining the keywords “autophagy”, “osteoarthritis”, and “plant”. The primary search criterion was the application of phytochemicals of different plant origin for the treatment of OA through autophagy. These phytochemicals can be classified as polyphenols, flavonoids, terpenoids, coumarins, saponins, and small molecule compounds. **Table 1** gives an overview of the resource profile and mechanisms of phytochemicals that mediate the autophagic pathway against OA, with species and family names according to the relevant literature based on www.theplantlist.org, http://www.plantsoftheworldonline.org/, http://mpns.kew.org/mpns-portal/ (Rivera et al., 2014).

2 AUTOPHAGY-MEDIATED CARTILAGE HOMEOSTASIS AND OA

Chondrocytes are the most dominant cells in cartilage tissue and play an important role in maintaining matrix integrity, and abnormal chondrocyte function is closely related to the development of OA. Chondrocytes play an important role in maintaining cartilage metabolic homeostasis by maintaining the stability of cartilage tissue and ECM (Kim and Blanco, 2007; Caramés et al., 2010; Charlier et al., 2019; Rim et al., 2020). When certain pathological factors act on the cartilage matrix and alter its structure, chondrocytes respond accordingly. However, the ability of articular chondrocytes to maintain normal cartilage matrix structure and integrity is limited and decreases with age (Martel-Pelletier et al., 2016). Molecular changes associated with aging of articular cartilage, as well as mechanical and inflammatory factors, can lead to elevated levels of reactive oxygen species (ROS), induce mitochondrial damage and ERS, severely impair chondrocytes and their ability to regulate ECM release, and may ultimately trigger the cascade of chondrocytes apoptosis (Wu et al., 2014; Bolduc et al., 2019). Dysfunction occurring in chondrocytes, including decreased survival (Loeser et al., 2016), inadequate ECM production (Mobasheri et al., 2017) and excessive activation of proteases (Kim et al., 2014) also accelerate cartilage degradation and disrupt joint microarchitectural integrity, leading to the development of OA.

Autophagy is an evolutionarily highly conserved degradation system that relies on the degradation of dysfunctional organelles and biomolecules by lysosomes under the regulation of autophagy-associated genes (ATG) to remove protein aggregates and dysfunctional organelles to maintain cellular homeostasis and protect cells from apoptosis (Levine and Kroemer, 2008; Mizushima et al., 2008; Nakamura and Yoshimori, 2017). When cells are exposed to abnormal physiological conditions, such as external stress, nutrient deficiency, hypoxia and ERS, autophagy is activated and plays a key role in regulating energy and nutrition and maintaining energy metabolism in the body (Duan et al., 2020). It was found that autophagy has a protective effect on cells in an inflammatory environment by regulating the body’s energy and nutrients and maintaining the body’s energy metabolism (Nakamura and Yoshimori, 2017; Yu et al., 2018). The most common marker

TABLE 1 | Phytochemicals improve cartilage homeostasis via mediated autophagy against OA *in vitro/in vivo*.

	Phytochemical	Plant species, family	Model	Dosage range	Active concentration	Signal pathways/Mechanisms	References
Polyphenols	Curcumin	*Curcuma longa* L., Zingiberaceae Martinov	*In vitro*, IL-1β induced rats chondrocytes	5 μM, 10 μM, 15 μM, and 20 μM	10 μM	MAPK/ERK1/2 signal pathway	Li et al. (2017a)
			In vitro, IL-1β induced rats chondrocytes	1.25–20 μM	10 μM	—	Chen et al. (2021)
			In vivo, DMM surgery mice	50 mg/kg *via* oral administration, once daily for 8 weeks	50 mg/kg	AKT/mTOR pathway	Zhang et al. (2018a)
			In vitro, IL-1β induced rats chondrocytes	10 μM	10 μM		
			In vivo, HFD rats	200 μg/kg body weight and 400 μg/kg body weight *via* joint injection	200 μg/kg body weight	E2F1/PITX1 pathway and AKT/mTOR pathway	Yao et al. (2021)
	Hydroxytyrosol	*Olea europaea* L., Oleaceae Hoffmanns. and Link	*In vitro*, TNF-αmice chondrocytes	0, 12.5, 25, 50, 100, 200 and 400 μM, last for 24 h	50 μM	SIRT6 pathway	Zhi et al. (2018)
			In vitro, H_2O_2 induced OA human chondrocytes	100 μM for 30 min	100 μM	SIRT1 pathway	Cetrullo et al. (2016)
	Resveratrol	*Vitis vinifera* L., Vitaceae Juss	*In vitro*, DMM surgery mice chondrocytes	125 mg *via* intra-articular injection for 8 w	125 mg	HIF-1α-dependent AMPK and mTOR signaling	Qin et al. (2017)
			In vivo, DMM surgery mice				
	Butein	*Butea monosperma (Lam.)* Kuntze, Fabaceae Lindl	*In vitro*, IL-1β induced TKA surgery human chondrocytes	0.6 μg/ml-10 μg/ml (or 2.25–36 μM) for 24 h	10 μg/ml (36 μM)	AMPK/TSC2/ULK1/mTOR pathway	Ansari et al. (2018a)
	Mangiferin	*Mangifera indica* L., Anacardiaceae R.Br	*In vivo*, DMM surgery mice	10 mg/kg once a day for 8 weeks	10 mg/kg	AMPK signaling pathway	Li et al. (2019b)
			In vitro, TBHP-induced chondrocytes from mice	0, 5, 10, 50, 100, 200 μM	100 μM		
	Delphinidin	*Aristotelia chilensis* (Molina) Stuntz, Elaeocarpaceae Juss	*In vitro*, H_2O_2 induced C28/I2 human chondrocytes	10–75 μM	40 μM	Nrf2 and NF-κB were activated	Lee et al. (2020)
	Punicalagin	*Punica granatum* L., Lythraceae J.St.-Hil	*In vitro*, TBHP induced mice chondrocytes	0–50 μg/ml	50 μg/ml	Autophagic flux in chondrocytes after TBHP treatment recovered	Kong et al. (2020)
			In vivo, DMM surgery mice	20 mg/kg via oral administration each day for 8 weeks	20 mg/kg		
			In vitro, rats chondrocytes	0, 25, 50 and 100 μM	50 μM	Foxo1/Prg4/HIF3α axis	Liu et al. (2021)
			In vivo, Rats with cut anterior cruciate ligament, medial collateral ligament and medial meniscus	10 mg/kg *via* oral administration for 12 weeks	10 mg/kg		
	(-)Epigallocatechin 3-Gallate	*Camellia sinensis* (L.) Kuntze, Theaceae Mirb. ex Ker Gawl	*In vivo,* ACLT surgery rats	10 μM EGCG by intra-articular injection once every 3 days for 5 weeks	10 μM	mTOR expression was reduced and LC3, Beclin-1 and p62 expression were increased	Huang et al. (2020)
	Chlorogenic acid	*Bauhinia macrantha* Oliv., Fabaceae Lindl	*In vitro,* Human chondrocyte C28/I2 cells	0, 50, 100, 200, 250, 400 μM	250 μM	Antioxidant response proteins Nrf2 and NF-κB were increased	Zada et al. (2021)
Flavonoids	Icariin	*Epimedium sagittatum* (Sieb. and Zucc.) Maxim., Berberidaceae Juss	*In vitro*, TNF-α induced rats chondrocytes	0, 3, 5, 7, 10, and 20 μM	10 μM	p65 nuclear translocation and IκBα protein degradation were inhibited	Mi et al. (2018)
			In vivo, ACTL surgery rats	20, 40, or 80 mg/kg/day by intraperitoneal injection for 4 consecutive weeks	20 mg/kg	PI3K/AKT/mTOR pathway	Tang et al. (2021)

(Continued on following page)

TABLE 1 | (*Continued*) Phytochemicals improve cartilage homeostasis via mediated autophagy against OA *in vitro/in vivo*.

	Phytochemical	Plant species, family	Model	Dosage range	Active concentration	Signal pathways/Mechanisms	References
			In vitro, chondrocytes from ACTL surgery rats	1–100 μM	80 μM		
	Baicalin	*Scutellaria baicalensis* Georgi, Lamiaceae Martinov	*In vitro*, IL-1β-induced chondrocytes from TKA surgery OA patients	20 μM	20 μM	miR-766–3p level was upregulated and AIFM1 expression was decreased	Li et al. (2020)
	Glabridin	*Glycyrrhiza glabra* L., Fabaceae Lindl	*In vitro,* human OA chondrocytes	0.01–10 μM	1 μM	mTOR pathway	Dai et al. (2021b)
			In vivo, ACLT surgery rats	1, 5, and 10 mg/kg for 4 or 8 weeks	1 mg/kg		
	Rhoifolin	*Rhus succedanea* L., Anacardiaceae R.Br	*In vitro,* IL-1β induced rats chondrocytes	0, 5, 10, and 20 μM	20 μM	P38/JNK pathway and PI3K/AKT/mTOR pathway	Yan et al. (2021)
			In vivo, ACLT surgery rats	20 μM intra-articular injection weekly for 8 weeks	20 μM		
	Eupatilin	*Artemisia absinthium* L., Asteraceae Bercht. and J.Presl	*In vitro,* IL-1β induced rats chondrocytes	0, 25, 50, 100 μM	25 μM	Senstrin2-dependent autophagy	Lou et al. (2019)
	Sinensetin	*Citrus* L., Phyllanthaceae Martinov	*In vitro,* TBHP induced mice chondrocytes	0, 10, 20, 30, 40, and 50 μM	10 μM	AMPK/mTOR signaling pathway	Zhou et al. (2021a)
			In vivo, DMM surgery mice	50 mg/kg by gavage for 8 w	50 mg/kg		
Terpenoids	Morroniside	*Corni Fructus,* Cornaceae Bercht. and J.Presl	*In vitro*, TKA surgery human chondrocytes	0, 1, 20, 200 μM	20 μM	PI3K/AKT/mTOR signal pathway	Xiao et al. (2020)
	Lycopene	*Solanum lycopersicum* L., Solanaceae Juss	*In vitro,* H_2O_2 induced SD rats chondrocytes	0.001–10 μM	0.1 μM	MAPK and PI3K/Akt/NF-κB axis	Wu et al. (2021)
	Celastrol	*Tripterygium wilfordii,* Celastraceae R.Br	*In vitro,* IL-1β induced SD rats chondrocytes	0–1.6 μM	0.2 μM	The expression of LC3-II and Beclin-1 increased	Feng et al. (2020)
			In vivo, ACLT surgery rats	0.5 mg/kg, 1 mg/kg by intraperitoneal injection for 12 w	0.5 mg/kg		
Coumarins	Isoimperatorin	*Angelica dahurica*, Apiaceae Lindl	*In vivo*, DMM surgery mice	500 mg/kg *via* oral admin-istration for 4 w	500 mg/kg	mTORC1 pathway	Ouyang et al. (2017)
			In vitro, DMM surgery mice chondrocytes	1–100 mM	1 μM		
	Isopsoralen	*Cullen corylifolium* (L.) Medik., Fabaceae Lindl	*In vitro,* IL-1β induced rats chondrocytes	5, 10, 20, and 40 μg/ml	20 μg/ml	LC3-II and LAMP-1 expression was significantly increased, but p62/SQSTM1 expression was significantly decreased	Chen et al. (2020b)
Saponin	Astragaloside IV	*Astragalus mongholicus* Bunge, Fabaceae Lindl	*In vitro*, IL-1β induced TKA surgery human chondrocytes	50 μg/ml	50 μg/ml	Protein expression of LC3-II/I was increased and that of P62/SQSTM1 was decreased	Liu et al. (2017)
	Huzhangoside D	*Clematis graveolens* Lindl., Ranunculaceae Juss	*In vivo,* ACLT surgery rats	17, 34, 68 mg/kg *via* intraperitoneal injection daily for 4 w	17 mg/kg	AKT and mTOR signaling pathway	Zhang et al. (2021)
Small molecules compounds	β-ecdysterone	*Achyranthes bidentata*, Amaranthaceae Juss	*In vivo*, MIA intraperitoneal injection induced OA rats	0.6 mg/kg, 0.8 mg/kg, and 1 mg/kg *via* subcutaneous injection twice a week for 4 weeks	0.6 mg/kg	PI3K/AKT/MTOR signal pathway	Tang et al. (2020)
			In vitro, DMM surgery mice chondrocytes	10, 20, 40 μM	10 μM		

(Continued on following page)

TABLE 1 | (*Continued*) Phytochemicals improve cartilage homeostasis via mediated autophagy against OA *in vitro/in vivo*.

Phytochemical	Plant species, family	Model	Dosage range	Active concentration	Signal pathways/Mechanisms	References
Dihydroartemisinin	*Artemisia annua* L., Asteraceae Bercht. and J.Presl	*In vitro*, TNF-α induced rats chondrocytes	0–10 μM	1 μM	LC3-II and ATG5 levels were increased and the expression of MMP-3 and -9, ADAMTS5, CCL-2 and -5, and CXCL1 was decreased. p65 and IκBα protein nuclear translocation and degradation were impaired	Jiang et al. (2016)
Shikimic Acid	*Artemisia absinthium* L., Asteraceae Bercht. and J.Presl	*In vitro*, IL-1β induced SW1353 human chondrocytes	0, 0.1,1,5,10, and 20 mM	0.1 mM	MAPK pathway	You et al. (2021)
		In vivo, ACLT surgery rats	20 mM in 100 μL *via* intra-articular injection	20 mM		
Sinomenium	*Sinomenium acutum* (Thunb.) Rehder a& E.H.Wilson, Menispermaceae	*In vitro*, IL-1β induced human chondrocytes	10 mM	10 mM	AMPK/mTOR signaling pathway	Chen et al. (2016)
		In vivo, ACLT surgery mice	5 mg/kg *via* intra-articular injection for 4 or 8 w	5 mg/kg		
Tetrahydrohyperforin	*Hypericum perforatum* L., Hypericaceae Juss	*In vivo*, mice indeced by intra-articular injection of collagenase solution	6 g/kg *via* oral administration once weekly for 6 w	6 g/kg	The levels of LC3-II, Beclin-1 and Atg5 were increased and The level of *p*-mTOR was decreased	Zhang et al. (2018b)
		In vitro, rats chondrocytes	50, 100, 150 and 200 μmol/L	50 μmol/L		

of autophagy activation is the conversion of microtubule-associated protein 1A/1B-light chain 3 (LC3) from LC3-I to LC3-II, a lipidated form of the former protein that allows LC3-II to adhere to the phagocytic membrane during autophagosome formation and extension (Mizushima and Yoshimori, 2007). Under normal cellular conditions, most LC3 proteins are expressed as cytoplasmic LC3-I, which is converted to LC3-II upon autophagy activation by binding to diethanolamine phosphate (PE) and dispersing in the outer and inner membranes of autophagosomes, and this conversion is widely used as an indicator of autophagy activation (Jiang et al., 2016; Ansari et al., 2017). Autophagy deficiency or lack of autophagy activation induces apoptosis (Hara et al., 2006). It has been found that the expression of autophagy regulatory factors and autophagy-related proteins was observed to be downregulated in articular cartilage isolated from OA animals or humans, accompanied by increased chondrocyte apoptosis, suggesting that impaired autophagy is a contributing factor in the development of OA (Taniguchi et al., 2009; Caramés et al., 2010; Vinatier et al., 2018). In addition, the capacity of cells to degrade damaged components by activating autophagy is limited, and excessive oxidative stress can exceed the limits of autophagy, leading to a severe decrease in autophagic flux and impaired function, which can lead to cellular senescence and apoptosis, resulting in the progression of OA (Roca-Agujetas et al., 2019). In early stage of OA, autophagy in chondrocytes and cartilage tissue is confirmed by the upregulation of the autophagy-associated protein LC3. However, the transient activation of autophagy is shown to be only a compensatory response to cellular stress. In late stage of OA, the compensatory response fails to offset oxidative stress and causes structural cellular damage accompanied by inhibition of autophagy (Portal-Núñez et al., 2016; Tang et al., 2020). Nevertheless, the activation of autophagy during the early development of OA is still positive for chondrocyte survival. When autophagy is activated, damaged mitochondria can be removed and intracellular ROS are reduced, protecting chondrocytes from the negative effects of OA. There is evidence that enhanced autophagy in chondrocytes can slow the progression of OA by affecting intracellular metabolic activity (Caramés et al., 2010; Barranco, 2015; Caramés et al., 2015; Luo et al., 2019). Consequently, autophagy plays an irreplaceable role in protecting chondrocytes from oxidative stress (Ansari et al., 2018b). **Figure 1** provides an overview of the mechanism of maintaining cartilage homeostasis through regulation of autophagy.

3 PHYTOCHEMICALS FOR THE TREATMENT OF OA BY PROMOTING AUTOPHAGY

Phytochemicals from traditional medicinal plants are inexpensive and widely available, and can exert anti-inflammatory and antioxidant effects with good pharmacological activity. In recent years, various phytochemicals have been used in the prevention and treatment of various diseases by modulating autophagic targets, such as cardiovascular diseases and cancer

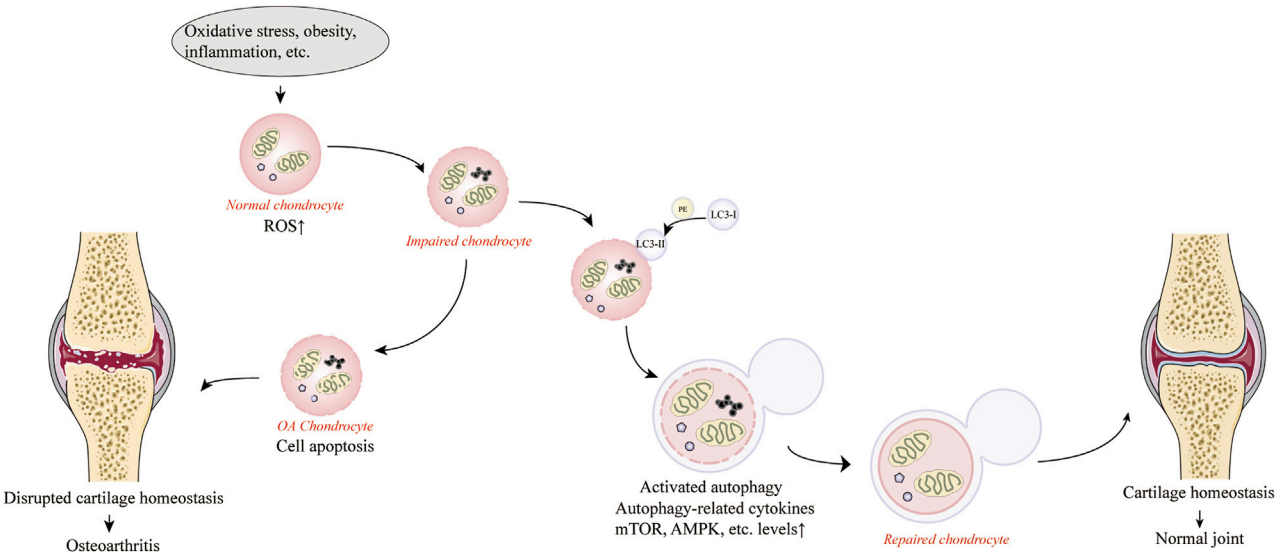

FIGURE 1 | Activation of autophagy against osteoarthritis by maintaining cartilage homeostasis. Produced using Servier Medical Art (smart.servier.com).

(Hong et al., 2020; Li et al., 2020; Luo et al., 2020). Therefore, it is expected that phytochemicals derived from medicinal plants may retard the development of OA by mediating autophagy. There is increasing evidence that phytochemicals can also target autophagic pathways to function as complementary and alternative drugs for OA treatment, and their mechanisms related to the treatment of OA through the autophagic pathway are receiving increasing attention (Hu et al., 2020; Liu et al., 2020; Yu et al., 2021). In this review, we have selected phytochemicals that have the potential to activate autophagic pathways mediating cartilage homeostasis against OA in recent years. The anti-osteoarthritis activity of these phytochemicals and their mechanistic effects are described in the following sections. **Figure 2** illustrates the autophagic pathways of phytochemicals against OA.

3.1 Polyphenols

Polyphenols, a large family of naturally occurring organic compounds characterized by multiples of phenol units, are widely distributed in numerous plants including vegetables, fruits, and botanical drugs (Salucci et al., 2017). It has been found that polyphenols are able to treat oxidative stress, inflammation and neurological diseases by mediating the autophagic pathway, and it has also been shown that polyphenols help to fight against OA (Varela-Eirín et al., 2020; Valsamidou et al., 2021). Here, we will summarize the existing scientific evidence gathered from *in vitro* and *in vivo* studies which support the beneficial effects of polyphenols on ameliorating OA by mediating the autophagic pathways.

3.1.1 Curcumin

Curcumin, a polyphenol derived from *Curcuma longa* L., has anti-inflammatory and antioxidant properties and functions as an anti-inflammatory therapeutic agent in Chinese medicine (Goel et al., 2008). Several studies have found that curcumin can treat OA by mediating autophagy-related pathways and thus improving the status of chondrocytes in an *in vitro* OA model. Li et al. treated mice primary chondrocytes with curcumin and observed that curcumin reduced the expression of autophagy markers LC3-II and Beclin-1 through suppressing mitogen-activated protein kinase/extracellular signal-regulated kinase 1/2 (MAPK/ERK1/2) signaling pathway, thereby inhibiting interleukin-1beta (IL-1β)-induced chondrocyte apoptosis and activation of cysteine aspartate protease-3 (Caspase-3), exerting its anti-inflammatory and anti-apoptotic effects (Li et al., 2017a). Similarly, Chen et al. also found that the curcumin pretreatment reduced IL-1β-induced apoptosis in rat primary chondrocytes through activation of autophagy and inhibition of nuclear factor-κ b (NF-κB) signaling pathway (Chen et al., 2021). In addition, curcumin has been found to activate autophagy and thus improve the function of chondrocytes *in vivo* models of OA. By establishing aging spontaneous OA and the destabilization of the medial meniscus (DMM) surgery-induced OA models in mice, Zhang et al. found that curcumin treatment promoted autophagy by suppressing the protein kinase B/mechanistic target of rapamycin kinase (AKT/mTOR) signaling pathway enhanced autophagy and reduced apoptosis and cartilage loss (Zhang et al., 2018a). Yao et al. established a rat model of OA by feeding a high-fat diet and injected curcumin into the knee joints of OA rats and found that the chondroprotective effect of curcumin may be achieved in part through inhibition of AKT/mTOR pathway autophagy (Yao et al., 2021). Besides, there is a study confirming that curcumin has been used clinically and has been shown to improve pain in patients with mild to moderate OA. But the limitations of curcumin being used in the clinic are mainly due to its low bioavailability and unstable metabolism in the body (Panahi et al., 2014). Curcumin showed low absorption and poor stability *in*

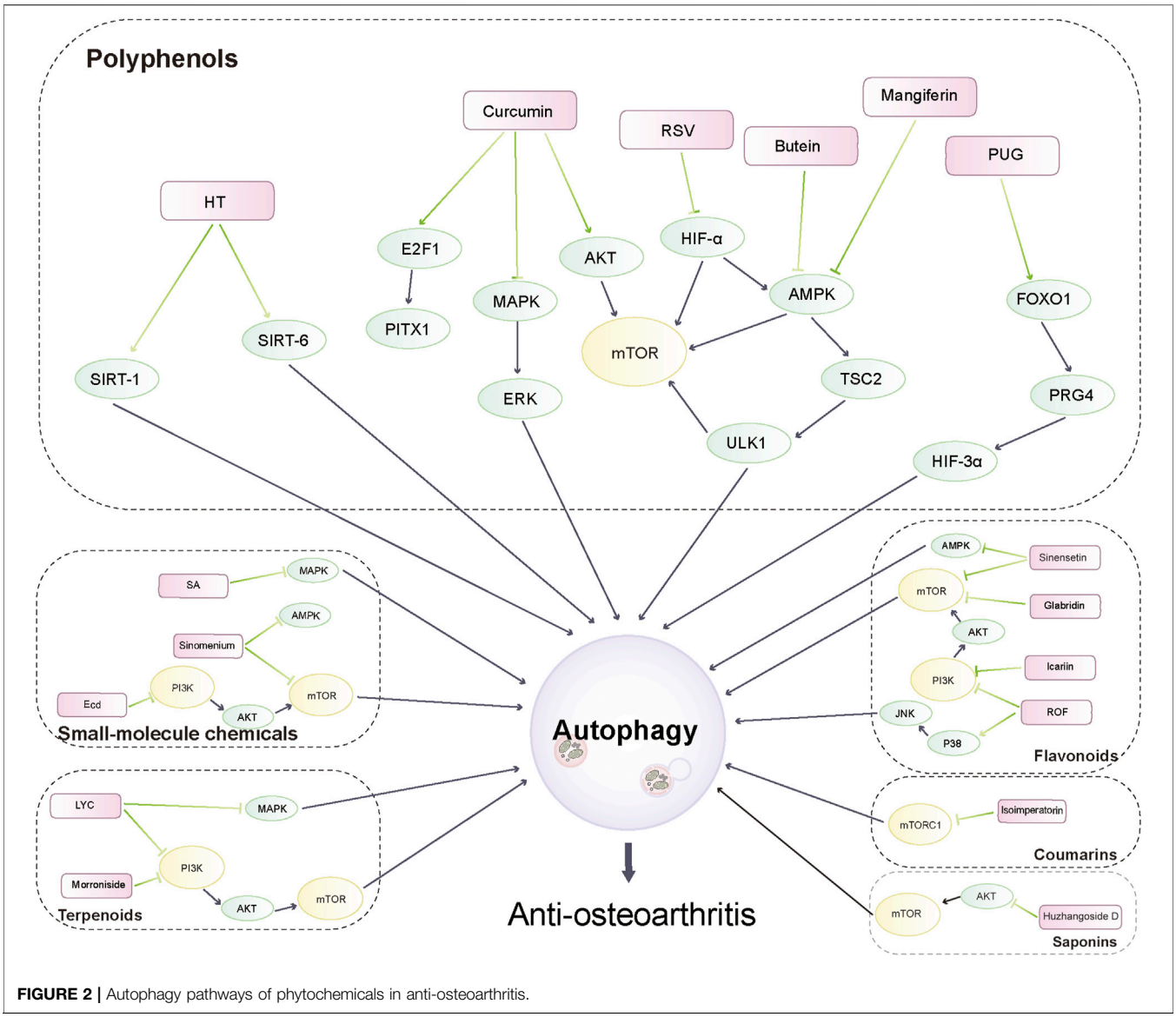

FIGURE 2 | Autophagy pathways of phytochemicals in anti-osteoarthritis.

vivo and *in vitro* environments (T1/2 < 5 min; F < 1%) (Yang et al., 2007). In addition, its solubility in water is limited, with the maximum solubility in pH 5.0 aqueous buffer only 11 ng/ml (Chen et al., 2015). It showed that orally administered curcumin at a dose of 1 g/kg only had 0.5 μg/ml maximum serum concentration, indicating only 1% oral bioavailability (Maiti et al., 2007). Current strategies to improve the bioavailability of curcumin are mainly to change the delivery method of curcumin, to modify it chemically or to combine it with other drugs (Prasad et al., 2014). In conclusion, curcumin, as an active ingredient derived from a natural drug that promotes autophagy, may have great promise in the treatment of OA through autophagy-mediated cartilage homeostasis.

3.1.2 Hydroxytyrosol

Olive oil is the main source of fat in the Mediterranean diet (Granados-Principal et al., 2010). Studies on animal models of arthritis (Musumeci et al., 2013; Rosillo et al., 2014; Silva et al., 2015) and some preliminary trials (Bohlooli et al., 2012; Takeda et al., 2013) suggest that treatment with olive oil or olive phenol-rich extracts may be beneficial for patients with OA. Hydroxytyrosol (HT), the main phenolic in *Olea europaea* L, has been of interest for its potent antioxidant capacity, and studies have been conducted to identify the health benefits of HT in the prevention or treatment of cardiovascular disease, diabetes and cancer (Granados-Principal et al., 2010; Hu et al., 2014). Relevant *in vitro* experiments revealed that HT can regulate autophagy and thus improve chondrocyte function. Cetrullo et al. found experimentally that HT increases autophagy markers through the induction of the Sirtuin-1 (SIRT-1) pathway, thus protecting human primary chondrocytes from DNA damage and cell death due to oxidative stress increased by hydrogen peroxide (Cetrullo et al., 2016). It has been shown that HT increased autophagy in chondrocytes and preosteoblasts and protected them from cell

death and oxidative damage (Aparicio-Soto et al., 2015). The results of Zhi et al. showed that HT may promote chondrocyte autophagy through Sirtuin-6 (SIRT6) and decreased Tumour Necrosis Factor alpha (TNF-α)-induced interleukin-1β (IL-1β) and interleukin-6 (IL-6) levels, thus protecting chondrocytes from TNF-α-induced inflammatory response and oxidative stress-induced DNA damage and cell death (Zhi et al., 2018). Such evidence suggests the potential of HT in preventing chondrocytes from being affected by OA through the relevant autophagic pathway. HT, a hydrophilic phenolic antioxidant, has broad potential for mediating autophagy in the treatment of OA (Cornwell and Ma, 2008).

3.1.3 Resveratrol

Resveratrol (RSV), an active substance derived from *Vitis vinifera* L, has long been used in traditional Chinese medicine, and some studies have demonstrated that RSV inhibits the inflammatory response to OA in both *in vivo* and *in vitro* models (Zhang et al., 2020). Recently, *in vitro* and *in vivo* studies have also revealed that RSV can improve chondrocyte function by mediating autophagy-related pathways, thereby delaying OA progression. Qin et al. demonstrated experimentally that intra-articular injections of RSV upregulated the expression of hypoxia-inducible factor-1 alpha (HIF-1α) and hypoxia-inducible factor-2 alpha (HIF-2α) by up-regulating the AMP-activated protein kinase (AMPK)/mTOR signaling pathway, thereby promoting chondrocyte autophagy and delayed the degeneration of articular cartilage in a DMM-induced OA model (Qin et al., 2017). Additionally, RSV has been used clinically and has been shown to improve pain conditions and knee function in patients with OA (Nguyen et al., 2017; Wong et al., 2017; Hussain et al., 2018). It is notable that there are some limitations to the utilization of resveratrol. First, the solubility of resveratrol is relatively low, 0.05 mg/ml when dissolved in water, and in addition, resveratrol is chemically unstable when exposed to the intrinsic enzymatic and PH environment of the gastric and intestinal tract, which reduces the low bioavailability after oral administration (Francioso et al., 2014; Robinson et al., 2015). However, RSV still has the potential to improve chondrocyte homeostasis in OA progression by mediating autophagy, thus emerging as a new therapeutic approach for OA.

3.1.4 Butein

Butein is a polyphenol derived primarily from *Butea monosperma* (Lam.) Kuntze. Plant extracts containing butein are traditionally used in Ayurvedic and Unani India as well as in Chinese medical systems to treat various human ailments. (Wang et al., 2014). Butein has been shown to inhibit the pro-inflammatory effects of IL-1β on chondrocytes (Zheng et al., 2017). Ansari treated IL-1β-induced human chondrocytes with butein and showed that butein activated autophagy through suppressing the AMPK/Tuberous sclerosis complex 2 (TSC2)/Unc-51-like kinase 1 (ULK1)/mTOR pathway and inhibited IL-6 expression in human chondrocytes, thereby protecting chondrocytes from OA (Ansari et al., 2018a). It has been found that Butein binds to human serum albumin (HSA) through hydrophobic interaction, thus successfully penetrating into the cell membrane to exert pharmacological effects (Padmavathi et al., 2017). As a potential therapeutic agent to improve chondrocyte homeostasis and thus treat and/or prevent OA through autophagy, butein deserves further investigation.

3.1.5 Mangiferin

Mangiferin, a natural polyphenol derived mainly from *Mangifera indica* L., is able to exert anti-inflammatory and antioxidant effects (Sellés et al., 2015), while it has been suggested that mangiferin may promote bone repair in endochondral osteogenesis by activating autophagy (Bai et al., 2018). Li et al. applied mangiferin treatment to reverse oxidative stress induced by tert-butyl hydroperoxide (TBHP) and alleviate chondrocyte apoptosis and ECM degradation in an *in vitro* experiment. *In vivo* experiments likewise confirmed that mangiferin could exert therapeutic effects on DMM-induced OA mice by activating autophagy. Their findings showed that mangiferin decreased mTOR activity and promoted phosphorylation of AMPK to activate autophagy in a time- and dose-dependent manner (Li et al., 2019b). This evidence demonstrates the ability of mangiferin to mitigate chondrocyte apoptosis and ECM degradation by regulating the autophagic pathway, thus exerting an anti-osteoarthritic effect. A clinical study found the concentration of mangiferin in plasma reached 38.64 ± 6.75 ng/ml approximately 1 h after oral administration of 0.9 g of mangiferin, with an apparent elimination half-life (t1/2) of 7.85 ± 1.72 h, further demonstrating its potential application in clinically mediated autophagy for the treatment of OA (Hou et al., 2012).

3.1.6 Delphinidin

The natural compound anthocyanins extracted from *Aristotelia chilensis* (Molina) Stuntz are used to treat OA and several diseases (Kong et al., 2003). Among the various anthocyanins, delphinidin is a special class of polyphenols that protects chondrocytes and inhibits the progression of OA by mediating relevant cellular pathways against oxidative stress (Haseeb et al., 2013). Delphinidin has been reported to inhibit IL-1-induced matrix metalloproteinases (MMPs) expression in human articular chondrocytes via suppressing NF-κB and ERK/MAPK pathways (Wongwichai et al., 2019). Lee et al. applied delphinidin to hydrogen peroxide (H_2O_2)-treated human chondrocytes and found that delphinidin could activate autophagy by up-regulating nuclear factor erythroid 2-related factor 2 (NRF2) and NF-κB pathways to protect chondrocytes from oxidative stress generated by H2O2 (Lee et al., 2020). Therefore, delphinidin may protect chondrocytes by inducing autophagy and thus stop the progression of OA, providing a new idea for the treatment of OA. The high hydrophilicity and instability of delphinidin may restrict its use in clinical practice, so it requires strategies to be developed to increase its bioavailability (Legeay et al., 2019).

3.1.7 Punicalagin

Punicalagin (PUG) is a hydrolyzable polyphenol extracted from *Punica granatum* L. with a wide range of biological activities and cytoprotective effects (Yan et al., 2016; Foroutanfar et al., 2020).

PUG has been reported to play a protective role in inhibiting apoptosis, and related studies have also shown that pomegranate glucoside is beneficial in the treatment of OA (Yu et al., 2019; Foroutanfar et al., 2020). Both *in vivo* and *in vitro* studies have shown that PUG can exert anti-osteoarthritic effects through activation of autophagy. Liu et al. found that PUG promotes autophagy through the forkhead box O1/proteoglycan 4 (FOXO1/Prg4)/HIF3α axis, inhibits inflammation and extracellular matrix degradation, and attenuates inflammatory damage caused by lipopolysaccharide (LPS) in rat chondrocytes (Liu et al., 2021). In addition, Kong injected PUG in a mouse DMM model and showed that PUG increased antioxidant enzymes and reduced the degradation of apoptotic proteins and ECM by mediating autophagy, thus effectively stopping the progression (Kong et al., 2020). Although preclinical studies have shown that PUG can reduces chondrocyte apoptosis and ECM degradation through mediating autophagy, its solubility is low and insufficient for effective use after oral administration, which greatly limits its clinical application (Cerdá et al., 2005). However, the bioavailability of PUG can be promoted using micronization techniques therefore PUG has the potential to fight OA by mediating autophagy, but further experimental confirmation is needed (Nyamba et al., 2021).

3.1.8 (-)-Epigallocatechin 3-Gallate

(-)-Epigallocatechin gallate (EGCG) is the most abundant bioactive polyphenol in *Camellia sinensis* (L.) Kuntze and has been shown to have anti-inflammatory and antioxidant effects (Luk et al., 2020). Related *in vitro* experiment found EGCG can attenuate extracellular matrix degradation and inflammation by inhibiting MMPs and TNF-α activation (Rasheed et al., 2009). In addition, Huang et al. observed that intra-articular injection of EGCG reduced cartilage degradation in an anterior cruciate ligament transection (ACLT)-induced OA rat model by regulating the expression levels of autophagy-related marker proteins, namely, decreasing mTOR expression and enhancing LC3, beclin-1, and p62 expression, thereby reducing chondrocyte inflammation and apoptosis (Huang et al., 2020). It has been shown that there is no toxicity in rats consuming up to 500 mg/kg/day doses of EGCG dietary (Isbrucker et al., 2006). And the bioavailability of EGCG at a dose of 800 mg/day showed a significant increase in healthy participants compared to a dose of 400 mg/day (Chow et al., 2003). Therefore, EGCG may be an alternative treatment for OA because of its high bioavailability and its ability to improve chondrocyte apoptosis and cartilage degeneration in OA rat models.

3.1.9 Chlorogenic Acid

Chlorogenic acid (CGA) is a natural polyphenolic compound from *Bauhinia macrantha* Oliv. with antioxidant properties that have been found to protect against oxidative stress by activating multiple signaling pathways in chondrocytes (Hoelzl et al., 2010; Chen et al., 2011). Zada et al. found that CGA protects against H2O2-induced oxidative stress by mediating autophagy while regulating antioxidant pathways such as NRF2 and NF-κB pathways, thereby protecting human chondrocytes from apoptosis and slow down the progression of OA (Zada et al., 2021). A study reported that the apparent bioavailability of oral CGA in rats was 27–33% (Farah et al., 2008). These results suggest that CGA can be used for drug development in OA by modulating autophagy for targeted treatment of OA.

3.2 Flavonoids

In recent years, researches have confirmed the beneficial effects of flavonoids to health, including their use in conditions related to autophagy, such as neurodegenerative diseases (Dai et al., 2021a; Pérez-Arancibia et al., 2021). A large number of experiments have shown that flavonoids and its derivatives can improve chondrocytes and thus combat against OA, which makes it possible to apply flavonoids in clinical studies (Basu et al., 2018; Ansari et al., 2020).

3.2.1 Icariin

Icariin, a flavonoid compound extracted from *Epimedium sagittatum* (Sieb and Zucc.) Maxim., has been shown to slow down the progression of OA by inhibiting the NF-κB pathway to attenuate the inflammatory response of chondrocytes (Hua et al., 2018) and by inhibiting the expression of MMP-13 and pro-inflammatory cytokines in chondrocytes (Zeng et al., 2014; Pan et al., 2017a; Sun et al., 2018). Related *in vivo* and *in vitro* experiments revealed its ability to protect chondrocytes from OA by activating autophagy. The results of Mi et al. showed that icariin protects chondrocytes from OA by inhibiting TNF-α-induced NF-κB signaling pathway to activate autophagy and significantly reduce apoptotic markers. In addition, icariin exerted the same effect as the Pyrrolidinedithiocarbamic acid (PDTC, NF-κB inhibitor) control, but it exerted a better anti-inflammatory effect in inhibiting the activation of NF-κB signaling pathway (Mi et al., 2018). Tang et al. administered icariin intraperitoneally to DMM surgery induced OA rats and found that it attenuated OA in a dose-dependent manner by downregulating phosphatidylinositol 3-kinase (PI3K)/AKT/mTOR signaling to activate autophagy in chondrocytes (Tang et al., 2021). Icariin has a low bioavailability due to its poor absorption, which poses additional limitations to its clinical application (Li et al., 2015). However, it has been found that the bioavailability of icariin can be improved by pharmacological methods (Zhang et al., 2012). Therefore, the studies on the activation of autophagy to maintain the homeostasis of chondrocytes by icariin are of guidance for the prevention and treatment of OA.

3.2.2 Baicalin

Baicalin, a principal flavonoid extracted from roots of *Scutellaria baicalensis* Georgi, has a wide range of biological activities such as anti-inflammatory and antioxidant (Wang et al., 2007; Lee et al., 2015), and some studies have shown that baicalin plays a role in improving OA progression (Pan et al., 2017b; Yang et al., 2018). Li et al. used baicalin to treat IL-1β-treated human OA chondrocytes, and the results showed that baicalin increased the promotion of autophagy flux and attenuated IL-1β-induced chondrocyte apoptosis and ECM degradation (Li et al., 2020). However, the bioavailability of baicalin was found to be very low (2.2%), therefore, how to improve the

bioavailability of baicalin is still a problem (Xing et al., 2005). Nevertheless, it is undeniable that baicalin is promising in regulating the autophagic pathway against chondrocyte apoptosis and endochondral homeostasis against OA.

3.2.3 Glabridin

Glabridin is a flavonoid derived from *Glycyrrhiza glabra* L. that exerts powerful antioxidant effects by removing free radicals and has been found to be comparable to vitamin E in terms of its antioxidant capacity (Fuhrman et al., 2000; Simmler et al., 2013). It has been used to prevent and treat pathological changes associated with free radical oxidation, such as cellular senescence (Veratti et al., 2011). In addition, glabridin has been found to enhance the function of osteoblasts thereby preventing osteoporosis and various bone and joint diseases (Choi, 2011). Dai et al. found a significant increase in LC3-II levels in human chondrocytes after the administration of glabridin, suggesting that it could protect them from oxidative stress, apoptosis by enhancing autophagy. *In vivo* experiments revealed that glabridin could activate autophagy, which is to reduce mTOR expression, and increase LC3-II levels attenuated ACLT-induced apoptosis in OA rats, thereby delaying their cartilage degeneration (Dai et al., 2021b). The clinical application of glabridin is limited due to its poor water solubility and therefore low bioavailability, but studies have shown that this situation can be improved by combining it with β-Lactoglobulin. (Wei et al., 2018). These results indicate the potential of glabridin in OA prevention and treatment as a potential drug for OA.

3.2.4 Rhoifolin

Rhoifolin (ROF) is a flavanone derived from *Rhus succedanea* L. that exhibits significant antioxidant and anti-inflammatory effects in a variety of diseases (Fang et al., 2020; Peng et al., 2020). *In vitro*, ROF attenuated osteoclast-stimulated osteolysis by inhibiting MAPK and NF-κB signaling pathways (Liao et al., 2019). Yan et al. showed that ROF significantly blocked phosphorylation of P38/JNK and PI3K/AKT/mTOR pathways to enhance autophagy and protected rat chondrocytes from IL-1β-induced inflammation and apoptosis. *In vivo*, intra-articular injection of ROF also significantly improved cartilage damage in a rat OA model, affirming the potential role of ROF in OA treatment by regulating autophagy (Yan et al., 2021). However, the optimal dose of ROF for *in vivo* application is unclear and needs to be further investigated.

3.2.5 Eupatilin

Eupatilin is a flavonoid derived from *Artemisia absinthium* L. that exerts anti-apoptotic and anti-inflammatory effects in a variety of diseases (Choi et al., 2008; Cai et al., 2012). Recent studies suggest that eupatilin may be useful in arthritis (Jeong et al., 2015; Kim et al., 2015). Lou et al. found that eupatilin attenuated IL -1β-induced apoptosis in rat chondrocytes by modulating autophagy-related protein levels, that is, by increasing senstrin2 and decreasing mTOR, which activated autophagy in a dose-dependent manner (Lou et al., 2019). Eupatilin at 33–85 mM exerts moderate toxic effects on human and mice cancer cells, but more eupatilin toxicity studies on chondrocytes are needed (Zater et al., 2016).

3.2.6 Sinensetin

Sinensetin is a polymethoxylated flavonoid derived from *Citrus* L. with potent anti-inflammatory activity (Han Jie et al., 2020). Sinensetin has been shown to mediate the AMPK/mTOR signaling pathway to promote autophagy and thereby treat liver cancer (Kim et al., 2020). *In vitro* experiments by Zhou et al. showed that Sinensetin activated the AMPK/mTOR signaling pathway in a time- and dose-dependent mannersignificantly improved the autophagy function of mice chondrocytes and inhibited TBHP-induced apoptosis in mouse chondrocytes. *In vivo* experiments yielded similar results, and Sinensetin protected against DMM-induced mice (Zhou et al., 2021b). These results provide evidence that Sinensetin could be a potential candidate for the treatment of OA.

3.3 Terpenoids

Terpenoids are the largest class of natural products, most of which are of plant origin, and their biological properties, mainly anti-proliferative and apoptotic, have been shown to play an important role in cancer prevention and health promotion through the promotion of autophagy (Martel et al., 2019; El-Baba et al., 2021). Therefore, plant-derived terpenoids components will provide a novel approach for mediating autophagy in the treatment of OA.

3.3.1 Morroniside

Corni Fructus (CF) is one of the most important botanical products in traditional Chinese medicine and its compound has been used clinically for a long time in the treatment of OA (Chen et al., 2014a). In latest years, some compounds extracted from CF such as cyclic enol ether glycosides and active ingredients have been found to have antioxidant and anti-inflammatory effects. Morroniside, an water-soluble iridoid glycoside derived from CF, has a variety of bioactive substances with antioxidant and anti-inflammatory effects (Park et al., 2009; Wang et al., 2010; Chen et al., 2014b). It has been shown in many *in vivo* and *in vitro* experiments that morroniside improves chondrocyte function by modulating autophagy to slow OA progression. Xiao et al. conducted *in vitro* experiments with human chondrocytes and showed that morroniside decreased the level of LC3 conversion in chondrocytes, thus promoting chondrocyte proliferation, survival and matrix synthesis. Interestingly, morroniside also inhibited the autophagic response of chondrocytes by promoting PI3K/AKT/mTOR signaling, while increasing the activity of AKT and mTOR. However, overexpression of autophagy genes in the experiment enhanced the positive regulation of cell proliferation, survival and matrix synthesis by morroniside, suggesting that activation of autophagy facilitates the protective effect of morroniside on chondrocytes (Xiao et al., 2020). Furthermore, Yu et al. established a mouse model of OA by DMM surgery and used primary mouse chondrocytes induced by morroniside treatment with IL-1β as *in vitro* subjects. Morroniside was found to slow down the progression of OA

by inhibiting the NF-κB signaling pathway and suppressing the expression of MMP-13, Caspase-1 and NOD-like receptor family pyrin domain containing 3 (NLRP3) (Yu et al., 2021). Similarly, Cheng et al. treated human osteoarthritic chondrocytes with morroniside for *in vitro* experiments and found that morroniside could promote cell survival and matrix synthesis, and also induced an experimental OA model in rats by anterior cruciate ligament severance combined with medial meniscectomy (Hayami et al., 2003; Zhao et al., 2014), and found that intra-articular injection of morroniside reduced cartilage damage in an experimental model of OA rats (Cheng et al., 2015). Therefore, some drugs with autophagy-activating effects may serve as effective supplements to morroniside in the treatment of OA.

3.3.2 Lycopene

Lycopene (LYC), a lipid-soluble carotenoid naturally found in *Solanum lycopersicum* L, is a potent antioxidant with potential chondroprotective effects (Sachdeva and Chopra, 2015; Wang et al., 2016). It is shown *in vitro* experiments by Wu et al. that LYC may enhance autophagy and inhibit H_2O_2-induced inflammation and apoptosis in rat chondrocytes by suppressing mTOR levels in part through inhibition of MAPK and PI3K/AKT/NF-κB axis (Wu et al., 2021), thus LYC has potential therapeutic implications for mediating autophagy in the treatment of OA.

3.3.3 Celastrol

Celastrol is a natural triterpenoid found in traditional Chinese medicine botanical drugs *Tripterygium wilfordii* (Yang et al., 2006). Owing to its powerful anti-inflammatoryand antioxidant properties, celastrol has been used to treat a variety of diseases (Kannaiyan et al., 2011). Feng et al. found that celastrol restored IL-1β-induced inhibition of autophagy in rat chondrocytes by inhibiting the NF-κB signaling pathway, increased the expression levels of LC3-II and Beclin-1, and ameliorated IL-1β-induced apoptosis in rat chondrocytes. In addition, celastrol decreased IL-1β-stimulated phosphorylation of IκBα and P65. The therapeutic effect of celastrol on OA articular cartilage was also confirmed in the ACLT rat OA model (Feng et al., 2020). Celastrol is poorly water soluble, but it has been studied to effectively improve its bioavailability through galactosylated liposomes (Chen et al., 2020a). These results suggest that celastrol has potential in the prevention and treatment of OA.

3.4 Coumarins

Coumarins are different species of plant-derived secondary metabolites that have anti-inflammatory and anti-apoptotic properties and have recently been found to treat cancer by mediating autophagy (Guo et al., 2019; Rodríguez-Hernández et al., 2020). Accordingly, it is possible that these plant-derived coumarins mediate the autophagic pathway for the treatment of OA.

3.4.1 Isoimperatorin

Isoimperatorin is an linear furanocoumarin isolated from the *Angelica dahurica* (Wei and Ito, 2006). It has been demonstrated that isoimperatorin may exert anti-osteoarthritic effects by inhibiting COX-2 production in a mouse model (Moon et al., 2008). Ouyang et al. found that isoimperatorin activated autophagy by downregulating the mTORC1 signaling pathway in a dose-dependent manner in mouse chondrocytes, and downregulated the expression of MMP13, Runt-related transcription factor 2 (Runx2), and Vascular endothelial growth factor (VEGF) expression of inflammatory factors, thereby ameliorating articular cartilage degeneration in a mouse DMM model (Ouyang et al., 2017). Thus, isoimperatorin activates autophagy in a dose-dependent manner to down-regulate the level of inflammatory factors in cartilage and thus anti-osteoarthritis. Isoimperatorin was found to have toxic effects on human tumor cell lines, but more data is needed on its effects on chondrocytes (Kim et al., 2007).

3.4.2 Isopsoralen

Isopsoralen is a linear furanocoumarin isolated from the fruit of *Cullen corylifolium* (L.) Medik. and has various pharmacological effects such as anti-inflammatory, anti-oxidative stress (Li et al., 2019c; Zhang et al., 2019). Isopsoralen has been found to promote chondrocyte differentiation (Li et al., 2012). A study by Chen et al. showed that isopsoralen significantly enhanced autophagic flux by reducing the expression of LC3-II and sqstm1/p62, which resulted in a protective effect against il-1β-induced apoptosis in rat chondrocytes (Chen et al., 2020b). isopsoralen deserves consideration as a therapeutic agent for OA.

3.5 Saponin

Saponins originating from different plants have also been found to exert anti-inflammatory and antioxidant activity through the mediation of autophagy and thus be used in the treatment of various diseases (Zhou et al., 2019; Luo et al., 2020). Saponins have potential in mediating autophagic pathways in the treatment of OA.

3.5.1 Astragaloside IV

Astragaloside IV (AST) is a unique active saponin compound extracted from *Astragalus mongholicus* Bunge, which has been found to protect against IL-1β-induced joint inflammation and cartilage damage (Wang and Chen, 2014). Liu et al. treated chondrocytes from OA patients induced by IL-1β with AST and demonstrated that AST increased chondrocyte autophagic flux, reversed the expression of LC-3II/I and p62, significantly inhibited IL-1β-induced apoptosis, and maintained cell viability (Liu et al., 2017). AST may be a new candidate for the treatment of OA because of its potential to mediate autophagy to regulate cartilage function. However, the gastrointestinal absorption of AST is very low, with a bioavailability of 2.2% in rats, thus limiting its clinical application (Gu et al., 2004). More research is needed to make it better applied in the clinical treatment of OA.

3.5.2 Huzhangoside D

Huzhangoside D is a saponin isolated from *Clematis graveolens* Lindl, the latter being used to treat inflammation (Kawata et al., 1998). Zhang et al. treated an ACLT-induced KOA rat model with huzhangoside D and found that huzhangoside D may activate autophagy through downregulation of AKT and mTOR signaling

pathway activity to activate autophagy, thereby upregulating the levels of autophagy-associated proteins beclin-1, ATG5, ATG7 and LC3. Meanwhile the levels of pro-inflammatory cytokines including TNF-α, IL-6 and IL-1β were decreased and the levels of anti-inflammatory cytokines such as IL-10 were increased, and the damage to cartilage structures and the function of cartilage in KOA rat models were restored to some extent (Zhang et al., 2021).

3.6 Small-Molecule Chemicals

In addition to the above phytochemicals, a number of small-molecule chemicals derived from plants, such as various natural compounds and compound analogues, have also been found to enhance autophagy to treat various diseases (Jang et al., 2019; Wu et al., 2020). These plant-derived small molecules would be able to mediate autophagy to treat OA, but more research is needed.

3.6.1 β-ecdysterone

β-ecdysterone (Ecd) is an estrogen analog isolated from *Achyranthes bidentata* with various physiological effects such as anti-fatigue, pro-proliferative and hypolipidemic (Xu et al., 2018). It was found that Ecd inhibited IL-1β-induced apoptosis and inflammation in rat chondrocytes by inhibiting the NF-κB signaling pathway (Zhang et al., 2014). Tang used Ecd to intervene in a rat OA model established by monoiodoacetic acid (MIA), and the results showed that Ecd may induce chondrogenesis through the down-regulation of PI3K/AKT/mTOR signaling pathway induced chondrocyte autophagy and downregulated the expression of PI3K, mTOR, and caspase-3, thereby reducing OA-like symptoms (Tang et al., 2020). Evidence related to Ecd improving chondrocyte homeostasis through mediated autophagy requires further examination.

3.6.2 Dihydroartemisinin

Dihydroartemisinin (DHA), a semisynthetic derivative of Artemisinin (ART), has fewer side effects than ART, the main phytochemical extracted from *Artemisia annua* L. (Tu, 1999). It has been shown that DHA can inhibit estrogen deficiency-induced osteoporosis and osteoblast remodeling (Zhou et al., 2016). Jiang et al. have found *in vitro* experiments that DHA inhibits TNF-α-induced NF- κB pathway activation and promote autophagy in rat chondrocytes thereby inhibiting chondrocyte catabolism and inflammatory factor levels, thus DHA has potential in improving OA through enhanced autophagy (Jiang et al., 2016). Currently, it has been found that the compounding of hydroxypropyl-beta-cyclodextrin (HPβCD) with DHA increases the solubility and stability of DHA, which makes it possible to apply DHA to clinical trials (Ansari et al., 2009).

3.6.3 Shikimic Acid

Shikimic acid (SA) is a hydroaromatic compound extracted from *Artemisia absinthium L*, which has been shown to have significant anti-inflammatory effects (Kolodziej et al., 2008). Another study showed that SA can inhibit osteoclastogenesis by inhibiting NF-κB and MAPK pathways, suggesting its potential role in the treatment of OA (Chen et al., 2018). *In vitro* and *in vivo* experiments have recently demonstrated that SA can delay OA progression by enhancing autophagy-mediated cartilage homeostasis. You et al. found that SA inhibited IL-1β-induced mitogen activation by inhibiting phosphorylation of ERK, p38, JNK, p65, and MAPK and NF-κB pathway activation and attenuated the expression of inflammatory and apoptotic factors, such as iNOS, COX2, MMPs and ADAMTS5, thereby alleviating IL-1β-induced inflammatory responses, dysregulation of cartilage anabolism and catabolism, and autophagic damage in human chondrocytes. In addition, *in vivo* experiments revealed that SA reduced cartilage erosion and proteoglycan loss in ACLT rats, thus providing new evidence for water-soluble SA to treat and prevent the development of OA (Steimer et al., 2015; You et al., 2021).

3.6.4 Sinomenium

Sinomenium (SIN) is a natural alkaloid extracted from the medicinal plant *Sinomenium acutum* (Thunb.) Rehder and E.H.Wilson, which decreases the protein level of MMP-13, a marker of cartilage degradation in rats, thereby resisting cartilage degradation, and blocks collagen-induced arthritis through NF-κB signaling and downregulates the expression of MMP13 (Ju et al., 2010; Sun et al., 2014). Chen et al. found that SIN improved IL-1β-induced degradation of the extracellular matrix in mouse chondrocytes at least in part through activation of autophagy. Similarly, by intra-articular injection of CM-SIN and GelMA in ACLT surgery-induced mice, SIN was also found to improve cartilage matrix degradation, at least in part, by inducing autophagy *in vivo* (Chen et al., 2016).

3.6.5 Tetrahydrohyperforin

Tetrahydrohyperforin (IDN5706) is a tetrahydro derivative of hyperforin, one of the main active components of *Hypericum perforatum* L. extracts, which has many properties, including anti-inflammatory and anti-tumor properties (Koeberle et al., 2011). *In vitro* studies by Zhang et al. demonstrated that IDN5706 decreased the levels of MMP-13 and IL-6 in OA rat chondrocytes. At the same time, the levels of LC3-II, Beclin-1 and Atg5 were increased and the levels of *p*-mTOR were decreased. IDN5706 was also found to attenuate the degeneration of OA rat model induced by intra-articular injection of collagenase solution articular cartilage through activation of autophagy (Zhang et al., 2018bbib_Zhang_et_al_2018a).

4 SUMMARY AND PROSPECT

In the development of OA, the activation of autophagy has positive significance for the survival of chondrocytes, and autophagy as a therapeutic target for OA has a broad clinical application prospect. Targeted application of drugs to regulate chondrocyte autophagy levels is expected to provide more options for the clinical treatment of OA. In recent years, plant extracts and phytochemicals isolated from the former have gradually gained popularity and attracted widespread attention. They have definite anti-osteoarthritic ability, which is mainly achieved by mediating relevant autophagy-related

pathways, and improving chondrocyte autophagy. Given the cost-effectiveness and wide availability of phytochemicals, and the growing awareness of their role in promoting chondrocyte autophagy and thus treating OA, research on improving OA is rapidly increasing. Phytochemicals emerge as an important source for the development of novel OA therapeutics, providing a valuable source of OA therapeutics, lead compounds or adjuvants for the discovery of new drugs that exert multifaceted biological activities in maintaining human health and preventing disease. However, except from curcumin and RSV (Chin, 2016; Nguyen et al., 2017), most of the current experimental designs are confined to preclinical studies such as cellular and animal experiments, and it remains unclear whether they can be applied in the clinics. Furthermore, there are still many issues to be solved in this field. First, *in vitro* experiments have demonstrated curcumin at concentrations of 25 μM and above is cytotoxic to primary chondrocytes after 5 days in culture, but most phytochemicals still lack validated clinical trials to demonstrate their toxicity (Clutterbuck et al., 2013). Second, some studies have demonstrated a dose-effect effect of curcumin, EGCG and HT in the improvement of chondrocyte function, so it is possible that different doses of phytochemicals have different efficacy in the treatment of OA, and there are still no comparative studies on the effectiveness of other phytochemicals with different doses (Chowdhury et al., 2008; Oliviero et al., 2013; Zhi et al., 2018). Third, it has been argued that phytochemicals such as curcumin, resveratrol, and EGCG may be pan-assay interference compounds (PAINS), that is, by interfering with various reactions in the assays, such as chemical aggregation, the presence of a reactive michael acceptor, and fluorescence activity, thus making the assays readout appear false positive rather than through specific compound/target interactions. Moreover, its experimental results are strongly influenced by the experimental conditions, such as the purity of the phytochemical extracts (Baell, 2016). The pharmacological effects of these phytochemicals in a variety of diseases have attracted widespread attention from researchers as a panaceas, but this invalid metabolic panaceas (IMPS) may lead to a waste of research resources in drug development, so further exploration in the control of experimental conditions and development is needed to minimize the effect of false positives (Bisson et al., 2016). Autophagy can be used as a protective mechanism to degrade and remove damaged organelles and proteins, and thus can be used to treat various aging-related diseases (Ren and Zhang, 2018). In oxidative stress environments, autophagy is activated to eliminating intracellular ROS to protect cells from apoptosis, as well as to prevent tissue inflammation by downregulating inflammation-related signals, reducing inflammatory cytokine expression, and promoting apoptotic corpse clearance (Levine et al., 2011; Yun et al., 2020). Current studies have shown that activation of autophagy can protect chondrocytes from oxidative stress and inflammation by down-regulating the levels of inflammation and oxidative stress-related proteins such as iNOS and MMPs and upregulating autophagy-related factors such as mTOR and AMPK to maintain the structural integrity of the cartilage matrix against early OA (Duan et al., 2020), but the role of autophagy in different periods of OA is different, and further studies are needed on the mechanism of autophagy activation on advanced OA and its effects. Besides, it has been shown by another study that curcumin has potential therapeutic potential for diseases such as viral infections by modulating APE1 and thus affecting the common redox response in the body, and therefore is not a PAINS (Li et al., 2019a). Since Apurinic/apyrimidinic endonuclease 1 (APE1) can promote autophagy, it is possible that phytochemicals like curcumin could enhance the regulation of APE1 by targeting autophagy to treat OA, thus avoiding becoming an IMPS and the failure of drug development due to false positives in its pharmacological effects, but the role of phytochemicals in mediating autophagy in different periods of OA and the specific molecular mechanisms of their anti-osteoarthritis function need to be further investigated, and further experimental demonstration on the existing basis is needed (Li et al., 2019d; Tang et al., 2019). Obviously, our review has the limitation that there is a risk of obtaining false-positive results. However, in the context of developing natural products with the potential to target the treatment of OA, our review remains a summary and critical evaluation based on the available evidence and provides a basis for further research and development. Therefore, the combined efforts of more relevant researchers and experts are needed to conduct systematic experimental design and experimental analysis and to establish an effective evaluation system so that phytochemicals can more effectively benefit patients with OA. It is hoped that increasingly extensive and well-designed pharmacological and clinical studies will enable safer and more rational use of these ancient botanical drugs based on conclusive evidence.

AUTHOR CONTRIBUTIONS

MS and XZ conceptualized the review. ZT drafted the manuscript, drew illustrations of autophagy-related pathways and processed them at the same time. MS and XZ revised and supplemented the manuscript. All the authors participated in writing and giving feedback on the manuscript. All authors have read and approved the final manuscript.

FUNDING

This work was supported by the Scientific research funding project of the Department of Education of Liaoning Province (LJC2019ST02), 2019 Outstanding Talents Support Plan for Higher Education Institutions in Liaoning Province (WR2019024) and the Scientific research funding project of the Department of Education of Liaoning Province (LJKZ1048).

REFERENCES

Ansari, M. T., Iqbal, I., and Sunderland, V. B. (2009). Dihydroartemisinin-cyclodextrin Complexation: Solubility and Stability. *Arch. Pharm. Res.* 32 (1), 155–165. doi:10.1007/s12272-009-1130-4

Ansari, M. Y., Ahmad, N., and Haqqi, T. M. (2018a). Butein Activates Autophagy through AMPK/TSC2/ULK1/mTOR Pathway to Inhibit IL-6 Expression in IL-1β Stimulated Human Chondrocytes. *Cell Physiol Biochem* 49 (3), 932–946. doi:10.1159/000493225

Ansari, M. Y., Ahmad, N., and Haqqi, T. M. (2020). Oxidative Stress and Inflammation in Osteoarthritis Pathogenesis: Role of Polyphenols. *Biomed. Pharmacother.* 129, 110452. doi:10.1016/j.biopha.2020.110452

Ansari, M. Y., Khan, N. M., Ahmad, I., and Haqqi, T. M. (2018b). Parkin Clearance of Dysfunctional Mitochondria Regulates ROS Levels and Increases Survival of Human Chondrocytes. *Osteoarthritis Cartilage* 26 (8), 1087–1097. doi:10.1016/j.joca.2017.07.020

Ansari, M. Y., Khan, N. M., and Haqqi, T. M. (2017). A Standardized Extract of Butea Monosperma (Lam.) Flowers Suppresses the IL-1β-induced Expression of IL-6 and Matrix-Metalloproteases by Activating Autophagy in Human Osteoarthritis Chondrocytes. *Biomed. Pharmacother.* 96, 198–207. doi:10.1016/j.biopha.2017.09.140

Aparicio-Soto, M., Sánchez-Fidalgo, S., González-Benjumea, A., Maya, I., Fernández-Bolaños, J. G., and Alarcón-de-la-Lastra, C. (2015). Naturally Occurring Hydroxytyrosol Derivatives: Hydroxytyrosyl Acetate and 3,4-dihydroxyphenylglycol Modulate Inflammatory Response in Murine Peritoneal Macrophages. Potential Utility as New Dietary Supplements. *J. Agric. Food Chem.* 63 (3), 836–846. doi:10.1021/jf503357s

Baell, J. B. (2016). Feeling Nature's PAINS: Natural Products, Natural Product Drugs, and Pan Assay Interference Compounds (PAINS). *J. Nat. Prod.* 79 (3), 616–628. doi:10.1021/acs.jnatprod.5b00947

Bai, Y., Liu, C., Fu, L., Gong, X., Dou, C., Cao, Z., et al. (2018). Mangiferin Enhances Endochondral Ossification-Based Bone Repair in Massive Bone Defect by Inducing Autophagy through Activating AMP-Activated Protein Kinase Signaling Pathway. *FASEB J.* 32 (8), 4573–4584. doi:10.1096/fj.201701411R

Barranco, C. (2015). Osteoarthritis: Activate Autophagy to Prevent Cartilage Degeneration? *Nat. Rev. Rheumatol.* 11 (3), 127. doi:10.1038/nrrheum.2015.12

Basu, A., Schell, J., and Scofield, R. H. (2018). Dietary Fruits and Arthritis. *Food Funct.* 9 (1), 70–77. doi:10.1039/c7fo01435j

Benderdour, M., Martel-Pelletier, J., Pelletier, J. P., Kapoor, M., Zunzunegui, M. V., and Fahmi, H. (2015). Cellular Aging, Senescence and Autophagy Processes in Osteoarthritis. *Curr. Aging Sci.* 8 (2), 147–157. doi:10.2174/1874609808666150727111530

Bert, J. M., and Bert, T. M. (2014). Nonoperative Treatment of Unicompartmental Arthritis: from Bracing to Injection. *Clin. Sports Med.* 33 (1), 1–10. doi:10.1016/j.csm.2013.08.002

Bisson, J., McAlpine, J. B., Friesen, J. B., Chen, S. N., Graham, J., and Pauli, G. F. (2016). Can Invalid Bioactives Undermine Natural Product-Based Drug Discovery? *J. Med. Chem.* 59 (5), 1671–1690. doi:10.1021/acs.jmedchem.5b01009

Bohlooli, S., Jastan, M., Nakhostin-Roohi, B., Mohammadi, S., and Baghaei, Z. (2012). A Pilot Double-Blinded, Randomized, Clinical Trial of Topical virgin Olive Oil versus Piroxicam Gel in Osteoarthritis of the Knee. *J. Clin. Rheumatol.* 18 (2), 99–101. doi:10.1097/RHU.0b013e31824a47b5

Bolduc, J. A., Collins, J. A., and Loeser, R. F. (2019). Reactive Oxygen Species, Aging and Articular Cartilage Homeostasis. *Free Radic. Biol. Med.* 132, 73–82. doi:10.1016/j.freeradbiomed.2018.08.038

Cai, M., Phan, P. T., Hong, J. G., Kim, D. H., Kim, J. M., Park, S. J., et al. (2012). The Neuroprotective Effect of Eupatilin against Ischemia/reperfusion-Induced Delayed Neuronal Damage in Mice. *Eur. J. Pharmacol.* 689 (1-3), 104–110. doi:10.1016/j.ejphar.2012.05.042

Cameron, M., and Chrubasik, S. (2014). Oral Herbal Therapies for Treating Osteoarthritis. *Cochrane Database Syst. Rev.* 5, CD002947. doi:10.1002/14651858.CD002947.pub2

Caramés, B., Olmer, M., Kiosses, W. B., and Lotz, M. K. (2015). The Relationship of Autophagy Defects to Cartilage Damage during Joint Aging in a Mouse Model. *Arthritis Rheumatol.* 67 (6), 1568–1576. doi:10.1002/art.39073

Caramés, B., Taniguchi, N., Otsuki, S., Blanco, F. J., and Lotz, M. (2010). Autophagy Is a Protective Mechanism in normal Cartilage, and its Aging-Related Loss Is Linked with Cell Death and Osteoarthritis. *Arthritis Rheum.* 62 (3), 791–801. doi:10.1002/art.27305

Cerdá, B., Tomás-Barberán, F. A., and Espín, J. C. (2005). Metabolism of Antioxidant and Chemopreventive Ellagitannins from Strawberries, Raspberries, Walnuts, and Oak-Aged Wine in Humans: Identification of Biomarkers and Individual Variability. *J. Agric. Food Chem.* 53 (2), 227–235.

Cetrullo, S., D'Adamo, S., Guidotti, S., Borzì, R. M., and Flamigni, F. (2016). Hydroxytyrosol Prevents Chondrocyte Death under Oxidative Stress by Inducing Autophagy through Sirtuin 1-dependent and -independent Mechanisms. *Biochim. Biophys. Acta* 1860 (6), 1181–1191. doi:10.1016/j.bbagen.2016.03.002

Charlier, E., Deroyer, C., Ciregia, F., Malaise, O., Neuville, S., Plener, Z., et al. (2019). Chondrocyte Dedifferentiation and Osteoarthritis (OA). *Biochem. Pharmacol.* 165, 49–65. doi:10.1016/j.bcp.2019.02.036

Chen, F. P., Chang, C. M., Hwang, S. J., Chen, Y. C., and Chen, F. J. (2014a). Chinese Herbal Prescriptions for Osteoarthritis in Taiwan: Analysis of National Health Insurance Dataset. *BMC Complement Altern. Med.* 14, 91. doi:10.1186/1472-6882-14-91

Chen, F. P., Li, B. S., and Tang, C. H. (2015). Nanocomplexation between Curcumin and Soy Protein Isolate: Influence on Curcumin Stability/bioaccessibility and *In Vitro* Protein Digestibility. *J. Agric. Food Chem.* 63 (13), 3559–3569. doi:10.1021/acs.jafc.5b00448

Chen, J. P., Xu, D. G., Yu, X. Y., Zhao, F. M., Xu, D. Q., Zhang, X., et al. (2014b). Discrepancy between the Effects of Morronside on Apoptosis in Human Embryonic Lung Fibroblast Cells and Lung Cancer A549 Cells. *Oncol. Lett.* 7 (4), 927–932. doi:10.3892/ol.2014.1850

Chen, P., Xia, C., Mei, S., Wang, J., Shan, Z., Lin, X., et al. (2016). Intra-articular Delivery of Sinomenium Encapsulated by Chitosan Microspheres and Photo-Crosslinked GelMA Hydrogel Ameliorates Osteoarthritis by Effectively Regulating Autophagy. *Biomaterials* 81, 1–13. doi:10.1016/j.biomaterials.2015.12.006

Chen, T., Zhou, R., Chen, Y., Fu, W., Wei, X., Ma, G., et al. (2021). Curcumin Ameliorates IL-1β-induced Apoptosis by Activating Autophagy and Inhibiting the NF-Kb Signaling Pathway in Rat Primary Articular Chondrocytes. *Cell Biol Int* 45 (5), 976–988. doi:10.1002/cbin.11541

Chen, W. P., Tang, J. L., Bao, J. P., Hu, P. F., Shi, Z. L., and Wu, L. D. (2011). Anti-arthritic Effects of Chlorogenic Acid in Interleukin-1β-Induced Rabbit Chondrocytes and a Rabbit Osteoarthritis Model. *Int. Immunopharmacol* 11 (1), 23–28. doi:10.1016/j.intimp.2010.09.021

Chen, X., Hu, X., Hu, J., Qiu, Z., Yuan, M., and Zheng, G. (2020a). Celastrol-Loaded Galactosylated Liposomes Effectively Inhibit AKT/c-Met-Triggered Rapid Hepatocarcinogenesis in Mice. *Mol. Pharm.* 17 (3), 738–747. doi:10.1021/acs.molpharmaceut.9b00428

Chen, X., Li, X., Zhai, X., Zhi, X., Cao, L., Qin, L., et al. (2018). Shikimic Acid Inhibits Osteoclastogenesis *In Vivo* and *In Vitro* by Blocking RANK/TRAF6 Association and Suppressing NF-Kb and MAPK Signaling Pathways. *Cell Physiol Biochem* 51 (6), 2858–2871. doi:10.1159/000496039

Chen, Z., Li, C., Qian, Y. H., Fu, Y., and Feng, Z. M. (2020b). Enhancement of Autophagy Flux by Isopsoralen Ameliorates Interleukin-1β-Stimulated Apoptosis in Rat Chondrocytes. *J. Asian Nat. Prod. Res.* 22 (2), 179–192. doi:10.1080/10286020.2018.1537265

Cheng, L., Zeng, G., Liu, Z., Zhang, B., Cui, X., Zhao, H., et al. (2015). Protein Kinase B and Extracellular Signal-Regulated Kinase Contribute to the Chondroprotective Effect of Morroniside on Osteoarthritis Chondrocytes. *J. Cell Mol Med* 19 (8), 1877–1886. doi:10.1111/jcmm.12559

Chin, K. Y., and Pang, K. L. (2017). Therapeutic Effects of Olive and its Derivatives on Osteoarthritis: From Bench to Bedside. *Nutrients* 9 (10). doi:10.3390/nu9101060

Chin, K. Y. (2016). The Spice for Joint Inflammation: Anti-inflammatory Role of Curcumin in Treating Osteoarthritis. *Drug Des. Devel Ther.* 10, 3029–3042. doi:10.2147/DDDT.S117432

Choi, E. J., Oh, H. M., Na, B. R., Ramesh, T. P., Lee, H. J., Choi, C. S., et al. (2008). Eupatilin Protects Gastric Epithelial Cells from Oxidative Damage and Down-Regulates Genes Responsible for the Cellular Oxidative Stress. *Pharm. Res.* 25 (6), 1355–1364. doi:10.1007/s11095-008-9531-5

Choi, E. M. (2011). Glabridin Protects Osteoblastic MC3T3-E1 Cells against Antimycin A Induced Cytotoxicity. *Chem. Biol. Interact* 193 (1), 71–78. doi:10.1016/j.cbi.2011.05.007

Chow, H. H., Cai, Y., Hakim, I. A., Crowell, J. A., Shahi, F., Brooks, C. A., et al. (2003). Pharmacokinetics and Safety of green tea Polyphenols after Multiple-Dose Administration of Epigallocatechin Gallate and Polyphenon E in Healthy Individuals. *Clin. Cancer Res.* 9 (9), 3312–3319.

Chowdhury, T. T., Salter, D. M., Bader, D. L., and Lee, D. A. (2008). Signal Transduction Pathways Involving P38 MAPK, JNK, NFkappaB and AP-1 Influences the Response of Chondrocytes Cultured in Agarose Constructs to IL-1beta and Dynamic Compression. *Inflamm. Res.* 57 (7), 306–313. doi:10.1007/s00011-007-7126-y

Clutterbuck, A. L., Allaway, D., Harris, P., and Mobasheri, A. (2013). Curcumin Reduces Prostaglandin E2, Matrix Metalloproteinase-3 and Proteoglycan Release in the Secretome of Interleukin 1β-Treated Articular Cartilage. *F1000Res* 2, 147. doi:10.12688/f1000research.2-147.v210.12688/f1000research.2-147.v1

Cornwell, D. G., and Ma, J. (2008). Nutritional Benefit of Olive Oil: The Biological Effects of Hydroxytyrosol and its Arylating Quinone Adducts. *J. Agric. Food Chem.* 56 (19), 8774–8786. doi:10.1021/jf8015877

Cutolo, M., Berenbaum, F., Hochberg, M., Punzi, L., and Reginster, J. Y. (2015). Commentary on Recent Therapeutic Guidelines for Osteoarthritis. *Semin. Arthritis Rheum.* 44 (6), 611–617. doi:10.1016/j.semarthrit.2014.12.003

Dai, B., Zhong, T., Chen, Z.-X., Chen, W., Zhang, N., Liu, X.-L., et al. (2021a10122). Myricetin Slows Liquid-Liquid Phase Separation of Tau and Activates ATG5-dependent Autophagy to Suppress Tau Toxicity. *J. Biol. Chem.* 297, 101222. doi:10.1016/j.jbc.2021.101222

Dai, J., Zhang, Y., Chen, D., Chen, D., Li, X., Wang, J., et al. (2021b). Glabridin Inhibits Osteoarthritis Development by Protecting Chondrocytes against Oxidative Stress, Apoptosis and Promoting mTOR Mediated Autophagy. *Life Sci.* 268, 118992. doi:10.1016/j.lfs.2020.118992

Doria, A., Gatto, M., and Punzi, L. (2013). Autophagy in Human Health and Disease. *N. Engl. J. Med.* 368 (19), 1845. doi:10.1056/NEJMc1303158

Duan, R., Xie, H., and Liu, Z. Z. (2020). The Role of Autophagy in Osteoarthritis. *Front Cell Dev Biol* 8, 608388. doi:10.3389/fcell.2020.608388

El-Baba, C., Baassiri, A., Kiriako, G., Dia, B., Fadlallah, S., Moodad, S., et al. (2021). Terpenoids' Anti-cancer Effects: Focus on Autophagy. *Apoptosis* 26 (9-10), 491–511. doi:10.1007/s10495-021-01684-y

Fang, J., Cao, Z., Song, X., Zhang, X., Mai, B., Wen, T., et al. (2020). Rhoifolin Alleviates Inflammation of Acute Inflammation Animal Models and LPS-Induced RAW264.7 Cells via IKKβ/NF-Kb Signaling Pathway. *Inflammation* 43 (6), 2191–2201. doi:10.1007/s10753-020-01286-x

Farah, A., Monteiro, M., Donangelo, C. M., and Lafay, S. (2008). Chlorogenic Acids from green Coffee Extract Are Highly Bioavailable in Humans. *J. Nutr.* 138 (12), 2309–2315. doi:10.3945/jn.108.095554

Feng, K., Chen, H., and Xu, C. (2020). Chondro-protective Effects of Celastrol on Osteoarthritis through Autophagy Activation and NF-Kb Signaling Pathway Inhibition. *Inflamm. Res.* 69 (4), 385–400. doi:10.1007/s00011-020-01327-z

Foroutanfar, A., Mehri, S., Kamyar, M., Tandisehpanah, Z., and Hosseinzadeh, H. (2020). Protective Effect of Punicalagin, the Main Polyphenol Compound of Pomegranate, against Acrylamide-Induced Neurotoxicity and Hepatotoxicity in Rats. *Phytother Res.* 34 (12), 3262–3272. doi:10.1002/ptr.6774

Francioso, A., Mastromarino, P., Masci, A., d'Erme, M., and Mosca, L. (2014). Chemistry, Stability and Bioavailability of Resveratrol. *Med. Chem.* 10 (3), 237–245. doi:10.2174/15734064113096660053

Fuhrman, B., Volkova, N., Rosenblat, M., and Aviram, M. (2000). Lycopene Synergistically Inhibits LDL Oxidation in Combination with Vitamin E, Glabridin, Rosmarinic Acid, Carnosic Acid, or Garlic. *Antioxid. Redox Signal* 2 (3), 491–506. doi:10.1089/15230860050192279

Goel, A., Kunnumakkara, A. B., and Aggarwal, B. B. (2008). Curcumin as "Curecumin": from Kitchen to Clinic. *Biochem. Pharmacol.* 75 (4), 787–809. doi:10.1016/j.bcp.2007.08.016

Goldring, M. B., and Otero, M. (2011). Inflammation in Osteoarthritis. *Curr. Opin. Rheumatol.* 23 (5), 471–478. doi:10.1097/BOR.0b013e328349c2b1

Granados-Principal, S., Quiles, J. L., Ramirez-Tortosa, C. L., Sanchez-Rovira, P., and Ramirez-Tortosa, M. C. (2010). Hydroxytyrosol: from Laboratory Investigations to Future Clinical Trials. *Nutr. Rev.* 68 (4), 191–206. doi:10.1111/j.1753-4887.2010.00278.x

Gu, Y., Wang, G., Pan, G., Fawcett, J. P., A, J., and Sun, J. (2004). Transport and Bioavailability Studies of Astragaloside IV, an Active Ingredient in Radix Astragali. *Basic Clin. Pharmacol. Toxicol.* 95 (6), 295–298. doi:10.1111/j.1742-7843.2004.t01-1-pto950508.x

Guo, H., He, Y., Bu, C., and Peng, Z. (2019). Antitumor and Apoptotic Effects of 5-methoxypsoralen in U87MG Human Glioma Cells and its Effect on Cell Cycle, Autophagy and PI3K/Akt Signaling Pathway. *Arch. Med. Sci.* 15 (6), 1530–1538. doi:10.5114/aoms.2019.81729

Han Jie, L., Jantan, I., Yusoff, S. D., Jalil, J., and Husain, K. (2020). Sinensetin: An Insight on its Pharmacological Activities, Mechanisms of Action and Toxicity. *Front Pharmacol.* 11, 553404. doi:10.3389/fphar.2020.553404

Hara, T., Nakamura, K., Matsui, M., Yamamoto, A., Nakahara, Y., Suzuki-Migishima, R., et al. (2006). Suppression of Basal Autophagy in Neural Cells Causes Neurodegenerative Disease in Mice. *Nature* 441 (7095), 885–889. doi:10.1038/nature04724

Haseeb, A., Chen, D., and Haqqi, T. M. (2013). Delphinidin Inhibits IL-1β-induced Activation of NF-Kb by Modulating the Phosphorylation of IRAK-1(Ser376) in Human Articular Chondrocytes. *Rheumatology (Oxford)* 52 (6), 998–1008. doi:10.1093/rheumatology/kes363

Hayami, T., Funaki, H., Yaoeda, K., Mitui, K., Yamagiwa, H., Tokunaga, K., et al. (2003). Expression of the Cartilage Derived Anti-angiogenic Factor Chondromodulin-I Decreases in the Early Stage of Experimental Osteoarthritis. *J. Rheumatol.* 30 (10), 2207–2217.

Hoelzl, C., Knasmüller, S., Wagner, K. H., Elbling, L., Huber, W., Kager, N., et al. (2010). Instant Coffee with High Chlorogenic Acid Levels Protects Humans against Oxidative Damage of Macromolecules. *Mol. Nutr. Food Res.* 54 (12), 1722–1733. doi:10.1002/mnfr.201000048

Hong, P., Liu, Q. W., Xie, Y., Zhang, Q. H., Liao, L., He, Q. Y., et al. (2020). Echinatin Suppresses Esophageal Cancer Tumor Growth and Invasion Through Inducing AKT/mTOR-Dependent Autophagy and Apoptosis. *Cell Death Dis.* 11 (7), 524. doi:10.1038/s41419-020-2730-7

Hou, S., Wang, F., Li, Y., Li, Y., Wang, M., Sun, D., et al. (2012). Pharmacokinetic Study of Mangiferin in Human Plasma after Oral Administration. *Food Chem.* 132 (1), 289–294. doi:10.1016/j.foodchem.2011.10.079

Hu, J., Zhou, J., Wu, J., Chen, Q., Du, W., Fu, F., et al. (2020). Loganin Ameliorates Cartilage Degeneration and Osteoarthritis Development in an Osteoarthritis Mouse Model through Inhibition of NF-Kb Activity and Pyroptosis in Chondrocytes. *J. Ethnopharmacol* 247, 112261. doi:10.1016/j.jep.2019.112261

Hu, T., He, X. W., Jiang, J. G., and Xu, X. L. (2014). Hydroxytyrosol and its Potential Therapeutic Effects. *J. Agric. Food Chem.* 62 (7), 1449–1455. doi:10.1021/jf405820v

Hua, W., Zhang, Y., Wu, X., Kang, L., Tu, J., Zhao, K., et al. (2018). Icariin Attenuates Interleukin-1β-Induced Inflammatory Response in Human Nucleus Pulposus Cells. *Curr. Pharm. Des.* 23 (39), 6071–6078. doi:10.2174/1381612823666170615112158

Huang, H. T., Cheng, T. L., Ho, C. J., Huang, H. H., Lu, C. C., Chuang, S. C., et al. (2020). Intra-Articular Injection of (-)-Epigallocatechin 3-Gallate to Attenuate Articular Cartilage Degeneration by Enhancing Autophagy in a Post-Traumatic Osteoarthritis Rat Model. *Antioxidants (Basel)* 10 (1). doi:10.3390/antiox10010008

Hunter, D. J., and Bierma-Zeinstra, S. (2019). Osteoarthritis. *Lancet* 393 (10182), 1745–1759. doi:10.1016/S0140-6736(19)30417-9

Hussain, S. A., Marouf, B. H., Ali, Z. S., and Ahmmad, R. S. (2018). Efficacy and Safety of Co-administration of Resveratrol with Meloxicam in Patients with Knee Osteoarthritis: a Pilot Interventional Study. *Clin. Interv. Aging* 13, 1621–1630. doi:10.2147/cia.S172758

Isbrucker, R. A., Edwards, J. A., Wolz, E., Davidovich, A., and Bausch, J. (2006). Safety Studies on Epigallocatechin Gallate (EGCG) Preparations. Part 2: Dermal, Acute and Short-Term Toxicity Studies. *Food Chem. Toxicol.* 44 (5), 636–650. doi:10.1016/j.fct.2005.11.003

Jang, H. J., Yang, K. E., Hwang, I. H., Huh, Y. H., Kim, D. J., Yoo, H. S., et al. (2019). Cordycepin Inhibits Human Ovarian Cancer by Inducing Autophagy and Apoptosis through Dickkopf-Related Protein 1/β-Catenin Signaling. *Am. J. Transl Res.* 11 (11), 6890–6906.

Jeong, J. H., Moon, S. J., Jhun, J. Y., Yang, E. J., Cho, M. L., and Min, J. K. (2015). Eupatilin Exerts Antinociceptive and Chondroprotective Properties in a Rat Model of Osteoarthritis by Downregulating Oxidative Damage and Catabolic

Activity in Chondrocytes. *PLoS One* 10 (6), e0130882. doi:10.1371/journal.pone.0130882

Jiang, J., Meng, Y., Hu, S., Botchway, B. O. A., Zhang, Y., and Liu, X. (2020). Saikosaponin D: A Potential Therapeutic Drug for Osteoarthritis. *J. Tissue Eng. Regen. Med.* 14 (8), 1175–1184. doi:10.1002/term.3090

Jiang, L. B., Meng, D. H., Lee, S. M., Liu, S. H., Xu, Q. T., Wang, Y., et al. (2016). Dihydroartemisinin Inhibits Catabolism in Rat Chondrocytes by Activating Autophagy via Inhibition of the NF-Kb Pathway. *Sci. Rep.* 6, 38979. doi:10.1038/srep38979

Jones, I. A., Togashi, R., Wilson, M. L., Heckmann, N., and Vangsness, C. T. (2019). Intra-articular Treatment Options for Knee Osteoarthritis. *Nat. Rev. Rheumatol.* 15 (2), 77–90. doi:10.1038/s41584-018-0123-4

Ju, X. D., Deng, M., Ao, Y. F., Yu, C. L., Wang, J. Q., Yu, J. K., et al. (2010). Protective Effect of Sinomenine on Cartilage Degradation and Chondrocytes Apoptosis. *Yakugaku Zasshi* 130 (8), 1053–1060. doi:10.1248/yakushi.130.1053

Kannaiyan, R., Shanmugam, M. K., and Sethi, G. (2011). Molecular Targets of Celastrol Derived from Thunder of God Vine: Potential Role in the Treatment of Inflammatory Disorders and Cancer. *Cancer Lett.* 303 (1), 9–20. doi:10.1016/j.canlet.2010.10.025

Kawata, Y., Kizu, H., and Tomimori, T. (1998). Studies on the Constituents of Clematis Species. VII. Triterpenoid Saponins from the Roots of Clematis Terniflora DC. Var. Robusta Tamura. *Chem. Pharm. Bull (Tokyo)* 46 (12), 1891–1900. doi:10.1248/cpb.46.1891

Khan, N. M., Ahmad, I., and Haqqi, T. M. (2018). Nrf2/ARE Pathway Attenuates Oxidative and Apoptotic Response in Human Osteoarthritis Chondrocytes by Activating ERK1/2/ELK1-P70S6K-P90RSK Signaling axis. *Free Radic. Biol. Med.* 116, 159–171. doi:10.1016/j.freeradbiomed.2018.01.013

Kim, H. A., and Blanco, F. J. (2007). Cell Death and Apoptosis in Osteoarthritic Cartilage. *Curr. Drug Targets* 8 (2), 333–345. doi:10.2174/138945007779940025

Kim, J., Kim, Y., Yi, H., Jung, H., Rim, Y. A., Park, N., et al. (2015). Eupatilin Ameliorates Collagen Induced Arthritis. *J. Korean Med. Sci.* 30 (3), 233–239. doi:10.3346/jkms.2015.30.3.233

Kim, J. H., Jeon, J., Shin, M., Won, Y., Lee, M., Kwak, J. S., et al. (2014). Regulation of the Catabolic cascade in Osteoarthritis by the Zinc-ZIP8-MTF1 axis. *Cell* 156 (4), 730–743. doi:10.1016/j.cell.2014.01.007

Kim, S. M., Ha, S. E., Lee, H. J., Rampogu, S., Vetrivel, P., Kim, H. H., et al. (2020). Sinensetin Induces Autophagic Cell Death through P53-Related AMPK/mTOR Signaling in Hepatocellular Carcinoma HepG2 Cells. *Nutrients* 12 (8). doi:10.3390/nu12082462

Kim, Y. K., Kim, Y. S., and Ryu, S. Y. (2007). Antiproliferative Effect of Furanocoumarins from the Root of Angelica Dahurica on Cultured Human Tumor Cell Lines. *Phytother Res.* 21 (3), 288–290. doi:10.1002/ptr.2043

Kloppenburg, M., and Berenbaum, F. (2020). Osteoarthritis Year in Review 2019: Epidemiology and Therapy. *Osteoarthritis Cartilage* 28 (3), 242–248. doi:10.1016/j.joca.2020.01.002

Koeberle, A., Rossi, A., Bauer, J., Dehm, F., Verotta, L., Northoff, H., et al. (2011). Hyperforin, an Anti-inflammatory Constituent from St. John's Wort, Inhibits Microsomal Prostaglandin E(2) Synthase-1 and Suppresses Prostaglandin E(2) Formation *In Vivo*. *Front Pharmacol.* 2, 7. doi:10.3389/fphar.2011.00007

Kolodziej, H., Radtke, O. A., and Kiderlen, A. F. (2008). Stimulus (Polyphenol, IFN-Gamma, LPS)-dependent Nitric Oxide Production and Antileishmanial Effects in RAW 264.7 Macrophages. *Phytochemistry* 69 (18), 3103–3110. doi:10.1016/j.phytochem.2007.11.012

Kong, J., Wang, J., Gong, X., Zheng, X., and Chen, T. (2020). Punicalagin Inhibits Tert-Butyl Hydroperoxide-Induced Apoptosis and Extracellular Matrix Degradation in Chondrocytes by Activating Autophagy and Ameliorates Murine Osteoarthritis. *Drug Des. Devel Ther.* 14, 5521–5533. doi:10.2147/DDDT.S282932

Kong, J. M., Chia, L. S., Goh, N. K., Chia, T. F., and Brouillard, R. (2003). Analysis and Biological Activities of Anthocyanins. *Phytochemistry* 64 (5), 923–933. doi:10.1016/s0031-9422(03)00438-2

Kraus, V. B., Blanco, F. J., Englund, M., Karsdal, M. A., and Lohmander, L. S. (2015). Call for Standardized Definitions of Osteoarthritis and Risk Stratification for Clinical Trials and Clinical Use. *Osteoarthritis Cartilage* 23 (8), 1233–1241. doi:10.1016/j.joca.2015.03.036

Lee, D. Y., Park, Y. J., Song, M. G., Kim, D. R., Zada, S., and Kim, D. H. (2020). Cytoprotective Effects of Delphinidin for Human Chondrocytes against Oxidative Stress through Activation of Autophagy. *Antioxidants (Basel)* 9 (1). doi:10.3390/antiox9010083

Lee, W., Ku, S. K., and Bae, J. S. (2015). Anti-inflammatory Effects of Baicalin, Baicalein, and Wogonin *In Vitro* and *In Vivo*. *Inflammation* 38 (1), 110–125. doi:10.1007/s10753-014-0013-0

Legeay, S., Trân, K., Abatuci, Y., Justiniano, H., Lugnier, C., Duval, O., et al. (2019). Design, Synthesis, Pharmacological Evaluation and Vascular Effects of Delphinidin Analogues. *Curr. Pharm. Des.* 24 (46), 5580–5589. doi:10.2174/1381612825666190206144913

Levine, B., and Kroemer, G. (2008). Autophagy in the Pathogenesis of Disease. *Cell* 132 (1), 27–42. doi:10.1016/j.cell.2007.12.018

Levine, B., Mizushima, N., and Virgin, H. W. (2011). Autophagy in Immunity and Inflammation. *Nature* 469 (7330), 323–335. doi:10.1038/nature09782

Li, C., Li, Q., Mei, Q., and Lu, T. (2015). Pharmacological Effects and Pharmacokinetic Properties of Icariin, the Major Bioactive Component in Herba Epimedii. *Life Sci.* 126, 57–68. doi:10.1016/j.lfs.2015.01.006

Li, H., Zhong, C., Wang, Q., Chen, W., and Yuan, Y. (2019a). Curcumin Is an APE1 Redox Inhibitor and Exhibits an Antiviral Activity against KSHV Replication and Pathogenesis. *Antivir. Res* 167, 98–103. doi:10.1016/j.antiviral.2019.04.011

Li, L., Eun, J. S., Nepal, M., Ryu, J. H., Cho, H. K., Choi, B. Y., et al. (2012). Isopsoralen Induces Differentiation of Prechondrogenic ATDC5 Cells via Activation of MAP Kinases and BMP-2 Signaling Pathways. *Biomol. Ther. (Seoul)* 20 (3), 299–305. doi:10.4062/biomolther.2012.20.3.299

Li, X., Feng, K., Li, J., Yu, D., Fan, Q., Tang, T., et al. (2017a). Curcumin Inhibits Apoptosis of Chondrocytes through Activation ERK1/2 Signaling Pathways Induced Autophagy. *Nutrients* 9 (4). doi:10.3390/nu9040414

Li, Y., Wu, Y., Jiang, K., Han, W., Zhang, J., Xie, L., et al. (2019b2019). Mangiferin Prevents TBHP-Induced Apoptosis and ECM Degradation in Mouse Osteoarthritic Chondrocytes via Restoring Autophagy and Ameliorates Murine Osteoarthritis. *Oxid Med. Cell Longev* 2019, 8783197. doi:10.1155/2019/8783197

Li, Y. P., Wu, B., Liang, J., and Li, F. (2019c). Isopsoralen Ameliorates H2O2-Induced Damage in Osteoblasts via Activating the Wnt/β-Catenin Pathway. *Exp. Ther. Med.* 18 (3), 1899–1906. doi:10.3892/etm.2019.7741

Li, Y. S., Xiao, W. F., and Luo, W. (2017b). Cellular Aging towards Osteoarthritis. *Mech. Ageing Dev.* 162, 80–84. doi:10.1016/j.mad.2016.12.012

Li, Z., Cheng, J., and Liu, J. (2020). Baicalin Protects Human OA Chondrocytes against IL-1β-Induced Apoptosis and ECM Degradation by Activating Autophagy via MiR-766-3p/AIFM1 Axis. *Drug Des. Devel Ther.* 14, 2645–2655. doi:10.2147/dddt.S255823

Li, Z., Wang, Y., Wu, L., Dong, Y., Zhang, J., Chen, F., et al. (2019d). Apurinic Endonuclease 1 Promotes the Cisplatin Resistance of Lung Cancer Cells by Inducing Parkin-mediated M-itophagy. *Oncol. Rep.* 42 (6), 2245–2254. doi:10.3892/or.2019.7345

Liao, S., Song, F., Feng, W., Ding, X., Yao, J., Song, H., et al. (2019). Rhoifolin Ameliorates Titanium Particle-Stimulated Osteolysis and Attenuates Osteoclastogenesis via RANKL-Induced NF-Kb and MAPK Pathways. *J. Cell Physiol* 234 (10), 17600–17611. doi:10.1002/jcp.28384

Liu, F., Li, L., Lu, W., Ding, Z., Huang, W., Li, Y. T., et al. (2020). Scutellarin Ameliorates Cartilage Degeneration in Osteoarthritis by Inhibiting the Wnt/β-Catenin and MAPK Signaling Pathways. *Int. Immunopharmacol* 78, 105954. doi:10.1016/j.intimp.2019.105954

Liu, F., Yang, H., Li, D., Wu, X., and Han, Q. (2021). Punicalagin Attenuates Osteoarthritis Progression via Regulating Foxo1/Prg4/HIF3α axis. *Bone* 152, 116070. doi:10.1016/j.bone.2021.116070

Liu, J., Meng, Q., Jing, H., and Zhou, S. (2017). Astragaloside IV Protects against Apoptosis in Human Degenerative Chondrocytes through Autophagy Activation. *Mol. Med. Rep.* 16 (3), 3269–3275. doi:10.3892/mmr.2017.6980

Loeser, R. F., Collins, J. A., and Diekman, B. O. (2016). Ageing and the Pathogenesis of Osteoarthritis. *Nat. Rev. Rheumatol.* 12 (7), 412–420. doi:10.1038/nrrheum.2016.65

Lou, Y., Wu, J., Liang, J., Yang, C., Wang, K., Wang, J., et al. (2019). Eupatilin Protects Chondrocytes from Apoptosis via Activating Sestrin2-dependent Autophagy. *Int. Immunopharmacol* 75, 105748. doi:10.1016/j.intimp.2019.105748

Luk, H. Y., Appell, C., Chyu, M. C., Chen, C. H., Wang, C. Y., Yang, R. S., et al. (2020). Impacts of Green Tea on Joint and Skeletal Muscle Health: Prospects of

Translational Nutrition. *Antioxidants (Basel)* 9 (11). doi:10.3390/antiox9111050

Luo, P., Gao, F., Niu, D., Sun, X., Song, Q., Guo, C., et al. (2019). The Role of Autophagy in Chondrocyte Metabolism and Osteoarthritis: A Comprehensive Research Review. *Biomed. Res. Int.* 2019, 5171602. doi:10.1155/2019/5171602

Luo, Y., Lu, S., Gao, Y., Yang, K., Wu, D., Xu, X., et al. (2020). Araloside C Attenuates Atherosclerosis by Modulating Macrophage Polarization via Sirt1-Mediated Autophagy. *Aging (Albany NY)* 12 (2), 1704–1724. doi:10.18632/aging.102708

Maiti, K., Mukherjee, K., Gantait, A., Saha, B. P., and Mukherjee, P. K. (2007). Curcumin-phospholipid Complex: Preparation, Therapeutic Evaluation and Pharmacokinetic Study in Rats. *Int. J. Pharm.* 330 (1-2), 155–163. doi:10.1016/j.ijpharm.2006.09.025

Mao, Q. Q., Xu, X. Y., Shang, A., Gan, R. Y., Wu, D. T., Atanasov, A. G., et al. (2020). Phytochemicals for the Prevention and Treatment of Gastric Cancer: Effects and Mechanisms. *Int. J. Mol. Sci.* 21 (2). doi:10.3390/ijms21020570

Martel, J., Ojcius, D. M., Ko, Y. F., Ke, P. Y., Wu, C. Y., Peng, H. H., et al. (2019). Hormetic Effects of Phytochemicals on Health and Longevity. *Trends Endocrinol. Metab.* 30 (6), 335–346. doi:10.1016/j.tem.2019.04.001

Martel-Pelletier, J., Barr, A. J., Cicuttini, F. M., Conaghan, P. G., Cooper, C., Goldring, M. B., et al. (2016). Osteoarthritis. *Nat. Rev. Dis. Primers* 2, 16072. doi:10.1038/nrdp.2016.72

Mi, B., Wang, J., Liu, Y., Liu, J., Hu, L., Panayi, A. C., et al. (2018). Icariin Activates Autophagy via Down-Regulation of the NF-Kb Signaling-Mediated Apoptosis in Chondrocytes. *Front Pharmacol.* 9, 605. doi:10.3389/fphar.2018.00605

Mizushima, N., Levine, B., Cuervo, A. M., and Klionsky, D. J. (2008). Autophagy Fights Disease through Cellular Self-Digestion. *Nature* 451 (7182), 1069–1075. doi:10.1038/nature06639

Mizushima, N., and Yoshimori, T. (2007). How to Interpret LC3 Immunoblotting. *Autophagy* 3 (6), 542–545. doi:10.4161/auto.4600

Mobasheri, A., Rayman, M. P., Gualillo, O., Sellam, J., van der Kraan, P., and Fearon, U. (2017). The Role of Metabolism in the Pathogenesis of Osteoarthritis. *Nat. Rev. Rheumatol.* 13 (5), 302–311. doi:10.1038/nrrheum.2017.50

Moon, T. C., Jin, M., Son, J. K., and Chang, H. W. (2008). The Effects of Isoimperatorin Isolated from Angelicae Dahuricae on Cyclooxygenase-2 and 5-lipoxygenase in Mouse Bone Marrow-Derived Mast Cells. *Arch. Pharm. Res.* 31 (2), 210–215. doi:10.1007/s12272-001-1143-0

Musumeci, G., Trovato, F. M., Pichler, K., Weinberg, A. M., Loreto, C., and Castrogiovanni, P. (2013). Extra-virgin Olive Oil Diet and Mild Physical Activity Prevent Cartilage Degeneration in an Osteoarthritis Model: an *In Vivo* and *In Vitro* Study on Lubricin Expression. *J. Nutr. Biochem.* 24 (12), 2064–2075. doi:10.1016/j.jnutbio.2013.07.007

Nakamura, S., and Yoshimori, T. (2017). New Insights into Autophagosome-Lysosome Fusion. *J. Cell Sci* 130 (7), 1209–1216. doi:10.1242/jcs.196352

Nelson, A. E. (2018). Osteoarthritis Year in Review 2017: Clinical. *Osteoarthritis Cartilage* 26 (3), 319–325. doi:10.1016/j.joca.2017.11.014

Netea-Maier, R. T., Plantinga, T. S., van de Veerdonk, F. L., Smit, J. W., and Netea, M. G. (2016). Modulation of Inflammation by Autophagy: Consequences for Human Disease. *Autophagy* 12 (2), 245–260. doi:10.1080/15548627.2015.1071759

Nguyen, C., Boutron, I., Baron, G., Coudeyre, E., Berenbaum, F., Poiraudeau, S., et al. (2017). Evolution of Pain at 3 Months by Oral Resveratrol in Knee Osteoarthritis (ARTHROL): Protocol for a Multicentre Randomised Double-Blind Placebo-Controlled Trial. *BMJ open* 7 (9), e017652. doi:10.1136/bmjopen-2017-017652

Nyamba, I., Lechanteur, A., Semdé, R., and Evrard, B. (2021). Physical Formulation Approaches for Improving Aqueous Solubility and Bioavailability of Ellagic Acid: A Review. *Eur. J. Pharm. Biopharm.* 159, 198–210. doi:10.1016/j.ejpb.2020.11.004

Oliviero, F., Sfriso, P., Scanu, A., Fiocco, U., Spinella, P., and Punzi, L. (2013). Epigallocatechin-3-gallate Reduces Inflammation Induced by Calcium Pyrophosphate Crystals *In Vitro*. *Front Pharmacol.* 4, 51. doi:10.3389/fphar.2013.00051

Ouyang, J., Jiang, H., Fang, H., Cui, W., and Cai, D. (2017). Isoimperatorin Ameliorates Osteoarthritis by Downregulating the Mammalian Target of Rapamycin C1 Signaling Pathway. *Mol. Med. Rep.* 16 (6), 9636–9644. doi:10.3892/mmr.2017.7777

Padmavathi, G., Roy, N. K., Bordoloi, D., Arfuso, F., Mishra, S., Sethi, G., et al. (2017). Butein in Health and Disease: A Comprehensive Review. *Phytomedicine* 25, 118–127. doi:10.1016/j.phymed.2016.12.002

Pan, L., Zhang, Y., Chen, N., and Yang, L. (2017a). Icariin Regulates Cellular Functions and Gene Expression of Osteoarthritis Patient-Derived Human Fibroblast-like Synoviocytes. *Int. J. Mol. Sci.* 18 (12). doi:10.3390/ijms18122656

Pan, Y., Chen, D., Lu, Q., Liu, L., Li, X., and Li, Z. (2017b). Baicalin Prevents the Apoptosis of Endplate Chondrocytes by Inhibiting the Oxidative Stress Induced by H2O2. *Mol. Med. Rep.* 16 (3), 2985–2991. doi:10.3892/mmr.2017.6904

Panahi, Y., Rahimnia, A. R., Sharafi, M., Alishiri, G., Saburi, A., and Sahebkar, A. (2014). Curcuminoid Treatment for Knee Osteoarthritis: a Randomized Double-Blind Placebo-Controlled Trial. *Phytother Res.* 28 (11), 1625–1631. doi:10.1002/ptr.5174

Park, C. H., Yamabe, N., Noh, J. S., Kang, K. S., Tanaka, T., and Yokozawa, T. (2009). The Beneficial Effects of Morroniside on the Inflammatory Response and Lipid Metabolism in the Liver of Db/db Mice. *Biol. Pharm. Bull* 32 (10), 1734–1740. doi:10.1248/bpb.32.1734

Peng, S., Hu, C., Liu, X., Lei, L., He, G., Xiong, C., et al. (2020). Rhoifolin Regulates Oxidative Stress and Proinflammatory Cytokine Levels in Freund's Adjuvant-Induced Rheumatoid Arthritis via Inhibition of NF-Kb. *Braz. J. Med. Biol. Res.* 53 (6), e9489. doi:10.1590/1414-431x20209489

Pérez-Arancibia, R., Ordoñez, J. L., Rivas, A., Pihán, P., Sagredo, A., Ahumada, U., et al. (2021). A Phenolic-Rich Extract from Ugni Molinae Berries Reduces Abnormal Protein Aggregation in a Cellular Model of Huntington's Disease. *PloS one* 16 (7), e0254834. doi:10.1371/journal.pone.0254834

Philp, A. M., Davis, E. T., and Jones, S. W. (2017). Developing Anti-inflammatory Therapeutics for Patients with Osteoarthritis. *Rheumatology (Oxford)* 56 (6), 869–881. doi:10.1093/rheumatology/kew278

Portal-Núñez, S., Esbrit, P., Alcaraz, M. J., and Largo, R. (2016). Oxidative Stress, Autophagy, Epigenetic Changes and Regulation by miRNAs as Potential Therapeutic Targets in Osteoarthritis. *Biochem. Pharmacol.* 108, 1–10. doi:10.1016/j.bcp.2015.12.012

Prasad, S., Tyagi, A. K., and Aggarwal, B. B. (2014). Recent Developments in Delivery, Bioavailability, Absorption and Metabolism of Curcumin: the golden Pigment from golden Spice. *Cancer Res. Treat* 46 (1), 2–18. doi:10.4143/crt.2014.46.1.2

Qin, N., Wei, L., Li, W., Yang, W., Cai, L., Qian, Z., et al. (2017). Local Intra-articular Injection of Resveratrol Delays Cartilage Degeneration in C57BL/6 Mice by Inducing Autophagy via AMPK/mTOR Pathway. *J. Pharmacol. Sci.* 134 (3), 166–174. doi:10.1016/j.jphs.2017.06.002

Ranjan, A., Ramachandran, S., Gupta, N., Kaushik, I., Wright, S., Srivastava, S., et al. (2019). Role of Phytochemicals in Cancer Prevention. *Int. J. Mol. Sci.* 20 (20). doi:10.3390/ijms20204981

Rasheed, Z., Anbazhagan, A. N., Akhtar, N., Ramamurthy, S., Voss, F. R., and Haqqi, T. M. (2009). Green tea Polyphenol Epigallocatechin-3-Gallate Inhibits Advanced Glycation End Product-Induced Expression of Tumor Necrosis Factor-Alpha and Matrix Metalloproteinase-13 in Human Chondrocytes. *Arthritis Res. Ther.* 11 (3), R71. doi:10.1186/ar2700

Ren, J., and Zhang, Y. (2018). Targeting Autophagy in Aging and Aging-Related Cardiovascular Diseases. *Trends Pharmacol. Sci.* 39 (12), 1064–1076. doi:10.1016/j.tips.2018.10.005

Rim, Y. A., Nam, Y., and Ju, J. H. (2020). The Role of Chondrocyte Hypertrophy and Senescence in Osteoarthritis Initiation and Progression. *Int. J. Mol. Sci.* 21 (7). doi:10.3390/ijms21072358

Rivera, D., Allkin, R., Obón, C., Alcaraz, F., Verpoorte, R., and Heinrich, M. (2014). What Is in a Name? the Need for Accurate Scientific Nomenclature for Plants. *J. Ethnopharmacol* 152 (3), 393–402. doi:10.1016/j.jep.2013.12.022

Robinson, K., Mock, C., and Liang, D. (2015). Pre-formulation Studies of Resveratrol. *Drug Dev. Ind. Pharm.* 41 (9), 1464–1469. doi:10.3109/03639045.2014.958753

Robinson, W. H., Lepus, C. M., Wang, Q., Raghu, H., Mao, R., Lindstrom, T. M., et al. (2016). Low-grade Inflammation as a Key Mediator of the Pathogenesis of Osteoarthritis. *Nat. Rev. Rheumatol.* 12 (10), 580–592. doi:10.1038/nrrheum.2016.136

Roca-Agujetas, V., de Dios, C., Lestón, L., Marí, M., Morales, A., and Colell, A. (2019). Recent Insights into the Mitochondrial Role in Autophagy and its

Regulation by Oxidative Stress. *Oxid Med. Cell Longev* 2019, 3809308. doi:10.1155/2019/3809308

Rodríguez-Hernández, K. D., Martínez, I., Reyes-Chilpa, R., and Espinoza, B. (2020). Mammea Type Coumarins Isolated from Calophyllum Brasiliense Induced Apoptotic Cell Death of Trypanosoma Cruzi through Mitochondrial Dysfunction, ROS Production and Cell Cycle Alterations. *Bioorg. Chem.* 100, 103894. doi:10.1016/j.bioorg.2020.103894

Rosillo, M. Á., Alcaraz, M. J., Sánchez-Hidalgo, M., Fernández-Bolaños, J. G., Alarcón-de-la-Lastra, C., and Ferrándiz, M. L. (2014). Anti-inflammatory and Joint Protective Effects of Extra-virgin Olive-Oil Polyphenol Extract in Experimental Arthritis. *J. Nutr. Biochem.* 25 (12), 1275–1281. doi:10.1016/j.jnutbio.2014.07.006

Sachdeva, A. K., and Chopra, K. (2015). Lycopene Abrogates Aβ(1-42)-Mediated Neuroinflammatory cascade in an Experimental Model of Alzheimer's Disease. *J. Nutr. Biochem.* 26 (7), 736–744. doi:10.1016/j.jnutbio.2015.01.012

Salucci, S., Burattini, S., Giordano, F. M., Lucarini, S., Diamantini, G., and Falcieri, E. (2017). Further Highlighting on the Prevention of Oxidative Damage by Polyphenol-Rich Wine Extracts. *J. Med. Food* 20 (4), 410–419. doi:10.1089/jmf.2016.0153

Sellés, A. J. N., Villa, D. G., and Rastrelli, L. (2015). Mango Polyphenols and its Protective Effects on Diseases Associated to Oxidative Stress. *Curr. Pharm. Biotechnol.* 16 (3), 272–280.

Silva, S., Sepodes, B., Rocha, J., Direito, R., Fernandes, A., Brites, D., et al. (2015). Protective Effects of Hydroxytyrosol-Supplemented Refined Olive Oil in Animal Models of Acute Inflammation and Rheumatoid Arthritis. *J. Nutr. Biochem.* 26 (4), 360–368. doi:10.1016/j.jnutbio.2014.11.011

Simmler, C., Pauli, G. F., and Chen, S. N. (2013). Phytochemistry and Biological Properties of Glabridin. *Fitoterapia* 90, 160–184. doi:10.1016/j.fitote.2013.07.003

Sofat, N., Ejindu, V., and Kiely, P. (2011). What Makes Osteoarthritis Painful? the Evidence for Local and central Pain Processing. *Rheumatology (Oxford)* 50 (12), 2157–2165. doi:10.1093/rheumatology/ker283

Sohn, M., Kim, K., Uddin, M. J., Lee, G., Hwang, I., Kang, H., et al. (2017). Delayed Treatment with Fenofibrate Protects against High-Fat Diet-Induced Kidney Injury in Mice: the Possible Role of AMPK Autophagy. *Am. J. Physiol. Ren. Physiol* 312 (2), F323–F334. doi:10.1152/ajprenal.00596.2015

Steimer, S. S., Berkemeier, T., Gilgen, A., Krieger, U. K., Peter, T., Shiraiwa, M., et al. (2015). Shikimic Acid Ozonolysis Kinetics of the Transition from Liquid Aqueous Solution to Highly Viscous Glass. *Phys. Chem. Chem. Phys.* 17 (46), 31101–31109. doi:10.1039/c5cp04544d

Sun, X., Deng, X., Cai, W., Li, W., Shen, Z., Jiang, T., et al. (2018). Icariin Inhibits LPS-Induced Cell Inflammatory Response by Promoting GRα Nuclear Translocation and Upregulating GRα Expression. *Life Sci.* 195, 33–43. doi:10.1016/j.lfs.2018.01.006

Sun, Y., Yao, Y., and Ding, C. Z. (2014). A Combination of Sinomenine and Methotrexate Reduces Joint Damage of Collagen Induced Arthritis in Rats by Modulating Osteoclast-Related Cytokines. *Int. Immunopharmacol* 18 (1), 135–141. doi:10.1016/j.intimp.2013.11.014

Takeda, R., Koike, T., Taniguchi, I., and Tanaka, K. (2013). Double-blind Placebo-Controlled Trial of Hydroxytyrosol of Olea Europaea on Pain in Gonarthrosis. *Phytomedicine* 20 (10), 861–864. doi:10.1016/j.phymed.2013.03.021

Tang, W., Lin, D., Chen, M., Li, Z., Zhang, W., Hu, W., et al. (2019). PTEN-mediated Mitophagy and APE1 Overexpression Protects against Cardiac Hypoxia/reoxygenation Injury. In Vitro *Cell Dev Biol Anim* 55 (9), 741–748. doi:10.1007/s11626-019-00389-6

Tang, Y., Li, Y., Xin, D., Chen, L., Xiong, Z., and Yu, X. (2021). Icariin Alleviates Osteoarthritis by Regulating Autophagy of Chondrocytes by Mediating PI3K/AKT/mTOR Signaling. *Bioengineered* 12 (1), 2984–2999. doi:10.1080/21655979.2021.1943602

Tang, Y., Mo, Y., Xin, D., Zeng, L., Yue, Z., and Xu, C. (2020). β-Ecdysterone Alleviates Osteoarthritis by Activating Autophagy in Chondrocytes through Regulating PI3K/AKT/mTOR Signal Pathway. *Am. J. Transl Res.* 12 (11), 7174–7186.

Taniguchi, N., Caramés, B., Ronfani, L., Ulmer, U., Komiya, S., Bianchi, M. E., et al. (2009). Aging-related Loss of the Chromatin Protein HMGB2 in Articular Cartilage Is Linked to Reduced Cellularity and Osteoarthritis. *Proc. Natl. Acad. Sci. U S A.* 106 (4), 1181–1186. doi:10.1073/pnas.0806062106

Togano, S., Yashiro, M., Masuda, G., Sugimoto, A., Miki, Y., Yamamoto, Y., et al. (2021). Gastric Cancer Stem Cells Survive in Stress Environments via Their Autophagy System. *Sci. Rep.* 11 (1), 20664. doi:10.1038/s41598-021-00155-3

Tu, Y. (1999). The Development of New Antimalarial Drugs: Qinghaosu and Dihydro-Qinghaosu. *Chin Med. J. (Engl)* 112 (11), 976–977.

Valsamidou, E., Gioxari, A., Amerikanou, C., Zoumpoulakis, P., Skarpas, G., and Kaliora, A. C. (2021). Dietary Interventions with Polyphenols in Osteoarthritis: A Systematic Review Directed from the Preclinical Data to Randomized Clinical Studies. *Nutrients* 13 (5). doi:10.3390/nu13051420

Varela-Eirín, M., Carpintero-Fernández, P., Sánchez-Temprano, A., Varela-Vázquez, A., Paíno, C. L., Casado-Díaz, A., et al. (2020). Senolytic Activity of Small Molecular Polyphenols from Olive Restores Chondrocyte Redifferentiation and Promotes a Pro-regenerative Environment in Osteoarthritis. *Aging* 12 (16), 15882–15905. doi:10.18632/aging.103801

Veratti, E., Rossi, T., Giudice, S., Benassi, L., Bertazzoni, G., Morini, D., et al. (2011). 18beta-glycyrrhetinic Acid and Glabridin Prevent Oxidative DNA Fragmentation in UVB-Irradiated Human Keratinocyte Cultures. *Anticancer Res.* 31 (6), 2209–2215.

Vinatier, C., Domínguez, E., Guicheux, J., and Caramés, B. (2018). Role of the Inflammation-Autophagy-Senescence Integrative Network in Osteoarthritis. *Front Physiol.* 9, 706. doi:10.3389/fphys.2018.00706

Wang, B., and Chen, M. Z. (2014). Astragaloside IV Possesses Antiarthritic Effect by Preventing Interleukin 1β-Induced Joint Inflammation and Cartilage Damage. *Arch. Pharm. Res.* 37 (6), 793–802. doi:10.1007/s12272-014-0336-2

Wang, C. Z., Mehendale, S. R., and Yuan, C. S. (2007). Commonly Used Antioxidant Botanicals: Active Constituents and Their Potential Role in Cardiovascular Illness. *Am. J. Chin Med.* 35 (4), 543–558. doi:10.1142/S0192415X07005053

Wang, T., and He, C. (2018). Pro-inflammatory Cytokines: The Link between Obesity and Osteoarthritis. *Cytokine Growth Factor Rev.* 44, 38–50. doi:10.1016/j.cytogfr.2018.10.002

Wang, W., Xu, J., Li, L., Wang, P., Ji, X., Ai, H., et al. (2010). Neuroprotective Effect of Morroniside on Focal Cerebral Ischemia in Rats. *Brain Res. Bull* 83 (5), 196–201. doi:10.1016/j.brainresbull.2010.07.003

Wang, Y., Smith, S., Teichtahl, A. J., Hodge, A. M., Wluka, A. E., Giles, G. G., et al. (2016). Association between Dietary Intake of Antioxidants and Prevalence of Femoral Head Cartilage Defects and Bone Marrow Lesions in Community-Based Adults. *J. Rheumatol.* 43 (10), 1885–1890. doi:10.3899/jrheum.160325

Wang, Z., Lee, Y., Eun, J. S., and Bae, E. J. (2014). Inhibition of Adipocyte Inflammation and Macrophage Chemotaxis by Butein. *Eur. J. Pharmacol.* 738, 40–48. doi:10.1016/j.ejphar.2014.05.031

Wei, Y., and Ito, Y. (2006). Preparative isolation of imperatorin, oxypeucedanin and isoimperatorin from traditional Chinese herb "Bai zhi"Angelica dahurica (Fisch. ex Hoffm) Benth. et Hook using multidimensional high-speed counter-current chromatography. *J. Chromatogr. A.* 1115 (1-2), 112–117. doi:10.1016/j.chroma.2006.02.081

Wei, Y., Vriesekoop, F., Yuan, Q., and Liang, H. (2018). β-Lactoglobulin as a Nanotransporter for Glabridin: Exploring the Binding Properties and Bioactivity Influences. *ACS Omega* 3 (9), 12246–12252. doi:10.1021/acsomega.8b01576

Wong, R. H. X., Evans, H. M., and Howe, P. R. C. (2017). Resveratrol Supplementation Reduces Pain Experience by Postmenopausal Women. *Menopause* 24 (8), 916–922. doi:10.1097/gme.0000000000000861

Wongwichai, T., Teeyakasem, P., Pruksakorn, D., Kongtawelert, P., and Pothacharoen, P. (2019). Anthocyanins and Metabolites from Purple rice Inhibit IL-1β-induced Matrix Metalloproteinases Expression in Human Articular Chondrocytes through the NF-Kb and ERK/MAPK Pathway. *Biomed. Pharmacother.* 112, 108610. doi:10.1016/j.biopha.2019.108610

Wu, L., Liu, H., Li, L., Liu, H., Cheng, Q., Li, H., et al. (2014). Mitochondrial Pathology in Osteoarthritic Chondrocytes. *Curr. Drug Targets* 15 (7), 710–719. doi:10.2174/1389450115666140417120305

Wu, X., Liu, Y., Zhang, E., Chen, J., Huang, X., Yan, H., et al. (2020). Dihydroartemisinin Modulates Apoptosis and Autophagy in Multiple Myeloma through the P38/MAPK and Wnt/β-Catenin Signaling Pathways. *Oxid Med. Cell Longev* 2020, 6096391. doi:10.1155/2020/6096391

Wu, Z., Zhang, X., Li, Z., Wen, Z., and Lin, Y. (2021). Activation of Autophagy Contributes to the Protective Effects of Lycopene against Oxidative Stress-Induced Apoptosis in Rat Chondrocytes. *Phytother Res.* 35 (7), 4032–4045. doi:10.1002/ptr.7127

Xiao, Z., Wang, J., Chen, S., and Feng, Y. (2020). Autophagy Promotion Enhances the Protective Effect of Morroniside on Human OA Chondrocyte. *Biosci. Biotechnol. Biochem.* 84 (5), 989–996. doi:10.1080/09168451.2020.1717925

Xing, J., Chen, X., and Zhong, D. (2005). Absorption and Enterohepatic Circulation of Baicalin in Rats. *Life Sci.* 78 (2), 140–146. doi:10.1016/j.lfs.2005.04.072

Xu, T., Niu, C., Zhang, X., and Dong, M. (2018). β-Ecdysterone Protects SH-Sy5y Cells against β-amyloid-induced Apoptosis via C-Jun N-Terminal Kinase- and Akt-Associated Complementary Pathways. *Lab Invest* 98 (4), 489–499. doi:10.1038/s41374-017-0009-0

Yan, C., Sun, W., Wang, X., Long, J., Liu, X., Feng, Z., et al. (2016). Punicalagin Attenuates Palmitate-Induced Lipotoxicity in HepG2 Cells by Activating the Keap1-Nrf2 Antioxidant Defense System. *Mol. Nutr. Food Res.* 60 (5), 1139–1149. doi:10.1002/mnfr.201500490

Yan, J., Ni, B., Sheng, G., Zhang, Y., Xiao, Y., Ma, Y., et al. (2021). Rhoifolin Ameliorates Osteoarthritis via Regulating Autophagy. *Front Pharmacol.* 12, 661072. doi:10.3389/fphar.2021.661072

Yang, H., Chen, D., Cui, Q. C., Yuan, X., and Dou, Q. P. (2006). Celastrol, a Triterpene Extracted from the Chinese "Thunder of God Vine," Is a Potent Proteasome Inhibitor and Suppresses Human Prostate Cancer Growth in Nude Mice. *Cancer Res.* 66 (9), 4758–4765. doi:10.1158/0008-5472.CAN-05-4529

Yang, K. Y., Lin, L. C., Tseng, T. Y., Wang, S. C., and Tsai, T. H. (2007). Oral Bioavailability of Curcumin in Rat and the Herbal Analysis from Curcuma Longa by LC-MS/MS. *J. Chromatogr. B Analyt Technol. Biomed. Life Sci.* 853 (1-2), 183–189. doi:10.1016/j.jchromb.2007.03.010

Yang, X., Zhang, Q., Gao, Z., Yu, C., and Zhang, L. (2018). Baicalin Alleviates IL-1β-induced Inflammatory Injury via Down-Regulating miR-126 in Chondrocytes. *Biomed. Pharmacother.* 99, 184–190. doi:10.1016/j.biopha.2018.01.041

Yao, J., Liu, X., Sun, Y., Dong, X., Liu, L., and Gu, H. (2021). Curcumin-Alleviated Osteoarthritic Progression in Rats Fed a High-Fat Diet by Inhibiting Apoptosis and Activating Autophagy via Modulation of MicroRNA-34a. *J. Inflamm. Res.* 14, 2317–2331. doi:10.2147/JIR.S312139

You, H., Zhang, R., Wang, L., Pan, Q., Mao, Z., and Huang, X. (2021). Chondro-Protective Effects of Shikimic Acid on Osteoarthritis via Restoring Impaired Autophagy and Suppressing the MAPK/NF-κB Signaling Pathway. *Front Pharmacol.* 12, 634822. doi:10.3389/fphar.2021.634822

Yu, H., Yao, S., Zhou, C., Fu, F., Luo, H., Du, W., et al. (2021). Morroniside Attenuates Apoptosis and Pyroptosis of Chondrocytes and Ameliorates Osteoarthritic Development by Inhibiting NF-Kb Signaling. *J. Ethnopharmacol* 266, 113447. doi:10.1016/j.jep.2020.113447

Yu, L., Chen, Y., and Tooze, S. A. (2018). Autophagy Pathway: Cellular and Molecular Mechanisms. *Autophagy* 14 (2), 207–215. doi:10.1080/15548627.2017.1378838

Yu, L. M., Dong, X., Xue, X. D., Zhang, J., Li, Z., Wu, H. J., et al. (2019). Protection of the Myocardium against Ischemia/reperfusion Injury by Punicalagin through an SIRT1-NRF-2-HO-1-dependent Mechanism. *Chem. Biol. Interact* 306, 152–162. doi:10.1016/j.cbi.2019.05.003

Yun, H. R., Jo, Y. H., Kim, J., Shin, Y., Kim, S. S., and Choi, T. G. (2020). Roles of Autophagy in Oxidative Stress. *Int. J. Mol. Sci.* 21 (9). doi:10.3390/ijms21093289

Zada, S., Pham, T. M., Hwang, J. S., Ahmed, M., Lai, T. H., Elashkar, O., et al. (2021). Chlorogenic Acid Protects Human Chondrocyte C28/I2 Cells from Oxidative Stress-Induced Cell Death through Activation of Autophagy. *Life Sci.* 285, 119968. doi:10.1016/j.lfs.2021.119968

Zater, H., Huet, J., Fontaine, V., Benayache, S., Stévigny, C., Duez, P., et al. (2016). Chemical Constituents, Cytotoxic, Antifungal and Antimicrobial Properties of Centaurea Diluta Ait. Subsp. Algeriensis (Coss. & Dur.) Maire. *Asian Pac. J. Trop. Med.* 9 (6), 554–561. doi:10.1016/j.apjtm.2016.04.016

Zeng, L., Wang, W., Rong, X. F., Zhong, Y., Jia, P., Zhou, G. Q., et al. (2014). Chondroprotective Effects and Multi-Target Mechanisms of Icariin in IL-1 Beta-Induced Human SW 1353 Chondrosarcoma Cells and a Rat Osteoarthritis Model. *Int. Immunopharmacol* 18 (1), 175–181. doi:10.1016/j.intimp.2013.11.021

Zhang, G., Cao, J., Yang, E., Liang, B., Ding, J., Liang, J., et al. (2018a). Curcumin Improves Age-Related and Surgically Induced Osteoarthritis by Promoting Autophagy in Mice. *Biosci. Rep.* 38 (4). doi:10.1042/bsr20171691

Zhang, G., Zhang, H., You, W., Tang, X., Li, X., and Gong, Z. (2020). Therapeutic Effect of Resveratrol in the Treatment of Osteoarthritis via the MALAT1/miR-9/nf-Kb Signaling Pathway. *Exp. Ther. Med.* 19 (3), 2343–2352. doi:10.3892/etm.2020.8471

Zhang, J., Wang, S., Rong, G., Cheng, F., Gui, B., and Shen, C. (2018b). Tetrahydrohyperforin Prevents Articular Cartilage Degeneration and Affects Autophagy in Rats with Osteoarthritis. *Exp. Ther. Med.* 15 (6), 5261–5268. doi:10.3892/etm.2018.6098

Zhang, R. J., Cai, C., Pang, J., Xu, X. L., and Li, G. W. (2021). Therapeutic Effect of Huzhangoside D in Rats with Knee Osteoarthritis Induced by Anterior Cruciate Ligament Transection. *Pharmacogn Mag.* 17 (73), 112.

Zhang, W., Ouyang, H., Dass, C. R., and Xu, J. (2016). Current Research on Pharmacologic and Regenerative Therapies for Osteoarthritis. *Bone Res.* 4, 15040. doi:10.1038/boneres.2015.40

Zhang, X., Xu, X., Xu, T., and Qin, S. (2014). β-Ecdysterone Suppresses Interleukin-1β-Induced Apoptosis and Inflammation in Rat Chondrocytes via Inhibition of NF-Kb Signaling Pathway. *Drug Dev. Res.* 75 (3), 195–201. doi:10.1002/ddr.21170

Zhang, Y., Wang, Q. S., Cui, Y. L., Meng, F. C., and Lin, K. M. (2012). Changes in the Intestinal Absorption Mechanism of Icariin in the Nanocavities of Cyclodextrins. *Int. J. Nanomedicine* 7, 4239–4249. doi:10.2147/IJN.S33014

Zhang, Y., Zhang, Y., Li, J., Chen, Y., Han, L., He, Q., et al. (2019). The Role of Hepatic Antioxidant Capacity and Hepatobiliary Transporter in Liver Injury Induced by Isopsoralen in Zebrafish Larvae. *Hum. Exp. Toxicol.* 38 (1), 36–44. doi:10.1177/0960327118774873

Zhang, Y. J., Gan, R. Y., Li, S., Zhou, Y., Li, A. N., Xu, D. P., et al. (2015). Antioxidant Phytochemicals for the Prevention and Treatment of Chronic Diseases. *Molecules* 20 (12), 21138–21156. doi:10.3390/molecules201219753

Zhao, H., Zhang, T., Xia, C., Shi, L., Wang, S., Zheng, X., et al. (2014). Berberine Ameliorates Cartilage Degeneration in Interleukin-1β-Stimulated Rat Chondrocytes and in a Rat Model of Osteoarthritis via Akt Signalling. *J. Cell Mol Med* 18 (2), 283–292. doi:10.1111/jcmm.12186

Zheng, W., Zhang, H., Jin, Y., Wang, Q., Chen, L., Feng, Z., et al. (2017). Butein Inhibits IL-1β-induced Inflammatory Response in Human Osteoarthritis Chondrocytes and Slows the Progression of Osteoarthritis in Mice. *Int. Immunopharmacol* 42, 1–10. doi:10.1016/j.intimp.2016.11.009

Zhi, L. Q., Yao, S. X., Liu, H. L., Li, M., Duan, N., and Ma, J. B. (2018). Hydroxytyrosol Inhibits the Inflammatory Response of Osteoarthritis Chondrocytes via SIRT6-Mediated Autophagy. *Mol. Med. Rep.* 17 (3), 4035–4042. doi:10.3892/mmr.2017.8353

Zhou, J.-c., Wang, J.-l., Ren, H.-z., and Shi, X.-l. (2021a). Autophagy Plays a Double-Edged Sword Role in Liver Diseases. *J. Physiol. Biochem.* 2021, 298. doi:10.1007/s13105-021-00844-7

Zhou, L., Liu, Q., Yang, M., Wang, T., Yao, J., Cheng, J., et al. (2016). Dihydroartemisinin, an Anti-malaria Drug, Suppresses Estrogen Deficiency-Induced Osteoporosis, Osteoclast Formation, and RANKL-Induced Signaling Pathways. *J. Bone Miner Res.* 31 (5), 964–974. doi:10.1002/jbmr.2771

Zhou, P., Xie, W., Meng, X., Zhai, Y., Dong, X., Zhang, X., et al. (2019). Notoginsenoside R1 Ameliorates Diabetic Retinopathy through PINK1-dependent Activation of Mitophagy. *Cells* 8 (3), 213. doi:10.3390/cells8030213

Zhou, W., Shi, Y., Wang, H., Yu, C., Zhu, H., and Wu, A. (2021b). Sinensetin Reduces Osteoarthritis Pathology in the Tert-Butyl Hydroperoxide-Treated Chondrocytes and the Destabilization of the Medial Meniscus Model Mice via the AMPK/mTOR Signaling Pathway. *Front Pharmacol.* 12, 713491. doi:10.3389/fphar.2021.713491

Conflict of Interest: The authors declare that the research was conducted in the absence of any commercial or financial relationships that could be construed as a potential conflict of interest.

Publisher's Note: All claims expressed in this article are solely those of the authors and do not necessarily represent those of their affiliated organizations, or those of the publisher, the editors and the reviewers. Any product that may be evaluated in this article, or claim that may be made by its manufacturer, is not guaranteed or endorsed by the publisher.

Copyright © 2021 Tian, Zhang and Sun. This is an open-access article distributed under the terms of the Creative Commons Attribution License (CC BY). The use, distribution or reproduction in other forums is permitted, provided the original author(s) and the copyright owner(s) are credited and that the original publication in this journal is cited, in accordance with accepted academic practice. No use, distribution or reproduction is permitted which does not comply with these terms.

frontiers in Pharmacology

ORIGINAL RESEARCH
published: 04 January 2022
doi: 10.3389/fphar.2021.797892

Effects of *Sparganii Rhizoma* on Osteoclast Formation and Osteoblast Differentiation and on an OVX-Induced Bone Loss Model

Sungyub Lee†, Minsun Kim†, Sooyeon Hong, Eom Ji Kim, Jae-Hyun Kim, Youngjoo Sohn and Hyuk-Sang Jung**

Department of Anatomy, College of Korean Medicine, Kyung Hee University, Seoul, South Korea

Postmenopausal osteoporosis is caused by an imbalance between osteoclasts and osteoblasts and causes severe bone loss. Osteoporotic medicines are classified into bone resorption inhibitors and bone formation promoters according to the mechanism of action. Long-term use of bisphosphonate and selective estrogen receptor modulators (SERMs) can cause severe side effects in postmenopausal osteoporosis patients. Therefore, it is important to find alternative natural products that reduce osteoclast activity and increase osteoblast formation. *Sparganii Rhizoma* (SR) is the dried tuberous rhizome of *Sparganium stoloniferum* Buchanan-Hamilton and is called "samreung" in Korea. However, to date, the effect of SR on osteoclast differentiation and the ovariectomized (OVX)-induced bone loss model has not been reported. *In vitro*, tartrate-resistant acid phosphatase (TRAP) staining, western blots, RT-PCR and other methods were used to examine the effect of SR on osteoclast differentiation and osteoblasts. *In vivo*, we confirmed the effect of SR in a model of OVX-induced postmenopausal osteoporosis. SR inhibited osteoclast differentiation and decreased the expression of TNF receptor-associated factor 6 (TRAF6), nuclear factor of activated T cells 1 (NFATc1) and c-Fos pathway. In addition, SR stimulates osteoblast differentiation and increased protein expression of the bone morphogenetic protein 2 (BMP-2)/SMAD signaling pathway. Moreover, SR protected against bone loss in OVX-induced rats. Our results appear to advance our knowledge of SR and successfully demonstrate its potential role as a osteoclastogenesis-inhibiting and osteogenesis-promoting herbal medicine for the treatment of postmenopausal osteoporosis.

Keywords: sparganii rhizoma, bone remodeling, osteoclast, osteoblast, ovariectomized

OPEN ACCESS

Edited by:
Daohua Xu,
Guangdong Medical University, China

Reviewed by:
Baosheng Boris Guo,
Nanjing University, China
Ronghua Zhang,
Jinan University, China

****Correspondence:***
Youngjoo Sohn
youngjoos@khu.ac.kr
Hyuk-Sang Jung
jhs@khu.ac.kr

†These authors have contributed equally to this work and share first authorship

Specialty section:
This article was submitted to Ethnopharmacology, a section of the journal Frontiers in Pharmacology

Received: *19 October 2021*
Accepted: *06 December 2021*
Published: *04 January 2022*

Citation:
Lee S, Kim M, Hong S, Kim EJ, Kim J-H, Sohn Y and Jung H-S (2022) Effects of Sparganii Rhizoma *on Osteoclast Formation and Osteoblast Differentiation and on an OVX-Induced Bone Loss Model. Front. Pharmacol. 12:797892. doi: 10.3389/fphar.2021.797892*

Abbreviations: ALP, alkaline phosphatase; ALT, alanine transferase; AST, aspartate aminotransferase; ATP6v0d2, ATPase H+ transporting v0 subunit d2; BMD, bone mineral density; BMP-2, bone morphogenetic protein 2; BV/TV, trabecular bone volume; CA2, carbonic anhydrase II; DC-STAMP, dendritic cell-specific transmembrane protein; H&E, hematoxylin and eosin; IHC, immunohistochemical; LC-MS, liquid chromatography–mass spectrometry; MAPK, mitogen-activated protein kinase; MMP-9, matrix metalloproteinase-9; NFATc1, nuclear factor of activated T cells 1; NF-κB, nuclear factor-κB; OSCAR, osteoclast-associated receptor; OVX, ovariectomized; RANKL, receptor activator of nuclear factor-κB ligand; RT-PCR, real-time polymerase chain reaction; RUNX-2, runt-related transcription factor 2; SERMs, selective estrogen receptor modulators; SR, Sparganii Rhizoma; Tb. sp, trabecular separation; Tb.N, trabecular number; Tb.Th, trabecular thickness; TRAP, tartrate-resistant acid phosphatase.

INTRODUCTION

Bone remodeling is maintained by a balance between bone resorption by osteoclasts and bone formation by osteoblasts (Matsuo and Irie, 2008). However, bone metabolic diseases such as osteoporosis and Paget's disease occur when bone formation is reduced due to a decrease in the activity of osteoblasts. Additionally, excessive activity of osteoclasts is increased or when the two factors act at the same time (Feng and McDonald, 2011). Osteoporosis is known to be associated with several factors (menopause and aging), and it is characterized by excessive bone loss, weakening of bone microstructure and increased risk of fracture (Sozen et al., 2017). Osteoporotic medicines are classified into bone resorption inhibitors and bone formation promoters according to the mechanism of action. For the treatment of osteoporosis, bone resorption inhibitors such as bisphosphonate and selective estrogen receptor modulators (SERMs) are mainly used (Kennel and Drake, 2009; Gu et al., 2016). However, bone resorption inhibitors cannot treat osteoporosis that has already progressed. In addition, long-term use of bisphosphonate and SERMs can cause severe side effects in postmenopausal osteoporosis patients, such as osteonecrosis of the jaw, atrial fibrillation, abnormal vaginal bleeding, hot flashes and atrophic vaginitis (Bamias et al., 2005; Gu et al., 2016). Thus, the discovery of alternative natural products that decrease osteoclast activity and increase osteoblast formation with fewer side effects than the current medications is crucial.

Osteoclasts are multinucleated giant cells derived from mononuclear and macrophage precursor cells (Collin-Osdoby and Osdoby, 2012). Receptor activator of nuclear factor-κB ligand (RANKL) plays a critical role in the differentiation of osteoclast precursor cells into mature osteoclasts (Suda et al., 1999). On the surface of osteoclasts, the binding receptor activator of nuclear factor-κB (RANK) to RANKL activates TNF receptor-associated factor 6 (TRAF6) (Clohisy et al., 2003). Then, activation of TRAF6 induces nuclear factor-κB (NF-κB) and mitogen-activated protein kinase (MAPK). These signaling pathways activate transcription factors such as nuclear factor of activated T cells 1 (NFATc1) and c-Fos (Galibert et al., 1998; Boyle et al., 2003). NFATc1 is essential for osteoclast differentiation and regulates the expression of osteoclast-related genes (Takayanagi et al., 2002; Kim and Kim, 2014). Osteoblasts are derived from mesenchymal stem cells and large cells responsible for bone synthesis and mineralization. Bone morphogenetic protein 2 (BMP-2) and runt-related transcription factor 2 (RUNX-2) are important transcription factors for osteoblast differentiation and bone formation (Liu et al., 2007). These transcription factors upregulate the expression of osteogenic markers such as alkaline phosphatase (ALP), bone sialoprotein (BSP) and collagen type 1 (COL1) (Liu et al., 2007).

Korean medicine has recently been spotlighted as an alternative medicine for various diseases due to its few side effects and high therapeutic effects (Yuan et al., 2016). *Sparganii Rhizoma* (SR) is the dried tuberous rhizome of *Sparganium stoloniferum* Buchanan-Hamilton and is called "samreung" in Korea (Jia et al., 2021). SR has been used as a traditional Korean medicine to treat patients with gynecological diseases such as uterine fibroids, blood stasis and dysmenorrhea (Zhao et al., 2018). The chemical components of SR have been identified as phenylpropanoids (such as ferulic acid, *p*-coumaric acid, caffeic acid), flavonoids (such as kaempherol, rutin, formononetin), coumarins (such as sparstolonin B), volatile oils (β-pinene, eucalyptol, myrtenol) and others (Jia et al., 2021). Among them, kaempferol, rutin, formononetin, ferulic acid, p-coumaric acid and caffeic acid were previously found to inhibit osteoclast differentiation (Kyung et al., 2008; Sagar et al., 2016; Doss et al., 2018; Kim et al., 2018; Liu et al., 2020; Ekeuku et al., 2021). Inflammation has been associated with metabolic bone diseases such as postmenopausal osteoporosis and rheumatoid arthritis. Previous studies have shown that estrogen deficiency promotes bone loss by inducing an increase in inflammatory cytokines such as IL-6 and TNF-α. The pro-inflammatory cytokines TNF-α and IL-6 are potent inducers of bone resorption. Previous studies have confirmed that TNF-α can promote RANKL-induced osteoclast formation *in vitro*. IL-1 promotes multinucleation of osteoclast precursors and enhances the ability of mature multinucleated cells to resorb bone. Therefore, it is suggested that increased expression of inflammatory cytokines is associated with osteoporosis (Ginaldi et al., 2005). Among the components of *p*-coumaric acid, caffeic acid, kaempferol, rutin, formononetin, and sparstolonin B have been proven to have anti-inflammatory effects through previous studies (Guardia et al., 2001; Pragasam et al., 2013; Kadioglu et al., 2015; Luo et al., 2019; Yepuri et al., 2019; Zielinska et al., 2021). Therefore, it was expected that SR would be effective for postmenopausal osteoporosis because of the pharmacological effects of SR, which have been traditionally used for female diseases, and the inhibition of osteoclast differentiation and anti-inflammatory effects of SR components. However, to date, the effect of SR on osteoclast differentiation and an ovariectomized (OVX)-induced bone loss model has not been reported. Therefore, this study was performed to explore the effects of SR on osteoclast differentiation and osteoblasts as well as the underlying mechanism and OVX-induced bone loss models.

MATERIALS AND METHODS

Reagents

Dulbecco's modified Eagle's medium (DMEM) was obtained from Welgene (Daejeon, Korea). Minimum essential medium Eagle alpha-modification (α-MEM), penicillin/streptomycin (P/S), Dulbecco's phosphate buffered saline (DPBS) and normal serum for immunohistochemistry were purchased from Gibco (Gaithersburg, MD, United States). Fetal bovine serum (FBS) was supplied by Atlas Biologicals (Fort Collins, CO, United States). RANKL was purchased from Peprotech (London, United Kingdom). Cell Counting Kit-8 (CCK-8; WST-8; 2-(2-methoxy-4-nitrophenyl)-3-(4-nitrophenyl)-5-(2,4-disulfophenyl)-2H-tetrazolium, monosodium salt) was purchased from Dojindo Molecular Technologies, Inc. (Japan, Kumamoto). Osteo assay stripwell plates were

purchased from Corning, Inc. (New York, NY, United States). Tartrate-resistant acid phosphatase (TRAP) kits, 4′,6-diamidino-2-phenylindol (DAPI), β-glycerophosphate and ascorbic acid, 17β-estradiol (E_2) and alendronate (ALN) were obtained from Sigma-Aldrich; Merck KGaA (Darmstadt, Germany). Acti-stain™ 488 Fluorescent Phalloidin was purchased from Cytoskeleton, Inc. (Denver, CO, United States). Primary antibodies against anti-TRAF6 (TRAF6; cat no: sc- 8409), anti-Lamin B (Lamin B; cat no: sc- 374015), anti-β-actin (Actin; cat no: 8432) and anti-c-Fos (c-Fos; cat no: sc-447) were purchased from Santa Cruz Biotechnology, Inc. (Santa Cruz, CA, United States). Anti-NFATc1 (NFATc1; cat no: 556602) was purchased from BD Pharmingen, Inc. (San Diego, CA, United States). Anti-RUNX-2 (RUNX-2; cat no: ab), anti-Osterix (Osterix; cat no: ab209484) and anti-SMAD 1/5/9 (SMAD1/5/9; cat no: ab80255) were purchased from Abcam (Cambridge, MA, United States). Anti-phosphorylated (p)-extracellular signal-regulated kinase (p-ERK; cat no: 4370S), anti-ERK (ERK; cat no: 4695S), anti-p-c-Jun N-terminal kinase (p-JNK; cat no: 4668S), anti-JNK (JNK; cat no: 9258S), anti-p-p38 (p-p38; cat no: 4511S), anti-p38 (p38; cat no: 9212L), anti-p-NF-κB (p-NF-κB; cat no: 3032S), anti-NF-κB (NF-κB; cat no: 8242S), anti-p-IκB (p-IκB; cat no: 2859S), anti-IκB (IκB; cat no: 4814S) and anti-phospho-SMAD1/5 (p-SMAD1/5; cat no: 9516S) was purchased from Cell Signaling Technology, Inc. (Danvers, MA, United States), and secondary antibodies were purchased from Jackson ImmunoResearch Laboratories, Inc. (West Grove, PA, United States). Masson-goldner trichrome kit was purchased from BioGnost (cat no: MGT-100T, Zagreb, Croatia, EU). Proteinase K was supplied by Thermo Fisher Scientific (Waltham, MA, United States). Biotinylated secondary antibody, ABC HRP Kit (Peroxidase, Standard) and 3,3′-diaminobenzidine (DAB) solution were purchased from Vector Labs (Burlingame, CA, United States).

Preparation of *Sparganii Rhizoma* Ethanol Extract

SR was purchased from Omniherb Co. (Yeoungcheon, Korea). A total of 150 g of the dried herbs was extracted in 80% ethanol for 2 weeks. The extracts were filtered using filter paper (no. 3; Whatman PLC; GE Healthcare). Then, the ethanol extract was evaporated using a vacuum concentrator. Then, the extract was filtered and evaporated using a vacuum to yield the powder (dried powder: 5.5 g), and the SR extract yield was 3.7%.

Cell Culture and Cell Cytotoxicity Assay

The RAW 264.7 macrophage line was obtained from the Korean Cell Line Bank (KCLB No. 40071; Seoul, Korea). RAW 264.7 cells were cultured in DMEM containing 10% FBS and 1% P/S in a 5% CO_2 incubator (Thermo Fisher; Waltham, MA) at 37°C. For determination of the effect of SR on RAW 264.7 cell cytotoxicity, cell viability was measured using the Cell Counting Kit-8 (CCK-8) assay. For the RAW 264.7 cell cytotoxicity assay, RAW 264.7 cells were seeded into 96-well plates at a density of 5×10^3 cells/well at 37°C for 24 h. Then, the cells were treated with SR (125, 250, 500, 1,000 μg/ml) at 37°C for 1 day. For the osteoclast cytotoxicity assay, RAW 264.7 cells were seeded in 96-well plates at a density of 5×10^3 cells/well at 37°C for 24 h. Then, the cells were treated with SR (125, 250, 500, 1,000 μg/ml) and kaempferol (209.5 ng/ml and 419 ng/ml) at 37°C for 5 days. The cytotoxicity of RAW 264.7 cells and osteoclasts were measured using the Cell Counting Kit-8 (CCK-8) assay. Thereafter, we added 10 μL of CCK-8 solution to each well, and the cells were incubated at 37°C for 2 h. At the end of the experiment, the optical densities (ODs) at 405 nm were detected using an enzyme-linked immunosorbent assay (ELISA) reader (VersaMax microplate reader; Molecular Devices, LLC).

MC3T3-E1 subclone 4 cells were obtained from the American Type Culture Collection (No. ATCC-CRL-2593, Manassas, VA). MC3T3-E1 cells were cultured in α-MEM (without ascorbic acid) containing 10% FBS and 1% P/S in a 5% CO_2 incubator at 37°C. For determination of the effect of SR on MC3T3-E1 cell cytotoxicity assay, MC3T3-E1 cells were seeded in a 96-well plate at a density of 1×10^4 cells/well overnight in a 5% CO_2 incubator at 37°C for 24 h, and then, the cells were treated with SR at various concentrations (125, 250, 500, 1,000 μg/ml) for 3, 7 and 14 days. For determination of the effect of kaempferol on MC3T3-E1 cell cytotoxicity assay, MC3T3-E1 cells were seeded in a 96-well plate at a density of 1×10^4 cells/well overnight in a 5% CO_2 incubator at 37°C for 24 h, and then, the cells were treated with kaempferol at various concentrations (41.9 ng/ml and 83.8 ng/ml) for 3 and 7 days. Thereafter, we added 10 μL of CCK-8 solution to each well, and the cells were incubated at 37°C for 2 h. Then, cell cytotoxicity was measured using enzyme-linked immunosorbent assays (ELISA; VersaMax, Molecular Devices, LLC, Sunnyvale, CA). Then, cell cytotoxicity was measured using the CCK-8 assay, and absorbance was detected with a microplate reader at 405 nm. Cytotoxicity is expressed as a percentage compared to that of the normal group, and values less than 90% were considered to indicate cytotoxicity.

TRAP Staining and TRAP Activity

To determine the effect of SR on osteoclast differentiation, we seeded RAW 264.7 cells in 24-well plates at a density of 1.5×10^4 cells/well and cultured them at 37°C for 24 h. Then, RAW 264.7 cells were replaced with α-MEM containing RANKL (100 ng/ml) and SR (125, 250, 500, 1,000 μg/ml) at 37°C for 5 days. The differentiation medium was replaced every 2 days. In order to compare the inhibitory effect of SR and kaempferol on osteoclast differentiation, RAW 264.7 cells were seeded in 24-well plates at a density of 1.5×10^4 cells/well and cultured them at 37°C for 24 h. Then, the medium was replaced with RANKL (100 ng/ml) and SR (500 and 1,000 μg/ml) or kaempferol (209.5 ng/ml and 419 ng/ml) at 37°C for 5 days. After the end of osteoclast differentiation, the cells were fixed with 10% formaldehyde at room temperature for 10 min. Then, tartrate-resistant acid phosphatase (TRAP) staining was performed using a TRAP kit. The stained cells were imaged with an inverted microscope (Olympus, Tokyo, Japan). Cells with more than three nuclei or more nuclei were considered TRAP-positive osteoclasts.

To investigate the effect of SR on TRAP activity in differentiation medium, we transferred 50 μL of differentiation medium to a new 96-well plate. Thereafter, an equal volume of TRAP solution [4.93 mg p-nitrophenyl phosphate (PNPP) in 750 ml of 0.5 M acetate solution and 150 ml of tartrate acid solution] was added to each well and cultured at 37°C for 1 h. Thereafter, the reaction was stopped using 0.5 M NaOH, and the level of TRAP activity was measured using an ELISA reader at 405 nm.

Pit Formation Assay and F-Actin Ring Staining

For analysis of the effect of SR on bone resorption, RAW 264.7 cells were seeded in osteoassay surface multiple well plates at a density of 5×10^3 cells/well and cultured for 24 h. The cells were treated with replacement α-MEM containing RANKL (100 ng/ml) and SR (125, 250, 500, 1,000 μg/ml) for 5 days. The differentiation medium was replaced every 2 days. Afterward, the cells were washed and removed using deionized water with 4% sodium hypochlorite. The pit area was captured with an inverted microscope and measured using ImageJ software, and pit area measurements expressed the absorption area as a percentage of the total area.

For determination of the effects of SR on F-actin ring formation, RAW 264.7 cells were seeded in a 96-well plate at a density of 5×10^3 cells/well and cultured for 24 h. RAW 264.7 cells were stimulated with RANKL (100 ng/ml) and SR (125, 250, 500, 1,000 μg/ml) at 37°C for 5 days. The cells were washed with phosphate-buffered saline (PBS) and fixed with 4% paraformaldehyde for 20 min. Then, the cells were permeabilized for 5 min with 0.1% Triton X-100. The cells were stained for Acti-stain™ 488 Fluorescent Phalloidin and DAPI for nuclei at room temperature in the dark for 30 min. Images were captured using fluorescence microscopy (Cellena, Logos Biosystems; magnification, ×200) and counted using ImageJ software version 1.46 (National Institutes of Health, Bethesda, MD).

Western Blotting Analysis

To the examination of the effect of SR on the expression of TRAF6/MAPK/NF-kB signaling pathway, RAW 264.7 cells were seeded in a 60 π dish at a density of 2×10^6 cells/well and cultured for 24 h. The cells were treated with α-MEM containing RANKL (100 ng/ml) and SR (125, 250, 500, 1,000 μg/ml) for 6 h. For determination of the effect of SR on the expression of NFATc1, c-Fos and MMP-9, RAW 264.7 cells were seeded in a 60 π dish at a density of 5×10^5 cells/well and cultured for 24 h. The cells were treated with α-MEM containing RANKL (100 ng/ml) and SR (125, 250, 500, 1,000 μg/ml) or kaempferol (209.5 ng/ml and 419 ng/ml) for 1 day. For determination of the effect of SR on the expression of osteoblast differentiation transcription factors, MC3T3-E1 cells were seeded in a 60 π dish at a density of 5×10^5 cells/well overnight in a 5% CO_2 incubator at 37°C for 24 h, and then, the cells were treated with SR (25, 50, 100, 200 μg/ml) or kaempferol (41.9 ng/ml and 83.8 ng/ml) for 2 days. Total protein was extracted using RIPA buffer (composition: 50 mM Tris-Cl, 150 mM NaCl, 1% NP-40, 0.5% sodium deoxycholate and 0.1% SDS). Then, the extracts were centrifuged at 4°C for 20 min (2,000 rpm). Nuclear protein was extracted using a nuclear extraction kit (Thermo Fisher Scientific, Waltham, MA, United States).

The supernatants were collected, and protein (30 μg) was quantized by using a BCA protein assay kit. Thirty micrograms of protein were then separated using 10% SDS-PAGE and transferred onto a nitrocellulose membrane for 1 h. Subsequently, the membrane was blocked with 5% skim milk in TBST (containing 0.1% Tween 20) for 1 h at room temperature and incubated with primary antibodies at 4°C overnight. The primary antibodies used were as follows: TRAF6 (dilution; 1: 1,000), p-NF-κB (dilution; 1:1,000), NF-κB (dilution; 1:1,000), p-IκB (dilution; 1:1,000), IκB (dilution; 1:1,000), Lamin B (dilution; 1:1,000), p-ERK (dilution; 1:1,000), ERK (dilution; 1: 1,000), p-JNK (dilution; 1:1,000), JNK (dilution; 1:1,000), p-p38 (dilution; 1:1,000), p38 (dilution; 1:1,000), NFATc1 (dilution; 1: 1,000), c-Fos (dilution; 1:200), β-actin (dilution; 1: 1,000), RUNX-2 (dilution; 1: 1,000), Osterix (dilution; 1: 1,000), SMAD1/5/9 (dilution; 1: 1,000) and p-SMAD1/5 (dilution; 1: 1,000). After 24 h, the membranes were washed three times with TBST and incubated with secondary antibodies at 37°C for 1 h. Then, the band was detected using electrochemiluminescence (ECL) solution. The protein levels were quantified by using ImageJ software version 1.46, and the resulting bands were normalized using a loading control.

Real-Time Polymerase Chain Reaction (RT-PCR)

For determination of the effect of SR on osteoclast-related genes, RAW 264.7 cells were seeded in 6-well plates at a density of 2×10^3 cells/well and cultured for 24 h. The cells were treated with α-MEM containing RANKL (100 ng/ml) and SR (125, 250, 500, 1,000 μg/ml) for 4 days. The differentiation medium was replaced every 2 days. Total RNA was extracted from TRIzol® reagent according to the manufacturer's instructions (Invitrogen, Carlsbad, CA, United States). Total RNA (2 μg) was quantized using a NanoDrop 2000 instrument (Thermo Scientific, United Kingdom). cDNA reverse transcription was performed using a reverse transcription kit (Invitrogen; Thermo Fisher Scientific, Inc.). PCR was performed using a C1000 Touch™ Thermal Cycler (Bio-Rad Laboratories, Inc.). PCR conditions were as follows: 94°C for 1 min (denaturation), 55–58°C for 30 s (annealing) and 72°C for 1 min (extension). The primers used were as **Table 1**. PCR products were separated by 1.2% agarose gel. The band was quantified by using ImageJ software version 1.46, and the resulting products were normalized using β-actin.

Alizarin Red S Staining

For determination of the effect of SR on osteoblast differentiation, MC3T3-E1 cells were seeded in 24-well plates at a density of 1×10^4 cells/well and cultured for 24 h. Cells were treated in osteogenic medium (α-MEM without ascorbic acid supplemented with 10 mM β-glycerophosphate and 25 μg/ml

TABLE 1 | Primer sequences for RT–PCR analysis.

Genes	Primer sequence	Accession no.	Cycle	Temperature
Nfatc1 (NFATc1)	F: TGC TCC TCC TCC TGC TGC TC R: CGT CTT CCA CCT CCA CGT CG	NM_198,429.2	32	58
Fos (c-Fos)	F: ATG GGC TCT CCT GTC AAC AC R: GGC TGC CAA AAT AAA CTC CA	NM_010234.3	33	58
Mmp9 (MMP-9)	F: CGA CTT TTG TGG TCT TCC CC R: TGA AGG TTT GGA ATC GAC CC	NM_013599.4	30	58
Tnfrsf11a (RNAK)	F: AAA CCT TGG ACC AAC TGC AC R: ACC ATC TTC TCC TCC CHA GT	NM_009399.3	32	53
Acp5 (TRAP)	F: ACT TCC CCA GCC CTT ACT ACC G R: TCA GCA CAT AGC CCA CAC CG	NM_007388.3	30	58
Ca2 (CA2)	F: CTC TCA GGA CAA TGC AGT GCT GA R: ATC CAG GTC ACA CAT TCC AGC A	NM_001357334.1	32	58
Oscar (OSCAR)	F: CTG CTG GTA ACG GAT CAG CTC CCC AGA R: CCA AGG AGC CAG AAC CTT CGA AAC T	NM_001290377.1	35	53
Atp6v0d2 (ATP6v0d2)	F: ATG GGG CCT TGC AAA AGA AAT CTG R: CGA CAG CGT CAA ACA AAG GCT TGT A	NM_175,406.3	30	58
Dcstamp (DC-STAMP)	F: TGG AAG TTC ACT TGA AAC TAC GTG R: CTCGGTTTCCCGTCAGCCTCTCTC	NM_001289506.1	40	63
Actb (β-actin)	F: TTC TAC AAT GAG CTG CGT GT R: CTC ATA GCT CTT CTC CAG GG	NM_008084.3	30	58

NFATc1, nuclear factor of activated T cells 1; MMP-9, matrix metalloproteinase-9; RANK, receptor activator of nuclear factor-κB; TRAP, tartrate-resistant acid phosphatase; CA2, carbonic anhydrase II; OSCAR, osteoclast-associated receptor; ATP6v0d2, ATPase H + Transporting V0 Subunit D2; DC-STAMP, dendritic cell-specific transmembrane protein.

ascorbic acid) and SR (25, 50, 100, 200 μg/ml) for 14 days. The cells were washed three times with PBS and fixed with 80% Et-OH for 1 h at 4°C. For Alizarin Red S staining, the cells were rinsed with distilled water (D.W) and stained with Alizarin Red solution for 5 min at room temperature, and images were captured using a camera. For quantification of the Alizarin Red S staining, 10% (v/w) cetylpyridinium chloride in sodium phosphate was added to each well and extracted for 10 min. The extract was measured using an ELISA reader at 570 nm.

Experimental Animals and Treatment

Eleven-week-old female Sprague Dawley (SD) rats were purchased from Nara Biotech (230–250 g; Seoul, Korea) and housed at 22 ± 2°C and a relative humidity of 53–55% under a 12 h light-dark cycle. Rats were placed in separate cages and provided *ad libitum* access to food and water. All animal experiments were approved by the Committee of the Kyung Hee University Laboratory Animal Center (approval number: KHSASP-21-185). For determination of the effect of SR on postmenopausal osteoporosis, OVX osteoporosis was induced. All animals were acclimatized for 1 week before surgery. For surgery, the animals were deeply anesthetized by 100% oxygen and 5% isoflurane. Both ovaries were removed in animals in the OVX group, and animals in the sham groups did not undergo removal of the ovaries and received the same stress. During the surgery, the isoflurane concentration was adjusted to 2–3%. After wound closure, the animals received intraperitoneal administration of gentamicin (4 mg/kg) for 3 postsurgical days.

Afterward, the animals were randomized into the following six groups (n = 8 each): sham group (sham operation; oral administration of deionized water (D.W)), OVX group (OVX-induced; oral administration of D. W), E_2 group (OVX-induced; oral administration of 100 μg/kg E_2), ALN group (OVX-induced; oral administration of 3 mg/kg ALN), SR-L group (OVX-induced; oral administration of 4.92 mg/kg SR) and SR-H group (OVX-induced; oral administration of 31.48 mg/kg SR). Doses for SR-L and SR-H were calculated based on the following theory: according to Korean medicine, a single dose of 8 g is recommended based on an average adult weight of 60 kg. Therefore, SR required 4.92 mg/kg. The animals in the SR-L group were treated with 4.92 mg/kg. Rats are known to have a metabolism 6.4 times faster than humans (Tschop et al., 2011; Nair and Jacob, 2016) Based on these results, the SR-H group was treated with a concentration 6.4 times higher than that of the SR-L group. Therefore, the SR-H group was treated with 31.48 mg/kg. E_2, ALN and SR were dissolved in vehicle administered for 8 weeks, and animal weight was measured once a week. The humanitarian termination points were as follows: 1) weight loss of more than 20% compared to that of the other rats; 2) difficulty eating due to uncomfortable walking; 3) severe infection and bleeding at the surgical site; 4) vomiting and hemoptysis; no animals exhibited abnormal behavior during the experiment. After 8 weeks, the rats were anesthetized with 100% oxygen and 5% isoflurane. For all animal sacrifices, lethal cardiac puncture up to 10 ml was performed (Beeton et al., 2007). After confirming that the heart had completely stopped, we performed cervical dislocation. Then, uterine samples were collected. We fixed the femur samples in 10% neutral buffered formalin (NBF). Blood samples were collected from the SD rats after sacrifice and centrifuged at 29,739 xg for 10 min.

Serum Levels of TRAP, ALP, AST and ALT

The extracted blood was stored at room temperature for 15 min and then centrifuged at 29,739 xg for 10 min to separate the

serum. The blood sample was stored at −4°C until the experiment. Serum TRAP activity was assessed in the same manner as described in a previous experimental method, and the serum expression of alkaline phosphatase (ALP), aspartate aminotransferase (AST) and alanine transferase (ALT) were performed by DKkorea (Seoul, Korea).

Micro-CT Analysis

The femurs were analyzed with a microcomputed tomography (micro-CT, SkyScan1176, Skyscan, Kontich, Belgium) system. The scanning parameters were set as follows: a 50 kV/200 μA, 8.9 μm pixels, an aluminum (Al) filter of 0.5 mm, and a 180° rotation angle with rotation steps of 0.4°. Bone microstructure, such as bone mineral density (BMD), trabecular bone volume (BV/TV), trabecular thickness (Tb.Th), trabecular number (Tb.N) and trabecular separation (Tb.sp), was analyzed with NRecon software (SkyScan version 1.6.10.1; Bruker Corporation, Billerica, MA).

Hematoxylin and Eosin (H&E) Staining, TRAP Staining and Masson-Goldner's Trichrome Staining

The femurs were decalcified with 10% ethylenediaminetetraacetic acid (EDTA) for 3 weeks, embedded in paraffin, and then sectioned using a microtome (5 μm-thick; Carl Zeiss AG). Tissue sections were mounted on a slide dryer for 1 day. H&E staining was performed to measure the trabecular area. The trabecular areas were captured in H&E-stained sections under a light microscope (Olympus Corporation, magnification, ×100) and its was measured with ImageJ version 1.46. To confirm the bone resorption and bone formation parameters in femoral tissues, we stained them using the TRAP and masson-goldner's trichrome staining kit according to the manufacturer's protocol. The stained tissues were captured under a light microscope (Olympus Corporation, magnification, ×100 and ×200). Bone resorption parameters such as osteoclast surface per bone surface (Oc.S/BS) and osteoclast number per bone surface (Oc.N/BS) and bone formation parameters such as Osteoblast surface per bone surface (Ob.S/BS), the osteoblast number per bone surface (Ob.N/BS) were measured with ImageJ version 1.46.

Immunohistochemical (IHC) Staining

For analysis of IHC staining, the tissues were deparaffinized by xylene. In addition, 0.3% hydrogen peroxide was used for 15 min to block endogenous peroxidase. Proteinase K (0.4 mg/ml) was used for antigen retrieval at 37°C for 30 min. After washes in PBS, section tissues were incubated with normal serum for 1 h and incubated with primary antibodies against CTK (1:100), NFATc1 (1:100) and BMP-2 (1:100) at 4°C overnight. Then, the tissues were washed with PBS and incubated with secondary antibodies for 1 h. The tissues were incubated with an ABC kit for 30 min, and the reaction was visualized with DAB solution. Counterstaining was performed with hematoxylin. The positive area was captured in the IHC staining sections under a light microscope (Olympus Corporation, magnification, ×100 and ×200).

Liquid Chromatography–Mass Spectrometry (LC-MS) Analysis

Kaempferol (HPLC purity>97%; cat. no. 60010; Sigma-Aldrich; Merck KGaA) is a well-known flavonoid compound in SR (Wang et al., 2012; Wang et al., 2013). A Waters e2695 system (Milford, MA, United States) equipped with an ACQUITY QDa Detector was used to analyze the sample and kaempferol. Separation was performed on an Xbridge-C18 with a C18 guard column (250 × 4.6 mm; 5 μm; Waters Corporation). The mobile phase consisted of acetonitrile (A) and H_2O with 1% acetic acid (B) and was run at 25°C for 40 min at a flow rate of 0.4 ml/min. The system was run with a gradient program: 0–40 min, 5–80% B. The sample injection volume was 10 μL. The mass spectrometer was fitted to an atmospheric pressure electrospray ionization (ESI) source operated in positive ion mode. The electrospray capillary voltage was set to 0.8 kV, and the cone voltage was 15 V. MS data were acquired in scan mode (mass range m/z 150–650).

Statistical Analyses

All quantitative data are presented as the mean ± SD values of three experiments. Differences between the control and treatment groups were analyzed using one-way ANOVA after Dunnett's post hoc tests. Statistical significance was considered at $p < 0.05$. Statistical analysis was performed using GraphPad PRISM (version 5.01, GraphPad Software, Inc., San Diego, United States).

RESULTS

Sparganii Rhizoma Decreased the Number of TRAP-Positive Cells and TRAP Activity

To confirm the viability of RAW 264.7 cells, we performed a CCK-8 assay. RAW 264.7 cells were treated with SR (125, 250, 500, 1,000 μg/ml) for 24 h, and the viability of RAW 264.7 cells was not affected after SR treatment. Then, to verify the cell viability in osteoclasts, we performed a CCK-8 assay. RAW 264.7 cells were treated with RANKL (100 ng/ml) and SR (125, 250, 500, 1,000 μg/ml) for 5 days, and the viability of osteoclasts was not affected after SR treatment. These results indicate that the osteoclast inhibitory effect of SR is not due to toxicity (**Figures 1A,B**). We conducted osteoclast experiments, as shown in **Figure 1C**. To examine the effect of SR on osteoclast differentiation in RAW 264.7 cells, we conducted TRAP staining and TRAP activity assays. As shown in **Figures 1D,E**, when only RANKL was added to RAW 264.7 cells, the number of multinucleated TRAP-positive cells stained red was increased. However, in the SR-treated cells, the number of multinucleated TRAP-positive cells stained red was decreased in a dose-dependent manner. In addition, TRAP activity in the differentiation medium was significantly decreased by SR treatment (**Figure 1F**).

Sparganii Rhizoma Reduced the Pit Area for Bone Resorption of the F-Actin Ring for Osteoclast Cytoskeletal Structure

To determine the effect of SR on bone resorption, we assessed the pit formation. As shown in **Figure 2A**, when only RANKL was

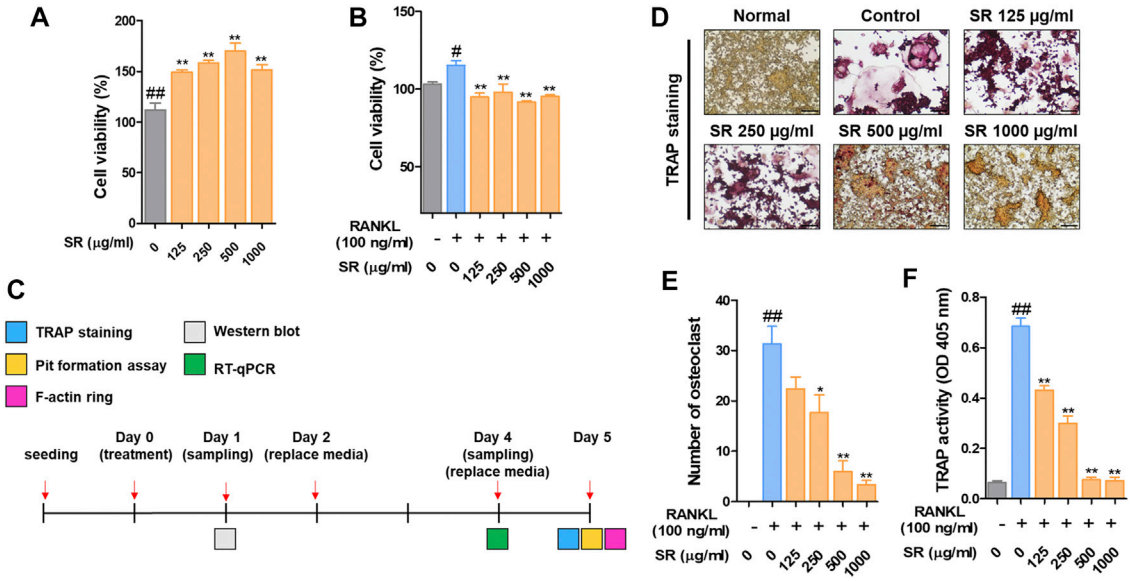

FIGURE 1 | The effects of SR on osteoclast differentiation and bone resorption in RANKL-induced RAW 264.7 cells. **(A)** RAW 264.7 cell viability was measured using a CCK-8 assay kit. **(B)** The effects of SR (0, 125, 250, 500, 1,000 μg/ml) on the viability of osteoclasts induced by RANKL using a CCK-8 assay kit. **(C)** *In vitro* experimental design to investigate the effect of SR on osteoclast differentiation. **(D)** TRAP-positive cells were stained using a TRAP kit. **(E)** A number of TRAP-positive cells with >3 nuclei were counted using an inverted microscope (magnification, ×100). **(F)** TRAP activity was measured using an ELISA reader. Data are presented as the mean ± SD of three independent experiments. Statistical analysis was performed using one-way ANOVA followed by Dunnett's post hoc test. $^{\#}p < 0.05$, $^{\#\#}p < 0.01$ vs. the normal group (untreated cells); $^{*}p < 0.05$, $^{**}p < 0.01$ vs. the RANKL only treatment group.

added to RAW 264.7 cells, the pit area was increased compared with that of the nontreated cells. However, in the SR-treated cells, the pit area was considerably decreased in a dose-dependent manner. Afterward, we examined F-actin ring formation. The F-actin ring was considerably increased in the RANKL-treated cells compared with the nontreated cells, and the F-actin ring was decreased in the SR-treated cells (**Figure 2B**). Consistent with these results, the SR-treated cells had a significantly decreased pit area and number of F-actin rings. SR was shown to have a significant inhibitory effect on the bone resorption and F-actin ring formation (**Figures 2C,D**).

Sparganii Rhizoma Decreased the Expression of TRAF6/NF-κB/MAPK Signaling Pathway

After demonstrating the inhibitory effect of SR on osteoclast differentiation, the role of SR on TRAF6/NF-κB signaling/MAPK signaling, an early transcription factor in osteoclast differentiation, was confirmed. As shown in **Figures 3A,B**, the expression of TRAF6 was significantly increased due to RANKL stimulation, and SR inhibited this increase. In addition, SR significantly inhibited nuclear translocation and phosphorylation of NF-κB and phosphorylation of IκB through RANKL stimulation and SR reduced the degradation of IκB induced by RANKL, but the difference was not significant. As presented in **Figures 3C,D**, RANKL stimulation significantly increased phosphorylation of ERK, JNK and p38, and SR significantly inhibited this increase.

Sparganii Rhizoma Inhibited Transcription Factors Related to Osteoclast Differentiation

To determine the expression of the transcription factors involved in the osteoclast differentiation effect of SR, we measured the expression levels of NFATc1 and c-Fos by western blots and RT-PCR. As shown in **Figure 4A**, after RANKL treatment, the protein expression of NFATc1 and c-Fos was increased; by comparison, the expression of NFATc1 and c-Fos was decreased by SR treatment. As a result of quantification using β-actin, the protein expression of NFATc1 and c-Fos was shown to be reduced upon SR treatment compared with RANKL treatment, consistent with the visual results (**Figure 4B**). In the RANKL treatment group, the mRNA expression of *Nfatc1* and *Fos* was increased compared to that in the nontreatment group. However, in the SR treatment group, the mRNA expression of *Nfatc1* and *Fos* declined dramatically compared to that in the RANKL treatment group (**Figure 4C**). As a result of quantification using *Actb*, the mRNA levels of *Nfatc1* and *Fos* were found to decrease upon SR treatment compared to those of the RANKL treatment group, consistent with the visual results (**Figure 4D**).

Sparganii Rhizoma Suppressed the Expression of Osteoclast-Related Genes

Matrix metalloproteinase-9 (MMP-9) is known as a factor related to osteoclast bone resorption. To determine the effect of SR on the expression of MMP-9, we performed Western blotting and RT-PCR. As shown in **Figures 5A,B**, after RANKL treatment, the

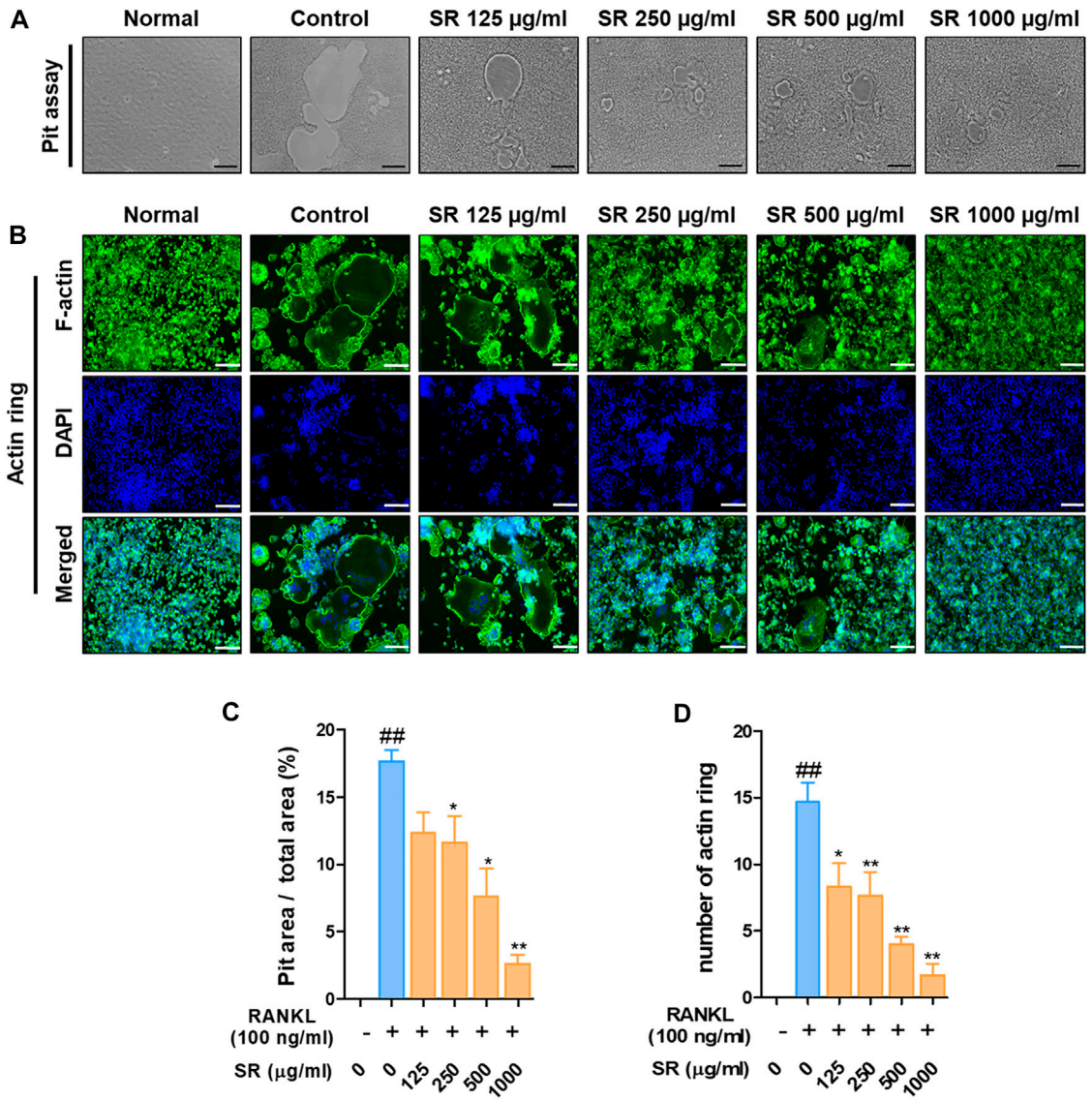

FIGURE 2 | The effects of SR on bone resorption and F-actin ring formation in RANKL-induced RAW 264.7 cells. **(A)** Pit formation was captured using an inverted microscope (magnification, ×100; scale bar, 200 μm). **(B)** F-actin rings were stained with fluorescent phalloidin (magnification, ×100; scale bar, 200 μm). **(C)** The pit area was measured using ImageJ software. Data are presented as the mean ± SD (standard error of the mean) of three independent experiments. **(D)** The number of F-actin rings was counted. Data are presented as the mean ± SD of three independent experiments. Statistical analysis was performed using one-way ANOVA followed by Dunnett's post hoc test. $^{\#\#}p < 0.01$ vs. the normal group (untreated cells); $^{*}p < 0.05$, $^{**}p < 0.01$ vs. the RANKL only treatment group.

protein and mRNA expression of MMP-9 was increased; by comparison, the expression of MMP-9 was decreased by SR treatment. To determine the effect of SR on the expression of osteoclast-related genes, which are bone resorption and osteoclast differentiation markers, we performed RT-PCR. As shown in **Figure 5C**, after RANKL treatment, the mRNA expression of osteoclast-related genes, such as RANK (*Tnfrsf11a*), TRAP (*Acp5*), carbonic anhydrase II (CA2/*Ca2*), osteoclast-associated receptor (OSCAR/*oscar*), ATPase H+ transporting v0 subunit d2 (ATP6v0d2/*Atp6v0d2*) and dendritic cell-specific transmembrane protein (DC-STAMP/*Dcstamp*), was increased, while the mRNA expression of osteoclast-related genes was considerably decreased by SR treatment. As a result of quantification using *Actb*, the mRNA levels were found to increase after RANKL treatment, and the expression of osteoclast-related genes was decreased by SR treatment (**Figure 5D**).

Sparganii Rhizoma Significantly Increased Osteoblast Differentiation in MC3T3-E1 Cells

To investigate the underlying mechanisms by which SR increases osteoblast differentiation, we examined the effects of SR in MC3T3-E1 cells. In this study, we initially examined the effect

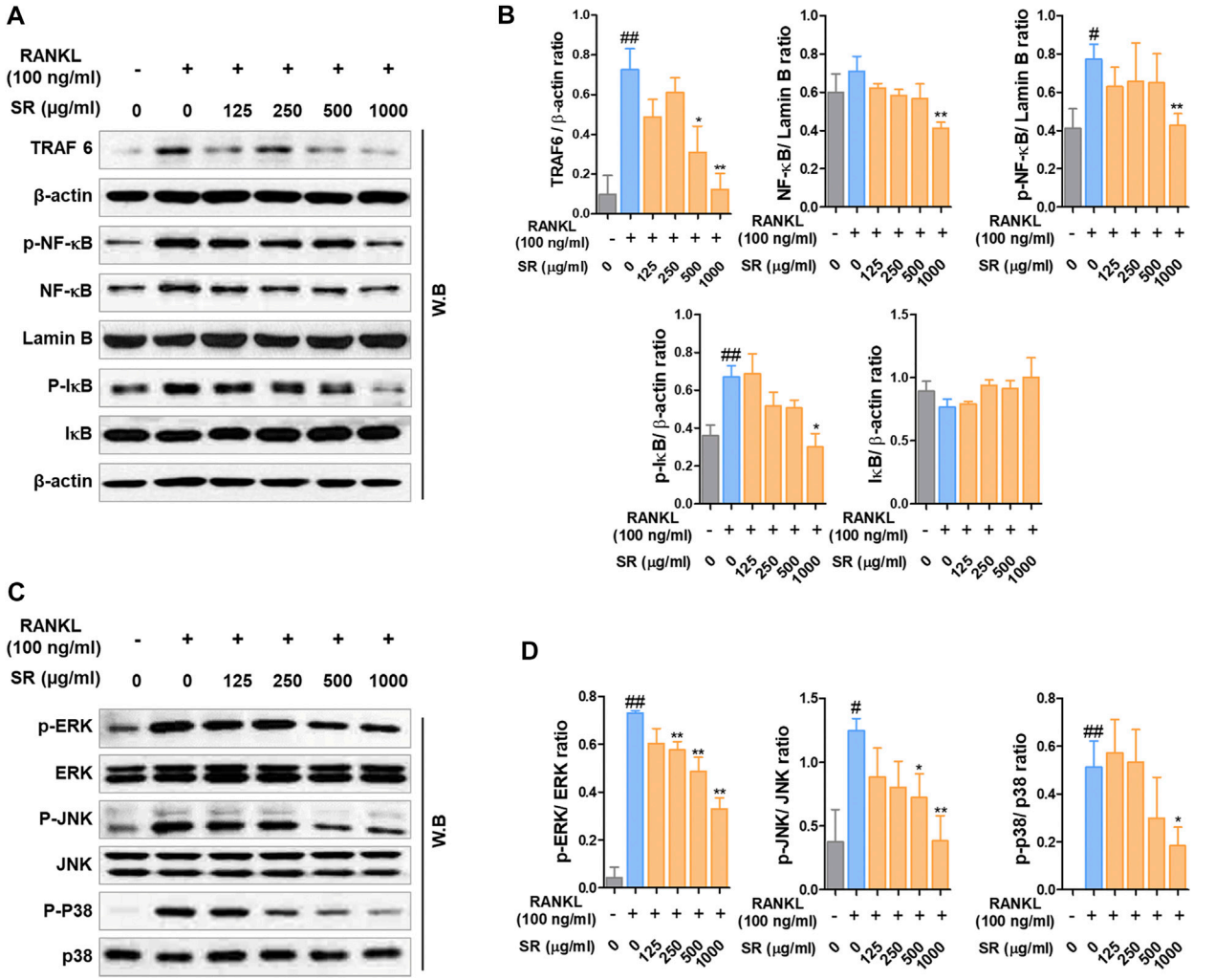

FIGURE 3 | The effects of SR on the expression of TRAF6, NF-κB and MAPK signaling pathway. **(A)** Protein expression levels of TRAF6, p-NF-κB, NF-κB, p-IκB and IκB were measured by western blotting. **(B)** TRAF6, p-IκB and IκB were normalized to that of β-actin, which was used as a loading control. p-NF-κB and NF-κB were normalized to that of Lamin B, which was used as a loading control. **(C)** Protein expression levels of p-ERK, p-JNK, p-p38 were measured by western blotting. The bands were normalized to that of ERK, JNK and p38. Data are presented as the mean ± SD of three independent experiments. Statistical analysis was performed using one-way ANOVA followed by Dunnett's post hoc test. $^{\#}p < 0.05$, $^{\#\#}p < 0.01$ vs. the normal group (untreated cells); $^{*}p < 0.05$, $^{**}p < 0.01$ vs. the RANKL only treatment group.

of SR treatment on MC3T3-E1 cell viability. The viability of MC3T3-E1 cells was not affected by treatment with SR for 3, 7 or 14 days (**Figure 6A**). Following 14 days of osteoblast differentiation, calcified nodules were formed at an earlier stage in the SR treatment group than in the osteogenic medium treatment group. Following 21 days of osteoblast differentiation, calcified nodules were increased by treatment with osteogenic medium compared with those of the growth medium treatment group. In addition, SR at concentrations of 100 and 200 μg/ml resulted in significantly increased calcified nodules compared with those of the osteogenic medium treatment (**Figure 6B**). Moreover, the absorbance of Alizarin Red S staining dye was significantly increased by SR treatment in a dose-dependent manner after 14 and 21 days compared with that of the osteogenic medium treatment group (**Figure 6C**). Afterward, the effect of SR on the osteoblast differentiation pathway at the protein level was verified. Therefore, as shown in **Figures 6D,E**, SR upregulated the protein expression of BMP-2, RUNX2 and Osterix and p-SMAD 1/5.

Change in Body and Uterine Weight and Serum Levels of TRAP, ALP, AST, and ALT

To investigate the effect of SR on the OVX-induced model, we orally administered SR to rats for 8 weeks. After 2 weeks, the OVX-induced group had an increased body weight compared with the sham group. In addition, the weight was not significantly different in the E_2, ALN, SR-L and SR-H groups compared to the OVX group (**Figure 7A**). As shown in **Figure 7B**, uterine weight was significantly reduced in the OVX group compared with the sham group. The E_2 group had

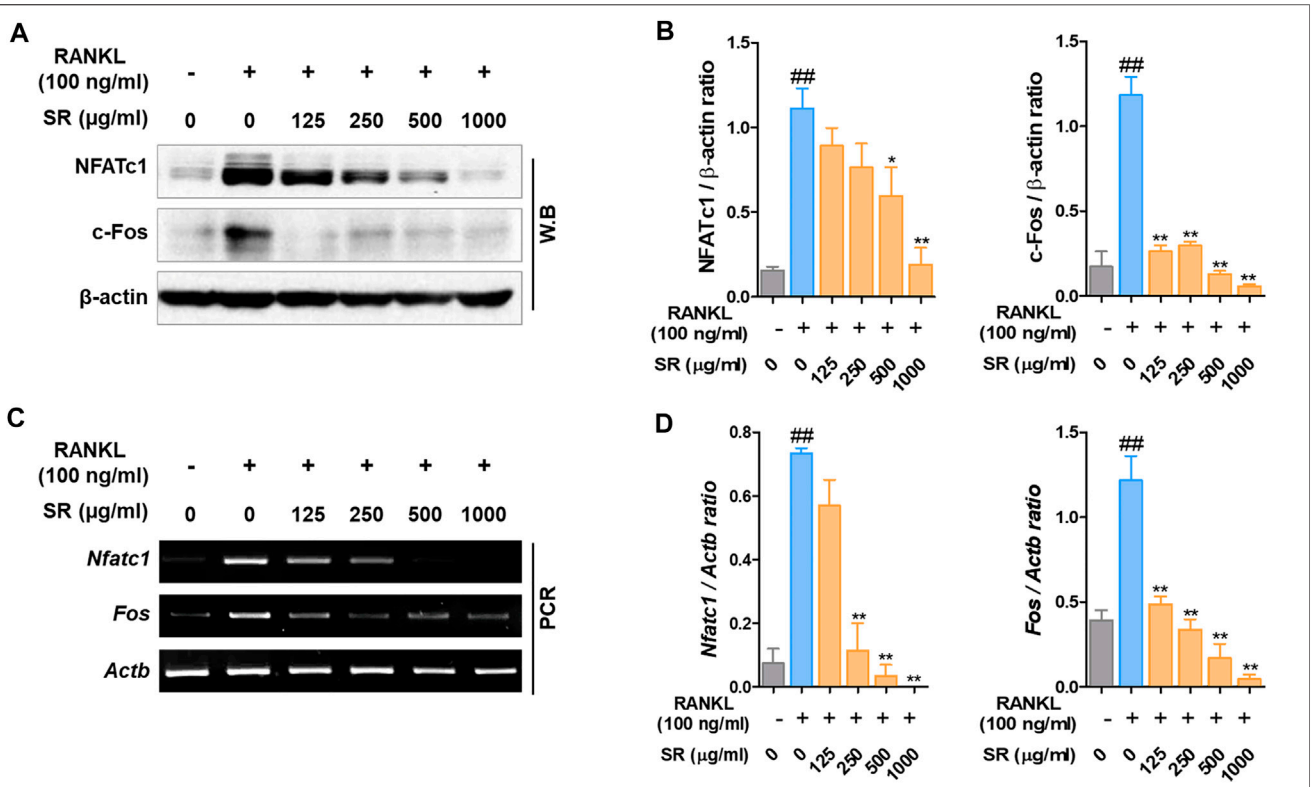

FIGURE 4 | The effects of SR on NFATc1 and c-Fos levels in RAW 264.7 cells. **(A)** Protein expression levels of NFATc1 and c-Fos were measured by western blotting. **(B)** The bands were normalized to that of β-actin, which was used as a loading control. **(C)** mRNA expression levels in *Nfatc1* and *Fos* were measured by RT-PCR. The bands were normalized to that of β-actin (*Actb*). Data are presented as the mean ± SD of three independent experiments. Statistical analysis was performed using one-way ANOVA followed by Dunnett's post hoc test. $^{\#\#}p < 0.01$ vs. the normal group (untreated cells); $^{*}p < 0.05$, $^{**}p < 0.01$ vs. the RANKL only treatment group.

decreased uterine weight, but the ALN, SR-L and SR-H groups did not show changes. Next, to determine the effect of SR on the levels of TRAP, ALP, AST, and ALT in serum, we performed ELISAs. After 8 weeks, the levels of TRAP were significantly decreased in the SR-H group. However, TRAP activity was unchanged in the E_2, ALN and SR-L groups (**Figure 7C**). The ALP levels were increased in the OVX-induced group compared with the sham group. The ALP levels were significantly decreased in the SR-L group and not significantly decreased in the E_2, ALN, and SR-H groups, but the ALP levels were decreased compared to those in the sham group (**Figure 7D**). To investigate hepatotoxicity by SR treatment, we analyzed AST and ALT as indicators of hepatotoxicity. The E_2, ALN and SR-L groups did not show hepatotoxicity compared with the OVX group, and the SR-H group had decreased levels of AST. In addition, the levels of ALT did not affect the E_2, ALN and SR-H groups. However, the levels of ALT were reduced in the SR-L group (**Figures 7E,F**).

Sparganii Rhizoma Prevents Bone Loss in the OVX-Induced Model

To confirm the change in bone metabolism in the OVX-induced model, we examined the femur using micro-CT. In the sagittal images, bone loss increased in the OVX group compared to the sham group. However, bone loss was decreased in the E_2, ALN, SR-L, and SR-H groups. The same result was found in the cross-sectional and 3D reconstruction images (**Figure 8A**). Next, we explored the effect of SR in bone microarchitecture. BMD, BV/TV and Tb.Th were significantly decreased in the OVX group compared with the sham group. The E_2, ALN, and SR groups had considerably increased BMD, BV/TV and Tb.Th values compared to the OVX group (**Figures 8B–D**). Tb. sp was significantly increased in the OVX group compared to the sham group, and the E_2, ALN and SR groups had decreased Tb. sp values compared to the OVX group (**Figure 8E**).

Sparganii Rhizoma Suppressed Trabecular Bone Loss and Osteoclast Formation and Increased Osteoblast Differentiation

To further verify the effect of SR on OVX-induced bone loss, we used histological staining by H&E staining. The results showed that trabecular bone loss was significantly increased in the OVX group compared with the sham group. However, trabecular bone loss was decreased in the E_2, ALN and SR groups compared with the OVX group (**Figures 9A,D**). We performed TRAP staining and masson-goldner's trichrome staining to measure the expression of

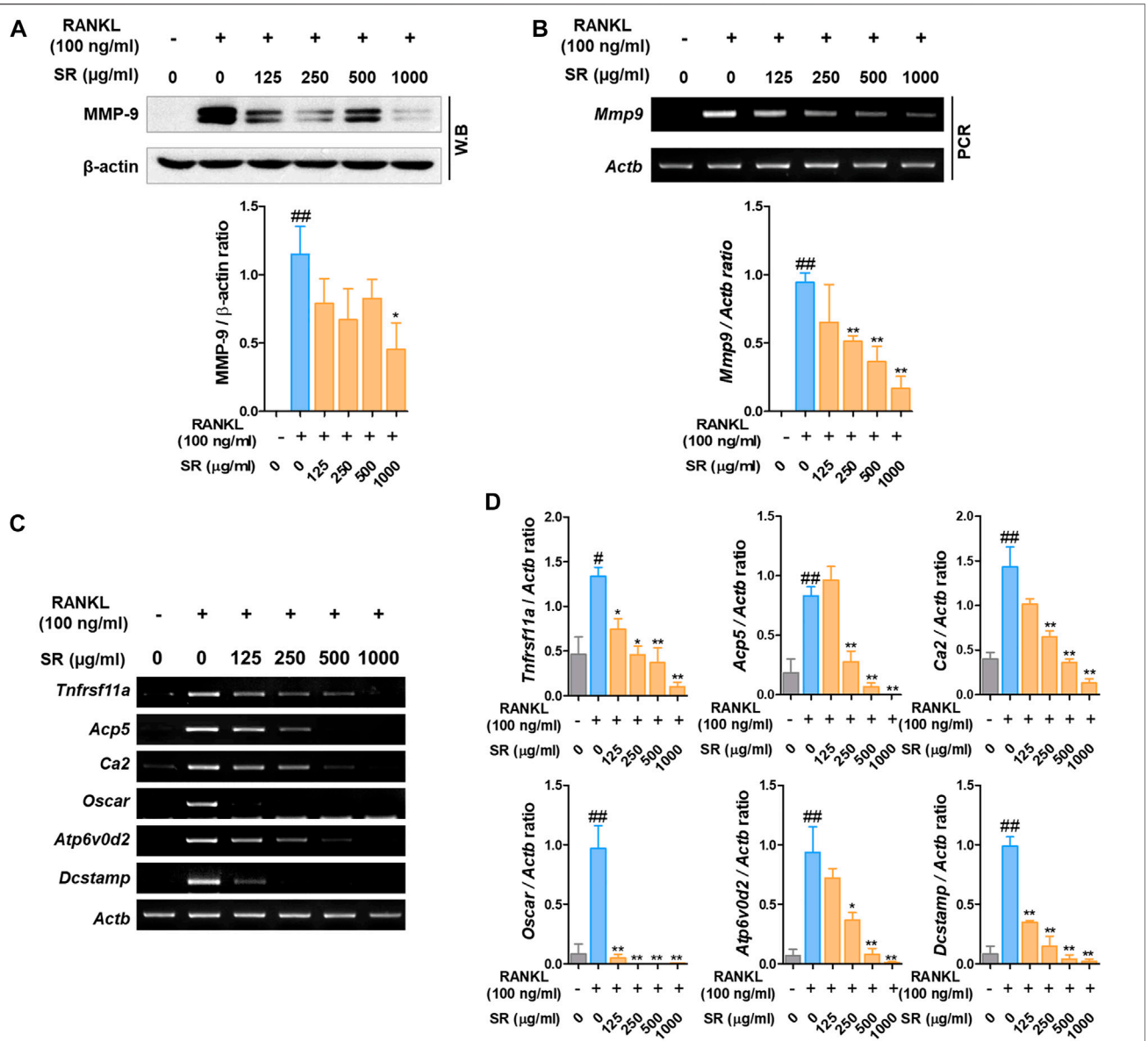

FIGURE 5 | The effects of SR on the expression of osteoclast-related genes in RANKL-induced RAW 264.7 cells. **(A)** Protein expression of MMP-9 was determined using Western blotting and **(B)** mRNA expression of MMP-9 (*Mmp9*) was determined using RT-PCR. The bands were normalized to that of β-actin (*Actb*). **(C)** mRNA expression of RANK (*Tnfrsf11a*), TRAP (*Acp5*), CA2 (*Ca2*), OSCAR (*Oscar*), ATP6v0d2 (*Atp6vod2*) and DC-STAMP (*Dcstamp*) was determined using RT-PCR. **(D)** The bands were normalized to that of β-actin (*Actb*). Data are presented as the mean ± SD of three independent experiments. Statistical analysis was performed using one-way ANOVA followed by Dunnett's post hoc test. $^{\#}p < 0.05$, $^{\#\#}p < 0.01$ vs. the normal group (untreated cells); $^{*}p < 0.05$, $^{**}p < 0.01$ vs. the RANKL only treatment group.

osteoclasts and osteoblasts in the femoral tissue, respectively. In addition, the surface and number of TRAP-positive cells in the OVX group increased compared to the sham group, and the surface and number of TRAP-positive cells in the E_2, ALN and SR groups decreased compared to the OVX group (**Figures 9B,E,F**). Also, the surface and number of osteoblasts was decreased in the OVX group compared to the sham group, and the surface and number of osteoblasts was increased in the E_2, ALN and SR groups compared to the OVX group (**Figures 9C,G,H**).

Sparganii Rhizoma Decreased the Number of CTK- and NFATc1-Positive Cells and Increased the Number of BMP2-Positive Cells

To determine the effect of SR on the number of CTK, NFATc1 and BMP-2 cells, we performed IHC staining. The number of CTK- and NFATc1-positive cells in the OVX group was notably higher than that in the sham group (**Figures**

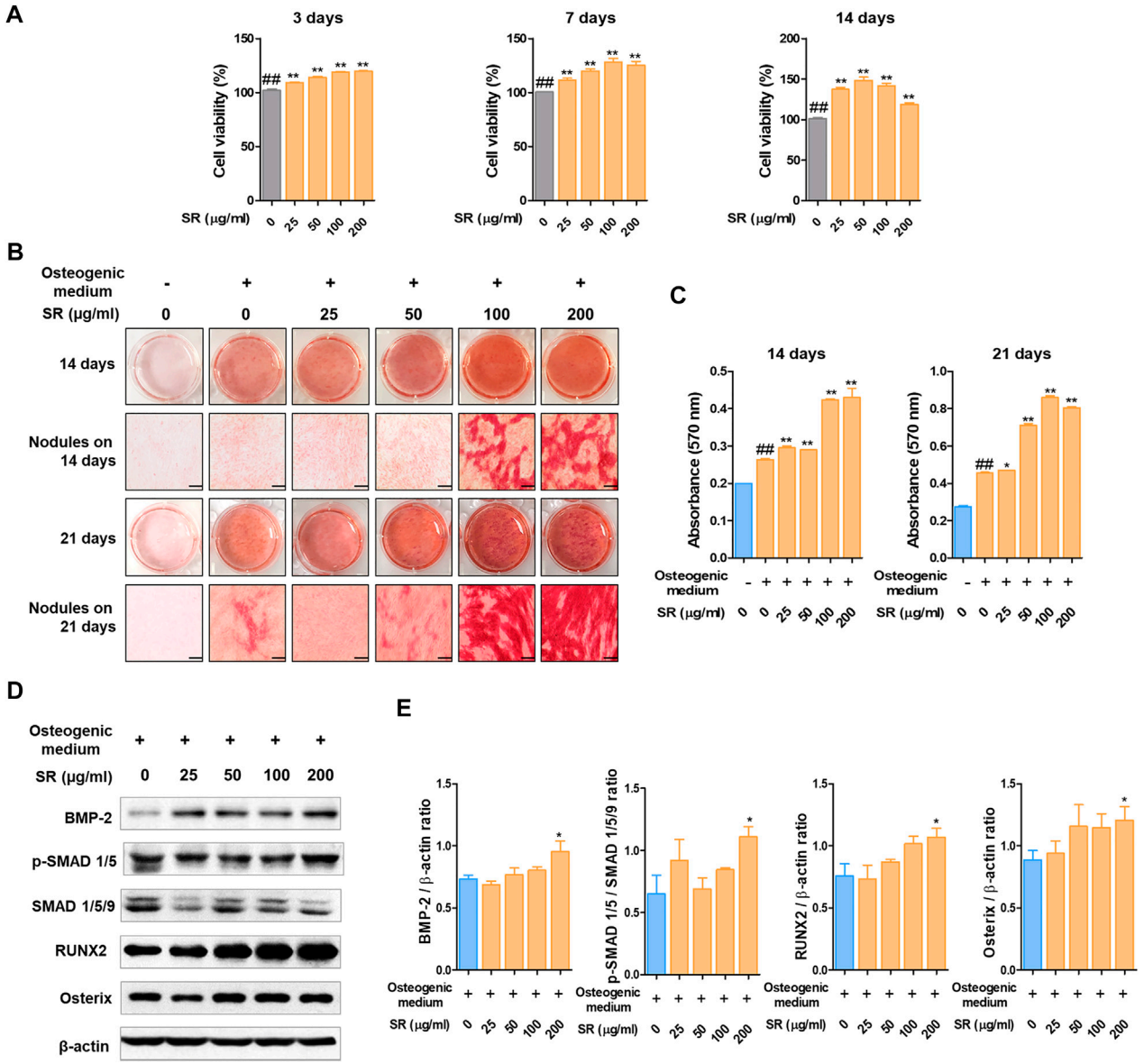

FIGURE 6 | The effects of SR on osteoblast differentiation. **(A)** MC3T3-E1 cell viability was analyzed by CCK-8 assays at 3, 7 and 14 days. **(B)** Calcified nodules produced by osteoblasts were stained with Alizarin Red S for 14 and 21 days. **(C)** The absorbance of Alizarin Red S staining dye was measured using an ELISA reader at 450 nm. **(D)** Protein expression levels of BMP-2, p-Smad 1/5, RUNX-2 and Osterix were measured by western blotting. **(E)** BMP-2, RUNX-2 and Osterix levels were normalized to that of β-actin. p-Smad 1/5 levels was normalized to that of Smad 1/5/9. Data are presented as the mean ± SD of three independent experiments. Statistical analysis was performed using one-way ANOVA followed by Dunnett's post hoc test. $^{\#\#}p < 0.01$ vs. the normal group (untreated cells); $^{*}p < 0.05$, $^{**}p < 0.01$ vs. the osteogenic medium-treated cells.

10A,B). However, the number of CTK- and NFATc1-positive cells was considerably reduced in the E_2, ALN and SR groups (**Figures 10D,E**). The number of BMP-2-positive cells in the OVX group was significantly decreased than that in the sham group. However, the number of BMP-2-positive cells was significantly increased in the E_2, ALN and SR groups (**Figures 10C,F**).

Identification of Kaempferol as an *Sparganii Rhizoma* Component

To determine the quality of SR, we conducted LC/MS analysis by measuring the content of a well-known compound of SR, kaempferol. Similar to the peaks of kaempferol, SR extract samples were detected at the same retention times, and kaempferol was identified as a component in the SR extract (**Figures 11A,B**).

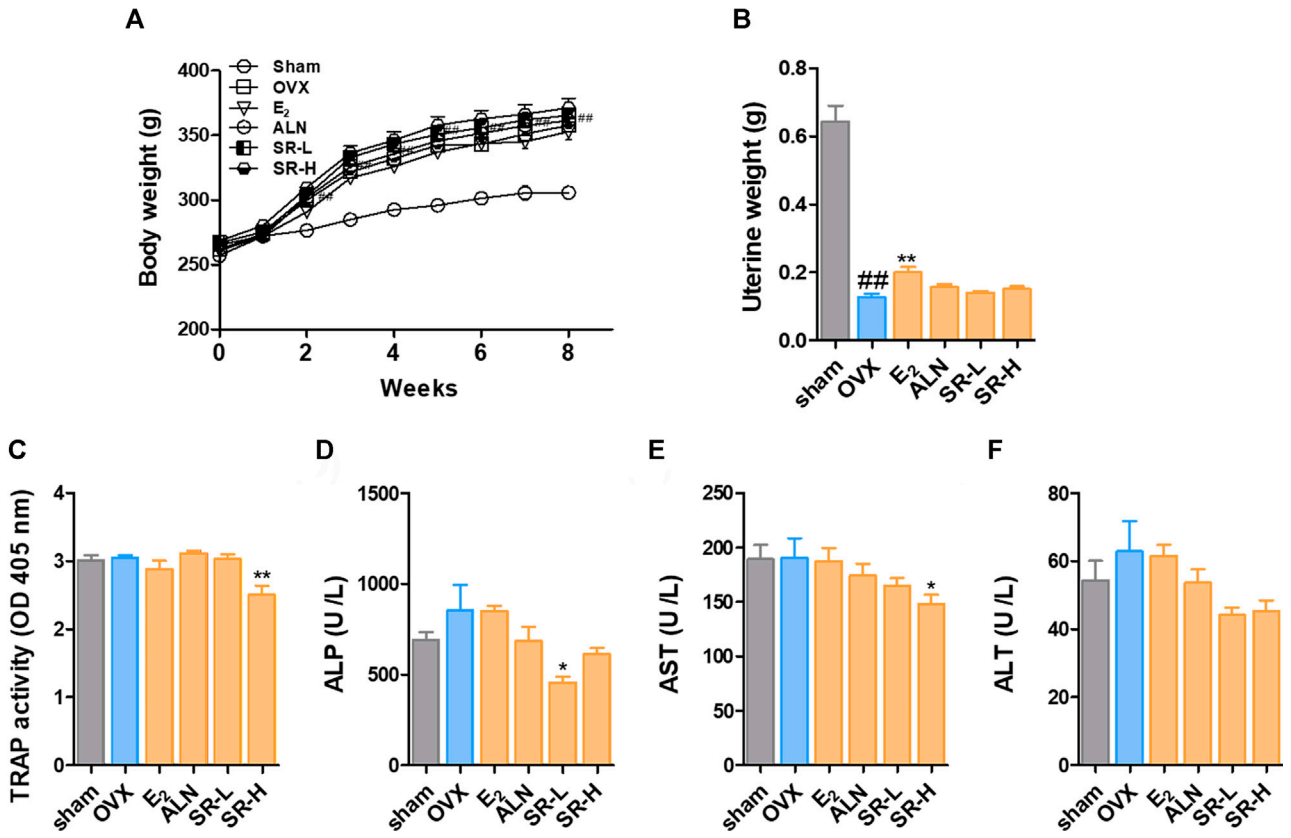

FIGURE 7 | Change in body weight and serum levels of TRAP, ALP, AST and ALT in the OVX model. **(A)** Body weight was measured once a week for 8 weeks. **(B)** The uterine weight was measured after sacrifice. The serum levels of **(C)** TRAP, **(D)** ALP, **(E)** AST, and **(F)** ALT were measured using an ELISA reader. The results are presented as the mean ± SEM of each experimental group (n = 8). Statistical analysis was performed using one-way ANOVA followed by Dunnett's post hoc test. $^{\#}p < 0.05$, $^{\#\#}p < 0.01$ vs. the normal group (sham-operation group); $^{*}p < 0.05$, $^{**}p < 0.01$ vs. the control group (OVX-induced group).

Comparison of Effects of *Sparganii Rhizoma* and Kaempferol on Osteoclasts and Osteoblasts

The positive results of kaempferol on osteoclasts and osteoblasts have been reported in various previous studies (Guo et al., 2012; Kim et al., 2018). In order to confirm whether the pharmacological effect of SR is dependent on kaempferol, the main component, we conducted osteoclast and osteoclast experiments based on the concentration of kaempferol contained in SR. Based on the LS-MS data, the content of kaempferol in 1 g of SR was 0.419 mg. Therefore, the amount of kaempferol contained in 1,000 μg/ml SR is 419 ng/ml, and the amount of kaempferol contained in 200 μg/ml SR is 83.8 ng/ml. As shown in **Figures 12A–C**, SR inhibited the differentiation and activity of osteoclasts as in the previous experimental results, but kaempferol had no effect on the number of osteoclasts and TRAP activity in the medium. The concentrations of SR and Kaempferol in the osteoclast experimental did not show cytotoxicity (**Figure 12D**). Protein expression of NFATc1/c-Fos also strongly inhibited SR, but kaempferol had no significant effect (**Figures 12E,F**). The concentrations of SR and kaempferol in the osteoblast experimental did not show cytotoxicity (**Figure 12G**). SR showed a significant increase in the expression of BMP-2, p-SMAD1/5, RUNX2 and Osterix, which are key factors for osteoblast differentiation, but kaempferol did not show a significant effect on the expression of these proteins. These results indicate that the concentration of kaempferol contained in SR does not have a significant effect on osteoclasts and osteoblasts. In addition, it means that the pharmacological effect of SR is not mediated by kaempferol, but is a comprehensive effect of various components constituting SR. Therefore, this study is considered to be different from the existing studies on kaempferol.

DISCUSSION

Osteoporosis is caused by an imbalance in bone remodeling. Therefore, it is important to inhibit the activity of osteoclasts or increase the activation of the differentiation of osteoblasts (Feng and McDonald, 2011). This study used two cell lines to evaluate the effects of SR on osteoclasts and osteoblasts. RAW 264.7 cells are derived from mouse monocytes/macrophages and are suitable for establishing an osteoclast differentiation model. MC3T3-E1 cells

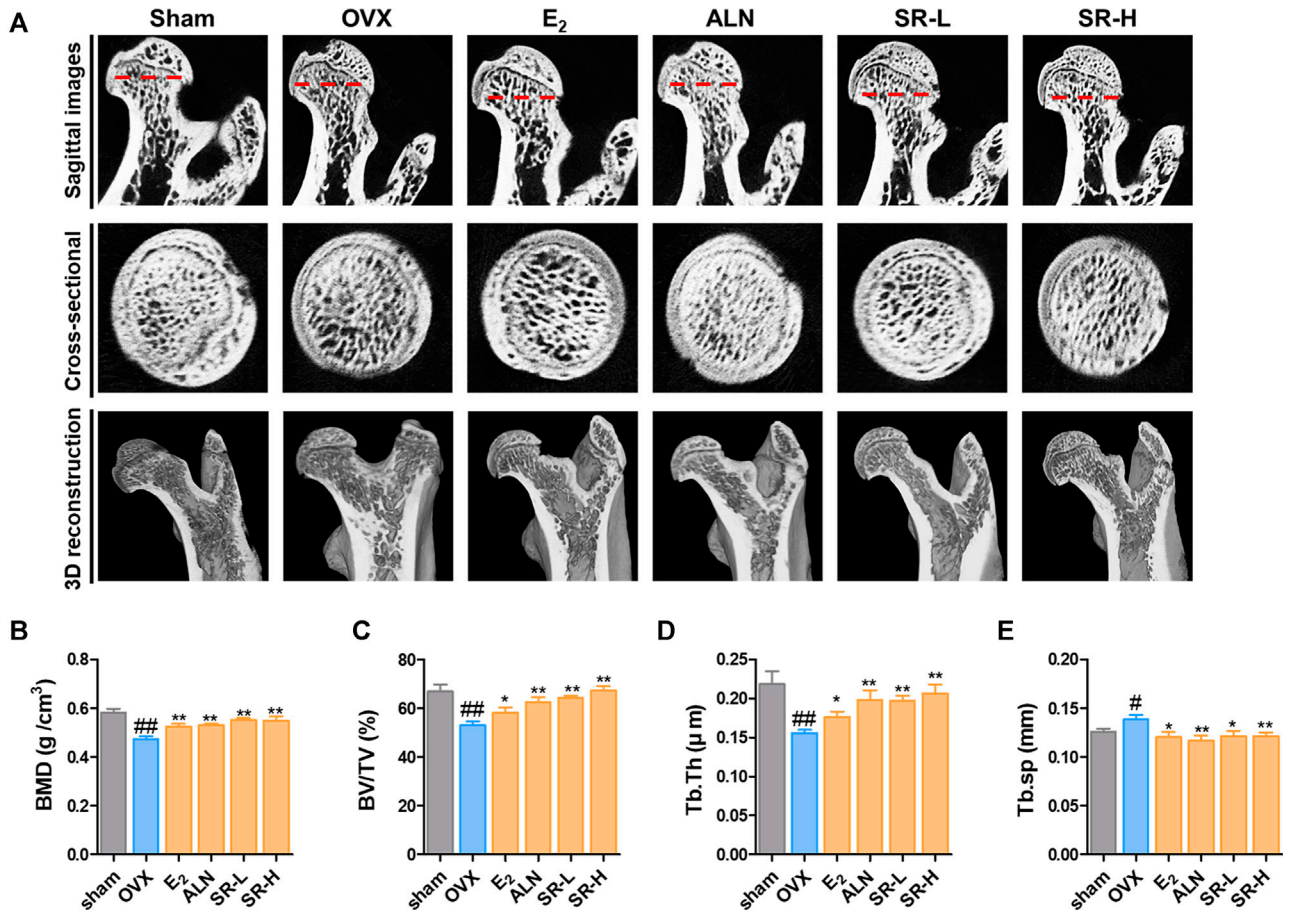

FIGURE 8 | Effects of SR on bone loss in the OVX-induced model. **(A)** Micro-CT analysis of the femurs. **(B)** BMD, **(C)** BV/TV, **(D)** Tb.Th and **(E)** Tb. sp of femurs were measured using micro-CT. The results are presented as the mean ± SEM of each experimental group (n = 8). Statistical analysis was performed using one-way ANOVA followed by Dunnett's post hoc test. $^{\#}p < 0.05$, $^{\#\#}p < 0.01$ vs. the normal group (sham-operation group); $^{*}p < 0.05$, $^{**}p < 0.01$ vs. the control group (OVX-induced group).

are osteoblast precursor cell lines derived from mouse calvaria. Experimental results *in vitro* demonstrated that SR inhibited osteoclast differentiation via the NFATc1/c-Fos signaling pathway. In addition, SR increased osteoblast differentiation via an upregulated BMP-2/RUNX-2 signaling pathway. *In vivo*, SR also inhibited bone loss in the OVX-induced model (**Figure 13**).

RAW 264.7 cells originate from hematopoietic precursors of the monocyte/macrophage lineage (Teitelbaum and Ross, 2003; Hartley et al., 2008). RAW 264.7 cells are known to be suitable for *in vitro* studies of osteoclast formation and function (Teitelbaum and Ross, 2003). TRAP is an iron-containing enzyme common to bones and the immune system. In addition, TRAP has been used as a representative histochemical marker for osteoclasts (Ballanti et al., 1997; Boyle et al., 2003). Pit formation assays are commonly used to examine osteoclast differentiation and bone resorption ability (Marchisio et al., 1984; Bradley and Oursler, 2008). In the present study, we demonstrated that SR significantly decreased the number of osteoclasts and activity and significantly reduced the pit area. Osteoclasts induce skeletal formation during the bone resorption process and attach to the bone. Additionally, osteoclast actin is organized into one large ring to separate the extracellular space. The formation of the actin ring is an important marker for the bone resorption of osteoclasts (Marchisio et al., 1984; Matsubara et al., 2017). The results of the current study showed that SR significantly decreased F-actin formation in RANKL-induced osteoclasts. Taken together, these results suggest that SR suppresses osteoclast differentiation, formation and resorption.

RANK, like many TNFR family proteins, transduces biochemical signals following recruitment of intracellular adapter TNF receptor-associated factor (TRAF) proteins, and TRAF6 plays an essential role in RANKL-mediated NF-κB activation (Armstrong et al., 2002). Previous studies have shown that TRAF6 deficiency inhibits RANKL-induced JNK and p38 activation (Lomaga et al., 1999). NF-κB translocates to the nucleus via RANKL-RANK binding and plays an important role in the early stage of osteoclast differentiation (Grande et al., 2015). Previous studies have shown that mice deficient in NF-κB1 and NF-κB2 cannot differentiate into osteoclasts, leading to osteopetrosis (Iotsova et al., 1997). The

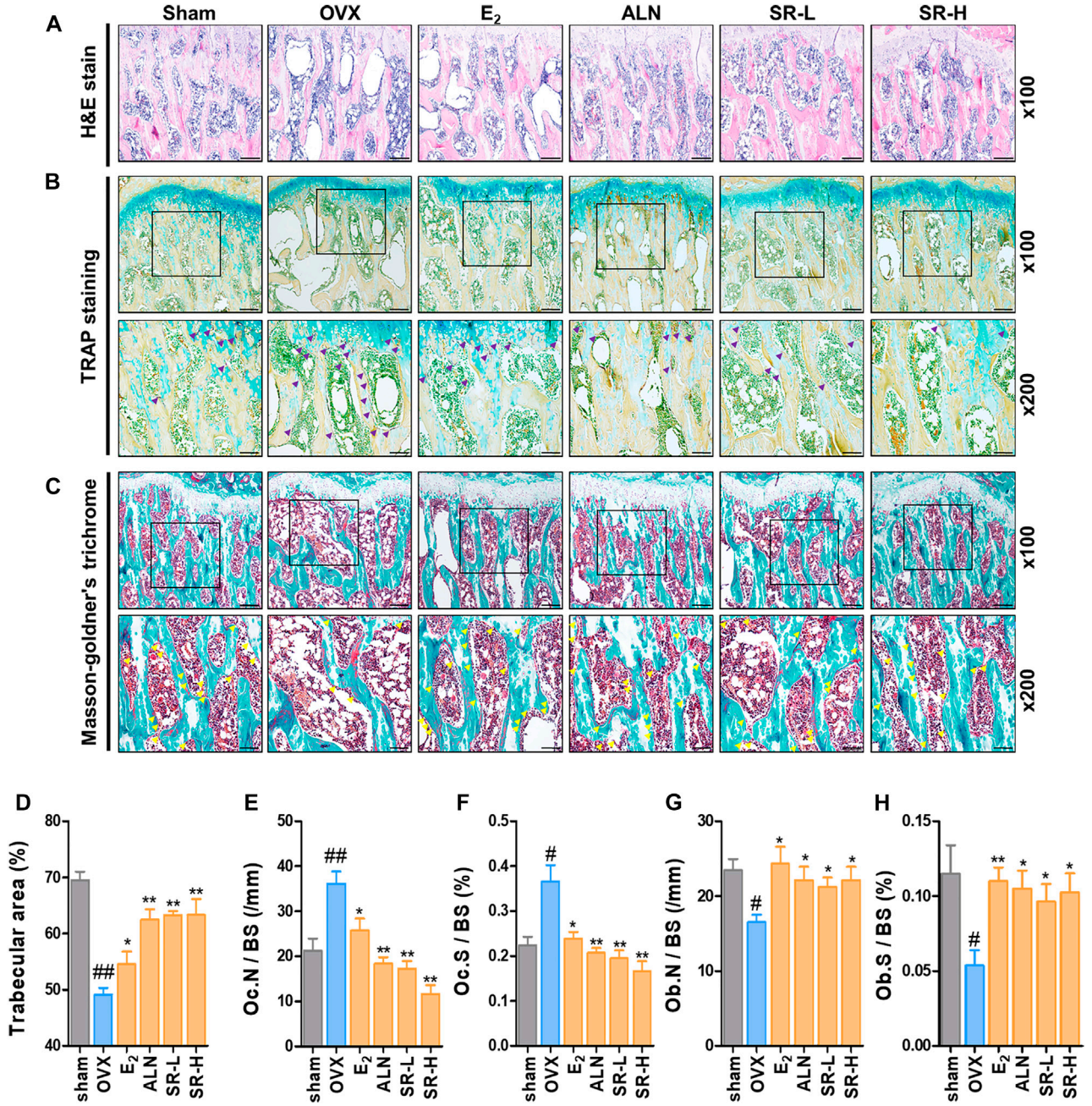

FIGURE 9 | Effect of SR on trabecular area, osteoclasts and osteoblast in the OVX-induced rats. **(A)** The trabecular area was measured using H&E staining of femur tissue. **(B)** The number of osteoclasts (purple) in the femoral tissue was verified through TRAP staining. **(C)** The number of osteoblasts (yellow) in the femoral tissue was measured through masson-goldner's trichrome staining. **(D)** Trabecular area, **(E)** Oc.N /BS (/mm). **(F)** Oc.S /BS (%). **(G)** Ob. N/BS and **(F)** Ob. S/BS were measured using ImageJ version 1.46. The results are presented as the mean ± SEM of each experimental group (n = 8). Statistical analysis was performed using one-way ANOVA followed by Dunnett's post hoc test. $^{\#\#}p < 0.01$, $^{\#}p < 0.05$ vs. the normal group (sham-operation group); $^{*}p < 0.05$, $^{**}p < 0.01$ vs. the control group (OVX-induced group).

MAPK signaling pathway is known to play an important role in osteoclast differentiation. ERK is associated with osteoclast survival, and JNK and p38 promote osteoclast differentiation (Matsumoto et al., 2000; Miyazaki et al., 2000). In this study, SR treatment reduced phosphorylation of IκB and NF-κB. In addition, SR treatment inhibited the MAPK signaling pathway by reducing phosphorylation of ERK, JNK and p38. These results suggest that SR can regulate osteoclast differentiation by inhibiting phosphorylation of NF-κB and MAPK.

Activation of the TRAF6, NF-κB and MAPK signaling pathways by the interaction of RANKL and RANK promotes the activation of several downstream transcription factors, such

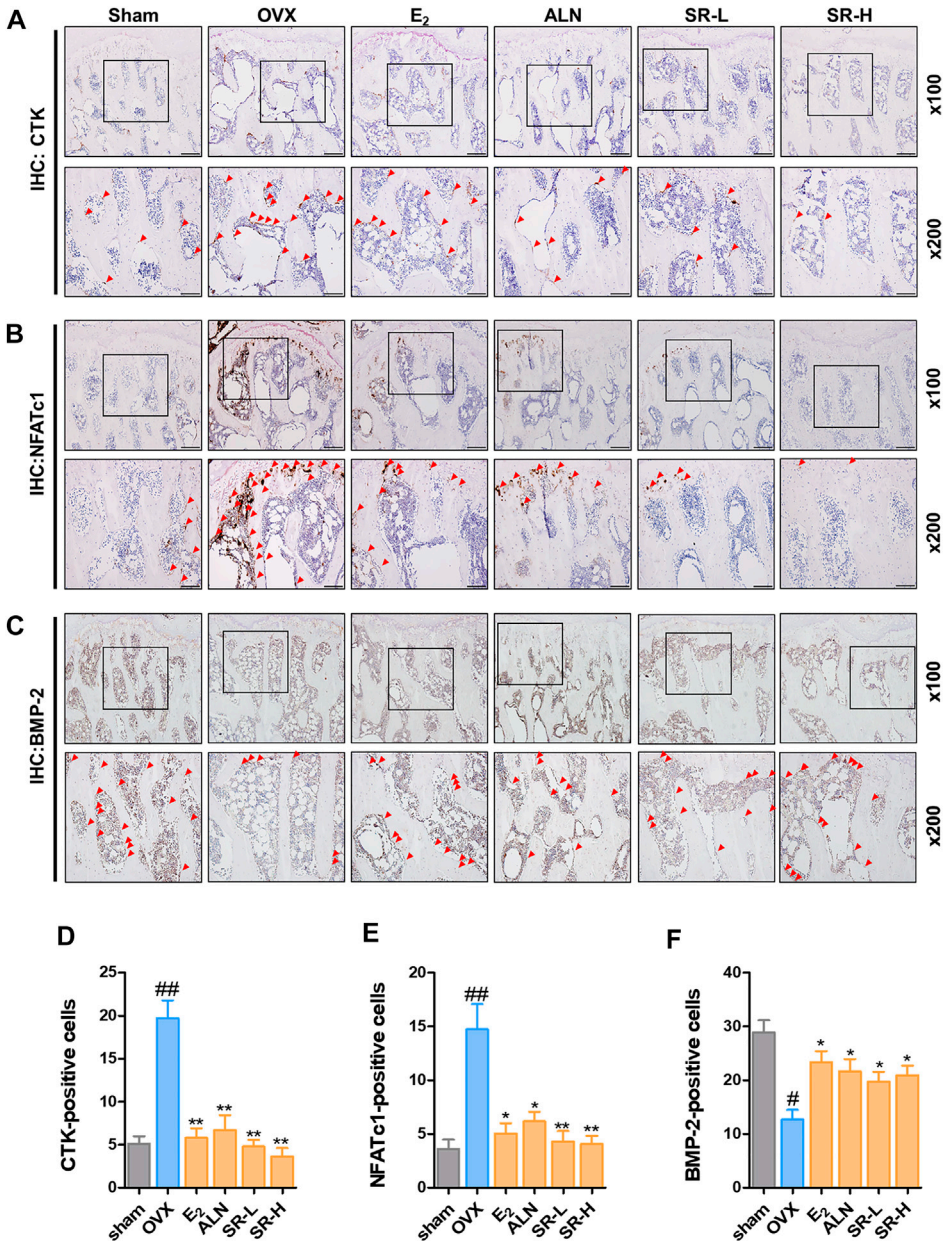

FIGURE 10 | Effect of SR on histopathological examination in the OVX-induced rats. **(A)** CTK-, **(B)** NFATc1- and **(C)** BMP-2-positive cells were measured using IHC staining. **(D)** The number of CTK- **(E)** NFATc1- and **(F)** BMP-2-positive cells was counted using ImageJ version 1.46. The results are presented as the mean ± SEM of each experimental group (n = 8). Statistical analysis was performed using one-way ANOVA followed by Dunnett's post hoc test. $^{\#\#}p < 0.01$, $^{\#}p < 0.05$ vs. the normal group (sham-operation group); $^{*}p < 0.05$, $^{**}p < 0.01$ vs. the control group (OVX-induced group).

as NFATc1 and c-Fos (Wada et al., 2006). In previous studies, overexpression of NFATc1 accelerated osteoclast differentiation and increased osteoclast formation independent of RANKL. NFATc1-deficient embryonic stem cells could not differentiate into osteoclasts, even in the presence of RANKL (Takayanagi et al., 2002; Kim and Kim, 2014). In addition, c-Fos deficiency causes severe osteoporosis due to a lack of osteoclasts (Arai et al., 2012). In this study, SR significantly inhibited the protein and mRNA expression of NFATc1 and c-Fos. These results indicate that SR can reduce osteoclast formation, differentiation and functions by inhibiting the NFATc1 and c-Fos signaling pathways.

RANK (*Tnfrsf11a*) is expressed on the surface of mature T cells and hematopoietic precursors. Activation of the *Tnfrsf11a* receptor triggers intracellular signaling mediated by the interaction of intracellular I, II and III domains, adapter proteins, and TNF receptor-related factors (TRAFs). RANK-deficient mice were characterized by severe osteopetrosis due

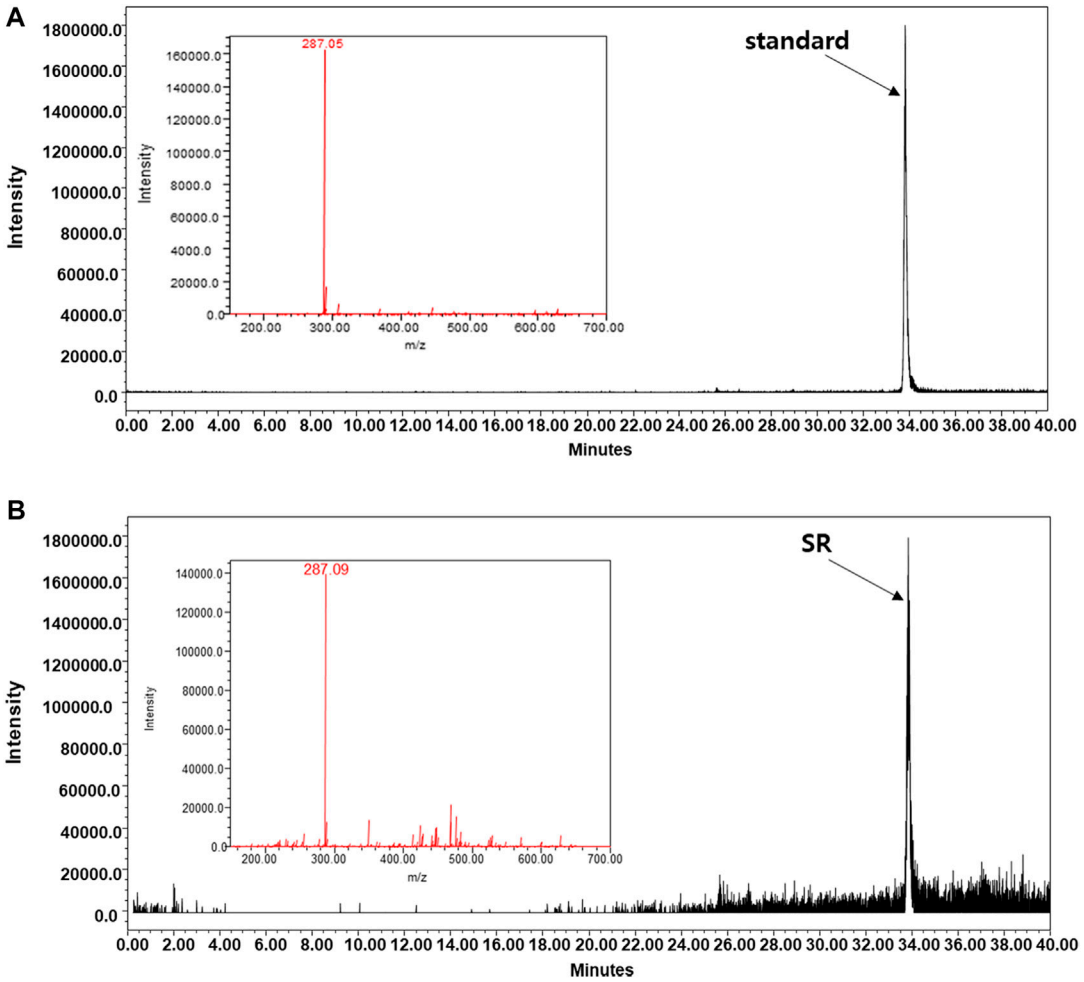

FIGURE 11 | LC-MS analysis was carried out using the A Waters e2695 system. Kaempferol was confirmed in the **(A)** standard and **(B)** SR extracts.

to blockade of osteoclast differentiation (Wong et al., 1997; Dougall et al., 1999). c-Fos and NFATc1 upregulate the expression of osteoclast-specific genes such as TRAP (*Acp5*), MMP-9 (*Mmp9*), CA2 (*ca2*), OCSAR (*Oscar*), ATP6vod2 (*Atp6v0d2*), and DC-STAMP (*Dcstamp*). *Acp5, Mmp9* and *Ca2* are involved in osteoclast differentiation, which promotes bone resorption (Zhao et al., 2010). Additionally, *Mmp9* has been shown to be important for bone development and repair (Colnot et al., 2003). *Ca2* affects the acidity of the bone surface, and its expression is upregulated by c-Fos signaling. When *CA2* is deficient, it has been found that nonfunctional osteoclasts cause osteoporosis (Sly et al., 1983; David et al., 2001). OSCAR is expressed in monocytes, macrophages, dendritic cells and osteoclasts and is a collagen-activating receptor that stimulates osteoclast differentiation. In a previous study, in the case of mononuclear cells from patients with high *Oscar* expression, the potential to differentiate into osteoclasts was improved compared to that of cells with low expression (Herman et al., 2008). Thus, *Oscar* is an important factor in osteoclast formation. *Atp6vod2* and *Dcstamp* are essential factors for cell-cell fusion (Kim et al., 2008). According to previous studies, *Atp6vod2*-deficient mice developed osteofossilosis due to abnormal osteoclast maturation (Lee et al., 2006). The osteoclasts isolated from *Dcstamp* knockout mice were osteoclasts with a single nucleus due to the lack of cell-cell fusion. In our study, SR inhibited the expression of osteoclast-specific genes (Yagi et al., 2005). These results demonstrated that SR suppressed osteoclast-specific genes through inhibition of c-Fos and NFATc1.

MC3T3-E1 cells were established from C57BL/6 mouse calvaria and are known to be suitable for *in vitro* experiments of osteoblast differentiation (Quarles et al., 1992). Alizarin Red S staining and Von Kossa staining are methods for staining calcium in mineralized nodule substrates. Calcified nodules are indicators of osteoblast differentiation (Puchtler et al., 1969; Bills et al., 1971). In this study, mineralized nodules increased in the osteogenic medium group compared with the growth medium group. SR significantly increased the calcified nodules in a concentration-dependent manner. These results indicate that SR plays an important role in promoting mineralization in MC3T3-E1 cells. The differentiation and maturation of osteoblasts is regulated by several factors. BMP-2 and RUNX-2 are key factors that induce bone development and promote

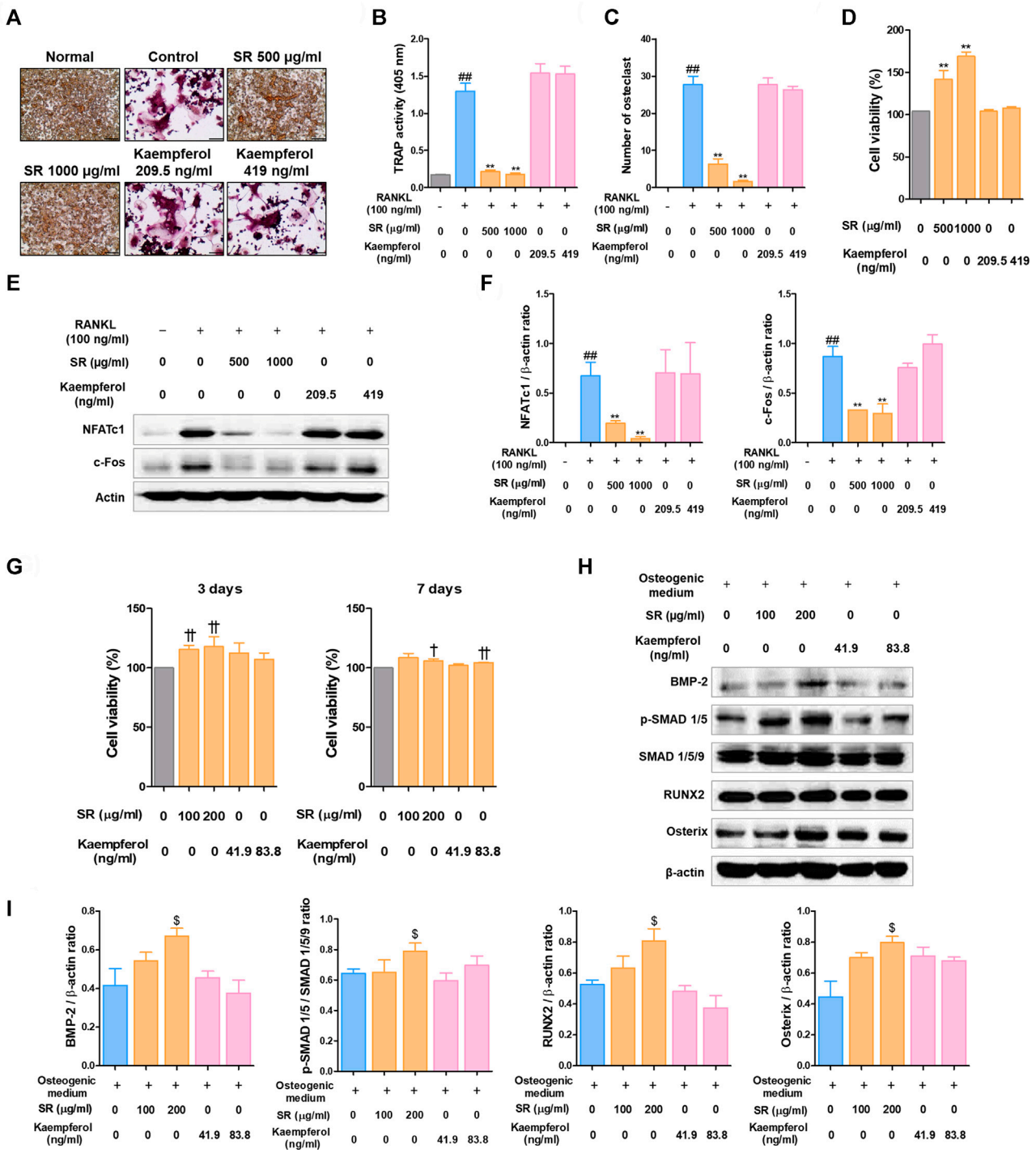

FIGURE 12 | Comparative analysis of pharmacological effects of SR and kaempferol on the differentiation of osteoclasts and osteoblasts. **(A)** TRAP-positive cells were stained using a TRAP kit. **(B)** TRAP activity was measured using an ELISA reader. **(C)** A number of TRAP-positive cells with >3 nuclei were counted using an inverted microscope (magnification, ×100). **(D)** RAW 264.7 cell viability was measured using a CCK-8 assay kit. **(E)** Protein expression levels of NFATc1 and c-Fos were measured by western blotting. **(F)** The bands were normalized to that of β-actin, which was used as a loading control. **(G)** MC3T3-E1 cell viability was analyzed by CCK-8 assays at 3 and 7 days. **(H)** Protein expression levels of BMP-2, p-Smad 1/5, RUNX-2 and Osterix were measured by western blotting. **(I)** BMP-2, RUNX-2 and Osterix levels were normalized to that of β-actin. p-Smad 1/5 levels was normalized to that of Smad 1/5/9. Data are presented as the mean ± SD of three independent experiments. Statistical analysis was performed using one-way ANOVA followed by Dunnett's post hoc test. $^{\#\#}p < 0.01$ vs. the normal group (untreated cells, RAW 264.7 cells); $^{*}p < 0.05$, $^{**}p < 0.01$ vs. the RANKL only treatment group. $^{\dagger}p < 0.05$, $^{\dagger\dagger}p < 0.01$ vs. the normal group (untreated cells, MC3T3-E1 cells); $^{\$}p < 0.05$ vs. the osteogenic medium-treated cells.

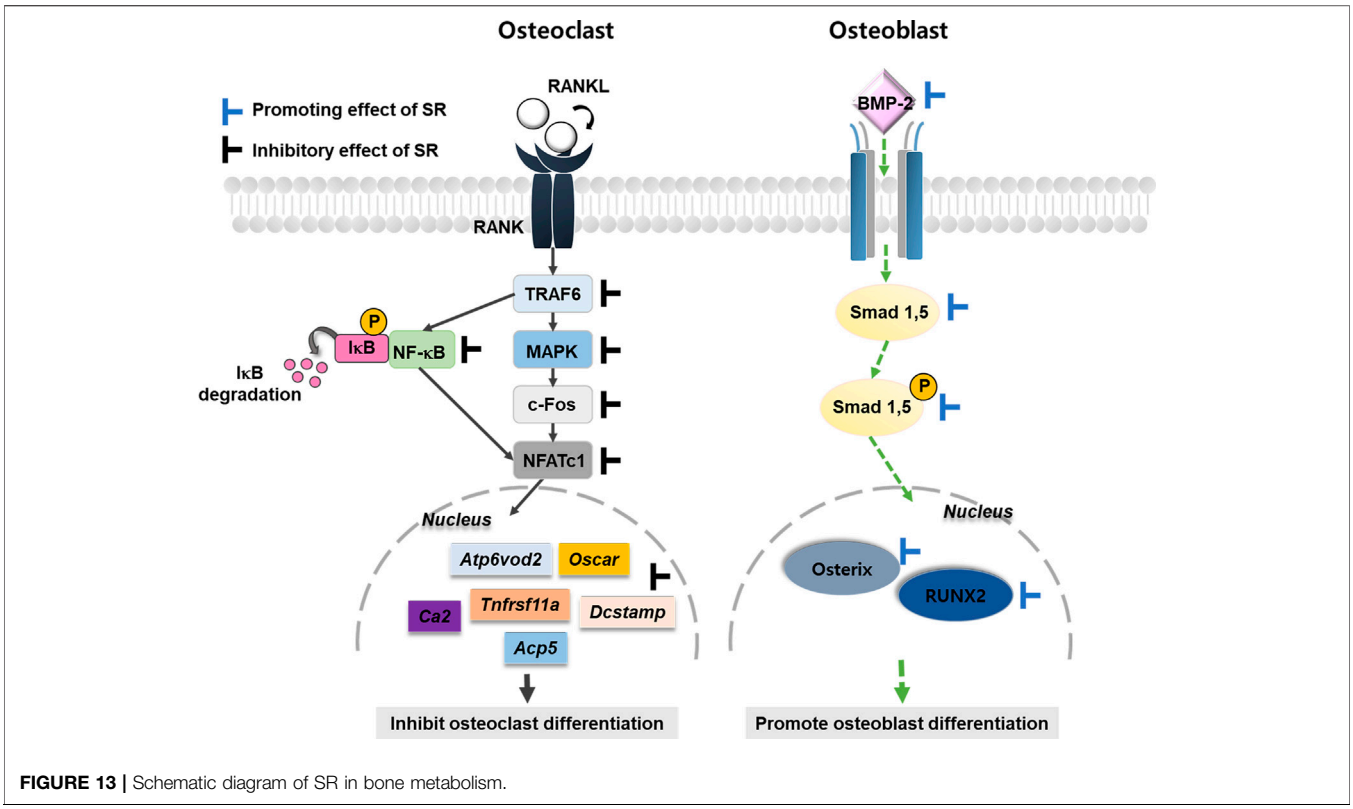

FIGURE 13 | Schematic diagram of SR in bone metabolism.

osteoblastic differentiation and bone formation. BMP-2 binds to receptors, resulting in the phosphorylation of SMAD, which then moves to the nucleus. Activated SAMD is translocated into the nucleus, and these signaling pathways activate RUNX-2. With increased RUNX2 activation, ALP (*Alpl*), COL1 (*COL1a1*) and BSP (*Ibsp*) are induced. Runx2 is an essential and important factor for osteoblast differentiation and chondrocyte maturation (Hay et al., 2001; Komori, 2010). Runx2-deficient mice lack osteoblasts and show little expression of bone matrix protein genes (Komori et al., 1997). Osterix is an osteoblast-specific transcription factor that activates a gene repertoire during osteoblast differentiation into mature osteoblasts and osteocytes. Osterix mutant embryos do not form bones and do not express osteoblast-specific marker genes (Cao et al., 2005; Sinha and Zhou, 2013). The results of the present study indicated that SR upregulates the expression of BMP-2, RUNX2 and Osterix and p-SAMD 1/5.

The OVX-induced rat model is mainly used in postmenopausal osteoporosis research and shares clinical characteristics with human osteoporosis. In a previous study, the OVX model showed an increase in body weight and atrophy of the uterus due to estrogen deficiency (Kalu, 1991; Eastell et al., 2016). In this study, the weight of the OVX group increased significantly from 2 weeks. In addition, uterine weight was significantly reduced in the OVX group compared to the sham group. These results indicate that the OVX model was successfully established. However, SR did not affect body or uterine weight. The results suggest that SR did not show an estrogen-like effect. Osteoclasts increase the levels of TRAP in the serum (Wronski et al., 1988). In this study, serum TRAP levels were increased in the OVX group compared to the sham group, but the difference was not significant. The reason for this small difference is not known, but it is assumed that this is a problem caused by the short experimental period. The ALP isoenzyme is derived from the bone and liver. ALP is a marker of osteoblast activity and bone formation and is involved in osteoblast metabolism. Therefore, when bone metabolism is rapid, such as in conditions with metabolic bone disease, the activity of osteoblasts increases with excessive osteoclast activity, and the concentration of ALP in the serum increases (Kuo and Chen, 2017; Kim M. et al., 2021). The ALP level in the OVX group increased compared to that in the sham group and decreased significantly in the SR-L group. In addition, the SR-H group had decreased ALP levels, but the decrease was not significant. These results suggest that the SR group had a reduced increase in ALP levels due to excessive osteoclast activity. AST and ALT are the most commonly used indicators of hepatotoxicity. High serum levels of AST and ALT indicate damage to hepatocytes (Ozer et al., 2008). In this study, ALT and AST were significantly decreased in the E_2, ALN, SR-L and SR-H groups. These results indicate that the E_2, ALN, SR-L and SR-H groups did not exhibit hepatotoxicity.

Quantitative evaluation of three-dimensional (3D) trabecular structural properties may improve the ability to understand the pharmaceutical properties of osteoporosis and to estimate bone properties. Micro-CT is a commonly used technique to understand the structural properties of bones (Jiang et al., 2000; Genant et al., 2008). BMD is an important indicator used to evaluate bone quality. In this study, micro-CT was

used to analyze the trabecular bone structure in rats. BV/TV is the area ratio of trabecular bone in the area of interest. Tb.Th is the average thickness of the trabecular trabeculae. Tb. Sp is the average distance of trabecular trabeculae (Small, 2005). In this study, BMD, BV/TV and Tb.Th were significantly decreased in the OVX group compared to the sham group. The E_2, ALN and SR groups had increased BMD, BV/TV and Tb.Th values compared with the OVX group. Tb. sp was significantly increased in the OVX group compared to the sham group. E_2, ALN and SR increased Tb. sp. in the OVX-induced rat model. Our data showed that SR significantly inhibited bone loss in the OVX-induced rat model.

Trabecular area and bone quality reduction is a common symptom in patients with osteoporosis. Therefore, the trabecular area was used as an important indicator of antiosteoporotic activity (Osterhoff et al., 2016). The OVX group had a decreased trabecular area compared with the sham group, and the OVX-induced reduced trabecular area was increased in the E_2, ALN and SR groups. Since estrogen deficiency through OVX causes abnormal activity of osteoclasts, TRAP staining in the femur is used to investigate the antiosteoporosis effect in various studies (Lee et al., 2019). In this study, the OVX group increased the number and area of TRAP-positive cells compared to the sham group, and SR inhibited this increase. The role of estradiol deficiency on osteoblast activation has been discussed in various researches. Confirming the study of Li et al., osteoblast activity was increased after OVX compared to the sham group (Li et al., 2019). Since it was found that the expression of estrogen suppresses the death of osteoblasts and prolongs the lifespan of osteoblasts, it is believed that the lack of estrogen due to menopause accelerates the death of osteoblasts (Bradford et al., 2010). Similar to Li's study, our results showed that osteoblast activity was decreased in the OVX group compared to the sham group, and the osteoblast activity was significantly increased in the SR group than the OVX group. The result of this study is that SR suppresses the decrease in osteoblast activity caused by estradiol deficiency, and it is considered that SR plays a positive role in osteoblast differentiation and activity, as in the cellular level results.

Immunohistochemical (IHC) staining is a staining method used to detect the presence of specific protein markers (Duraiyan et al., 2012; Kim et al., 2020; Kim M. et al., 2021). In our study, the number of CTK-, NFATc1- and BMP-2-positive cells was evaluated by IHC staining. We found that the OVX group had elevated numbers of CTK- and NFATc1-positive cells in the OVX-induced rat model, while E_2, ALN and SR treatment reduced their expression levels. In addition, the number of BMP-2-positive cells was decreased due to OVX, and it was confirmed that this expression was increased through E_2, ALN and SR treatment. These experimental results indicated that SR inhibits osteoclast differentiation and increases osteoblast activity in the OVX-induced osteoporosis model, and this effect is mediated by NFATc1 and BMP-2 similar to the *in vitro* experimental results.

The present study had several limitations. 1) Osteoporosis occurs for various reasons, including menopause, aging, inflammation, and steroid overdose (Sozen et al., 2017). In this study, only the effects of SR on postmenopausal osteoporosis were verified. In particular, the osteoblast differentiation-promoting effect of SR is expected to be effective in senile osteoporosis caused by metabolic deterioration due to aging. In the future, it will be expected to have research value to investigate the anti-osteoporosis effect of SR in aged rat or mice with an aging phenotype such as senescence-accelerated mouse prone 6 (SAMP6) (Azuma et al., 2018). 2) Another limitation is that the mechanism analysis of osteoclasts and osteoblasts has been confined. Various previous studies have demonstrated that the TRAF6/MAPK/NF-κB/NFATc1/c-Fos mechanism is representative as the mechanism for inducing osteoclast differentiation (Wong et al., 1998; Mizukami et al., 2002). However, including this, the mTOR/Akt mechanism involved in osteoclast survival (Tiedemann et al., 2017) and the OSCAR-stimulated calcium signaling mechanism were also found to be involved in the differentiation and activity of osteoclasts (Barrow et al., 2011). However, in this study, the pharmacological effects of SR on these mechanisms were not investigated. In addition, as for the osteoblast differentiation mechanism, various intracellular mechanisms such as Wnt/β-catenin canonical mechanisms exist (Pai et al., 2017), but this study only investigated the effect of SR on the BMP-2/SMAD mechanism and the expression of RUNX2. It is considered that the limitations of this study occurred during the initial construction stage of the experiment. We do not know the effect of SR on some of the mechanisms because we selected and conducted experiments on mechanisms that were found to play a major role in the differentiation/activation of osteoclasts and osteoblasts through preliminary investigation. In the future, if the role of SR on the expression of all factors in osteoclasts and osteoblasts is identified through experiments such as bioinformatic analysis, it is expected that it will be helpful in understanding the mechanism of bone metabolism control of SR. 3) Antagonists are useful in explaining the mechanism of each cell and have been utilized in various studies. For example, OPG and denosumab are representative antagonists that inhibit osteoclast differentiation by regulating RANKL (Schieferdecker et al., 2014) and, noggin and chordin are antagonists that inhibit osteoblast activity by inhibiting the BMP-2 mechanism (Glister et al., 2018), These antagonists are useful in explaining the mechanism of each cell and have been utilized in various studies (Gu et al., 2016; Kim JH. et al., 2021). However, this study did not include antagonist-related studies. Our results in osteoclast experiments do not appear to inhibit osteoclast differentiation by directly binding and then inactivating RANKL in SR. SR down-regulates NFATc1/c-Fos signaling activated after RANKL-RANK binding and activates osteoclast differentiation and inhibition. Therefore, it is expected that the use of antagonists will not be of great help in the mechanism analysis. However, the role of SR in upregulating the BMP-2 mechanism is thought to be useful to explain and understand such a mechanism if an in-depth study was conducted using noggin (antagonist of bmp-2). In the future, further study of SR using these antagonists is considered as a meaningful study that can more clearly explain the mechanism of action of osteoclasts and osteoblasts in SR. iv) The cellular concentration of SR used in this study was determined by referring to the toxicity verification through CCK-8 and previous study (Liu et al., 2020). However, these concentrations are a high

concentration relative to the concentration in the consensus document of ethnopharmacology (Heinrich et al., 2020). Because this may introduce artefacts in the model used, it is recommended to study appropriate dose levels in future studies.

CONCLUSION

In summary, SR inhibited osteoclast differentiation, function, and bone resorption through the TRAF6/MAPK/NF-κB/NFATc1/c-Fos pathways and stimulates osteoblast differentiation by increased protein expression of the BMP-2/samd signaling pathway. Moreover, SR protected against bone loss in OVX-induced rats. However, the concentration used in the verification test of SR's osteoclast inhibitory ability is likely to produce artefacts, so it is recommended to study the appropriate drug dose level reflecting the drug-extract ratio and other basic pharmaceutical parameters in the future. Nevertheless, our results appear to advance our knowledge of SR and successfully demonstrate its potential role as a osteoclastogenesis-inhibiting and osteogenesis-promoting herbal medicine for the treatment of postmenopausal osteoporosis.

DATA AVAILABILITY STATEMENT

The original contributions presented in the study are included in the article/**Supplementary Material**, further inquiries can be directed to the corresponding authors.

ETHICS STATEMENT

The animal study was reviewed and approved by the KHSASP-21–185.

AUTHOR CONTRIBUTIONS

YS and H-SJ designed the study. SL and MK performed all experiments, verified the analytical data and wrote the manuscript. SH and EK assisted with the *in vivo* experiments. J-HK, YS, and H-SJ helped to draft the manuscript. All authors read and approved the final manuscript.

FUNDING

This research was supported by a grant from the Korea Health Technology R&D Project through the Korea Health Industry Development Institute (KHIDI), funded by the Ministry of Health and Welfare, Republic of Korea (Grant Number: HF21C0092).

SUPPLEMENTARY MATERIAL

The Supplementary Material for this article can be found online at: https://www.frontiersin.org/articles/10.3389/fphar.2021.797892/full#supplementary-material

REFERENCES

Arai, A., Mizoguchi, T., Harada, S., Kobayashi, Y., Nakamichi, Y., Yasuda, H., et al. (2012). Fos Plays an Essential Role in the Upregulation of RANK Expression in Osteoclast Precursors within the Bone Microenvironment. *J. Cel Sci* 125 (Pt 12), 2910–2917. doi:10.1242/jcs.099986

Armstrong, A. P., Tometsko, M. E., Glaccum, M., Sutherland, C. L., Cosman, D., and Dougall, W. C. (2002). A RANK/TRAF6-dependent Signal Transduction Pathway Is Essential for Osteoclast Cytoskeletal Organization and Resorptive Function. *J. Biol. Chem.* 277 (46), 44347–44356. doi:10.1074/jbc.M202009200

Azuma, K., Zhou, Q., and Kubo, K. Y. (2018). Morphological and Molecular Characterization of the Senile Osteoporosis in Senescence-Accelerated Mouse Prone 6 (SAMP6). *Med. Mol. Morphol.* 51 (3), 139–146. doi:10.1007/s00795-018-0188-9

Ballanti, P., Minisola, S., Pacitti, M. T., Scarnecchia, L., Rosso, R., Mazzuoli, G. F., et al. (1997). Tartrate-resistant Acid Phosphate Activity as Osteoclastic Marker: Sensitivity of Cytochemical Assessment and Serum Assay in Comparison with Standardized Osteoclast Histomorphometry. *Osteoporos. Int.* 7 (1), 39–43. doi:10.1007/BF01623458

Bamias, A., Kastritis, E., Bamia, C., Moulopoulos, L. A., Melakopoulos, I., Bozas, G., et al. (2005). Osteonecrosis of the Jaw in Cancer after Treatment with Bisphosphonates: Incidence and Risk Factors. *J. Clin. Oncol.* 23 (34), 8580–8587. doi:10.1200/JCO.2005.02.8670

Barrow, A. D., Raynal, N., Andersen, T. L., Slatter, D. A., Bihan, D., Pugh, N., et al. (2011). OSCAR Is a Collagen Receptor that Costimulates Osteoclastogenesis in DAP12-Deficient Humans and Mice. *J. Clin. Invest.* 121 (9), 3505–3516. doi:10.1172/JCI45913

Beeton, C., Garcia, A., and Chandy, K. G. (2007). Drawing Blood from Rats through the Saphenous Vein and by Cardiac Puncture. *J. Vis. Exp.* 7, 266. doi:10.3791/266

Bills, C. E., Eisenberg, H., and Pallante, S. L. (1971). Complexes of organic acids with calcium phosphate: the von Kossa stain as a clue to the composition of bone mineral. *Johns Hopkins Med. J.* 128 (4), 194–207.

Boyle, W. J., Simonet, W. S., and Lacey, D. L. (2003). Osteoclast Differentiation and Activation. *Nature* 423 (6937), 337–342. doi:10.1038/nature01658

Bradford, P. G., Gerace, K. V., Roland, R. L., and Chrzan, B. G. (2010). Estrogen Regulation of Apoptosis in Osteoblasts. *Physiol. Behav.* 99 (2), 181–185. doi:10.1016/j.physbeh.2009.04.025

Bradley, E. W., and Oursler, M. J. (2008). Osteoclast Culture and Resorption Assays. *Methods Mol. Biol.* 455, 19–35. doi:10.1007/978-1-59745-104-8_2

Cao, Y., Zhou, Z., de Crombrugghe, B., Nakashima, K., Guan, H., Duan, X., et al. (2005). Osterix, a Transcription Factor for Osteoblast Differentiation, Mediates Antitumor Activity in Murine Osteosarcoma. *Cancer Res.* 65 (4), 1124–1128. doi:10.1158/0008-5472.CAN-04-2128

Clohisy, J. C., Frazier, E., Hirayama, T., and Abu-Amer, Y. (2003). RANKL Is an Essential Cytokine Mediator of Polymethylmethacrylate Particle-Induced Osteoclastogenesis. *J. Orthop. Res.* 21 (2), 202–212. doi:10.1016/S0736-0266(02)00133-X

Collin-Osdoby, P., and Osdoby, P. (2012). RANKL-mediated Osteoclast Formation from Murine RAW 264.7 Cells. *Methods Mol. Biol.* 816, 187–202. doi:10.1007/978-1-61779-415-5_13

Colnot, C., Thompson, Z., Miclau, T., Werb, Z., and Helms, J. A. (2003). Altered Fracture Repair in the Absence of MMP9. *Development* 130 (17), 4123–4133. doi:10.1242/dev.00559

David, J. P., Rincon, M., Neff, L., Horne, W. C., and Baron, R. (2001). Carbonic Anhydrase II Is an AP-1 Target Gene in Osteoclasts. *J. Cel Physiol* 188 (1), 89–97. doi:10.1002/jcp.1099

Doss, H. M., Samarpita, S., Ganesan, R., and Rasool, M. (2018). Ferulic Acid, a Dietary Polyphenol Suppresses Osteoclast Differentiation and Bone Erosion via the Inhibition of RANKL Dependent NF-Kb Signalling Pathway. *Life Sci.* 207, 284–295. doi:10.1016/j.lfs.2018.06.013

Dougall, W. C., Glaccum, M., Charrier, K., Rohrbach, K., Brasel, K., De Smedt, T., et al. (1999). RANK Is Essential for Osteoclast and Lymph Node Development. *Genes Dev.* 13 (18), 2412–2424. doi:10.1101/gad.13.18.2412

Duraiyan, J., Govindarajan, R., Kaliyappan, K., and Palanisamy, M. (2012). Applications of Immunohistochemistry. *J. Pharm. Bioallied Sci.* 4 (Suppl. 2), S307–S309. doi:10.4103/0975-7406.100281

Eastell, R., O'Neill, T. W., Hofbauer, L. C., Langdahl, B., Reid, I. R., Gold, D. T., et al. (2016). Postmenopausal Osteoporosis. *Nat. Rev. Dis. Primers* 2, 16069. doi:10.1038/nrdp.2016.69

Ekeuku, S. O., Pang, K. L., and Chin, K. Y. (2021). Effects of Caffeic Acid and its Derivatives on Bone: A Systematic Review. *Drug Des. Devel Ther.* 15, 259–275. doi:10.2147/DDDT.S287280

Feng, X., and McDonald, J. M. (2011). Disorders of Bone Remodeling. *Annu. Rev. Pathol.* 6, 121–145. doi:10.1146/annurev-pathol-011110-130203

Galibert, L., Tometsko, M. E., Anderson, D. M., Cosman, D., and Dougall, W. C. (1998). The Involvement of Multiple Tumor Necrosis Factor Receptor (TNFR)-associated Factors in the Signaling Mechanisms of Receptor Activator of NF-kappaB, a Member of the TNFR Superfamily. *J. Biol. Chem.* 273 (51), 34120–34127. doi:10.1074/jbc.273.51.34120

Genant, H. K., Engelke, K., and Prevrhal, S. (2008). Advanced CT Bone Imaging in Osteoporosis. *Rheumatology (Oxford)* 47 (Suppl. 4), iv9–16. doi:10.1093/rheumatology/ken180

Ginaldi, L., Di Benedetto, M. C., and De Martinis, M. (2005). Osteoporosis, Inflammation and Ageing. *Immun. Ageing* 2, 14. doi:10.1186/1742-4933-2-14

Glister, C., Regan, S. L., Samir, M., and Knight, P. G. (2019). Gremlin, Noggin, Chordin and Follistatin Differentially Modulate BMP-Induced Suppression of Androgen Secretion by Bovine Ovarian Theca Cells. *J. Mol. Endocrinol.* 62, 15–25. doi:10.1530/JME-18-0198

Grande, R., Pacella, S., Di Giulio, M., Rapino, M., Di Valerio, V., Cellini, L., et al. (2015). NF-kB Mediated Down-Regulation of Collagen Synthesis upon HEMA (2-hydroxyethyl Methacrylate) Treatment of Primary Human Gingival Fibroblast/Streptococcus Mutans Co-cultured Cells. *Clin. Oral Investig.* 19 (4), 841–849. doi:10.1007/s00784-014-1304-4

Gu, Y., Zhou, J., Wang, Q., Fan, W., and Yin, G. (2016). Ginsenoside Rg1 Promotes Osteogenic Differentiation of rBMSCs and Healing of Rat Tibial Fractures through Regulation of GR-dependent BMP-2/SMAD Signaling. *Sci. Rep.* 6, 25282. doi:10.1038/srep25282

Guardia, T., Rotelli, A. E., Juarez, A. O., and Pelzer, L. E. (2001). Anti-inflammatory Properties of Plant Flavonoids. Effects of Rutin, Quercetin and Hesperidin on Adjuvant Arthritis in Rat. *Farmaco* 56 (9), 683–687. doi:10.1016/s0014-827x(01)01111-9

Guo, A. J., Choi, R. C., Zheng, K. Y., Chen, V. P., Dong, T. T., Wang, Z. T., et al. (2012). Kaempferol as a Flavonoid Induces Osteoblastic Differentiation via Estrogen Receptor Signaling. *Chin. Med.* 7, 10. doi:10.1186/1749-8546-7-10

Hartley, J. W., Evans, L. H., Green, K. Y., Naghashfar, Z., Macias, A. R., Zerfas, P. M., et al. (2008). Expression of Infectious Murine Leukemia Viruses by RAW264.7 Cells, a Potential Complication for Studies with a Widely Used Mouse Macrophage Cell Line. *Retrovirology* 5, 1. doi:10.1186/1742-4690-5-1

Haÿ, E., Lemonnier, J., Fromigué, O., and Marie, P. J. (2001). Bone Morphogenetic Protein-2 Promotes Osteoblast Apoptosis through a Smad-independent, Protein Kinase C-dependent Signaling Pathway. *J. Biol. Chem.* 276 (31), 29028–29036. doi:10.1074/jbc.M011265200

Heinrich, M., Appendino, G., Efferth, T., Fürst, R., Izzo, A. A., Kayser, O., et al. (2020). Best Practice in Research - Overcoming Common Challenges in Phytopharmacological Research. *J. Ethnopharmacol* 246, 112230. doi:10.1016/j.jep.2019.112230

Herman, S., Müller, R. B., Krönke, G., Zwerina, J., Redlich, K., Hueber, A. J., et al. (2008). Induction of Osteoclast-Associated Receptor, a Key Osteoclast Costimulation Molecule, in Rheumatoid Arthritis. *Arthritis Rheum.* 58 (10), 3041–3050. doi:10.1002/art.23943

Iotsova, V., Caamaño, J., Loy, J., Yang, Y., Lewin, A., and Bravo, R. (1997). Osteopetrosis in Mice Lacking NF-kappaB1 and NF-kappaB2. *Nat. Med.* 3 (11), 1285–1289. doi:10.1038/nm1197-1285

Jia, J., Li, X., Ren, X., Liu, X., Wang, Y., Dong, Y., et al. (2021). Sparganii Rhizoma: A Review of Traditional Clinical Application, Processing, Phytochemistry, Pharmacology, and Toxicity. *J. Ethnopharmacol* 268, 113571. doi:10.1016/j.jep.2020.113571

Jiang, Y., Zhao, J., White, D. L., and Genant, H. K. (2000). Micro CT and Micro MR Imaging of 3D Architecture of Animal Skeleton. *J. Musculoskelet. Neuronal Interact* 1 (1), 45–51.

Kadioglu, O., Nass, J., Saeed, M. E., Schuler, B., and Efferth, T. (2015). Kaempferol Is an Anti-inflammatory Compound with Activity towards NF-Kb Pathway Proteins. *Anticancer Res.* 35 (5), 2645–2650.

Kalu, D. N. (1991). The Ovariectomized Rat Model of Postmenopausal Bone Loss. *Bone Miner* 15 (3), 175–191. doi:10.1016/0169-6009(91)90124-i

Kennel, K. A., and Drake, M. T. (2009). Adverse Effects of Bisphosphonates: Implications for Osteoporosis Management. *Mayo Clin. Proc.* 84 (7), 632–638. doi:10.1016/S0025-6196(11)60752-0

Kim, C. J., Shin, S. H., Kim, B. J., Kim, C. H., Kim, J. H., Kang, H. M., et al. (2018). The Effects of Kaempferol-Inhibited Autophagy on Osteoclast Formation. *Int. J. Mol. Sci.* 19 (1), 125. doi:10.3390/ijms19010125

Kim, J. H., Kim, M., Hong, S., Kim, E. Y., Lee, H., Jung, H. S., et al. (2021a). Albiflorin Promotes Osteoblast Differentiation and Healing of Rat Femoral Fractures through Enhancing BMP-2/Smad and Wnt/β-Catenin Signaling. *Front. Pharmacol.* 12, 690113. doi:10.3389/fphar.2021.690113

Kim, J. H., and Kim, N. (2014). Regulation of NFATc1 in Osteoclast Differentiation. *J. Bone Metab.* 21 (4), 233–241. doi:10.11005/jbm.2014.21.4.233

Kim, K., Lee, S. H., Ha Kim, J., Choi, Y., and Kim, N. (2008). NFATc1 Induces Osteoclast Fusion via Up-Regulation of Atp6v0d2 and the Dendritic Cell-specific Transmembrane Protein (DC-STAMP). *Mol. Endocrinol.* 22 (1), 176–185. doi:10.1210/me.2007-0237

Kim, M., Kim, H. S., Kim, J. H., Kim, E. Y., Lee, B., Lee, S. Y., et al. (2020). Chaenomelis Fructus Inhibits Osteoclast Differentiation by Suppressing NFATc1 Expression and Prevents Ovariectomy-Induced Osteoporosis. *BMC Complement. Med. Ther.* 20 (1), 35. doi:10.1186/s12906-020-2841-9

Kim, M., Kim, J.-H., Hong, S., Kwon, B., Kim, E.-Y., Jung, H.-S., et al. (2021b). Effects of Melandrium Firmum Rohrbach on RANKL-induced O-steoclast D-ifferentiation and OVX R-ats. *Mol. Med. Rep.* 24 (2), 610. doi:10.3892/mmr.2021.12248

Komori, T. (2010). Regulation of Osteoblast Differentiation by Runx2. *Adv. Exp. Med. Biol.* 658, 43–49. doi:10.1007/978-1-4419-1050-9_5

Komori, T., Yagi, H., Nomura, S., Yamaguchi, A., Sasaki, K., Deguchi, K., et al. (1997). Targeted Disruption of Cbfa1 Results in a Complete Lack of Bone Formation Owing to Maturational Arrest of Osteoblasts. *Cell* 89 (5), 755–764. doi:10.1016/s0092-8674(00)80258-5

Kuo, T. R., and Chen, C. H. (2017). Bone Biomarker for the Clinical Assessment of Osteoporosis: Recent Developments and Future Perspectives. *Biomark Res.* 5, 18. doi:10.1186/s40364-017-0097-4

Kyung, T. W., Lee, J. E., Shin, H. H., and Choi, H. S. (2008). Rutin Inhibits Osteoclast Formation by Decreasing Reactive Oxygen Species and TNF-Alpha by Inhibiting Activation of NF-kappaB. *Exp. Mol. Med.* 40 (1), 52–58. doi:10.3858/emm.2008.40.1.52

Lee, K. Y., Kim, J. H., Kim, E. Y., Yeom, M., Jung, H. S., and Sohn, Y. (2019). Water Extract of Cnidii Rhizoma Suppresses RANKL-Induced Osteoclastogenesis in RAW 264.7 Cell by Inhibiting NFATc1/c-Fos Signaling and Prevents Ovariectomized Bone Loss in SD-rat. *BMC Complement. Altern. Med.* 19 (1), 207. doi:10.1186/s12906-019-2611-8

Lee, S. H., Rho, J., Jeong, D., Sul, J. Y., Kim, T., Kim, N., et al. (2006). V-ATPase V0 Subunit D2-Deficient Mice Exhibit Impaired Osteoclast Fusion and Increased Bone Formation. *Nat. Med.* 12 (12), 1403–1409. doi:10.1038/nm1514

Li, J., Li, X., Liu, D., Hamamura, K., Wan, Q., Na, S., et al. (2019). eIF2α Signaling Regulates Autophagy of Osteoblasts and the Development of Osteoclasts in OVX Mice. *Cell Death Dis* 10 (12), 921. doi:10.1038/s41419-019-2159-z

Liu, M., Zhao, L., Han, L., Li, H., Shi, Y., Cui, J., et al. (2020). Discovery and Identification of Proangiogenic Chemical Markers from Gastrodiae Rhizoma Based on Zebrafish Model and Metabolomics Approach. *Phytochem. Anal.* 31 (6), 835–845. doi:10.1002/pca.2949

Liu, T., Gao, Y., Sakamoto, K., Minamizato, T., Furukawa, K., Tsukazaki, T., et al. (2007). BMP-2 Promotes Differentiation of Osteoblasts and Chondroblasts in Runx2-Deficient Cell Lines. *J. Cel Physiol* 211 (3), 728–735. doi:10.1002/jcp.20988

Lomaga, M. A., Yeh, W. C., Sarosi, I., Duncan, G. S., Furlonger, C., Ho, A., et al. (1999). TRAF6 Deficiency Results in Osteopetrosis and Defective Interleukin-1, CD40, and LPS Signaling. *Genes Dev.* 13 (8), 1015–1024. doi:10.1101/gad.13.8.1015

Luo, L., Zhou, J., Zhao, H., Fan, M., and Gao, W. (2019). The Anti-inflammatory Effects of Formononetin and Ononin on Lipopolysaccharide-Induced Zebrafish Models Based on Lipidomics and Targeted Transcriptomics. *Metabolomics* 15 (12), 153. doi:10.1007/s11306-019-1614-2

Marchisio, P. C., Cirillo, D., Naldini, L., Primavera, M. V., Teti, A., and Zambonin-Zallone, A. (1984). Cell-substratum Interaction of Cultured Avian Osteoclasts

Is Mediated by Specific Adhesion Structures. *J. Cel Biol* 99 (5), 1696–1705. doi:10.1083/jcb.99.5.1696

Matsubara, T., Kinbara, M., Maeda, T., Yoshizawa, M., Kokabu, S., and Takano Yamamoto, T. (2017). Regulation of Osteoclast Differentiation and Actin Ring Formation by the Cytolinker Protein Plectin. *Biochem. Biophys. Res. Commun.* 489 (4), 472–476. doi:10.1016/j.bbrc.2017.05.174

Matsumoto, M., Sudo, T., Saito, T., Osada, H., and Tsujimoto, M. (2000). Involvement of P38 Mitogen-Activated Protein Kinase Signaling Pathway in Osteoclastogenesis Mediated by Receptor Activator of NF-Kappa B Ligand (RANKL). *J. Biol. Chem.* 275 (40), 31155–31161. doi:10.1074/jbc.M001229200

Matsuo, K., and Irie, N. (2008). Osteoclast-osteoblast Communication. *Arch. Biochem. Biophys.* 473 (2), 201–209. doi:10.1016/j.abb.2008.03.027

Miyazaki, T., Katagiri, H., Kanegae, Y., Takayanagi, H., Sawada, Y., Yamamoto, A., et al. (2000). Reciprocal Role of ERK and NF-kappaB Pathways in Survival and Activation of Osteoclasts. *J. Cel Biol* 148 (2), 333–342. doi:10.1083/jcb.148.2.333

Mizukami, J., Takaesu, G., Akatsuka, H., Sakurai, H., Ninomiya-Tsuji, J., Matsumoto, K., et al. (2002). Receptor Activator of NF-kappaB Ligand (RANKL) Activates TAK1 Mitogen-Activated Protein Kinase Kinase Kinase through a Signaling Complex Containing RANK, TAB2, and TRAF6. *Mol. Cel Biol* 22 (4), 992–1000. doi:10.1128/MCB.22.4.992-1000.2002

Nair, A. B., and Jacob, S. (2016). A Simple Practice Guide for Dose Conversion between Animals and Human. *J. Basic Clin. Pharm.* 7 (2), 27–31. doi:10.4103/0976-0105.177703

Osterhoff, G., Morgan, E. F., Shefelbine, S. J., Karim, L., McNamara, L. M., and Augat, P. (2016). Bone Mechanical Properties and Changes with Osteoporosis. *Injury* 47 (Suppl. 2), S11–S20. doi:10.1016/S0020-1383(16)47003-8

Ozer, J., Ratner, M., Shaw, M., Bailey, W., and Schomaker, S. (2008). The Current State of Serum Biomarkers of Hepatotoxicity. *Toxicology* 245 (3), 194–205. doi:10.1016/j.tox.2007.11.021

Pai, S. G., Carneiro, B. A., Mota, J. M., Costa, R., Leite, C. A., Barroso-Sousa, R., et al. (2017). Wnt/beta-catenin Pathway: Modulating Anticancer Immune Response. *J. Hematol. Oncol.* 10 (1), 101. doi:10.1186/s13045-017-0471-6

Pragasam, S. J., Venkatesan, V., and Rasool, M. (2013). Immunomodulatory and Anti-inflammatory Effect of P-Coumaric Acid, a Common Dietary Polyphenol on Experimental Inflammation in Rats. *Inflammation* 36 (1), 169–176. doi:10.1007/s10753-012-9532-8

Puchtler, H., Meloan, S. N., and Terry, M. S. (1969). On the History and Mechanism of Alizarin and Alizarin Red S Stains for Calcium. *J. Histochem. Cytochem.* 17 (2), 110–124. doi:10.1177/17.2.110

Quarles, L. D., Yohay, D. A., Lever, L. W., Caton, R., and Wenstrup, R. J. (1992). Distinct Proliferative and Differentiated Stages of Murine MC3T3-E1 Cells in Culture: an *In Vitro* Model of Osteoblast Development. *J. Bone Miner Res.* 7 (6), 683–692. doi:10.1002/jbmr.5650070613

Sagar, T., Rantlha, M., Kruger, M. C., Coetzee, M., and Deepak, V. (2016). Ferulic Acid Impairs Osteoclast Fusion and Exacerbates Survival of Mature Osteoclasts. *Cytotechnology* 68 (5), 1963–1972. doi:10.1007/s10616-016-0009-8

Schieferdecker, A., Voigt, M., Riecken, K., Braig, F., Schinke, T., Loges, S., et al. (2014). Denosumab Mimics the Natural Decoy Receptor Osteoprotegerin by Interacting with its Major Binding Site on RANKL. *Oncotarget* 5 (16), 6647–6653. doi:10.18632/oncotarget.2160

Sinha, K. M., and Zhou, X. (2013). Genetic and Molecular Control of Osterix in Skeletal Formation. *J. Cel Biochem* 114 (5), 975–984. doi:10.1002/jcb.24439

Sly, W. S., Hewett-Emmett, D., Whyte, M. P., Yu, Y. S., and Tashian, R. E. (1983). Carbonic Anhydrase II Deficiency Identified as the Primary Defect in the Autosomal Recessive Syndrome of Osteopetrosis with Renal Tubular Acidosis and Cerebral Calcification. *Proc. Natl. Acad. Sci. U S A.* 80 (9), 2752–2756. doi:10.1073/pnas.80.9.2752

Small, R. E. (2005). Uses and Limitations of Bone Mineral Density Measurements in the Management of Osteoporosis. *MedGenMed* 7 (2), 3.

Sözen, T., Özışık, L., and Başaran, N. Ç. (2017). An Overview and Management of Osteoporosis. *Eur. J. Rheumatol.* 4 (1), 46–56. doi:10.5152/eurjrheum.2016.048

Suda, T., Takahashi, N., Udagawa, N., Jimi, E., Gillespie, M. T., and Martin, T. J. (1999). Modulation of Osteoclast Differentiation and Function by the New Members of the Tumor Necrosis Factor Receptor and Ligand Families. *Endocr. Rev.* 20 (3), 345–357. doi:10.1210/edrv.20.3.0367

Takayanagi, H., Kim, S., Koga, T., Nishina, H., Isshiki, M., Yoshida, H., et al. (2002). Induction and Activation of the Transcription Factor NFATc1 (NFAT2) Integrate RANKL Signaling in Terminal Differentiation of Osteoclasts. *Dev. Cel* 3 (6), 889–901. doi:10.1016/s1534-5807(02)00369-6

Teitelbaum, S. L., and Ross, F. P. (2003). Genetic Regulation of Osteoclast Development and Function. *Nat. Rev. Genet.* 4 (8), 638–649. doi:10.1038/nrg1122

Tiedemann, K., Le Nihouannen, D., Fong, J. E., Hussein, O., Barralet, J. E., and Komarova, S. V. (2017). Regulation of Osteoclast Growth and Fusion by mTOR/raptor and mTOR/rictor/Akt. *Front Cel Dev Biol* 5, 54. doi:10.3389/fcell.2017.00054

Tschöp, M. H., Speakman, J. R., Arch, J. R., Auwerx, J., Brüning, J. C., Chan, L., et al. (2011). A Guide to Analysis of Mouse Energy Metabolism. *Nat. Methods* 9 (1), 57–63. doi:10.1038/nmeth.1806

Wada, T., Nakashima, T., Hiroshi, N., and Penninger, J. M. (2006). RANKL-RANK Signaling in Osteoclastogenesis and Bone Disease. *Trends Mol. Med.* 12 (1), 17–25. doi:10.1016/j.molmed.2005.11.007

Wang, X., Wu, Q., Wu, Y., Chen, G., Yue, W., and Liang, Q. (2012). Response Surface Optimized Ultrasonic-Assisted Extraction of Flavonoids from Sparganii Rhizoma and Evaluation of Their *In Vitro* Antioxidant Activities. *Molecules* 17 (6), 6769–6783. doi:10.3390/molecules17066769

Wang, X., Wu, Q. N., Wu, Y., Wu, C., Yue, W., and Liang, Q. (2013). Determination of Seven Phenolic Compounds in Rhizoma Sparganii by RP-HPLC. *J. Chromatogr. Sci.* 51 (4), 371–375. doi:10.1093/chromsci/bms150

Wong, B. R., Josien, R., Lee, S. Y., Sauter, B., Li, H. L., Steinman, R. M., et al. (1997). TRANCE (Tumor Necrosis Factor [TNF]-Related Activation-Induced Cytokine), a New TNF Family Member Predominantly Expressed in T Cells, Is a Dendritic Cell-specific Survival Factor. *J. Exp. Med.* 186 (12), 2075–2080. doi:10.1084/jem.186.12.2075

Wong, B. R., Josien, R., Lee, S. Y., Vologodskaia, M., Steinman, R. M., and Choi, Y. (1998). The TRAF Family of Signal Transducers Mediates NF-kappaB Activation by the TRANCE Receptor. *J. Biol. Chem.* 273 (43), 28355–28359. doi:10.1074/jbc.273.43.28355

Wronski, T. J., Cintrón, M., and Dann, L. M. (1988). Temporal Relationship between Bone Loss and Increased Bone Turnover in Ovariectomized Rats. *Calcif Tissue Int.* 43 (3), 179–183. doi:10.1007/BF02571317

Yagi, M., Miyamoto, T., Sawatani, Y., Iwamoto, K., Hosogane, N., Fujita, N., et al. (2005). DC-STAMP Is Essential for Cell-Cell Fusion in Osteoclasts and Foreign Body Giant Cells. *J. Exp. Med.* 202 (3), 345–351. doi:10.1084/jem.20050645

Yepuri, N., Dhawan, R., Cooney, M., Pruekprasert, N., Meng, Q., and Cooney, R. N. (2019). Sparstolonin B: A Unique Anti-inflammatory Agent. *Shock* 52 (6), 568–576. doi:10.1097/SHK.0000000000001326

Yuan, H., Ma, Q., Ye, L., and Piao, G. (2016). The Traditional Medicine and Modern Medicine from Natural Products. *Molecules* 21 (5), 559. doi:10.3390/molecules21050559

Zhao, M. M., Gu, R., Fan, J. Y., Zeng, Y., Cao, Y., Wang, W. Q., et al. (2018). Research Progress of Tibetan Medicine "Zha-Xun". *Zhongguo Zhong Yao Za Zhi* 43 (8), 1554–1562. doi:10.19540/j.cnki.cjcmm.20180122.001

Zhao, Q., Wang, X., Liu, Y., He, A., and Jia, R. (2010). NFATc1: Functions in Osteoclasts. *Int. J. Biochem. Cel Biol* 42 (5), 576–579. doi:10.1016/j.biocel.2009.12.018

Zielińska, D., Zieliński, H., Laparra-Llopis, J. M., Szawara-Nowak, D., Honke, J., and Giménez-Bastida, J. A. (2021). Caffeic Acid Modulates Processes Associated with Intestinal Inflammation. *Nutrients* 13 (2), 554. doi:10.3390/nu13020554

Conflict of Interest: The authors declare that the research was conducted in the absence of any commercial or financial relationships that could be construed as a potential conflict of interest.

Publisher's Note: All claims expressed in this article are solely those of the authors and do not necessarily represent those of their affiliated organizations, or those of the publisher, the editors and the reviewers. Any product that may be evaluated in this article, or claim that may be made by its manufacturer, is not guaranteed or endorsed by the publisher.

Copyright © 2022 Lee, Kim, Hong, Kim, Kim, Sohn and Jung. This is an open-access article distributed under the terms of the Creative Commons Attribution License (CC BY). The use, distribution or reproduction in other forums is permitted, provided the original author(s) and the copyright owner(s) are credited and that the original publication in this journal is cited, in accordance with accepted academic practice. No use, distribution or reproduction is permitted which does not comply with these terms.

frontiers in Pharmacology

REVIEW
published: 19 January 2022
doi: 10.3389/fphar.2021.830331

The Effects of Crocin on Bone and Cartilage Diseases

Shayan Vafaei[1], *Xuming Wu*[2], *Jiajie Tu*[2]* *and Seyed Noureddin Nematollahi-mahani*[1]*

[1]Department of Anatomical Science, School of Medicine, Kerman University of Medical Sciences, Kerman, Iran, [2]Key Laboratory of Anti-Inflammatory and Immune Medicine, Anhui Collaborative Innovation Center of Anti-Inflammatory and Immune Medicine, Institute of Clinical Pharmacology, Anhui Medical University, Ministry of Education, Hefei, China

Crocin, the main biologically active carotenoid of saffron, generally is derived from the dried trifid stigma of *Crocus sativus* L. Many studies have demonstrated that crocin has several therapeutic effects on biological systems through its anti-oxidant and anti-inflammatory properties. The wide range of crocin activities is believed to be because of its ability to anchor to many proteins, triggering some cellular pathways responsible for cell proliferation and differentiation. It also has therapeutic potentials in arthritis, osteoarthritis, rheumatoid arthritis, and articular pain probably due to its anti-inflammatory properties. Anti-apoptotic effects, as well as osteoclast inhibition effects of crocin, have suggested it as a natural substance to treat osteoporosis and degenerative disease of bone and cartilage. Different mechanisms underlying crocin effects on bone and cartilage repair have been investigated, but remain to be fully elucidated. The present review aims to undertake current knowledge on the effects of crocin on bone and cartilage degenerative diseases with an emphasis on its proliferative and differentiative properties in mesenchymal stem cells.

Keywords: crocin, bone, cartilage, inflammation, cell differentiation

OPEN ACCESS

Edited by:
Longhuo Wu,
Gannan Medical University, China

Reviewed by:
Yujie Deng,
Guangzhou Regenerative Medicine and Health Guangdong Laboratory, China
Albert Hoi Hung Cheung,
The Chinese University of Hong Kong, China
Chen Zhu,
Anhui Provincial Hospital, China

***Correspondence:**
Jiajie Tu
tujiajie@ahmu.edu.cn
Seyed Noureddin Nematollahi-mahani
nnematollahi@kmu.ac.ir

Specialty section:
This article was submitted to Ethnopharmacology, a section of the journal Frontiers in Pharmacology

Received: *07 December 2021*
Accepted: *28 December 2021*
Published: *19 January 2022*

Citation:
Vafaei S, Wu X, Tu J and Nematollahi-mahani SN (2022) The Effects of Crocin on Bone and Cartilage Diseases. Front. Pharmacol. 12:830331. doi: 10.3389/fphar.2021.830331

INTRODUCTION

Crocus sativus L. (*C. sativus* L.) is one of about 88 species from the *Crocus* genus, which is part of the Iridaceae family. It is well known in herbal medicine and has attracted the attention of researchers because of its properties, especially its anti-inflammatory and proliferative capacities in bone and cartilage destructive diseases (Ríos et al., 1996; Mollazadeh et al., 2015). This plant is mainly cultivated in Iran, China, India, Azerbaijan, Turkey, Morocco, Greece, Spain, Italy, Mexico, and other places (Xue, 1982; Alavizadeh and Hosseinzadeh, 2014). It is a perennial herb that grows up to about 20 cm and usually produces 2-3 blue-purple flowers (Melnyk et al., 2010). The dried stigma, called saffron, is the most widely used part (Gismondi et al., 2012; Winterhalter and Straubinger, 2000). Because of the distinguished color, odor, and flavor, it is used as a food coloring and flavoring substances (Winterhalter and Straubinger, 2000; Caballero-Ortega et al., 2007; Mollazadeh et al., 2015). Carotenoids, the main metabolites of saffron, are responsible for the red color, smell, and bitterness (Srivastava et al., 2010; Gismondi et al., 2012). Water-soluble carotenoids can affect certain cellular pathways and molecules because of their ability to bind to a wide range of proteins, including membrane proteins, transcription factors, mitochondrial proteins, structural proteins, and enzymes (Hosseinzadeh et al., 2014; Li S et al., 2017). Among these biologically active components, there are four well-established ingredients that are likely responsible for the therapeutic potential of saffron, including crocin, crocetin, safranal, and picrocrocin (Pfander and Schurtenberger, 1982; Tsimidou and Tsatsaroni, 1993; Liakopoulou-Kyriakides and Kyriakides, 2002; Srivastava et al., 2010; Gohari et al., 2013; Hosseinzadeh and Nassiri-Asl, 2013). Crocin has five proper subsets; the principal one in

FIGURE 1 | The picture of *C. Sativus L.*, saffron and crocin (molecular structure).

saffron is α-crocin (Alonso et al., 2001; Ordoudi et al., 2015). Chemical studies have shown that crocin is a diester composed of the disaccharide gentiobiose and the dicarboxylic acid crocetin (**Figure 1**) (Alavizadeh and Hosseinzadeh, 2014). In the past, saffron was used as a sexual stimulant, and as a treatment for infertility and impotence (Asadi et al., 2014). Recent studies have revealed other therapeutic and pharmacological activities of saffron, such as neuroprotective (Baghishani et al., 2018; Haeri et al., 2019), neurogenetic (Ebrahimi et al., 2021), antidepressant (Shafiee et al., 2018), anti-apoptotic (Vafaei et al., 2020), antioxidant (Altinoz et al., 2016; Hatziagapiou et al., 2019), and anti-inflammatory (Nam et al., 2010; Lv et al., 2016) effects. Crocin is one of essential ingredients that responsible for the therapeutic effects of saffron. Specifically, the antioxidative properties of crocin involve several signaling pathways and molecules. For example, it modulates GPx, GST, CAT, and SOD (Korani et al., 2019), inhibits reactive oxygen species (ROS) and interacts with peroxidase (Mostafavinia et al., 2016). Overall, it inhibits free radicals (Ebadi, 2006) and affects certain pathways, such as CREB signaling (Zheng et al., 2007). Crocin also has anti-inflammatory properties via the downregulation of inflammatory marker levels such as interleukin (IL)-1ß, IL-6, tumor necrosis factor (TNF)-α, and insulin-like growth factor (IGF)-1, or through modulation of signaling pathways such as PI3K/Akt and Nuclear factor-kappa B (NF-κB) (Deng et al., 2018; Xie et al., 2019). It has been shown that crocin can polarize macrophages to the M2 (anti-inflammatory) phenotype by suppressing the p38 and JNK pathways. Therefore, its anti-inflammatory effects are associated with this pathway, in addition to other pathways (Zhu et al., 2019). Furthermore, crocin is metabolized in the liver and exerts protective effects on liver toxicity induced by morphine (Salahshoor et al., 2016) and nicotine (Jalili et al., 2015).

METHODS

Crocin exerts its effects under various conditions, and its antioxidant and anti-inflammatory properties contribute to the treatment of various diseases, including bone and cartilage inflammation. In this review, we summarized studies published through 2021 on the effect of crocin on bone and cartilage diseases. We chose crocin, bone, cartilage, and inflammation as keywords. The related articles were collected from online literature resources such as Web of Knowledge, PubMed, Scopus, and Google Scholar.

ROLE OF CROCIN IN BONE AND CARTILAGE DISEASES

Crocin and Osteoarthritis

One of the most common joint diseases worldwide is osteoarthritis (OA), which is considered the main cause of disability in elderly people and often presents with pain and limited movement (Krasnokutsky et al., 2007; Silverwood et al., 2015; Dubin, 2016). OA severity varies from localized to chronic inflammation (Feldmann, 2001) and leads to joint cartilage degeneration, synovitis, and even bone remodeling (Benazzo et al., 2016). OA is reinforced by several factors such as obesity, age, trauma, mechanical stress, oxidative stress, and inflammation (Chen D. et al., 2017; Lim et al., 2017; Min et al., 2018; Yoo et al., 2018). In mild and severe OA, symptoms of inflammation are pronounced (Sinkov and Cymet, 2003), and inflammatory cytokines, including IL-2, interferon (IFN)-γ, TNF-α, and IL-1ß, are thought to be involved in the pathology (Goldring, 2000; Linton and Fazio, 2003; Chen D. et al., 2017). Overall, inflammatory cytokines lead to NF-κB signaling pathway activation, which can induce expression of matrix-degrading enzymes, such as matrix metalloproteinase (MMP) and C-reactive protein (CRP) 5, and increase erythrocyte sedimentation rate (ESR), which are involved in cartilage degeneration and osteoarthritis (Pennock et al., 2007; Sakkas and Platsoucas, 2007; Mohamadpour et al., 2013; Chen D. et al., 2017). MMPs, especially MMP1 and MMP3, destroy the extracellular matrix, thereby disrupting normal joint performance and leading to OA progression (Largo et al., 2003; Tardif et al., 2004; Burrage et al., 2006; Takaishi et al., 2008). Researchers have shown that the anti-inflammatory properties of crocin have a therapeutic effect on OA. In the study by Lei et al., OA rats were administered 30 mg/kg crocin daily for 10 days.

TABLE 1 | Brief summary of studies on crocin and OA.

Reference	Models/Crocin doses	Main results	Conclusion
Lei et al. (2017)	Rats/30 mg/kg daily for 10 days	Decrease in joint pain, IL-6 level, LPO, and Nrf2 expression; increase in CS activity, MHC IIα expression, glutathione production, and glutathione peroxidase activity	Crocin reduces OA symptoms by affecting oxidative stress, inflammation, and JNK activity
Ding et al. (2013)	chondrocyte culture, and 5–100 μM (50–1,000 mg/ml) intra-articular injection	Repression of IL-1ß, downregulation of mRNA and protein expression of MMP-1, -3 and -13	Crocin reduces inflammation *in-vitro* and regenerates rabbit knee cartilage
(K. Li et al., 2015)	NP cells/10–100 μM (100–1,000 mg/ml)	Decrease MMP-1, -3, and -13 overexpression, IL-1β, TNF-α, IL-6, and iNOS, and inhibit MAPK and JNK pathways	Crocin reduces inflammation *in-vitro* and *ex-vivo*
Poursamimi et al. (2020)	OA patients/15 mg tabs/day for 4 months	Decrease CRP and IL-17, increase regulatory T cells, shifted Treg/Th17 ratio towards regulatory T cells	Crocin decreases inflammation in OA patients

After treatment, joint pain, IL-6 level, muscular lipid peroxidation (LPO), and Nrf2 levels were decreased, while citrate synthase (CS) activity, myosin heavy chain (MHC) IIα expression, glutathione production, and glutathione peroxidase activity were increased. They concluded that crocin could reduce OA symptoms by alleviating oxidative stress and inflammation and inhibiting JNK activity, which is an interesting property for OA treatment (Lei et al., 2017). A study by Ding et al. demonstrated the chondrogenic effects of crocin. In their study, crocin repressed IL-1ß expression and reduced the synthesis of MMP-1, -3, and -13 in chondrocytes, probably by blocking the NF-κB pathway. In the *in vivo* phase of their study, intra-articular injections of crocin were performed, and the results showed that crocin can reduce cartilage degeneration in OA-induced rabbit knees (Ding et al., 2013). In a study conducted by Li et al. on the anti-inflammatory effects of crocin on rat intervertebral discs, nucleus pulposus cells were isolated from rats and treated with different doses of crocin. Crocin reduced MMP-1, -3, and -13 overexpression, pro-inflammatory factors including IL-1β, TNF-α, IL-6, and inducible nitric oxide synthase (iNOS), and inhibited mitogen-activated protein kinase (MAPK) and JNK pathways (K. Li et al., 2015). In a clinical trial conducted by Poursamim et al., 40 patients with OA received Krocina (crocin tablets, 15 mg/daily) or placebo for 4 months. The results demonstrated that crocin reduced serum CRP and IL-17 levels. In addition, the number of regulatory T cells increased while the number of T helper and $CD8^+$ cells decreased in crocin- and placebo-treated individuals, respectively. Finally, in the crocin group, the Treg/Th17 ratio shifted towards regulatory T cells (Poursamimi et al., 2020). The aforementioned reports demonstrate the possible curative potential of crocin on OA, which makes this herbal plant an appropriate candidate for OA treatment. In **Table 1**, a summary of studies on crocin and OA is presented.

Crocin and Rheumatoid Arthritis

Rheumatoid arthritis (RA) is a chronic autoimmune disease characterized by synovitis and degeneration of the cartilage and underlying bone, which can lead to lasting joint disorders (Turco, 1963; Nakken et al., 2017; Dreher et al., 2019). In this comprehensive disease, joint symptoms are most prevalent, which develop and progress through inflammation (Hamerman, 1966; CADTH Common Drug Reviews, 2015; Borthwick, 2016; Szekanecz et al., 2016). Studies have demonstrated a pivotal role for inflammatory cytokines, including TNF-α, IL-1β, and IL-6, in RA initiation and progression (Benucci et al., 2012; do Prado et al., 2016; Duesterdieck-Zellmer et al., 2012; Furman et al., 2014; Giacomelli et al., 2016; Hreggvidsdottir et al., 2014; G.; Li et al., 2016). Similar to the above studies, there are some reports demonstrating the probable roles of oxidative stress in RA development (Kacsur et al., 2002; Meki et al., 2009; Filaire and Toumi, 2012; Radhakrishnan et al., 2014). Studies have also shown that some signaling pathways can affect the progression and prognosis of RA, including Wnt/β-catenin signaling pathways. The Wnt/β-catenin pathway can regulate inflammatory cytokine secretion, which can affect fibroblast-like synoviocyte (FLS) proliferation and give rise to bone metabolism/destruction (Brunt et al., 2018; Liang et al., 2019; Macedo et al., 2019; Wang et al., 2020; Miao et al., 2021). When the Wnt signaling pathway is activated, pro-inflammatory cytokines, including TNF-α and IL-1β, are produced (Wu et al., 2017; Brunt and Scholpp, 2018; Yuan et al., 2018). NF-κB, which acts as an RA initiator, is another important molecule involved in RA pathogenesis (Gilston et al., 1997; Makarov, 2001). It has been suggested that NF-κB activation occurs prior to type II collagen-induced arthritis (CIA), which is associated with autoimmunity to type II collagen, B cells, and T cells, especially Th17, macrophages, and cytokines (Mulherin et al., 1996; Ehinger et al., 2001; Murphy et al., 2003; Roman-Blas and Jimenez, 2006; Zhu et al., 2010; Hu et al., 2013; Al-Zifzaf et al., 2015). Given the inflammatory nature of RA initiation, and the anti-inflammatory effects of crocin, studies have been designed to understand the possible effects of crocin on RA inhibition and treatment. In a study by Hemshekhar et al., in 2012, 10–20 mg/kg crocin was administered for 15 consecutive days in a rat model of arthritis. They demonstrated that crocin modulates the serum levels of enzymatic and non-enzymatic inflammatory cytokines, including MMP-13, MMP-3, MMP-9, HAases, TNF-α, IL-1β, NF-κB, IL-6, COX-2, and PGE2, as well as ROS mediators, which were increased in the RA-induced rats. Furthermore, crocin also increased the levels of GSH, SOD, CAT, and GST. In addition, inhibiting the exoglycosidases cathepsin-D and tartrate-resistant acid phosphatase in the bones adjacent to the joints by crocin protected bone resorption (Hemshekhar et al., 2012). Rathore et al. administered three doses of crocin (25, 50, and 100 mg/kg) for 47 days in a mouse model of RA. They observed a reduction in TNF-α and IL-1β levels and an increase in SOD and GR activity

TABLE 2 | Brief summary of studies on crocin and RA.

Reference	Models/Crocin doses	Main results	Conclusion
Hemshekhar et al. (2012)	Rats/10–20 mg/kg daily for 15 days	Decreased MMP-13, MMP-3, MMP-9, HAases, TNF-a, IL-1b, NF-κB, IL-6, COX-2, PGE2 and ROS. Impression GSH, SOD, CAT, and GST. Inhibited levels of the exoglycosidases cathepsin-D, and tartrate-resistant acid phosphatase	Reduced RA symptoms by regulating oxidative stress, inflammation, and the levels of exoglycosidases, cathepsin-D and tartrate-resistant acid phosphatase
Rathore et al. (2015)	Mice/25, 50 and 100 mg/kg for 47 days	Reduction in TNF-α and IL-1β levels, increase in SOD and GR activity in 50 and 100 mg/kg treatments	Reduced inflammation and oxidative stress in 50 and 100 mg/kg treatments
Hu et al. (2019)	Rats/160 mg/kg for 14 days	Decreased paw swelling and ankle diameters, joint, spleen, and thymus inflammation, and levels of TNF-α and TGF-β1	Reduced RA symptoms and complications by reducing inflammation
Liu et al. (2018)	Rats/40 mg/kg for 15 days	MMP-1, -3, and -13 protein expression levels were decreased and decreasing inflammatory cytokines similar to previous studies	Reduced RA by reducing inflammation
Li X et al. (2017)	Rats/6.25–25 mg/kg	Reduction in iNOS and decrease in inflammatory cytokines similar to previous studies	Crocin has positive effects on RA-induced rats
Li L et al. (2018)	Synoviocytes/500 μM (5,000 mg/ml)	Reduced TNF-α, IL-1β, IL-6, *p*-IκBα, *p*-IκB kinase α/β, and p65 expression	Crocin had anti-inflammatory and anti-arthritic effects *in-vitro* and *in-vivo* through NF-κB signaling
(Wang et al., 2020)	Rats/50 and 100 mg/kg	Reduced pain-related cytokines and glial activation by affecting Wnt/β-catenin and the Wnt signaling pathway	Reduced neuropathic pain in RA-induced rats

when higher doses were administered (Rathore et al., 2015). Hu et al. injected 160 mg/kg crocin for 14 days into RA-induced rats. Paw swelling and ankle diameters in crocin-treated rats were significantly decreased as compared to controls. Histological analysis also showed that inflammation was reduced in the joints and other organs, such as the spleen. In addition, TNF-α and TGF-β1 levels decreased in synovial tissues (Hu et al., 2019). In a similar study, Liu et al. showed that the anti-inflammatory and anti-arthritic effects of 40 mg/kg crocin lasted for 15 days. Their study showed that MMP-1, -3, and -13 protein expression levels were decreased in RA-induced rats (Liu et al., 2018). At the same time, Li et al. showed similar results, in addition to a reduction in iNOS production. This study, along with others, showed that crocin has positive effects on RA-induced rats (Li X et al., 2017). In an *in vitro* study, Li et al. demonstrated that 500 μM (5,000 mg/ml) of crocin reduced the levels of TNF-α, IL-1β, and IL-6 in human FLS. In addition, crocin caused lower levels of *p*-IκBα, *p*-IκB kinase α/β, and p65 expression, demonstrating its effect on the NF-κB pathway. The *in vivo* phase of their study showed that crocin can decrease TNF-α, IL-1β, and IL-6 serum levels, and that NF-κB signaling could suppress inflammation in FLS in RA-induced mice (Li L et al., 2018). Wang et al. showed that crocin inhibits Wnt/β-catenin and the Wnt signaling pathway to reduce pain-related cytokines, and glial activation may reduce neuropathic pain in RA-induced rats (J. F. Wang et al., 2020). Collectively, crocin may be an efficient treatment for RA and is effective for its associated secondary complications. **Table 2** summarizes these studies.

Crocin and Osteoporosis

Osteoporosis (OP) is a progressive systemic skeletal disorder characterized by a reduction in bone mass and deterioration of bone tissue, which occurs following an imbalance of bone formation/absorption, leading to bone fragility. The risk of bone fractures, morbidity, and mortality increases in OP, which increases treatment expenses as well (NHI, 2001; Todd and Robinson, 2003; Bliuc et al., 2009; Bawa, 2010). There are numerous factors that contribute to OP pathogenesis, including metabolic syndrome (MetS), which involves abnormal glucose metabolism, dyslipidemia, hypertension, and abdominal obesity (Zhou et al., 2013). In MetS, fat tissue secretes inflammatory factors and hyperglycemia results in an increase in glycation end products, which leads to a reduction in bone mineral density (BMD) (Yamaguchi, 2014). Due to the positive effects of crocin on hypertension, body fat balance, and MetS, along with its anti-inflammatory properties, crocin as a potential treatment for osteoporosis should receive more attention (Sheng et al., 2006; Imenshahidi et al., 2015; Shafiee et al., 2017). In a study by Algandaby, 5 and 10 mg/kg crocin was administered to a rat model of metabolic syndrome-induced osteoporosis. In the crocin treatment group, bone tissue was histologically protected against OP effects, bone formation markers including serum alkaline phosphatase and osteocalcin increased, and bone resorption markers, including tartrate-resistant acid phosphatase and collagen cross-linking carboxyterminal telopeptide, were inhibited. In addition, crocin reduced TNF-α and IL-6 serum levels and oxidative stress in the epiphyseal tissue of rats. These results demonstrated that crocin may protect against MetS-induced osteoporosis (Algandaby, 2019). Another cause of OP is hormone (including estrogen, testosterone, and parathyroid hormone) deficiency, which usually effects cancerous bone and can cause a reduction in BMD. OP is more common in women than in men, and women over 50 years of age are more vulnerable to causes of OP, likely because of estrogen deficiency in the postmenopausal period (Hunter and Sambrook, 2000; Marcus, 2002; Johnell and Kanis, 2006; Sugerman, 2014; Noh et al., 2020). Cao et al. studied the effects of 5–20 mg/kg/day of crocin for 12 weeks in ovariectomized rats. They demonstrated that crocin protected rats from reduced BMD in L4 vertebrae and femurs, and prevented deterioration of the trabecular microarchitecture in rats caused by ovariectomy. A significant reduction in skeletal remodeling, as evidenced by lower levels of bone turnover markers, was also observed. Oxidative stress factors in the

TABLE 3 | Brief summary of studies on crocin and OP.

Reference	Models/Crocin doses	Main results	Conclusion
Algandaby, (2019)	Rats/5–10 mg/kg daily for 12 weeks orally	Protected from histological changes in bone, increased serum alkaline phosphatase and osteocalcin, decreased tartrate-resistant acid phosphatase and collagen cross-linking carboxyterminal telopeptide and TNF-α and IL-6 oxidative stress	Crocin may be effective against MetS-induced osteoporosis
Cao et al. (2014)	Rats/5–20 mg/kg daily for 12 weeks	Reduction in skeletal remodeling and oxidative stress factors, increase in BMD and trabecular microarchitecture	Administration of crocin for 14 weeks can prevent OP in rats
Nie et al. (2019)	MC3T3-E1 cell line/ 100 μM (1,000 mg/ml)	Upregulated expression levels of Bcl-2 and Cyt C, and downregulated caspase-9, caspase-3, Bcl-2-associated X protein, and cytoplasmic Cyt C, and increased levels of ROS and intracellular Ca2+	Crocin may have a therapeutic effect on dexamethasone-induced apoptosis of osteoblasts via inhibition of the ROS/ Ca2+-mediated mitochondrial pathway *in-vitro*

serum or bone tissue returned to near-normal conditions. Collectively, these results demonstrated that crocin administration can prevent OP in rats (Cao et al., 2014). In an *in vitro* study by Nie et al., crocin was used to protect against glucocorticoid-induced osteoporosis and osteonecrosis by inhibiting the ROS/Ca^{2+}-mediated mitochondrial pathway. They showed that crocin decreases mitochondrial transmembrane potential and increases ROS and intracellular Ca^{2+} levels following induction of OP by dexamethasone in osteoblasts. In addition, the expression levels of B-cell lymphoma-2(Bcl-2) and mitochondrial cytochrome c (Cyt-C) were upregulated, and cleaved caspase-9, cleaved caspase-3, Bcl-2-associated X protein, and cytoplasmic Cyt C were downregulated by crocin (Nie et al., 2019). Taken together, these studies demonstrated that crocin is a potential medicine for OP treatment. **Table 3** shows the relationship between crocin and OP.

Effects of Crocin on Cell Differentiation

Bone regeneration is a complex procedure that occurs in abnormal conditions, such as bone degenerative diseases and fractures, but is insufficient and inefficient in some circumstances (Marzona and Pavolini, 2009; Dimitriou et al., 2011). Following the inflammatory phase of bone defects, there is a proliferative phase called the mesenchymal activation phase. During this phase, mesenchymal stem cells (MSCs) differentiate into chondrocytes and osteoblasts, which facilitate bone regeneration, either through endochondral ossification or intramembranous ossification (Knight and Hankenson, 2013). Bony tissue cells include osteoclasts, osteoblasts, and osteocytes, which are involved in bone regeneration and remodeling. These cells are derived from MSCs depending on the environmental stimulants that coordinate bone formation and bone absorption (Boyle et al., 2003; Zaminy et al., 2008; Knight and Hankenson, 2013; Noh et al., 2020). For example, studies have demonstrated that bone marrow MSCs (BMSCs) as multipotent stem cells can differentiate into bone and cartilage cells. This occurs through the expression of different growth factors, including platelet-derived growth factor (PDGF), bone morphogenetic proteins (BMPs), and transforming growth factor-β(TGF-β), and likely via the ERK and JNK MAPK signaling pathways. However, these growth factors are highly limited in these cells owing to rapid degradation and high cytotoxicity, as well as the high financial cost of these factors; thus, it is desirable to investigate novel osteoblastic inducers, especially natural products (Friedman et al., 2006; Fan et al., 2011; Mostafa et al., 2012; Yu et al., 2012; Udalamaththa et al., 2016; Li C et al., 2017). Baharara et al. (2014) reported successful differentiation of BMSCs into osteoblasts following treatment with crocin, which was confirmed by an increase in alkaline phosphatase (ALP) activity, cell mineralization, and osteocalcin gene expression (Baharara et al., 2014). Kalalinia et al. (2018) demonstrated that 12.5–50 μM (125–500 mg/ml) crocin is not cytotoxic based on the MTT assay and IC_{50} calculation. Moreover, at these concentrations, it may enhance osteogenesis in BMSCs, as measured by ALZ intensity, ALP activity, and ALP mRNA expression. Thus, crocin can be considered a safe substance to promote the osteogenic differentiation of BMSCs (Kalalinia et al., 2018). Li et al. (2017) also studied the osteogenic effect of crocin both *in vitro* and *in vivo*. For the *in vitro* study, they treated human BMSCs with crocin and demonstrated an increase in ALP activity and calcium nodule formation (assayed by alizarin red S staining). In addition, they treated male rats with femoral head osteonecrosis with crocin and showed considerable histopathological changes in the femoral head tissues with H&E staining. Western blotting and q-PCR assays showed an increase in the expression levels of RUNX2, COL1A1, and OCN, and a decrease in GSK-3β phosphorylation in both bone tissue and BMSCs after treatment with crocin, in a dose-dependent manner. These researchers suggested that crocin has potential for use in the treatment of osteogenic diseases in the future (B. Li et al., 2020). Koski et al. administered crocin over 7 weeks to human fetal osteoblasts and observed an increase in cell proliferation. In addition, crocin decreased human osteosarcoma (MG-63) cells viability *in vitro*. In contrast, the *in vivo* application of crocin showed pro-apoptotic and anti-inflammatory effects in a rat model of femoral inflammation. These results suggest that crocin may have a therapeutic effect on osteosarcoma regulation and potential for use in wound healing during bone tissue regeneration (Koski et al., 2020). Studies have shown that in some diseases involving bone degeneration and dysregulation of bone homeostasis besides osteogenesis, the influence of osteoclast formation and osteo-immunomodulation is important (Chen et al., 2017b; Chen

TABLE 4 | Studies on the effect of crocin on osteoblastic differentiation.

Reference	Models/Crocin doses	Main results	Conclusion
Baharara et al. (2014)	BMSCs/60–80 μM (600–800 mg/ml)	Increased alkaline phosphatase (ALP) activity, cell mineralization, and osteocalcin gene expression	crocin may have effect on osteoblastic differentiation of BMSCs
Kalalinia et al. (2018)	BMSCs/12.5–50 μM (125–500 mg/ml)	Increased ALZ intensity, ALP activity, and ALP mRNA expression, was not cytotoxic using MTT test and IC_{50} calculation	Crocin can be considered a safe substance to promote osteogenic differentiation of BMSCs
(B. Li et al., 2020)	hBMSCs/10–50 μM (10–500 mg/ml)	Increased LAP activity, calcium nodules, and RUNX2, COL1A1, and OCN expression, decreased GSK- 3β phosphorylation	Crocin is effective in *in-vitro* and *in-vivo* osteogenic models
Zhu et al. (2019)	M2 macrophages and BMSCs/40 and 80 μM (400–800 mg/ml)	Promoted M2 phenotype that was decreased in anti-inflammatory cytokine-induced osteogenic differentiation of BMSCs in co-culture with pre-treated macrophages through inhibition of p38 and c-Jun N-terminal kinase signaling	Crocin has therapeutic potential for bone degenerative diseases through induction of M2 macrophage polarization, resulting in inflammation reduction and osteogenic differentiation of BMSCs
Koski et al. (2020)	hFOBs and MG-63 cell line, Rats/ 45 μg (450 mg/ml)	Increased osteoblast proliferation and decreased osteosarcoma viability and pro-apoptotic and anti-inflammatory effects *in-vivo*	Crocin has a potential therapeutic effect on osteosarcoma regulation and uses for wound healing during bone tissue regeneration

TABLE 5 | Studies on the effect of crocin on osteoclastic inhibition.

Reference	Models/Crocin doses	Main results	Conclusion
Fu et al. (2017)	BMMs/100 μM (1,000 mg/ml)	Inhibition of RANKL, downregulation of NF-κB pathway, and reduction of NFATc1, c-Fos and cathepsin levels	Crocin suppresses osteoclast differentiation and function and inhibits bone resorption activity
Shi et al. (2018)	BMMs/10–40 μM (100–400 mg/ml)	Downregulation of NFATc1, c-Fos and cathepsin K, inhibition of κBα degradation, NF-κB p65 subunit nuclear translocation suppression, and JNK activation resulted in inhibition of RANKL	Crocin downregulates osteoclast differentiation via inhibition of JNK and NF-κB signaling pathways and decreases osteoclastogenesis in BMMs
Suh et al. (2019)	RAW264.7 cell line/ 2–10 μM (20–100 mg/ml)	Decreased gene expression levels of TRAF6, Akt2, ERK1, OSTM1, and MMP-9	Crocin decreases osteoclast function and differentiation and bone resorption *in-vitro*, as well reduction in bone resorption activity of osteoclasts

et al., 2017c). On the other hand, M2 macrophages (anti-inflammatory macrophages) secrete cytokines such as BMP-2 that contribute to osteogenesis (Yuan et al., 2017). Note that crocin may be effective in macrophage polarization and promotion of the M2 phenotype (Li J et al., 2018). Zhu et al. showed that crocin promoted macrophage polarization toward the M2 phenotype and reduced the expression of anti-inflammatory cytokines *in vitro* and *in vivo*. In addition, pre-treatment of macrophages with crocin induced the osteogenic differentiation of BMSCs in co-culture media. This is probably due to the inhibition of p38 and c-Jun N-terminal kinase signaling. This study indicated that crocin has therapeutic potential for bone degenerative disease by inducing M2 macrophage polarization, which results in inflammation reduction and osteogenic differentiation of BMSCs (Zhu et al., 2019). The above-mentioned studies have emphasized that crocin may have a positive effect on osteogenesis by promoting osteoblastic differentiation. A summary of these studies is provided in **Table 4**.

In some pathological conditions related to bone loss-associated diseases (osteoporosis, arthritis, osteomyelitis, etc.), osteoclast cells are activated, leading to bone resorption. Under similar conditions, an imbalance occurs between osteoblast activities (leading to bone formation) and osteoclast activities (leading to bone resorption) (Boyle et al., 2003; Walsh and Gravallese, 2010; Redlich and Smolen, 2012). Stimulation of hematopoietic stem cells (HSCs) by inflammatory cytokines, such as IL-1, IL-6, and TNF-α (which are inhibited by crocin, as mentioned above) or other factors such as monocyte/ macrophage colony-stimulating factor (M-CSF) and activation of receptor activator of nuclear factor kappaB (RANK) with its ligand (RANKL) can lead to osteoclast differentiation (Udagawa et al., 1999; Azuma et al., 2000; Teitelbaum, 2000; Ross, 2006; Walsh and Gravallese, 2010; Redlich and Smolen, 2012; Yamashita et al., 2012; Xu and Teitelbaum, 2013; Yokota et al., 2014). Studies have indicated that RANKL, a membrane protein of the TNF family, plays a role in osteoclast differentiation (Yasuda et al., 1998; Takayanagi et al., 2000; Roodman, 2006). RANKL is expressed on osteoblast cell membranes in response to stimulatory factors and then engages RANK on osteoclast cell membranes, along with activation of the NF-κB and MAPK signaling pathways. The final product of these cascades is the expression of tartrate-resistant acid phosphatase (TRAP) and other enzymes, which are involved in osteoclast-mediated bone resorption (Asagiri and Takayanagi, 2007). Fu et al. demonstrated that crocin suppresses osteoclast differentiation and function by directly inhibiting RANKL in bone marrow-derived macrophages (BMM). Downregulation of the NF-κB pathway and reduction in

osteoclast-specific gene expression, including NFATc1, c-Fos, and cathepsin, are involved, leading to inhibition of bone resorption activity (Fu et al., 2017). A similar study by Shi et al. demonstrated that crocin downregulates osteoclast differentiation via inhibition of JNK and NF-κB signaling pathways in BMM cells *in vitro*. In the crocin-treated group, osteoclast markers including NFATc1, c-Fos, and cathepsin K, were downregulated. An inhibitor of κBα degradation and NF-κB p65 subunit nuclear translocation was suppressed, while c-Jun N-terminal kinase (JNK) was activated, resulting in the inhibition of RANKL in BMM. These results demonstrated that crocin decreased osteoclastogenesis in BMM (Shi et al., 2018). Suh et al. showed that crocin treatment decreased gene expression of TRAF6, Akt2, ERK1, OSTM1, and MMP-9, which are related to osteoclast differentiation and function and bone resorption *in vitro*, as well as a reduction in bone resorption activity of osteoclasts (Suh et al., 2019). These studies demonstrate the potential therapeutic effect of crocin on osteoclast and bone resorption dysfunction, as well as bone loss-associated diseases. A summary of these studies is provided in **Table 5**.

CONCLUSION

Studies have shown that crocin, the main biologically active component of saffron, has anti-inflammatory and antioxidant effects. In addition, crocin has potential therapeutic effects on bone and cartilage diseases that involve inflammation and accumulation of free radicals, including OA, RA, and osteoporosis. Crocin can reduce oxidative stress and inflammatory cytokines via inhibiting molecular pathways include Wnt, MAPK and JNK signaling pathway. It modulates PI3K/Akt and NF-κB signaling pathways and polarizes macrophages to the M2 (anti-inflammatory) phenotype by suppressing the p38 and JNK pathways. Crocin also has proliferative and anti-apoptotic effects, especially on osteoblasts, and positive effects on osteoblastic differentiation of MSCs, while it also inhibits osteoclast activity. These data suggest promising potential therapeutic use of crocin in bone degenerative and bone-loss diseases, which require more precise laboratories and clinical trials. For example, crocin in high doses exhibited a cytotoxic effect and acts as an apoptotic promotor (Li et al., 2013), so it seems that further researches are needed to the determination of proper crocin dosage for both *in-vitro* and *in-vivo* studies. Also, the molecular mechanisms of various crocin effects are not recognized very well yet, so future studies may need to clarify the molecular mechanisms that they are involved. Overall regarding the beneficial effects of crocin in bone and cartilage diseases and due to lack of human studies in crocin effects in this field, the need for human trials is felt and future studies can be done in this research area.

AUTHOR CONTRIBUTIONS

JT and SN-M conceived this manuscript. SV drafted this manuscript. XW revised this manuscript.

FUNDING

This study was supported by the National Natural Science Foundation of China (31900616) and the Project of Improvement of Scientific Ability of Anhui Medical University (2020xkjT009).

REFERENCES

Al-Zifzaf, D. S., El Bakry, S. A., Shawarby, L. A., Ghaffar, A. Y. A., Amer, H. A., et al. (2015). FoxP3+T Regulatory Cells in Rheumatoid Arthritis and the Imbalance of the Treg/TH17 Cytokine axis. *The Egypt. Rheumatologist* 37 (1), 7–15. doi:10.1016/j.ejr.2014.06.004

Alavizadeh, S. H., and Hosseinzadeh, H. (2014). Bioactivity Assessment and Toxicity of Crocin: a Comprehensive Review. *Food Chem. Toxicol.* 64, 65–80. doi:10.1016/j.fct.2013.11.016

Algandaby, M. M. (2019). Crocin Attenuates Metabolic Syndrome-Induced Osteoporosis in Rats. *J. Food Biochem.* 43 (7), e12895. doi:10.1111/jfbc.12895

Alonso, G. L., Salinas, M. R., Garijo, J., and Sánchez-fernández, M. A. (2001). Composition of Crocins and Picrocrocin from Spanish Saffron (Crocus Sativus L.). *J. Food Qual.* 24 (3), 219–233. doi:10.1111/j.1745-4557.2001.tb00604.x

Altinoz, E., Ozmen, T., Oner, Z., Elbe, H., Erdemli, M. E., and Bag, H. G. (2016). Effect of Crocin on Oxidative Stress in Recovery from Single Bout of Swimming Exercise in Rats. *Gen. Physiol. Biophys.* 35 (1), 87–94. doi:10.4149/gpb_2015018

Asadi, M. H., Zafari, F., Sarveazad, A., Abbasi, M., Safa, M., Koruji, M., et al. (2014). Saffron Improves Epididymal Sperm Parameters in Rats Exposed to Cadmium. *Nephrourol Mon* 6 (1), e12125. doi:10.5812/numonthly.12125

Asagiri, M., and Takayanagi, H. (2007). The Molecular Understanding of Osteoclast Differentiation. *Bone* 40 (2), 251–264. doi:10.1016/j.bone.2006.09.023

Azuma, Y., Kaji, K., Katogi, R., Takeshita, S., and Kudo, A. (2000). Tumor Necrosis Factor-Alpha Induces Differentiation of and Bone Resorption by Osteoclasts. *J. Biol. Chem.* 275 (7), 4858–4864. doi:10.1074/jbc.275.7.4858

Baghishani, F., Mohammadipour, A., Hosseinzadeh, H., Hosseini, M., and Ebrahimzadeh-Bideskan, A. (2018). The Effects of Tramadol Administration on Hippocampal Cell Apoptosis, Learning and Memory in Adult Rats and Neuroprotective Effects of Crocin. *Metab. Brain Dis.* 33 (3), 907–916. doi:10.1007/s11011-018-0194-6

Bawa, S. (2010). The Significance of Soy Protein and Soy Bioactive Compounds in the Prophylaxis and Treatment of Osteoporosis. *J. Osteoporos.* 2010, 891058. doi:10.4061/2010/891058

Benazzo, F., Perticarini, L., Padolino, A., Castelli, A., Gifuni, P., Lovato, M., et al. (2016). A multi-centre, Open Label, Long-Term Follow-Up Study to Evaluate the Benefits of a New Viscoelastic Hydrogel (Hymovis®) in the Treatment of Knee Osteoarthritis. *Eur. Rev. Med. Pharmacol. Sci.* 20 (5), 959–968.

Benucci, M., Saviola, G., Baiardi, P., Manfredi, M., Sarzi Puttini, P., and Atzeni, F. (2012). Determinants of Risk Infection during Therapy with Anti TNF-Alpha Blocking Agents in Rheumatoid Arthritis. *Open Rheumatol. J.* 6, 33–37. doi:10.2174/1874312901206010033

Bliuc, D., Nguyen, N. D., Milch, V. E., Nguyen, T. V., Eisman, J. A., and Center, J. R. (2009). Mortality Risk Associated with Low-Trauma Osteoporotic Fracture and Subsequent Fracture in Men and Women. *Jama* 301 (5), 513–521. doi:10.1001/jama.2009.50

Borthwick, L. A. (2016). The IL-1 Cytokine Family and its Role in Inflammation and Fibrosis in the Lung. *Semin. Immunopathol* 38 (4), 517–534. doi:10.1007/s00281-016-0559-z

Boyle, W. J., Simonet, W. S., and Lacey, D. L. (2003). Osteoclast Differentiation and Activation. *Nature* 423 (6937), 337–342. doi:10.1038/nature01658

Brunt, L., and Scholpp, S. (2018). The Function of Endocytosis in Wnt Signaling. *Cell Mol Life Sci* 75 (5), 785–795. doi:10.1007/s00018-017-2654-2

Burrage, P. S., Mix, K. S., and Brinckerhoff, C. E. (2006). Matrix Metalloproteinases: Role in Arthritis. *Front. Biosci.* 11, 529–543. doi:10.2741/1817

Caballero-Ortega, H., Pereda-Miranda, R., and Abdullaev, F. I. (2007). HPLC Quantification of Major Active Components from 11 Different Saffron (Crocus Sativus L.) Sources. *Food Chem.* 100 (3), 1126–1131. doi:10.1016/j.foodchem.2005.11.020

CADTH Common Drug Reviews (2015). In Golimumab (Simponi) IV: In Combination with Methotrexate (MTX) for the Treatment of Adult Patients with Moderately to Severely Active Rheumatoid Arthritis. *Ottawa (On) Can. Agency Drugs Tech. Health Copyright © CADTH*, 26962595.

Cao, P. C., Xiao, W. X., Yan, Y. B., Zhao, X., Liu, S., Feng, J., et al. (2014). Preventive Effect of Crocin on Osteoporosis in an Ovariectomized Rat Model. *Evid. Based Complement. Alternat Med.* 2014, 825181. doi:10.1155/2014/825181

Chen, D., Shen, J., Zhao, W., Wang, T., Han, L., Hamilton, J. L., et al. (2017a). Osteoarthritis: toward a Comprehensive Understanding of Pathological Mechanism. *Bone Res.* 5, 16044. doi:10.1038/boneres.2016.44

Chen, Z., Bachhuka, A., Han, S., Wei, F., Lu, S., Visalakshan, R. M., et al. (2017b). Tuning Chemistry and Topography of Nanoengineered Surfaces to Manipulate Immune Response for Bone Regeneration Applications. *ACS Nano* 11 (5), 4494–4506. doi:10.1021/acsnano.6b07808

Chen, Z., Ni, S., Han, S., Crawford, R., Lu, S., Wei, F., et al. (2017c). Nanoporous Microstructures Mediate Osteogenesis by Modulating the Osteo-Immune Response of Macrophages. *Nanoscale* 9 (2), 706–718. doi:10.1039/C6NR06421C

de Sousa, L. M., dos Santos Alves, J. M., da Silva Martins, C., Pereira, K. M. A., Goes, P., and Gondim, D. V. (2019). Immunoexpression of Canonical Wnt and NF-Kb Signaling Pathways in the Temporomandibular Joint of Arthritic Rats. *Inflamm. Res.* 68, 889–900. doi:10.1007/s00011-019-01274-4

Deng, M., Li, D., Zhang, Y., Zhou, G., Liu, W., Cao, Y., et al. (2018). Protective Effect of Crocin on Ultraviolet B-induced D-ermal F-ibroblast P-hotoaging. *Mol. Med. Rep.* 18 (2), 1439–1446. doi:10.3892/mmr.2018.9150

Dimitriou, R., Jones, E., McGonagle, D., and Giannoudis, P. V. (2011). Bone Regeneration: Current Concepts and Future Directions. *BMC Med.* 9, 66. doi:10.1186/1741-7015-9-66

Ding, Q., Zhong, H., Qi, Y., Cheng, Y., Li, W., Yan, S., et al. (2013). Anti-arthritic Effects of Crocin in Interleukin-1β-Treated Articular Chondrocytes and Cartilage in a Rabbit Osteoarthritic Model. *Inflamm. Res.* 62 (1), 17–25. doi:10.1007/s00011-012-0546-3

do Prado, A. D., Bisi, M. C., Piovesan, D. M., Bredemeier, M., Batista, T. S., Petersen, L., et al. (2016). Ultrasound Power Doppler Synovitis Is Associated with Plasma IL-6 in Established Rheumatoid Arthritis. *Cytokine* 83, 27–32. doi:10.1016/j.cyto.2016.03.014

Dreher, M., Kosz, M., and Schwarting, A. (2019). Physical Activity, Exercise and Nutrition in Rheumatism : Adjuvant Treatment Options for Inflammatory-Rheumatic Diseases. *Orthopade* 48 (11), 917–926. doi:10.1007/s00132-019-03808-4

Dubin, A. (2016). Managing Osteoarthritis and Other Chronic Musculoskeletal Pain Disorders. *Med. Clin. North. Am.* 100 (1), 143–150. doi:10.1016/j.mcna.2015.08.008

Duesterdieck-Zellmer, K. F., Driscoll, N., and Ott, J. F. (2012). Concentration-dependent Effects of Tiludronate on Equine Articular Cartilage Explants Incubated with and without Interleukin-1β. *Am. J. Vet. Res.* 73 (10), 1530–1539. doi:10.2460/ajvr.73.10.1530

Ebadi, M. (2006). *Pharmacodynamic Basis of Herbal Medicine*. 2nd Ed. Boca Raton, Florida, United States: CRC Press.

Ebrahimi, B., Vafaei, S., Rastegar-Moghaddam, S. H. R., Hosseini, M., Tajik Yabr, F., and Mohammadipour, A. (2021). Crocin Administration from Childhood to Adulthood Increases Hippocampal Neurogenesis and Synaptogenesis in Male MiceJournal of Kerman University of Medical Sciences. *J. Kerman Univ. Med. Sci.* 28 (3), 243–251. doi:10.22062/jkmu.2021.91664

Ehinger, M., Vestberg, M., Johansson, A. C., Johannesson, M., Svensson, A., and Holmdahl, R. (2001). Influence of CD4 or CD8 Deficiency on Collagen-Induced Arthritis. *Immunology* 103 (3), 291–300. doi:10.1046/j.1365-2567.2001.01257.x

Fan, J. J., Cao, L. G., Wu, T., Wang, D. X., Jin, D., Jiang, S., et al. (2011). The Dose-Effect of Icariin on the Proliferation and Osteogenic Differentiation of Human Bone Mesenchymal Stem Cells. *Molecules* 16 (12), 10123–10133. doi:10.3390/molecules161210123

Feldmann, M. (2001). Pathogenesis of Arthritis: Recent Research Progress. *Nat. Immunol.* 2 (9), 771–773. doi:10.1038/ni0901-771

Filaire, E., and Toumi, H. (2012). Reactive Oxygen Species and Exercise on Bone Metabolism: Friend or Enemy? *Jt. Bone Spine* 79 (4), 341–346. doi:10.1016/j.jbspin.2012.03.007

Friedman, M. S., Long, M. W., and Hankenson, K. D. (2006). Osteogenic Differentiation of Human Mesenchymal Stem Cells Is Regulated by Bone Morphogenetic Protein-6. *J. Cel Biochem* 98 (3), 538–554. doi:10.1002/jcb.20719

Fu, L., Pan, F., and Jiao, Y. (2017). Crocin Inhibits RANKL-Induced Osteoclast Formation and Bone Resorption by Suppressing NF-Kb Signaling Pathway Activation. *Immunobiology* 222 (4), 597–603. doi:10.1016/j.imbio.2016.11.009

Furman, B. D., Mangiapani, D. S., Zeitler, E., Bailey, K. N., Horne, P. H., Huebner, J. L., et al. (2014). Targeting Pro-inflammatory Cytokines Following Joint Injury: Acute Intra-articular Inhibition of Interleukin-1 Following Knee Injury Prevents post-traumatic Arthritis. *Arthritis Res. Ther.* 16 (3), R134. doi:10.1186/ar4591

Giacomelli, R., Ruscitti, P., Alvaro, S., Ciccia, F., Liakouli, V., Di Benedetto, P., et al. (2016). IL-1β at the Crossroad between Rheumatoid Arthritis and Type 2 Diabetes: May We Kill Two Birds with One Stone? *Expert Rev. Clin. Immunol.* 12 (8), 849–855. doi:10.1586/1744666x.2016.1168293

Gilston, V., Jones, H. W., Soo, C. C., Coumbe, A., Blades, S., Kaltschmidt, C., et al. (1997). NF-kappa B Activation in Human Knee-Joint Synovial Tissue during the Early Stage of Joint Inflammation. *Biochem. Soc. Trans.* 25 (3), 518. doi:10.1042/bst025518s

Gismondi, A., Serio, M., Canuti, L., and Canini, A. (2012). Biochemical, Antioxidant and Antineoplastic Properties of Italian Saffron (*Crocus Sativus L. %J Am. J. Plant Sci.* 03 (11), 8. doi:10.4236/ajps.2012.311190

Gohari, A. R., Saeidnia, S., and Mahmoodabadi, M. K. (2013). An Overview on Saffron, Phytochemicals, and Medicinal Properties. *Pharmacogn Rev.* 7 (13), 61–66. doi:10.4103/0973-7847.112850

Goldring, M. B. (2000). Osteoarthritis and Cartilage: the Role of Cytokines. *Curr. Rheumatol. Rep.* 2 (6), 459–465. doi:10.1007/s11926-000-0021-y

Haeri, P., Mohammadipour, A., Heidari, Z., and Ebrahimzadeh-Bideskan, A. (2019). Neuroprotective Effect of Crocin on Substantia Nigra in MPTP-Induced Parkinson's Disease Model of Mice. *Anat. Sci. Int.* 94 (1), 119–127. doi:10.1007/s12565-018-0457-7

Hamerman, D. (1966). New Thoughts on the Pathogenesis of Rheumatoid Arthritis. *Am. J. Med.* 40 (1), 1–9. doi:10.1016/0002-9343(66)90181-1

Hatziagapiou, K., Kakouri, E., Lambrou, G. I., Bethanis, K., and Tarantilis, P. A. (2019). Antioxidant Properties of Crocus Sativus L. And its Constituents and Relevance to Neurodegenerative Diseases; Focus on Alzheimer's and Parkinson's Disease. *Curr. Neuropharmacol* 17 (4), 377–402. doi:10.2174/1570159x16666180321095705

Hemshekhar, M., Sebastin Santhosh, M., Sunitha, K., Thushara, R. M., Kemparaju, K., Rangappa, K. S., et al. (2012). A Dietary Colorant Crocin Mitigates Arthritis and Associated Secondary Complications by Modulating Cartilage Deteriorating Enzymes, Inflammatory Mediators and Antioxidant Status. *Biochimie* 94 (12), 2723–2733. doi:10.1016/j.biochi.2012.08.013

Hosseinzadeh, H., Mehri, S., Heshmati, A., Ramezani, M., Sahebkar, A., and Abnous, K. (2014). Proteomic Screening of Molecular Targets of Crocin. *Daru* 22 (1), 5. doi:10.1186/2008-2231-22-5

Hosseinzadeh, H., and Nassiri-Asl, M. (2013). Avicenna's (Ibn Sina) the Canon of Medicine and Saffron (Crocus Sativus): a Review. *Phytother Res.* 27 (4), 475–483. doi:10.1002/ptr.4784

Hreggvidsdottir, H. S., Noordenbos, T., and Baeten, D. L. (2014). Inflammatory Pathways in Spondyloarthritis. *Mol. Immunol.* 57 (1), 28–37. doi:10.1016/j.molimm.2013.07.016

Hu, Y., Cheng, W., Cai, W., Yue, Y., Li, J., and Zhang, P. (2013). Advances in Research on Animal Models of Rheumatoid Arthritis. *Clin. Rheumatol.* 32 (2), 161–165. doi:10.1007/s10067-012-2041-1

Hu, Y., Liu, X., Xia, Q., Yin, T., Bai, C., Wang, Z., et al. (2019). Comparative Anti-arthritic Investigation of Iridoid Glycosides and Crocetin Derivatives from

Gardenia Jasminoides Ellis in Freund's Complete Adjuvant-Induced Arthritis in Rats. *Phytomedicine* 53, 223–233. doi:10.1016/j.phymed.2018.07.005

Hunter, D. J., and Sambrook, P. N. (2000). Bone Loss. Epidemiology of Bone Loss. *Arthritis Res.* 2 (6), 441–445. doi:10.1186/ar125

Imenshahidi, M., Razavi, M., Faal, A., Gholampoor, A., Mousavi, S., and Hosseinzadeh, H. (2015). The Effect of Chronic Administration of Safranal on Systolic Blood Pressure in Rats. *Iranian J. Pharm. Res.* 14 (2), 585–590. doi:10.22037/ijpr.2015.1669

Jalili, C., Tabatabaei, H., Kakaberiei, S., Roshankhah, S., and Salahshoor, M. R. (2015). Protective Role of Crocin against Nicotine-Induced Damages on Male Mice Liver. *Int. J. Prev. Med.* 6, 92. doi:10.4103/2008-7802.165203

Javad, B., Tayebe, R., Shahrokhabadi Khadijeh, N., and Maryam, N. (2014). Effects of Crocus Sativus Lextract and Vitamin D3 on *In Vitro* Osteogenesis of Mecenchymal Stem Cells. *Int. J. Cell Mol. Biotechnol.* 2014, 1–10. doi:10.5899/2014/ijcmb-00012

Johnell, O., and Kanis, J. A. (2006). An Estimate of the Worldwide Prevalence and Disability Associated with Osteoporotic Fractures. *Osteoporos. Int.* 17 (12), 1726–1733. doi:10.1007/s00198-006-0172-4

Kacsur, C., Mader, R., Ben-Amotz, A., and Levy, Y. (2002). Plasma Anti-oxidants and Rheumatoid Arthritis. *Harefuah* 141 (2), 148–223.

Kalalinia, F., Ghasim, H., Amel Farzad, S., Pishavar, E., Ramezani, M., and Hashemi, M. (2018). Comparison of the Effect of Crocin and Crocetin, Two Major Compounds Extracted from Saffron, on Osteogenic Differentiation of Mesenchymal Stem Cells. *Life Sci.* 208, 262–267. doi:10.1016/j.lfs.2018.07.043

Knight, M. N., and Hankenson, K. D. (2013). Mesenchymal Stem Cells in Bone Regeneration. *Adv. Wound Care (New Rochelle)* 2 (6), 306–316. doi:10.1089/wound.2012.0420

Korani, S., Korani, M., Sathyapalan, T., and Sahebkar, A. (2019). Therapeutic Effects of Crocin in Autoimmune Diseases: A Review. *Biofactors* 45 (6), 835–843. doi:10.1002/biof.1557

Koski, C., Sarkar, N., and Bose, S. (2020). Cytotoxic and Osteogenic Effects of Crocin and Bicarbonate from Calcium Phosphates for Potential Chemopreventative and Anti-inflammatory Applications *In Vitro* and *In Vivo*. *J. Mater. Chem. B* 8 (10), 2048–2062. doi:10.1039/c9tb01462d

Krasnokutsky, S., Samuels, J., and Abramson, S. B. (2007). Osteoarthritis in 2007. *Bull. NYU Hosp. Jt. Dis.* 65 (3), 222–228.

Largo, R., Alvarez-Soria, M. A., Díez-Ortego, I., Calvo, E., Sánchez-Pernaute, O., Egido, J., et al. (2003). Glucosamine Inhibits IL-1beta-induced NFkappaB Activation in Human Osteoarthritic Chondrocytes. *Osteoarthritis Cartilage* 11 (4), 290–298. doi:10.1016/s1063-4584(03)00028-1

Lei, M., Guo, C., Hua, L., Xue, S., Yu, D., Zhang, C., et al. (2017). Crocin Attenuates Joint Pain and Muscle Dysfunction in Osteoarthritis Rat. *Inflammation* 40 (6), 2086–2093. doi:10.1007/s10753-017-0648-8

Li, B., Qin, K., Wang, B., Liu, B., Yu, W., Li, Z., et al. (2020). Crocin Promotes Osteogenesis Differentiation of Bone Marrow Mesenchymal Stem Cells. In Vitro *Cel Dev Biol Anim* 56 (8), 680–688. doi:10.1007/s11626-020-00487-w

Li, C., Wei, G. J., Xu, L., Rong, J. S., Tao, S. Q., and Wang, Y. S. (2017). The Involvement of Senescence Induced by the Telomere Shortness in the Decline of Osteogenic Differentiation in BMSCs. *Eur. Rev. Med. Pharmacol. Sci.* 21 (5), 1117–1124.

Li, G., Wu, Y., Jia, H., Tang, L., Huang, R., Peng, Y., et al. (2016). Establishment and Evaluation of a Transgenic Mouse Model of Arthritis Induced by Overexpressing Human Tumor Necrosis Factor Alpha. *Biol. Open* 5 (4), 418–423. doi:10.1242/bio.016279

Li, J., Lei, H. T., Cao, L., Mi, Y. N., Li, S., and Cao, Y. X. (2018). Crocin Alleviates Coronary Atherosclerosis via Inhibiting Lipid Synthesis and Inducing M2 Macrophage Polarization. *Int. Immunopharmacol* 55, 120–127. doi:10.1016/j.intimp.2017.11.037

Li, K., Li, Y., Ma, Z., and Zhao, J. (2015). Crocin Exerts Anti-inflammatory and Anti-catabolic Effects on Rat Intervertebral Discs by Suppressing the Activation of JNK. *Int. J. Mol. Med.* 36 (5), 1291–1299. doi:10.3892/ijmm.2015.2359

Li, L., Zhang, H., Jin, S., and Liu, C. (2018). Effects of Crocin on Inflammatory Activities in Human Fibroblast-like Synoviocytes and Collagen-Induced Arthritis in Mice. *Immunol. Res.* 66 (3), 406–413. doi:10.1007/s12026-018-8999-2

Li, S., Liu, X., Lei, J., Yang, J., Tian, P., and Gao, Y. (2017). Crocin Protects Podocytes against Oxidative Stress and Inflammation Induced by High Glucose through Inhibition of NF-Kb. *Cell Physiol Biochem* 42 (4), 1481–1492. doi:10.1159/000479212

Li, X., Huang, T., Jiang, G., Gong, W., Qian, H., and Zou, C. (2013). Synergistic Apoptotic Effect of Crocin and Cisplatin on Osteosarcoma Cells via Caspase Induced Apoptosis. *Toxicol. Lett.* 221 (3), 197–204. doi:10.1016/j.toxlet.2013.06.233

Li, X., Jiang, C., and Zhu, W. (2017). Crocin Reduces the Inflammation Response in Rheumatoid Arthritis. *Biosci. Biotechnol. Biochem.* 81 (5), 891–898. doi:10.1080/09168451.2016.1263145

Liakopoulou-Kyriakides, M., and Kyriakidis, D. A. (2002). "Croscus Sativus-Biological Active Constitutents,". Editor R. Atta ur (Amsterdam, Netherlands: Elsevier), Vol. 26, 293–312. doi:10.1016/s1572-5995(02)80009-6*Studies in Natural Products Chemistry*

Liang, J. J., Li, H. R., Chen, Y., Zhang, C., Chen, D. G., Liang, Z. C., et al. (2019). Diallyl Trisulfide Can Induce Fibroblast-like Synovial Apoptosis and Has a Therapeutic Effect on Collagen-Induced Arthritis in Mice via Blocking NF-Kb and Wnt Pathways. *Int. Immunopharmacol* 71, 132–138. doi:10.1016/j.intimp.2019.03.024

Lim, H. A., Song, E. K., Seon, J. K., Park, K. S., Shin, Y. J., and Yang, H. Y. (2017). Causes of Aseptic Persistent Pain after Total Knee Arthroplasty. *Clin. Orthop. Surg.* 9 (1), 50–56. doi:10.4055/cios.2017.9.1.50

Linton, M. F., and Fazio, S. (2003). Macrophages, Inflammation, and Atherosclerosis. *Int. J. Obes. Relat. Metab. Disord.* 27 (Suppl. l), S35–S40. doi:10.1038/sj.ijo.0802498

Liu, W., Sun, Y., Cheng, Z., Guo, Y., Liu, P., and Wen, Y. (2018). Crocin Exerts Anti-inflammatory and Anti-arthritic Effects on Type II Collagen-Induced Arthritis in Rats. *Pharm. Biol.* 56 (1), 209–216. doi:10.1080/13880209.2018.1448874

Lv, B., Huo, F., Zhu, Z., Xu, Z., Dang, X., Chen, T., et al. (2016). Crocin Upregulates CX3CR1 Expression by Suppressing NF-Kb/yy1 Signaling and Inhibiting Lipopolysaccharide-Induced Microglial Activation. *Neurochem. Res.* 41 (8), 1949–1957. doi:10.1007/s11064-016-1905-1

Makarov, S. S. (2001). NF-kappa B in Rheumatoid Arthritis: a Pivotal Regulator of Inflammation, Hyperplasia, and Tissue Destruction. *Arthritis Res.* 3 (4), 200–206. doi:10.1186/ar300

Marcus, R. (2002). An Expanded Overview of Postmenopausal Osteoporosis. *J. Musculoskelet. Neuronal Interact* 2 (3), 195–197.

Marzona, L., and Pavolini, B. (2009). Play and Players in Bone Fracture Healing Match. *Clin. Cases Miner Bone Metab.* 6 (2), 159–162.

Meki, A. R., Hamed, E. A., and Ezam, K. A. (2009). Effect of green tea Extract and Vitamin C on Oxidant or Antioxidant Status of Rheumatoid Arthritis Rat Model. *Indian J. Clin. Biochem.* 24 (3), 280–287. doi:10.1007/s12291-009-0053-7

Melnyk, J. P., Wang, S., and Marcone, M. F. (2010). Chemical and Biological Properties of the World's Most Expensive Spice: Saffron. *Food Res. Int.* 43 (8), 1981–1989. doi:10.1016/j.foodres.2010.07.033

Miao, C., Bai, L., Yang, Y., and Huang, J. (2021). Dysregulation of lncRNAs in Rheumatoid Arthritis: Biomarkers, Pathogenesis and Potential Therapeutic Targets. *Front. Pharmacol.* 12, 652751. doi:10.3389/fphar.2021.652751

Min, B. W., Kang, C. S., Lee, K. J., Bae, K. C., Cho, C. H., Choi, J. H., et al. (2018). Radiographic Progression of Osteoarthritis after Rotational Acetabular Osteotomy: Minimum 10-Year Follow-Up Outcome According to the Tönnis Grade. *Clin. Orthop. Surg.* 10 (3), 299–306. doi:10.4055/cios.2018.10.3.299

Mohamadpour, A. H., Ayati, Z., Parizadeh, M. R., Rajbai, O., and Hosseinzadeh, H. (2013). Safety Evaluation of Crocin (A Constituent of Saffron) Tablets in Healthy Volunteers. *Iran J. Basic Med. Sci.* 16 (1), 39–46.

Mollazadeh, H., Emami, S. A., and Hosseinzadeh, H. (2015). Razi's Al-Hawi and Saffron (Crocus Sativus): a Review. *Iran J. Basic Med. Sci.* 18 (12), 1153–1166.

Mostafa, N. Z., Fitzsimmons, R., Major, P. W., Adesida, A., Jomha, N., Jiang, H., et al. (2012). Osteogenic Differentiation of Human Mesenchymal Stem Cells Cultured with Dexamethasone, Vitamin D3, Basic Fibroblast Growth Factor, and Bone Morphogenetic Protein-2. *Connect. Tissue Res.* 53 (2), 117–131. doi:10.3109/03008207.2011.611601

Mostafavinia, S. E., Khorashadizadeh, M., and Hoshyar, R. (2016). Antiproliferative and Proapoptotic Effects of Crocin Combined with Hyperthermia on Human Breast Cancer Cells. *DNA Cel Biol* 35 (7), 340–347. doi:10.1089/dna.2015.3208

Mulherin, D., Fitzgerald, O., and Bresnihan, B. (1996). Synovial Tissue Macrophage Populations and Articular Damage in Rheumatoid Arthritis. *Arthritis Rheum.* 39 (1), 115–124. doi:10.1002/art.1780390116

Murphy, C. A., Langrish, C. L., Chen, Y., Blumenschein, W., McClanahan, T., Kastelein, R. A., et al. (2003). Divergent Pro- and Antiinflammatory Roles for IL-23 and IL-12 in Joint Autoimmune Inflammation. *J. Exp. Med.* 198 (12), 1951–1957. doi:10.1084/jem.20030896

Nakken, B., Papp, G., Bosnes, V., Zeher, M., Nagy, G., and Szodoray, P. (2017). Biomarkers for Rheumatoid Arthritis: From Molecular Processes to Diagnostic Applications-Current Concepts and Future Perspectives. *Immunol. Lett.* 189, 13–18. doi:10.1016/j.imlet.2017.05.010

Nam, K. N., Park, Y. M., Jung, H. J., Lee, J. Y., Min, B. D., Park, S. U., et al. (2010). Anti-inflammatory Effects of Crocin and Crocetin in Rat Brain Microglial Cells. *Eur. J. Pharmacol.* 648 (1-3), 110–116. doi:10.1016/j.ejphar.2010.09.003

NHI (2001). Osteoporosis Prevention, Diagnosis, and Therapy. *Jama* 285 (6), 785–795. doi:10.1001/jama.285.6.785

Nie, Z., Deng, S., Zhang, L., Chen, S., Lu, Q., and Peng, H. (2019). Crocin Protects against Dexamethasone-induced O-steoblast A-poptosis by I-nhibiting the ROS/Ca2+-mediated M-itochondrial P-athway. *Mol. Med. Rep.* 20 (1), 401–408. doi:10.3892/mmr.2019.10267

Noh, J.-Y., Yang, Y., and Jung, H. (2020). Molecular Mechanisms and Emerging Therapeutics for Osteoporosis. *Ijms* 21, 7623. doi:10.3390/ijms21207623

Ordoudi, S. A., Kyriakoudi, A., and Tsimidou, M. Z. (2015). Enhanced Bioaccessibility of Crocetin Sugar Esters from Saffron in Infusions Rich in Natural Phenolic Antioxidants. *Molecules* 20 (10), 17760–17774. doi:10.3390/molecules201017760

Pennock, A. T., Robertson, C. M., Emmerson, B. C., Harwood, F. L., and Amiel, D. (2007). Role of Apoptotic and Matrix-Degrading Genes in Articular Cartilage and Meniscus of Mature and Aged Rabbits during Development of Osteoarthritis. *Arthritis Rheum.* 56 (5), 1529–1536. doi:10.1002/art.22523

Pfander, H., and Schurtenberger, H. (1982). Biosynthesis of C20-Carotenoids in Crocus Sativus. *Phytochemistry* 21 (5), 1039–1042. doi:10.1016/S0031-9422(00)82412-7

Poursamimi, J., Shariati-Sarabi, Z., Tavakkol-Afshari, J., Mohajeri, S. A., Ghoryani, M., and Mohammadi, M. (2020). Immunoregulatory Effects of Krocina, a Herbal Medicine Made of Crocin, on Osteoarthritis Patients: A Successful Clinical Trial in Iran. *Ijaai* 19 (3), 253–263. doi:10.18502/ijaai.v19i3.3453

Radhakrishnan, A., Tudawe, D., Chakravarthi, S., Chiew, G. S., and Haleagrahara, N. (2014). Effect of γ-tocotrienol in Counteracting Oxidative Stress and Joint Damage in Collagen-Induced Arthritis in Rats. *Exp. Ther. Med.* 7 (5), 1408–1414. doi:10.3892/etm.2014.1592

Rathore, B., Jaggi, K., Thakur, S., Mathur, A., and Mahdi, A. A. (2015). Anti-inflammatory Activity of Crocus Sativus Extract in Experimental Arthritis. *Int. J. Pharm. Sci. Res.* 6, 1473–1478. doi:10.13040/IJPSR.0975-8232.6(4).1473-78

Redlich, K., and Smolen, J. S. (2012). Inflammatory Bone Loss: Pathogenesis and Therapeutic Intervention. *Nat. Rev. Drug Discov.* 11 (3), 234–250. doi:10.1038/nrd3669

Ríos, J. L., Recio, M. C., Giner, R. M., and Máñez, S. (1996). An Update Review of Saffron and its Active Constituents. *Phytother. Res.* 10 (3), 189–193. doi:10.1002/(SICI)1099-1573(199605)10:3<189:AID-PTR754>3.0.CO;2-C

Roman-Blas, J. A., and Jimenez, S. A. (2006). NF-kappaB as a Potential Therapeutic Target in Osteoarthritis and Rheumatoid Arthritis. *Osteoarthritis Cartilage* 14 (9), 839–848. doi:10.1016/j.joca.2006.04.008

Roodman, G. D. (2006). Regulation of Osteoclast Differentiation. *Ann. N. Y Acad. Sci.* 1068, 100–109. doi:10.1196/annals.1346.013

Ross, F. P. (2006). M-CSF, C-Fms, and Signaling in Osteoclasts and Their Precursors. *Ann. N. Y Acad. Sci.* 1068 (1), 110–116. doi:10.1196/annals.1346.014

Sakkas, L. I., and Platsoucas, C. D. (2007). The Role of T Cells in the Pathogenesis of Osteoarthritis. *Arthritis Rheum.* 56 (2), 409–424. doi:10.1002/art.22369

Salahshoor, M. R., Khashiadeh, M., Roshankhah, S., Kakabaraei, S., and Jalili, C. (2016). Protective Effect of Crocin on Liver Toxicity Induced by Morphine. *Res. Pharm. Sci.* 11 (2), 120–129.

Shafiee, M., Moghaddam, N. S. A., Tousi, M., Avan, A., Ryzhikov, M., et al. (2017). Saffron against Components of Metabolic Syndrome: Current Status and Prospective. *J. Agric. Food Chem.* 65 (50), 10837–10843. doi:10.1021/acs.jafc.7b03762

Shafiee, M., Arekhi, S., Omranzadeh, A., and Sahebkar, A. (2018). Saffron in the Treatment of Depression, Anxiety and Other Mental Disorders: Current Evidence and Potential Mechanisms of Action. *J. Affect Disord.* 227, 330–337. doi:10.1016/j.jad.2017.11.020

Sheng, L., Qian, Z., Zheng, S., and Xi, L. (2006). Mechanism of Hypolipidemic Effect of Crocin in Rats: Crocin Inhibits Pancreatic Lipase. *Eur. J. Pharmacol.* 543 (1-3), 116–122. doi:10.1016/j.ejphar.2006.05.038

Shi, L., Zhao, S., Chen, Q., Wu, Y., Zhang, J., and Li, N. (2018). Crocin Inhibits RANKL induced Osteoclastogenesis by Regulating JNK and NFκB Signaling Pathways. *Mol. Med. Rep.* 17 (6), 7947–7951. doi:10.3892/mmr.2018.8835

Silverwood, V., Blagojevic-Bucknall, M., Jinks, C., Jordan, J. L., Protheroe, J., and Jordan, K. P. (2015). Current Evidence on Risk Factors for Knee Osteoarthritis in Older Adults: a Systematic Review and Meta-Analysis. *Osteoarthritis Cartilage* 23 (4), 507–515. doi:10.1016/j.joca.2014.11.019

Sinkov, V., and Cymet, T. (2003). Osteoarthritis: Understanding the Pathophysiology, Genetics, and Treatments. *J. Natl. Med. Assoc.* 95 (6), 475–482.

Srivastava, R., Ahmed, H., Dixit, R. K., Dharamveerand Saraf, S. A. (2010). Crocus Sativus L.: A Comprehensive Review. *Pharmacogn Rev.* 4 (8), 200–208. doi:10.4103/0973-7847.70919

Sugerman, D. T., and Jin, J. (2014). JAMA Patient page. Talking to Your Doctor about Tests, Treatments, and Their Costs. *JAMA* 312 (1), 2178. doi:10.1001/jama.2013.28300910.1001/jama.2014.3693

Suh, K. S., Chon, S., Jung, W. W., and Choi, E. M. (2019). Crocin Attenuates Methylglyoxal-Induced Osteoclast Dysfunction by Regulating Glyoxalase, Oxidative Stress, and Mitochondrial Function. *Food Chem. Toxicol.* 124, 367–373. doi:10.1016/j.fct.2018.12.031

Szekanecz, Z., Kerekes, G., Végh, E., Kardos, Z., Baráth, Z., Tamási, L., et al. (2016). Autoimmune Atherosclerosis in 3D: How it Develops, How to Diagnose and what to Do. *Autoimmun. Rev.* 15 (7), 756–769. doi:10.1016/j.autrev.2016.03.014

Takaishi, H., Kimura, T., Dalal, S., Okada, Y., and D'Armiento, J. (2008). Joint Diseases and Matrix Metalloproteinases: a Role for MMP-13. *Curr. Pharm. Biotechnol.* 9 (1), 47–54. doi:10.2174/138920108783497659

Takayanagi, H., Iizuka, H., Juji, T., Nakagawa, T., Yamamoto, A., Miyazaki, T., et al. (2000). Involvement of Receptor Activator of Nuclear Factor kappaB Ligand/osteoclast Differentiation Factor in Osteoclastogenesis from Synoviocytes in Rheumatoid Arthritis. *Arthritis Rheum.* 43 (2), 259–269. doi:10.1002/1529-0131(200002)43:2<259:Aid-anr4>3.0.Co;2-w

Tardif, G., Reboul, P., Pelletier, J. P., and Martel-Pelletier, J. (2004). Ten Years in the Life of an Enzyme: the story of the Human MMP-13 (Collagenase-3). *Mod. Rheumatol.* 14 (3), 197–204. doi:10.1007/s10165-004-0292-7

Teitelbaum, S. L. (2000). Bone Resorption by Osteoclasts. *Science* 289 (5484), 1504–1508. doi:10.1126/science.289.5484.1504

Todd, J. A., and Robinson, R. J. (2003). Osteoporosis and Exercise. *Postgrad. Med. J.* 79 (932), 320–323. doi:10.1136/pmj.79.932.320

Tsimidou, M., and Tsatsaroni, E. (1993). Stability of Saffron Pigments in Aqueous Extracts. *J. Food Sci.* 58 (5), 1073–1075. doi:10.1111/j.1365-2621.1993.tb06116.x

Turco, G. L. (1963). RHEUMATOID ARTHRITIS. *Aggiorn Clinico Ter* 4, 1–56.

Udagawa, N., Takahashi, N., Jimi, E., Matsuzaki, K., Tsurukai, T., Itoh, K., et al. (1999). Osteoblasts/stromal Cells Stimulate Osteoclast Activation through Expression of Osteoclast Differentiation Factor/RANKL but Not Macrophage colony-stimulating Factor: Receptor Activator of NF-Kappa B Ligand. *Bone* 25 (5), 517–523. doi:10.1016/S8756-3282(99)00210-0

Udalamaththa, V. L., Jayasinghe, C. D., and Udagama, P. V. (2016). Potential Role of Herbal Remedies in Stem Cell Therapy: Proliferation and Differentiation of Human Mesenchymal Stromal Cells. *Stem Cel Res Ther* 7 (1), 110. doi:10.1186/s13287-016-0366-4

Vafaei, S., Motejaded, F., and Ebrahimzadeh-bideskan, A. (2020). Protective Effect of Crocin on Electromagnetic Field-Induced Testicular Damage and Heat Shock Protein A2 Expression in Male BALB/c Mice. *Iran J. Basic Med. Sci.* 23 (1), 102–110. doi:10.22038/ijbms.2019.38896.9229

Walsh, N. C., and Gravallese, E. M. (2010). Bone Remodeling in Rheumatic Disease: a Question of Balance. *Immunol. Rev.* 233 (1), 301–312. doi:10.1111/j.0105-2896.2009.00857.x

Wang, J. F., Xu, H. J., He, Z. L., Yin, Q., and Cheng, W. (2020). Crocin Alleviates Pain Hyperalgesia in AIA Rats by Inhibiting the Spinal Wnt5a/β-Catenin

Signaling Pathway and Glial Activation. *Neural Plast.* 2020, 4297483. doi:10.1155/2020/4297483

Winterhalter, P., and Straubinger, M. (2000). Saffron-renewed Interest in an Ancient Spice. *Food Rev. Int.* 16 (1), 39–59. doi:10.1081/FRI-100100281

Wu, T., Zhang, J., Geng, M., Tang, S. J., Zhang, W., and Shu, J. (2017). Nucleoside Reverse Transcriptase Inhibitors (NRTIs) Induce Proinflammatory Cytokines in the CNS via Wnt5a Signaling. *Sci. Rep.* 7 (1), 4117. doi:10.1038/s41598-017-03446-w

Xie, Y., He, Q., Chen, H., Lin, Z., Xu, Y., and Yang, C. (2019). Crocin Ameliorates Chronic Obstructive Pulmonary Disease-Induced Depression via PI3K/Akt Mediated Suppression of Inflammation. *Eur. J. Pharmacol.* 862, 172640. doi:10.1016/j.ejphar.2019.172640

Xu, F., and Teitelbaum, S. L. (2013). Osteoclasts: New Insights. *Bone Res.* 1 (1), 11–26. doi:10.4248/BR201301003

Xue, X. H. (1982). Cultivation of Crocus Sativus. *Zhong Yao Tong Bao* 7 (4), 3–4.

Yamaguchi, T. (2014). Updates on Lifestyle-Related Diseases and Bone Metabolism. The Metabolic Syndrome and Bone Metabolism. *Clin. Calcium* 24 (11), 1599–1604.

Yamashita, T., Takahashi, N., and Udagawa, N. (2012). New Roles of Osteoblasts Involved in Osteoclast Differentiation. *World J. Orthop.* 3 (11), 175–181. doi:10.5312/wjo.v3.i11.175

Yasuda, H., Shima, N., Nakagawa, N., Yamaguchi, K., Kinosaki, M., Mochizuki, S., et al. (1998). Osteoclast Differentiation Factor Is a Ligand for Osteoprotegerin/osteoclastogenesis-Inhibitory Factor and Is Identical to TRANCE/RANKL. *Proc. Natl. Acad. Sci. U S A.* 95 (7), 3597–3602. doi:10.1073/pnas.95.7.3597

Yokota, K., Sato, K., Miyazaki, T., Kitaura, H., Kayama, H., Miyoshi, F., et al. (2014). Combination of Tumor Necrosis Factor α and Interleukin-6 Induces Mouse Osteoclast-like Cells with Bone Resorption Activity Both *In Vitro* and *In Vivo*. *Arthritis Rheumatol.* 66 (1), 121–129. doi:10.1002/art.38218

Yoo, J. H., Oh, H. C., Park, S. H., Kim, J. K., and Kim, S. H. (2018). Does Obesity Affect Clinical and Radiological Outcomes in Minimally Invasive Total Knee Arthroplasty? Minimum 5-Year Follow-Up of Minimally Invasive TKA in Obese Patients. *Clin. Orthop. Surg.* 10 (3), 315–321. doi:10.4055/cios.2018.10.3.315

Yu, Y., Mu, J., Fan, Z., Lei, G., Yan, M., Wang, S., et al. (2012). Insulin-like Growth Factor 1 Enhances the Proliferation and Osteogenic Differentiation of Human Periodontal Ligament Stem Cells via ERK and JNK MAPK Pathways. *Histochem. Cel Biol* 137 (4), 513–525. doi:10.1007/s00418-011-0908-x

Yuan, S., Shi, Y., Guo, K., and Tang, S. J. (2018). Nucleoside Reverse Transcriptase Inhibitors (NRTIs) Induce Pathological Pain through Wnt5a-Mediated Neuroinflammation in Aging Mice. *J. Neuroimmune Pharmacol.* 13 (2), 230–236. doi:10.1007/s11481-018-9777-6

Yuan, X., Cao, H., Wang, J., Tang, K., Li, B., Zhao, Y., et al. (2017). Immunomodulatory Effects of Calcium and Strontium Co-doped Titanium Oxides on Osteogenesis. *Front. Immunol.* 8, 1196. doi:10.3389/fimmu.2017.01196

Zaminy, A., Ragerdi Kashani, I., Barbarestani, M., Hedayatpour, A., Mahmoudi, R., and Farzaneh Nejad, A. (2008). Osteogenic Differentiation of Rat Mesenchymal Stem Cells from Adipose Tissue in Comparison with Bone Marrow Mesenchymal Stem Cells: Melatonin as a Differentiation Factor. *Iran Biomed. J.* 12 (3), 133–141.

Zheng, Y. Q., Liu, J. X., Wang, J. N., and Xu, L. (2007). Effects of Crocin on Reperfusion-Induced Oxidative/nitrative Injury to Cerebral Microvessels after Global Cerebral Ischemia. *Brain Res.* 1138, 86–94. doi:10.1016/j.brainres.2006.12.064

Zhou, J., Zhang, Q., Yuan, X., Wang, J., Li, C., Sheng, H., et al. (2013). Association between Metabolic Syndrome and Osteoporosis: a Meta-Analysis. *Bone* 57 (1), 30–35. doi:10.1016/j.bone.2013.07.013

Zhu, J., Yamane, H., and Paul, W. E. (2010). Differentiation of Effector CD4 T Cell Populations (*). *Annu. Rev. Immunol.* 28, 445–489. doi:10.1146/annurev-immunol-030409-101212

Zhu, K., Yang, C., Dai, H., Li, J., Liu, W., Luo, Y., et al. (2019). Crocin Inhibits Titanium Particle-Induced Inflammation and Promotes Osteogenesis by Regulating Macrophage Polarization. *Int. Immunopharmacol* 76, 105865. doi:10.1016/j.intimp.2019.105865

Conflict of Interest: The authors declare that the research was conducted in the absence of any commercial or financial relationships that could be construed as a potential conflict of interest.

Publisher's Note: All claims expressed in this article are solely those of the authors and do not necessarily represent those of their affiliated organizations, or those of the publisher, the editors and the reviewers. Any product that may be evaluated in this article, or claim that may be made by its manufacturer, is not guaranteed or endorsed by the publisher.

Copyright © 2022 Vafaei, Wu, Tu and Nematollahi-mahani. This is an open-access article distributed under the terms of the Creative Commons Attribution License (CC BY). The use, distribution or reproduction in other forums is permitted, provided the original author(s) and the copyright owner(s) are credited and that the original publication in this journal is cited, in accordance with accepted academic practice. No use, distribution or reproduction is permitted which does not comply with these terms.

frontiers in Pharmacology

REVIEW
published: 31 January 2022
doi: 10.3389/fphar.2021.789311

Botanical Drug Extracts Combined With Biomaterial Carriers for Osteoarthritis Cartilage Degeneration Treatment: A Review of 10Years of Research

Panyun Mu[1], Jie Feng[1], Yimei Hu[2], Feng Xiong[1], Xu Ma[1] and Linling Tian[1]*

[1]Department of Clinical Medicine, Chengdu University of Traditional Chinese Medicine, Chengdu, China, [2]Department of Orthopedics, Hospital of Chengdu University of Traditional Chinese Medicine, Chengdu, China

Osteoarthritis (OA) is a long-term chronic arthrosis disease which is usually characterized by pain, swelling, joint stiffness, reduced range of motion, and other clinical manifestations and even results in disability in severe cases. The main pathological manifestation of OA is the degeneration of cartilage. However, due to the special physiological structure of the cartilage, once damaged, it is unable to repair itself, which is one of the challenges of treating OA clinically. Abundant studies have reported the application of cartilage tissue engineering in OA cartilage repair. Among them, cell combined with biological carrier implantation has unique advantages. However, cell senescence, death and dedifferentiation are some problems when cultured *in vitro*. Botanical drug remedies for OA have a long history in many countries in Asia. In fact, botanical drug extracts (BDEs) have great potential in anti-inflammatory, antioxidant, antiaging, and other properties, and many studies have confirmed their effects. BDEs combined with cartilage tissue engineering has attracted increasing attention in recent years. In this review, we will explain in detail how cartilage tissue engineering materials and BDEs play a role in cartilage repair, as well as the current research status.

Keywords: osteoarthritis, botanical drug, extracts, cartilage, tissue engineering, biomaterial carriers

OPEN ACCESS

Edited by:
Longhuo Wu,
Gannan Medical University, China

Reviewed by:
Qingjia Chi,
Wuhan University of Technology, China
Maurice Collins,
University of Limerick, Ireland

****Correspondence:***
Yimei Hu
huyimei@cdutcm.edu.cn

Specialty section:
This article was submitted to Ethnopharmacology, a section of the journal Frontiers in Pharmacology

Received: *04 October 2021*
Accepted: *08 December 2021*
Published: *31 January 2022*

Citation:
Mu P, Feng J, Hu Y, Xiong F, Ma X and Tian L (2022) Botanical Drug Extracts Combined With Biomaterial Carriers for Osteoarthritis Cartilage Degeneration Treatment: A Review of 10 Years of Research. Front. Pharmacol. 12:789311. doi: 10.3389/fphar.2021.789311

1 INTRODUCTION

Osteoarthritis (OA) is a progressive arthrosis disease (Crivelli et al., 2019), the main pathophysiological features of which include cartilage defects, synovitis, osteophyte formation, and subchondral bone damage (Yeh et al., 2015; Wang et al., 2018). OA patients suffer from joint pain and stiffness, difficulty in movement, and ultimately disability (Wang et al., 2018; Jin, 2020), which significantly affects their quality of life (Rahimi et al., 2021), especially for the elderly (Kann et al., 2016), and places a huge economic burden on their families and society (Wang et al., 2018; Jin, 2020). According to the World Health Organization, more than 10% of people under the age of 60 worldwide suffer from OA (Wang et al., 2018). By 2032, the number of people over the age of 45 suffering from OA will increase from 25 to 29%, and the peak of incidence will be around the age of 75 (Qin et al., 2020).

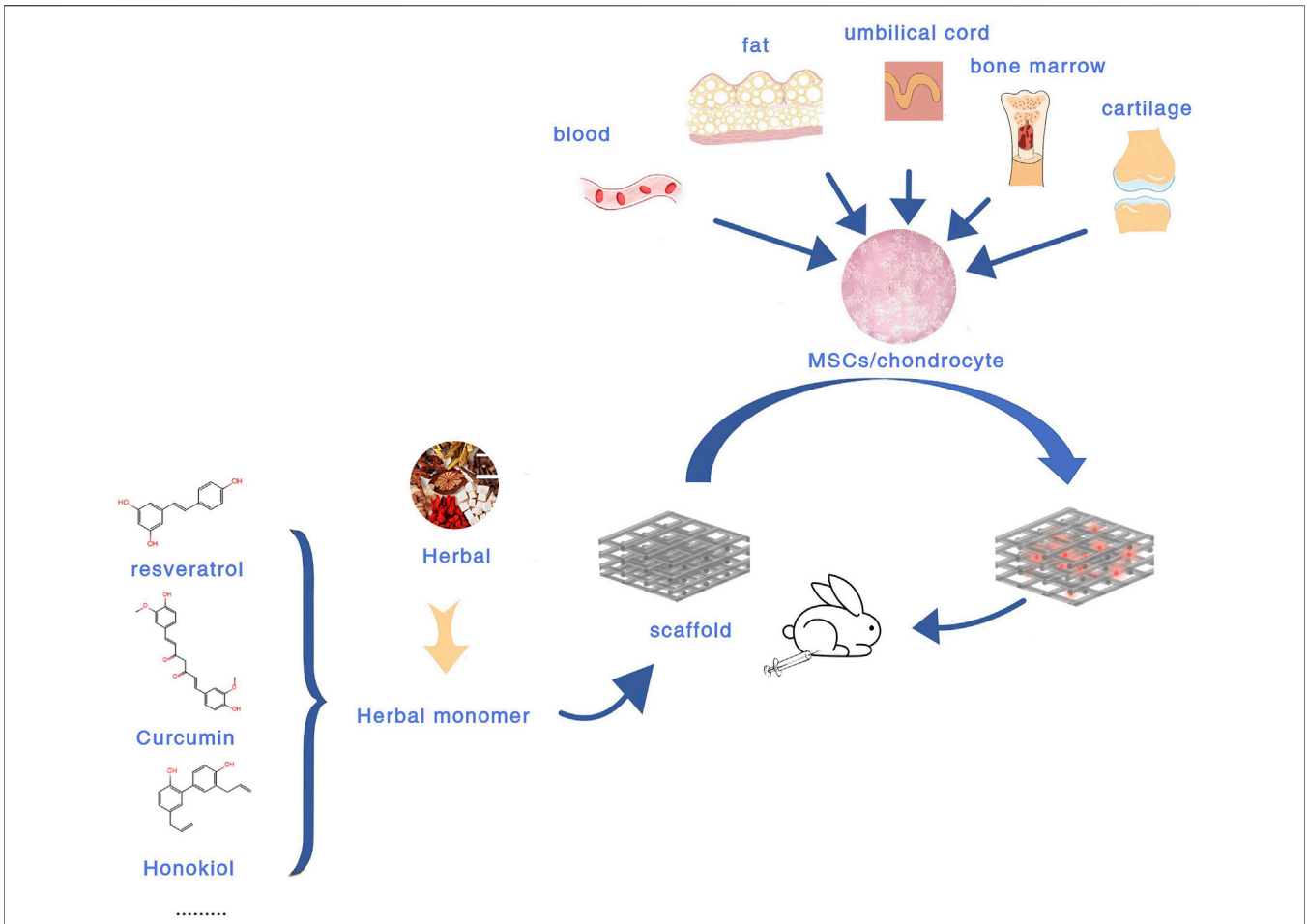

FIGURE 1 | Experimental flow chart of IA injection of BDEs-loaded biomaterial scaffolds.

1.1 Ultrastructure of Bone and Joint, and Pathogenesis of OA

In a joint, the articular cartilage, calcified cartilage, subchondral cortex, and trabecular bone form biological complexes called "osteochondral units" (Goldring and Goldring, 2016). The articular cartilage is mainly composed of extracellular matrix (ECM) and chondrocytes (1–2%). The ECM consists mainly of Type II collagen (COL2), glycosaminoglycan (GAG), aggrecan (ACAN), elastin fibrils, and 70% water (Goldring and Goldring, 2016; Jin, 2020) and provides tensile and elastic force for the articular cartilage (Crivelli et al., 2019) to maintain the proper biomechanical function of the joint. The development, maintenance, and repair of the ECM are controlled by chondrocytes derived from highly specialized and metabolically active mesenchymal stem cells (MSCs). The shape, number, and size of chondrocytes, stiffness of the cartilage, ECM composition, and content of proteoglycan, COL2, and water in the ECM vary with the anatomical regions of the articular cartilage (Rai et al., 2017)

Articular cartilage can be damaged by daily wear and abnormal mechanical load (Xia et al., 2014). With the progression of OA, a disintegrin and metalloproteinase with thrombospondin motifs 5 (ADAMTS5) and matrix metalloproteinase 13 (MMP13) are the main enzymes causing cartilage damage (Wang et al., 2013; Miller et al., 2016; Jin et al., 2020a). In the early stages of OA, inflammatory stimuli induce the cartilage and synovial cells to secrete these enzymes. Steoarthritic chondrocytes mediate the production of inflammatory mediators, including interleukin 1 (IL-1), tumor necrosis factor (TNF), prostaglandins, and nitric oxide (NO) through the nuclear factor-kappa B (NF-κB) signaling pathway (Charlier et al., 2019). IL-1β and TNF-α are effective inducers of matrix metalloproteinases (MMPs). Among them, proteases MMP1, MMP3, and MMP13 inhibit proteoglycan and collagen synthesis, mediate chondrocyte apoptosis, and promote cartilage inflammation (Abramson, 2008; Blanco et al., 2011; Oliveira Silva et al., 2020).

1.2 Treatment Status of Osteoarthritis

The lack of vascular and aneural tissue in articular cartilage gives it a limited intrinsic self-repair ability (Sheu et al., 2013; Lima et al., 2019), which makes the treatment of articular cartilage

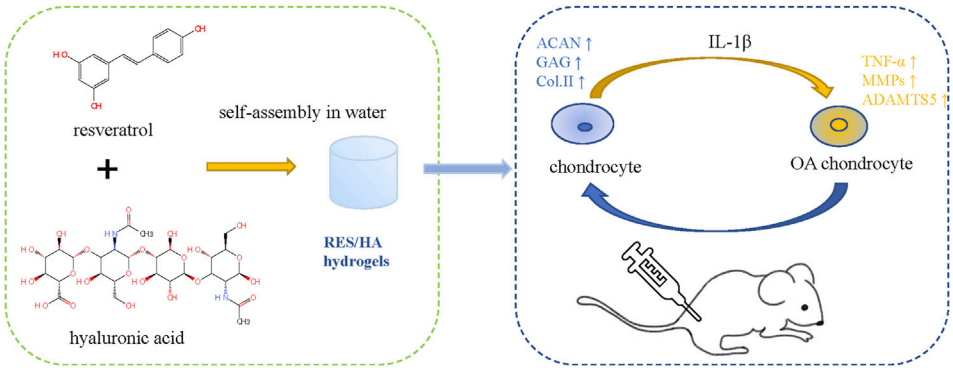

FIGURE 2 | Schematic diagram of chondrocyte regulation of HA-based hydrogel combined with BDEs.

defects an extremely difficult clinical problem (Makris et al., 2015). The current methods include conservative and nonconservative treatments. The conservative treatments include non-pharmacologic, pharmacologic, and alternative therapies (Madry et al., 2011; Kang et al., 2020), while nonconservative therapeutic strategies mainly include bone marrow stimulation (Frehner and Benthien, 2018), autologous or allogeneic osteochondral transplantation (Bugbee et al., 2016; Di Martino et al., 2021), autologous chondrocyte implantation, and periosteum transplantation (Mistry et al., 2017). Although such treatments have been widely used in clinical practice, they still have obvious and inevitable limitations and deficiencies (Vinatier and Guicheux, 2016; Xu et al., 2020).

Drug therapies include nonsteroidal anti-inflammatory drugs (NSAIDs), opioids, and glucocorticoids. Most therapies are limited to symptomatic treatment aiming at relieving pain and improving joint function rather than inhibiting the progression of OA (Jin, 2020). However, the long-term use of such drugs can cause serious adverse reactions such as gastrointestinal reactions and osteoporosis (Crivelli et al., 2019; Shi et al., 2019). Beyond oral administration, other routes have been developed for the treatment of OA. Different from other diseases, OA is limited to one or more joints, which offers a special opportunity for local intra-articular (IA) drug injection. IA allows the delivery of therapeutic drugs directly to the diseased joint at very high concentrations; moreover, it limits the absorption of drugs into the systemic circulation, which reduces systemic toxicity. Thus, compared with the systemic approach, a smaller dose can achieve a therapeutic effect similar to that of oral administration (Burt et al., 2009; Jones et al., 2019). IA injections of hyaluronic acid (HA) or glucocorticoids have been used to relieve knee OA (KOA) pain (Berenbaum et al., 2012). However, the main limitation of IA injection is the rapid elimination of the drug from the articular cavity. Studies have shown that small-molecule drugs (MW < 10 kDa) can be removed from the synovial fluid by lymphatic drainage within 5 h of injection (Zhang et al., 2018; Jones et al., 2019), and thus multiple injections are required, which can lead to infection or joint disability. To control the release rate over a long period of time, a new biology-based drug delivery vector is needed (Chen et al., 2012).

Compared with the above treatment methods, tissue engineering composed of scaffolds, cells, and favorable growth factors has become the most promising treatment strategy for cartilage repair (Xu et al., 2020). Biodegradable tissue engineering scaffolds have attracted great attention in recent years by virtue of their many advantages (Ming et al., 2018). At the same time, tissue engineering methods are preferred for severe cartilage defects, congenital abnormalities, and elderly patients with limited inherent ability (Lima et al., 2019). Currently, there are various biomaterial scaffolds for cartilage defects, including hydrogels, nanoparticles, microspheres, liposomes, and so on (Lima et al., 2019; Jin, 2020; Xu et al., 2020). In terms of cell selection, the current research shows that chondrocytes and MSCs remain the main sources of seed cells in cartilage repair (Xu et al., 2020). However, the main drawback of using autologous chondrocytes is that when cultured *in vitro*, they are prone to dedifferentiate and develop into a fibroblast phenotype (Vinatier and Guicheux, 2016). (**Figure 1** Experimental flow chart of intra-articular injection of BDEs loaded biomaterial scaffolds).

Growth factors play essential regulatory roles in cartilage development (Lecanda et al., 1997; Chen et al., 2020a). The most effective growth factor for inducing cartilage formation is transforming growth factor β (TGF-β) (Makris et al., 2015). However, *in vivo* studies have shown that under continuous stimulation by TGF-β1, adverse reactions such as synovial fibrosis, endochondral osteogenesis, and hypertrophic scarring were observed. On the other hand, growth factors can only release their maximum potential at the injured site and can easily become inactivated under physiological conditions (Chen et al., 2020a). Moreover, the use of growth factors is limited due to their complex extraction process, high cost, and low yield (Wildemann et al., 2007). At present, it is urgent to explore a simple, effective, safe, and cheap bioactive substance to replace growth factors and meet the actual demands of cartilage repair (Kankala et al., 2018; Jin, 2020).

There are many reviews on the repair of cartilage defects. Based on preclinical and clinical studies, Theodoridis et al. (2021) reviewed the research status and limitations of cartilage tissue engineering as a cartilage repair strategy from the aspects of

biomaterial selection, cell implantation, scaffold performance and structure, local biological stimulation, etc. Makris et al. (2015) reviewed the current clinical use of articular cartilage surface defect repair technologies and the status of preclinical research on stent-based acellular or chondrocyte implantation technologies. Murphy et al. (2019) mainly discussed the repair technology of meniscus injury and the protective effects of meniscus repair on cartilage. Herbal therapy for OA has been reported in many related studies, and botanical drug extracts (BDEs) combined with scaffolds in the treatment of OA have also been the subject of a large number of studies. Compared to growth factors, BDEs have a wider range of sources, more accessibility, and greater cost-efficiency. Various studies have demonstrated their anti-inflammatory, antioxidant, and cartilage protection properties. Many practices have studied the use of herbs in biotechnology in treating rheumatoid arthritis (RA) and OA (Buhrmann et al., 2020). However, the combination of BDEs with cartilage tissue engineering is rarely used in clinical practice and is mostly done in preclinical research. In this review, we will explain in detail how cartilage tissue engineering materials and BDEs play a role in cartilage repair, as well as the current research status (**Figure 2** Schematic diagram of chondrocyte regulation of HA - based hydrogel combined with BDEs).

1.3 Botanical Drug Extracts

In the latest guidelines for OA, NSAIDs are recommended as a high-grade evidence-based therapy (Bannuru et al., 2019), but patients are prone to adverse reactions after taking such drugs. In recent years, certain advancements have been made in the treatment of OA with botanical drug remedies. In relevant meta-analyses, it has been found that botanical drug can relieve pain and improve the range of motion in patients with KOA (Cameron and Chrubasik, 2014), and the incidence of adverse reactions is low (Chen et al., 2016a). We searched in the PubMed database for "osteoarthritis," "arthritis," "tissue engineering," "cartilage tissue engineering," "biomaterials, Chinese herbal medicine," "scaffolds," "nanoparticles," and "hydrogels." Reviews, conference papers, and studies (those did not include both BDEs and carriers) were excluded. Finally, 31 related articles were selected through reading headlines, abstracts, and full texts. We then classified the BDEs in the literature (including flavonoids, polyphenols, alkaloids, saponins, and others). By summarizing the effect of plant drug extract combined with biomaterial carrier on the repair of OA cartilage injury, its mechanism, and current research status, we provide a theoretical basis for ideas and directions of future research.

2 FLAVONOIDS

2.1 Quercetin

Quercetin (QUE), an abundant bioflavonoid, is widely distributed in the plant kingdom as a secondary plant metabolite. It is also a common component of the human diet, being found in onions, apples, and so on (Andres et al., 2018). QUE has effective antioxidant, antiproliferative, and free radical scavenging properties (Yeung et al., 2021), as well as being able to alleviate pain (Britti et al., 2017) caused by arthritis (Kanzaki et al., 2012; Wei et al., 2019). A large amount of evidence shows that QUE can delay the occurrence and development of OA (Britti et al., 2017; Feng et al., 2019a; Hu et al., 2019; Ma et al., 2019). In the animal model of OA, QUE can raise the production of superoxide dismutase (SOD), attenuate reactive oxygen species (ROS) levels, reduce inflammation and oxidative stress, improve antioxidant defense, maintain the integrity of joint cartilage ECM, and reduce symptoms and arthritis (Qiu et al., 2018; Wei et al., 2019). QUE can inhibit the expression of chondrocyte matrix degradation protease and inflammatory mediators, reduce cartilage degradation and apoptosis in OA rats, and promote cartilage synthesis (Hu et al., 2019). Siard et al. (2016) showed that QUE significantly reduces the production of inflammatory cytokines by lymphocytes and is even more effective than common NSAIDs. However, due to its low bioavailability of oral administration, studies have reported no significant improvement in the treatment of arthritis with QUE (Bae et al., 2009; Javadi et al., 2014). Mok et al. (2020) injected QUE-loaded polypeptide-based hydrogel, namely methoxy-poly(ethylene glycol)-l-poly(alanine) (mPEG-PA), into the knee joints of OA rats and found that the gradual release of QUE from the mPEG-PA hydrogel could be sustained over 28 days; in addition, the limb idleness index (LII) of the rats was significantly decreased after treatment with QUE (50 μg) hydrogel at 4 and 8 weeks (−0.27, −0.31). The Osteoarthritis Research Society International (OARSI) score shows that the international score of the QUE hydrogel group (50 μg) was significantly lower than that of the control group ($p < 0.01$). These results suggest that the continuous use of QUE hydrogel (50 μg) can relieve OA symptoms and delay the progression of KOA.

2.2 Hesperetin

Hesperetin (Hes), a flavonoid in the flavanone class extracted from citrus fruit (Muhammad et al., 2019), can inhibit osteoclast formation and promote the differentiation of osteoblasts, giving it potential for treating bone-related diseases (Ouyang et al., 2019). HES also has antioxidant and anti-inflammatory properties. The antioxidant activity of HES not only is limited to scavenging free radicals but also enhances the defense ability of antioxidant cells through the ERK/Nrf2 signaling pathway (Parhiz et al., 2015). Lin et al. (2020) found the anti-inflammatory effect of HES in OA lies in inhibiting the IL-1β–induced expression of inflammatory factors, downregulating MMP13 and ADAMTS5, and upregulating COL2 and protein aggregation. There has been only one animal study that used HES combined with a cartilage tissue engineering scaffold. Ouyang et al. (2019) loaded HES into nanoparticles (HGdPDW). HGdPDW promoted the expression of ACAN, Sox9, and COL2A1 after IL-1β stimulation for 3 days ($p < 0.05$) but inhibited the expression of MMP13 and COL10A1 ($p < 0.05$), thus reducing apoptosis and inflammatory response. Magnetic resonance imaging (MRI)/ Interactive Video Information System (IVIS) bipeak imaging confirmed that HGdPDW has low cytotoxic and chondrogenic binding ability. HGdPDW treatment increases the

articular cartilage thickness of the knee, preserves proteoglycan and collagen, and alleviates the progressive degeneration of articular cartilage *in vivo*. In addition, it can significantly improve the OARSI score of anterior cruciate ligament transection (ACLT) in OA mice ($p < 0.05$).

2.3 Icariin

Icariin (ICA), the main component of *Epimedii Folium* (*Epimedium brevicornu* Maxim., *Epimedium sagittatum* (Sieb. et Zucc.) Maxim., *Epimedium pubescens* Maxim., or *Epimedium koreanum* Nakai), is a typical flavonoid compound with anti-inflammatory, anti-oxidative (Zuo et al., 2019), and bone-protective properties (Wang et al., 2020). ICA can treat OA through multiple pathways and targets. It increases the vitality of chondrocytes through reducing the inflammatory damage caused by NF-κB/HIF-2α signaling (Wang et al., 2020); regulates chondrocyte autophagy by mediating the PI3K/Akt/mTOR pathway (Tang et al., 2021) and inhibiting NF-κB; alleviates OA by inhibiting inflammatory cytokines and chondrocyte apoptosis (Liu et al., 2018a; Mi et al., 2018); upregulates the proliferation, osteogenic, and chondrogenic differentiation of bone marrow–derived MSCs (BMSCs); and protects BMSCs from apoptosis through the mitogen-activated protein kinase (MAPK) signaling pathway (Liu et al., 2020a). In a study on ICA and human OA fibroblast-like synoviocytes, it was found that ICA could inhibit the expression of IL-1β, MMP4, and glucose-regulated protein 78 (GRP78), which further reduces the inflammatory response (Pan et al., 2017). Thus, ICA is an effective candidate drug for the treatment of articular cartilage injury, and due to its low price, easy access, and reparative effects on osteochondral defects, it has earned the increasing attention of researchers.

There are two animal studies that used ICA combined with cartilage tissue engineering scaffolds. Kankala et al. (2018) printed porous three-dimensional (3D) sodium alginate (SA) and gel scaffolds with excellent mechanical strength. They then studied the physical characterizations and cytocompatibility of the scaffolds, and the effects of ICA on the growth of chondrocytes. With the extension of the incubation time *in vitro*, the content of GAG in chondrocytes increased gradually, and ICA (10 μg/ml) could significantly accelerate GAG secretion. However, there is no relevant animal model of OA to further verify the reparative effects of ICA combined with stents on OA cartilage defects. Li et al. (2012) used ICA/Type I collagen (ICA/COL) hydrogel encapsulated neonatal rabbit chondrocytes to construct engineering grafts. The results showed that ICA could significantly upregulate the expression of ACAN, Sox9, and COL2 (from 99.7 to 248%), upregulate the synthesis of GAG and COL2, and accelerate the formation of cartilage tissue in the cell hydrogel structure. It could even improve the reparative efficiency of supercritical osteochondral defects in adult rabbit models and promote the fusion of newly formed cartilage and subchondral bone. Thus, ICA is a promising compound for cartilage repair and serves as a substitute for certain growth factors (**Table 1**).

3 POLYPHENOLS

3.1 Resveratrol

Resveratrol (RES) is a phytochemical found in grape and *Reynoutria japonica* Houtt. which acts on several cellular signaling pathways and has anti-inflammatory, antioxidant, and antiaging properties (Limagne et al., 2016; Wang et al., 2016; Oz et al., 2019; Yeung et al., 2019; Yuce et al., 2021). Elmali et al. (2007) showed that the IA injection of RES could mitigate synovitis cell infiltration and cartilage damage through the histopathological evaluation of the rabbit arthritis model. RES can prevent the degradation of proteoglycan and ACAN in cartilage tissue induced by advanced glycation end products (AGEs) (Liu et al., 2010); upregulate the expression of COL2; downregulate the expression of inducible NO synthase (iNOS) and MMP13 (Li et al., 2015); reduce the accumulation of ROS and hypoxia inducible factor-α (HIF-1α); and inhibit the MAPK signaling pathway to prevent inflammation and degeneration of the joints (Yang et al., 2018). RES can also effectively reverse IL-1β–induced catabolic and inflammatory responses (Gu et al., 2017) and significantly prevent OA cartilage damage by activating sirtuin 1 (SIRT1) to inhibit the expression of HIF-2α and catabolic factors (Li et al., 2015; Wang et al., 2016; Abed et al., 2017). In addition, RES has a protective effect on subchondral bone, which is manifested in the promotion of the Wnt/β-catenin and ERK1/2 signaling pathways to boost mesenchymal cell differentiation into osteoblasts (Abed et al., 2017).

Qin et al. (2017) have shown that the IA injection of RES promotes chondrocyte autophagy (*via* regulating the HIF-1α–dependent MAPK/mTOR signaling pathway) and delays cartilage degeneration induced by medial meniscal instability surgery. Dietary RES supplementation can reduce paw edema and erythema in collagen-induced arthritis–OA (CIA-OA) model rats and mitigate the invasion of inflammatory cells and cartilage degeneration around the joints (Oz et al., 2019). The intraperitoneal injection of RES (5 or 10 mg/kg) in monosodium iodoacetate–induced arthritis–OA (MIA-OA) rats significantly reduced mechanical, thermal, and cold hyperalgesia and increased vertical and horizontal movements (Wang et al., 2016). At the same time, a clinical study showed that treatment with RES improved WOMAC scores (pain, stiffness, and body function) (Hussain et al., 2018). These results suggest that RES may be a potential analgesic agent that can reduce pain and discomfort in KOA patients and improve their general condition and life quality. The anti-inflammatory effects of RES have been studied in both humans and animals. Due to the weak oral bioavailability of RES, we hope to develop different administration methods in order to obtain good results in clinical treatment (Kotha et al., 2006).

There are six studies that used RES combined with cartilage tissue engineering scaffolds to treat OA. Kann et al. (2016) encapsulated RES and curcumin (CUR) in lipid-core nanocapsules and studied their interaction with the human primary chondrocytes. Due to the different solubilities of CUR and RES, the lower solubility accompanied faster release from the nanocapsules. The combination of the two can achieve the effect

TABLE 1 | The effect of flavonoids combined with carriers on OA cartilage repair.

Research (author & year)	BDEs	Carrier	Gene expression		Cartilage repair effects		Other evaluations	Research conclusion
			Inhibition	Promote	Imaging evaluations	Tissue sections		
Ouyang et al. (2019)	Hes	Gd2(CO3) 3-PNs	IL-6, TNF-α, NO, iNOS, MMPs, Bax	Col.II, Bcl-2, ACAN, Sox9	Cartilage affinity of synthesized NPs based on MRI/IVIS	Cartilage thickness, caspase-3 expression, and OARSI score	TLR2/NF-κB/Akt signaling pathway	HGdPDW could effectively target cartilage and protect chondrocytes from apoptosis and inflammation
Mok (2018)	Que	MPIP				OARSI score	LIIs (OA-related pain), Krenn score (synovial inflammation)	Sustained delivery of Que (50 μg) could provide symptom relief and also delay the progression of KOA
Kankala et al. (2018)	ICA	SA/gel		GAG			The distribution of chondrocytes on the scaffold surface (by CLSM)	SA/gel composite scaffold addition of ICA further promoted cell proliferation and differentiation
Li et al. (2012)	ICA	Col-CH		Col.I, Col.II, GAG, ACAN, Sox9	Restoration of osteochondral defects by direct observation	Restoration of the osteochondral defects and cartilage thickness	The morphology of chondrocytes encapsulated in hydrogels (by CLSM)	ICA can promote cartilage repair and cartilage tissue formation

CLSM, confocal laser scanning microscopic; EE, Encapsulation efficiency; ILLs, limb idleness index; IVIS, Interactive Video Information System; PNs, polydopamine nanoparticles; MPIP, methoxy-poly(ethylene glycol)-l-poly(alanine); Col-CH, collagen type I cell–hydrogel.

of rapid initial treatment (by RES) and prolonged treatment (by CUR). By virtue of its rapid release, RES can quickly clear ROS produced in OA rats induced by sodium nitroprusside (SNP) and reduce NO expression, thereby protecting the chondrocytes. Coradini et al. (2015) also studied the synergistic effects of RES and CUR using intraperitoneal injections instead of IA injections. RES and CUR were co-encapsulated in lipid core nano-capsules and intraperitoneally injected into Complete Freund's adjuvant (CFA)–induced arthritis rats. The results showed that co-encapsulated polyphenols were safe and nontoxic when injected *in vivo* and could significantly reduce foot swelling in arthritic rats ($p < 0.05$), with an amplitude of 37–55%. In addition, co-encapsulated polyphenols alleviated cartilage damage by significantly reducing synovial membrane fibrosis and cartilage and bone loss ($p < 0.05$). Ming et al. (2018) used the microfluidic technique to select the optimum concentration of chondrocytes cultured by RES and then studied the reparative effects of RES and drug-loaded polylactic acid (PLA)/gelatin nano-scaffolds on cartilage defects. They reported that the best concentration of RES was 114.281 mol/L. Nanofiber scaffolds have good elasticity, mechanical strength, and compression recovery ability and can play a supporting role in the repair of cartilage defects. The results of animal experiments also showed that the PLA/gelatin 3D nano-scaffold could promote the repair of cartilage defects. RES (114.281 mol/L) loaded inside the scaffold could greatly promote the differentiation of chondrocytes and formation of cartilage, and maintain the normal structure of the new cartilage, with good cartilage defect reparative effects and improved OA treatment effects. Qin et al. (2020) prepared RES-loaded silica aerogel (RSA) using the sol–gel method. In simulated gastric juice (pH = 2.0) and a phosphate buffer (pH = 7.4) at 37°C, the release of RSA lasted for more than 6 h, and the release amount reached 90 and 80%, respectively. Preliminary *in vitro* toxicity tests showed that RSA had good biocompatibility and stability. Combined with the anti-inflammatory effects of RES, it shows great potential for treating OA. Sheu et al. (2013) prepared an oxidized HA (Oxi-HA)/RES hydrogel, which showed good biocompatibility. The Oxi-HA/Res hydrogel could upregulate the gene expression of COL2, aggrecan, and Sox9; promote ECM synthesis; downregulate the gene expression of IL-1B, MMP1, MMP3, and MMP13; and reduce inflammation and injury induced by lipopolysaccharides. The Oxi-HA/Res hydrogel may be a potential chondrocyte carrier for the treatment of cartilage defects. However, this study only carried out *in vitro* experiments, so further *in vivo* research is necessary to determine possible clinical application in the future. Kamel et al. (2019) prepared a mixed micellar system using poloxamer (P188:P407 = 2:1), then subjected it to *in vitro* and *in vivo* evaluation, and compared the curative effects of MM3, PLA-coated MM3, and drug suspension. PLA-coated MM3 had the best ability to eliminate knee edema, and MM3 had the best ability to remove TNF-α. The addition of PLA coating can increase drug retention and reduce drug clearance from the synovial fluid. Histological studies have shown that articular and synovial structures can be restored through IA injection of drug-loaded micellar nano-systems. In addition, it can also reduce the symptoms of joint swelling in OA rats (**Table 2**).

3.2 Curcumin

CUR, a bioactive polyphenolic, is a natural BDEs which is mainly extracted from the rhizome of turmeric (*Curcuma longa L.*) (Feng et al., 2019b). CUR has significant antioxidant and free radical scavenging effects and is traditionally considered to possess anti-inflammatory, anticancer, antioxidant, antiangiogenesis, and anti-radiation properties (Aggarwal et al., 2013; Tasneem et al., 2019; Hasanzadeh et al., 2020).

Numerous previous studies have shown that CUR can inhibit chondrocyte apoptosis (Zhang et al., 2016; Henrotin et al., 2019). Its molecular mechanisms are not only associated with the inhibition of cell proliferation and metastasis but also associated with the downregulation of various factors such as TNF-α, IL-1β, and protease levels (Khayyal et al., 2018; Wang et al., 2019). Extensive research has revealed that CUR can exhibit anti-inflammatory effects on OA *via* suppressing the NF-κB signaling pathway, IL-1β, IL-6, IL-18, iNOS, prostaglandin E2 (PGE_2), and cyclooxygenase-2 (COX-2) (Chin, 2016; Zhang et al., 2016; Qiu et al., 2020). Chondrocyte apoptosis in OA is related to oxidative and endoplasmic reticulum (ER) stress (Feng et al., 2019b). Feng et al. (2019b) demonstrated that CUR protected rat chondrocytes from apoptosis by promoting SIRT1 expression and inhibiting ER stress and its related PERK-eIF2α-ATF4-CHOP signaling pathway.

Yang et al. (2007) compared the routes of oral and intravenous administration of CUR and found that due to the very low oral bioavailability of CUR, its maximum plasma concentration (500 mg/kg) is much lower than that of intravenous injection (10 mg/kg) (0.06 vs. 0.36 μg), and so a very high dose (>10 g/day) is required for oral administration to reach the plasma concentration recommended in the preclinical study (Belcaro et al., 2010; Gupte et al., 2019). A clinical study showed that CUR and low-dose ibuprofen had the same effect in reducing OA pain (Kuptniratsaikul et al., 2014; Gupte et al., 2019). A meta-analysis showed that the use of CUR as a dietary supplement was better than glucosamine (GA) and chondroitin in improving OA in the knee joints, hip joints, and hands in the short term (Liu et al., 2018b). Other studies have also shown that CUR can reduce OA pain and improve joint function while reducing the risk of adverse events (Panahi et al., 2014; Bannuru et al., 2018; Zeng et al., 2021) and can serve to decrease the use of NSAIDs which has more adverse effects (Grover and Samson, 2016; Wang et al., 2021a). At present, there are many methods, such as nanoparticles, liposomes, micelles, and phospholipid complexes, which can extend drug release time and increase permeability and resistance to clearance (Anand et al., 2007; Wang et al., 2019).

There are five studies that used CUR combined with a cartilage tissue engineering scaffold to treat OA. Kang et al. (2020) added CUR to the hydrophobic main chain of poly(β-amino ester) (PAE) to prepare anti-inflammatory polymeric prodrug of CUR (ACP) and found that amphiphilic ACP dissociated under acidic conditions. The potential of ACP micelles as a targeted therapeutic agent for inflammatory disease was investigated using an MIA-OA rat model due to the pathological characteristics of OA joints, such as low pH (6.6–7.1) and high ROS levels. In an acidic environment, the CUR release rate of ACP was very fast, 95% in 7 days, showing that it can play a role in accelerated drug treatment. ACP could significantly scavenge H_2O_2 and had no cytotoxicity when the concentration was lower than 100 μg/ml. ACP could also significantly inhibit the levels of TNF-α and IL-1β, with a stronger effect than that of free CUR. After treatment with ACP micelles, the articular surface of MIA-OA rats was smooth, the cartilage structure was intact, and the expression of proteoglycan, ACAN, and collagen protein was strong. The results showed that ACP micelles had strong anti-inflammatory and anti-arthritis properties. Yeh et al. (2015) used soybean phosphatidylcholines as a liposome formulation and compared the particle size, encapsulation efficiency, liposome stability, and cellular uptake of CUR/bisdemethoxycurcumin (BDMC)–loaded liposomes. The results showed that the encapsulation rates of CUR and BDMC in the liposomes were 69.5 and 71.4% respectively, and the particle size of the liposomes was stable after formation. Both liposomes inhibited macrophage inflammation and osteoclast differential activity. Compared with free drugs (such as CUR and BDMC), CUR-like liposomes (CUR-LIP) showed less cytotoxicity and a higher drug uptake rate. CUR-LIP can inhibit the proliferation of osteoclasts and maintain the differentiation function of osteoblasts by increasing the ratio of osteoprotectin (OPG)/NF-κB ligand receptor activator (RANKL), downregulating MMP3 and COX-2 induced by IL-1β. Therefore, CUR liposomes may delay the progression of OA.

Crivelli et al. (2019) prepared silk fibroin nanoparticles (SFNs) using the desolvation method, then tested empty and drug-loaded [with CUR or celecoxib (CXB)] nanoparticles for their ROS scavenging activity, hemolysis, cytotoxicity, and anti-inflammatory effects in an OA *in vitro* model. The results indicated that CUR-SFNs exhibited a synergistic antioxidant effect. SFNs encapsulation could reduce the cytotoxicity of free drugs. CXB, a selective COX-2 inhibitor, is the first choice in the treatment of OA pain, but the long-term high-dosage use of CXB may cause serious cardiotoxicity and renal complications. On the contrary, CUR can reduce OA-related inflammation without obvious side effects. When free CUR was added to SFNs, its antioxidant activity increased from 80 to 90%, while CBX showed no significant difference. Based on these findings, it can be speculated that the combination of SFNs and CUR has synergistic antioxidant effects. At high concentrations, the anti-inflammatory effects of SFNs/CUR (400 μg/ml) are greater than those of SFNs/CXB (800 μg/ml). Therefore, we believe that SFNs/CUR is more suitable for the treatment of OA than SFNs/CXB. Of course, more *in vivo* and preclinical studies are needed to verify this view.

Wang et al. (2018) prepared HA/chitosan nanoparticles (cNP) for the delivery of CUR to investigate their effect on OA treatment. The results showed that the optimal drug loading of HA/cNP for CUR was 38.44%, which showed a good sustained release effect. CUR delivered by HA/cNP inhibiting the inflammation and chondrocyte apoptosis of OA may be mediated by inhibiting the NF-κB pathway and expression of MMP1 and MMP13, and increasing the expression of COL2. Ratanavaraporn et al. (2017) prepared gelatin/silk fibroin microspheres loaded with CUR for use in the anti-inflammatory treatment of MIA-OA rats. The results showed that the encapsulation efficiency of CUR by gelatin/silk fibroin (30/70) microspheres reached 59%, the encapsulation amount of CUR microspheres was about 2 μg/mg. CUR-coated gelatin/silk fibroin (30/70) microspheres reduced serum IL-6 levels and delayed the degeneration of joint and synovial tissue cells. These results indicate that the CUR-sustained release system

TABLE 2 | The effect of RES combined with carriers on OA cartilage repair.

Research (author & year)	BDEs	Carrier	Gene expression		Cartilage repair effects		Other evaluations	Research conclusion
			Inhibition	Promote	Imaging evaluations	Tissue sections		
Kann et al. (2016)	CUR and RES	PC-NPs	NO		No mention	No mention	Microscopy; cell viability testing	Polyphenols combined with nanocapsules can significantly reduce the level of NO, protect joint cells, and prevent apoptosis
Coradini et al. (2015)	CUR and RES	Lipid-core nanocapsules			No mention	Significantly attenuation of fibrosis in the synovial membrane, cartilage, and bone loss		
Ming et al. (2018)	RES	PLA-gel			Significant articular cartilage repair effect were assessed by general observation and microCT	A smooth and thick cartilage surface and a clear structure were observed by hematoxylin and eosin staining, Safranin-O Fast Green staining, Alcian blue staining, and toluene staining		PLA/gelatin 3D nano scaffolds loaded with RES can greatly promote the formation of cartilage
Qin et al. (2020)	RES	SiA			No mention	No mention	Surface morphology analysis, FTIR analysis, Raman analysis	RSA has biocompatibility and stability; Combined with the anti-inflammatory effect of RES, it shows a good potential in the treatment of OA
Sheu et al. (2013)	RES	HA	IL-1β, MMPs, Col.I	Col.II, ACAN, Sox9	No mention	No mention	MTT, FTIR, and TNBS assays	Oxi-HA/RES hydrogel is biocompatible with chondrocytes, allowing ECM synthesis and reducing LPS-induced inflammation and injury
Kamel et al. (2019)	RES	PLA-P	TNF-α					RES-loaded mixed micellar nanosystems reduce the severity of cartilage injury and synovitis

EE, Encapsulation efficiency; FTIR, Fourier transform infrared; PLA-P, PLA-coated poloxamer; HA, hyaluronic acid hydrogel; SiA, silica aerogel; PLA-gel, PLA/gelatine nano-scaffold; PC-NPs, poly(ε-caprolactone) nanocarriers; MTT, MTT assay; TNBS, trinitrobenzene sulfonate assay.

can be used for the local anti-inflammatory treatment of OA with reduced trauma.

3.3 Epigallocatechin-3-Gallate

Epigallocatechin-3-gallate (EGCG), a major extract of green tea [*Camellia sinensis* (L.) Kuntze], accounts for approximately 40–60% of green tea polyphenols (Zheng et al., 2019). EGCG can inhibit the activation of p38 MAPK and c-Jun N-terminal kinase (JNK) (Singh et al., 2003) and significantly reduce the levels of TNF-α and MMP13 in human chondrocytes stimulated by AGEs (Rasheed et al., 2016). With both anti-inflammatory and antioxidant properties (Akhtar and Haqqi, 2011), EGCG inhibits COX-2 and PGE_2 production *via* the upregulation of hsa-miR-199a-3p expression (Ahmed et al., 2002; Ownby et al., 2014; Jhang et al., 2016), inhibits IL-1β–induced ADAMTS5 expression (Rasheed et al., 2016), and cartilage and proteoglycan degradation (Heinecke et al., 2010). Mice treated with EGCG showed OA-related pain relief (Leong et al., 2014), indicating that EGCG can not only delay the progression of OA but also relieve its symptoms. Natarajan et al. (2015) verified the cartilage protective effects of EGCG through the IA injection of polyphenols, but it requires repeated injections, which is not popular in clinical medicine.

There are two animal studies that used EGCG combined with cartilage tissue engineering scaffolds. GA, an amino monosaccharide, is an important component of polyglucosamine which is found mainly in the cartilage matrix and synovial fluid. Its protective effects on cartilage are mainly inhibiting proteoglycan degradation, stimulating proteoglycan synthesis, inhibiting the activation of inflammatory cells, activating chondrocytes and synovial cells, and restoring joint function. Zheng et al. (2019) studied the effect mechanism of an EGCG-GA mixture and EGCG-GA-casein protein nanoparticles (EGCG-NPs) in OA rats. The results showed that EGCG, as a plant polyphenol, could significantly promote the effects of GA; nanoparticles (NPs) could significantly improve the stability of EGCG; and EGCG combined with NPs could inhibit TNF-α, IL-1β, IL-6, and IL-8 expression in OA rats, inhibit synovial hyperplasia and inflammatory cell infiltration, and effectively

alleviate inflammation. It could also improve erythema and swelling around the joints in OA rats. The other study combined EGCG with HA and gelatin to create a composite hydrogel in order to explore the anti-inflammatory and cartilage protective effects of an EGCG-loaded composite hydrogel in the treatment of OA *in vivo* and *in vitro* (Jin et al., 2020b). After adding EGCG to the hydrogel, the cytotoxicity of EGCG was eliminated and it showed good biodegradability. Moreover, the expression of IL-1β, TNF-α, MMP13, and ADAMTS5 were significantly downregulated. Under *in vitro* experiment conditions, EGCG could promote the growth and differentiation of chondrocytes. After 4 weeks of injection into the joints of OA rats, no significant differences were observed in the surface or thickness of the cartilage between the injected rats and control rats. Therefore, we believe that EGCG combined with material scaffolds will be a promising tissue engineering strategy for repairing cartilage defects in OA.

3.4 Honokiol

Honokiol (HON) is a phenolic compound extracted from *Magnolia officinalis* Rehder & E.H.Wilson (Kim et al., 2010). *In vitro* studies of macrophages and neutrophils showed that HON had anti-inflammatory effects (Munroe et al., 2007). Other previous studies showed that HON may have a cartilage protective effect (Chen et al., 2014; Wu et al., 2017a). In the CIA-OA mice, the oral administration of magnolol and HON could block the production of IL-17, MMPs, RANKL, and NO in inflammatory joints and reduce serum TNF-α and IL-1β to inhibit inflammation, cartilage degeneration, and bone erosion (Kim et al., 2010) with no liver or kidney damage. However, its oral bioavailability is low, and only 1% can be absorbed. Moreover, HON can inhibit the levels of PGE_2, NO, TGF-β1, and IL-6, the protein expression of COX-2 and iNOS, and the phosphorylation of Akt, IκB-α, and NF-kB, upregulated by IF-1β (Li et al., 2011; Chen et al., 2014). The results of Park et al. (2017) showed that HON could inhibit the osteoclastic effect mediated by RANKL. In addition, HON promotes the chondrogenesis of human umbilical cord MSCs and inhibits inflammation by blocking the NF-κB pathway (Wu et al., 2017a). There is only one animal study that uses HON combined with a cartilage tissue engineering scaffold. Zhu et al. (2020) showed that HON significantly inhibited the release of pro-inflammatory cytokines TNF-α, IL-1B, and IL-6 stimulated by lipopolysaccharide (LPS). *In vivo*, a scaffold containing HON was implanted into the cartilage defect area. After 8 weeks, the defect area was filled with COL2-positive cartilage tissue with an intact tide line structure, and the cartilage had become hard and smooth. Meanwhile, the ratio of the bone volume to tissue volume (BV: TV) was significantly increased. These results show that HON combined with a scaffold can promote the regeneration of hyaline cartilage and bone tissue in osteochondral defects (**Table 3**).

4 ALKALOIDS

4.1 Brucine

Brucine (BRU) is a major effective component of *Strychnos nux-vomica* L. (Wu et al., 2017b), with high toxicity (Liu et al., 2015a; Lu et al., 2020). *S. nux-vomica* L. has a long history of clinical application in herbal medicine, especially in the treatment of RA and OA. BRU has anti-inflammatory and analgesic effects (Yin et al., 2003) and can significantly inhibit LPS-induced PGE_2 production (Liu et al., 2015a; Lu et al., 2020). BRU can effectively promote chondrocyte regeneration and repair cartilage damage caused by OA. Although BRU is highly effective in the treatment of OA, its potential use is severely limited due to its high toxicity; with its good lipid solubility, it can easily penetrate the blood–brain barrier and cause serious toxicity to the central nervous system if distributed in the brain (Gao et al., 2021). Its oral administration can also cause gastrointestinal irritation and systemic toxicity (Liu et al., 2015a; Lu et al., 2020). Until now, BRU has not been used clinically or studied in clinical trials. Therefore, new drug delivery systems are urgently needed to reduce the side effects (Liu et al., 2015a; Lu et al., 2020). There is only one animal study that used BRU combined with a cartilage tissue engineering scaffold. To determine the feasibility of IA injection, Chen et al. (2012) evaluated a BRU-loaded microsphere/thermally responsive hydrogel (BMH) combination system in such aspects as drug release, pharmacodynamics, and biocompatibility. The results showed that the entrapment rate of this system was 98.60% w/w with an average particle size of 0.9–4.5 μm. The sustained release cycle of BMH was 7 days. They established a rabbit OA model through the IA injection of collagenase and studied the therapeutic effects of this strategy on OA by IA injection. Histological assessment showed that BMH reduced the number of fibroblasts and improved synovial integrity during cartilage defect repair, and the pharmacodynamic results revealed that BMH could protect OA joints from degradation by suppressing TNF-α and IL-1β levels.

4.2 Sinomenium

Sinomenium (SIN) is a BDE extracted and purified from the plant *Sinomenium acutum* (Thunb.) Rehder & E.H.Wilson (Chen et al., 2016b), which has anti-rheumatism, anti-inflammatory, and anti-pain effects (Wu et al., 2019a; Jiang et al., 2020). Clinically, SIN is widely used to treat patients with RA (Zhao et al., 2012). By activating the Nrf2/HO-1 signaling pathway and inhibiting NF-κB activity, SIN can reduce the protein levels of ADAMTS5 and MMPs in rats (Wu et al., 2019b), inhibit inflammation and ECM degradation, and play a role in cartilage protection (Wu et al., 2019a). In addition, SIN downregulates iNOS, COX-2, NO, PGE_2, TNF-α, and IL-6 induced by IL-1β (Wu et al., 2019a), suggesting that it protects chondrocytes by promoting autophagy and preventing cartilage degradation, thereby reducing the clinical symptoms of arthritis. However, few studies have evaluated the availability of SIN in the treatment of OA. There is only one animal study that used SIN combined with a cartilage tissue engineering scaffold. Chen et al. (2016b) evaluated the therapeutic effects of SIN coated with chitosan microspheres (CM-SIN) on OA by IA injection. Both *in vivo* and *in vitro* studies showed that SIN could partially induce autophagy to inhibit the degradation of the cartilage matrix induced by IL-1β. SIN downregulates the mRNA expression of cartilage degradation markers MMP13 and ADAMTS5 and upregulates

TABLE 3 | The effect of polyphenol active ingredients combined with carriers on OA cartilage repair.

Research (author & year)	BDEs	Carrier	Gene expression		Cartilage repair effects		Other evaluations	Research conclusion
			Inhibition	Promote	Imaging evaluations	Tissue sections		
Kang et al. (2020)	CUR	PEG	IL-1β, TNF-α	Col.II, ACAN, Sox9	No mention	Smooth surface with structural integrity of cartilage, along with strong expression of proteoglycan, ACAN, and collagen, was observed by H&E, Masson's trichrome, Safranin-O, and ACAN staining		ACP micelles inhibit TNF-α and IL-1 β, significant protection of joint structure from arthritis
Yeh et al. (2015)	CUR	SPC-liposome	TRAP, cathepsin K, NO, MMPs, COX-2	OPG/RANKL	No mention	No mention	OPG/RANKL signaling pathway	CUR-loaded liposomes can inhibit macrophage inflammation and osteoclast differentiation, which may slow down the progression of OA
Crivelli et al. (2019)	CUR	SNPs	IL-6, RANTES, ROS, NO		No mention	No mention	FTIR, DSC, TGA, SEM	CUR and SFNs showed synergistic antioxidant effect
Wang et al. (2019)	CUR	HA/cNP	MMPs, NF-κB	Col.II	Improved articular surface injury in OA rats by general observation *via* a microscope	The knee joint surface was smooth, and the cells were regularly arranged in OA rats by H&E staining, toluidine blue staining, Safranin-O Fast Green staining	UV assay; flow cytometry; western blot analysis	HA/cNP and CUR may suppress inflammation and chondrocyte apoptosis in KOA *via* repression of the NF-κB pathway
Ratanavaraporn et al. (2017)	CUR	Gel/SMs	IL-6		Sign of OA was not observed in the treatment group *via* X-ray	Histologic and histochemical grading of articular joint and synovial tissue change of OA rats treated with CUR-loaded gel/SMs was significantly better than in other groups	Radiographic, histological examination	CUR gel/SMs have potential anti-inflammatory effect on OA joint in rats
Jin. (2020)	EGCG	HA/gel	IL-1β, TNF-α, ADAMTS5, MMPs	Col.II, ACAN, Sox9	No mention	In 5% HTG-E group, cartilage surface and thickness were completely intact, showing no signs of wear and tear		HTG hydrogel can promote the accumulation of ECM, and it has anti-inflammatory and cartilage protective ability after loading EGCG
Zheng et al. (2019)	EGCG	EGC-NPs	IL-1β, IL-6, TNF-α		The therapeutic effect of the EGC-NPs was significantly better than that of the EGCG-GA mixture and comparable to the antiarthritic effect of celecoxib by a radiographic evaluation and scoring system	Combined with EGCG, GA can effectively promote its antiarthritic effects		The anti-inflammatory effect of EGC-NPs was significantly higher than that of the EGCG-GA mixture
Zhu et al. (2020)	HON	ECM/PGDH	IL-1β, IL-6, TNF-α	Col.I, Col.II, BV: TV, Tb.Th	In the group in which the defect was repaired with PEGDA/ECM/HON scaffold, the surfaces of the defect were smooth and the defect region displayed an intact tideline structure *via* micro-CT	The defects in the PEGDA/ECM/HON group were mostly filled with cartilage tissue positive for COL2, indicating regeneration of hyaline cartilage-like tissue		Scaffolds combined with HON promoted the regeneration of hyaline cartilage and subchondral bone

EE, Encapsulation efficiency; CFA, Complete Freund's adjuvant; H&E, hematoxylin and eosin; SNP, sodium nitroprusside; FTIR, Fourier transform infrared; Tb.Th, trabecular thickness; HA/cNP, HA/chitosan nanoparticles; gel/SMs, gelatin/Thai silk fibroin microspheres; HA/gel, HA/gelatin hybrid hydrogel; ECM/PGDH, 3D-printed ECM/polyethylene glycol diacrylate hydrogel; SNPs, silk fibroin nanoparticles; PEG, poly(ethylene glycol); HA, hyaluronic acid hydrogel; PC-NPs, poly(ε-caprolactone) nanocarriers; UV, ultraviolet; DSC, Differential scanning calorimetry; TGA/DSC 1, Simultaneous thermogravimetric analysis; SEM, scanning electron microscopy; HTG, HA/gelatin; SPC, Soybean phosphatidylcholine; TRAP, tartrate-resistant acid phosphatase; HTG-E, EGCG-loaded HA/gelatin; EGC-NPs, EGCG-GA-Casein Nanoparticles.

the expression of ECM components COL2A1 and ACAN. After the IA injection of CM-SIN for 4 and 8 weeks, the OARSI score of OA mice was significantly reduced ($p < 0.01$), cartilage degeneration was improved, and OA progression was delayed.

4.3 Berberine

Berberine (BBR) is an active component isolated from *Coptis chinensis* Franch.("Huanglian" in Chinese) (Neag et al., 2018). BBR has obvious immunosuppressive, anticancer (Mishra et al., 2019), and anti-inflammatory effects (Hu et al., 2011; Zhou et al., 2015a; Belwal et al., 2020). It has been shown that BBR can activate the Wnt/β-catenin signaling pathway in OA rats (Zhou et al., 2016a). Wnt signaling molecules play an important role in the process of osteogenesis (Wong et al., 2020), so it can be speculated that BBR can upregulate the Wnt signaling pathway and promote the reconstruction of the subchondral bone. BBR has also been reported to enhance autophagy levels in chondrocytes (Chen et al., 2018). BBR significantly inhibits IL-1β–induced inflammation by inhibiting the NF-κB signaling pathway in human OA chondrocytes (Zhou et al., 2016b; Lu et al., 2019) and significantly inhibits the IL-1β–induced expression of MMP3, MMP13 (Moon et al., 2011; Belwal et al., 2020), iNOS, and COX-2, and the production of NO and E2. In addition, BBR inhibits apoptosis and promotes the proliferation of SNP-stimulated chondrocytes in rats and OA rats (Zhou et al., 2015b; Zhou et al., 2017). BBR also promotes articular chondrocyte survival and stroma formation by activating Akt signaling (Zhao et al., 2014; Liu et al., 2015b). However, BBR has poor water solubility, low bioavailability, and a short biological half-life, so it is necessary to design a continuous delivery system to improve its utilization.

There are three animal studies that used BBR combined with cartilage tissue engineering scaffolds. Chen et al. (2018) investigated the effects of a combined BBR and sodium hyaluronate/SA (HA/SA) scaffold on cartilage repair. *In vitro*, the scaffold sizes ranged from 100 to 200 μm, and all BBR was released within 72 h. HA/SA-IPN scaffolds combined with BBR can activate the Wnt/β-catenin signaling pathway to promote the osteogenesis differentiation of BMSCs and increase the bone volume to tissue volume ratio (BV/TV). Meanwhile, the cartilage defect surface of the BBR and scaffold group was smooth and filled with thicker hyaline cartilage–like tissue. *In vivo*, BBR significantly increased the level of autophagy marker LC3, downregulated MMP13 and ADAMTS5, and upregulated COL2A1 and ACAN. These results suggest that BBR inhibits the degradation of the cartilage matrix by enhancing autophagy and promoting cartilage regeneration. We believe that this system can regenerate not only cartilage but also subchondral bone simultaneously, which is a promising strategy for osteochondral defect repair. Zhou et al. (2015a) successfully synthesized CNs for the sustained release of BBR using the ionic cross-linking method and established an OA rat model by ACLT combined with medial meniscal resection (ACLT + MMx). *In vitro*, the CNs could continuously release BBR, with good stability, uniform morphology and structure, good particle size and appropriate Zeta potential, and encapsulate a large amount of BBR. In the ACLT + MMx rat model, BBR significantly downregulated the mRNA expression of caspase-3 and Bax and upregulated the mRNA expression of Bcl-2. The Mankin score was used for histopathological scoring, and the results showed that the BBR-CNs group was significantly better than the model group in structural changes, chondrocyte changes, tide mark, and safranin staining ($p < 0.001$), and the cartilage damage of OA rats was reversed. These results suggest that the IA administration of BBR-CNs may be an effective treatment for OA. Zhou et al. (2017) successfully synthesized a new type of BBR-loaded chitosan microspheres (CMs) with an encapsulation efficiency of 100.8 ± 2.7 mg/g. CMs loaded with BBR significantly inhibited the protein expression levels of caspase-3, disintegrin, ADAMTS5, and MMP13 induced by SNP, which confirmed its antiapoptotic activity. However, they did not conduct further animal model tests to verify the system's effectiveness *in vivo*.

4.4 Colchicine

Colchicine (CLC) is a water-soluble alkaloid extracted from *Colchicum autumnale* L. (Mohamed et al., 2020) and the first therapy of choice in gout treatment (Letter, 1974). Due to its anti-inflammatory and anti-fibrosis properties (Leung et al., 2018), CLC is used not only in the treatment of arthritis but also as a remedy to treat numerous skin conditions (Sullivan et al., 1998), Familial Mediterranean fever (Knieper et al., 2017), Behcet's disease (Nava et al., 2014), cirrhosis (Kershenobich et al., 1988; Gong and Gluud, 2004; Rambaldi and Gluud, 2005), and certain carcinomas (Mohamed et al., 2020). Clinical studies have shown that CLC can significantly improve symptoms in KOA patients (Das et al., 2002). However, a study by Leung et al. (2018) showed that CLC (0.5 mg, twice daily, orally, 16 weeks) did not reduce KOA symptoms but reduced the inflammatory and high bone turnover biomarkers associated with OA severity and risk of progression. The oral administration of CLC has certain limitations due to its extensive first-pass effects, poor bioavailability, and severe gastrointestinal side effects (Abdulbaqi et al., 2018). At the same time, the intravenous administration of CLC can cause serious or even fatal effects such as cell loss, tissue necrosis, and intravascular coagulation transmission (Evans et al., 1996; Abdulbaqi et al., 2018), and its intravenous administration is prohibited. In addition, the high water and poor skin permeability of CLC pose challenges for its transdermal delivery (Mohamed et al., 2020). Most importantly, the chronic and progressive nature of OA requires frequent administration. Thus, in order to ensure better safety and effectiveness, it is urgent to find an alternative administration route for CLC (Marwah et al., 2016).

There is only one animal study that used CLC combined with a cartilage tissue engineering scaffold. Mohamed et al. (2020) developed novel CLC transdermal delivery systems to conquer such obstacles. Compared with the drug suspension liquid, the patch increased the drug flux and penetration level for more than 24 h. The therapeutic effects of the CLC patch on the MIA-OA rat model showed that CLC improved exercise ability, increased the blood glutathione level, and significantly reduced the malondialdehyde, NO, TNF-α, and COX-2 levels. The histopathological evaluation of the rats' knee joints showed

that rats treated with CLC patches showed similar near-normal structures, regular smooth cartilage surfaces, and dense bone joint lumens when compared to those of the control group. These results show that the CLC preparation had good protective and therapeutic effects on bone tissue damage caused by MIA-OA (**Table 4**).

5 OTHERS

5.1 Ginger Extract

Ginger is the rhizome of *Zingiber officinale* Roscoe, and its extract can inhibit the mitochondrial pathway of cell apoptosis (Hosseinzadeh et al., 2017). When inflammation causes apoptosis of articular chondrocytes in OA, the value of apoptosis mitochondrial pathway marker Bax/Bcl-2 increases (Lee et al., 2004). Numerous studies have shown that the treatment of OA with ginger extract (GINE) is effective and safe (Bliddal et al., 2000; Leach and Kumar, 2008; Bartels et al., 2015; Rondanelli et al., 2020). Experimental studies found that 0.01, 0.5, 1, 5, 10, 25, 50, and 100 μg/ml of GINE was nontoxic to C28I2 chondrocytes, and 5 and 25 μg/ml of GINE can reduce the ROS production, upregulate the expression of antioxidant enzymes GPx-1, GPx-3, GPx-4, and SOD1, reduce the value of Bax/Bcl-2, inhibit the activation of caspase-3, inhibit the apoptosis mitochondrial pathway signal stimulated by IL-1β, and reduce apoptosis of human C28I2 chondrocytes (Hosseinzadeh et al., 2017; Li et al., 2020). However, the oral administration of GINE can cause gastrointestinal reactions, poor absorption, rapid metabolism, and the elimination of the active compound, and GINE itself has low bioavailability. Therefore, several studies have suggested that its transdermal administration is safer than oral (Amorndoljai et al., 2015).

There is only one clinical study that used GINE combined with a cartilage tissue engineering carrier. Amorndoljai et al. (2015) prepared a topical liniment by combining GINE and nanostructured lipid carrier (NLC). About 60 KOA patients (aged 50–75 years) were included afterward and applied this liniment three times per day. After 12 weeks of treatment, the GINE nanoparticles significantly improved the patients' overall assessment, knee pain, symptoms, daily activity, physical activity, and quality of life, and their Knee Injury and Osteoarthritis Outcome Score (KOOS), Index of Severity for Osteoarthritis (ISOA), and Patient's Global Assessment (PGA) results were statistically significant ($p < 0.05$). There were no safety problems or adverse events.

5.2 Cordycepin

Cordycepin (3′-deoxyadenosine) (COR) is a nucleoside analog isolated from *Cordyceps militaris* (L.) Fr., which occupies a notable place in traditional medicine. In recent years, many studies have verified that COR has anticancer, antiangiogenesis, antiaging, and other pharmacological effects (Khan and Tania, 2020). It has also been found that COR can induce cell apoptosis and autophagy. Moreover, a recent study has shown that COR significantly inhibited the production of PGE_2 and NO and decreased the production of MMP13, IL-6, iNOS, and COX-2 in OA chondrocytes induced by IL-1β (Hu et al., 2014). These clues suggest that COR inhibits TGF-β activity, induces autophagy, and prevents cartilage degradation to protect the chondrocytes (Ying et al., 2014; Ashraf et al., 2019; Tao et al., 2020). It is suggested that COR may be a potential candidate drug for the prevention of OA. However, few studies have evaluated its efficacy in the treatment of OA (Xia et al., 2017).

There is only one animal study that used COR combined with a cartilage tissue engineering carrier. Xia et al. (2017) investigated the synergistic effects of hydrogel and COR on the promotion of chondrocyte autophagy, both *in vivo* and *in vitro*. All of the CMs-encapsulated COR (CM-COR) was released in phosphate-buffered saline within 72 h. COR decreased the mRNA expression of MMP13 and ADAMTS5 and increased the mRNA expression of COL2A1 and ACAN. In addition, COR significantly increased the expression of LC3-positive chondrocytes in cartilage tissue, suggesting that COR can activate autophagy to prevent IL-1β–induced cartilage degradation. After receiving CM-COR + hydrogel, cartilage degeneration decreased, the OARSI score reached 3.4 ± 0.3, and the progression of OA was delayed to the greatest extent.

5.3 Tetramethylpyrazine/Ligustrazine

Tetramethylpyrazine (TMP), also called ligustrazine (LIG), is a botanical extract component separated from *Conioselinum anthriscoides* "Chuanxiong," which has strong anti-inflammatory (Wei et al., 2016; Chen et al., 2017) and cartilage protection properties (Ju et al., 2010). In recent years, TMP has proven to be an effective candidate for the treatment of OA (Zhang et al., 2018) as it can reduce IL-1β–induced GAG degradation, MMP3 mRNA expression, and IL-1–induced cartilage and chondrocyte degeneration, thereby improving chondrocyte activity and inhibiting their apoptosis. ROS and the apoptotic mitochondrial pathways influence articular cartilage degeneration in OA (Kim and Blanco, 2007; Musumeci et al., 2015). Furthermore, TMP scavenges cytotoxic ROS to maintain the mitochondrial membrane potential and downregulate caspase-3 activity (Ju et al., 2010). However, TMP is quickly erased from the articular cavity after IA injection, so multiple injections are required to maintain the curative effect, which may lead to the inflammation and infection of local tissues. Reducing the number of injections is the key to increasing patient compliance (Zhang et al., 2018).

There are three animal studies that used TMP/LIG combined with cartilage tissue engineering carriers. Zhang et al. (2018) evaluated the curative effects of TMP microspheres on joint swelling and histological analysis in a papain-induced OA rat model. The drug loading of freeze-dried microspheres (81.36 ± 1.15%) was greater than that of vacuum-dried microspheres (8.22 ± 0.19%). The freeze-dried microspheres had a particle size of about 10 μm and excellent sustained release properties, effectively able to extend the release time of the drug in the articular cavity to 30 days (4.7 times more than the TMP solution). TMP microspheres were also superior to the TMP solution in improving the range of motion and swelling of OA

TABLE 4 | The effect of alkaloid active ingredients combined with carriers on OA cartilage repair.

Research (author & year)	BDEs	Carrier	Gene expression		Cartilage repair effects		Other evaluations	Research conclusion
			Inhibition	Promote	Imaging evaluations	Tissue sections		
Chen et al. (2012)	BRU	MH	IL-1β, TNF-α		The severity of OA was milder in the BMH group than in the saline group *via* gross pathological observation	The number of fibroblasts was significantly decreased and the integrity of synovium was improved in the BS and BMH groups than in the saline group	X-ray (release profiles of BRU), SEM, FX imaging	BRU-loaded MH can inhibit the expression of TNF- α and IL-1β to protect OA joint
Chen (2015)	SIN	CM/ GelMA	IL-1β, ADAMTS5	Col.II, ACAN, LC3	No mention	The combination of CM-SIN and GelMA hydrogel retarded the progression of surgically induced OA, while each of these components alone also had a mild beneficial effect according to the OARSI score	SEM, RT-PCR	SIN combined with scaffolds can improve the progression of surgically induced OA by promoting autophagy
Mohamed et al. (2020)	CLC	MSN	IL-1β, NO, COX-2		No mention	the rats group treated with formula 2 showed nearly normal architecture like normal control with a regular smooth surface	TEM, FTIR, FE-SEM	COL-MSN/hydrogel patch is an effective, safe, and convenient treatment for OA
Chen et al. (2018)	BBR	HA/SA	ADAMTS5, MMPs	Col.II, ACAN, BV/ TV, Wnt/β-catenin, LC3	The defect surface became smooth in the group of scaffold + BER, by general observation, and the results of the micro-CT scans demonstrated that much more calcified tissue was produced at 4 and 8 weeks post-surgery in the defect regions implanted with the scaffold in combination with BER than in those implanted with the scaffold without BER	The OA mice treated with BER showed better cartilage surfaces with cracks and a markedly lower OARSI score compared to that of the untreated OA mice		BER combined with HA/SA can activate Wnt signaling pathway, repair subchondral bone, and promote autophagy to protect the cartilage
Zhou et al. (2015a)	BBR	CNs	Bax, caspase-3	Bcl-2	The cartilage damage in the OA + BBR–loaded CNs group was significantly reversed by general observation	Mankin scores revealed that BBR-loaded CNs treatment antagonized a stronger effect on the amelioration of cartilage damage		BBR-loaded CNs further showed anti-apoptosis activity in the treatment of OA
Zhou et al. (2017)	BBR	CMs	ADAMTS5, MMPs, caspase-3		No mention	No mention		BBR-CMs showed enhanced anti-apoptotic and chondroprotective effects on the treatment of OA

SEM, scanning electron microscopy; LC3, 1A/1B-light chain 3; RT-PCR, real-time polymerase chain reaction; TEM, transmission electron microscopy; BMSCs, bone marrow–derived MSCs; MMx, medial menisci resection; MH, chitosan–glycerol–borax microsphere/thermally responsive hydrogel; CM/GelMA, chitosan microspheres and photo-cross-linked gelatin methacryloyl hydrogel; MSN, mesoporous silica nanoparticles/hydrogel; HA/SA, hyaluronate and SA scaffold; CNs, chitosan nanoparticles; CMs, chitosan microspheres; BS, brucine solution; BER, berberine.

joints and promoting the repair of cartilage defects. TMP microspheres showed powerful advantages in reducing drug dose, limiting injection times, and improving efficacy. Two other similar studies showed that a combination of nanoparticles and LIG could improve bioavailability and targeting, and effectively reduce synovial MMP levels and NF-κB expression upstream of the NF-κB signaling pathway, thereby alleviating KOA and reducing adverse reactions (Ji et al., 2021). The combination of TMP and nanoparticles can lengthen the retention in the articular cavity, enhance the concentration of

TMP, and improve the anti-inflammatory effects while avoiding systemic toxicity (Li et al., 2021).

5.4 Andrographolide

Andrographolide (AG) is a major plant extract of *Andrographis paniculata* (Burm. f.) Nees, which is known for its antioxidant and anti-inflammatory effects (Burgos et al., 2020; Kulsirirat et al., 2021a). A double-blind, randomized, placebo-controlled study also found AG (300 and 600 mg/day) to be effective and safe in relieving pain in patients with mild to moderate KOA (Hancke et al., 2019). The pharmacological mechanism may be as follows: AG suppresses synovial inflammation *via* the regulation of TNF-α receptor 2 (TNF-R2) trafficking (Wang et al., 2021b); activates the Keap1-Nrf2-ARE pathway, and increases cell proliferation inhibited by H_2O_2 and antioxidant enzyme activity to alleviate the oxidative stress damage of chondrocytes (Li et al., 2018); specifically, AG can promote the osteogenesis and chondrogenesis of human suprapatellar fat pad–derived MSCs (Kulsirirat et al., 2021b), and it inhibits the activation of NF-κB and MMP13 expression stimulated by IL-1β in the chondrocytes (Ding et al., 2013; Chen et al., 2020b). However, the low water solubility and high lipid solubility of AG reduce its bioavailability and thus limit its oral absorption (He et al., 2021). Therefore, a continuous delivery system is needed to maximize the pharmacological benefits of AG.

There are two animal studies that used AG combined with a cartilage tissue engineering carrier. He et al. (2021) used an OA rat model to verify the anti-inflammatory and cartilage protection ability of AG combined with mesoporous silica nanoparticles (AG-MSNs). The results showed drug encapsulation efficiency of 43.39 ± 0.33% and drug loading capacity of 22.38 ± 0.71%, while at pH = 5.6, AG could be released continuously for 48 h with an accumulated release rate of about 80%. AG-MSNs prevented the IL-1β–mediated upregulation of MMP3 and MMP13 (64.66 and 67.33%). AG and AG-MSNs showed remarkable anti-inflammatory properties, decreasing the damage to chondrocytes stimulated by IL-1β. It is noteworthy that pH-responsive polyacrylic acid (PAA)–loaded Ag-MSNs was superior to AG-MSNs in the OARSI score, cartilage protection effects, and anti-inflammatory effects. In addition, Kulsirirat et al. (2021a) showed that combined use of a gelatin-based hydrogel with AG-NPs significantly extended the duration for more than 1 month. Unfortunately, only the *in vivo* sustained release time of the drug delivery system was reported, and no analysis of cartilage defect repair was performed.

5.5 Celastrol

Celastrol (CSL) is a pentacyclic triterpenoid extracted from *Tripterygium wilfordii* Hook. f., which has been widely used to treat RA (Song et al., 2019), systemic lupus erythematosus (Xinqiang et al., 2020), and cancer (Wang et al., 2007). Previous studies have shown that CSL can block IL-1β and TNF secretion in OA animals and eliminate the infiltration and proliferation of immune cells, thereby preventing cartilage and bone defects (Liu et al., 2020b). In different types of cells, CSL can inhibit IKK complex phosphorylation IκBα, one of the key steps of NF-κB activation (Jin et al., 2020a). The NF-κB signaling pathway is a typical signaling pathway involved in the development of OA pathobiology. The NF-κB transcription factor can induce cartilage degradation and promote the secretion of a variety of degradation enzymes such as MMPs and ADAMTS, which play a key role in the degradation of ECM structural proteins (Feng et al., 2020). However, the clinical application of CSL is limited due to its systemic toxicity and poor bioavailability caused by its low water solubility (13.25 ± 0.83 μg/ml at 37°C) (Wang et al., 2007). There is only one animal study that used CSL combined with a cartilage tissue engineering carrier. Jin et al. (2020a) verified an anti-inflammatory therapy against KOA through the IA injection of hollow mesoporous silica NPs loaded with CSL. the NPs largely improved the dissolution rate of CSL to 73.99% (from 12.96%). When pH = 6, the release of CSL was triggered, exerting an anti-inflammatory effect, cartilage protective effect through the prevention of COL2 degradation, and downregulation of MMP3 and MMP13 expression.

5.6 11-Keto-β-Boswellic Acid

Numerous studies on the pharmacological properties of *Boswellia serrata* Roxb. gum-resin extract 11-keto-β-boswellic acid (KBA) have shown its therapeutic effects on inflammatory diseases such as OA, RA, inflammatory bowel disease, and cancer (Bairwa and Jachak, 2016; Efferth and Oesch, 2020). KBA downregulates pro-inflammatory cytokines such as TNF-α, IL-1, IL-2, IL-4, IL-6, and IFN-γ and increases the phagocytosis of macrophages. The inhibitory effect of KBA on 5-lipoxygenase could lead to a decrease in leukotriene production. Various chronic inflammatory diseases are associated with increased leukotriene activity (Ammon, 2010; Efferth and Oesch, 2020). However, the pharmacological activity of KBA is limited by its low oral bioavailability, low water solubility and high Phase I metabolism (Bairwa and Jachak, 2016). There is only one animal study that used KBA combined with a cartilage tissue engineering carrier. Bairwa and Jachak (2016) developed an oral preparation of KBA nanoparticles (KBA-NPs) to improve its bioavailability and anti-inflammatory activity. The particle size was 152.6 nm, the polydispersity index was 0.194, the encapsulation rate was 79.7%, and the cumulative release of KBA was 61.5% at 72 h. Compared with KBA suspension (34.9%), the inhibition rate of KBA-NPs on rat foot swelling at 5 h was 60.8%, and the bioavailability and anti-inflammatory activity of KBA-NPs were increased by seven times and 1.7 times, respectively. The increased anti-inflammatory activity of KBA-NPs may be due to its increased bioavailability. However, the study did not report the effects of the administration system on cartilage defect repair (**Table 5**).

6 A SUMMARY OF THE APPLICATION OF BOTANICAL DRUG EXTRACTS AND CARRIERS IN THE REPAIR OF CARTILAGE DEFECTS

6.1 Preparation of Carriers

Scaffolding is of great significance in cartilage tissue engineering. It is worth noting that electrostatic spinning technology and 3D

printing technology are the hot spots in cartilage tissue engineering at present.

Ming et al. (2018) prepared PLA/gelatin 3D nanofiber sponge loaded with resveratrol (RES) using the electrostatic spinning technology reported by Chen (Chen et al., 2016c; Chen et al., 2016d). First, 0.1 g of PLA and 0.75 g of gelatin were mixed in 9 ml of 1,1,1,3,3,3-hexafluoro-2-propanol with a mass ratio of 1:5 of gelatin to PLA and stirred at room temperature for 5 h to prepare the PLA/gelatin solution. RES was then added, and the mixture was dissolved in 0.1 ml of ethanol and stirred until uniform. The mixed solution was then loaded into a stainless-steel needle at a flow rate of 3 ml/h at an applied voltage of 15 kV. The distance between the needle and the collector was 10 cm. All the collected PLA/gelatin nanofiber membranes were placed in a vacuum overnight to remove the residual solvents. The nanofiber membranes prepared as above were cut into small pieces (0.5 × 0.5 cm), then 1 g of the membranes was weighed and added to 100 ml of tert-Butanol and dispersed by a homogenizer at a speed of 10,000 r/min for 20 min. The dispersed nanofibers were then poured into a 24-well cell culture plate and freeze-dried for 24 h, and the freeze-dried 3D nanofiber sponge was heated in air at 190°C for 2 h for cross-linking in order to obtain the final scaffold.

Kann et al. (2016) dissolved 2 g of SA and 6 g of gelatin (SA/gel, 1:3 ratio) in 50 ml of ddH_2O to preprocess the colloid solution. The 3D printer parameters were set as follows: printing pressure of 0.20–0.40 MPa, line spacing of 0.3–1.2 mm, printing diameter of 210–510 μm, printing speed of 4–16 mm/s, and printing temperature of 200°C, kept constant throughout the printing process. The printed SA/gel composite scaffold was promptly soaked in 5% $CaCl_2$ for 30 min for rapid solidification, then soaked in 2% glutaraldehyde for 24 h for cross-linking. Residual glutaraldehyde was removed *via* l-glutamate treatment, and the scaffold was freeze-dried. In addition, Zhu et al. (Zhu et al., 2020) first prepared acellular cartilage polyethylene diacrylate (PEGDA)/ECM hydrogel using the optical cross-linking method, then prepared PEGDA/ECM 3D ink *via* dynamic projection stereophotography. Moreover, many preparation methods for drug-loading material scaffolds have been widely used in cartilage tissue engineering, such as hydrogel prepared by chemical or photo cross-linking (Goldring and Goldring, 2016) (Rai et al., 2017), aerogel prepared *via* the sol–gel method (Xia et al., 2014), membrane hydroliposomes (Wang et al., 2013) and NPs prepared by ion cross-linking (Miller et al., 2016).

6.2 Combination of Botanical Drug Extracts and Carriers

Through an analysis of the relevant literature, the combination of extracts and carriers is classified into two categories according to the different periods of ingredient addition: reactive combination and cell culture.

I. Reactive combination: This is the method chosen for many studies (Charlier et al., 2019; Jin et al., 2020a; Oliveira Silva et al., 2020). The combination is carried out through a series of chemical reactions between the BDEs and the carrier material preparation. For example, Sheu et al. (Goldring and Goldring, 2016) dissolved RES and HMDI in a dry tetrahydrofuran solution, slowly heated it to 50°C for 50 h, then gradually added H_2O to the reaction mixture (over 30 min) to generate RES-HMDI-NH_2. Oxi-hyaluronan (OXI-HA) solution was then mixed with the RES-HMDI-NH_2 solution to form an Oxi-HA-RES solution. Finally, the oxidized HA/RES hydrogel was prepared. II. Cell culture: Considering the cytotoxicity of some ingredients, this method is more suitable for confirming safe and nontoxic BDEs, so there are fewer studies. Kann et al. (2016) incubated cells in a normal medium for 24 h. After the cells had adhered normally, they took the medium out and replaced it with a medium containing ICA. After incubation for 1, 3, 5, and 7 days, they observed the cell proliferation. Finally, cells cultured with the extracts were planted on the carrier.

A total of 31 reports were included in this review, among which 12 were not studied in animal models, 17 were tested by IA injection, one was tested by intraperitoneal injection, and the remaining one was a clinical trial. In the selection of carriers, nanoparticles, microspheres, hydrogels, and 3D printed carriers are chosen. It is noteworthy that due to the pathological relationship between low pH and OA, acid-sensitive hydrogels prepared from mesoporous silica are superior in drug release, anti-inflammatory, and cartilage defect repair properties. The combination of cartilage tissue engineering materials improves the bioavailability of BDEs, prolongs the time of drug action, and alleviates adverse reactions.

We can find that almost all BDEs that can be used to treat OA have anti-inflammatory and antioxidant effects. Among them, CUR, BBR, and HON can not only protect cartilage but also promote the formation of subchondral bone, which is more suitable for the treatment of patients with subchondral bone damage in the advanced stages of OA. In addition, for BRU and CLC, we need to develop more appropriate administration systems to reduce their toxicity. Aside from anti-inflammatory and cartilage protective effects, Hes, SIN, and COR can also induce autophagy *in vivo* to mitigate the degradation of the cartilage matrix. At present, RES and CUR are the most studied BDEs, but they are still in the animal experiment stage. Further studies are required to confirm our hypotheses on how to further improve efficacy and whether they are clinically feasible (**Table 6**).

7 CONCLUSION

This article reviews the role of BDEs combined with biomaterial carriers in the treatment of OA and the repair of cartilage degeneration in recent 10 years. Many studies have shown that BDEs play an anti-inflammatory, anti-oxidation, and cartilage protection role by inhibiting the expression of pro-inflammatory factors (IL-1β, IL-6, and TNF-α) and matrix degrading enzymes (MMP1, MMP3, MMP13, and COX-2), and removing oxidative stress substances such as NO, ROS, and H_2O_2. They can also promote the repair of cartilage degeneration and delay the progress of OA by regulating chondrocyte autophagy. Some BDEs (e.g. RES, CUR, ICA, and Hes) can also promote the

TABLE 5 | The effect of other effective components of traditional Chinese medicine combined with carriers on OA cartilage repair.

Research (author & year)	BDEs	Carrier	Gene expression		Cartilage repair effects		Research conclusion
			Inhibition	Promote	Imaging evaluations	Tissue sections	
Amorndoljai et al. (2015)	GINE	NLC			No mention	No mention	GINE nanoparticles alleviated joint pain, improved symptoms of KOA
He et al. (2021)	AG	MSNs-PAA	IL-1β, MMPs	Col.II, GAG, ACAN	AG@MSNs-PAA displayed minimal changes in cartilage compared to the other three ACLT groups by general observation	Matrix vertical fissures, thinner cartilage as well as minor surface destabilization were observed	AG@MSNs-PAA can effectively inhibit the development of OA
Kulsirirat et al. (2021a)	AG	PLGA-NPs			No mention	No mention	AG-NPs-PLGA can prolong the duration to improve the therapeutic efficacy
Xia et al. (2017)	COR	CM-HAMA	IL-1β, MMPs, ADAMTS5	Col.II, LC3, ACAN	No mention	In comparison with IL1-β–treated cartilage, cartilage that was simultaneously treated with IL1-β and COR exhibited more Safranin-O–positive proteoglycan	COR improves cartilage matrix degradation by inducing autophagy
Zhang (2017)	TMP	PLGA-Ms			No mention	The cartilage damage was improved in the treatment group compared to the untreated OA model; the cartilage layer recovered integrity and chondrocytes arranged in normal	IA injection of TMP microspheres can effectively relieve inflammatory symptoms
Jin et al. (2020a)	CSL	MSNs-Cs	IL-1β, IL-6, TNF-α, MMPs, NF-κB		A profoundly reduced knee swelling and improvement in synovial inflammation and cartilage integrity were demonstrated in the CSL@ HMSNs-CS group by MRI	A dramatic improvement in pathological changes, such as smooth cartilage surface, undulating tide line, and cartilage thickness was observed in the CSL@HMSNs-CS group	HMSNs-Cs can improve the solubility and bioavailability of CSL
Bairwa and Jachak, 2016	KBA	PLAG-NPs			No mention	No mention	The bioavailability and anti-inflammatory activity of KBA in KBA-NPs were increased

AG@MSNs-PAA, andrographolide-loaded mesoporous silica nanoparticles with pH-responsive PAA; PLGA, poly(lactic-co-glycolic acid); PLGA-NPs, PLGA nanoparticle–gelatin hydrogel; CM, chitosan microspheres; HAMA, HA methacrylate; PLGA-Ms, PLGA microspheres; MSNs-Cs, mesoporous silica nanoparticles-chitosan; PLAG-NPs, PLAG–polyvinyl alcohol nanoparticles; HMSNS-Cs, Hollow mesoporous silica nanoparticles capped with chitosan; CSL@HMSNs-CS, celastrol loaded HMSNS-Cs.

production of COL2 in the cartilage ECM, thus promoting the production of hyaline cartilage (instead of fibrocartilage) at the defect site, which is very beneficial to the recovery of normal joint function. In addition, a few BDEs, such as CUR, HON, and BBR, play an osteogenic role through OPG/RANKL and Wnt/β-catenin signaling pathways and promote the repair of subchondral bone defects, so they are more suitable for the injury of subchondral bone involved in late OA. At present, the clinical drugs used for OA treatment are mostly limited to symptomatic treatment to relieve joint pain and improve joint function. Comparatively, BDEs can not only improve the joint function and eliminate clinical symptoms but also promote the repair of damaged cartilage in multiple ways and targets, and delay the progress of OA.

Since the progression of OA is a long-term, chronic process, the patients need long-term administration. However, oral administration has poor bioavailability and long-term oral administration can cause some serious adverse reactions. On the contrary, local IA injection or drug carrier implantation greatly improves drug utilization and reduces systemic response. Compared with local injection of pure BDEs, the sustained-release effect of the biomaterial carrier can enhance the retention time of the drug in the joints and enable the drug to function stably for a long time. So how to choose IA injection or drug carrier implantation? The attributes of OA determine a long-term treatment and delaying the progress of OA is the focus of the current clinical treatment. In combination with the included studies, it is more appropriate to select IA injection of drug-carrying biomaterial carriers (hydrogels, nanoparticles, microspheres, etc.) when cartilage damage is not serious in the early and middle stages of OA. Because it is easier to perform than surgical treatment, long-term and repeated injection therapy is possible. For the damage involving subchondral bone in the late stage of OA, the drug carrier implantation is recommended. Compared with the current clinical knee replacement for patients with late OA, drug carrier implantation is theoretically more conducive to the recovery of joint function in patients without worrying about prosthetic wear.

TABLE 6 | A summary of key advancements in the field.

Category	Key advancements	References
Herbal monomer	CUR and RES are the most used herbal monomers in cartilage repair, and the optimal concentration of RES is 114.281 mol/L	Ming et al. (2018)
	Coencapsulated RES and CUR in lipomolecular nanocapsules, improved the photostability of RES and the *in vitro* antioxidant activity of both polyphenols	Coradini et al. (2015), Kann et al. (2016)
	CUR, BBR, and HON can not only protect cartilage but also promote the formation of subchondral bone	Chen et al. (2012), Yeh et al. (2015), Zhu et al. (2020)
	Both BRU and CLC have severe biotoxicity, pay attention to test its safety	Chen et al. (2012), Mohamed et al. (2020)
	Hes, SIN, and COR can induce autophagy *in vivo* to improve the degradation of the cartilage matrix	Chen (2015), Xia et al. (2017), Ouyang et al. (2019)
Carriers	GD2(CO3)3@PDA—a gadolinium (III) (Gd3+) containing MRI contrast agent coated with PDA, a good drug carrier for the targeted delivery of OA drugs to lesion sites	Ouyang et al. (2019)
	Prepared a high porosity 3D scaffold based on cellular responsive polymer ink SA and gelatin (SA-gel, 1:3)	Kankala et al. (2018)
	The use of PLA can enhance the bioabsorbability and drug carrying capacity of nanoparticles	Kamel et al. (2019)
	Microfluidic drug screening device can effectively screen the drug concentration required for cell culture	Ming et al. (2018)
	The thermosensitive composite hydrogel prepared with chitosan as temperature-sensitive material can change the distribution of drugs in the joint cavity, increase the concentration of drugs in the joint cavity, and delay the retention of drugs in the target region	Chen et al. (2012)
	PAE can be used to achieve controlled drug release at low PH, and the positively charged PAE can interact with the GAG in the cartilage by electrostatic interaction to achieve targeted drug delivery	Kang (2019)
	AG@MSNs-PAA nanoplatform formed by modified MSNs and pH-responsive PAA is favorable for sustained release in the OA environment	Jin (2020), He et al. (2021)

PDA, polydopamine; AG@MSNs-PAA, andrographolide-loaded mesoporous silica nanoparticles with pH-responsive PAA.

However, long-term repeated injections tend to cause local infection and reduce patient compliance. Therefore, the optimal injection cycle, dose, and times of IA injection need further study and confirmation. It is worth noting that IA injection means that the injection has certain fluidity, so how to improve its biological response, targeting, and mechanical properties is a problem that researchers need to further explore. In addition, because of the irregularity of cartilage damage, the degradability of drug carrier, the biomechanical characteristics of local knee joints, and the different structures of cartilage layers in OA patients, the structural distribution of each layer, the optimal degradation rate, the compatibility and adhesion between the carriers and surrounding tissues need further research during stent fabrication.

It is found in the included studies that almost all researchers chose chondrocytes rather than MSCs in the selection of seed cells. However, many studies have confirmed that MSCs as seed cells are more suitable for cartilage repair. Then, whether BDEs can promote or induce the differentiation of MSCs into chondrocytes and the related mechanism of action are also questions worthy of consideration. In addition, because the mechanism of action of most BDEs (some having certain toxicity) has not been fully understood yet, the rejection reaction of the body, as well as the changes in the biological environment, chemical stimulation, and microenvironment in the damaged area, researchers need to further study and confirm the selection and manufacture of materials; the selection, dose, concentration, etc. of BDEs. At present, all *in vivo* animal studies have confirmed the effectiveness and safety of BDEs combined with biomaterial carriers, but there is no related clinical experiment to further verify their effectiveness and safety. Therefore, more relevant studies are needed to address the current problems.

AUTHOR CONTRIBUTIONS

PM and YH confirmed the review direction; PM and JF consulted and screened relevant literature, and XM, FX, and LT assisted in data extraction; PM completed the design of manuscript writing, pictures, tables, etc.; YH put forward suggestions on the revision of the manuscript and confirmed the final draft.

FUNDING

The research is funded by Sichuan Provincial Administration of Traditional Chinese Medicine, with the project number 2021MS454, and the special fund for 100 Talents Program of the First Affiliated Hospital of Chengdu University of TCM, with the project number 20-Y14.

ACKNOWLEDGMENTS

The authors thank all participants for their help during the writing of the article and thank the central administration of Sichuan Province and the Affiliated Hospital of Chengdu University of Traditional Chinese Medicine for their financial support.

SUPPLEMENTARY MATERIAL

The Supplementary Material for this article can be found online at: https://www.frontiersin.org/articles/10.3389/fphar.2021.789311/full#supplementary-material

REFERENCES

Abdulbaqi, I. M., Darwis, Y., Assi, R. A., and Khan, N. A. K. (2018). Transethosomal Gels as Carriers for the Transdermal Delivery of Colchicine: Statistical Optimization, Characterization, and *Ex Vivo* Evaluation. *Drug Des. Devel Ther.* 12, 795–813. doi:10.2147/DDDT.S158018

Abed, É., Delalandre, A., and Lajeunesse, D. (2017). Beneficial Effect of Resveratrol on Phenotypic Features and Activity of Osteoarthritic Osteoblasts. *Arthritis Res. Ther.* 19 (1), 151. doi:10.1186/s13075-017-1365-2

Abramson, S. B. (2008). Osteoarthritis and Nitric Oxide. *Osteoarthritis Cartilage* 16 Suppl 2, S15–S20. doi:10.1016/S1063-4584(08)60008-4

Aggarwal, B. B., Gupta, S. C., and Sung, B. (2013). Curcumin: an Orally Bioavailable Blocker of TNF and Other Pro-inflammatory Biomarkers. *Br. J. Pharmacol.* 169 (8), 1672–1692. doi:10.1111/bph.12131

Ahmed, S., Rahman, A., Hasnain, A., Lalonde, M., Goldberg, V. M., and Haqqi, T. M. (2002). Green tea Polyphenol Epigallocatechin-3-Gallate Inhibits the IL-1 Beta-Induced Activity and Expression of Cyclooxygenase-2 and Nitric Oxide Synthase-2 in Human Chondrocytes. *Free Radic. Biol. Med.* 33 (8), 1097–1105. doi:10.1016/s0891-5849(02)01004-3

Akhtar, N., and Haqqi, T. M. (2011). Epigallocatechin-3-gallate Suppresses the Global Interleukin-1beta-Induced Inflammatory Response in Human Chondrocytes. *Arthritis Res. Ther.* 13 (3), R93. doi:10.1186/ar3368

Ammon, H. P. (2010). Modulation of the Immune System by Boswellia Serrata Extracts and Boswellic Acids. *Phytomedicine* 17 (11), 862–867. doi:10.1016/j.phymed.2010.03.003

Amorndoljai, P., Taneepanichskul, S., Niempoog, S., and Nimmannit, U. (2015). Improving of Knee Osteoarthritic Symptom by the Local Application of Ginger Extract Nanoparticles: A Preliminary Report with Short Term Follow-Up. *J. Med. Assoc. Thai* 98 (9), 871–877.

Anand, P., Kunnumakkara, A. B., Newman, R. A., and Aggarwal, B. B. (2007). Bioavailability of Curcumin: Problems and Promises. *Mol. Pharm.* 4 (6), 807–818. doi:10.1021/mp700113r

Andres, S., Pevny, S., Ziegenhagen, R., Bakhiya, N., Schäfer, B., Hirsch-Ernst, K. I., et al. (2018). Safety Aspects of the Use of Quercetin as a Dietary Supplement. *Mol. Nutr. Food Res.* 62 (1). doi:10.1002/mnfr.201700447

Ashraf, S., Radhi, M., Gowler, P., Burston, J. J., Gandhi, R. D., Thorn, G. J., et al. (2019). The Polyadenylation Inhibitor Cordycepin Reduces Pain, Inflammation and Joint Pathology in Rodent Models of Osteoarthritis. *Sci. Rep.* 9 (1), 4696. doi:10.1038/s41598-019-41140-1

Bae, S. C., Jung, W. J., Lee, E. J., Yu, R., and Sung, M. K. (2009). Effects of Antioxidant Supplements Intervention on the Level of Plasma Inflammatory Molecules and Disease Severity of Rheumatoid Arthritis Patients. *J. Am. Coll. Nutr.* 28 (1), 56–62. doi:10.1080/07315724.2009.10719762

Bairwa, K., and Jachak, S. M. (2016). Nanoparticle Formulation of 11-Keto-β-Boswellic Acid (KBA): Anti-inflammatory Activity and *In Vivo* Pharmacokinetics. *Pharm. Biol.* 54 (12), 2909–2916. doi:10.1080/13880209.2016.1194437

Bannuru, R. R., Osani, M. C., Al-Eid, F., and Wang, C. (2018). Efficacy of Curcumin and Boswellia for Knee Osteoarthritis: Systematic Review and Meta-Analysis. *Semin. Arthritis Rheum.* 48 (3), 416–429. doi:10.1016/j.semarthrit.2018.03.001

Bannuru, R. R., Osani, M. C., Vaysbrot, E. E., Arden, N. K., Bennell, K., Bierma-Zeinstra, S. M. A., et al. (2019). OARSI Guidelines for the Non-surgical Management of Knee, Hip, and Polyarticular Osteoarthritis. *Osteoarthritis Cartilage* 27 (11), 1578–1589. doi:10.1016/j.joca.2019.06.011

Bartels, E. M., Folmer, V. N., Bliddal, H., Altman, R. D., Juhl, C., Tarp, S., et al. (2015). Efficacy and Safety of Ginger in Osteoarthritis Patients: a Meta-Analysis of Randomized Placebo-Controlled Trials. *Osteoarthritis Cartilage* 23 (1), 13–21. doi:10.1016/j.joca.2014.09.024

Belcaro, G., Cesarone, M. R., Dugall, M., Pellegrini, L., Ledda, A., Grossi, M. G., et al. (2010). Efficacy and Safety of Meriva®, a Curcumin-Phosphatidylcholine Complex, during Extended Administration in Osteoarthritis Patients. *Altern. Med. Rev.* 15 (4), 337–344.

Belwal, T., Bisht, A., Devkota, H. P., Ullah, H., Khan, H., Pandey, A., et al. (2020). Phytopharmacology and Clinical Updates of Berberis Species against Diabetes and Other Metabolic Diseases. *Front. Pharmacol.* 11, 41. doi:10.3389/fphar.2020.00041

Berenbaum, F., Grifka, J., Cazzaniga, S., D'Amato, M., Giacovelli, G., Chevalier, X., et al. (2012). A Randomised, Double-Blind, Controlled Trial Comparing Two Intra-articular Hyaluronic Acid Preparations Differing by Their Molecular Weight in Symptomatic Knee Osteoarthritis. *Ann. Rheum. Dis.* 71 (9), 1454–1460. doi:10.1136/annrheumdis-2011-200972

Blanco, F. J., Rego, I., and Ruiz-Romero, C. (2011). The Role of Mitochondria in Osteoarthritis. *Nat. Rev. Rheumatol.* 7 (3), 161–169. doi:10.1038/nrrheum.2010.213

Bliddal, H., Rosetzsky, A., Schlichting, P., Weidner, M. S., Andersen, L. A., Ibfelt, H. H., et al. (2000). A Randomized, Placebo-Controlled, Cross-Over Study of Ginger Extracts and Ibuprofen in Osteoarthritis. *Osteoarthritis Cartilage* 8 (1), 9–12. doi:10.1053/joca.1999.0264

Britti, D., Crupi, R., Impellizzeri, D., Gugliandolo, E., Fusco, R., Schievano, C., et al. (2017). A Novel Composite Formulation of Palmitoylethanolamide and Quercetin Decreases Inflammation and Relieves Pain in Inflammatory and Osteoarthritic Pain Models. *BMC Vet. Res.* 13 (1), 229. doi:10.1186/s12917-017-1151-z

Bugbee, W. D., Pallante-Kichura, A. L., Görtz, S., Amiel, D., and Sah, R. (2016). Osteochondral Allograft Transplantation in Cartilage Repair: Graft Storage Paradigm, Translational Models, and Clinical Applications. *J. Orthop. Res.* 34 (1), 31–38. doi:10.1002/jor.22998

Buhrmann, C., Honarvar, A., Setayeshmehr, M., Karbasi, S., Shakibaei, M., and Valiani, A. (2020). Herbal Remedies as Potential in Cartilage Tissue Engineering: An Overview of New Therapeutic Approaches and Strategies. *Molecules* 25 (13). doi:10.3390/molecules25133075

Burgos, R. A., Alarcón, P., Quiroga, J., Manosalva, C., and Hancke, J. (2020). Andrographolide, an Anti-inflammatory Multitarget Drug: All Roads Lead to Cellular Metabolism. *Molecules* 26 (1). doi:10.3390/molecules26010005

Burt, H. M., Tsallas, A., Gilchrist, S., and Liang, L. S. (2009). Intra-articular Drug Delivery Systems: Overcoming the Shortcomings of Joint Disease Therapy. *Expert Opin. Drug Deliv.* 6 (1), 17–26. doi:10.1517/17425240802647259

Cameron, M., and Chrubasik, S. (2014). Oral Herbal Therapies for Treating Osteoarthritis. *Cochrane Database Syst. Rev.* 5 (5), Cd002947. doi:10.1002/14651858.CD002947.pub2

Charlier, E., Deroyer, C., Ciregia, F., Malaise, O., Neuville, S., Plener, Z., et al. (2019). Chondrocyte Dedifferentiation and Osteoarthritis (OA). *Biochem. Pharmacol.* 165, 49–65. doi:10.1016/j.bcp.2019.02.036

Chen, B., Zhan, H., Marszalek, J., Chung, M., Lin, X., Zhang, M., et al. (2016a). Traditional Chinese Medications for Knee Osteoarthritis Pain: A Meta-Analysis of Randomized Controlled Trials. *Am. J. Chin. Med.* 44 (4), 677–703. doi:10.1142/S0192415X16500373

Chen, P., Xia, C., Mei, S., Wang, J., Shan, Z., Lin, X., et al. (2016b). Intra-articular Delivery of Sinomenium Encapsulated by Chitosan Microspheres and Photo-Crosslinked GelMA Hydrogel Ameliorates Osteoarthritis by Effectively Regulating Autophagy. *Biomaterials* 81, 1–13. doi:10.1016/j.biomaterials.2015.12.006

Chen, W., Chen, S., Morsi, Y., El-Hamshary, H., El-Newhy, M., Fan, C., et al. (2016c). Superabsorbent 3D Scaffold Based on Electrospun Nanofibers for Cartilage Tissue Engineering. *ACS Appl. Mater. Interfaces* 8 (37), 24415–25415.

Chen, W., Ma, J., Zhu, L., Morsi, Y., Ei-Hamshary, H., Al-Deyab, S. S., et al. (2016d). Superelastic, Superabsorbent and 3D Nanofiber-Assembled Scaffold for Tissue Engineering. *Colloids Surf B Biointerfaces* 142, 165–172.

Chen, L., Liu, J., Guan, M., Zhou, T., Duan, X., and Xiang, Z. (2020). Growth Factor and its Polymer Scaffold-Based Delivery System for Cartilage Tissue Engineering. *Int. J. Nanomedicine* 15, 6097–6111. doi:10.2147/IJN.S249829

Chen, L., Liu, T., Wang, Q., and Liu, J. (2017). Anti-inflammatory Effect of Combined Tetramethylpyrazine, Resveratrol and Curcumin *In Vivo*. *BMC Complement. Altern. Med.* 17 (1), 233. doi:10.1186/s12906-017-1739-7

Chen, P., Xia, C., Mo, J., Mei, S., Lin, X., and Fan, S. (2018). Interpenetrating Polymer Network Scaffold of Sodium Hyaluronate and Sodium Alginate Combined with Berberine for Osteochondral Defect Regeneration. *Mater. Sci. Eng. C Mater. Biol. Appl.* 91, 190–200. doi:10.1016/j.msec.2018.05.034

Chen, S., Luo, Z., and Chen, X. (2020). Andrographolide Mitigates Cartilage Damage via miR-27-3p-Modulated Matrix Metalloproteinase13 Repression. *J. Gene Med.* 22 (8), e3187. doi:10.1002/jgm.3187

Chen, Y. J., Tsai, K. S., Chan, D. C., Lan, K. C., Chen, C. F., Yang, R. S., et al. (2014). Honokiol, a Low Molecular Weight Natural Product, Prevents Inflammatory

Response and Cartilage Matrix Degradation in Human Osteoarthritis Chondrocytes. *J. Orthop. Res.* 32 (4), 573–580. doi:10.1002/jor.22577

Chen, Z. P., Liu, W., Liu, D., Xiao, Y. Y., Chen, H. X., Chen, J., et al. (2012). Development of Brucine-Loaded Microsphere/thermally Responsive Hydrogel Combination System for Intra-articular Administration. *J. Control. Release* 162 (3), 628–635. doi:10.1016/j.jconrel.2012.07.037

Chin, K. Y. (2016). The Spice for Joint Inflammation: Anti-inflammatory Role of Curcumin in Treating Osteoarthritis. *Drug Des. Devel Ther.* 10, 3029–3042. doi:10.2147/DDDT.S117432

Coradini, K., Friedrich, R. B., Fonseca, F. N., Vencato, M. S., Andrade, D. F., Oliveira, C. M., et al. (2015). A Novel Approach to Arthritis Treatment Based on Resveratrol and Curcumin Co-encapsulated in Lipid-Core Nanocapsules: *In Vivo* Studies. *Eur. J. Pharm. Sci.* 78, 163–170. doi:10.1016/j.ejps.2015.07.012

Crivelli, B., Bari, E., Perteghella, S., Catenacci, L., Sorrenti, M., Mocchi, M., et al. (2019). Silk Fibroin Nanoparticles for Celecoxib and Curcumin Delivery: ROS-Scavenging and Anti-inflammatory Activities in an *In Vitro* Model of Osteoarthritis. *Eur. J. Pharm. Biopharm.* 137, 37–45. doi:10.1016/j.ejpb.2019.02.008

Das, S. K., Mishra, K., Ramakrishnan, S., Srivastava, R., Agarwal, G. G., Singh, R., et al. (2002). A Randomized Controlled Trial to Evaluate the Slow-Acting Symptom Modifying Effects of a Regimen Containing Colchicine in a Subset of Patients with Osteoarthritis of the Knee. *Osteoarthritis Cartilage* 10 (4), 247–252. doi:10.1053/joca.2002.0516

Di Martino, A., Silva, S., Andriolo, L., Merli, G., Reale, D., Zaffagnini, S., et al. (2021). Osteochondral Autograft Transplantation versus Autologous Bone-Cartilage Paste Grafting for the Treatment of Knee Osteochondritis Dissecans. *Int. Orthop.* 45 (2), 453–461. doi:10.1007/s00264-020-04804-6

Ding, Q. H., Ji, X. W., Cheng, Y., Yu, Y. Q., Qi, Y. Y., and Wang, X. H. (2013). Inhibition of Matrix Metalloproteinases and Inducible Nitric Oxide Synthase by Andrographolide in Human Osteoarthritic Chondrocytes. *Mod. Rheumatol.* 23 (6), 1124–1132. doi:10.1007/s10165-012-0807-6

Efferth, T., and Oesch, F. (2020). Anti-inflammatory and Anti-cancer Activities of Frankincense: Targets, Treatments and Toxicities. *Semin. Cancer Biol.* doi:10.1016/j.semcancer.2020.01.015

Elmali, N., Baysal, O., Harma, A., Esenkaya, I., and Mizrak, B. (2007). Effects of Resveratrol in Inflammatory Arthritis. *Inflammation* 30 (1-2), 1–6. doi:10.1007/s10753-006-9012-0

Evans, T. I., Wheeler, M. T., Small, R. E., Breitbach, S. A., Sanders, K. M., and Roberts, W. N. (1996). A Comprehensive Investigation of Inpatient Intravenous Colchicine Use Shows More Education Is Needed. *J. Rheumatol.* 23 (1), 143–148.

Feng, K., Chen, H., and Xu, C. (2020). Chondro-protective Effects of Celastrol on Osteoarthritis through Autophagy Activation and NF-Kb Signaling Pathway Inhibition. *Inflamm. Res.* 69 (4), 385–400. doi:10.1007/s00011-020-01327-z

Feng, K., Chen, Z., Pengcheng, L., Zhang, S., and Wang, X. (2019). Quercetin Attenuates Oxidative Stress-Induced Apoptosis via SIRT1/AMPK-Mediated Inhibition of ER Stress in Rat Chondrocytes and Prevents the Progression of Osteoarthritis in a Rat Model. *J. Cel Physiol* 234 (10), 18192–18205. doi:10.1002/jcp.28452

Feng, K., Ge, Y., Chen, Z., Li, X., Liu, Z., Li, X., et al. (2019). Curcumin Inhibits the PERK-eIF2α-CHOP Pathway through Promoting SIRT1 Expression in Oxidative Stress-Induced Rat Chondrocytes and Ameliorates Osteoarthritis Progression in a Rat Model. *Oxid Med. Cel Longev* 2019, 8574386. doi:10.1155/2019/8574386

Frehner, F., and Benthien, J. P. (2018). Microfracture: State of the Art in Cartilage Surgery? *Cartilage* 9 (4), 339–345. doi:10.1177/1947603517700956

Gao, L., Lin, Y., Wang, S., Lin, L., Lu, D., Zhao, Y., et al. (2021). Chronotoxicity of Semen Strychni Is Associated with Circadian Metabolism and Transport in Mice. *J. Pharm. Pharmacol.* 73 (3), 398–409. doi:10.1093/jpp/rgaa007

Goldring, S. R., and Goldring, M. B. (2016). Changes in the Osteochondral Unit during Osteoarthritis: Structure, Function and Cartilage-Bone Crosstalk. *Nat. Rev. Rheumatol.* 12 (11), 632–644. doi:10.1038/nrrheum.2016.148

Gong, Y., and Gluud, C. (2004). Colchicine for Primary Biliary Cirrhosis. *Cochrane Database Syst. Rev.* (2), Cd004481. doi:10.1002/14651858.CD004481.pub2

Grover, A. K., and Samson, S. E. (2016). Benefits of Antioxidant Supplements for Knee Osteoarthritis: Rationale and Reality. *Nutr. J.* 15, 1. doi:10.1186/s12937-015-0115-z

Gu, H., Jiao, Y., Yu, X., Li, X., Wang, W., Ding, L., et al. (2017). Resveratrol Inhibits the IL-1β-induced Expression of MMP-13 and IL-6 in Human Articular Chondrocytes via TLR4/MyD88-dependent and -independent Signaling Cascades. *Int. J. Mol. Med.* 39 (3), 734–740. doi:10.3892/ijmm.2017.2885

Gupte, P. A., Giramkar, S. A., Harke, S. M., Kulkarni, S. K., Deshmukh, A. P., Hingorani, L. L., et al. (2019). Evaluation of the Efficacy and Safety of Capsule Longvida® Optimized Curcumin (Solid Lipid Curcumin Particles) in Knee Osteoarthritis: a Pilot Clinical Study. *J. Inflamm. Res.* 12, 145–152. doi:10.2147/JIR.S205390

Hancke, J. L., Srivastav, S., Cáceres, D. D., and Burgos, R. A. (2019). A Double-Blind, Randomized, Placebo-Controlled Study to Assess the Efficacy of Andrographis Paniculata Standardized Extract (ParActin®) on Pain Reduction in Subjects with Knee Osteoarthritis. *Phytother Res.* 33 (5), 1469–1479. doi:10.1002/ptr.6339

Hasanzadeh, S., Read, M. I., Bland, A. R., Majeed, M., Jamialahmadi, T., and Sahebkar, A. (2020). Curcumin: an Inflammasome Silencer. *Pharmacol. Res.* 159, 104921. doi:10.1016/j.phrs.2020.104921

He, M., Qin, Z., Liang, X., He, X., Zhu, B., Lu, Z., et al. (2021). A pH-Responsive Mesoporous Silica Nanoparticles-Based Drug Delivery System with Controlled Release of Andrographolide for OA Treatment. *Regen. Biomater.* 8 (4), rbab020. doi:10.1093/rb/rbab020

Heinecke, L. F., Grzanna, M. W., Au, A. Y., Mochal, C. A., Rashmir-Raven, A., and Frondoza, C. G. (2010). Inhibition of Cyclooxygenase-2 Expression and Prostaglandin E2 Production in Chondrocytes by Avocado Soybean Unsaponifiables and Epigallocatechin Gallate. *Osteoarthritis Cartilage* 18 (2), 220–227. doi:10.1016/j.joca.2009.08.015

Henrotin, Y., Malaise, M., Wittoek, R., de Vlam, K., Brasseur, J. P., Luyten, F. P., et al. (2019). Bio-optimized Curcuma Longa Extract Is Efficient on Knee Osteoarthritis Pain: a Double-Blind Multicenter Randomized Placebo Controlled Three-Arm Study. *Arthritis Res. Ther.* 21 (1), 179. doi:10.1186/s13075-019-1960-5

Hosseinzadeh, A., Bahrampour Juybari, K., Fatemi, M. J., Kamarul, T., Bagheri, A., Tekiyehmaroof, N., et al. (2017). Protective Effect of Ginger (Zingiber Officinale Roscoe) Extract against Oxidative Stress and Mitochondrial Apoptosis Induced by Interleukin-1β in Cultured Chondrocytes. *Cells Tissues Organs* 204 (5-6), 241–250. doi:10.1159/000479789

Hu, P., Chen, W., Bao, J., Jiang, L., and Wu, L. (2014). Cordycepin Modulates Inflammatory and Catabolic Gene Expression in Interleukin-1beta-Induced Human Chondrocytes from Advanced-Stage Osteoarthritis: an *In Vitro* Study. *Int. J. Clin. Exp. Pathol.* 7 (10), 6575–6584.

Hu, P. F., Chen, W. P., Tang, J. L., Bao, J. P., and Wu, L. D. (2011). Protective Effects of Berberine in an Experimental Rat Osteoarthritis Model. *Phytother Res.* 25 (6), 878–885. doi:10.1002/ptr.3359

Hu, Y., Gui, Z., Zhou, Y., Xia, L., Lin, K., and Xu, Y. (2019). Quercetin Alleviates Rat Osteoarthritis by Inhibiting Inflammation and Apoptosis of Chondrocytes, Modulating Synovial Macrophages Polarization to M2 Macrophages. *Free Radic. Biol. Med.* 145, 146–160. doi:10.1016/j.freeradbiomed.2019.09.024

Hussain, S. A., Marouf, B. H., Ali, Z. S., and Ahmmad, R. S. (2018). Efficacy and Safety of Co-administration of Resveratrol with Meloxicam in Patients with Knee Osteoarthritis: a Pilot Interventional Study. *Clin. Interv. Aging* 13, 1621–1630. doi:10.2147/CIA.S172758

Javadi, F., Eghtesadi, S., Ahmadzadeh, A., Aryaeian, N., Zabihiyeganeh, M., Foroushani, A. R., et al. (2014). The Effect of Quercetin on Plasma Oxidative Status, C-Reactive Protein and Blood Pressure in Women with Rheumatoid Arthritis. *Int. J. Prev. Med.* 5 (3), 293–301.

Jhang, J. J., Lu, C. C., and Yen, G. C. (2016). Epigallocatechin Gallate Inhibits Urate Crystals-Induced Peritoneal Inflammation in C57BL/6 Mice. *Mol. Nutr. Food Res.* 60 (10), 2297–2303. doi:10.1002/mnfr.201600106

Ji, L., Li, W., Qian, W., Feng, S., Shi, H., Wang, Y., et al. (2021). The Role of Nanoparticles-Mediated Ligustrazine in the Treatment of Knee Osteoarthritis and its Effect on Matrix Metalloproteinases and Upstream NF-Kb Signaling Pathway in Knee Osteoarthritis. *J. Nanosci Nanotechnol* 21 (2), 1372–1377. doi:10.1166/jnn.2021.18647

Jiang, W., Fan, W., Gao, T., Li, T., Yin, Z., Guo, H., et al. (2020). Analgesic Mechanism of Sinomenine against Chronic Pain. *Pain Res. Manag.* 2020, 1876862. doi:10.1155/2020/1876862

Jin, G. Z. (2020). Current Nanoparticle-Based Technologies for Osteoarthritis Therapy. *Nanomaterials (Basel)* 10 (12). doi:10.3390/nano10122368

Jin, T., Wu, D., Liu, X. M., Xu, J. T., Ma, B. J., Ji, Y., et al. (2020). Intra-articular Delivery of Celastrol by Hollow Mesoporous Silica Nanoparticles for pH-Sensitive Anti-inflammatory Therapy against Knee Osteoarthritis. *J. Nanobiotechnology* 18 (1), 94. doi:10.1186/s12951-020-00651-0

Jin, Y., Koh, R. H., Kim, S. H., Kim, K. M., Park, G. K., and Hwang, N. S. (2020). Injectable Anti-inflammatory Hyaluronic Acid Hydrogel for Osteoarthritic Cartilage Repair. *Mater. Sci. Eng. C Mater. Biol. Appl.* 115, 111096. doi:10.1016/j.msec.2020.111096

Jones, I. A., Togashi, R., Wilson, M. L., Heckmann, N., and Vangsness, C. T., Jr (2019). Intra-articular Treatment Options for Knee Osteoarthritis. *Nat. Rev. Rheumatol.* 15 (2), 77–90. doi:10.1038/s41584-018-0123-4

Ju, X. D., Deng, M., Ao, Y. F., Yu, C. L., Wang, J. Q., Yu, J. K., et al. (2010). The Protective Effect of Tetramethylpyrazine on Cartilage Explants and Chondrocytes. *J. Ethnopharmacol* 132 (2), 414–420. doi:10.1016/j.jep.2010.08.020

Kamel, R., Abbas, H., and Shaffie, N. M. (2019). Development and Evaluation of PLA-Coated Co-micellar Nanosystem of Resveratrol for the Intra-articular Treatment of Arthritis. *Int. J. Pharm.* 569, 118560. doi:10.1016/j.ijpharm.2019.118560

Kang, C., Jung, E., Hyeon, H., Seon, S., and Lee, D. (2020). Acid-activatable Polymeric Curcumin Nanoparticles as Therapeutic Agents for Osteoarthritis. *Nanomedicine* 23, 102104. doi:10.1016/j.nano.2019.102104

Kankala, R. K., Lu, F. J., Liu, C. G., Zhang, S. S., Chen, A. Z., and Wang, S. B. (2018). Effect of Icariin on Engineered 3D-Printed Porous Scaffolds for Cartilage Repair. *Materials (Basel)* 11 (8). doi:10.3390/ma11081390

Kann, B., Spengler, C., Coradini, K., Rigo, L. A., Bennink, M. L., Jacobs, K., et al. (2016). Intracellular Delivery of Poorly Soluble Polyphenols: Elucidating the Interplay of Self-Assembling Nanocarriers and Human Chondrocytes. *Anal. Chem.* 88 (14), 7014–7022. doi:10.1021/acs.analchem.6b00199

Kanzaki, N., Saito, K., Maeda, A., Kitagawa, Y., Kiso, Y., Watanabe, K., et al. (2012). Effect of a Dietary Supplement Containing Glucosamine Hydrochloride, Chondroitin Sulfate and Quercetin Glycosides on Symptomatic Knee Osteoarthritis: a Randomized, Double-Blind, Placebo-Controlled Study. *J. Sci. Food Agric.* 92 (4), 862–869. doi:10.1002/jsfa.4660

Kershenobich, D., Vargas, F., Garcia-Tsao, G., Perez Tamayo, R., Gent, M., and Rojkind, M. (1988). Colchicine in the Treatment of Cirrhosis of the Liver. *N. Engl. J. Med.* 318 (26), 1709–1713. doi:10.1056/NEJM198806303182602

Khan, M. A., and Tania, M. (2020). Cordycepin in Anticancer Research: Molecular Mechanism of Therapeutic Effects. *Curr. Med. Chem.* 27 (6), 983–996. doi:10.2174/0929867325666181001105749

Khayyal, M. T., El-Hazek, R. M., El-Sabbagh, W. A., Frank, J., Behnam, D., and Abdel-Tawab, M. (2018). Micellar Solubilisation Enhances the Antiinflammatory Activities of Curcumin and Boswellic Acids in Rats with Adjuvant-Induced Arthritis. *Nutrition* 54, 189–196. doi:10.1016/j.nut.2018.03.055

Kim, H. A., and Blanco, F. J. (2007). Cell Death and Apoptosis in Osteoarthritic Cartilage. *Curr. Drug Targets* 8 (2), 333–345. doi:10.2174/138945007779940025

Kim, K. R., Park, K. K., Chun, K. S., and Chung, W. Y. (2010). Honokiol Inhibits the Progression of Collagen-Induced Arthritis by Reducing Levels of Pro-inflammatory Cytokines and Matrix Metalloproteinases and Blocking Oxidative Tissue Damage. *J. Pharmacol. Sci.* 114 (1), 69–78. doi:10.1254/jphs.10070fp

Knieper, A. M., Klotsche, J., Lainka, E., Berger, T., Dressler, F., Jansson, A. F., et al. (2017). Familial Mediterranean Fever in Children and Adolescents: Factors for Colchicine Dosage and Predicting Parameters for Dose Increase. *Rheumatology (Oxford)* 56 (9), 1597–1606. doi:10.1093/rheumatology/kex222

Kotha, A., Sekharam, M., Cilenti, L., Siddiquee, K., Khaled, A., Zervos, A. S., et al. (2006). Resveratrol Inhibits Src and Stat3 Signaling and Induces the Apoptosis of Malignant Cells Containing Activated Stat3 Protein. *Mol. Cancer Ther.* 5 (3), 621–629. doi:10.1158/1535-7163.MCT-05-0268

Kulsirirat, T., Honsawek, S., Takeda-Morishita, M., Sinchaipanid, N., Udomsinprasert, W., Leanpolchareanchai, J., et al. (2021). The Effects of Andrographolide on the Enhancement of Chondrogenesis and Osteogenesis in Human Suprapatellar Fat Pad Derived Mesenchymal Stem Cells. *Molecules* 26 (7). doi:10.3390/molecules26071831

Kulsirirat, T., Sathirakul, K., Kamei, N., and Takeda-Morishita, M. (2021). The *In Vitro* and *In Vivo* Study of Novel Formulation of Andrographolide PLGA Nanoparticle Embedded into Gelatin-Based Hydrogel to Prolong Delivery and Extend Residence Time in Joint. *Int. J. Pharm.* 602, 120618. doi:10.1016/j.ijpharm.2021.120618

Kuptniratsaikul, V., Dajpratham, P., Taechaarpornkul, W., Buntragulpoontawee, M., Lukkanapichonchut, P., Chootip, C., et al. (2014). Efficacy and Safety of Curcuma Domestica Extracts Compared with Ibuprofen in Patients with Knee Osteoarthritis: a Multicenter Study. *Clin. Interv. Aging* 9, 451–458. doi:10.2147/CIA.S58535

Leach, M. J., and Kumar, S. (2008). The Clinical Effectiveness of Ginger (Zingiber Officinale) in Adults with Osteoarthritis. *JBI Libr. Syst. Rev.* 6 (8), 310–323. doi:10.11124/01938924-200806080-00001

Lecanda, F., Avioli, L. V., and Cheng, S. L. (1997). Regulation of Bone Matrix Protein Expression and Induction of Differentiation of Human Osteoblasts and Human Bone Marrow Stromal Cells by Bone Morphogenetic Protein-2. *J. Cel Biochem* 67 (3), 386–396. doi:10.1002/(sici)1097-4644(19971201)67:3<386:aid-jcb10>3.0.co;2-b

Lee, S. W., Lee, H. J., Chung, W. T., Choi, S. M., Rhyu, S. H., Kim, D. K., et al. (2004). TRAIL Induces Apoptosis of Chondrocytes and Influences the Pathogenesis of Experimentally Induced Rat Osteoarthritis. *Arthritis Rheum.* 50 (2), 534–542. doi:10.1002/art.20052

Leong, D. J., Choudhury, M., Hanstein, R., Hirsh, D. M., Kim, S. J., Majeska, R. J., et al. (2014). Green tea Polyphenol Treatment Is Chondroprotective, Anti-inflammatory and Palliative in a Mouse post-traumatic Osteoarthritis Model. *Arthritis Res. Ther.* 16 (6), 508. doi:10.1186/s13075-014-0508-y

Letter, M. (1974). Letter: Gouty Arthritis and Colchicine. *N. Engl. J. Med.* 291 (13), 681–682. doi:10.1056/NEJM197409262911320

Leung, Y. Y., Haaland, B., Huebner, J. L., Wong, S. B. S., Tjai, M., Wang, C., et al. (2018). Colchicine Lack of Effectiveness in Symptom and Inflammation Modification in Knee Osteoarthritis (COLKOA): a Randomized Controlled Trial. *Osteoarthritis Cartilage* 26 (5), 631–640. doi:10.1016/j.joca.2018.01.026

Li, B., Jiang, T., Liu, H., Miao, Z., Fang, D., Zheng, L., et al. (2018). Andrographolide Protects Chondrocytes from Oxidative Stress Injury by Activation of the Keap1-Nrf2-Are Signaling Pathway. *J. Cel Physiol* 234 (1), 561–571. doi:10.1002/jcp.26769

Li, D., Yuan, T., Zhang, X., Xiao, Y., Wang, R., Fan, Y., et al. (2012). Icariin: a Potential Promoting Compound for Cartilage Tissue Engineering. *Osteoarthritis Cartilage* 20 (12), 1647–1656. doi:10.1016/j.joca.2012.08.009

Li, H., Zhuo, H., Yin, D., Li, W., Zhang, Y., Li, P., et al. (2021). Intra-Articular Injection of a Nanosuspension of Tetramethylpyrazine Dihydroxynaphthalenate for Stronger and Longer-Lasting Effects against Osteoarthritis. *J. Biomed. Nanotechnol* 17 (6), 1199–1207. doi:10.1166/jbn.2021.3094

Li, J., Shao, X., Wu, L., Feng, T., Jin, C., Fang, M., et al. (2011). Honokiol: an Effective Inhibitor of Tumor Necrosis Factor-α-Induced Up-Regulation of Inflammatory Cytokine and Chemokine Production in Human Synovial Fibroblasts. *Acta Biochim. Biophys. Sin (Shanghai)* 43 (5), 380–386. doi:10.1093/abbs/gmr027

Li, W., Cai, L., Zhang, Y., Cui, L., and Shen, G. (2015). Intra-articular Resveratrol Injection Prevents Osteoarthritis Progression in a Mouse Model by Activating SIRT1 and Thereby Silencing HIF-2α. *J. Orthop. Res.* 33 (7), 1061–1070. doi:10.1002/jor.22859

Li, Z., Cheng, J., and Liu, J. (2020). Baicalin Protects Human OA Chondrocytes against IL-1β-Induced Apoptosis and ECM Degradation by Activating Autophagy via MiR-766-3p/AIFM1 Axis. *Drug Des. Devel Ther.* 14, 2645–2655. doi:10.2147/DDDT.S255823

Lima, A. C., Ferreira, H., Reis, R. L., and Neves, N. M. (2019). Biodegradable Polymers: an Update on Drug Delivery in Bone and Cartilage Diseases. *Expert Opin. Drug Deliv.* 16 (8), 795–813. doi:10.1080/17425247.2019.1635117

Limagne, E., Lançon, A., Delmas, D., Cherkaoui-Malki, M., and Latruffe, N. (2016). Resveratrol Interferes with IL1-β-Induced Pro-inflammatory Paracrine Interaction between Primary Chondrocytes and Macrophages. *Nutrients* 8 (5). doi:10.3390/nu8050280

Lin, Z., Fu, C., Yan, Z., Wu, Y., Zhan, J., Lou, Z., et al. (2020). The Protective Effect of Hesperetin in Osteoarthritis: an *In Vitro* and *In Vivo* Study. *Food Funct.* 11 (3), 2654–2666. doi:10.1039/c9fo02552a

Liu, D., Tang, W., Zhang, H., Huang, H., Zhang, Z., Tang, D., et al. (2020). Icariin Protects Rabbit BMSCs against OGD-Induced Apoptosis by Inhibiting ERs-Mediated Autophagy via MAPK Signaling Pathway. *Life Sci.* 253, 117730. doi:10.1016/j.lfs.2020.117730

Liu, D. D., Zhang, B. L., Yang, J. B., and Zhou, K. (2020). Celastrol Ameliorates Endoplasmic Stress-Mediated Apoptosis of Osteoarthritis via Regulating ATF-6/CHOP Signalling Pathway. *J. Pharm. Pharmacol.* 72 (6), 826–835. doi:10.1111/jphp.13250

Liu, F., Wang, X., Han, X., Tan, X., and Kang, W. (2015). Cytotoxicity and DNA Interaction of Brucine and Strychnine-Two Alkaloids of Semen Strychni. *Int. J. Biol. Macromol* 77, 92–98. doi:10.1016/j.ijbiomac.2015.03.017

Liu, F. C., Hung, L. F., Wu, W. L., Chang, D. M., Huang, C. Y., Lai, J. H., et al. (2010). Chondroprotective Effects and Mechanisms of Resveratrol in Advanced Glycation End Products-Stimulated Chondrocytes. *Arthritis Res. Ther.* 12 (5), R167. doi:10.1186/ar3127

Liu, S. C., Lee, H. P., Hung, C. Y., Tsai, C. H., Li, T. M., and Tang, C. H. (2015). Berberine Attenuates CCN2-Induced IL-1β Expression and Prevents Cartilage Degradation in a Rat Model of Osteoarthritis. *Toxicol. Appl. Pharmacol.* 289 (1), 20–29. doi:10.1016/j.taap.2015.08.020

Liu, X., Machado, G. C., Eyles, J. P., Ravi, V., and Hunter, D. J. (2018). Dietary Supplements for Treating Osteoarthritis: a Systematic Review and Meta-Analysis. *Br. J. Sports Med.* 52 (3), 167–175. doi:10.1136/bjsports-2016-097333

Liu, Y., Mi, B., Lv, H., Liu, J., Xiong, Y., Hu, L., et al. (2018). Shared KEGG Pathways of Icariin-Targeted Genes and Osteoarthritis. *J. Cel Biochem.*

Lu, L., Hu, J., Wu, Q., An, Y., Cui, W., Wang, J., et al. (2019). Berberine Prevents Human Nucleus Pulposus Cells from IL-1β-induced E-xtracellular M-atrix D-egradation and A-poptosis by I-nhibiting the NF-κB P-athway. *Int. J. Mol. Med.* 43 (4), 1679–1686. doi:10.3892/ijmm.2019.4105

Lu, L., Huang, R., Wu, Y., Jin, J. M., Chen, H. Z., Zhang, L. J., et al. (2020). Brucine: A Review of Phytochemistry, Pharmacology, and Toxicology. *Front. Pharmacol.* 11, 377. doi:10.3389/fphar.2020.00377

Ma, D., Yu, T., Peng, L., Wang, L., Liao, Z., and Xu, W. (2019). PIM1, CYP1B1, and HSPA2 Targeted by Quercetin Play Important Roles in Osteoarthritis Treatment by Achyranthes Bidentata. *Evid. Based Complement. Alternat Med.* 2019, 1205942. doi:10.1155/2019/1205942

Madry, H., Grün, U. W., and Knutsen, G. (2011). Cartilage Repair and Joint Preservation: Medical and Surgical Treatment Options. *Dtsch Arztebl Int.* 108 (40), 669–677. doi:10.3238/arztebl.2011.0669

Makris, E. A., Gomoll, A. H., Malizos, K. N., Hu, J. C., and Athanasiou, K. A. (2015). Repair and Tissue Engineering Techniques for Articular Cartilage. *Nat. Rev. Rheumatol.* 11 (1), 21–34. doi:10.1038/nrrheum.2014.157

Marwah, H., Garg, T., Goyal, A. K., and Rath, G. (2016). Permeation Enhancer Strategies in Transdermal Drug Delivery. *Drug Deliv.* 23 (2), 564–578. doi:10.3109/10717544.2014.935532

Mi, B., Wang, J., Liu, Y., Liu, J., Hu, L., Panayi, A. C., et al. (2018). Icariin Activates Autophagy via Down-Regulation of the NF-Kb Signaling-Mediated Apoptosis in Chondrocytes. *Front. Pharmacol.* 9, 605. doi:10.3389/fphar.2018.00605

Miller, R. E., Tran, P. B., Ishihara, S., Larkin, J., and Malfait, A. M. (2016). Therapeutic Effects of an Anti-ADAMTS-5 Antibody on Joint Damage and Mechanical Allodynia in a Murine Model of Osteoarthritis. *Osteoarthritis Cartilage* 24 (2), 299–306. doi:10.1016/j.joca.2015.09.005

Ming, L., Zhipeng, Y., Fei, Y., Feng, R., Jian, W., Baoguo, J., et al. (2018). Microfluidic-based Screening of Resveratrol and Drug-Loading PLA/Gelatine Nano-Scaffold for the Repair of Cartilage Defect. *Artif. Cell Nanomed Biotechnol* 46 (Suppl. 1), 336–346. doi:10.1080/21691401.2017.1423498

Mishra, S., Verma, S. S., Rai, V., Awasthee, N., Chava, S., Hui, K. M., et al. (2019). Long Non-coding RNAs Are Emerging Targets of Phytochemicals for Cancer and Other Chronic Diseases. *Cell Mol Life Sci* 76 (10), 1947–1966. doi:10.1007/s00018-019-03053-0

Mistry, H., Connock, M., Pink, J., Shyangdan, D., Clar, C., Royle, P., et al. (2017). Autologous Chondrocyte Implantation in the Knee: Systematic Review and Economic Evaluation. *Health Technol. Assess.* 21 (6), 1–294. doi:10.3310/hta21060

Mohamed, A. L., Elmotasem, H., and Salama, A. A. A. (2020). Colchicine Mesoporous Silica Nanoparticles/hydrogel Composite Loaded Cotton Patches as a New Encapsulator System for Transdermal Osteoarthritis Management. *Int. J. Biol. Macromol* 164, 1149–1163. doi:10.1016/j.ijbiomac.2020.07.133

Mok, S. W., Fu, S. C., Cheuk, Y. C., Chu, I. M., Chan, K. M., Qin, L., et al. (2020). Intra-Articular Delivery of Quercetin Using Thermosensitive Hydrogel Attenuate Cartilage Degradation in an Osteoarthritis Rat Model. *Cartilage* 11 (4), 490–499. doi:10.1177/1947603518796550

Moon, P. D., Jeong, H. S., Chun, C. S., and Kim, H. M. (2011). Baekjeolyusin-tang and its Active Component Berberine Block the Release of Collagen and Proteoglycan from IL-1β-stimulated Rabbit Cartilage and Down-Regulate Matrix Metalloproteinases in Rabbit Chondrocytes. *Phytother Res.* 25 (6), 844–850. doi:10.1002/ptr.3353

Muhammad, T., Ikram, M., Ullah, R., Rehman, S. U., and Kim, M. O. (2019). Hesperetin, a Citrus Flavonoid, Attenuates LPS-Induced Neuroinflammation, Apoptosis and Memory Impairments by Modulating TLR4/NF-Kb Signaling. *Nutrients* 11 (3). doi:10.3390/nu11030648

Munroe, M. E., Arbiser, J. L., and Bishop, G. A. (2007). Honokiol, a Natural Plant Product, Inhibits Inflammatory Signals and Alleviates Inflammatory Arthritis. *J. Immunol.* 179 (2), 753–763. doi:10.4049/jimmunol.179.2.753

Murphy, C. A., Garg, A. K., Silva-Correia, J., Reis, R. L., Oliveira, J. M., and Collins, M. N. (2019). The Meniscus in Normal and Osteoarthritic Tissues: Facing the Structure Property Challenges and Current Treatment Trends. *Annu. Rev. Biomed. Eng.* 21, 495–521. doi:10.1146/annurev-bioeng-060418-052547

Musumeci, G., Castrogiovanni, P., Trovato, F. M., Weinberg, A. M., Al-Wasiyah, M. K., Alqahtani, M. H., et al. (2015). Biomarkers of Chondrocyte Apoptosis and Autophagy in Osteoarthritis. *Int. J. Mol. Sci.* 16 (9), 20560–20575. doi:10.3390/ijms160920560

Natarajan, V., Madhan, B., and Tiku, M. L. (2015). Intra-Articular Injections of Polyphenols Protect Articular Cartilage from Inflammation-Induced Degradation: Suggesting a Potential Role in Cartilage Therapeutics. *PLoS One* 10 (6), e0127165. doi:10.1371/journal.pone.0127165

Nava, F., Ghilotti, F., Maggi, L., Hatemi, G., Del Bianco, A., Merlo, C., et al. (2014). Biologics, Colchicine, Corticosteroids, Immunosuppressants and Interferon-Alpha for Neuro-Behçet's Syndrome. *Cochrane Database Syst. Rev.* (12), Cd010729. doi:10.1002/14651858.CD010729.pub2

Neag, M. A., Mocan, A., Echeverría, J., Pop, R. M., Bocsan, C. I., Crişan, G., et al. (2018). Berberine: Botanical Occurrence, Traditional Uses, Extraction Methods, and Relevance in Cardiovascular, Metabolic, Hepatic, and Renal Disorders. *Front. Pharmacol.* 9, 557. doi:10.3389/fphar.2018.00557

Oliveira Silva, M., Gregory, J. L., Ansari, N., and Stok, K. S. (2020). Molecular Signaling Interactions and Transport at the Osteochondral Interface: A Review. *Front Cel Dev Biol* 8, 750. doi:10.3389/fcell.2020.00750

Ouyang, Z., Tan, T., Liu, C., Duan, J., Wang, W., Guo, X., et al. (2019). Targeted Delivery of Hesperetin to Cartilage Attenuates Osteoarthritis by Bimodal Imaging with Gd2(CO3)3@PDA Nanoparticles via TLR-2/nf-κB/Akt Signaling. *Biomaterials* 205, 50–63. doi:10.1016/j.biomaterials.2019.03.018

Ownby, S. L., Fortuno, L. V., Au, A. Y., Grzanna, M. W., Rashmir-Raven, A. M., and Frondoza, C. G. (2014). Expression of Pro-inflammatory Mediators Is Inhibited by an Avocado/soybean Unsaponifiables and Epigallocatechin Gallate Combination. *J. Inflamm. (Lond)* 11 (1), 8. doi:10.1186/1476-9255-11-8

Oz, B., Yildirim, A., Yolbas, S., Celik, Z. B., Etem, E. O., Deniz, G., et al. (2019). Resveratrol Inhibits Src Tyrosine Kinase, STAT3, and Wnt Signaling Pathway in Collagen Induced Arthritis Model. *BioFactors* 45 (1), 69–74. doi:10.1002/biof.1463

Pan, L., Zhang, Y., Chen, N., and Yang, L. (2017). Icariin Regulates Cellular Functions and Gene Expression of Osteoarthritis Patient-Derived Human Fibroblast-like Synoviocytes. *Int. J. Mol. Sci.* 18 (12). doi:10.3390/ijms18122656

Panahi, Y., Rahimnia, A. R., Sharafi, M., Alishiri, G., Saburi, A., and Sahebkar, A. (2014). Curcuminoid Treatment for Knee Osteoarthritis: a Randomized Double-Blind Placebo-Controlled Trial. *Phytother Res.* 28 (11), 1625–1631. doi:10.1002/ptr.5174

Parhiz, H., Roohbakhsh, A., Soltani, F., Rezaee, R., and Iranshahi, M. (2015). Antioxidant and Anti-inflammatory Properties of the Citrus Flavonoids Hesperidin and Hesperetin: an Updated Review of Their Molecular Mechanisms and Experimental Models. *Phytother Res.* 29 (3), 323–331. doi:10.1002/ptr.5256

Park, K. R., Kim, J. Y., Kim, E. C., Yun, H. M., and Hong, J. T. (2017). RANKL-induced Osteoclastogenesis Is Suppressed by 4-O-Methylhonokiol in Bone Marrow-Derived Macrophages. *Arch. Pharm. Res.* 40 (8), 933–942. doi:10.1007/s12272-017-0932-z

Qin, L., He, Y., Zhao, X., Zhang, T., Qin, Y., and Du, A. (2020). Preparation, Characterization, and *In Vitro* Sustained Release Profile of Resveratrol-Loaded Silica Aerogel. *Molecules* 25 (12). doi:10.3390/molecules25122752

Qin, N., Wei, L., Li, W., Yang, W., Cai, L., Qian, Z., et al. (2017). Local Intra-articular Injection of Resveratrol Delays Cartilage Degeneration in C57BL/6 Mice by Inducing Autophagy via AMPK/mTOR Pathway. *J. Pharmacol. Sci.* 134 (3), 166–174. doi:10.1016/j.jphs.2017.06.002

Qiu, B., Xu, X., Yi, P., and Hao, Y. (2020). Curcumin Reinforces MSC-Derived Exosomes in Attenuating Osteoarthritis via Modulating the miR-124/nf-kB and miR-143/ROCK1/TLR9 Signalling Pathways. *J. Cel Mol Med* 24 (18), 10855–10865. doi:10.1111/jcmm.15714

Qiu, L., Luo, Y., and Chen, X. (2018). Quercetin Attenuates Mitochondrial Dysfunction and Biogenesis via Upregulated AMPK/SIRT1 Signaling Pathway in OA Rats. *Biomed. Pharmacother.* 103, 1585–1591. doi:10.1016/j.biopha.2018.05.003

Rahimi, M., Charmi, G., Matyjaszewski, K., Banquy, X., and Pietrasik, J. (2021). Recent Developments in Natural and Synthetic Polymeric Drug Delivery Systems Used for the Treatment of Osteoarthritis. *Acta Biomater.* 123, 31–50. doi:10.1016/j.actbio.2021.01.003

Rai, V., Dilisio, M. F., Dietz, N. E., and Agrawal, D. K. (2017). Recent Strategies in Cartilage Repair: A Systemic Review of the Scaffold Development and Tissue Engineering. *J. Biomed. Mater. Res. A.* 105 (8), 2343–2354. doi:10.1002/jbm.a.36087

Rambaldi, A., and Gluud, C. (2005). Colchicine for Alcoholic and Non-alcoholic Liver Fibrosis and Cirrhosis. *Cochrane Database Syst. Rev.* (2), Cd002148. doi:10.1002/14651858.CD002148.pub2

Rasheed, Z., Rasheed, N., and Al-Shobaili, H. A. (2016). Epigallocatechin-3-O-gallate Up-Regulates microRNA-199a-3p Expression by Down-Regulating the Expression of Cyclooxygenase-2 in Stimulated Human Osteoarthritis Chondrocytes. *J. Cel Mol Med* 20 (12), 2241–2248. doi:10.1111/jcmm.12897

Ratanavaraporn, J., Soontornvipart, K., Shuangshoti, S., Shuangshoti, S., and Damrongsakkul, S. (2017). Localized Delivery of Curcumin from Injectable Gelatin/Thai Silk Fibroin Microspheres for Anti-inflammatory Treatment of Osteoarthritis in a Rat Model. *Inflammopharmacology* 25 (2), 211–221. doi:10.1007/s10787-017-0318-3

Rondanelli, M., Riva, A., Allegrini, P., Faliva, M. A., Naso, M., Peroni, G., et al. (2020). The Use of a New Food-Grade Lecithin Formulation of Highly Standardized Ginger (Zingiber Officinale) and Acmella Oleracea Extracts for the Treatment of Pain and Inflammation in a Group of Subjects with Moderate Knee Osteoarthritis. *J. Pain Res.* 13, 761–770. doi:10.2147/JPR.S214488

Sheu, S. Y., Chen, W. S., Sun, J. S., Lin, F. H., and Wu, T. (2013). Biological Characterization of Oxidized Hyaluronic Acid/resveratrol Hydrogel for Cartilage Tissue Engineering. *J. Biomed. Mater. Res. A.* 101 (12), 3457–3466. doi:10.1002/jbm.a.34653

Shi, Y., Hu, X., Cheng, J., Zhang, X., Zhao, F., Shi, W., et al. (2019). A Small Molecule Promotes Cartilage Extracellular Matrix Generation and Inhibits Osteoarthritis Development. *Nat. Commun.* 10 (1), 1914. doi:10.1038/s41467-019-09839-x

Siard, M. H., McMurry, K. E., and Adams, A. A. (2016). Effects of Polyphenols Including Curcuminoids, Resveratrol, Quercetin, Pterostilbene, and Hydroxypterostilbene on Lymphocyte Pro-inflammatory Cytokine Production of Senior Horses *In Vitro*. *Vet. Immunol. Immunopathol* 173, 50–59. doi:10.1016/j.vetimm.2016.04.001

Singh, R., Ahmed, S., Malemud, C. J., Goldberg, V. M., and Haqqi, T. M. (2003). Epigallocatechin-3-gallate Selectively Inhibits Interleukin-1beta-Induced Activation of Mitogen Activated Protein Kinase Subgroup C-Jun N-Terminal Kinase in Human Osteoarthritis Chondrocytes. *J. Orthop. Res.* 21 (1), 102–109. doi:10.1016/S0736-0266(02)00089-X

Song, X., Zhang, Y., Dai, E., Du, H., and Wang, L. (2019). Mechanism of Action of Celastrol against Rheumatoid Arthritis: A Network Pharmacology Analysis. *Int. Immunopharmacol* 74, 105725. doi:10.1016/j.intimp.2019.105725

Sullivan, T. P., King, L. E., Jr., and Boyd, A. S. (1998). Colchicine in Dermatology. *J. Am. Acad. Dermatol.* 39 (6), 993–999. doi:10.1016/s0190-9622(98)70275-0

Tang, Y., Li, Y., Xin, D., Chen, L., Xiong, Z., and Yu, X. (2021). Icariin Alleviates Osteoarthritis by Regulating Autophagy of Chondrocytes by Mediating PI3K/AKT/mTOR Signaling. *Bioengineered* 12 (1), 2984–2999. doi:10.1080/21655979.2021.1943602

Tao, X. M., Liu, P. F., Gu, H. Y., Lian, D. B., Gao, L., Tao, W. W., et al. (2020). Cordycepin Alleviates Anterior Cruciate Ligament Transection (ACLT)-Induced Knee Osteoarthritis through Regulating TGF-β Activity and Autophagy. *Drug Des. Devel Ther.* 14, 2809–2817. doi:10.2147/DDDT.S251893

Tasneem, S., Liu, B., Li, B., Choudhary, M. I., and Wang, W. (2019). Molecular Pharmacology of Inflammation: Medicinal Plants as Anti-inflammatory Agents. *Pharmacol. Res.* 139, 126–140. doi:10.1016/j.phrs.2018.11.001

Theodoridis, K., Manthou, M. E., Aggelidou, E., and Kritis, A. (2021). *Vivo Cartilage Regeneration with Cell-Seeded Natural Biomaterial Scaffold Implants: 15-Year Study*. Chengdu, China: Tissue Eng Part B Rev.

Vinatier, C., and Guicheux, J. (2016). Cartilage Tissue Engineering: From Biomaterials and Stem Cells to Osteoarthritis Treatments. *Ann. Phys. Rehabil. Med.* 59 (3), 139–144. doi:10.1016/j.rehab.2016.03.002

Wang, D., Miller, S. C., Liu, X. M., Anderson, B., Wang, X. S., and Goldring, S. R. (2007). Novel Dexamethasone-HPMA Copolymer Conjugate and its Potential Application in Treatment of Rheumatoid Arthritis. *Arthritis Res. Ther.* 9 (1), R2. doi:10.1186/ar2106

Wang, J., Wang, X., Cao, Y., Huang, T., Song, D. X., and Tao, H. R. (2018). Therapeutic Potential of Hyaluronic Acid/chitosan Nanoparticles for the Delivery of Curcuminoid in Knee Osteoarthritis and an *In Vitro* Evaluation in Chondrocytes. *Int. J. Mol. Med.* 42 (5), 2604–2614. doi:10.3892/ijmm.2018.3817

Wang, M., Sampson, E. R., Jin, H., Li, J., Ke, Q. H., Im, H. J., et al. (2013). MMP13 Is a Critical Target Gene during the Progression of Osteoarthritis. *Arthritis Res. Ther.* 15 (1), R5. doi:10.1186/ar4133

Wang, P., Meng, Q., Wang, W., Zhang, S., Xiong, X., Qin, S., et al. (2020). Icariin Inhibits the Inflammation through Down-Regulating NF-Kb/hif-2α Signal Pathways in Chondrocytes. *Biosci. Rep.* 40 (11). doi:10.1042/BSR20203107

Wang, Q., Ye, C., Sun, S., Li, R., Shi, X., Wang, S., et al. (2019). Curcumin Attenuates Collagen-Induced Rat Arthritis via Anti-inflammatory and Apoptotic Effects. *Int. Immunopharmacol* 72, 292–300. doi:10.1016/j.intimp.2019.04.027

Wang, R., Li, J., Xu, X., Xu, J., Jiang, H., Lv, Z., et al. (2021). Andrographolide Attenuates Synovial Inflammation of Osteoarthritis by Interacting with Tumor Necrosis Factor Receptor 2 Trafficking in a Rat Model. *J. Orthop. Translat* 29, 89–99. doi:10.1016/j.jot.2021.05.001

Wang, Z., Singh, A., Jones, G., Winzenberg, T., Ding, C., Chopra, A., et al. (2021). Efficacy and Safety of Turmeric Extracts for the Treatment of Knee Osteoarthritis: a Systematic Review and Meta-Analysis of Randomised Controlled Trials. *Curr. Rheumatol. Rep.* 23 (2), 11. doi:10.1007/s11926-020-00975-8

Wang, Z. M., Chen, Y. C., and Wang, D. P. (2016). Resveratrol, a Natural Antioxidant, Protects Monosodium Iodoacetate-Induced Osteoarthritic Pain in Rats. *Biomed. Pharmacother.* 83, 763–770. doi:10.1016/j.biopha.2016.06.050

Wei, B., Zhang, Y., Tang, L., Ji, Y., Yan, C., and Zhang, X. (2019). Protective Effects of Quercetin against Inflammation and Oxidative Stress in a Rabbit Model of Knee Osteoarthritis. *Drug Dev. Res.* 80 (3), 360–367. doi:10.1002/ddr.21510

Wei, Y., Liu, J., Zhang, H., Du, X., Luo, Q., Sun, J., et al. (2016). Ligustrazine Attenuates Inflammation and the Associated Chemokines and Receptors in Ovalbumine-Induced Mouse Asthma Model. *Environ. Toxicol. Pharmacol.* 46, 55–61. doi:10.1016/j.etap.2016.07.005

Wildemann, B., Kadow-Romacker, A., Haas, N. P., and Schmidmaier, G. (2007). Quantification of Various Growth Factors in Different Demineralized Bone Matrix Preparations. *J. Biomed. Mater. Res. A.* 81 (2), 437–442. doi:10.1002/jbm.a.31085

Wong, S. K., Chin, K. Y., and Ima-Nirwana, S. (2020). Berberine and Musculoskeletal Disorders: The Therapeutic Potential and Underlying Molecular Mechanisms. *Phytomedicine* 73, 152892. doi:10.1016/j.phymed.2019.152892

Wu, H., Yin, Z., Wang, L., Li, F., and Qiu, Y. (2017). Honokiol Improved Chondrogenesis and Suppressed Inflammation in Human Umbilical Cord Derived Mesenchymal Stem Cells via Blocking Nuclear Factor-Kb Pathway. *BMC Cel Biol* 18 (1), 29. doi:10.1186/s12860-017-0145-9

Wu, P., Liang, Q., Feng, P., Li, C., Yang, C., Liang, H., et al. (2017). A Novel Brucine Gel Transdermal Delivery System Designed for Anti-inflammatory and Analgesic Activities. *Int. J. Mol. Sci.* 18 (4). doi:10.3390/ijms18040757

Wu, Y., Lin, Z., Yan, Z., Wang, Z., Fu, X., and Yu, K. (2019). Sinomenine Contributes to the Inhibition of the Inflammatory Response and the Improvement of Osteoarthritis in Mouse-Cartilage Cells by Acting on the Nrf2/HO-1 and NF-Kb Signaling Pathways. *Int. Immunopharmacol* 75, 105715. doi:10.1016/j.intimp.2019.105715

Wu, Y., Lin, Z., Yan, Z., Wang, Z., Fu, X., and Yu, K. (2019). Sinomenine Contributes to the Inhibition of the Inflammatory Response and the

Improvement of Osteoarthritis in Mouse-Cartilage Cells by Acting on the Nrf2/HO-1 and NF-Kb Signaling Pathways. *Int. Immunopharmacol* 75, 105715. doi:10.1016/j.intimp.2019.105715

Xia, B., Di Chen, C., Zhang, J., Hu, S., Jin, H., and Tong, P. (2014). Osteoarthritis Pathogenesis: a Review of Molecular Mechanisms. *Calcif Tissue Int.* 95 (6), 495–505. doi:10.1007/s00223-014-9917-9

Xia, C., Chen, P., Mei, S., Ning, L., Lei, C., Wang, J., et al. (2017). Photo-crosslinked HAMA Hydrogel with Cordycepin Encapsulated Chitosan Microspheres for Osteoarthritis Treatment. *Oncotarget* 8 (2), 2835–2849. doi:10.18632/oncotarget.13748

Xinqiang, S., Yu, Z., Ningning, Y., Erqin, D., Lei, W., and Hongtao, D. (2020). Molecular Mechanism of Celastrol in the Treatment of Systemic Lupus Erythematosus Based on Network Pharmacology and Molecular Docking Technology. *Life Sci.* 240, 117063. doi:10.1016/j.lfs.2019.117063

Xu, B., Ye, J., Yuan, F. Z., Zhang, J. Y., Chen, Y. R., Fan, B. S., et al. (2020). Advances of Stem Cell-Laden Hydrogels with Biomimetic Microenvironment for Osteochondral Repair. *Front. Bioeng. Biotechnol.* 8, 247. doi:10.3389/fbioe.2020.00247

Yang, G., Chang, C. C., Yang, Y., Yuan, L., Xu, L., Ho, C. T., et al. (2018). Resveratrol Alleviates Rheumatoid Arthritis via Reducing ROS and Inflammation, Inhibiting MAPK Signaling Pathways, and Suppressing Angiogenesis. *J. Agric. Food Chem.* 66 (49), 12953–12960. doi:10.1021/acs.jafc.8b05047

Yang, K. Y., Lin, L. C., Tseng, T. Y., Wang, S. C., and Tsai, T. H. (2007). Oral Bioavailability of Curcumin in Rat and the Herbal Analysis from Curcuma Longa by LC-MS/MS. *J. Chromatogr. B Analyt Technol. Biomed. Life Sci.* 853 (1-2), 183–189. doi:10.1016/j.jchromb.2007.03.010

Yeh, C. C., Su, Y. H., Lin, Y. J., Chen, P. J., Shi, C. S., Chen, C. N., et al. (2015). Evaluation of the Protective Effects of Curcuminoid (Curcumin and Bisdemethoxycurcumin)-Loaded Liposomes against Bone Turnover in a Cell-Based Model of Osteoarthritis. *Drug Des. Devel Ther.* 9, 2285–2300. doi:10.2147/DDDT.S78277

Yeung, A. W. K., Aggarwal, B. B., Orhan, I. E., Barreca, D., Battino, M., Belwal, T., et al. (2019). Resveratrol, a Popular Dietary Supplement for Human and Animal Health: Quantitative Research Literature Analysis - a Review. *Anim. Sci. Pap. Rep.* 37 (2), 103–118.

Yeung, A. W. K., Choudhary, N., Tewari, D., El-Demerdash, A., Horbanczuk, O. K., Das, N., et al. (2021). Quercetin: Total-Scale Literature Landscape Analysis of a Valuable Nutraceutical with Numerous Potential Applications in the Promotion of Human and Animal Health - a Review. *Anim. Sci. Pap. Rep.* 39 (3), 199–212.

Yin, W., Wang, T. S., Yin, F. Z., and Cai, B. C. (2003). Analgesic and Anti-inflammatory Properties of Brucine and Brucine N-Oxide Extracted from Seeds of Strychnos Nux-Vomica. *J. Ethnopharmacol* 88 (2-3), 205–214. doi:10.1016/s0378-8741(03)00224-1

Ying, X., Peng, L., Chen, H., Shen, Y., Yu, K., and Cheng, S. (2014). Cordycepin Prevented IL-β-induced Expression of Inflammatory Mediators in Human Osteoarthritis Chondrocytes. *Int. Orthop.* 38 (7), 1519–1526. doi:10.1007/s00264-013-2219-4

Yuce, P., Hosgor, H., Rencber, S. F., and Yazir, Y. (2021). Effects of Intra-articular Resveratrol Injections on Cartilage Destruction and Synovial Inflammation in Experimental Temporomandibular Joint Osteoarthritis. *J. Oral Maxillofac. Surg.* 79 (2), 344–e12. doi:10.1016/j.joms.2020.09.015

Zeng, L., Yu, G., Hao, W., Yang, K., and Chen, H. (2021). The Efficacy and Safety of Curcuma Longa Extract and Curcumin Supplements on Osteoarthritis: a Systematic Review and Meta-Analysis. *Biosci. Rep.* 41 (6). doi:10.1042/BSR20210817

Zhang, X., Shi, Y., Zhang, Z., Yang, Z., and Huang, G. (2018). Intra-articular Delivery of Tetramethylpyrazine Microspheres with Enhanced Articular Cavity Retention for Treating Osteoarthritis. *Asian J. Pharm. Sci.* 13 (3), 229–238. doi:10.1016/j.ajps.2017.12.007

Zhang, Z., Leong, D. J., Xu, L., He, Z., Wang, A., Navati, M., et al. (2016). Curcumin Slows Osteoarthritis Progression and Relieves Osteoarthritis-Associated Pain Symptoms in a post-traumatic Osteoarthritis Mouse Model. *Arthritis Res. Ther.* 18 (1), 128. doi:10.1186/s13075-016-1025-y

Zhao, H., Zhang, T., Xia, C., Shi, L., Wang, S., Zheng, X., et al. (2014). Berberine Ameliorates Cartilage Degeneration in Interleukin-1β-Stimulated Rat Chondrocytes and in a Rat Model of Osteoarthritis via Akt Signalling. *J. Cel Mol Med* 18 (2), 283–292. doi:10.1111/jcmm.12186

Zhao, X. X., Peng, C., Zhang, H., and Qin, L. P. (2012). Sinomenium Acutum: a Review of Chemistry, Pharmacology, Pharmacokinetics, and Clinical Use. *Pharm. Biol.* 50 (8), 1053–1061. doi:10.3109/13880209.2012.656847

Zheng, Y., Xiao, L., Yu, C., Jin, P., Qin, D., Xu, Y., et al. (2019). Enhanced Antiarthritic Efficacy by Nanoparticles of (-)-Epigallocatechin Gallate-Glucosamine-Casein. *J. Agric. Food Chem.* 67 (23), 6476–6486. doi:10.1021/acs.jafc.9b02075

Zhou, K., Hu, L., Liao, W., Yin, D., and Rui, F. (2016). Coptisine Prevented IL-β-Induced Expression of Inflammatory Mediators in Chondrocytes. *Inflammation* 39 (4), 1558–1565. doi:10.1007/s10753-016-0391-6

Zhou, Y., Liu, S., Ming, J., Li, Y., Deng, M., and He, B. (2017). Sustained Release Effects of Berberine-Loaded Chitosan Microspheres on *In Vitro* Chondrocyte Culture. *Drug Dev. Ind. Pharm.* 43 (10), 1703–1714. doi:10.1080/03639045.2017.1339076

Zhou, Y., Liu, S. Q., Yu, L., He, B., Wu, S. H., Zhao, Q., et al. (2015). Berberine Prevents Nitric Oxide-Induced Rat Chondrocyte Apoptosis and Cartilage Degeneration in a Rat Osteoarthritis Model via AMPK and P38 MAPK Signaling. *Apoptosis* 20 (9), 1187–1199. doi:10.1007/s10495-015-1152-y

Zhou, Y., Tao, H., Li, Y., Deng, M., He, B., Xia, S., et al. (2016). Berberine Promotes Proliferation of Sodium Nitroprusside-Stimulated Rat Chondrocytes and Osteoarthritic Rat Cartilage via Wnt/β-Catenin Pathway. *Eur. J. Pharmacol.* 789, 109–118. doi:10.1016/j.ejphar.2016.07.027

Zhou, Y., Liu, S.-q., Peng, H., Yu, L., He, B., and Zhao, Q. (2015). *In Vivo* anti-apoptosis Activity of Novel Berberine-Loaded Chitosan Nanoparticles Effectively Ameliorates Osteoarthritis. *Int. Immunopharmacology* 28 (1), 34–43. doi:10.1016/j.intimp.2015.05.014

Zhu, S., Chen, P., Chen, Y., Li, M., Chen, C., and Lu, H. (2020). 3D-Printed Extracellular Matrix/Polyethylene Glycol Diacrylate Hydrogel Incorporating the Anti-inflammatory Phytomolecule Honokiol for Regeneration of Osteochondral Defects. *Am. J. Sports Med.* 48 (11), 2808–2818. doi:10.1177/0363546520941842

Zuo, S., Zou, W., Wu, R. M., Yang, J., Fan, J. N., Zhao, X. K., et al. (2019). Icariin Alleviates IL-1β-Induced Matrix Degradation by Activating the Nrf2/ARE Pathway in Human Chondrocytes. *Drug Des. Devel Ther.* 13, 3949–3961. doi:10.2147/DDDT.S203094

Conflict of Interest: The authors declare that the research was conducted in the absence of any commercial or financial relationships that could be construed as a potential conflict of interest.

Publisher's Note: All claims expressed in this article are solely those of the authors and do not necessarily represent those of their affiliated organizations, or those of the publisher, the editors, and the reviewers. Any product that may be evaluated in this article, or claim that may be made by its manufacturer, is not guaranteed or endorsed by the publisher.

Copyright © 2022 Mu, Feng, Hu, Xiong, Ma and Tian. This is an open-access article distributed under the terms of the Creative Commons Attribution License (CC BY). The use, distribution or reproduction in other forums is permitted, provided the original author(s) and the copyright owner(s) are credited and that the original publication in this journal is cited, in accordance with accepted academic practice. No use, distribution or reproduction is permitted which does not comply with these terms.

frontiers in Pharmacology

ORIGINAL RESEARCH
published: 04 February 2022
doi: 10.3389/fphar.2021.772944

Eucommia, Cuscuta, and Drynaria Extracts Ameliorate Glucocorticoid-Induced Osteoporosis by Inhibiting Osteoclastogenesis Through PI3K/Akt Pathway

Junwen Han[1†], Li Li[2†], Chen Zhang[3], Qianqian Huang[4], Shanglong Wang[2], Wenyu Li[2], Jiancheng Zong[2], Lijie Li[5], Zhen Zhao[6], Zengliang Zhang[7], Zimin Liu[2], Qi Wang[8]* and Yuanyuan Shi[9]**

[1]College of Traditional Chinese Medicine, Beijing University of Chinese Medicine, Beijing, China, [2]Chenland Nutritionals, Inc., Irvine, CA, United States, [3]School of Life Sciences, Beijing University of Chinese Medicine, Beijing, China, [4]Beijing University of Chinese Medicine Affiliated Third Hospital, Beijing, China, [5]Qingdao Engineering Vocational College Dongzhang Community, Qingdao, China, [6]Pathology and Laboratory Medicine, Weill Cornell Medical College, New York, NY, United States, [7]Traditional Chinese Medicine College, Inner Mongolia Medicine University, Hohhot, China, [8]National Institute of Chinese Constitution and Preventive Medicine, Beijing, China, [9]Shenzhen Research Institute, Beijing University of Chinese Medicine, Shenzhen, China

Osteoporosis is one of the most common diseases in the world which resulted in heavy socioeconomic burden and a public health threat. Glucocorticoid-induced osteoporosis (GIO) is the most common secondary reason of osteoporosis. Therapeutic strategies using traditional Chinese medicine are under investigation for osteoporosis, with efforts to improve efficacy and clarify the mechanism. The combination of Eucommia, Cuscuta, and Drynaria is widely used in traditional Chinese decoction for osteoporosis treatment, but the experimental efficacy and mechanism are still unclear. Administration of E.C.D. extracts (Eucommia, Cuscuta, and Drynaria) in experimental GIO rats resulted in decreased urinal calcium, phosphorus loss, and decreased expression of RANKL, CTX in serum, increased serum calcium, phosphorus, and OPG level. E.C.D. extracts also improved bone density, structural integrity, and biomechanical function in experimental GIO rats. These finding were associated with E.C.D. extracts' treatment efficacy to GIO *in vivo*. The balance between osteoclast and osteoblast activity is essential for bone remodeling and bone related disease. The E.C.D. extracts inhibited Raw 264.7 cell differentiation to osteoclast *in vitro*. On the other hand, it promoted OPG expression of bone marrow mesenchymal stromal cells (MSCs) which can suppress the osteoclast genesis. E.C.D. extracts also increased the Wnt1 and Runx2 expression which are related to osteoblast formation. It also regulated the paracrine effect of MSC to inhibit osteoclast differentiation. The analysis of HPLC and comprehensive pharmacology identified the constituents of E.C.D. extracts and the potential osteoporosis-related targets mediated by E.C.D. extracts. The KEGG enrichment analysis suggested that PI3K/Akt pathway may be involved in the regulation osteoclast genesis by E.C.D. extracts and the result of Western blot of *vitro* assays proved it. Collectively, these data demonstrate E.C.D. extracts can inhibit osteoclast differentiation to foster experimental osteoporosis both *in vivo* and *in vitro* and it may exert the function of inhibiting osteoclast differentiation through PI3K/Akt pathway.

Keywords: Eucommia, Cuscuta, Drynaria, Traditional Chinese medicine, Osteoporosis, Osteoclast, PI3K/Akt

OPEN ACCESS

Edited by:
Longhuo Wu,
Gannan Medical University, China

Reviewed by:
Xuqiang Liu,
The First Affiliated Hospital of Nanchang University, China
Lianjie Shi,
Peking University, China
Yu-Mi Yang,
Yonsei University, South Korea

****Correspondence:***
Zimin Liu
dliu@chenland.com
Qi Wang
wangqi710@126.com
Yuanyuan Shi
yshi@bucm.edu.cn

[†]These authors have contributed equally to this work and share first authorship

Specialty section:
This article was submitted to Ethnopharmacology, a section of the journal Frontiers in Pharmacology

Received: *09 September 2021*
Accepted: *23 December 2021*
Published: *04 February 2022*

Citation:
Han J, Li L, Zhang C, Huang Q, Wang S, Li W, Zong J, Li L, Zhao Z, Zhang Z, Liu Z, Wang Q and Shi Y (2022) Eucommia, Cuscuta, and Drynaria Extracts Ameliorate Glucocorticoid-Induced Osteoporosis by Inhibiting Osteoclastogenesis Through PI3K/Akt Pathway. Front. Pharmacol. 12:772944. doi: 10.3389/fphar.2021.772944

INTRODUCTION

Bone remodeling is a dynamic process in which activated osteoclasts resorb bone and osteoblasts generate a bone matrix that undergoes mineralization (Sözen et al., 2017). This biological process repairs micro-damages that develop in bone during daily activity and protects skeletal strength (Sambrook and Cooper, 2006). When the balance of bone remodeling is disrupted, bone resorption is greater than bone formation, resulting in osteoporosis. Glucocorticoids (GC) are widely used in clinic, but they also bring serious side effects, one of which is glucocorticoid-induced osteoporosis (GIO) (Long, 2020). GIO is the most common secondary reason of osteoporosis. Fractures could occur in as many as 30–50% of patients who have received chronic glucocorticoid therapy (Canalis et al., 2007). The direct mechanism of GIO is upregulating PPARγR2 and RANKL expression and decreasing OPG expression, which results in bone resorption (Compston, 2018).

As more mechanisms of osteoporosis were discovered and novel techniques had been developed to help better understand about the micro-structure of bone, there are several effective therapies for osteoporosis treatment including bisphosphonates, elective estrogen, and RANKL inhibitor such as denosumab (Khosla and Hofbauer, 2017; Choksi et al., 2018), as well as teriparatide (Chotiyarnwong and McCloskey, 2020). Despite multiple therapies having been applied to clinical treatment, there are still high fracture risks and side effects of patients who have osteoporosis (Khosla and Hofbauer, 2017). The side effects and long-term effects of the novel drugs drive the development of new therapy.

The structure of bone is made of three parts: cells (osteocytes, osteoblasts, and osteoclasts), organic components (matrix proteins), and nonorganic components (calcium and hydroxyapatite) (Buehring et al., 2013). Bone's metabolism balance largely depends on the activity of osteoclast and osteoblast. Osteoclast origins from hematopoietic mononuclear cell while osteoblast origins from bone marrow mesenchymal stromal cell (MSC) (Chen et al., 2016; Andrzejewska et al., 2019). The classic pathway published before is RANKL/OPG pathway which regulates osteoclast differentiation and osteoblast genesis (Silva and Branco, 2011; Tobeiha et al., 2020). However, the upstream targets and other proteins are gradually discovered playing important roles in bone metabolism (Armas and Recker, 2012). The phosphatidylinositol 3-kinase (PI3K)/Akt signaling pathway regulates a broad range of biological processes including cell proliferation, growth, and anti-apoptosis (Ersahin et al., 2015). PI3K/Akt signaling pathway also has been shown to regulate osteoclast differentiation (Yeon et al., 2019; Cui et al., 2020). However, the downstream proteins which can be regulated by PI3K/Akt are abundant and not clearly clarified. Thus, to find the specific pathway that regulates the bone metabolism is important.

Eucommia, Cuscuta, and Drynaria (E.C.D.) are widely used as a combination and play a synergy in traditional Chinese medicine (TCM) decoction for osteoporosis treatment (Jia et al., 2012; He et al., 2019). The combination of E.C.D. is an important component in many decoctions and prescriptions in orthopedics such as Zhuang Jin Xu Gu Dan (<Shang Ke Da Cheng>, Qing Dynasty), Tu Si Zi Wan, etc. The combination of E.C.D. is also published to treat weakness of the feet and knees (Sang Shurong, 1993). <Zheng Zhi Zhun Sheng • Yang Yi> (Volume 2, Ming Dynasty) records the Drynaria pill using the combination of E.C.D. to treat flaccidity and arthralgia. <Bai Yi Xuan Fang> (Song Dynasty) use the combination of Eucommia and Cuscuta to treat low back pain. For bio-pharmacology study, Eucommia extracts were published to alleviate osteoporosis in rats and regulate osteoblast differentiation through the Shp2/PI3K/Akt pathway (Zhou et al., 2016). Mo H. et al. reported Cuscuta can modulate RANKL/OPG (Mo et al., 2019). Drynaria was proved to suppress the RANKL signal to inhibit osteoclast differentiation (Lin et al., 2013). The combination of E.C.D. has been developed as an adjunct to dietary supplements for treating osteoporosis (EuBone, Batch No.BH201-20201013-01, Product code: T-4005-1). It is also applying for a patent of novel formula to promote bone repair (patent application number: 2020105750230). Even though there is a lot of evidence of therapeutic application of the combination of E.C.D. in osteoporosis treatment, the efficacy of the combination of E.C.D. in experimental models and the further mechanism are still not clearly clarified. Thus, we proposed that E.C.D. extracts can alleviate experimental osteoporosis by regulating bone metabolism balance.

MATERIALS AND METHODS

Preparation of E.C.D. Extracts

Eucommia (*Eucommia ulmoides Oliv.*) was purchased from Anhui Zhiliang Traditional Chinese Medicine Decoction Pieces Co., LTD. Cuscuta (*Cuscuta chinensis Lam*) and Drynaria (*Davallia trichomanoides Blume*) were purchased from Bozhou Traditional Chinese Medicine Commodity Trading Center Co., LTD. Raw medicinal materials were identified by HPLC according to the method developed by Alkemist Las IDTSOP-72-01 in the U.S (**Supplementary Figure S1**). The E.C.D. extracts were made from ground Eucommia, Cuscuta, and Drynaria at a ratio of 6:1:3 (the ratio is based on the calculation of pharmacopoeia recommended dosage and extracts rate) into powder and sieved through a 20-mesh sieve. The extraction process of counter-current extraction (CCE) was based on a previous publication (He et al., 2017). Briefly, 5 L of 95% ethanol was added to 500 g of dried powder. Then, the mixture was extracted twice at room temperature (each time was 60 min). The extract was then filtered and condensed under vacuum, and then further dried using a freeze-dryer. For *vitro* delivery, E.C.D. extracts were dissolved in DMSO solution (100 mg/ml) and sonicated for 1 h in room temperature then centrifuged 3,000 rpm for 10 min. The supernatant was taken and diluted in DMEM medium in different doses for further experiment.

Animals

A total of 40 2-month-old female Wistar rats, weight 200 ± 20 g, were used in the present study. Rats were housed in room temperature (25°C) with 60% humidity and a 12-h light/dark cycle in the Laboratory Animal Department (4 rats per cage). After adaptation for 1 week, rats were randomly divided into five groups (n = 8 per group). The rats in the Vehicle group received saline intramuscular injection twice/week and saline by gavage 7 days/week. Other rats were proceeded of prednisolone hydride (4.5 mg/kg) intramuscular injection twice/week to induce GIO. After GC administration rats received either saline (GC group) or E.C.D. extracts of 90 mg/kg/day (E.C.D.-L group), or E.C.D. extracts of 135 mg/kg/day (E.C.D.-M group), or E.C.D. extracts of 180 mg/kg/day (E.C.D.-H group) by gavage for 7 day/week. The body weight and temperature of each rat was measured every week. 8 weeks later, rats were placed in a metabolic cage to collect overnight urine. The 24-h urine of rat was centrifuged at 3,500 rpm/min 4oC for 15 min, the supernatant was separated, and stored in a −80°C refrigerator for further test. The rats were then scarified, and the blood was collected from each rat. Collected blood was centrifuged at 2,000 rpm for 20 min to collect serum. Femurs of two sides were also collected and filled in saline and stored at −20°C for measurement of bone mineral content (BMC), bone mineral density (BMD), trabecular microarchitecture by micro-CT, and bone biomechanical quality by a three-point bending test.

Cytokine Analysis of Serum and Urine

Serum calcium and phosphorus concentration were measured by Siemens ADVIA 2400 blood biochemical analyzer. Urine calcium and phosphorus concentration were analyzed by standard colorimetric methods using commercial kits (ZhongSheng BeiKong Biotechnology and Science, PRC) and analyzed by a Cobas Integra 400 Plus automatic biochemical analyzer (Roche Diagnostics, Switzerland). Serum Osteocalcin, CTX, OPG, and RANKL concentration were determined using rat ELISA kit (R&D, United States; for details, see **Supplementary Table S2**).

Histology and H&E Staining

Rats were sacrificed 8 weeks following GC or saline administration. After a biomechanical test, the right femur was processed in 10% EDTA for bone demineralization of 8 weeks. The EDTA decalcified liquid was replaced every 3 days. Then the bone was fixed in 10% formalin, processed, embedded in paraffin, and sectioned (5 μm). Bone sections were assessed by hematoxylin and eosin (H&E) stain (abcam, Catalog number: ab245880) following the company's manuscript. The TRAP staining was performed using a Trap Stain Kit (Servicebio, Catalog number: G1050). The images were observed by Olympus BX51 light microscopy (Olympus, Japan).

Biomechanical Testing

The attached muscle and connective tissue of the right femur were removed. The right femur then was subjected to the 3-point bending test using a Lloyd material testing machine (LR5K; J.J. Lloyd Instruments, Southampton, United Kingdom). The femora specimens were placed on their lateral surface on the two supports of the bending apparatus. The bending load was applied at a rate of 1.0 mm/s (span 15 mm, transverse distance 2–3 mm) on the midpoint of the femora diaphysis until failure of the bone specimen. The breaking strength indexes including maximal load (Fmax) and elastic load (Fp) were measured.

Microtomographic Histomorphometry by Micro-CT

The left femur was thoroughly dissected from soft tissue and then was fixed with 4% paraformaldehyde for 24 h, and subsequently washed with 10% saccharose solution. A total of 12 h later, microtomography of the proximal femur was performed by micro-CT camera scanner (Bruker, Skyscan1174). Three-dimensional images of each proximal femur were acquired with a voxel size of 10.34 μm in all spatial directions. A cone-beam-type desktop micro-CT system was used to quantify structural parameters of the femur. The analytical conditions were 80 kV with 800 μA, and the spatial resolution was 14 μm according to the protocol of largetube-14 μm-150 min-SS for about 500 consecutives sections. For all femurs, a cylinder region of interest (ROI, diameter 3 mm × height 4 mm) was chosen to reconstruct three-dimensional images using Micview software. After thresholding, trabecular thickness (Tb.Th), trabecular number (Tb.N), trabecular separation (Tb.Sp), bone volume/total volume (BV/TV), structural model index (SMI), and bone mineral density (BMD) were determined.

Liquid Chromatography Mass Spectrometry Analysis

We performed HPLC analyses for the identification of chemical fingerprints presented in E.C.D. extracts. Briefly, the E.C.D. extracts were dissolved in methanol (1 g/ml) and then sonicated for 1 h. The extracts-methanol mixture was centrifuged at 12,000 rpm for 10 min and supernatant was taken and then diluted 1:10 with methanol. The sample was ready for HPLC analysis.

The Dionex Ultimate 3000 U. UPLC system was made up of LTQ-Orbitrap XL (Thermo Fisher Scientific, San Jose, CA) controlled by Xcalibur software (Version 2.1), a binary pump, an autosampler, a solvent degasser, and a thermostatic column compartment (Thermo Fisher Scientific, United States) were used for analysis component of CuraUltrad. Mass spectrometer (MS) detection was performed on a Q Exactive™ Plus mass spectrometer (Thermo Fisher Scientific, United States) equipped with an electrospray ionization source (ESI).

All chromatographic separations were performed on a Waters Acquity UPLC BDS C18 column (150 mm × 2.4 mm, 2.74 μm). The column temperature was 35°C, the flow rate was 0 ml/min. The mobile phase consisted of acetonitrile (A) and 0.1% formic acid aqueous solution (B) at a flow rate of 0.3 ml/min, with gradient elution as follows: 0– min, 95% B; 3– min, 95%–25% B; 45–45. min, 25%–95% B; 45.1–50 min, 95% B.

In negative and positive ion modes, the mass conditions were set. Briefly, the gas of sheath and auxiliary was nitrogen. The flow rates were 40 arbitrary units and 20 arbitrary units, respectively. The capillary temperature was 320°C. The sheath gas flow rate was 35.0 μL/min. The aux gas flow rate was 10 μL/min. The sweep gas flow rate was 10 μL/min. The positive ion spray voltage was 3.5 KV while the negative ion spray voltage was 3.0 KV. In addition, the mass scanning range was m/z 120-1800.

The Analysis of Constituents of E.C.D. Extracts

The information of published constituents of Eucommia, Cuscuta, and Drynaria was collected based on TCMSP database (https://old.tcmsp-e.com/tcmsp.php). The molecular 2D files of these constituents were downloaded from the ChemSpider database (http://www.chemspider.com/) and were saved in mol format. The mass spectra of E.C.D. extracts were recorded across the range of m/z 120-1800. All the data were processed using Xcalibur software version 2.7. The constituents of E.C.D. extracts found in mass spectra were compared with published information and the TCMSP database then the molecular information was recorded in **Supplementary Data Sheet S1**.

The Prediction of E.C.D. Extracts Related Targets

The predicted proteins targeted by E.C.D. extracts were screened using MedChem Studio software based on the mass spectrometry analysis. Briefly, the identified constituents of E.C.D. were input into the SwissTargetPrediction database (http://www.swisstargetprediction.ch/). We picked the targets of ingredients of E.C.D. with high confidence score (≥1) and recorded the target information.

Network Construction and Analysis

Known therapeutic targets for osteoporosis were collected from GeneCards database (http://www.genecards.org/), OMIM database (https://www.omim.org/). and DrugBank database (http://www.drugbank.ca/). After integrating data from several databases and removing duplicate data, we took the intersection of the verified constituents target of E.C.D. based on previous analysis and the therapeutic targets of osteoporosis. The constituents–targets network was constructed using Cytoscape software (Verson 3.8.2, Boston, MA) and Java analysis.

Pathway Enrichment Analysis

Kyoto Encyclopedia of Genes and Genomes (KEGG) pathways analysis was undertaken to explore the potential functions of the pivotal target proteins involved in the E.C.D extracts-mediated treatment of osteoporosis using DAVID Bioinformatics Resources 6.8 (https://david.abcc.ncifcrf.gov/home.jsp). Relevant pathways with the false discovery rate (FDR)-corrected p-value < 0.05 were considered statistically significant. Other parameters were set as the default values. Meanwhile, the biological process (BP), cellular components (CC), and molecular function (MF) of target protein involved were also analyzed.

Cells

The murine Raw264.7 cell line was purchased from Xie He Hospital, Beijing, China. The cells were cultured in DMEM medium (Geibo, Catalog number: 11,995-065) with 10% fetal bovine serum (FBS) and 1% penicillin/streptomycin/L-glutamine (P.S.G.). The cells of passage 11-15 were used in the experiment. The murine bone marrow MSC was harvested from C57BL/6 male mice, 6 weeks of age. Briefly, the mice were sacrificed by broken vertebral column. The tibia and femur were isolated and then washed by PBS. The bone was crushed and washed 4 times with PBS. Collection of PBS was centrifuged at 1500 rpm for 10 min. Then 0.1% Collagenase I (Worthington, Catalog number: LS004194) and 0.25% Collagenase II (Worthington, Catalog number: LS004174) were added to bone fragments and the mixture was incubated in a 37 oC shaker for 1 h. Supernatant was collected and then centrifuged in 1500 rpm for 10 min. The cells from two steps were seeded in 100 mm dish for 3 days. MSC was cultured using MesenCult™ Expansion Kit (Mouse) (STEMCELL, Catalog number: 05513). MesenPure™ (STEMCELL, Catalog number: 05510) was used to keep MSC homogeneous and maintain robust proliferation, differentiation, and colony formation capacity. Passage 4-6 of MSC was used in this experiment.

CCK8 Assay

The Cell Counting Kit-8 (Biorigin, Catalog number: BN15201) was used for this experiment. Basically, Raw264.7 cells or MSCs were seeded in 96-well plate overnight. Then E.C.D. extracts of different doses were added to each well and co-incubated for 24 h or 48 h. Then the medium was replaced and 10 μL CCK was added to each well maintained at 37°C in a humidified 5% CO_2 atmosphere for 1 h. The OD number was read in 450 nm.

Osteoclast Differentiation Assay

RAW 264.7 cells were cultured at a density of 2×10^5 cells/well in 6-well plates in the presence of 50 ng/ml recombinant mouse RANKL (Novoprotein, Catalog number: CR06, China) and 50 ng/ml recombinant mouse M-CSF (Novoprotein, Catalog number: CB34, China). M-CSF and RANKL (C/R) were replenished every 2 days. Cultures were maintained at 37°C in a humidified 5% CO_2 atmosphere. At the same time, E.C.D. extracts (1 μg/ml, 50 μg/ml, 200 μg/ml) or MSC CM or E.C.D. pre-treated MSC CM were added for 48 h, 96 h, or 5 days.

RNA Extraction and qPCR

The E.C.D. extracts were added to Raw264.7 cells or mouse bone marrow derived MSCs at different doses (1 μg/ml, 50 μg/ml, 200 μg/ml). RNA was harvested after 48 h incubation. The RNA was extracted with Trizol Reagent (QIAzol, Catalog number: 79306). Reverse transcription (RT) was conducted using Evo M-MLV RT kit with gDNA Clean for qPCR II (Accurate Biology, Catalog number: AG11711). Real-time amplification of complementary cDNA was conducted in a Rotor-Gene 3000 System (Corbett Research, Mortlake, Australia) with the 2X Realab Green PCR Fast mixture (Universal) (LABLEAD, Catalog number: R0202-03). The primers of mouse used are as follows:

NFATc1, 5′-TCATCCT GTCCAACACCAAA-3′(Forward) and 5′-TCACCCTGGTGTTCTTCC TC-3′(Reverse); TRAP, 5′-CAGCAGCC AAGGAGGACTAC-3′(Forward) and 5′-ACA TAGCCCACACCGTTC TC-3′(Reverse); RANKL, 5′-TGTACT TTCGAGCGCAGATG-3′ (Forward) and 5′-AGGCTTGTTTCA TCCTCCTG-3′ (Reverse); Runx2, 5′-CGA CAG TCC CAA CTT CCT GT-3′ (Forward) and 5′-CGG TAA CCA CAG TCC CAT CT-3′(Reverse); Wnt1, 5′-CTTCGGCAAGATCGTCAAC-3′(Forward) and 5′-CTGCCTCGTTGTTGTGAAG-3′(Reverse); OPG, 5′-ACAGTTTGCCTGGGACCAAA-3′ (Forward) and 5′-TC ACAGAGGTCAATGTCTTGGA-3′(Reverse).

Protein Extraction and Western Blot

The E.C.D. extracts were added to Raw264.7 cells with C/R (50 ng/ml) stimulation at different dose (1 μg/ml, 50 μg/ml, 200 μg/ml). After 48 h or 96 h, the protein was harvested by RIPA buffer (APPPLYGEN, Catalog number: C1055) with protease inhibitor (10X) and phosphatase inhibitor (10X). The protein concentration was measured by BCA assay (APPPLYGEN, Catalog number: P1511) following the company's manual. After adding loading buffer (5×), the lysed protein was boiled at 100°C for 10 min and then equal protein concentration was electrophoresed on 8 or 12% gels. Antibodies for blotting (NFATc1, RANKL, TRAP, PI3K, p-Akt, Akt, p-P38, P38, GAPDH) are detailed in **Supplementary Table S1**. Protein expression was assessed using ImageJ software.

Tartrate-Resistant Acid Phosphate Staining Assay

The Raw264.7 cells were cultured in 96-well plate at the density of 5X10^3 cells/well. The C/R of 50 ng/ml were added for 5 days, and medium was changed every other day. E.C.D. extracts of different concentrations were added in the meantime. Then the TRAP staining was performed following the company's manual (Servicebio, Catalog number: G1050). Briefly, cells were fixed by 4% paraformaldehyde then permeabilized by 0.2% Triton X-100. The TRAP working solution was added and then incubated in 37°C for 2 h. The TRAP staining was observed under light microscope and the number of TRAP positive cells with ≥ 3 nuclei was counted.

F-Actin Assay

The Raw264.7 cells were cultured in 35 mm dish at the density of 1X10^5 cells/dish. The C/R of 50 ng/ml were added for 5 days and E.C.D. extracts were added at the same time. Five days later, the F-actin staining was performed using Rhodamine Phalloidin Reagent (abcam, Catalog number: ab235138) as suggested by the manufacturer. Basically, the cells were fixed by 4% formaldehyde at room temperature for 30 min and then permeabilized by 0.1% Triton X-100 for 5 min 1X Phalloidin conjugate working solution was added and incubated at room temperature for 90 min. The DAPI was added for 10 min to stain nuclei. After adding mounting media, the cells were observed using Olympus FV3000 confocal microscope fitted with a filter at Ex/Em = 546/575 nm.

Bone Resorption Assay

The bovine bone slices (0.4 mm) were put in a 96-well plate, and the Raw264.7 cells were cultured on the bone slice at the density of 1X10^3 cells/well overnight. The C/R of 50 ng/ml were added for 7 days and E.C.D. extracts were added at the same time. The medium was changed every 3 days. After 7 days, the cells were washed off with 10% sodium hypochlorite for 5 min and washed 3 times with distilled water. The bone resorption pit was observed under the light microscope. Then the bone slices were stained using 1% toluidine blue at room temperature for 30 min and washed 3 times with distilled water. The resorption pit was photographed under the light microscope and the percentage of resorption area was assessed using ImageJ software (Fu et al., 2013; Sapkota et al., 2015; Zeng et al., 2016; Liao et al., 2021).

PI3K Inhibition Assay

The PI3K inhibitor (LY294002) (Kao et al., 2005; Zhao et al., 2015) was purchased from Apexbio (Catalog number: LY294002). LY294002 was added to Raw264.7 cells to reach the final concentration of 30 μM. After 2 h, LY294002 was removed and then C/R of 50 ng/ml were added for another 48 h. Then the protein was harvested and assessed by Western blot.

Preparation of MSC Conditioned Medium

Mouse bone marrow MSCs from P5-P6 were cultured to 80–90% confluence. The E.C.D. extracts (1 μg/ml, 50 μg/ml, 200 μg/ml) or PBS (same volume) were added to medium for 48 h. The pre-treated MSCs were washed with PBS, then replenished with supplement-free DMEM medium. After 24 h, the CM was collected, and centrifuged at 2000 rpm for 5 min to remove cell debris. The CM was then kept at −80°C until use.

Statistical Analysis

For comparisons between two groups, we used Student's unpaired *t* test. For analysis of more than two groups, one-way or two-way analysis of variance (ANOVA) was performed. When data were not normally distributed, non-parametric analyses were performed using Kruskal-Wallis testing. Comparisons of weight change was made by analyzing the area of curves, then two-way ANOVA was performed to assess for differences in weight changes. Statistical significance was accepted at $p < 0.05$.

RESULTS

E.C.D. Extracts Protected Body Weight Loss, Calcium and Phosphate Loss of Experimental GIO Rats

Osteoporosis usually results in low weight, calcium loss, and fragile bones (Lane et al., 2000). To assess the therapeutic effects of E.C.D. extracts *in vivo*, we inducted GIO in rats and

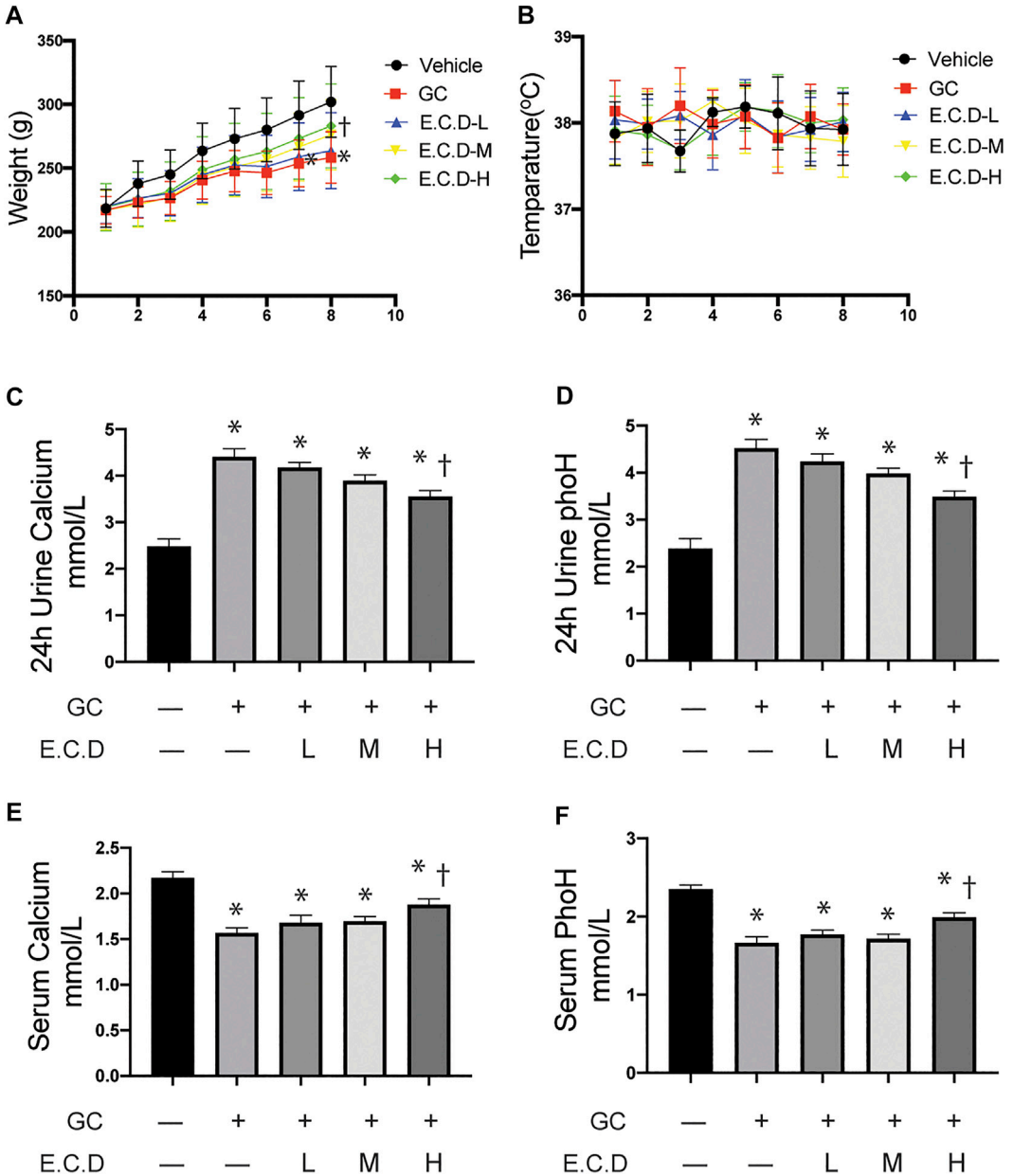

FIGURE 1 | E.C.D. extracts protected body weight loss, and calcium and phosphorus loss of GIO rats. **(A)** Rats were randomly divided into five group, $n = 8$ in each group: Vehicle group (black, dot), GC group (red, square), E.C.D.-L group (blue, triangle), E.C.D.-M group (yellow, down triangle), E.C.D.-H group (green, diamond). The change of body weight from Week 0 to Week 8 was recorded. * GC group vs. Vehicle group, † E.C.D.-H group vs. GC group, $p < 0.05$. **(B)** The temperature of rats was recorded every week (0-8) with no significant difference between each group. **(C,D)** The 24-h urine calcium and phosphorus (phoH) were collected 8 weeks after GC administration, $n = 8$ in each group. **(E,F)** The serum calcium and phosphorus (phoH) were measured 8 weeks after GC administration, $n = 8$ in each group. Data was analyzed as mean ± SEM, * vs. Vehicle group (GC–E.C.D.–), † vs. GC group (GC + E.C.D. –), $p < 0.05$.

processed E.C.D. extracts by gavage. Rats after GC administration gained less body weight (red line, square, **Figure 1A**) as weeks increased compared to rats in the Vehicle group (black line, circle), while rats that received E.C.D. extracts displayed increased body weight compared with rats in the GC group. With the dose of E.C.D. extracts increasing, the weight improvement efficacy is more dramatic. At week 8, rats receiving E.C.D. extracts of high dose (green line, diamond) gained more weight than rats in the GC group. Assessment of urine and serum revealed increased calcium and phosphorus loss in urine (**Figures 1C,D**) while decreased calcium and phosphorus levels in serum (**Figures 1E,F**) of rats in the GC group compared with rats in the Vehicle group, which was rescued when rats

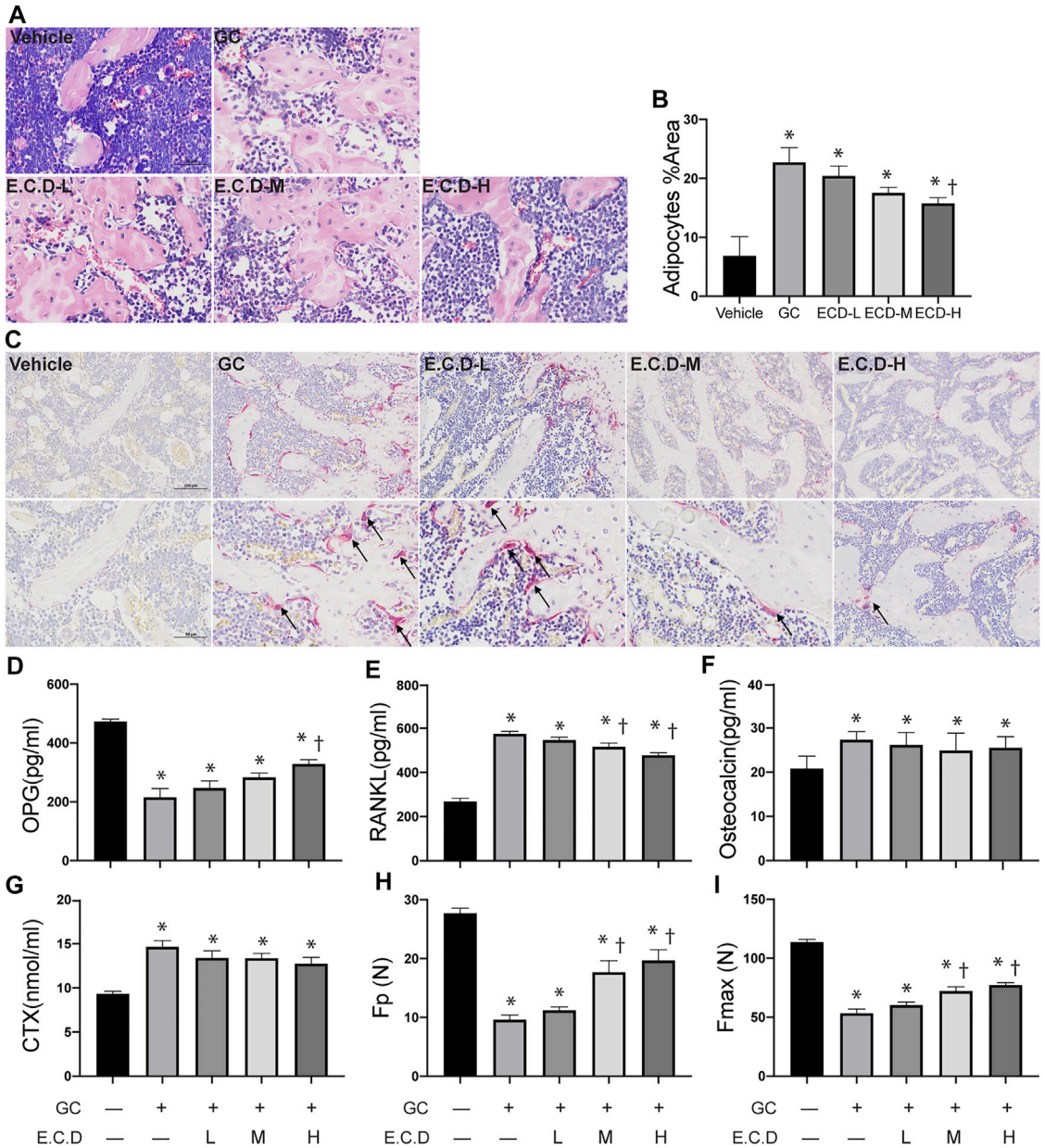

FIGURE 2 | E.C.D. extracts restored the bone marrow structure and regulated cytokine of bone resorption and regeneration. **(A)** H&E staining was performed with femur of rats in five groups: Vehicle group (left upper panel), GC group (middle upper panel), B.C.D.–L group (left lower panel), B.C.D.–M group (middle lower panel), and B.C.D.–H group (right lower panel). **(B)** The quantitative adipocytes area in bone marrow for five groups, $n = 3$ in each group. **(C)** TRAP staining was assessed for five groups, upper panel is X200 magnification, lower panel is X400 magnification. The black arrow pointed to TRAP positive osteoclasts. **(D–G)** The OPG, RANKL, osteocalcin, and CTX level in rats' serum were measured 8 weeks after GC administration, $n = 8$ in each group. **(H,I)** The Fp and Fmax of bone were assessed, $n = 8$ in each group. Data were analyzed as mean ± SEM, * vs. Vehicle group (GC–E.C.D.–), † vs. GC group (GC + E.C.D. –), $p < 0.05$.

received E.C.D. extracts treatment. As the dose increased, rats restored the serum calcium and phosphorus concentration (**Figures 1E,F**). The level of calcium and phosphorus in urine (**Figures 1C,D**) was decreased by E.C.D. extracts of high dose. These data indicated that E.C.D. extracts can protect the loss of calcium and phosphorus and weight decrease in experimental GIO rats. The temperature (**Figure 1B**) of rats during the experiment fluctuated without significant differentiation.

E.C.D. Extracts Restored the Bone Marrow Structure and Regulated Cytokine of Bone Resorption and Regeneration

The bone marrow deterioration was examined using H&E staining (Yang et al., 2020). In H&E staining (**Figure 2A**) the bone marrow cavity of the GC group was significantly enlarged with more light stained area composed by adipocytes compared with the Vehicle group, which was ameliorated by E.C.D. extracts treatment. The percentage of adipocytes area was quantified (**Figure 2B**) and E.C.D. extracts of high dose significantly decreased the adipocytes infiltration in bone marrow compared with the GC group. The TRAP staining (Bai et al., 2005) was performed to assess the activity of osteoclast (**Figure 2C**). After GC administration there were more osteoclast accumulation in trabeculae which was reversed by E.C.D. extracts treatment. The cytokine and chemokine in serum revealed the metabolism of osteoclast and osteoblast (Boyce and Xing, 2008). Bone remodeling is regulated by a crosstalk between bone-forming osteoblasts and bone-resorbing osteoclasts (Kim et al., 2020). OPG was synthesized by osteoblasts which inhibited osteoclast differentiation. The activation of RANKL-RANK signal could stimulate osteoclast formation. The OPG, RANKL, osteocalcin (an indicator of spontaneous bone loss) (Brown et al., 1984), and CTX (a bone resorption marker) (Iba et al., 2008) levels were measured by ELISA (**Figures 2D–G**). GC administration resulted in decreased OPG (related to osteoblast genesis) while increased RANKL, osteocalcin, and CTX (related to osteoclast genesis). Administration of E.C.D. extracts improved the OPG expression (E.C.D.-H group) and decreased RANKL expression (E.C.D.-M group and E.C.D.-H group) in serum compared with the GC group. But E.C.D. extracts did not decrease expression of osteocalcin and CTX in serum. The biomechanical function of bone is important to evaluate osteoporosis. The maximum load (Fmax) and elastic load (Fp) were dramatically decreased in rats of the GC group compared with the Vehicle group (**Figures 2H,I**). The E.C.D. extracts of medium and high dose treatment significantly increased the Fmax and Fp compared with the GC group.

E.C.D. Extracts Improved the Integrity of Bone Structure and Increased Bone Density by Micro-CT Scan

3-D trabecular structural characteristics can help us understand the pathophysiology of osteoporosis. The compact trabecular bone structure was shown in the Vehicle group compared with decreased trabeculae volume and abnormal morphologies like scattered structure or fracture of the GC group (**Figure 3A**). E.C.D. extracts treatment improved the integrity and continuity of trabecular structure. Multi-angle and multi-section of bone structure was assessed by mico-CT and shown in **Supplementary Figure S2**. We further measured the bone volume/total volume (BV/TV), trabecular thickness (Tb.Th), and trabecular number (Tb.N) by micro-CT, which can reflect the trabecular bone volume, thickness, and number. GC administration remarkably decreased the volume of the trabecular, which reverted by E.C.D. extracts treatment in medium and high dose (**Figure 3B**). The number of trabecular also decreased in the GC group but E.C.D. extracts treatment did not improve it (**Figure 3E**). E.C.D. extracts also can improve trabecular thickness which was thinner in the GC group (**Figure 3C**). The trabecular separation (Tb.Sp) indicates the average width of the medullary cavity between the trabeculae, suggesting increased bone resorption. GC administration markedly increased Tb.Sp in rats compared with the Vehicle group (**Figure 3D**), while E.C.D. extracts (E.C.D.-H group) significantly reduced Tb.Sp compared with the GC group. The structural model index (SMI) reflects the rods and plates of trabecular. When osteoporosis occurs, the trabecular bone changes from a plate shape to a rod shape, resulting in SMI increasing. In our study, GC increased SMI (**Figure 3F**) compared with the Vehicle rats, which was decreased when the rats were treated with E.C.D. extracts (E.C.D.-H group). Bone mineral density (BMD) was dramatically reduced by GC administration compared with the Vehicle group, which was rescued by E.C.D. extracts (**Figure 3G**). With increased dosage, the BMD improved.

E.C.D. Extracts Inhibited Osteoclast Differentiation *in vitro*

The abnormal activation of osteoclast differentiation is one of the key reasons to induce osteoporosis. To first assess if E.C.D. extracts affect the growth properties of cells, we first processed the CCK8 assay. Interestingly, E.C.D. extracts improved cell viability and the efficacy enhanced as dose increased both in 24 and in 48 h without toxicity (**Figures 4C,D**). Next, the osteoclast differentiation was induced by adding C/R (50 ng/ml) to Raw264.7 cells. We evaluated TRAP staining and F-actin assay after 5 days. TRAP staining is used to stain tartrate-resistant acid phosphatase in osteoclasts. Raw264.7 cell is a small circle monocyte (left panel, **Figure 4A**). After C/R stimulation, Raw264.7 cell differentiated into osteoclast which displayed large and multinucleated morphology with TRAP positive staining (red color, left second panel). E.C.D. extracts inhibited osteoclast differentiation with less TRAP positive multinucleated cells (right three panel). The ratio of TRAP positive cells with $\geq$ 3 nuclei of total cells was quantified (**Figure 4E**). There are more TRAP positive cells after C/R stimulation compared with the CTRL group, and E.C.D. extracts significantly reduced the number of TRAP positive cells compared with the C/R group. Actin ring is a characteristic actin structure that is essential for bone resorption by osteoclasts. Differentiated osteoclasts after C/R stimulation showed bright circle red fluorescence Actin ring with multiple nuclei inside (left second panel, **Figure 4B**). Raw264.7 cells with E.C.D. extracts of 1 μg/ml and 50 μg/ml treatment also displayed Actin ring with multiple nuclei. E.C.D. extracts of 200 μg/ml reversed osteoclast differentiation (right panel) with no multinucleated osteoclast with F-actin positive staining. The bone resorption assay was also assessed (**Supplementary Figure S3**). Treatment of E.C.D. extracts was shown to reduce the area of resorption pit on bovine bone slices

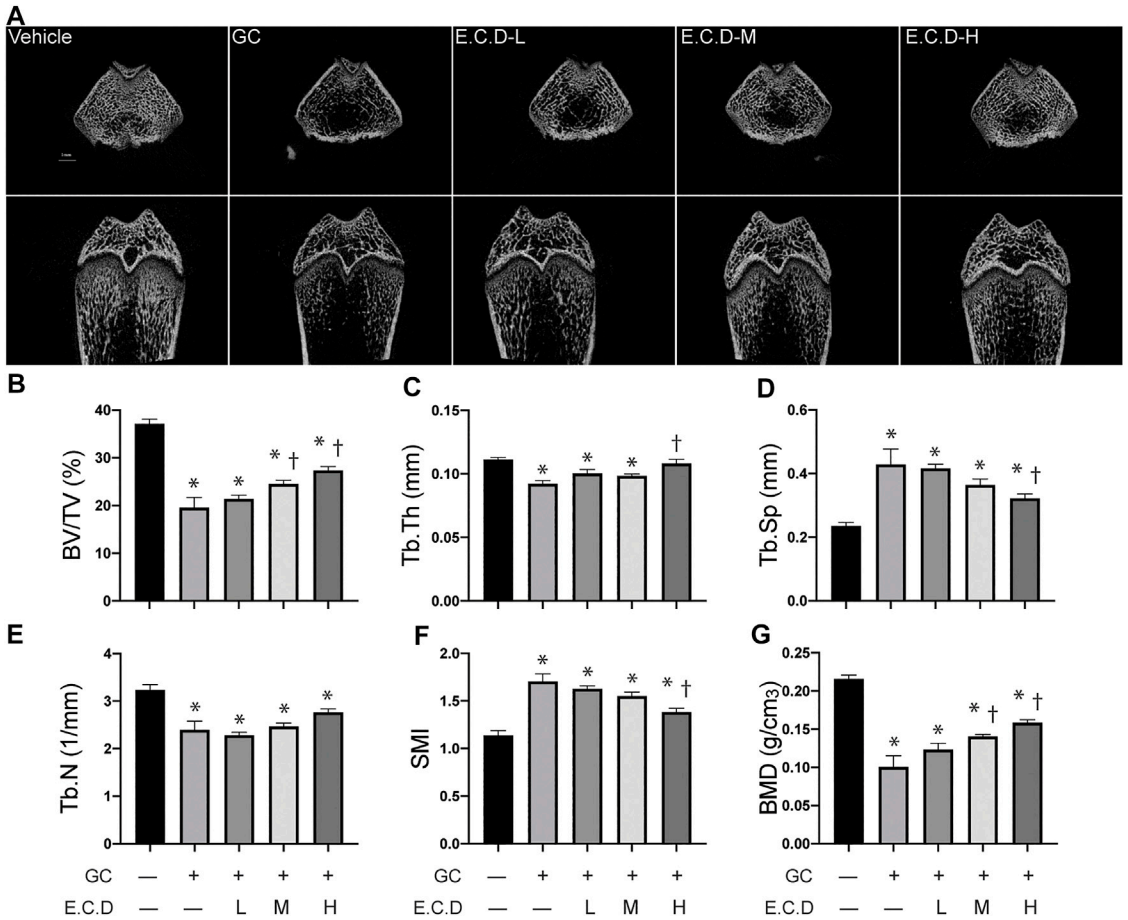

FIGURE 3 | E.C.D. extracts improved the integrity of bone structure and increased bone density by micro-CT scan. **(A)** The micro-CT scan was processed to assess the micro-structure and the biomechanics of rats. The upper panel was the transverse section of the femur, and the lower panel was the longitudinal section of the femur. The scale bar was labeled as 1 mm. **(B–G)** Bone volume/total volume (BV/TV), trabecular thickness (Tb.Th), trabecular separation (Tb.Sp), trabecular number (Tb.N), structural model index (SMI), and bone mineral density (BMD) were measured 8 weeks after GC administration of rats. The columns from left to right are Vehicle group, GC group, B.C.D.–L group, B.C.D.–M group and B.C.D.–H group, respectively, $n = 8$ in each group. Data were analyzed as mean ± SEM, * vs. Vehicle group (GC–E.C.D.–), † vs. GC group (GC + E.C.D. –), $p < 0.05$.

compared with the C/R group and the treatment function of E.C.D. extracts was dose-dependent that 200 μg/ml and 50 μg/ml E.C.D. extracts decreased more resorption area compared with E.C.D. extracts of 1 μg/ml. TRAP, NFATc1, and RANKL are important markers for osteoclast formation. We assessed these genes expression by qPCR. After C/R stimulation, the expression of TRAP, NFATc1, and RANKL were dramatically increased compared with the CTRL (**Figures 4F–H**). While these changes were reversed by E.C.D. extracts in three doses (1 μg/ml, 50 μg/ml, and 200 μg/ml). Moreover, as dose increased, the functional efficacy of E.C.D. extracts in inhibiting osteoclast differentiation increased. To further verify the hypothesis, we harvested the protein from Raw264.7 cells in 48 and 96 h, then the immunoblotting was performed, using GAPDH expression for normalization (**Figure 4I**). The expression of TRAP was increased in 48 and 96 h after C/R stimulation, which was reverted by E.C.D. extracts of 50 μg/ml and 200 μg/ml. C/R stimulation also increased NFATc1 expression in 96 h compared with CTRL (Raw264.7 cells without C/R stimulation), which were eliminated by E.C.D. extracts administration in doses of 1 μg/ml, 50 μg/ml, and 200 μg/ml. The expression of RANKL was increased in the C/R group both in 48 and 96 h compared with the CTRL group, and E.C.D. extracts of 50 μg/ml and 200 μg/ml significantly decreased it compared with the C/R group. These immunoblotting data indicated that E.C.D. extracts contributed to the inhibition of osteoclast differentiation, and the function is better in high doses (50 μg/ml and 200 μg/ml) than low doses (1 μg/ml).

E.C.D. Extracts Promoted OPG Expression of MSC and Regulated the Paracrine Effect of MSC to Inhibit Osteoclastogenesis of Raw264.7 Cells

The bone metabolism is a cross-talking and dynamic process. After we proved the efficacy of E.C.D. extracts on inhibition of

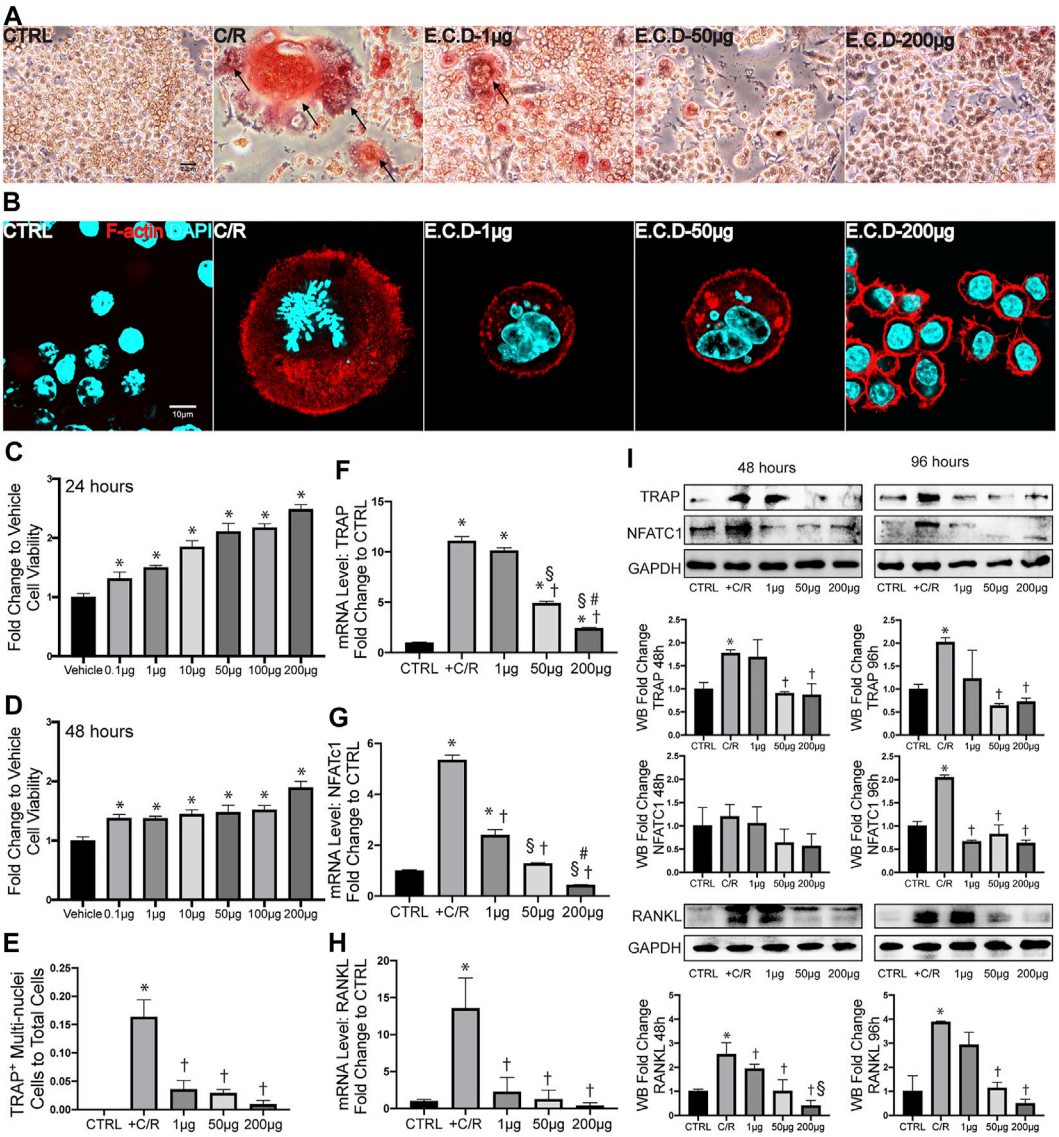

FIGURE 4 | E.C.D. extracts inhibited osteoclast differentiation *in vitro*. **(A)** TRAP staining assay displayed TRAP positive cells in Raw264.7 cells at Day 5 after C/R stimulation. The black arrow points to a mature osteoclast. The scale bar is labeled as 20 μm. **(E)** The quantitative percentage of mature osteoclasts in total cells was assessed, $n = 3$ in each group. **(B)** F-actin staining was assessed at Day 5 after C/R induction. F-actin was stained ared color and DAPI was blue. The bright actin ring was formed in the C/R group, E.C.D.-L, and E.C.D.-M group. The scale bar is labeled as 10 μm. **(C,D)** To assess the toxicity of E.C.D. extracts to cells, we performed CCK8 assay *in vitro*. The Raw264.7 cells were seeded in 96-well plate (Vehicle group, first column from left) and the E.C.D. extracts in different doses were added (second column to seventh column from left). The CCK8 assay was measured 24 and 48 h later. $n = 5$ in each group. Data were analyzed as mean ± SEM, * vs. Vehicle group, $p < 0.05$. **(F–H)** The mRNA expression level of TRAP, NFATc1, and RANKL were measured 48 h after C/R stimulation, $n = 3$ in each group. **(I)** The protein level of TRAP, NFATc1, and RANKL were assessed at 48 and 96 h after C/R stimulation. The immunoblotting was shown in the upper panel and quantity of densitometric values fold change was shown in the lower panel. $n = 3$ in each group. Data were analyzed as mean ± SEM, * vs. CTRL group, † vs. + C/R group, § vs. 1 μg group, # vs. 50 μg group, $p < 0.05$.

osteoclast differentiation, whether it plays a positive or a negative role on osteoblast genesis is also under investigation. Thus, we harvested MSC from mice bone marrow of tibia and femur (**Figure 5A**) and cultured them until passage 5. The CCK8 assay was assessed to clarify the function of E.C.D. extracts on MSC viability (**Figures 5B,C**). E.C.D. extracts of high dose (50 μg/ml and 200 μg/ml) improved MSCs viability on both 24 and 48 h. The OPG level and other genes related to osteoblast genesis were assessed by qPCR. Interestingly, the E.C.D. in low dose (1 μg/ml) dramatically increased OPG expression in MSCs (**Figure 5D**), while E.C.D. of 50 μg/ml still increased the OPG level but was a little bit lower than 1 μg/ml. As the dose increased to 200 μg/ml, the function of promoting OPG was lost (**Figure 5D**). The Wnt and Runx signaling are related to osteoblast formation (Komori, 2018; Komori, 2019; Karadeniz et al., 2020). Runx2 can induce Sp7, which is an essential transcription factor for osteoblast

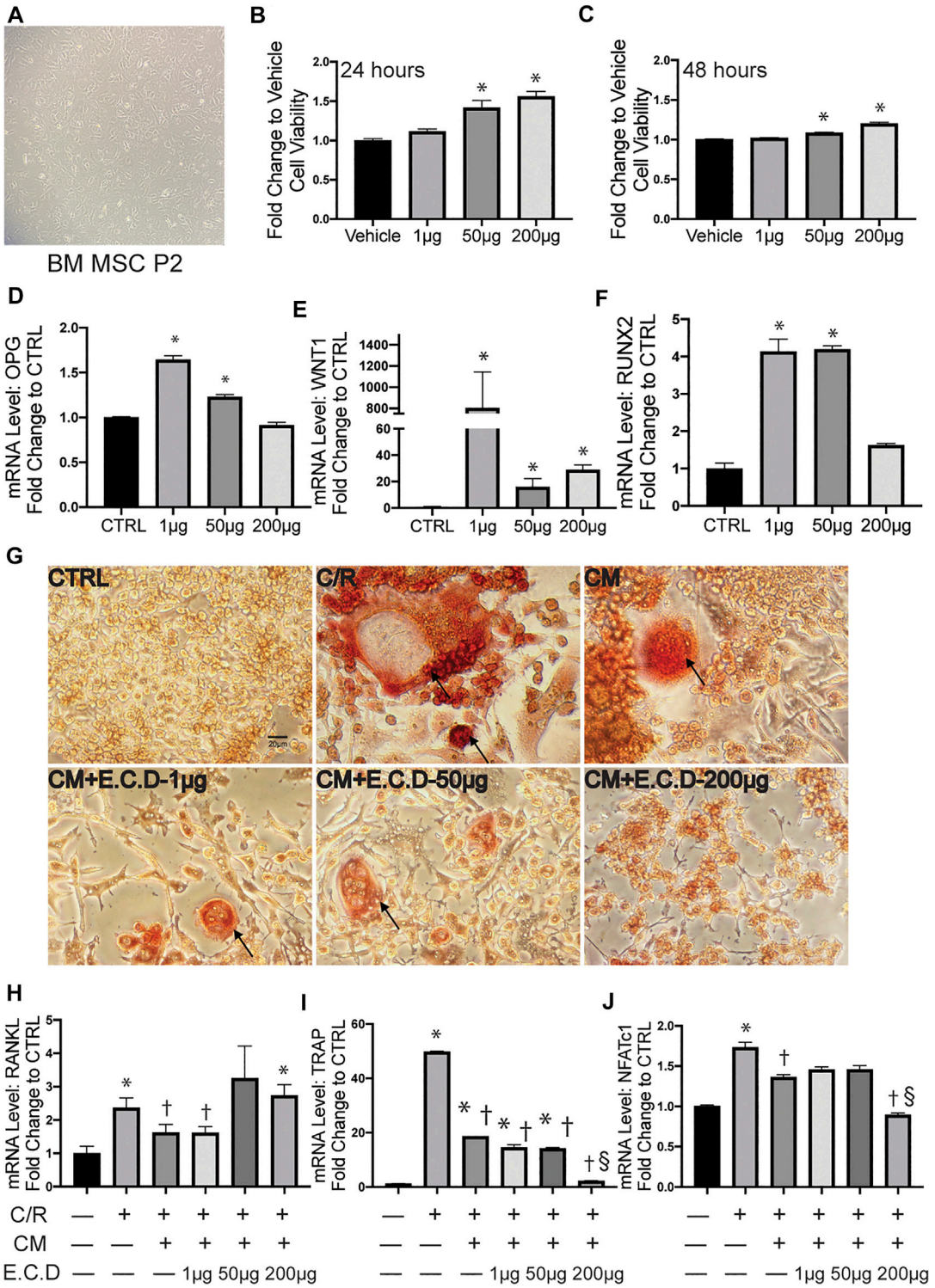

FIGURE 5 | E.C.D. extracts promoted OPG expression of MSC and regulated paracrine effect of MSC to inhibit osteoclastogenesis of Raw264.7 cells. **(A)** The mice bone marrow MSC was harvested and cultured for expansion. **(B,C)** The toxicity of E.C.D. extracts to MSC was assessed by CCK8 assay. The MSCs were cultured in 96-well plate (Vehicle group), the E.C.D. extracts were added in different doses of 1 μg/ml, 50 μg/ml, and 200 μg/ml (1 μg, 50 μg, and 200 μg group, respectively). $n = 5$ in each group, data were analyzed as mean ± SEM, * vs. Vehicle group. **(D–F)** The mRNA level of OPG, Wnt1, and Runx2 were analyzed by adding different doses of E.C.D. extracts to MSC. $n = 3$ in each group. Data were analyzed as mean ± SEM, * vs. CTRL group, $p < 0.05$. (**G**) TRAP staining was assessed 5 days after C/R stimulation, the MSC CM, CM pretreated with E.C.D. extracts of 1 μg/ml, 50 μg/ml, and 200 μg/ml were added with C/R. The black arrow points to a mature osteoclast.

(*Continued*)

FIGURE 5 | The scale bar is labeled as 20 μm. **(H–J)** The paracrine function of MSC mediated by E.C.D. extracts was assessed. The MSC was treated with E.C.D. extracts and then the conditioned medium (CM) was harvested. The C/R stimulated Raw264.7 cells were treated with CM without being preconditioned with E.C.D. extracts, CM preconditioned with 1 μg/ml or 50 μg/ml or 200 μg/ml E.C.D. extracts. $n = 3$ in each group. Data were analyzed as mean ± SEM, * vs. CTRL group (first column from left), † vs. + C/R group (second column from left), § vs. CM group (third column from left). $p < 0.05$.

differentiation. For Wnt1, E.C.D. extracts in low dose (1 μg/ml) dramatically increased Wnt1 expression in MSC, E.C.D. extracts with 50 μg/ml and 200 μg/ml can increase Wnt1 level but lower than 1 μg/ml (**Figure 5E**). For Runx2, E.C.D. extracts with 1 μg/ml and 50 μg/ml significantly enhanced Runx2 level in MSC, but E.C.D. extracts of 200 μg/ml lost the function (**Figure 5F**). To further understand the regulating function of E.C.D. extracts on MSC paracrine effect in mediating osteoclast differentiation, we treated MSC with E.C.D. extracts for 48 h then harvested preconditioned medium (CM) of MSC. The CM of MSC was used in osteoclast differentiation assay, and TRAP staining was assessed (**Figure 5G**). Addition of C/R to cells greatly enhanced the number of TRAP positive cells, which was reversed by adding MSC CM. CM pretreated with E.C.D. extracts also decreased TRAP positive cells. The CM of MSC showed the function of decreasing NFATc1, TRAP, and RANKL expression of Raw264.7 cells (**Figures 5H–J**) compared with the C/R group. The CM of MSC pre-treated with E.C.D. extracts (200 μg/ml) decreased expression of TRAP and NFATc1 (**Figures 5I,J**) compared with the C/R group and better than the CM group (CM without re-treating with E.C.D. extracts). These data demonstrated that E.C.D. extracts also can inhibit osteoclast differentiation by regulating MSC's paracrine effect. Interestingly, when we use CM of MSC pre-treated with E.C.D. extracts of high dose (200 μg/ml) treated Raw264.7 cells, the function of inhibiting RANKL expression is lost (**Figure 5H**).

HPLC Analysis Identified Constituents of the E.C.D. Extracts

The samples were scanned in the negative and positive iron model (**Figures 6A,B**). The HPLC displayed strong signals, high peak capacity, and reproducibility for retention time. We collected a total of 250 constituents of E.C.D. based on the TCMSP database. Comparing with the molecular weight and structure of published constituents, we identified 72 constituents of E.C.D. extracts (47, 8, 23 from Eucommia, Cuscuta, and Drynaria respectively, 6 constituents exist in 2 herbs), including Eucommiol, Quercetin, Kaempferol, Hyperin, Eriodictyol (**Figure 6C**), and other constituents (shown in **Supplementary Data Sheet S1**).

The Integrated Network Pharmacology Analysis Indicated the Potential Targets Mediated by E.C.D. Extracts in Treating Osteoporosis

The targets mediated by identified constituents of E.C.D. extracts were analyzed by Swiss Target Prediction. Meanwhile, we collected 4576 targets related to osteoporosis from DrugBank database, OMIM database, and GeneCards database. Comparing with published information of osteoporosis related targets, 44 targets mediated by the constituents of E.C.D. extracts had been identified with the potential of treating osteoporosis (**Figure 7A**). The 44 targets were mapped to a total of 101 pathways using the DAVID database. Unrelated pathways, such as "Pathways in cancer" were excluded. The pathways that satisfied the criteria (p-value <0.05, count>8, removing other disease-related pathways) were listed (**Figure7B**). Herbs-constituents-targets osteoporosis-related pathway network was constructed (**Figure 7A**). Three components of E.C.D. extracts related to 38 constituents, mediating 41 osteoporosis-related targets. The top nine pathways with the largest number of enrichment targets were considered as the main biological processes involved in osteoporosis treatment. They are the PI3K/Akt pathway, thyroid hormone pathway, HIF-1 pathway, FoxO pathway, estrogen pathway, Rap1 pathway, ErbB pathway, prolactin pathway, and Ras pathway. We next elucidate the biological process (BP), molecular function (MF), and cellular components (CC) of E.C.D. extracts involved in **Figure 7C**. For BP analysis, the main hubs play an important role on upregulating cell proliferation and downregulating cell apoptosis, positively regulating protein phosphorylation and PI3K signaling pathway. The main molecular function related to the targets are protein binding, enzyme binding, zinc ion binding, and transcription factor binding. Collecting KEGG pathway analysis, BP, MF, and CC analysis together, these data indicated E.C.D. extracts may exert therapeutic effect on osteoporosis through PI3K/Akt signaling pathway.

E.C.D. Extracts Inhibited Osteoclast Differentiation Through Regulating PI3k/Akt Pathway

The potential targets and pathways of E.C.D. extracts in mediating GIO were further verified by Western blot *in vitro*. PI3K is a protein usually promoting cell survival and proliferation. In many diseases, PI3K/Akt pathway regulates the abnormal stimulation of biological activities to induce a pathology process. In osteoporosis, a published paper showed abnormal activity of PI3K/Akt pathway can stimulate osteoclast differentiation (Lukert and Raisz, 1990). Raw264.7 cells expressed more PI3K after C/R stimulation (**Figure 8A**), while E.C.D. extracts down regulated the expression of PI3K. The quantitative bar graph (**Figure 8B**) of PI3K indicated that both 1 μg/ml, 50 μg/ml, and 200 μg/ml E.C.D. extracts can significantly inhibit PI3K expression. C/R induction also increased phosphorated Akt (**Figure 8C**), which was reversed by E.C.D. extracts administration in three doses (**Figure 8D**). To further verify that the PI3K/Akt pathway regulates osteoclast differentiation, we added one group with PI3K inhibitor (LY294002) (third column from left, **Figures 8A,C,E**).

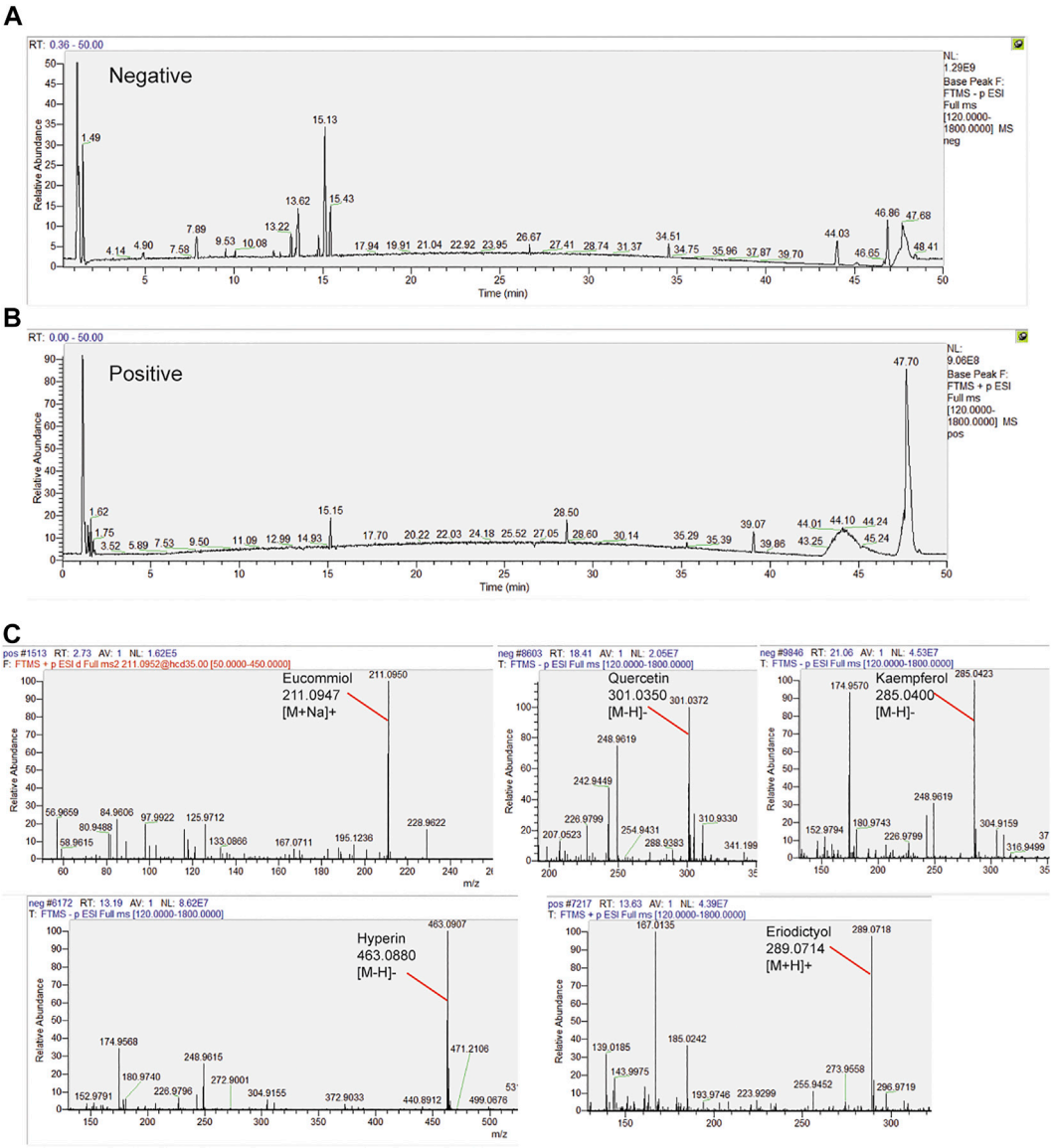

FIGURE 6 | HPLC analysis identified constituents in the E.C.D. extracts. **(A,B)** Total ion chromatogram analyzed in positive and negative ion modes for E.C.D. extracts. **(C)** E.C.D. extracts constituent analysis: Eucommiol, Quercetin, Kaempferol, Hyperin, and Eriodictyol.

LY294002 significantly inhibited PI3K expression (**Figure 8B**) and it also decreased phosphorated Akt (**Figure 8D**). We further assessed the RANKL expression regulated by LY294002. The Western blot result indicated that the level of RANKL was down regulated by the LY294002 (**Figure 8E**). The P38(MAPK) was also assessed as another signaling protein to promote osteoclast differentiation. After C/R stimulation, Raw264.7 cells expressed more p-P38 (phosphorated P38) compared with CTRL (**Supplementary Figure S4E**). E.C.D. extracts decreased p-P38 expression compared with the C/R group with significance in 50 μg/ml and 200 μg/ml (**Supplementary Figure S4F**). These data indicate that E.C.D. extracts inhibit osteoclast differentiation through regulating PI3K/Akt pathway and have the potential to regulate MAPK.

DISCUSSION

Glucocorticoid-induced osteoporosis (GIO) is the most common secondary cause of osteoporosis which results in server morbidity (Compston, 2018). Glucocorticoids can increase the production of M-CSF and RANKL which promote osteoclast differentiation and decrease production of osteoprotegerin (OPG) by osteoblastic cells (Swanson et al., 2006). Even though there are several choices for osteoporosis management, the clinical therapy remains suboptimal. For osteoporosis treatment, estrogen is selected for the treatment of OP patients with obvious menopausal symptoms and long-term use is not recommended (Fait, 2019). Bisphosphonates are currently the most commonly used medication for osteoporosis treatment such as alendronate, risedronate, and zoledronic acid (Qaseem et al.,

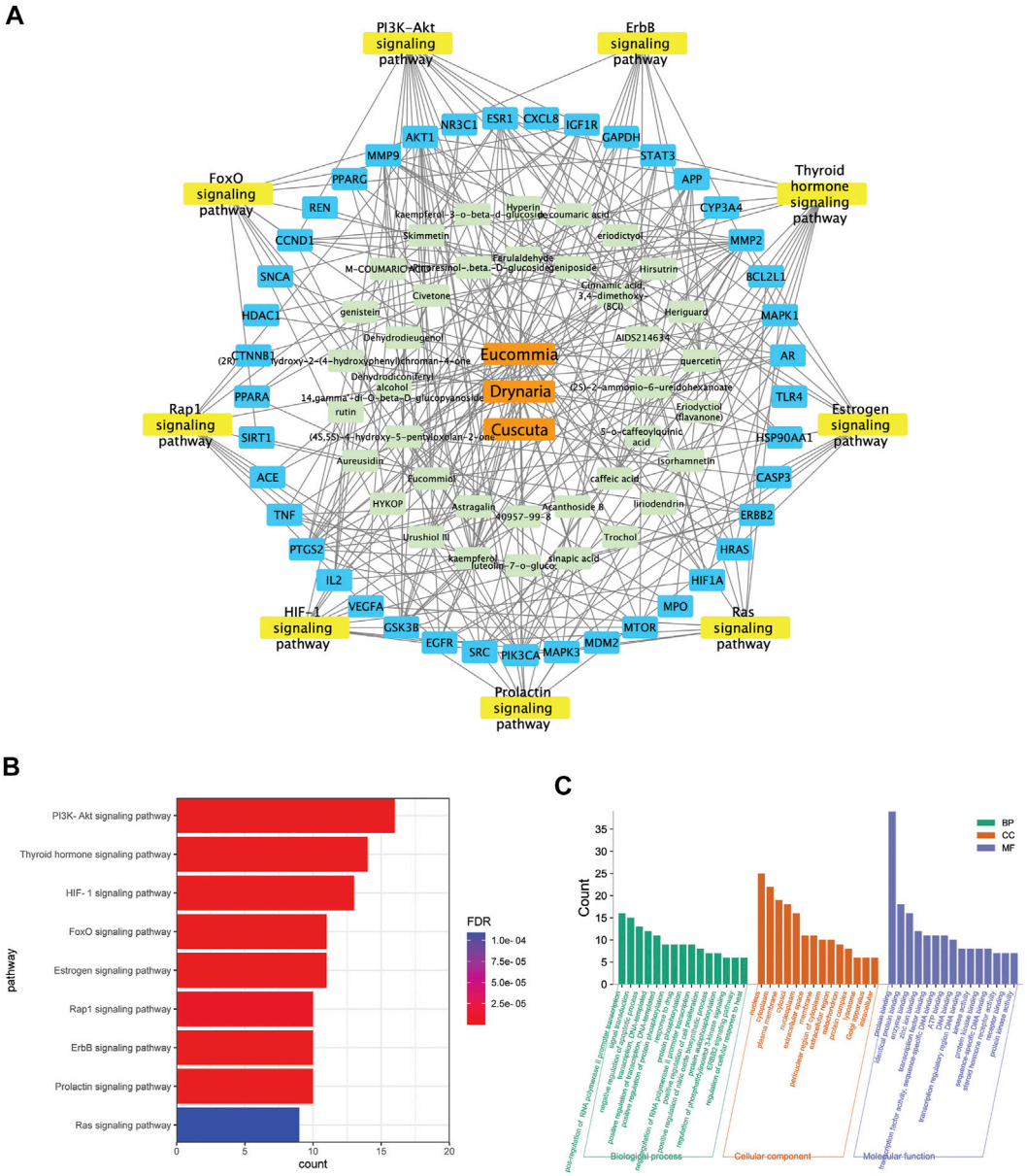

FIGURE 7 | The integrated network pharmacology analysis indicated the potential targets mediated by E.C.D. extracts in treating osteoporosis. **(A)** E.C.D. extracts–constituent–osteoporosis related targets–pathway network. **(B)** The potential pathways in treating osteoporosis by E.C.D. extracts performed by KEGG enrichment analysis. $p < 0.05$, the count of enrichment related targets decreases from top to bottom. **(C)** The biological process (BP), molecular function (MF), and cellular components (CC) analysis of targets mediated by E.C.D. extracts. $p < 0.05$, the count of related targets decreases from left to right.

2017). However, it has the risk of osteonecrosis of the jaw and atypical femoral fracture (Adler et al., 2016). Denosumab is also used as the first recommended approval drug to prevent osteoporosis. It works as a RANK binding inhibitor to reduce bone resorption (Miller, 2009). However, the clinical study found discontinuation of denosumab can cause rapid bone loss and increase the risk of multiple rebound-related vertebral fractures (RAVF) (Anastasilakis et al., 2021). The ideal strategy to treat osteoporosis is to both inhibit osteoclast and promote osteoblast formation. Existing treatments mostly focus on inhibiting bone desorption with side effects for long-term use.

The use of TCM as a potential treatment strategy for osteoporosis is an evolving field of investigation. Published literature and clinical trials provided evidence of efficacy of TCM herbs in experimental and clinical osteoporosis treatment (An et al., 2016; Wang et al., 2017). However, there is still a lack of strong experimental evidence and mechanism elaboration of TCM treatment. More effective therapy is under investigation. In the present study, we elaborated the efficacy of E.C.D. extracts in treating experimental GIO rats. GIO results in an overactive osteoclast and bone resorption in rats, with low levels of calcium and phosphorus in serum. The calcium and

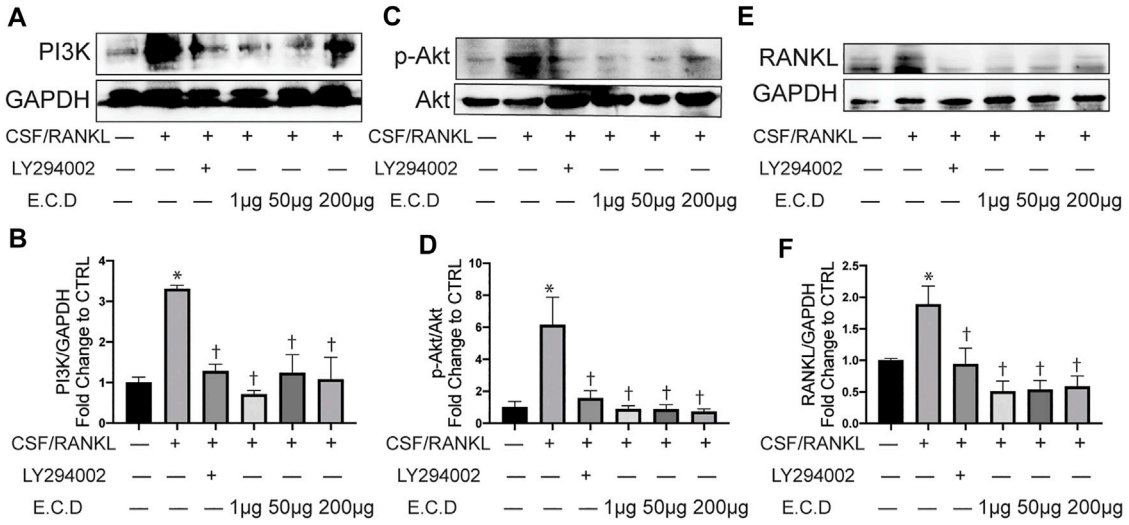

FIGURE 8 | E.C.D. extracts inhibited osteoclast differentiation through regulating PI3k/Akt pathway. PI3K inhibitor (LY294002) was added 2 h before C/R induction. Raw264.7 cells were stimulated with C/R. E.C.D. extracts in different doses (1 μg/ml, 50 μg/ml, 200 μg/ml) were added at the same time for 48 h. **(A)** Representative Western blotting images of PI3K and GAPDH. **(B)** Fold changes in relative densitometric values of PI3K. **(C)** Representative Western blotting images of p-Akt and Akt. **(D)** Fold changes in relative densitometric values of p-Akt. **(E)** Representative Western blotting images of RANKL and GAPDH. **(F)** Fold changes in relative densitometric values of RANKL. $n = 3$, data was analyzed as mean ± SEM, * vs. CTRL group (CSF/RANKL–LY294002– E.C.D–), † vs. C/R group (CSF/RANKL + LY294002–E.C.D–), $p < 0.05$.

phosphorus were lost from urine which results in a decreased level in serum. Moreover, the GC administration resulted in weight decrease of rats. In our study, E.C.D. extracts treatment protected the weight loss of rats after GC administration. With the doses increasing, the protecting function improved. Meanwhile, the level of calcium and phosphorus in serum were improved by E.C.D. extracts compared with the GC group. The dose of E.C.D. extracts effected the therapeutic function. With the dose increasing, E.C.D. extracts are more effective. Apart from protecting loss of serum calcium and phosphorus, the cytokines in serum also reflected the bone metabolism balance. E.C.D. extracts with high dose significantly decreased the osteoclast-related cytokine release RANKL and increased the osteoblast-related cytokine OPG. The bone histology also showed the trabecular bone destruction and bone marrow loss in the GC group. E.C.D. extracts effectively improved the bone structural elasticity and hardness of GIO rats based on the bone biomechanical measurement. Bone strength depends on all three factors: bone geometry, thickness, and density (Buehring et al., 2013). The micro-CT scan helped to further understand the effect of E.C.D. extracts on bone microstructure and bone strength of experimental GIO rats, which indicated E.C.D. extracts dramatically improved the integrity, thickness, and density of bone in GIO rats.

Currently, most treatments in clinic for osteoporosis are phosphate supplements or targeting through regulating bone metabolism by RANKL/OPG pathway (Compston et al., 2019). MAPK/NF-κB and Wnt/GSK-3β/β-catenin signaling pathway are also demonstrated to play important roles in osteoclast genesis (An et al., 2019; Wang et al., 2020). Xiao L. et al. found Puerarin can suppress osteoclastogenesis via inhibition of TRAF6/ROS-dependent MAPK/NF-κB signaling pathways (Masanobu, 2014) in ovariectomy (OVX)-induced osteoporosis model mice. Even though several signaling pathways are shown as a critical effector for osteoclast formation, there is still under investigation the mediation of TCM to potential signaling pathway during osteoclast formation. The natural herbs are usually more difficult to be clarified in a specific pathway which regulates biological metabolism because of its complex components especially for compound. To further understand the mechanism of the function of E.C.D. extracts alleviating osteoporosis, we processed HPLC analysis and investigated the potential targets mediated by E.C.D. extracts which have the potential to treat osteoporosis. The potential targets of E.C.D. extracts which may mediate the signaling pathway to treat osteoporosis were analyzed by the network pharmacology analysis. KEGG enriched pathway indicated E.C.D. extracts have the identified constituents which mostly targeted proteins in the PI3K/Akt pathway. The PI3K/Akt pathway is a crucial signaling pathway regulating cell proliferation and survival. Jang Bae Moon et al. demonstrated PI3K/Akt/GSK3β/NFATc1 signaling pathway regulates osteoclast differentiation (Moon et al., 2012). Wu L et al. found PI3K/Akt/Blimp1 signaling pathway promotes osteoclast formation (Wu et al., 2017). Tsubaki et al. (2014) found inhibition of PI3K/Akt pathways can suppress osteoclast formation. Activation of PI3K/Akt signaling cascade plays a crucial role in hyperactivation of osteoclasts in osteoporosis. For our study, to verify our hypothesis, we used PI3K inhibitor (LY294002) to pretreat Raw264.7 cells before C/R stimulation. The Western blot results indicated E.C.D. extracts inhibited PI3K expression and phosphorated Akt. At the same time, inhibition of the PI3K/Akt pathway decreased RANKL expression. Therefore, we believe E.C.D. extracts exert

function of inhibiting osteoclastogenesis through regulating the PI3K/Akt signaling pathway.

Finally, our experiment also has limitations. We demonstrated that E.C.D. extracts can alleviate experimental GIO *in vivo* and inhibit osteoclast differentiation through regulating the PI3K/Akt pathway *in vitro*. However, the bone metabolism depends on two biological processes: bone resorption by osteoclast and bone formation of osteoblast. We found E.C.D. extracts increased the OPG expression *in vivo* and promoted MSC proliferation and expression of OPG, Wnt1, and Runx2 (the protein related to osteoblast formation) *in vitro*. However, more experiments need to be conducted in the future to demonstrate this hypothesis. Also, based on a published paper, the PI3K/Akt pathway also regulates osteoblast genesis, the mechanism of E.C.D. extracts in mediating osteoblast by the PI3K/Akt pathway still need to be clarified.

The combination of Eucommia, Cuscuta, and Drynaria is widely used in TCM decoction for osteoporosis treatment. However, there are rare studies investigating the osteoporosis treatment efficacy of the combination and further clarify the mechanism. Our work proved that E.C.D. extracts have the significant efficacy in treating experimental GIO rats *in vivo*. Moreover, we processed a series of experiments *in vitro* to clarify the potential biological mechanism. Our work suggested E.C.D. extracts can down-regulate PI3K/Akt pathway to inhibit osteoclastogenesis and have therapeutic efficacy in GIO rats. It provides a novel perspective for GIO treatment in the future.

DATA AVAILABILITY STATEMENT

The original contributions presented in the study are included in the article/**Supplementary Material**. Further inquiries can be directed to the corresponding authors.

ETHICS STATEMENT

The animal study was reviewed and approved by the Laboratory Animal Ethics Committee Nanjing BIOGENE Biotech. Co. Ltd.

AUTHOR CONTRIBUTIONS

JH: Collection and assembly of data, data analysis and interpretation, manuscript writing and approval. LL: Conception and design, data analysis, and interpretation. CZ, QH: HPLC analysis, integrated network pharmacology analysis. SW: Conception and design. WL, JZ, and LJL: Collection and assembly of data, approval of manuscript. ZZ and ZL: Conception and design, approval of manuscript. QW: Conception and design, data analysis and interpretation, approval of manuscript. YS: Conception and design, data analysis and interpretation, financial support, and final approval of manuscript.

FUNDING

This work was supported by a grant from the medical security and capacity building of traditional Chinese medicine in 2020 (0332000000131). This work was also funded by company Chenland Nutritionals, Inc.

SUPPLEMENTARY MATERIAL

The Supplementary Material for this article can be found online at: https://www.frontiersin.org/articles/10.3389/fphar.2021.772944/full#supplementary-material

Supplementary Figure S1 | (A) Fingerprint of Eucommia extract. **(B)** Fingerprint of Cuscuta extract. **(C)** Fingerprint of Drynaria extract.

Supplementary Figure S2 | Micro-CT images of femur of GIO rats.

Supplementary Figure S3 | E.C.D. extracts reduced the resorption area on bone slices. **(A)** Representative phase contract images of bone resorption pit. The black arrow pointed to the resorption pit. **(B)** Representative images of toluidine blue staining of bone resorption pit. The black arrow pointed to dark blue staining of the resorption pit. **(C)** The percentage area of bone resorption pit was assessed by Image J. $n = 3$ in each group. Data was analyzed as mean ± SEM, * vs. CTRL group, † vs. +C/R group, $P<0.05$.

Supplementary Figure S4 | (A,C,E) Western blot images of PI3K, GAPDH, p-Akt, Akt, p-P38, and P38. **(B,D,F)** Quantitative protein expression of PI3K, p-Akt, and p-P38. $n = 3$ in each group. Data was analyzed as mean ± SEM, * vs. CTRL group, † vs. +C/R group, $P<0.05$.

REFERENCES

Long, X. (2020). Puerarin alleviates osteoporosis in the ovariectomy-induced mice by suppressing osteoclastogenesis via inhibition of TRAF6/ROS-dependent MAPK/NF-κB signaling pathways. *Aging* 12 (21), 21706–21729. doi:10.18632/aging.103976

Lukert, B. P., and Raisz, L. G. (1990). Glucocorticoid-induced osteoporosis: pathogenesis and management. *Annals of internal medicine* 112 (5), 352–364. doi:10.7326/0003-4819-112-5-352

Masanobu, T. (2014) Nitrogen-containing bisphosphonates inhibit RANKL- and M-CSF-induced osteoclast formation through the inhibition of ERK1/2 and Akt activation. *Journal of biomedical science* 21, 1. doi:10.1186/1423-0127-21-10

Adler, R. A., El-Hajj Fuleihan, G., Bauer, D. C., Camacho, P. M., Clarke, B. L., Clines, G. A., et al. (2016). Managing Osteoporosis in Patients on Long-Term Bisphosphonate Treatment: Report of a Task Force of the American Society for Bone and Mineral Research. *J. Bone Miner Res.* 31 (1), 16–35. doi:10.1002/jbmr.2708

An, J., Yang, H., Zhang, Q., Liu, C., Zhao, J., Zhang, L., et al. (2016). Natural Products for Treatment of Osteoporosis: The Effects and Mechanisms on Promoting Osteoblast-Mediated Bone Formation. *Life Sci.* 147, 46–58. doi:10.1016/j.lfs.2016.01.024

An, Y., Zhang, H., Wang, C., Jiao, F., Xu, H., Wang, X., et al. (2019). Activation of ROS/MAPKs/NF-κB/NLRP3 and Inhibition of Efferocytosis in Osteoclast-Mediated Diabetic Osteoporosis. *FASEB J* 33 (11), 12515–12527. doi:10.1096/fj.201802805RR

Anastasilakis, A. D., Polyzos, S. A., Makras, P., Trovas, G., Yavropoulou, M. P., and Tournis, S. (2021). Efficacy of Antiosteoporotic Medications in Patients with Rebound-Associated Fractures after Denosumab Discontinuation. *J. Clin. Densitom.* 24 (4), 591–596. doi:10.1016/j.jocd.2021.01.006

Andrzejewska, A., Lukomska, B., and Janowski, M. (2019). Concise Review: Mesenchymal Stem Cells: From Roots to Boost. *Stem Cells* 37 (7), 855–864. doi:10.1002/stem.3016

Armas, L. A., and Recker, R. R. (2012). Pathophysiology of Osteoporosis: New Mechanistic Insights. *Endocrinol. Metab. Clin. North. Am.* 41 (3), 475–486. doi:10.1016/j.ecl.2012.04.006

Bai, S., Kitaura, H., Zhao, H., Chen, J., Müller, J. M., Schüle, R., et al. (2005). FHL2 Inhibits the Activated Osteoclast in a TRAF6-Dependent Manner. *J. Clin. Invest.* 115 (10), 2742–2751. doi:10.1172/JCI24921

Boyce, B. F., and Xing, L. (2008). Functions of RANKL/RANK/OPG in Bone Modeling and Remodeling. *Arch. Biochem. Biophys.* 473 (2), 139–146. doi:10.1016/j.abb.2008.03.018

Brown, J. P., Delmas, P. D., Malaval, L., Edouard, C., Chapuy, M. C., and Meunier, P. J. (1984). Serum Bone Gla-Protein: A Specific Marker for Bone Formation in Postmenopausal Osteoporosis. *Lancet* 1 (8386), 1091–1093. doi:10.1016/s0140-6736(84)92506-6

Buehring, B., Viswanathan, R., Binkley, N., and Busse, W. (2013). Glucocorticoid-Induced Osteoporosis: An Update on Effects and Management. *J. Allergy Clin. Immunol.* 132 (5), 1019–1030. doi:10.1016/j.jaci.2013.08.040

Canalis, E., Mazziotti, G., Giustina, A., and Bilezikian, J. P. (2007). Glucocorticoid-Induced Osteoporosis: Pathophysiology and Therapy. *Osteoporos. Int.* 18 (10), 1319–1328. doi:10.1007/s00198-007-0394-0

Chen, Q., Shou, P., Zheng, C., Jiang, M., Cao, G., Yang, Q., et al. (2016). Fate Decision of Mesenchymal Stem Cells: Adipocytes or Osteoblasts? *Cell Death Differ* 23 (7), 1128–1139. doi:10.1038/cdd.2015.168

Choksi, P., Jepsen, K. J., and Clines, G. A. (2018). The Challenges of Diagnosing Osteoporosis and the Limitations of Currently Available Tools. *Clin. Diabetes Endocrinol.* 4, 12. doi:10.1186/s40842-018-0062-7

Chotiyarnwong, P., and McCloskey, E. V. (2020). Pathogenesis of Glucocorticoid-Induced Osteoporosis and Options for Treatment. *Nat. Rev. Endocrinol.* 16 (8), 437–447. doi:10.1038/s41574-020-0341-0

Compston, J. (2018). Glucocorticoid-Induced Osteoporosis: An Update. *Endocrine* 61 (1), 7–16. doi:10.1007/s12020-018-1588-2

Compston, J. E., McClung, M. R., and Leslie, W. D. (2019). Osteoporosis. *Lancet* 393 (10169), 364–376. doi:10.1016/s0140-6736(18)32112-3

Cui, J., Li, X., Wang, S., Su, Y., Chen, X., Cao, L., et al. (2020). Triptolide Prevents Bone Loss via Suppressing Osteoclastogenesis through Inhibiting PI3K-AKT-NFATc1 Pathway. *J. Cel Mol Med* 24 (11), 6149–6161. doi:10.1111/jcmm.15229

Ersahin, T., Tuncbag, N., and Cetin-Atalay, R. (2015). The PI3K/AKT/mTOR Interactive Pathway. *Mol. Biosyst.* 11 (7), 1946–1954. doi:10.1039/c5mb00101c

Fait, T. (2019). Menopause Hormone Therapy: Latest Developments and Clinical Practice. *Drugs Context* 8, 212551. doi:10.7573/dic.212551

Fu, Y. X., Gu, J. H., Zhang, Y. R., Tong, X. S., Zhao, H. Y., Yuan, Y., et al. (2013). Osteoprotegerin Influences the Bone Resorption Activity of Osteoclasts. *Int. J. Mol. Med.* 31 (6), 1411–1417. doi:10.3892/ijmm.2013.1329

He, J., Li, X., Wang, Z., Bennett, S., Chen, K., Xiao, Z., et al. (2019). Therapeutic Anabolic and Anticatabolic Benefits of Natural Chinese Medicines for the Treatment of Osteoporosis. *Front. Pharmacol.* 10, 1344. doi:10.3389/fphar.2019.01344

He, L., Guan, Q. Q., Peng, L. C., Chen, K. L., and Chai, X. S. (2017). Improvement of Alkali Efficiency for Purification of Dissolving Pulp by a Modified Cold Caustic Extraction Process. *Carbohydr. Polym.* 178, 412–417. doi:10.1016/j.carbpol.2017.09.085

Iba, K., Takada, J., Hatakeyama, N., Ozasa, Y., Wada, T., and Yamashita, T. (2008). Changes in Urinary NTX Levels in Patients with Primary Osteoporosis Undergoing Long-Term Bisphosphonate Treatment. *J. Orthop. Sci.* 13 (5), 438–441. doi:10.1007/s00776-008-1265-z

Jia, M., Nie, Y., Cao, D. P., Xue, Y. Y., Wang, J. S., Zhao, L., et al. (2012). Potential Antiosteoporotic Agents from Plants: a Comprehensive Review. *Evid. Based Complement. Alternat Med.* 2012, 364604. doi:10.1155/2012/364604

Kao, S. J., Lei, H. C., Kuo, C. T., Chang, M. S., Chen, B. C., Chang, Y. C., et al. (2005). Lipoteichoic Acid Induces Nuclear Factor-KappaB Activation and Nitric Oxide Synthase Expression via Phosphatidylinositol 3-Kinase, Akt, and P38 MAPK in RAW 264.7 Macrophages. *Immunology* 115 (3), 366–374. doi:10.1111/j.1365-2567.2005.02160.x

Karadeniz, F., Oh, J. H., Lee, J. I., Seo, Y., and Kong, C. S. (2020). 3,5-Dicaffeoyl-epi-Quinic Acid from Atriplex Gmelinii Enhances the Osteoblast Differentiation of Bone Marrow-Derived Human Mesenchymal Stromal Cells via WnT/BMP Signaling and Suppresses Adipocyte Differentiation via AMPK Activation. *Phytomedicine* 71, 153225. doi:10.1016/j.phymed.2020.153225

Khosla, S., and Hofbauer, L. C. (2017). Osteoporosis Treatment: Recent Developments and Ongoing Challenges. *Lancet Diabetes Endocrinol.* 5 (11), 898–907. doi:10.1016/S2213-8587(17)30188-2

Kim, J. M., Lin, C., Stavre, Z., Greenblatt, M. B., and Shim, J. H. (2020). Osteoblast-Osteoclast Communication and Bone Homeostasis. *Cells* 9 (9). doi:10.3390/cells9092073

Komori, T. (2019). Regulation of Proliferation, Differentiation and Functions of Osteoblasts by Runx2. *Int. J. Mol. Sci.* 20 (7), 1694. doi:10.3390/ijms20071694

Komori, T. (2018). Runx2, an Inducer of Osteoblast and Chondrocyte Differentiation. *Histochem. Cel Biol* 149 (4), 313–323. doi:10.1007/s00418-018-1640-6

Lane, J. M., Russell, L., and Khan, S. N. (2000). Osteoporosis. *Clin. Orthop. Relat. Res.* 372, 139–150. doi:10.1097/00003086-200003000-00016

Liao, R., Feng, Z., Li, W., Liu, R., Xu, X., Yao, S., et al. (2021). Interleukin-1 Induces Receptor Activator of Nuclear Factor-Kb Ligand-Independent Osteoclast Differentiation in RAW264.7 Cells. *Exp. Ther. Med.* 21 (6), 640. doi:10.3892/etm.2021.10072

Lin, T. H., Yang, R. S., Wang, K. C., Lu, D. H., Liou, H. C., Ma, Y., et al. (2013). Ethanol Extracts of Fresh Davallia Formosana (WL1101) Inhibit Osteoclast Differentiation by Suppressing RANKL-Induced Nuclear Factor- κ B Activation. *Evid. Based Complement. Alternat Med.* 2013, 647189. doi:10.1155/2013/647189

Miller, P. D. (2009). Denosumab: Anti-RANKL Antibody. *Curr. Osteoporos. Rep.* 7 (1), 18–22. doi:10.1007/s11914-009-0004-5

Mo, H., Zhang, N., Li, H., Li, F., and Pu, R. (2019). Beneficial Effects of Cuscuta Chinensis Extract on Glucocorticoid-Induced Osteoporosis through Modulation of RANKL/OPG Signals. *Braz. J. Med. Biol. Res.* 52 (12), e8754. doi:10.1590/1414-431X20198754

Moon, J. B., Kim, J. H., Kim, K., Youn, B. U., Ko, A., Lee, S. Y., et al. (2012). Akt Induces Osteoclast Differentiation through Regulating the GSK3β/NFATc1 Signaling Cascade. *J. Immunol.* 188 (1), 163–169. doi:10.4049/jimmunol.1101254

Qaseem, A., Forciea, M. A., McLean, R. M., and Denberg, T. D. (2017). Treatment of Low Bone Density or Osteoporosis to Prevent Fractures in Men and Women: A Clinical Practice Guideline Update from the American College of Physicians. *Ann. Intern. Med.* 166 (11), 818–839. doi:10.7326/M15-1361

Sambrook, P., and Cooper, C. (2006). Osteoporosis. *The Lancet* 367 (9527), 2010–2018. doi:10.1016/s0140-6736(06)68891-0

Sang Shurong, Y. L. (1993). *Wonderful Recipe for Nourishing Kidney and Longevity*. Harbin: Heilongjiang Science and Technology Press, 04. [ISBN Number] 7-5388-2170-8.

Sapkota, M., Li, L., Choi, H., Gerwick, W. H., and Soh, Y. (2015). Bromo-Honaucin A Inhibits Osteoclastogenic Differentiation in RAW 264.7 Cells via Akt and ERK Signaling Pathways. *Eur. J. Pharmacol.* 769, 100–109. doi:10.1016/j.ejphar.2015.11.003

Silva, I., and Branco, J. C. (2011). Rank/Rankl/opg: Literature Review. *Acta Reumatol Port* 36 (3), 209–218.

Sözen, T., Özışık, L., and Başaran, N. Ç. (2017). An Overview and Management of Osteoporosis. *Eur. J. Rheumatol.* 4 (1), 46–56. doi:10.5152/eurjrheum.2016.048

Swanson, C., Lorentzon, M., Conaway, H. H., and Lerner, U. H. (2006). Glucocorticoid Regulation of Osteoclast Differentiation and Expression of Receptor Activator of Nuclear Factor-KappaB (NF-KappaB) Ligand, Osteoprotegerin, and Receptor Activator of NF-kappaB in Mouse Calvarial Bones. *Endocrinology* 147 (7), 3613–3622. doi:10.1210/en.2005-0717

Tobeiha, M., Moghadasian, M. H., Amin, N., and Jafarnejad, S. (2020). RANKL/RANK/OPG Pathway: A Mechanism Involved in Exercise-Induced Bone Remodeling. *Biomed. Res. Int.* 2020, 6910312. doi:10.1155/2020/6910312

Tsubaki, M., Komai, M., Itoh, T., Imano, M., Sakamoto, K., Shimaoka, H., et al. (2014). Nitrogen-Containing Bisphosphonates Inhibit RANKL- and M-CSF-Induced Osteoclast Formation through the Inhibition of ERK1/2 and Akt Activation. *J. Biomed. Sci.* 21 (1), 10. doi:10.1186/1423-0127-21-10

Wang, T., Liu, Q., Tjhioe, W., Zhao, J., Lu, A., Zhang, G., et al. (2017). Therapeutic Potential and Outlook of Alternative Medicine for Osteoporosis. *Curr. Drug Targets* 18 (9), 1051–1068. doi:10.2174/1389450118666170321105425

Wang, Y., Chen, J., Chen, J., Dong, C., Yan, X., Zhu, Z., et al. (2020). Daphnetin Ameliorates Glucocorticoid-Induced Osteoporosis via Activation of Wnt/GSK-3β/β-Catenin Signaling. *Toxicol. Appl. Pharmacol.* 409, 115333. doi:10.1016/j.taap.2020.115333

Wu, L., Guo, Q., Yang, J., and Ni, B. (2017). Tumor Necrosis Factor Alpha Promotes Osteoclast Formation via PI3K/Akt Pathway-Mediated Blimp1 Expression Upregulation. *J. Cel Biochem* 118 (6), 1308–1315. doi:10.1002/jcb.25672

Yang, Y., Yu, T., Tang, H., Ren, Z., Li, Q., Jia, J., et al. (2020). Ganoderma Lucidum Immune Modulator Protein rLZ-8 Could Prevent and Reverse Bone Loss in Glucocorticoids-Induced Osteoporosis Rat Model. *Front. Pharmacol.* 11, 731. doi:10.3389/fphar.2020.00731

Yeon, J. T., Kim, K. J., Son, Y. J., Park, S. J., and Kim, S. H. (2019). Idelalisib Inhibits Osteoclast Differentiation and Pre-Osteoclast Migration by Blocking the PI3Kδ-Akt-C-Fos/NFATc1 Signaling Cascade. *Arch. Pharm. Res.* 42 (8), 712–721. doi:10.1007/s12272-019-01163-8

Zeng, X. Z., He, L. G., Wang, S., Wang, K., Zhang, Y. Y., Tao, L., et al. (2016). Aconine Inhibits RANKL-Induced Osteoclast Differentiation in RAW264.7 Cells by Suppressing NF-Kb and NFATc1 Activation and DC-STAMP Expression. *Acta Pharmacol. Sin* 37 (2), 255–263. doi:10.1038/aps.2015.85

Zhao, C., Sun, W., Zhang, P., Ling, S., Li, Y., Zhao, D., et al. (2015). miR-214 Promotes Osteoclastogenesis by Targeting Pten/PI3k/Akt Pathway. *RNA Biol.* 12 (3), 343–353. doi:10.1080/15476286.2015.1017205

Zhou, R. P., Lin, S. J., Wan, W. B., Zuo, H. L., Yao, F. F., Ruan, H. B., et al. (2016). Chlorogenic Acid Prevents Osteoporosis by Shp2/PI3K/Akt Pathway in Ovariectomized Rats. *PLoS One* 11 (12), e0166751. doi:10.1371/journal.pone.0166751

Conflict of Interest: Author LL, SW, WL, JZ, and ZL were employed by the company Chenland Nutritionals, Inc.

The remaining authors declare that the research was conducted in the absence of any commercial or financial relationships that could be construed as a potential conflict of interest.

The authors declare that this study received funding from company henland Nutritionals, Inc. The funder had the following involvement with the study: study design, decision to submit it.

Publisher's Note: All claims expressed in this article are solely those of the authors and do not necessarily represent those of their affiliated organizations, or those of the publisher, the editors, and the reviewers. Any product that may be evaluated in this article, or claim that may be made by its manufacturer, is not guaranteed or endorsed by the publisher.

Copyright © 2022 Han, Li, Zhang, Huang, Wang, Li, Zong, Li, Zhao, Zhang, Liu, Wang and Shi. This is an open-access article distributed under the terms of the Creative Commons Attribution License (CC BY). The use, distribution or reproduction in other forums is permitted, provided the original author(s) and the copyright owner(s) are credited and that the original publication in this journal is cited, in accordance with accepted academic practice. No use, distribution or reproduction is permitted which does not comply with these terms.

frontiers in Pharmacology

ORIGINAL RESEARCH
published: 09 March 2022
doi: 10.3389/fphar.2022.803880

Mogrol Attenuates Osteoclast Formation and Bone Resorption by Inhibiting the TRAF6/MAPK/NF-κB Signaling Pathway *In vitro* and Protects Against Osteoporosis in Postmenopausal Mice

Yongjie Chen[1,2†], Linlin Zhang[1†], Zongguang Li[1†], Zuoxing Wu[3], Xixi Lin[3], Na Li[2,3], Rong Shen[2], Guojun Wei[1], Naichun Yu[1], Fengqing Gong[1], Gang Rui[4], Ren Xu[2,3,5]* and Guangrong Ji[1,2]**

[1]Department of Orthopedics Surgery, Xiang'an Hospital of Xiamen University, School of Medicine, Xiamen University, Xiamen, China, [2]Fujian Provincial Key Laboratory of Organ and Tissue Regeneration, School of Medicine, Xiamen University, Xiamen, China, [3]State Key Laboratory of Cellular Stress Biology, School of Medicine, Xiamen University, Xiamen, China, [4]Department of Orthopedic Surgery, The First Affiliated Hospital of Xiamen University, Xiamen, China, [5]Guangxi Key Laboratory of Regenerative Medicine, Research Centre for Regenerative Medicine, Guangxi Medical University, Nanning, China

Osteoporosis is a serious public health problem that results in fragility fractures, especially in postmenopausal women. Because the current therapeutic strategy for osteoporosis has various side effects, a safer and more effective treatment is worth exploring. It is important to examine natural plant extracts during new drug design due to low toxicity. Mogrol is an aglycon of mogroside, which is the active component of *Siraitia grosvenorii* (Swingle) and exhibits anti-inflammatory, anticancer and neuroprotective effects. Here, we demonstrated that mogrol dose-dependently inhibited osteoclast formation and function. To confirm the mechanism, RNA sequencing (RNA-seq), real-time PCR (RT–PCR), immunofluorescence and Western blotting were performed. The RNA-seq data revealed that mogrol had an effect on genes involved in osteoclastogenesis. Furthermore, RT–PCR indicated that mogrol suppressed osteoclastogenesis-related gene expression, including CTSK, ACP5, MMP9 and DC-STAMP, in RANKL-induced bone marrow macrophages Western blotting demonstrated that mogrol suppressed osteoclast formation by blocking TNF receptor-associated factor 6 (TRAF6)-dependent activation of the mitogen-activated protein kinase nuclear factor-B (NF-κB) signaling pathway, which decreased two vital downstream transcription factors, the nuclear factor of activated T cells calcineurin-dependent 1 (NFATc1) and c-Fos proteins expression. Furthermore, mogrol dramatically reduced bone mass loss in postmenopausal mice. In conclusion, these data showed that mogrol may be a promising procedure for osteoporosis prevention or therapy.

Keywords: osteoporosis, osteoclast, mogrol, TRAF6, RANKL, MAPK, NF-κB

OPEN ACCESS

Edited by:
Daohua Xu,
Guangdong Medical University, China

Reviewed by:
Ting Zheng,
Qilu University of Technology, China
Weizong Weng,
Second Military Medical University, China

***Correspondence:**
Ren Xu
xuren526@xmu.edu.cn
Gang Rui
reigang@163.com
Guangrong Ji
jiguangrong@sina.cn

†These authors have contributed equally to this work and share first authorship

Specialty section:
This article was submitted to Ethnopharmacology, a section of the journal Frontiers in Pharmacology

Received: *28 October 2021*
Accepted: *08 February 2022*
Published: *09 March 2022*

Citation:
Chen Y, Zhang L, Li Z, Wu Z, Lin X, Li N, Shen R, Wei G, Yu N, Gong F, Rui G, Xu R and Ji G (2022) Mogrol Attenuates Osteoclast Formation and Bone Resorption by Inhibiting the TRAF6/MAPK/NF-κB Signaling Pathway In vitro and Protects Against Osteoporosis in Postmenopausal Mice. Front. Pharmacol. 13:803880. doi: 10.3389/fphar.2022.803880

INTRODUCTION

Osteoporosis is a condition that affects bone density and strength, as well as microarchitecture, resulting in fragility fractures of the hip, vertebrae, and wrist (NIH Consensus Development Panel on Osteoporosis Prevention Diagnosis and Theraphy, 2001). Approximately 25% of all women aged 65 or older are affected by osteoporosis, and rapid rates of bone loss occur postmenopausal (Ensrud and Crandall, 2017). Fractures of the hip and spine caused by osteoporosis increase the risk of fatal consequences such pneumonia and thromboembolic illness (Center et al., 1999). Therefore, osteoporosis has been one of the main health problems of postmenopausal women.

Inhibiting resorption or increasing bone formation has been selected as the main therapeutic strategy for osteoporosis. In bone-forming treatments, teriparatide and abaloparatide are the main drugs. However, nausea, headache and dizziness are common side effects of teriparatide or abaloparatide (Miller et al., 2016). Furthermore, several preclinical investigations have demonstrated that these medications enhance the incidence of osteosarcoma by concentration-dependently in rats (Vahle et al., 2008; Jolette et al., 2017). Antiresorptive medicines, such as asisphosphonates, RANKL antibodies, and selective estrogen receptor modulators (SERMs), target osteoclasts, inducing their apoptosis or inhibiting their formation or recruitment (Langdahl, 2021).

Osteoclasts are the primary agents of bone resorption. A sealing zone would be created after osteoclasts bind to the bone surface via $\alpha v\beta_3$ integrin. A highly acidic microenvironment is maintained by the proton pumps and chloride channels of osteoclasts, which facilitates the catalytic activity of cathepsin K, which is a sort of lysosomal protease that breaks down collagens. Osteoclasts originate from monocytes and macrophage-derived cells that are maintained by macrophage colony-stimulating factor (M-CSF). The formation of osteoclast precursor cells to mature osteoclasts highly dependent on RANKL. Following RANKL stimulation of RANK, the key regulatory transcription factors and enzymes were activated, resulting in the promotion of osteoclast differentiation, fusion, and proliferation. TRAF6, for example, is activated when RANKL binds to RANK, which has been found to activate the protein kinase TGF-β-activated kinase (TAK1) (Xia et al., 2009). TAK1 then activated the canonical IκB kinase (IKK) complex. NF-κB, protein kinase Tp12 and mitogen-activated protein (MAP) kinase kinases (MKKs) are activated in response to IKK activation (Beinke et al., 2004; Lopez-Pelaez et al., 2014). When activated, MKKs activate c-Jun N-terminal kinases and p38 MAP kinases. MEK1 and MEK2 are activated by activated Tp12, which stimulates extracellular signal-regulated kinase 1 (ERK1) and ERK2 (Strickson et al., 2017). After activating the MAPK and NF-κB signaling pathways, NFATc1, a critical regulator of osteoclastogenesis, is eventually increased (Asagiri et al., 2005). These antiresorptive drugs treat osteoporosis by inhibiting different osteoclast physiologies. Although these drugs are effective, long-term administration is limited due to their side effects (Siris et al., 2009).

It is meaningful to find derived chemical agents or compounds that possess antiresorptive properties. Mogrol is an aglycon of mogroside, which is the active ingredient of *Siraitia grosvenorii* (Swingle). As an herbaceous native plant, *Siraitia grosvenorii* (Swingle) is a sugar substitute or traditional Chinese medicine for alleviating lung congestion, dry coughs and colds in China (Li et al., 2014). Mogrol has several pharmacological characteristics, including anti-inflammatory effects by activating AMPK signaling (Liang et al., 2021), antileukemic effects via ERK and STAT3 inhibition (Liu et al., 2015), and neuroprotective effects by inhibiting NF-κB signaling (Chen et al., 2019). Despite its great array of biological advantages, it is unknown whether mogrol affects osteoporosis and osteoclasts. This research found that mogrol suppressed the production and activity of osteoclasts derived from BMMs *in vitro*. Additionally, we also demonstrated that mogrol blocked TRAF6 recruitment, reduced MAPK and NF-B signaling activation, and ultimately restricted NFATC1 and c-FOS expression. Furthermore, we further observed that mogrol treatment reduced bone loss in mice after ovariectomy (ovaries were removed) (OVX). In summary, the outcomes of this research indicate that mogrol may promise an application for preventing or treating osteoporosis.

MATERIALS AND METHODS

Mice and Reagents

C57BL/6J mice were acquired from Xiamen University's Study Animal Center, and all animal investigations were authorized by Xiamen University's Animal Care and Use Committee (XMULAC20210037). Chengdu Must Biotechnology (Chengdu, China) have supplied mogrol with a purity >98%. Dimethylsulfoxide (DMSO) was used to dissolve mogrol. Biological Industries (BI, Beit Haemek, Israel) supplied alpha-modified Eagle's medium (α-MEM) and penicillin–streptomycin solution. Gibco (Thermo Fisher Scientific, Waltham, United States) supplemented with fetal bovine serum (FBS). Recombinant M-CSF and RANKL were acquired from R&D Systems (Minneapolis, MN, United States). Cell Signaling Technology (Danvers, United States) provided antibodies (p-ERK, ERK, p-P38, P38, p-JNK, JNK, p-P65, P65, and IκBα). Antibodies against c-FOS and TRAF6 were obtained from Abcam (Cambridge, United Kingdom). Anti-NFATc1 antibody was acquired from Santa Cruz Biotechnology (CA, United States). Anti-GAPDH antibody was purchased from Proteintech (Wuhan, China). Dojindo (Kyushu Island, Japan) provided Cell Counting Kit-8 (CCK-8). Beyotime Biotechnology, Ltd. (Shanghai, China) provided Annexin V-FITC apoptosis kits.

Cell Culture and Differentiation Assay

BMMs were flushed from the hind leg of C57BL/6J mice aged 6 weeks and then cultivated with complete α-MEM and 25 ng/ml M-CSF. After 3 days, the media was replenished. BMMs were then digested and planted at a density of 6×10^3 cells/well onto 96-well plates and cultivated overnight. After adherence, 30 ng/ml RANKL was used to initiate BMMs differentiation and various

TABLE 1 | The primer sets used are as follows.

ACP5	Forward: 5′-TGTGGCCATCTTTATGCT-3′ Reverse: 5′-GTCATTTCTTTGGGGCTT-3′
DC-STAMP	Forward: 5′-CTTGCAACCTAAGGGCAA AG-3′ Reverse: 5′-TCA ACAGCTCTGTCGTGA CC-3′
ATP6V0d2	Forward: 5′-GTGAGACCTTGGAAGACCTGAA-3′ Reverse: 5′-GAGAAATGTGCTCAGGGGCT-3′
MMP-9	Forward: 5′-CGTGTCTGGAGATTCGACTTGA-3′ Reverse: 5′-TTGGAAACTCACACGCCAGA-3′
CTSK	Forward: 5′-GGCCAACTCAAGAAGAAAAC3′ Reverse: 5′GTGCTTGCTTCCCTTCTGG-3′
β-Actin	Forward: 5′-TCTGCTGGAAGGTGGACAGT-3′ Reverse: 5′-CCTCTATGCCAACACAGTGC-3′

Abbreviations: ACP5, acid phosphatase 5; ATP6V0d2, ATPase H+ transporting V0 subunit D2; CTSK, cathepsin K; DC-STAMP, dendritic cell-specific transmembrane protein; MMP-9, matrix metallopeptidase 9.

doses of mogrol was used to simultaneously treat these cells. Every 2 days, the cultural media were changed. Tartrate-resistant acid phosphatase (TRAP) was utilized to stain the cells fixed with 4% paraformaldehyde (PFA) on the fifth day. For the purpose of determining which stage of osteoclastogenesis was suppressed, BMMs were cultivated with mogrol and RANKL for 1, 3, or 5 days. At 6th day, the TRAP staining was conducted. Under a microscope (Olympus IX51, Japan), TRAP-positive cells with three or more nuclei were regarded as mature osteoclasts.

Cytotoxicity Assay

CCK-8 and flow cytometry were conducted to oberve the cytotoxic impact of mogrol on BMMs. For cell viability analysis, BMMs were treated with or without varying doses of mogrol (2.5, 5, 10, 20, 40, 80, or 160 μM). After 48 or 96 h of culture, cells were treated with CCK-8 solution for 2 h before being scanned with a multimode scanner at 450 nm (Biotek, United States). Apoptotic cell death caused by mogrol was quantified utilizing an Annexin-V-FITC apoptosis detection kit. BMMs were seeded onto 10 cm disks incubated with mogrol (or 0.1% DMSO) after being allowed to adhere for 48 h. FITC-labeled Annexin V and PI were utilized to incubate the cells for 15 min after being digested, washed and resuspended, and then examined using flow cytometry (Beckman, United States).

Immunofluorescence Staining

F-actin staining was used to explore whether mogrol affected the actin cytoskeleton. BMMs stimulated with RANKL were cultured with 20 μM mogrol on 35 mm confocal plates for 5 days, and the control group was treated with 0.1% DMSO. Next, 4% PFA was used to fix these cells, which were then permeabilized with 0.1% Triton X-100 and incubated with 3% bovine serum albumin (BSA). Following these preceding processes, rhodamine-conjugated phalloidin was tuilzed to stain the cells, and their nuclei were counterstain by 4′,6-diamidino-2-phenylindole (DAPI). BMMs were incubated overnight without or with RANKL and/or mogrol to detect the intracellular localization of P65. The cells were treated with a P65 antibody (1:200) and a secondary antibody (1:1,000) following fixation and permeabilization. DAPI was used to counterstain the nuclei. On a confocal fluorescence microscope (Leica, Germany), we analyzed the fluorescence of podosomal belts and the intracellular location of P65. Quantitative analysis of F-actin length was performed using ImageJ software.

Bone Resorption Analysis

BMMs were planted on bovine bone slices with stimulation of 30 ng/ml RANKL for 5 days. After forming mature osteoclasts, cells were then incubated with varying doses of mogrol (0, 5, 10, 20 μM) for 3–4 days. Scanning electron microscopy was used to examine and capture resorption on bone slices. The resorption pit was calculated using ImageJ software.

RNA-Seq and RT–PCR

Total RNA was extracted from BMMs that had been stimulated with 30 ng/ml RANKL and treated without or with 20 μM mogrol for 5 days using an RNA isolation kit (Vazyme, Nanjing, China) based on the manufacturer's protocol. GENEWIZ, Inc. (Suzhou, Jiangsu, China) prepared and sequenced RNA libraries on an Illumina HiSeq platform. We obtained reference genome sequences indexed by Hisat2 (v2.0.1) and gene model annotation files for related species from genome websites such as UCSC, NCBI, and ENSEMBL. Hisat2 software was used to align clean data to the reference genome. Differential expression analysis was performed using DESeq2 Bioconductor software. Dispersion and logarithmic fold change estimates were computed using data-driven prior distributions, and the Padj of genes was adjusted to 0.05 to identify genes that were differentially expressed between the two groups of subjects. GOSeq (v1.34.1) was used to categorize Gene Ontology (GO) items and generate a list of enriched genes with Padj values < 0.05. Using in-house scripts, we identified significantly differentially expressed genes in KEGG pathway annotations.

RT–PCR was utilized to examine osteoclastogenesis marker gene expression. BMMs were cultured with complete α-MEM containing 25 ng/ml M-CSF, 30 ng/ml RANKL and various dose of mogrol (0, 5, 10, 20 μM) in 6-well plates. At the fifth day, total RNA was isolated utilizing an RNA isolation kit. Five hundred nanograms of RNA was utilized to reverse transcribe complementary DNA (cDNA) by Vazyme's HiScript II Q RT SuperMix (Nanjing, China) for qPCR. The cDNA was then used as a template for qPCR, and ChamQ Universal SYBR qPCR Master Mix (Vazyme, Nanjing, China) was used to examine gene expression. The $2^{-\triangle\triangle CT}$ method was used to normalize the expression of the identified genes to that of β-actin. **Table 1** contains the primer sequences.

Western Blotting

To observe the impact of mogrol on early RANKL-stimulated signaling events over a short time course, BMMs were fasted for 4 h, pretreated with or without 20 μM mogrol, and then activated by 50 ng/ml RANKL at 0, 5, 10, 20, 30, or 60 min in 6-well plates. To study late RANKL-stimulated signaling events, BMMs were cultured with or without 20 μM mogrol for 0, 1, 3, or 5 days with stimulation of RANKL. Total cellular proteins were extracted,

separated and transferred to nitrocellulose membranes, which were then treated overnight at 4°C with moderate shaking with primary antibodies after being blocked for 1 h with 5% BSA. After rinsing the membranes, secondary antibodies conjugated to horseradish peroxidase (HRP) (CST, Danvers, MA, United States) were added to the blots. After incubation for 1 h, the membranes were submitted to chemiluminescence (Beijing Sage Creation, China).

OVX Mouse Model

Eighteen female C5BL/6J mice aged 12 weeks were prepped to establish an OVX mouse model and then randomly split into 3 groups ($n = 6$): sham (without surgery), OVX and mogrol group (with surgery plus 10 mg/kg mogrol). After the mice were anesthetized with isoflurane, all mice underwent OVX operations or sham. A 0.5–0.8 cm incision was made in the midline of the back to remove the ovaries. One week after surgery, the mice of the sham or OVX group were administered intraperitoneally normal saline, and the mice of the mogrol group were injected 10 mg/kg mogrol intraperitoneally every second day. At 7th week, all of the mice were sacrificed. For future experiments, the femurs were collected and preserved in 70% ethyl alcohol.

Micro-Computed Tomography (CT) Analysis

After scanning each femur using micro-CT (SkyScan, United States), the images were utilized to generate three-dimensional (3D) reconstructions of the femur. Testing parameters: 60 kV (source voltage), 160 μA (source current), rotation step of 0.4°, AI 0.25 mm filter and a pixel size of 10 μm. The NRecon program was utilized to reconstruct the images from micro-CT scans. The region of interest (ROI) of trabecular bone was set at 0.5 mm above the distal femur growth plate and 1 mm in length, while the cortical bone ROI was defined as 1 mm in height in the midpiece, and binarization was performed using a constant threshold (80–255). With the use of the cTAn program, some parameters were analyzed, including bone volume/tissue volume (BV/TV), trabecular thickness (Tb. Th), trabecular separation (Tb. Sp), trabecular number (Tb. N), bone surface/bone volume (BS/BV), and cross-sectional thickness (Cs.th).

Histological Assessment

The femurs were then dehydrated with gradient alcohol, infiltrated with a solution containing benzoylperoside, nonylphenolpolyglykoletheracetate, and methyl methacrylate, and finally embedded in methyl methacrylate (Hahn et al., 1991). Then, the blocks were sliced into 7 μm sections for von Kossa staining or 5 μm sections for TRAP staining. Images were acquired by light microscopy (Olympus, Japan) and analyzed by Osteomeasure (OsteoMetrics, Inc., United States). In von Kossa staining, the bone parameter BV/TV was used for analysis. While The osteoclast surface/bone surface area (Oc. S/BS) and the number of osteoclasts/bone perimeter (N. Oc/B) were analyzed by TRAP staining.

Statistical Analysis

All data in this research are shown as the mean ± standard deviation (SD). Student's t test was used to compare two groups, and one-way analysis of variance (ANOVA) with Dunnett's (each group compared with the control group) or Tukey's post hoc tests (each group compared with every other group) were employed for multiple comparisons. All data were acquired from at least three independent experiments. The results with $^{*}p < 0.05$, $^{**}p < 0.01$ or $^{***}p < 0.001$ were regarded as statistically significant.

RESULTS

Mogrol Suppressed RANKL-Stimulated Osteoclastogenesis Without Cytotoxicity

The toxicity of mogrol on BMMs was first investigated at 48 and 96 h. The CCK-8 assay revealed that mogrol (**Figure 1A**) had no cytotoxic effects at concentrations below 40 μM (**Figure 1B**). However, mogrol suppressed the proliferation of BMMs at a concentration of 80 μM and had a significant cytotoxic impact on BMMs at a concentration of 160 μM. Furthermore, there was no impact on BMM apoptosis in response to 20 μM mogrol for 48 h (**Figure 1C**). To demonstrate whether mogrol inhibits osteoclastogenesis, BMMs were cultivated with various dose of mogrol (0, 5, 10, 20 μM) with stimulation of RANKL. Multinucleated cells (three or more nuclei) stained for TRAP activity were regarded as mature osteoclasts. Mogrol inhibited osteoclast formation by dose-dependently. TRAP-positive multinucleated osteoclasts decreased from 236.67 ± 37.07/well in the absence of mogrol to 20.0 ± 6.08/well in the presence of 20 μM mogrol. Meanwhile, mogrol treatment significantly decreased the osteoclast area and quantity of multinucleated osteoclasts (5–10 or 10~) by dose-dependently (**Figures 2A,B**). Therefore, 20 μM mogrol could inhibit osteoclast formation without cytotoxic effects. Next, BMMs activated with RANKL were cultured with or without 20 μM mogrol for 1, 3, or 5 days to demonstrate which stage of osteoclast formation was impacted. The findings indicated that mogrol's inhibitory effect on osteoclast formation was particularly effective in the early stages (Days 1–3) (**Figures 2C,D**).

Mogrol Inhibited Osteoclast Bone Resorption

The impact of mogrol on the function of osteoclast was next examined by staining F-actin rings with rhodamine-phalloidin to look for morphological alterations in the osteoclast cytoskeleton linked to bone resorption. BMMs were cultivated with or without of 20 μM mogrol for 5 days with stimulation of RANKL, and immunofluorescence staining was performed. (**Figure 3A**). The F-actin data indicated that 20 μM mogrol considerably minified the podosomal belt, which was compatible with the retardation of osteoclast differentiation. Then, to investigate whether mogrol suppresses osteoclast bone resorption in bovine bone slices, mature osteoclasts were generated from BMMs under RANKL stimulation and cultured with 0, 5, 10, or 20 μM mogrol. Scanning electron microscopy has been utilized to observe the slices (**Figure 3C**), and the bone resorption areas were quantified using ImageJ software. As shown in **Figure 3B**, mogrol significantly decreased the resorption

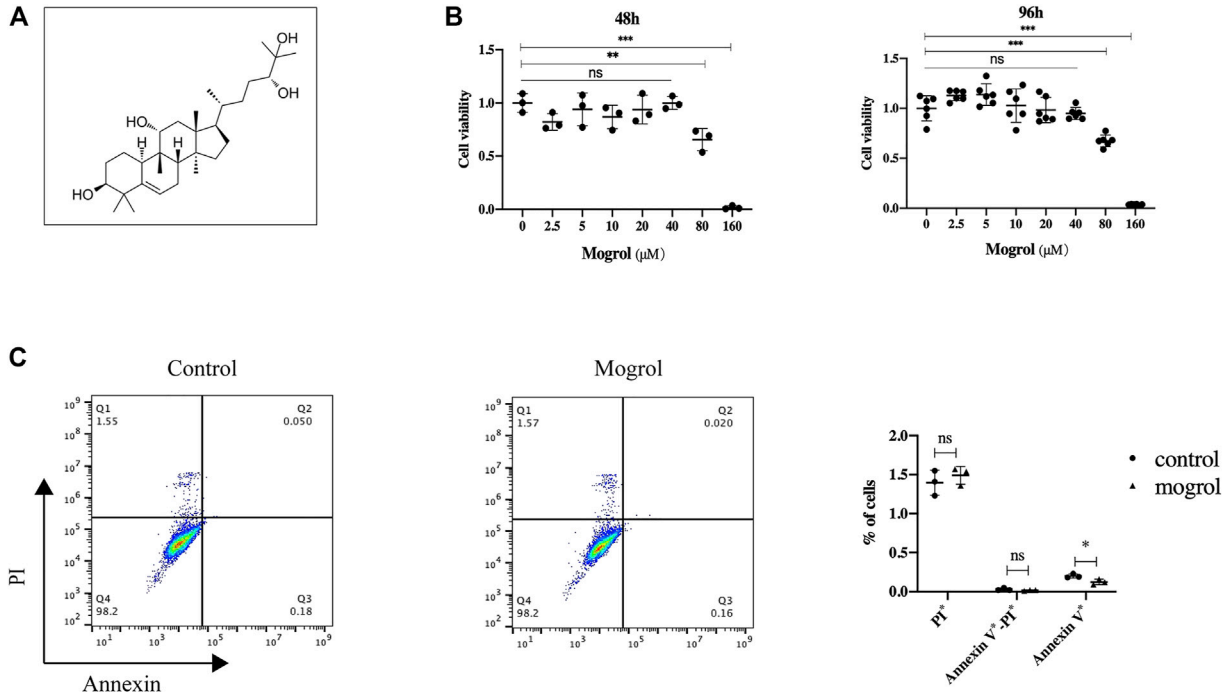

FIGURE 1 | Mogrol has no toxic effect on BMMs. **(A)** Mogrol's chemical structure. **(B)** After culturing for 48 or 96 h, a CCK-8 assay was conducted to study the impact of mogrol on BMM proliferation ($n = 6$). **(C)** Flow cytometry was utilized to analyze apoptosis of BMMs treated with 20 μM mogrol for 48 h. The histograms show the percentages of apoptotic and dead cells.

area by dose-dependently, indicating that mogrol inhibits osteoclast resorption function.

RNA-Seq Results

To examine how gene expression in RANKL-induced BMMs was altered by mogrol, RNA-seq was used to perform comprehensive gene expression analysis on BMMs induced by RANKL and cultured without or with mogrol for 5 days. The RNA-seq data revealed that in mogrol-treated cells, 64 genes were dramatically reduced <50%, while another 45 genes were considerably upregulated by > 2-fold compared to control cells (**Figure 4A**). Osteoclastogenesis suppressive genes such as lilrb4a and Fcgr3 (Onuora, 2015) were among the 45 upregulated genes, while CTSK, an osteoclast-specific gene, was among the 64 downregulated genes. Additionally, the expression of other osteoclastogenesis genes, including MMP9, OSCAR and ACP5, were lower in mogrol-treated cells. (**Figure 4B**). The GO analyses indicated that the biological processes innate immune response or the negative regulation of inflammation were enriched among the differentially expressed genes in mogrol-treated cells (**Figure 4C**). KEGG analyses also showed that the mogrol affected osteoclast differentiation (**Figure 4D**).

Mogrol Inhibited Osteoclast-Specific Gene Expression

RT–PCR was utilized to confirm osteoclastogenesis marker genes expression, such as MMP9, CTSK, ATP6v0d2, ACP5, and DC-STAMP. The findings indicated that 20 μM mogrol dramatically decreased these gene expression during osteoclast development. (**Figure 4E**).

Mogrol Suppressed the MAPK/NF-κB Signaling Pathway

The impact of mogrol on the MAPK and NF-κB signaling pathways was investigated using western blotting to determine the mechanism by which mogrol suppresses osteoclastogenesis. Western blotting indicated that the phosphorylation of JNK and p38 were dramatically suppressed by mogrol at 10 min, while ERK phosphorylation was inhibited at 5 or 10 min (**Figures 5A,B**). Meanwhile, mogrol inhibited the phosphorylation of P65 at 5 or 10 min and suppressed the degradation of IκBα at 5 min (**Figures 5C,D**). Immunofluorescence staining confirmed this discovery, showing that mogrol efficiently blocked P65 nuclear translocation, which is required for NF-κB activation (**Figure 5G**).

Mogrol Inhibited Osteoclastogenesis Proteins Expression

Subsequently, c-FOS and NFATc1 were selected to demonstrate the effect of mogrol on downstream transcription factors. BMMs activated with RANKL were cultivated with or without 20 μM mogrol for 0, 1, 3, and

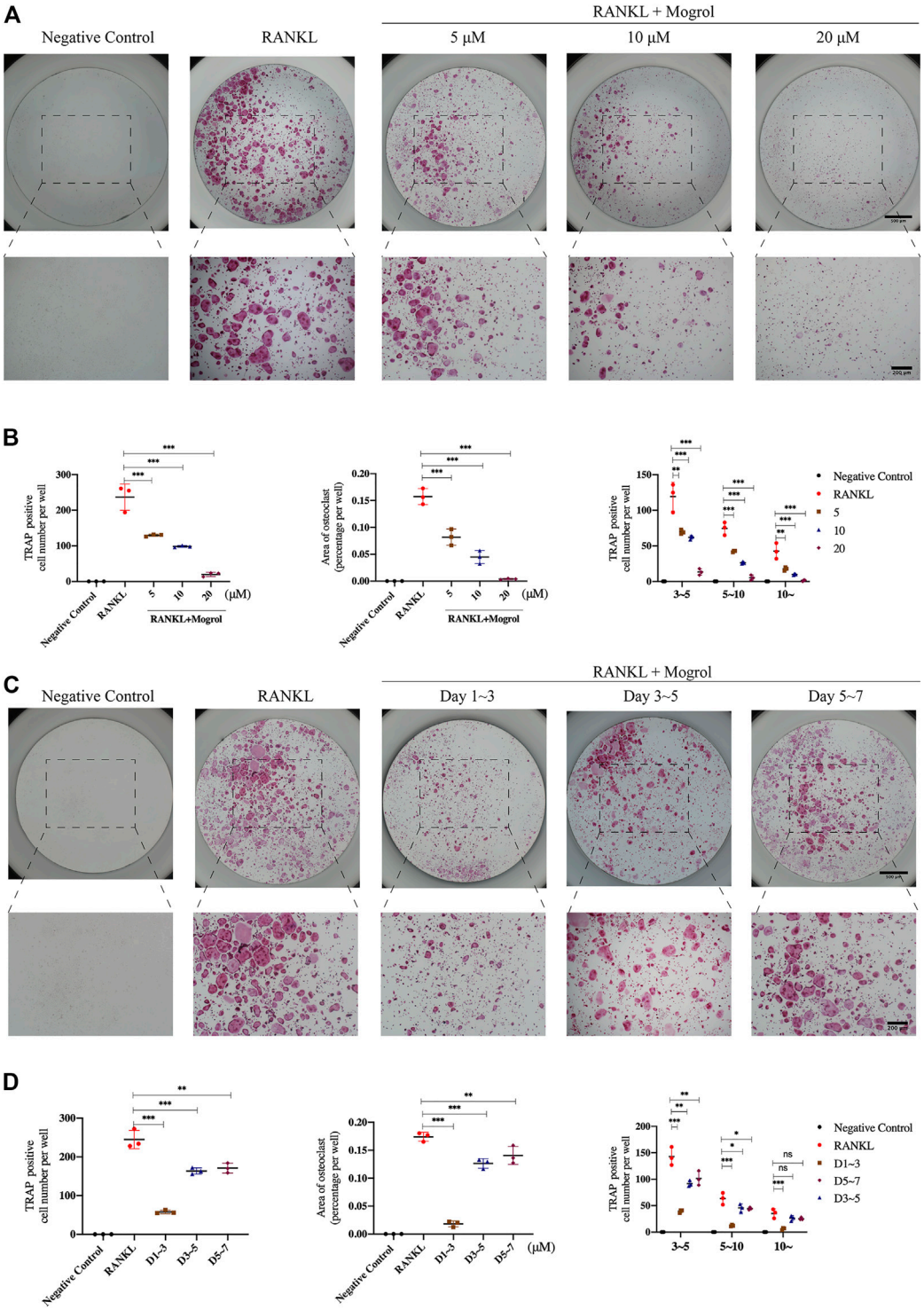

FIGURE 2 | Mogrol attenuated RANKL-activated osteoclastogenesis by time- and dose-dependently. **(A)** BMMs cultured with 0, 5, 10, or 20 μM mogrol with the stimulation of 30 ng/ml RANKL (or not). After 5 days, these cells were fixed and stained with TRAP (n = 3). **(B)** TRAP-positive multinucleated (there or more) cells were regarded as mature osteoclasts. Quantity, area and size of mature osteoclasts were quantified and analyzed. **(C)** Images of TRAP staining of BMMs stimulated without (negative control group) or with RANKL and treated without (positive control group) or with 20 μM for 1, 3, and 5 days (n = 3). **(D)** Osteoclast number, osteoclast area, and osteoclast size were all quantified.

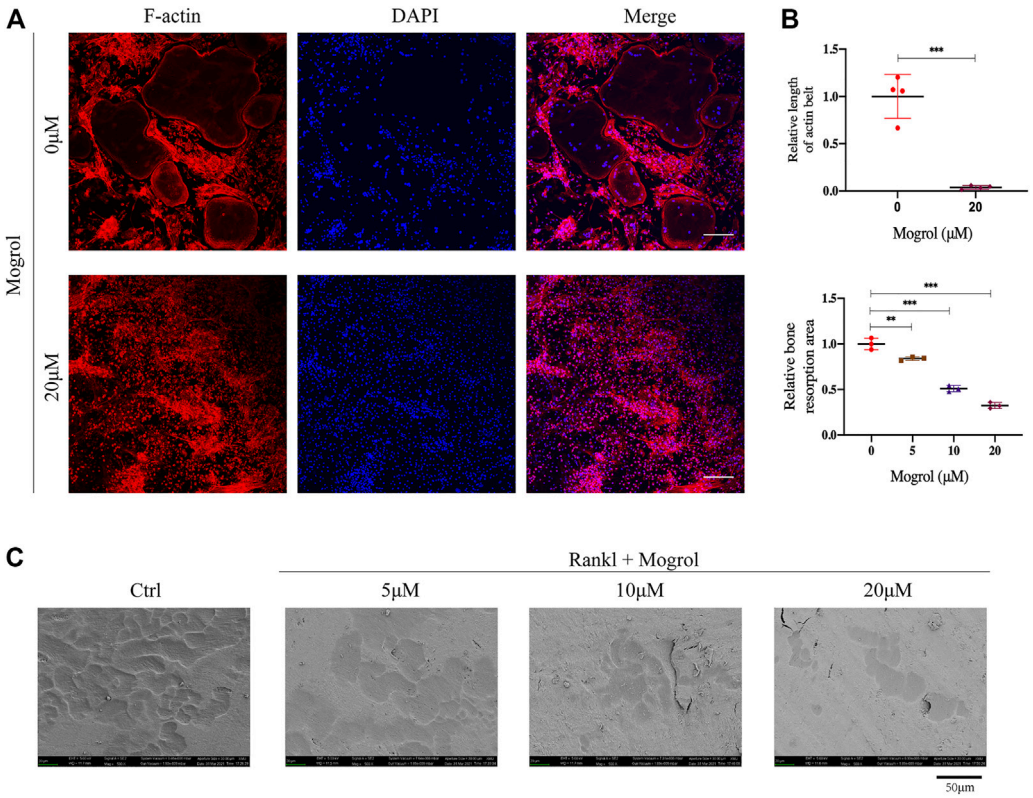

FIGURE 3 | Mogrol inhibited the formation of the podosomal belt and bone resorption. **(A)** BMMs were cultivated with (or without) 20 μM mogrol with stimulation of 30 ng/ml RANKL. After 5 days, rhodamine-conjugated phalloidin was utilized to stain the podosomal belts of osteoclasts, and DAPI were used to label their nuclei ($n = 3$), scale **(B)** Images of the bone resorptive area captured by scanning electron microscopy. ($n = 3$). **(C)** ImageJ software was utilized to measure the resorption pit area and F-actin belt length. bar = 100 μm.

5 days. The results suggested that RANKL activation increased c-FOS and NFATc1 protein expression, but mogrol substantially reduced their expression at 1 day (**Figures 5E,F**). In addition, mogrol suppressed TRAF6 and Siglec-15 expression at 3 or 5 days (**Figures 5E–H**).

Mogrol Relieved Bone Mass Loss in OVX Mice

Due to the encouraging findings obtained *in vitro*, the OVX mouse model was subsequently conducted to observe the inhibitory the effect of mogrol on osteoclasts *in vivo*. Mice were administered mogrol or normal saline every second day for 42 days. Micro-CT 3D reconstructions indicated that mogrol decreased bone loss of femurs in OVX mice. The quantitative analysis of micro-CT showed that the parameters BV/TV, Tb. Th, Tb. N and Cs. th of vehicle group were lower than sham group, while Tb. Sp and BS/BV were higher. However, BV/TV, Tb. Th, Tb. The N and Cs. th of the mogrol group were considerably higher than those of the vehicle group, while the BS/BV was inversely lower (**Figures 6A,B**). Histological assessment was conducted to further demonstrate the protective impact of Mogrol against bone loss after OVX. The Von Kossa results demonstrated that the BV/TV of the vehicle group was much lower than that of the sham group, while the BV/TV of the mogrol group was dramatically higher than that of the vehicle group (**Figures 7A,C**). Additionally, immunohistochemistry TRAP staining of femurs was used to assess the mogrol's impact on osteoclasts in OVX mice. As shown in **Figures 7B,C**, Oc. The S/BS and N. Oc/B of the mogrol group were substantially lower than those of the vehicle group. The results of animal study suggested that mogrol might dramatically attenuate bone mass loss in OVX mice.

DISCUSSION

Osteoporosis is the most common chronic bone metabolic condition and affects at least 200 million individuals globally over the age of 60 (Lane, 2006). As a result, there are more than 9 million fractures annually worldwide, with approximately one fracture every 3 s, due to osteoporosis. In particular, up to 40% of postmenopausal women suffer from osteoporosis (De Martinis et al., 2021). Moreover, 61% of osteoporotic fractures, including 70% of hip fractures, occur in women (Johnell and Kanis, 2006). Bone mineral density (BMD) is utilized in the clinic to identify and assess osteoporosis, which has a heritability of 0.6–0.8. Numerous osteoporosis susceptibility loci, including ESR1,

B

Gene symbol	Log2 fold change	p-value
Lilr4b	1.127	8.73E-99
Fcgr3	1.085	5.95E-30
Lilrb4a	1.051	2.64E-90
CTSK	-1.116	4.10E-57
ACP5	-0.952	6.50E-49
Oscar	-0.776	1.45E-43
siglec15	-0.724	5.84E-08
MMP-9	-0.527	1.25E-08
Atp6v0d2	-0.413	6.56E-24

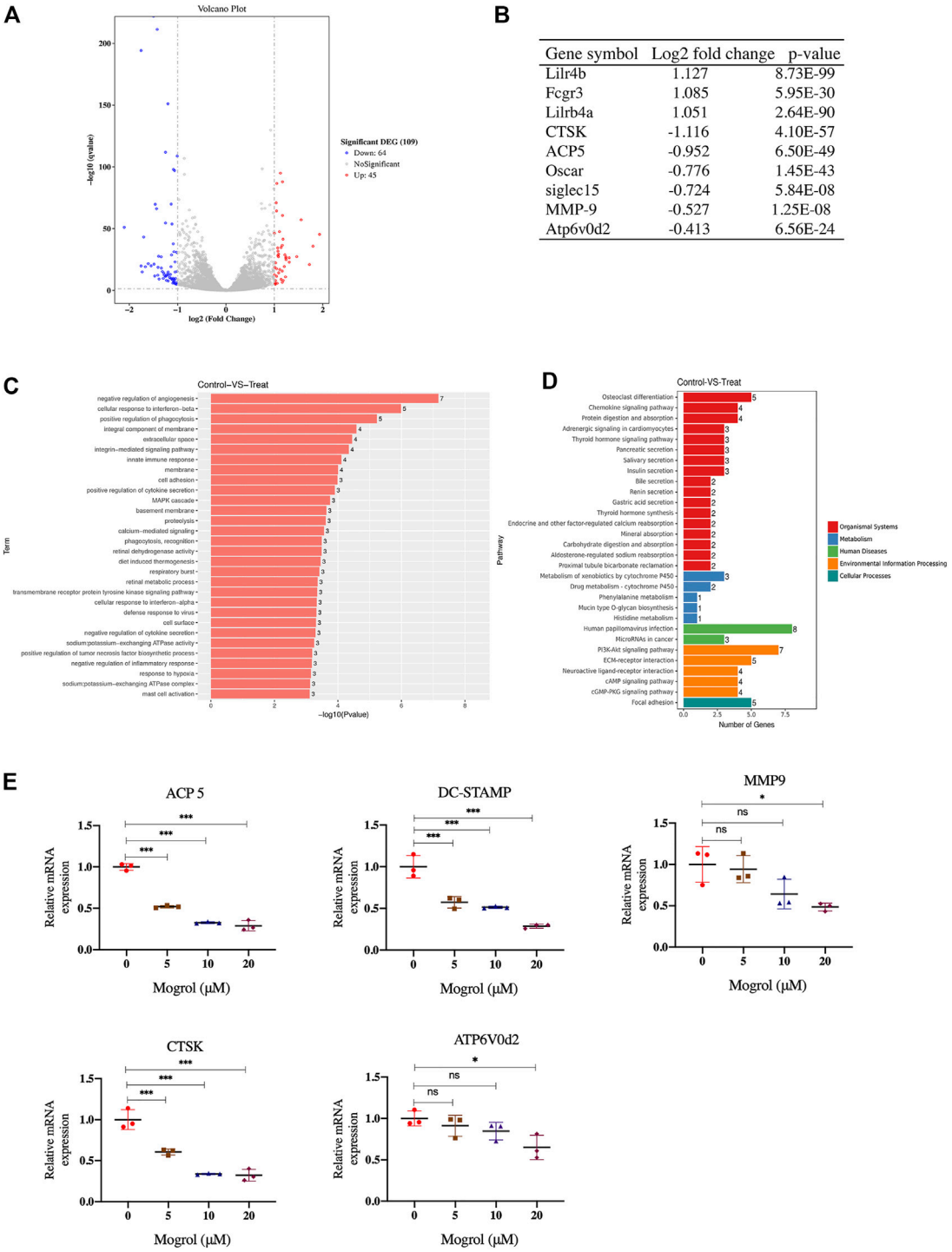

FIGURE 4 | RNA-seq analysis and osteoclast marker gene expression examined by RT–PCR. Identification of genes that are regulated by mogrol. RNA was extracted from BMMs cultured with or without mogrol treatment for 5 days under RANKL stimulation. **(A)** Volcano plots of RNA-seq data in mogrol-treated BMMs compared to control BMMs. **(B)** The log2-fold change and *p* value of some osteoclastogenesis-related genes. **(C,D)** Gene Ontology. **(C)** GO terms are displayed by gene *p* values. **(D)** KEGG pathways in the differentially expressed genes are illustrated by gene numbers. **(E)** Mogrol inhibits osteoclastogenesis marker gene expression. The expression levels of *ACP5, DC-STAMP, MMP9, CTSK and ATP6V0d2* were measured using RT–PCR.

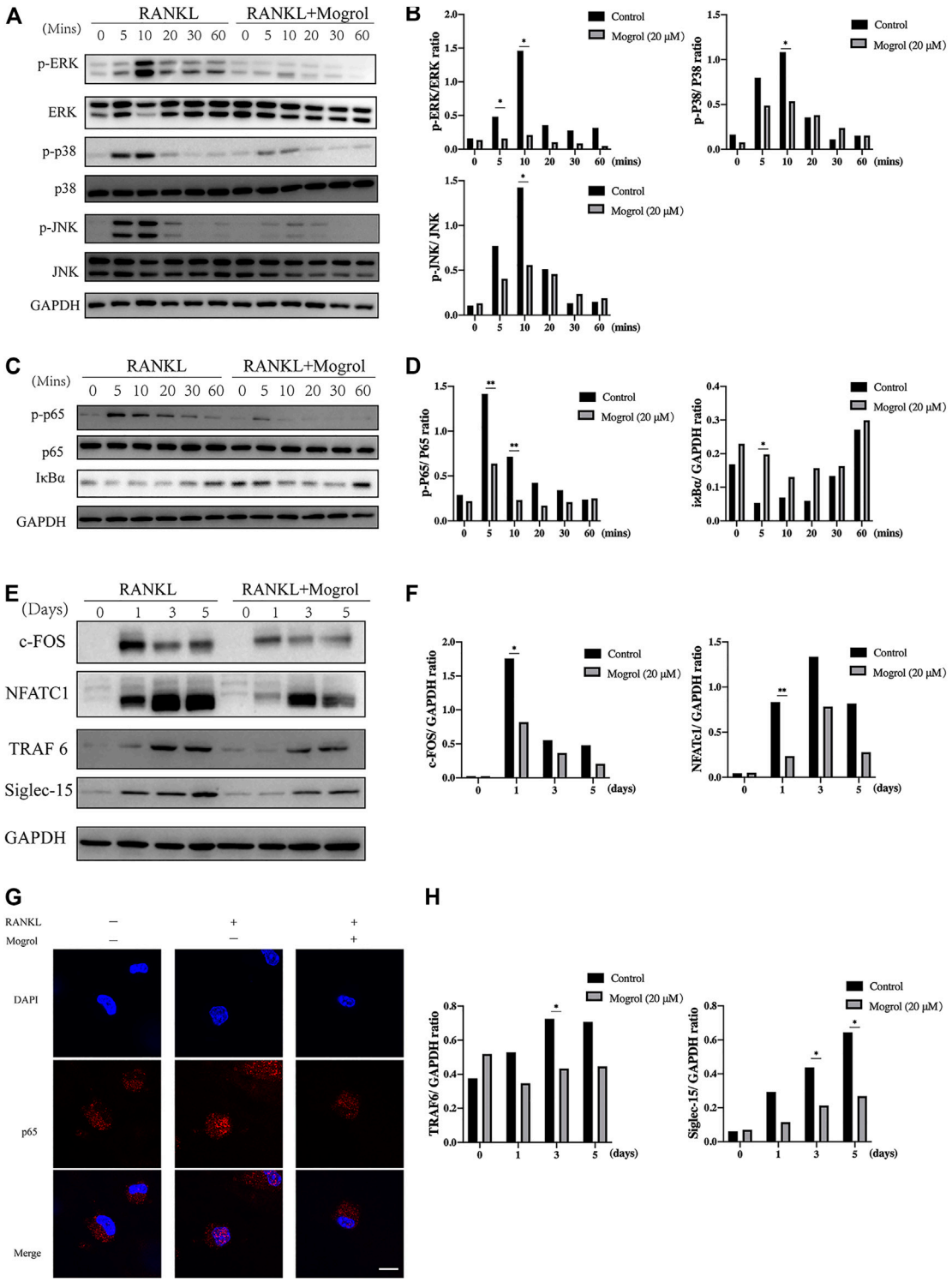

FIGURE 5 | Mogrol inhibited the RANKL-dependent TRAF6/NF-κB/MAPK signaling pathways. **(A)** The impact of mogrol on RANKL-induced activation of ERK, JNK, and p38. BMMs were starved for 4 h with or without 20 μM mogrol following activation with 50 ng/ml RANKL at various time points (0, 5, 10, 20, 30, or 60 min). Specific antibodies were employed to identify the total and phosphorylated forms of ERK, JNK, and P38. **(B)** Phosphorylated ERK, JNK, and P38 Gy levels were quantified and normalized to total proteins. **(C)** RANKL-induced NF-κB p65 phosphorylation and IκBα degradation after mogrol treatment. **(D)** Using ImageJ, the gray levels of p65 or IκBα were measured and normalized to GAPDH ($n = 3$). **(E)** BMMs were cultivated with or without mogrol for 0, 1, 3, and 5 days with the stimulation of RANKL. The proteins were identified with antibodies against NFATc1, c-Fos, TRAF6, Siglec-15, or GAPDH. **(F,H)** The relative expression of NFATc1, c-Fos, TRAF6 and Siglec-15 normalized to GAPDH was quantified by the gray level using ImageJ. **(G)** Nuclear translocation of P65 was determined by immunofluorescence staining using a p65 antibody and secondary antibody (red) and observed using a confocal fluorescence microscope. Scale bar = 50 μm.

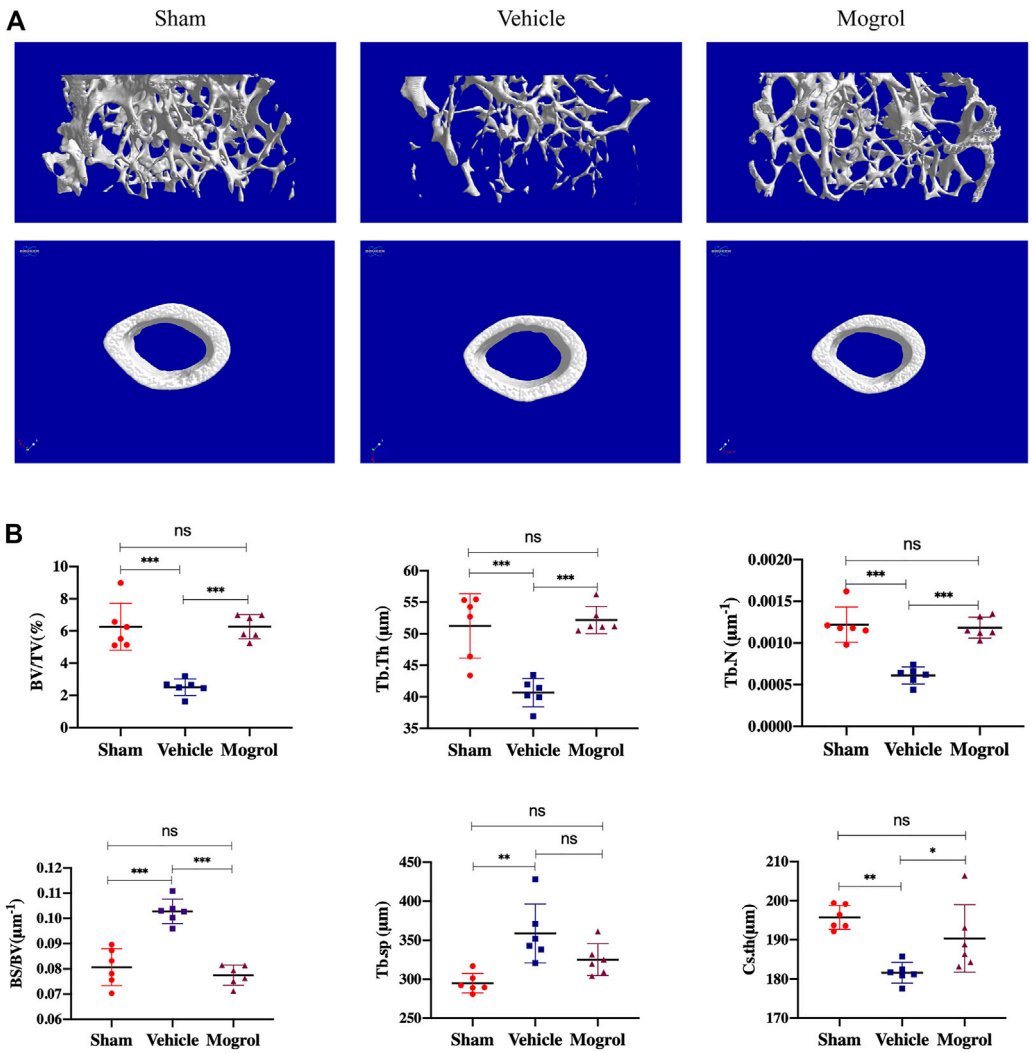

FIGURE 6 | Mogrol inhibited bone mass loss in OVX mice. **(A)** 3D reconstructions of images from micro-CT scans for femurs from sham, vehicle, and mogrol groups. **(B)** Bone parameter quantitative analysis, comprising BV/TV, BS/BV, Tb. Th, Tb. N, Tb. Sp, and Cs. th. (*n* = 6).

LRP4, DAAM2, WNT 16, and SOX 6, have been found and investigated using multiomics techniques based on systems genetics and genomics. Of note, drugs targeting susceptibility loci are more effective in clinical trials than those without genetic support (Yang et al., 2020). In addition to genomics studies, single-cell RNA sequencing (scRNA-Seq) has been used in osteoporosis research. For example, multipotent human skeletal stem cells are capable of forming bone and cartilage by scRNA-Seq. Due to its superiority, scRNA-Seq supports the viability of exploring the underlying cellular mechanisms of osteoporosis (Chan et al., 2018). Additionally, the gut microbiota which affects bone metabolism is receiving increasing attention in osteoporosis research (Chen et al., 2017).

For osteoporosis treatment, different drugs have been exploited. These drugs include bisphosphonates, RANKL antibodies, SERMs, and bone-anabolic agents. However, side effects such as esophageal irritation, thromboembolic disease, hypercalcemia, and renal toxicity limit the use of these drugs (Curry et al., 2018; Langdahl, 2021). These side effects prevent osteoporosis patients from taking these anti-osteoporosis drugs, particularly bisphosphonates (Khosla and Hofbauer, 2017). As a result, there is still a need to discover new medications that are free of these adverse effects and could be applied long-term. Recently, natural plant extracts have been an attractive alternative drug for osteoporosis due to their low toxicity (Zhan et al., 2019; Lin et al., 2020; Wang et al., 2021). Our study showed that mogrol, an aglycon of mogroside extracted from *Siraitia grosvenorii* (Swingle), has an inhibitory impact on osteoclast differentiation and function *in vitro* and protects against bone mass loss in postmenopausal mice.

RANKL, a member of the tumor necrosis factor superfamily, is produced by osteoblasts and osteocytes in the skeletal system (Suda et al., 1999; Nakashima et al., 2011). When RANKL binds to RANK, which is abundantly expressed in preosteoclasts, it

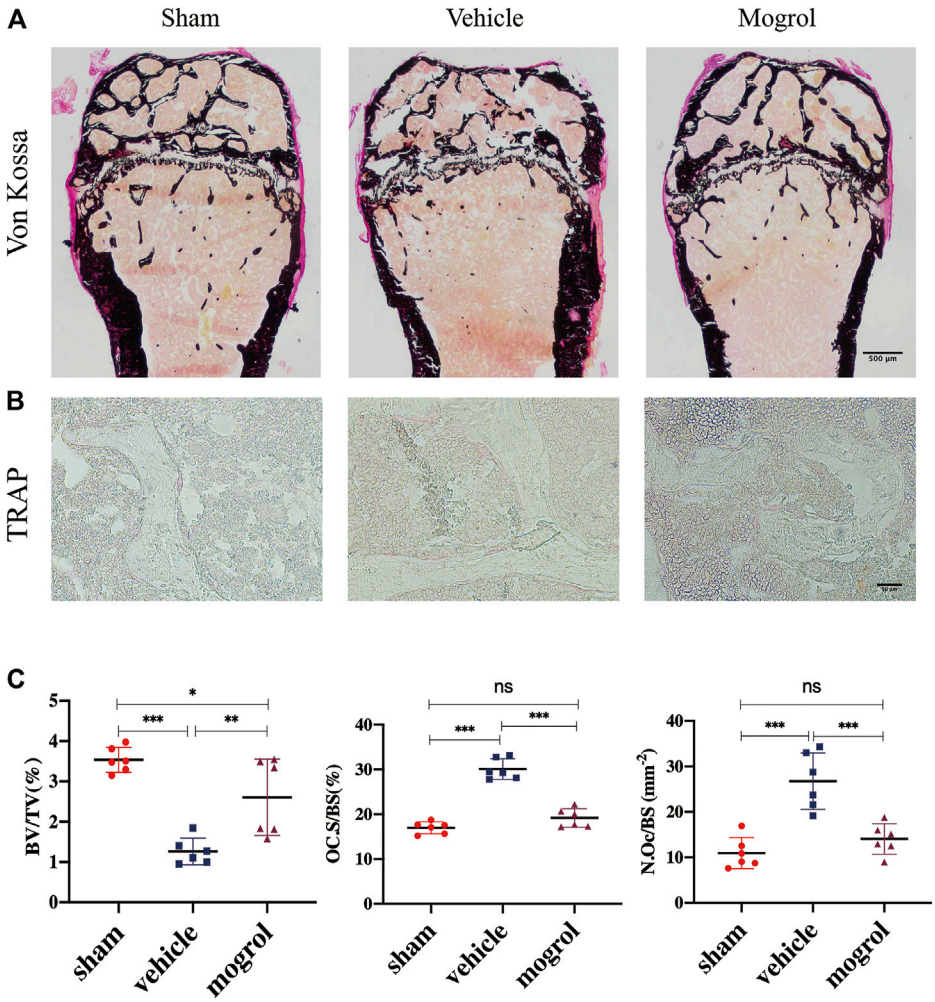

FIGURE 7 | Mogrol relieved bone mass loss in OVX mice by suppressing osteoclast differentiation or activity. **(A)** Images of Von Kossa staining of the femurs. **(B)** Images of TRAP staining. **(C)** Quantitative analysis of BV/TV in Von Vossa, Oc. S/BS, and N. Oc/B in TRAP staining (n = 6).

results in an increase in TRAF6, which further stimulates downstream signaling pathways during osteoclastogenesis (Kobayashi et al., 2001). For example, in the NF-κB signaling pathways, the recruitment of TRAF6 induces the phosphorylation of IκBα, leading to its subsequent degradation. Following IκBα breakdown, P65 is phosphorylated and transported from the cytoplasm to the nucleus, activating downstream transcription factors during osteoclastogenesis. (Jimi et al., 2019). It has been demonstrated that mogrol exerted neuroprotection against memory impairment and neuroinflammation by inhibiting the NF-κB signaling pathway (Chen et al., 2019). As shown by western blotting, mogrol inhibited IκBα protein degradation and p65 phosphorylation. Furthermore, the immunofluorescence staining results demonstrated that mogrol blocked RANKL-activated p65 nuclear translocation. These results demonstrated that mogrol inhibited the NF-κB signaling pathway to suppress osteoclast formation.

RANKL also activates the MAPK signaling pathway, which is comprised of the proteins JNK, P38, and ERK during osteoclastogenesis. Concurrent with NF-κB signaling pathway activation, TRAF6 recruitment induces the formation of a complex including TAK-1 and TAB. TAK1 stimulates IKKs and MKKs, resulting in the phosphorylation of JNK1, JNK2, and p38 MAP kinases. IKKβ activates protein kinase Tpl2 (MAP3K8) as a component of the IKK complex, and subsequently MEK1 and MEK2 are activated (MAP or ERK) (Strickson et al., 2017). Previously published research established that mogrol inhibited leukemia cell proliferation by suppressing ERK1/2 phosphorylation (Liu et al., 2015). Our Western blotting analysis indicated that mogrol suppressed the phosphorylation of ERK, P38 or JNK in the MAPK signaling pathway. Therefore, the NF-κB and MAPK signaling pathways were blocked by mogrol. We next demonstrated that mogrol reduced the levels of TRAF6 in BMMs using western blotting. Mogrol, on the other hand, has a suppressive impact on TRAF6. TRAF6-related downstream

signaling pathways, including MAPK, NF-κB, and ROS, are regulated by K63- or K48-linked ubiquitination. K63-linked ubiquitination of TRAF6 activates TAK-1, which is upstream of MAPKs and the NF-κB pathway, as described above. Act1 was identified to mediate K63-linked ubiquitination of TRAF6 (Wu et al., 2015). In contrast, TRAF6 degradation is promoted by K48-linked ubiquitination, which suppresses RANKL-induced osteoclastogenesis. Different molecules, such as IPMK, RNF19a and TRIM38, were identified as regulators of the K48-linked ubiquitination of TRAF6 (Kim et al., 2017; Wu et al., 2017). Recent research has discovered that some natural extracts promote TRAF6 degradation by enhancing K48-linked ubiquitination, such as icartin (Tan et al., 2017) and curcumenol, which suppress IPMK (Wang et al., 2021). There is a possibility that mogrol inhibits osteoclastogenesis by affecting the regulator of K63- or K48-linked ubiquitination. Nevertheless, further research on the underlying mechanism is required.

The c-Fos and Jun proteins, downstream of the NF-κB and MAPK signaling pathways, were dimerized to form AP-1, which was recruited to the promoter region of the NFATc1 gene to induce its expression, which subsequently promoted a variety of osteoclastogenic genes expression, such as Dcstamp, Atp6v0d2, ACP5, MMP9 and Ctsk. To determine how expression was altered by mogrol in RANKL-induced BMMs, RNA-seq was conducted. The RNA-seq results demonstrated that mogrol may be related to osteoclast differentiation, such as by upregulating the osteoclast inhibitory factors lilirb4a and fcgr3 or downregulating osteoclastogenesis-related genes such as ACP5, Dcstamp, MMP9 and Ctsk. Then, using real-time PCR, we demonstrated that mogrol reduced osteoclastogenic gene expression in BMMs. Consistent with the osteoclastogenesis results, mogrol decreased NFATc1 and c-Fos expression. Thus, we hypothesized that mogrol blocks osteoclast formation by inhibiting the NF-κB and MAPK signaling pathways by reducing TRAF6. Interestingly, we found that mogrol also suppressed Siglec-15 expression. Siglec-15 appears to promote the activation of ERK, AKT, or PI3K to modulate osteoclast differentiation as a member of the Siglec family of glycan-recognition proteins. Murine BMM and human osteoclast precursor differentiation into osteoclasts was suppressed by utilizing anti-Siglec-15 antibodies. There are still undisclosed signaling pathways regulated by Siglec-15 in osteoclast differentiation. Mogrol inhibited osteoclast fusion, as shown by TRAP staining, which was consistent with the western blot findings showing Siglec-15 suppression. However, it is unclear whether the inhibitory effect of mogrol on Siglec-15 is due to direct influences or reductions in the number of mature osteoclasts. It is worthwhile to further explore.

Finally, we also showed that intraperitoneal treatment with mogrol relieved bone mass loss in OVX mice *via* suppressing osteoclast activity, according to micro-CT and histological assessment. Interestingly, mogrol also rescued bone cortex thinning induced by OVX. Estrogen is essential for bone development and remodeling. Menopause or surgical ovariectomy results in trabecular and cortical bone loss by increasing osteoclast production and function. Endocortical resorption was increased after estrogen withdrawal in cortical bone (Väänänen and Härkönen, 1996). In addition, the production of inflammatory cytokines and RANKL promote cortical bone erosion by stimulating osteoclast differentiation and resorptive activity in bone disorders (Schett and Gravallese, 2012). These results indicated that osteoclasts are an important factor in bone metabolism. As shown in our results, in OVX mice, mogrol reduced cortical and trabecular bone loss, likely by inhibiting osteoclast development and activity *in vivo*. Notably, though a single dose treatment for OVX-mediated bone loss is limited, this is a first study to assess the effect of mogrol in pathological animal model of postmenopausal osteoporosis in detail. Additionally, due to the pharmacodynamics and pharmacokinetics of mogrol are largely unclear, further studies focusing on the magnitude of mogrol need to address the optimization of dosing and delivery strategies for ameliorating bone loss.

In conclusion, our study indicated that mogrol suppresses osteoclastogenesis and resorption by inhibiting the RANKL-dependent TRAF6/NF-κB/MAPK signaling pathway and relieved bone mass loss in postmenopausal mice. These findings demonstrate that mogrol could be an attractive natural extract to be used as a nontoxic drug for treating osteoclast-mediated osteolytic disorders such as osteoporosis.

DATA AVAILABILITY STATEMENT

The data presented in the study are deposited in the GEO repository, accession number GSE196742.

ETHICS STATEMENT

The animal study was reviewed and approved by Animal Care and Use Committee of Xiamen University (XMULAC20210037).

AUTHOR CONTRIBUTIONS

RX, GJ, and GR designed this study. YC, LZ, and ZL implemented research and drafted this manuscript. ZW, XL, NL, RS, GW, NY, and FG provided valuable opinions and assistance in the process of the research. RX and GJ supervised this study and revised this manuscript.

FUNDING

This study was supported by National Key R&D Program of China (2020YFA0112900 to RX), the National Natural Science Foundation of China (82074233 to GJ, 81902283 to GW

81972034 and 92068104 to RX), Scientific Research Foundation for Advanced Talents of Xiang'an hospital of Xiamen university (PM201809170009 to GJ), and Young Investigator Research Program of Xiang'an Hospital of Xiamen university (PM202103050009 to YC).

SUPPLEMENTARY MATERIAL

The Supplementary Material for this article can be found online at: https://www.frontiersin.org/articles/10.3389/fphar.2022.803880/full#supplementary-material

REFERENCES

Asagiri, M., Sato, K., Usami, T., Ochi, S., Nishina, H., Yoshida, H., et al. (2005). Autoamplification of NFATc1 Expression Determines its Essential Role in Bone Homeostasis. *J. Exp. Med.* 202, 1261–1269. doi:10.1084/jem.20051150

Beinke, S., Robinson, M. J., Hugunin, M., and Ley, S. C. (2004). Lipopolysaccharide Activation of the TPL-2/MEK/extracellular Signal-Regulated Kinase Mitogen-Activated Protein Kinase cascade Is Regulated by IkappaB Kinase-Induced Proteolysis of NF-kappaB1 P105. *Mol. Cel. Biol.* 24, 9658–9667. doi:10.1128/mcb.24.21.9658-9667.2004

Center, J. R., Nguyen, T. V., Schneider, D., Sambrook, P. N., and Eisman, J. A. (1999). Mortality after All Major Types of Osteoporotic Fracture in Men and Women: an Observational Study. *Lancet* 353, 878–882. doi:10.1016/s0140-6736(98)09075-8

Chan, C. K. F., Gulati, G. S., Sinha, R., Tompkins, J. V., Lopez, M., Carter, A. C., et al. (2018). Identification of the Human Skeletal Stem Cell. *Cell* 175, 43–e21. doi:10.1016/j.cell.2018.07.029

Chen, G., Liu, C., Meng, G., Zhang, C., Chen, F., Tang, S., et al. (2019). Neuroprotective Effect of Mogrol against Aβ1-42-induced Memory Impairment Neuroinflammation and Apoptosis in Mice. *J. Pharm. Pharmacol.* 71, 869–877. doi:10.1111/jphp.13056

Chen, Y. C., Greenbaum, J., Shen, H., and Deng, H. W. (2017). Association between Gut Microbiota and Bone Health: Potential Mechanisms and Prospective. *J. Clin. Endocrinol. Metab.* 102, 3635–3646. doi:10.1210/jc.2017-00513

Curry, S. J., Curry, S. J., Krist, A. H., Owens, D. K., Barry, M. J., Caughey, A. B., et al. (2018). Screening for Osteoporosis to Prevent Fractures: US Preventive Services Task Force Recommendation Statement. *Jama* 319, 2521–2531. doi:10.1001/jama.2018.7498

De Martinis, M., Sirufo, M. M., Polsinelli, M., Placidi, G., Di Silvestre, D., and Ginaldi, L. (2021). Gender Differences in Osteoporosis: A Single-Center Observational Study. *World J. Mens Health* 39, 750–759. doi:10.5534/wjmh.200099

Ensrud, K. E., and Crandall, C. J. (2017). Osteoporosis. *Ann. Intern. Med.* 167, Itc17–itc32. doi:10.7326/aitc201708010

Hahn, M., Vogel, M., and Delling, G. (1991). Undecalcified Preparation of Bone Tissue: Report of Technical Experience and Development of New Methods. *Virchows Arch. A. Pathol. Anat. Histopathol.* 418, 1–7. doi:10.1007/bf01600238

Jimi, E., Takakura, N., Hiura, F., Nakamura, I., and Hirata-Tsuchiya, S. (2019). The Role of NF-Kb in Physiological Bone Development and Inflammatory Bone Diseases: Is NF-Kb Inhibition "Killing Two Birds with One Stone"? *Cells* 8. doi:10.3390/cells8121636

Johnell, O., and Kanis, J. A. (2006). An Estimate of the Worldwide Prevalence and Disability Associated with Osteoporotic Fractures. *Osteoporos. Int.* 17, 1726–1733. doi:10.1007/s00198-006-0172-4

Jolette, J., Attalla, B., Varela, A., Long, G. G., Mellal, N., Trimm, S., et al. (2017). Comparing the Incidence of Bone Tumors in Rats Chronically Exposed to the Selective PTH Type 1 Receptor Agonist Abaloparatide or PTH(1-34). *Regul. Toxicol. Pharmacol.* 86, 356–365. doi:10.1016/j.yrtph.2017.04.001

Kalervo Väänänen, H., and Härkönen, P. L. (1996). Estrogen and Bone Metabolism. *Maturitas* 23 (Suppl. l), S65–S69. doi:10.1016/0378-5122(96)01015-8

Khosla, S., and Hofbauer, L. C. (2017). Osteoporosis Treatment: Recent Developments and Ongoing Challenges. *Lancet Diabetes Endocrinol.* 5, 898–907. doi:10.1016/s2213-8587(17)30188-2

Kim, E., Beon, J., Lee, S., Park, S. J., Ahn, H., Kim, M. G., et al. (2017). Inositol Polyphosphate Multikinase Promotes Toll-like Receptor-Induced Inflammation by Stabilizing TRAF6. *Sci. Adv.* 3, e1602296. doi:10.1126/sciadv.1602296

Kobayashi, N., Kadono, Y., Naito, A., Matsumoto, K., Yamamoto, T., Tanaka, S., et al. (2001). Segregation of TRAF6-Mediated Signaling Pathways Clarifies its Role in Osteoclastogenesis. *Embo J.* 20, 1271–1280. doi:10.1093/emboj/20.6.1271

Lane, N. E. (2006). Epidemiology, Etiology, and Diagnosis of Osteoporosis. *Am. J. Obstet. Gynecol.* 194, S3–S11. doi:10.1016/j.ajog.2005.08.047

Langdahl, B. L. (2021). Overview of Treatment Approaches to Osteoporosis. *Br. J. Pharmacol.* 178, 1891–1906. doi:10.1111/bph.15024

Li, C., Lin, L. M., Sui, F., Wang, Z. M., Huo, H. R., Dai, L., et al. (2014). Chemistry and Pharmacology of Siraitia Grosvenorii: a Review. *Chin. J. Nat. Med.* 12, 89–102. doi:10.1016/s1875-5364(14)60015-7

Liang, H., Cheng, R., Wang, J., Xie, H., Li, R., Shimizu, K., et al. (2021). Mogrol, an Aglycone of Mogrosides, Attenuates Ulcerative Colitis by Promoting AMPK Activation. *Phytomedicine* 81, 153427. doi:10.1016/j.phymed.2020.153427

Lin, X., Yuan, G., Li, Z., Zhou, M., Hu, X., Song, F., et al. (2020). Ellagic Acid Protects Ovariectomy-Induced Bone Loss in Mice by Inhibiting Osteoclast Differentiation and Bone Resorption. *J. Cel. Physiol.* 235, 5951–5961. doi:10.1002/jcp.29520

Liu, C., Zeng, Y., Dai, L. H., Cai, T. Y., Zhu, Y. M., Dou, D. Q., et al. (2015). Mogrol Represents a Novel Leukemia Therapeutic, via ERK and STAT3 Inhibition. *Am. J. Cancer Res.* 5, 1308–1318.

Lopez-Pelaez, M., Lamont, D. J., Peggie, M., Shpiro, N., Gray, N. S., and Cohen, P. (2014). Protein Kinase IKKβ-Catalyzed Phosphorylation of IRF5 at Ser462 Induces its Dimerization and Nuclear Translocation in Myeloid Cells. *Proc. Natl. Acad. Sci. U S A.* 111, 17432–17437. doi:10.1073/pnas.1418399111

Miller, P. D., Hattersley, G., Riis, B. J., Williams, G. C., Lau, E., Russo, L. A., et al. (2016). Effect of Abaloparatide vs Placebo on New Vertebral Fractures in Postmenopausal Women with Osteoporosis: A Randomized Clinical Trial. *Jama* 316, 722–733. doi:10.1001/jama.2016.11136

Nakashima, T., Hayashi, M., Fukunaga, T., Kurata, K., Oh-Hora, M., Feng, J. Q., et al. (2011). Evidence for Osteocyte Regulation of Bone Homeostasis through RANKL Expression. *Nat. Med.* 17, 1231–1234. doi:10.1038/nm.2452

NIH Consensus Development Panel on Osteoporosis Prevention, Diagnosis, and Therapy (2001). March 7-29, 2000: Highlights of the Conference. *South. Med. J.* 94, 569–573. doi:10.1001/jama.285.6.785

Onuora, S. (2015). Osteoimmunology: IgG Immune Complexes Directly Regulate Bone Homeostasis. *Nat. Rev. Rheumatol.* 11, 257. doi:10.1038/nrrheum.2015.51

Schett, G., and Gravallese, E. (2012). Bone Erosion in Rheumatoid Arthritis: Mechanisms, Diagnosis and Treatment. *Nat. Rev. Rheumatol.* 8, 656–664. doi:10.1038/nrrheum.2012.153

Siris, E. S., Selby, P. L., Saag, K. G., Borgström, F., Herings, R. M., and Silverman, S. L. (2009). Impact of Osteoporosis Treatment Adherence on Fracture Rates in North America and Europe. *Am. J. Med.* 122, S3–S13. doi:10.1016/j.amjmed.2008.12.002

Strickson, S., Emmerich, C. H., Goh, E. T. H., Zhang, J., Kelsall, I. R., Macartney, T., et al. (2017). Roles of the TRAF6 and Pellino E3 Ligases in MyD88 and RANKL Signaling. *Proc. Natl. Acad. Sci. U S A.* 114, E3481–e3489. doi:10.1073/pnas.1702367114

Suda, T., Takahashi, N., Udagawa, N., Jimi, E., Gillespie, M. T., and Martin, T. J. (1999). Modulation of Osteoclast Differentiation and Function by the New Members of the Tumor Necrosis Factor Receptor and Ligand Families. *Endocr. Rev.* 20, 345–357. doi:10.1210/edrv.20.3.0367

Tan, E. M., Li, L., Indran, I. R., Chew, N., and Yong, E. L. (2017). TRAF6 Mediates Suppression of Osteoclastogenesis and Prevention of Ovariectomy-Induced Bone Loss by a Novel Prenylflavonoid. *J. Bone Miner. Res.* 32, 846–860. doi:10.1002/jbmr.3031

Vahle, J. L., Zuehlke, U., Schmidt, A., Westmore, M., Chen, P., and Sato, M. (2008). Lack of Bone Neoplasms and Persistence of Bone Efficacy in Cynomolgus Macaques after Long-Term Treatment with Teriparatide [rhPTH(1-34)]. *J. Bone Miner. Res.* 23, 2033–2039. doi:10.1359/jbmr.080807

Wang, S., Ma, Q., Xie, Z., Shen, Y., Zheng, B., Jiang, C., et al. (2021). An Antioxidant Sesquiterpene Inhibits Osteoclastogenesis via Blocking IPMK/

TRAF6 and Counteracts OVX-Induced Osteoporosis in Mice. *J. Bone Miner. Res.* 36, 1850–1865. doi:10.1002/jbmr.4328

Wu, C., Su, Z., Lin, M., Ou, J., Zhao, W., Cui, J., et al. (2017). NLRP11 Attenuates Toll-like Receptor Signalling by Targeting TRAF6 for Degradation via the Ubiquitin Ligase RNF19A. *Nat. Commun.* 8, 1977. doi:10.1038/s41467-017-02073-3

Wu, N. L., Huang, D. Y., Tsou, H. N., Lin, Y. C., and Lin, W. W. (2015). Syk Mediates IL-17-induced CCL20 Expression by Targeting Act1-dependent K63-Linked Ubiquitination of TRAF6. *J. Invest. Dermatol.* 135, 490–498. doi:10.1038/jid.2014.383

Xia, Z. P., Sun, L., Chen, X., Pineda, G., Jiang, X., Adhikari, A., et al. (2009). Direct Activation of Protein Kinases by Unanchored Polyubiquitin Chains. *Nature* 461, 114–119. doi:10.1038/nature08247

Yang, T. L., Shen, H., Liu, A., Dong, S. S., Zhang, L., Deng, F. Y., et al. (2020). A Road Map for Understanding Molecular and Genetic Determinants of Osteoporosis. *Nat. Rev. Endocrinol.* 16, 91–103. doi:10.1038/s41574-019-0282-7

Zhan, Y., Liang, J., Tian, K., Che, Z., Wang, Z., Yang, X., et al. (2019). Vindoline Inhibits RANKL-Induced Osteoclastogenesis and Prevents Ovariectomy-Induced Bone Loss in Mice. *Front. Pharmacol.* 10, 1587. doi:10.3389/fphar.2019.01587

Conflict of Interest: The authors declare that the research was conducted in the absence of any commercial or financial relationships that could be construed as a potential conflict of interest.

Publisher's Note: All claims expressed in this article are solely those of the authors and do not necessarily represent those of their affiliated organizations, or those of the publisher, the editors and the reviewers. Any product that may be evaluated in this article, or claim that may be made by its manufacturer, is not guaranteed or endorsed by the publisher.

Copyright © 2022 Chen, Zhang, Li, Wu, Lin, Li, Shen, Wei, Yu, Gong, Rui, Xu and Ji. This is an open-access article distributed under the terms of the Creative Commons Attribution License (CC BY). The use, distribution or reproduction in other forums is permitted, provided the original author(s) and the copyright owner(s) are credited and that the original publication in this journal is cited, in accordance with accepted academic practice. No use, distribution or reproduction is permitted which does not comply with these terms.

frontiers in Pharmacology

ORIGINAL RESEARCH
published: 24 March 2022
doi: 10.3389/fphar.2022.851956

Identification of Polysaccharides From *Dipsacus asperoides* and Their Effects on Osteoblast Proliferation and Differentiation in a High-Glucose Environment

Duoduo Xu[1], *Jia Liu*[1†], *Wei Zheng*[2], *Qipin Gao*[3], *Yang Gao*[3]* *and Xiangyang Leng*[2]*

[1]Country School of Pharmacy, Changchun University of Chinese Medicine, Changchun, China, [2]The Affiliated Hospital, Changchun University of Chinese Medicine, Changchun, China, [3]Jilin Ginseng Academy, Changchun University of Chinese Medicine, Changchun, China

OPEN ACCESS

Edited by:
Longhuo Wu,
Gannan Medical University, China

Reviewed by:
Zhong-Ji Qian,
Guangdong Ocean University, China
Haixia Chen,
Tianjin University, China

***Correspondence:**
Xiangyang Leng
cz_lengxy@sina.com
Yang Gao
gaoyang-1979@hotmail.com

[†]These authors have contributed equally to this work

Specialty section:
This article was submitted to Ethnopharmacology, a section of the journal Frontiers in Pharmacology

Received: 10 January 2022
Accepted: 15 February 2022
Published: 24 March 2022

Citation:
Xu D, Liu J, Zheng W, Gao Q, Gao Y and Leng X (2022) Identification of Polysaccharides From Dipsacus asperoides and Their Effects on Osteoblast Proliferation and Differentiation in a High-Glucose Environment. Front. Pharmacol. 13:851956. doi: 10.3389/fphar.2022.851956

Polysaccharides (DAI-1 and DAI-2) from *Dipsacus asperoides (D. asperoides)* were obtained using mixed-bed ion exchange resin and Sephadex G-50 column chromatography following which their properties, structures, and activities were investigated. The results showed that DAI-1 and DAI-2 were homogeneous in nature, with glucose the only constituent, and had molecular masses of 17 and 4 kDa, respectively. Methylation analysis indicated that the backbones of DAI-1 and DAI-2 were mainly composed of (1→6)-linked glucose residues. DAI-1 possessed a small number of side chains and a branch point of (1→3, 6)-glucose, while DAI-2 lacked branching. Activity assays demonstrated that exposing osteoblasts to different DAI-1 concentrations (25, 50, or 100 μg/mL) in a high-glucose environment induced cell proliferation and led to a significant increase in bone morphogenetic protein 2 (BMP-2) and runt-related transcription factor 2 (Runx2) expressions at both the mRNA and protein levels. Moreover, DAI-1 treatment significantly increased alkaline phosphatase (ALP) and osteocalcin (OCN) activities in osteoblasts. Combined, our results suggested that DAI-1 may promote osteoblast proliferation and differentiation in a high-glucose environment.

Keywords: *Dipsacus asperoides* polysaccharide, extraction and separation, structure identification, osteoblast, proliferation and differentiation

INTRODUCTION

Osteoporosis (OP) is a chronic systemic metabolic bone disease characterized by bone loss, degeneration of bone microstructure, and increased bone fragility. The associated symptoms include bone pain, brittle bone-associated fractures, and paralysis. Although OP mainly affects the health of middle-aged and older adults, postmenopausal women and people with diabetes are also often prone to this condition (Compston et al., 2019).

Recent evidence has indicated that osteoblast activity is a key factor influencing OP development. Osteoblasts differentiate into mature osteoblasts in a three-stage process that involves proliferation, differentiation, and mineralization. Differentiation is required for osteoblast maturation, which is important for both bone formation and osteoblast function (Cicuéndez et al., 2017). Bone morphogenetic protein 2 (BMP-2) plays a key role in bone

formation and osteogenic differentiation. Specifically, the BMP-2 signaling pathway stimulates the synthesis and secretion of bone extracellular matrix. In addition, BMP-2 induces osteoblast differentiation by activating the Smad signaling pathway and regulating osteoblast-related gene expression. Runt-related transcription factor 2 (Runx2) is another key transcription factor for osteogenic gene expression and osteoblast differentiation, and greatly influences skeletal maturity and turnover. Runx2 serves as a necessary BMP-2 osteogenesis target gene, binding to specific sequences within the promoter regions of osteoblast-specific genes and regulating their expression (Lecanda et al., 1997; Gilbert et al., 2002). Furthermore, Runx2 promotes the expression of osteoblast-specific genes, including osteocalcin (OCN) and alkaline phosphatase (ALP) (Johnson et al., 2000; Pujari-Palmer et al., 2016). Diabetes is a predisposing factor for the development of OP. Intriguingly, numerous studies on the effects of hyperglycemia on bone health have shown that this condition can inhibit osteoblast activity to some extent, not only by suppressing osteoblast proliferation and differentiation, but also by downregulating the expression of osteogenesis-related genes and proteins (Zhen et al., 2010).

Polysaccharides are natural macromolecular compounds present in the cell membranes of higher plants and animals, as well as in the cell walls of microorganisms (Zhao et al., 2017). Until recently, polysaccharides have largely been thought of as mere energy storage molecules, structural materials, or impurities for removal. However, research attention has increasingly focused on polysaccharides, as they have recently been shown to participate in a wide range of processes, including cell and molecular recognition, fertilization, growth, inflammation, autoimmunity, and the malignant transformation of tumor cells. Owing to their low toxicity, polysaccharides are currently utilized as ingredients of natural drugs and numerous health care products (Wasser, 2002; Hou et al., 2021).

D. asperoides is a commonly administered Chinese herbal medicine composed primarily of saponins, alkaloids, flavonoids, volatile oils, and polysaccharides (Li et al., 2017). *D. asperoides* is often used in China to treat OP and other bone diseases, and has achieved good clinical effects. However, the active components underlying its bone health-promoting effects are unknown, and studies investigating the effects of *D. asperoides* on OP have mainly focused on its saponin contents. *D. asperoides* polysaccharides have been reported to exert a range of health-promoting effects, including enhanced immunity and anti-tumor activities (Zhang et al., 1997; Cong et al., 2013; Park et al., 2019; Sun et al., 2019) and there is little research on OP. In this study, we first extracted and isolated *D. asperoides* polysaccharides and characterized their structures. Then, we investigated the effects of the isolated polysaccharides on osteoblast damage induced by a high-glucose environment. Our results lay a foundation for future studies exploring the beneficial activities of *D. asperoides* polysaccharides on human health.

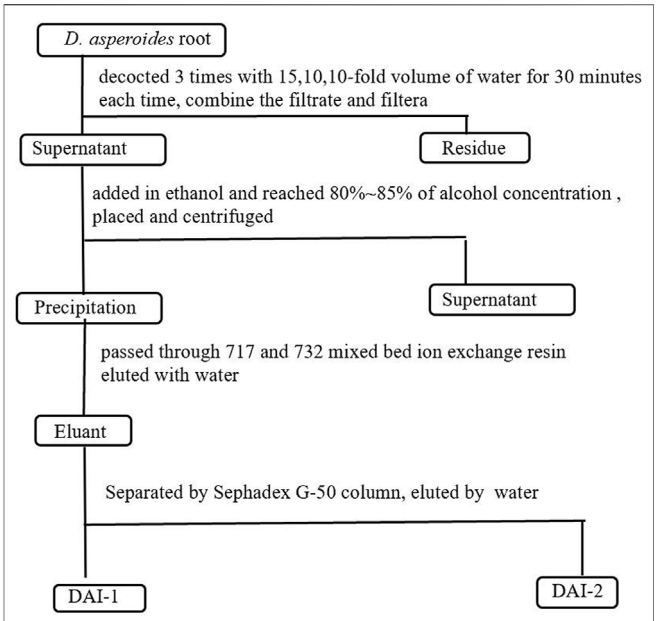

FIGURE 1 | Schematic of the process used for the extraction and isolation of *D. asperoides* polysaccharides.

MATERIALS AND METHODS

Materials and Chemicals

D. asperoides samples were obtained from Jishen Pharmacy (Jilin, China) and were identified by Professor Gao as dry roots of *Dipsacus asper* Wall. ex Henry. T-series dextran standards and those of nine monosaccharides were obtained from Fluka Chemical Co. (Everett, WA, United States). Sephadex G-50 was purchased from GE Healthcare Ltd. (Chalfront St., Guiles, UK). Ion exchange resins (717 and 732) were purchased from Tianjin Xijinna Environmental Protection Material Technology Co., Ltd. (Tianjin, China).

Isolation and Purification of *D. asperoides* Polysaccharides

D. asperoides root material (500 g) was weighed, crushed, and soaked in a 10-fold volume of water for 2 h. For the first extraction, a 15-fold volume of water (based on the original total volume) was added, following which the mixture was decocted for 30 min, filtered, and the filtrate was retained. For the second and third extractions, a 10-fold volume (based on the original total volume) of water was added each time before decocting the mixture. The decocted mixtures were filtered and the filtrates from each extraction were retained. The three filtrates were combined and concentrated. A 95% ethanol solution was slowly added to the concentrated solution with gentle stirring until the alcohol concentration reached 80–85%. After allowing to stand for 24 h, the mixture was centrifuged and a pellet containing the precipitate was retained and dried. Next, the Sevage method (Navarini et al., 1999) was repeatedly

employed to remove protein from the precipitate to yield a crude polysaccharide (DA) preparation. After dissolving in water, this crude polysaccharide preparation was passed through 717 and 732 mixed-bed ion exchange resin, and the bound material was eluted with water. Eluants were collected, pooled, and concentrated to generate a polysaccharide preparation designated as DAI. This preparation was further separated and purified using medium-pressure preparative liquid chromatography (CHEETAH MP, Agela, Tianjin, China) with a Sephadex G-50 column (5 × 50 cm), followed by elution using distilled water. The main DAI-1 and DAI-2 fractions were generated from pooled fractions, after which pooled DAI-1 and DAI-2 fractions were concentrated and lyophilized. The above experimental process is shown in **Figure 1**.

Assays of Neutral Sugar, Uronic Acid, and Protein Contents

The neutral sugar contents of DAI-1 and DAI-2 were measured using a phenol–sulfuric acid method (Dubois et al., 2002). Uronic acid content was determined using the *m*-hydroxydiphenyl method (Blumenkrantz and Asboe-Hansen, 1973). Protein analysis was performed using the Bradford method (Bradford, 1976).

Monosaccharide Composition Analysis

High-performance liquid chromatography (HPLC) combined with pre-column derivatization was used to determine the sugar composition of DAI-1 and DAI-2. DAI-1 (2 mg), DAI-2 (2 mg), and monosaccharide standard (1 mg) were separately derivatized according to a published method (Xu D. et al., 2016). After derivatization, the sample was dissolved in methanol, and 10 μL of the solution was injected into an Agilent 1200 HPLC system (CA, United States) equipped with a C_{18} column (4.6 μm × 250 mm). Gradient elution was performed using potassium phosphate (0.025 mol/L, pH 6.8) and acetonitrile as the mobile phase. Detection was conducted at a wavelength of 250 nm and a chromatogram was generated.

Molecular Mass Analysis

The molecular mass of DAI-1 and DAI-2 was determined using an HPLC system (Shimadzu, Tokyo, Japan) equipped with a refractive index detector fitted with a Sepax SRT SEC-100 (7.8 × 300 mm, DE, United States) chromatographic column. For the mobile phase, 0.7% Na_2SO_4 was used. GPC software (China) was used to calculate the molecular mass based on the calibration curve for dextran of different molecular masses.

Methylation Analysis

Samples were fully methylated according to the modified Ciucanu method (Needs and Selvendran, 1993) and then analyzed by Fourier transform infrared spectroscopy(IR, PerkinElmer Co., Ltd., Waltham, MA, United States) to assess methylation completion. The methylated product further acetylated to generate partially methylated and partially acetylated products that were analyzed using a gas chromatography-mass spectrometry (GC–MS) system (Agilent 6890 N/5975B) equipped with a DB-1 capillary column (30 m × 0.25 mm). The temperatures of the injection port and ion source were 200 and 250°C, respectively. The programmed heating method was as previously described (Xu D. et al., 2016). The results were analyzed based on ion flow and mass spectrographic results.

IR Spectroscopy

Powdered polysaccharide samples were compressed with KBr to generate a solid tablet that was analyzed *via* IR Spectroscopy within the wavelength range of 400–4000 cm^{-1}.

Effects of DAI-1and DAI-2 on Proliferation and Differentiation of Osteoblasts in High Glucose Environment

Cell Culture

The MC3T3-E1 cell line, which is derived from mouse embryonic osteoblast precursor cells, was purchased from ATCC (Rockefeller, MD, United States). The cells were cultured in Gibco Dulbecco's modified Eagle's medium (DMEM) containing 10% fetal bovine serum (Thermo, Rockford, IL, United States), penicillin (105 U/mL), and streptomycin (100 mg/L) (Sigma-Aldrich, St. Louis, MO, United States) in a humidified incubator with 5% CO_2 at 37°C. The culture medium was renewed every 2–3 days.

Determination of the Rates of Glucose-Mediated Inhibition of Osteoblast Proliferation Using a CCK-8 Assay

Cells were diluted to 1 × 10^5/mL in DMEM and 100 μL of the suspension was added per well of a 96-well culture plate. Once cells had completely adhered to the wells, glucose solutions of different concentrations in serum-free medium were added to the wells followed by culture for 24, 48, and 72 h. Cells without glucose treatment served as controls. After discarding the culture medium, 10 μL of CCK-8 solution was added to each well and the plate was then incubated for 1 h. After the addition of DMSO, the optical density (OD) was measured for each well using microplate reader (Thermo, Rockford, IL, United States) at 450 nm. The absorbance values were used to calculate the rates of glucose-induced inhibition of cell proliferation.

Effects of DAI-1 and DAI-2 on MC3T3-E1 Cell Viability

MC3T3-E1 cells (100 μL) in the logarithmic phase were seeded in a 96-well plate at a density of 1 × 10^5 cells/mL. Once cells had adhered to the wells, the plate was divided into a control group (DMEM), a glucose model group (75 mmol/L glucose), and three polysaccharide treatment groups (75 mmol/L glucose +25, 50, or 100 μg/mL polysaccharide). Cell viability was measured *via* CCK-8 assay after 48 and 72 h of culture.

Determination of ALP and OCN Activities by ELISA

Cells were inoculated into a 6-well plate and cultured for 48 h, following which the culture medium was discarded, 100 μL 0.2% Triton X-100 was added to each well, the supernatants were

TABLE 1 | The base of primers for quantitative real-time RT-PCR.

Genes	Forward primer (5-3)	Reverse primer (5-3)
BMP-2	CCTGGGCGGCGCGGCCGGCCTCATT	AGCCGGTGGTCTGGGGCGGGCGCT
Runx2	GGGGCAGTCATAACTGGGTT	GCGTGGGAACAGGTCACTTA
GAPDH	TTGTGCAGTGCCAGCCTCGTCCCG	TGCCACTGCAAATGGCAGCCCTGGT

collected after centrifugation, and protein concentrations were determined using the BCA method. ALP and OCN activities were subsequently determined using a kit according to the manufacturer's instructions. After color development, the OD was measured at 405 and 450 nm using a microplate reader.

Determination of BMP-2 and Runx2 Levels by Western Blotting

Cells (5×10^6 per well) from each group were incubated in separate culture bottles. After 48 h of incubation, the cells were harvested, total protein was extracted, and protein concentrations were measured using a BCA kit (Takara Bio Inc., Shiga, Japan). Next, equal amounts (80 μg) of boiled protein were separated by 4–20% sodium dodecyl sulfate–polyacrylamide gel electrophoresis (SDS–PAGE) using GAPDH as the internal loading reference and then transferred to a polyvinylidene fluoride (PVDF) membrane (Schleicher and Schuell, Keene, NH, United States). After blocking in 5% skimmed milk for 2 h at room temperature, the membrane was incubated with primary antibody (anti-BMP-2, anti-Runx2, or anti-GAPDH, diluted 1:2000) (Proteintech Co., Manchester, UK) at 4°C overnight, washed, and then incubated with horseradish peroxidase (HRP)-labeled goat anti-mouse IgG or goat anti-rabbit IgG (1:2,000, Santa Cruz Biotechnology, Inc., Dallas, TX, United States). Band intensities were measured after detection using enhanced chemiluminescence (ECL) reagent (Thermo).

Quantitative PCR Assays for BMP-2 and Runx2 mRNA Expression Levels

Osteoblasts were inoculated in 12-well plates at 1×10^5 cells/well and, after 2 days of polysaccharide treatment, total RNA was extracted from the five groups of osteoblasts. First-strand cDNA was synthesized from 1 μg of total RNA and was subsequently used for real-time fluorescent quantitative PCR. The mRNA expression levels of BMP-2 and Runx2 were detected using an ABI 7300 Real-time PCR System (Thermo). The primers used to amplify the BMP-2 and Runx2 sequences were synthesized by Chongqing Eternal Biotechnology Co., Ltd. and are listed in **Table 1**. The cycling conditions were as follows: denaturation at 95°C for 30 s, followed by 40 cycles of denaturation at 95°C for 5 s, annealing at 60°C for 30–34 s, and extension at 95°C for 15 s. Rq and Ct values were used for statistical analysis.

Statistical Analysis

Data were expressed as means ± SD. Differences among groups were analyzed using one-way analysis of variance (ANOVA) with the Cochran-Armitage test; dose-effect trend analysis was conducted using SAS software. Differences were considered significant at $p < 0.05$.

RESULTS

Extraction and Purification of DAI-1 and DAI-2

Crude polysaccharide preparations of *D. asperoides* were isolated *via* water extraction and alcohol precipitation, with a final yield of 28.3%. Determination of physical and chemical properties indicated that these extracts mainly contained neutral polysaccharides, proteins, and other water-soluble impurities, with almost no acid sugar. Accordingly, free protein and other impurities in the crude polysaccharide were removed using 717 and 732 mixed-bed ion exchange resin, and the DAI were further purified using Sephadex G-50 columns. The elution curve is shown in **Figure 2A**.

Basic Properties of DAI-1 and DAI-2

The sugar contents of DAI-1 and DAI-2 were 98.3 and 99.1%, respectively, with almost no acid sugar or protein being detected. The absence of nucleic acid and protein was further confirmed by the lack of absorption peaks at 260 and 280 nm. Sugar composition analysis further showed that these polysaccharide preparations contained only glucose (**Figures 2A,B**). For molecular mass determination, DAI-1 and DAI-2 presented with single, sharp absorbance peaks, indicating that they were homogeneous polysaccharides and had molecular masses of 17 and 4 kDa, respectively.

Methylation Analysis

Determination of polysaccharide structure has always been a difficult challenge in polysaccharide research. Although nuclear magnetic spectroscopy is increasingly used for the determination of polysaccharide structure, analysis of methylation remains an important method for this purpose as it can provide a large amount of information, such as details regarding the types and proportions of sugar residues. Methylation results for DAI-1 and DAI-2 were deduced by analyzing information within specific mass spectra regions, as outlined in the ion flow diagram in **Table 2**. Data analysis indicated that DAI-1 contains three types of glycosidic linkages in a molar ratio that reflects the presence of a few side chains, whereas DAI-2 is a linear (unbranched) polysaccharide. The numbers of ends and branches for DAI-1 were the same, thereby confirming that this result was reasonable, while (1→6) linkages between glucose

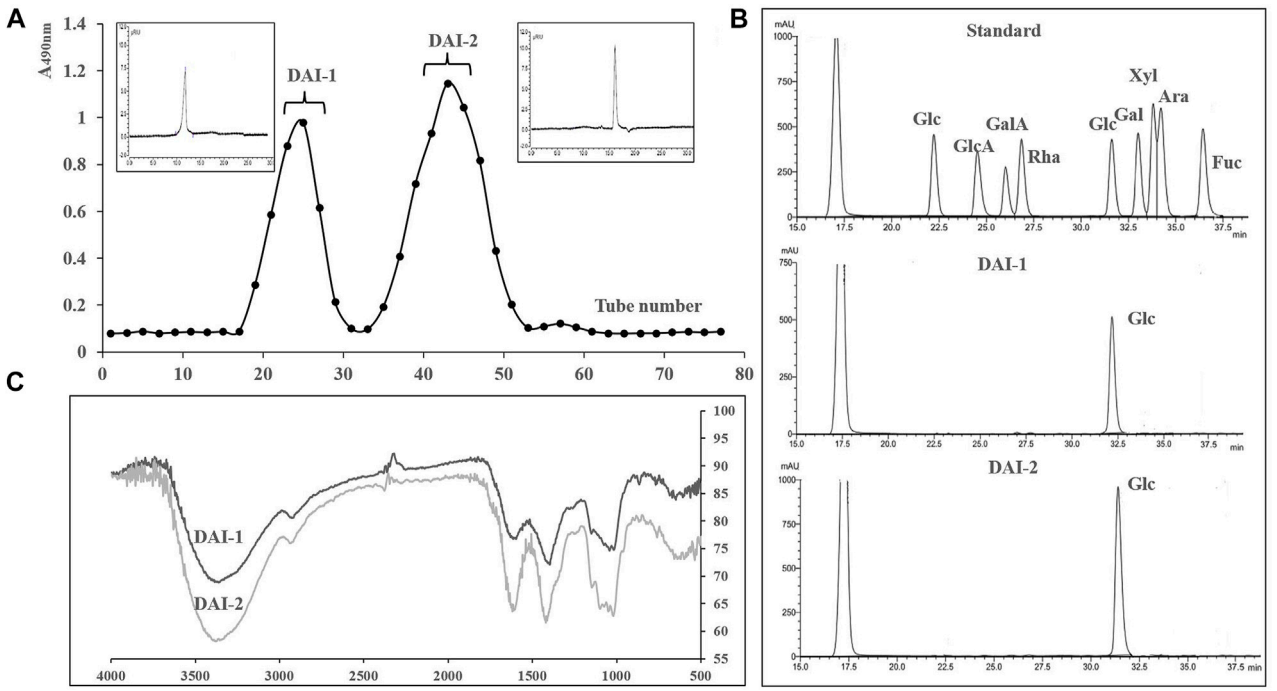

FIGURE 2 | The elution curve for DAI-1 and DAI-2 passed through Sephadex G 50 columns. The upper left and upper right panels correspond to their gel permeation chromatograms **(A)**. Liquid chromatograms of DAI-1, DAI-2, and monosaccharide standards **(B)**. Infrared chromatograms of DAI-1 and DAI-2 **(C)**.

TABLE 2 | Methylation analysis data of DAI-1 and DAI-2.

Polysaccharide	Retention time	Methylated sugar	Molar ratio	Deduced linkage pattern	Main mass spectrum fragment ion
DAI-1	20.2	2,3,4,6-Me_4- Glc	4.9	T- Glc*p*-(1→	87,101,117,129,161,205
	24.5	2,4,6- Me_3- Glc	40.2	→3)- Glc*p*-(1→	87,101,117,129,161,233
	30.4	2,4- Me_3- Glc	4.9	→3,6)- Glc*p*-(1→	87,117,129,189,233,261
DAI-2	20.2	2,4,6-Me4- Glc	1.6	→3)- Glc*p*-(1→	87,101,117,129,161,233
	24.5	2,3,4- Me3- Glc	6.0	→6)- Glc*p*-(1→	87,101,117,129,161,189,233

Note: Glc stands for glucose.

residues comprised the main linkage type detected in both DAI-1 and DAI-2.

IR Analysis

The IR chromatograms of DAI-1 and DAI-2 were similar and contained absorption peaks characteristic of polysaccharides (**Figure 2C**). Taking DAI-1 IR spectra as an example, the absorbance band at 3371 cm^{-1} in the IR chromatogram is characteristic for the O-H stretching vibration associated with polysaccharides; the weak band at approximately 2927 cm^{-1} corresponds to the C-H stretching vibration of carbohydrates; the 1597 cm^{-1} band corresponds to a C-O stretching vibration; and the absorption bands at 1408 cm^{-1} were associated with C-O stretching vibration. The strong band at 1016 cm^{-1} indicated that DAI-1 possessed a pyran-type structure (Gong et al., 2017). Additional absorption bands at approximately 866 and 738 cm^{-1} indicated that the sugar units of DAI-1 assumed *ß*- and *a*-configurations, respectively (Zhao et al., 2014).

Effects of DAI-1and DAI-2 Treatment on Osteoblast Proliferation and Differentiation

Determination of the Effects of Different Glucose Concentrations on Osteoblast Growth Rates

As shown in **Figure 3A**, osteoblast growth was inhibited in a manner that was dependent on the glucose dose and culture duration. When glucose was administered at the concentration of 25 mmol/L for 24 h, osteoblast growth was significantly inhibited. At the concentration of 100 mmol/L, the inhibition rate reached approximately 35%. At the glucose concentrations of 50 and 75 mmol/L, the rate of osteoblast growth inhibition ranged from 40–60% after 48 h of treatment,

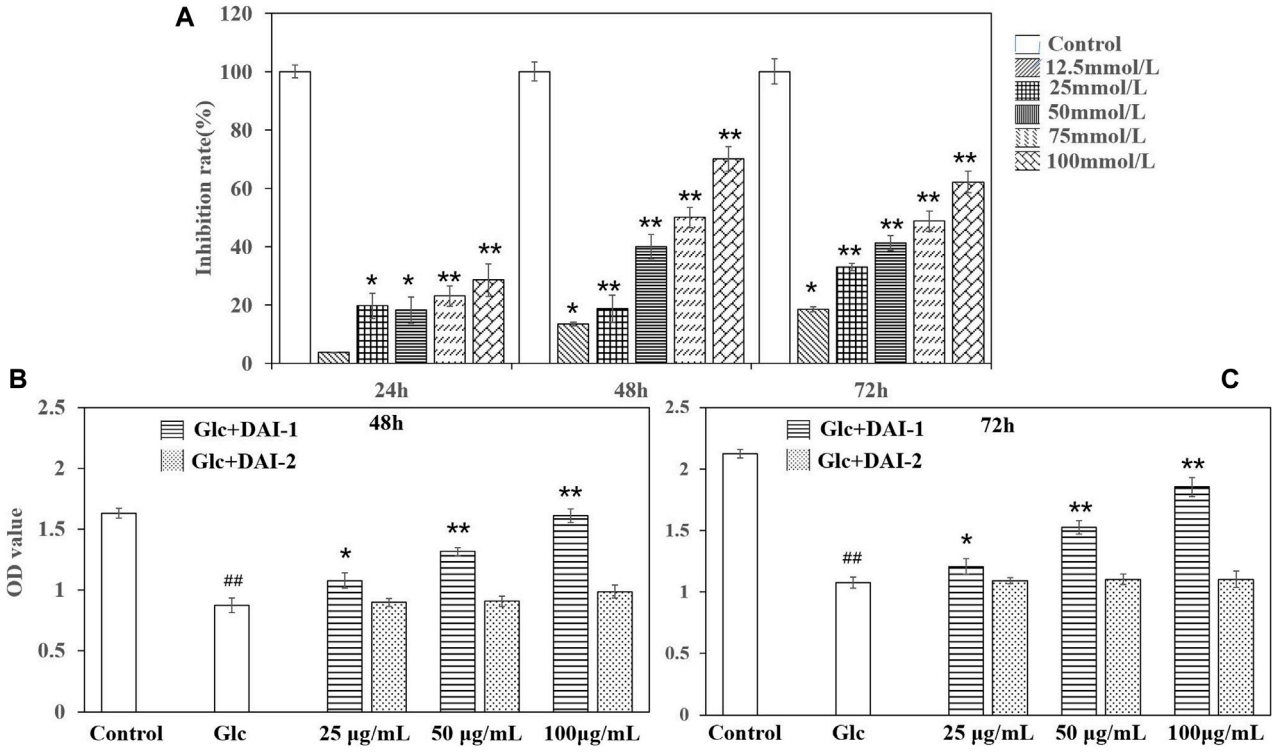

FIGURE 3 | The effects of different glucose concentrations on osteoblast growth rates **(A)**. *: $p < 0.05$, **: $p < 0.01$, for high-glucose group (represented by 'Glc' in the figure) *vs*. the control group (represented by 'Control' in the figure). The effects of exposing osteoblasts to DAI-1 and DAI-2 under a high-glucose environment for 48 h **(B)** and 72 h **(C)**. ##: $p < 0.01$, for high-glucose group *vs*. the control group; *: $p < 0.05$, **: $p < 0.01$, for the DAI-1and DAI-2 treated group *vs*. high-glucose group.

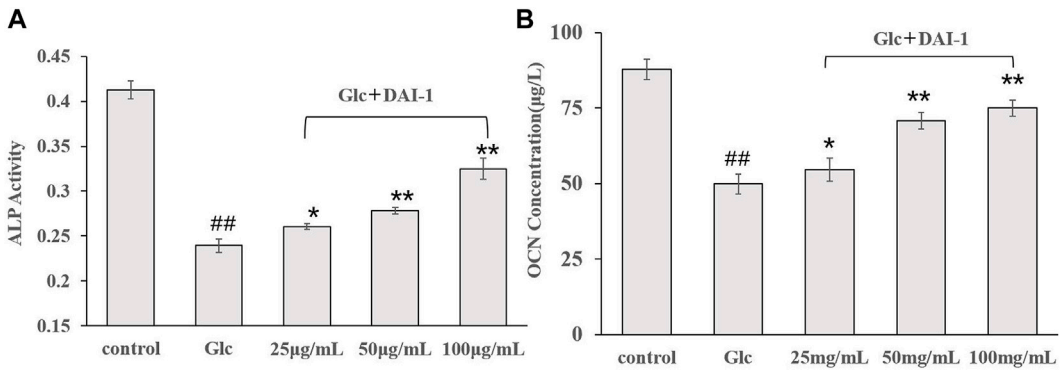

FIGURE 4 | The effects of DAI-1 on alkaline phosphatase (ALP) **(A)** and osteocalcin (OCN) **(B)** in osteoblasts exposed to high glucose concentrations. Osteoblasts were cultured in different conditioned media for 48 h, following which ALP and OCN activities were determined. ##: $p < 0.01$, for high-glucose group *vs*. the control group; *: $p < 0.05$, **: $p < 0.01$, for the DAI-1and DAI-2 treated group *vs*. high-glucose group.

similar to that seen at 72 h. Considering factors such as incubation time, we selected the glucose concentration of 75 mmol/L and treatment for 48 h as the modeling parameters in this experiment as this resulted in a stable osteoblast growth inhibition rate of between 40 and 60%.

Effects of DAI-1 and DAI-2 on the Proliferative Ability of MC3T3-E1 Cells Exposed to a High Glucose Concentration

The effects of DAI-1 and DAI-2 treatment on the proliferation of MC3T3-E1 cells after exposure to high glucose concentrations are

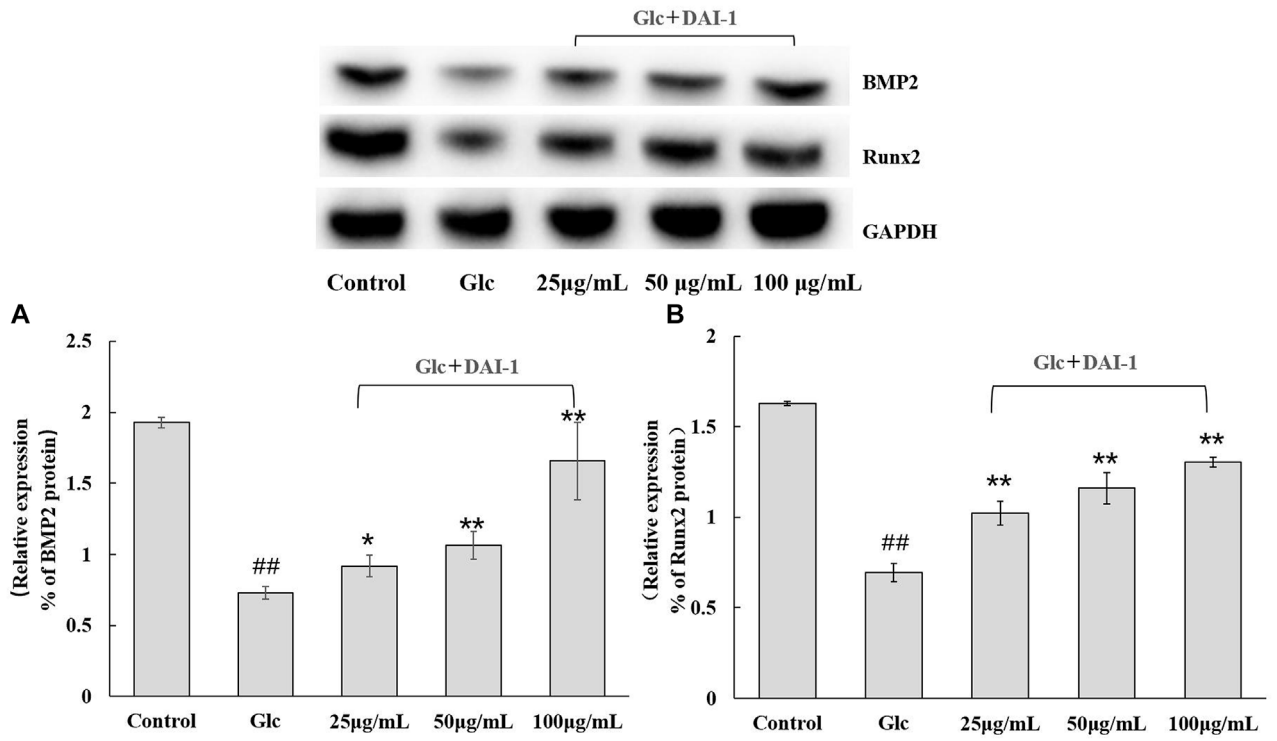

FIGURE 5 | The effect of DAI-1 on the relative protein expression of the osteoblast differentiation-related factors BMP-2 **(A)** and Runx2 **(B)** in a high-glucose environment. After 48 h of treatment, the protein levels of BMP-2 and Runx2 in osteoblasts were quantified by western blot. GAPDH served as a loading control. ##: $p <$ 0.01, for high-glucose group *vs*. the control group; *: $p < 0.05$, **: $p < 0.01$, for the DAI-1and DAI-2 treated group *vs*. high-glucose group.

shown in **Figures 3B,C**. Cells treated with low, medium and high doses of DAI-1 exhibited significantly increased cell proliferation compared with that in cells treated with glucose only, with increases of 1.23-, 1.50-, and 2.11-fold after 48 h of treatment and 1.12-, 1.42-, and 1.72-fold after 72 h of treatment, respectively, thus providing evidence of a dose-dependent effect for DAI-1. In contrast, compared with cells treated with glucose only, exposure to DAI-2 did not affect ($p > 0.05$) osteoblast proliferation in a high-glucose environment irrespective of the concentration used or duration of treatment (48 or 72 h).

Effects of DAI-1 and DAI-2 Treatment on ALP and OCN Activities as Determined by ELISA

ALP activity is an important marker of early-stage osteoblast differentiation and a functional indicator of osteoblast differentiation status, while OCN is a marker of late osteoblast differentiation and a key regulator of bone mineralization. The effects of DAI-1 on ALP and OCN activities in MC3T3-E1 cells exposed to high-glucose conditions are shown in **Figure 4**. Compared with the control group, ALP and OCN activities in the high-glucose treatment group showed a significant decline after 48 h (ALP: 0.57-fold, $p = 1.56 \times 10^{-5}$; OCN: 0.57-fold, $p = 4.31 \times 10^{-5}$, respectively). In contrast, ALP and OCN activities increased significantly in the DAI-1-treated groups; compared with cells treated with glucose only, those exposed to glucose plus low, middle, or high DAI-1 concentrations displayed changes of 1.09- ($p = 0.012$), 1.17- ($p = 0.00118$), and 1.36-fold ($p = 0.000459$), respectively, in ALP activity and 1.08- ($p = 0.03294$), 1.42- ($p = 0.00015$), and 1.50-fold ($p = 7.29 \times 10^{-5}$) in OCN activity. These results indicated that DAI-1 dose-dependently promoted ALP and OCN activities in ME3T3-E1 cells in a high-glucose environment. As observed for the proliferation effect, DAI-2 did not significantly affect ALP or OC activities in osteoblasts under a high-glucose environment regardless of the concentration used ($p > 0.05$). This indicated that DAI-2 had no effect on osteoblast differentiation.

DAI-1 and DAI-2 Inhibited the Protein Expression of BMP-2 and Runx2 in Osteoblasts Exposed to High-Glucose Conditions

The protein expression levels of BMP-2 and Runx2 in osteoblasts were monitored after 48 h of DAI-1 treatment in a high-glucose environment (**Figure 5**). No significant difference ($p > 0.05$) in the levels of these proteins were found between the high-glucose treatment group and the group exposed to glucose and DAI-2 (data not shown) in osteoblasts. The expression levels of BMP-2 and Runx2 in the high-glucose treatment group were significantly lower than those of the control group (0.38-fold [$p = 3.5 \times 10^{-6}$] and 0.42-fold [$p = 6.0 \times 10^{-6}$], respectively). In contrast, DAI-1 treatment upregulated the protein expression levels of BMP-2 and Runx2 [1.25- ($p = 0.021$), 1.46- ($p = 0.0059$), and 2.27-fold ($p = 0.0043$); and 1.47- ($p = 0.0023$), 1.67- ($p = 0.0012$), and 1.88-fold ($p = 4.7 \times 10^{-5}$), respectively, for the low, medium, and high

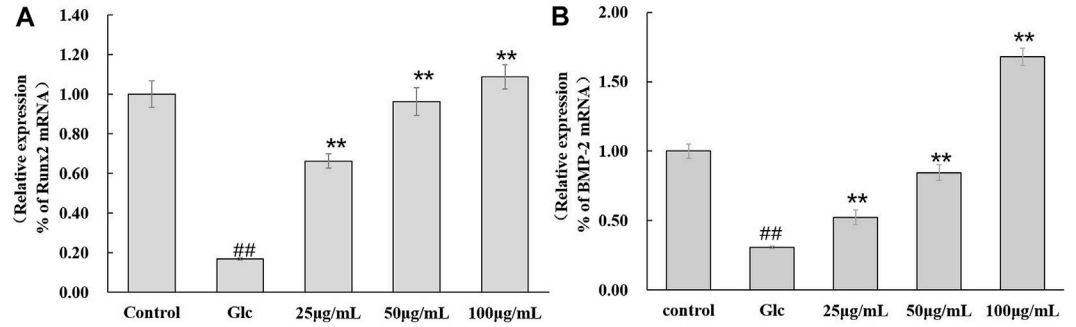

FIGURE 6 | The effect of DAI-1 on the relative mRNA expression of the osteoblast differentiation-related factors Runx2 **(A)** and BMP-2 **(B)** in a high-glucose environment. After 48 h of treatment, the transcription levels of Runx2 and BMP-2 in osteoblasts were quantified using quantitative real-time PCR. $^{\#\#}$: $p < 0.01$, for high-glucose group *vs*.the control group; *: $p < 0.05$, **: $p < 0.01$, for the DAI-1and DAI-2 treated group *vs*. high-glucose group.

DAI-1 concentrations]. These data demonstrated that DAI-1 treatment could markedly reverse the high-glucose-induced inhibition of BMP-2 and Runx2 protein expression.

DAI-1 and DAI-2 Inhibited the mRNA Expression of BMP-2 and Runx2 in Osteoblasts Under High-Glucose Conditions

The effect of DAI-1 treatment on BMP-2 and Runx2 mRNA levels is shown in **Figure 6**. After 48 h of culture, glucose treatment led to a decrease in the mRNA expression levels of BMP-2 (0.31-fold, $p = 3.0 \times 10^{-5}$) and Runx2 (0.17-fold, $p = 2.3 \times 10^{-5}$) relative to those in the control group. Compared with cells treated with glucose only, those exposed to glucose plus a high DAI-1 concentration displayed the greatest increases in BMP-2 (5.5-fold, $p = 2.5 \times 10^{-5}$) and Runx2 (1.1-fold, $p = 0.0003$) mRNA expression. Meanwhile, no significant difference in the mRNA expression of BMP-2 and Runx2 was observed with DAI-2 treatment ($p > 0.05$, data not shown).

DISCUSSION

Our findings showed that exposure to DAI-1, but not DAI-2, could promote osteoblast proliferation and differentiation in a high-glucose environment. This result was likely closely related to differences in the structure of the two polysaccharides. The molecular weight, monosaccharide composition, glycosidic bond, advanced structure and other structural characteristics of polysaccharides can affect the activity of polysaccharides (Ryoyama et al., 2014; Xiao et al., 2014; Xu F. et al., 2016). We have previously shown that the molecular mass of *Tremella* polysaccharide is the decisive factor affecting its immune activity (Gao et al., 2020). In this experiment, although DAI-1 and DAI-2 have the same composition and type of sugar residue, they differ in molecular mass and the presence/absence of branched chains. Future studies should focus on investigating the effect of polysaccharide structure on osteoblast activity.

Diabetic OP is a disorder of bone metabolism caused by long-term exposure to high-glucose conditions and has been associated with impaired osteoblast function. Osteoblasts, key regulators of bone formation, have important functions in bone matrix synthesis and secretion, bone mineralization, and bone remodeling. When osteoblast function is compromised or osteoblast numbers are reduced, the bone resorption rate exceeds the rate of bone formation, leading to decreased bone mass and, consequently, OP. Osteoblast differentiation, an important stage of bone formation, comprises three main phases, namely, cell proliferation, extracellular matrix maturation, and mineralization. Intriguingly, a high-glucose environment can repress the expression of genes and proteins related to osteogenic differentiation, resulting in the inhibition of osteoblast proliferation and differentiation.

ALP is a reliable marker of the early stage of osteoblast differentiation and serves as a functional indicator of osteoblast differentiation. ALP plays a major role in calcification *in vivo* and its positively correlated with osteoblast maturation status. Another osteoblast marker, OCN, is associated with the bone mineralization process during late osteoblast differentiation. Importantly, ALP and OCN activities undergo specific changes that are characteristic of each type of OP, and thus have greater sensitivity and specificity for use in monitoring osteoblast differentiation when compared with other osteoblast-associated markers (Song et al., 2009; Guzman et al., 2012; Runyan et al., 2012; Kopf et al., 2014). Meanwhile, the BMP-2/Smad/Runx2/Osterix signaling pathway plays an important role in osteoblast differentiation and the synthesis and secretion of extracellular matrix components. Runx2 protein regulates the expression of its corresponding gene when BMP signals are transmitted *via* the phosphorylation of Smad1/5/8, important regulators of osteoblast differentiation and bone development. As a transcription factor, Runx2 can also promote the expression of genes encoding osteoblast-specific proteins (e.g., OCN).

In this study, we isolated DAI-1 from *D. asperoides*, a traditional Chinese medicine used for tonifying kidney and strengthening bone, and characterized its structure. Under high-glucose conditions, osteoblasts (MC3T3-E1 cells) exposed to DAI-1 exhibited a significant increase in BMP-2 and Runx2

expression at both the mRNA and protein levels. Moreover, DAI-1 treatment reversed the loss of the activities of ALP and OCN resulting from exposure to a high-glucose environment. Our data suggest that DAI-1 treatment may reverse the inhibition of MC3T3-E1 cell proliferation and differentiation induced by high levels of glucose, effects that are likely mediated through the stimulation of the BMP-2/Smad/Runx2/Osterix signaling pathway.

DATA AVAILABILITY STATEMENT

The datasets used and/or analyzed during the current study are available from the corresponding author on reasonable request.

AUTHOR CONTRIBUTIONS

DX and JL designed performed the research. WZ analyzed data. YG and XL conceived the project. QG and XL reviewed and wrote the manuscript.

FUNDING

This study was supported by grants from Jilin Provincial Department of science and technology of China (Nos. 20190304018YY and 20210401058YY), and the TCM Clinical Research Center for Bone diseases of Jilin Province (Grant No. 20180623048TC).

REFERENCES

Blumenkrantz, N., and Asboe-Hansen, G. (1973). New Method for Quantitative Determination of Uronic Acids. *Anal. Biochem.* 54 (2), 484–489. doi:10.1016/0003-2697(73)90377-1

Bradford, M. M. (1976). A Rapid and Sensitive Method for the Quantitation of Microgram Quantities of Protein Utilizing the Principle of Protein-Dye Binding. *Anal. Biochem.* 72, 248–254. doi:10.1006/abio.1976.9999

Cicuéndez, M., Silva, V. S., Hortigüela, M. J., Matesanz, M. C., Vila, M., and Portolés, M. T. (2017). MC3T3-E1 Pre-osteoblast Response and Differentiation after Graphene Oxide Nanosheet Uptake. *Colloids Surf. B Biointerfaces* 158, 33–40. doi:10.1016/j.colsurfb.2017.06.019

Compston, J. E., Mcclung, M. R., and Leslie, W. D., and (2019). Osteoporosis. *Lancet* 393, 364–376. doi:10.1016/S0140-6736(18)32112-3

Cong, G., Cui, L., Zang, M., and Hao, L. (2013). Attenuation of Renal Ischemia/reperfusion Injury by a Polysaccharide from the Roots of Dipsacus Asperoides. *Int. J. Biol. Macromol* 56, 14–19. doi:10.1016/j.ijbiomac.2012.12.024

Dubois, M., Gilles, K. A., Hamilton, J. K., Rebers, P. A., and Smith, F. (2002). Colorimetric Method for Determination of Sugars and Related Substances. *Anal. Chem.* 28, 350–356. doi:10.1021/ac60111a017

Gao, Y., Yang, X., Zheng, W., Gao, M., Gao, Q., and Xu, D. (2020). Preparation, Characterization, and Cytokine-Stimulating Activity of Oligosaccharides from Tremella Fuciformis Berk. *J. Food Biochem.* 44, e13212. doi:10.1111/jfbc.13212

Gilbert, L., He, X., Farmer, P., Rubin, J., Drissi, H., van Wijnen, A. J., et al. (2002). Expression of the Osteoblast Differentiation Factor RUNX2 (Cbfa1/AML3/Pebp2alpha A) Is Inhibited by Tumor Necrosis Factor-Alpha. *J. Biol. Chem.* 277 (4), 2695–2701. doi:10.1074/jbc.M106339200

Gong, Y., Zhang, J., Gao, F., Zhou, J., Xiang, Z., Zhou, C., et al. (2017). Structure Features and *In Vitro* Hypoglycemic Activities of Polysaccharides from Different Species of Maidong. *Carbohydr. Polym.* 173, 215–222. doi:10.1016/j.carbpol.2017.05.076

Guzman, A., Zelman-Femiak, M., Boergermann, J. H., Paschkowsky, S., Kreuzaler, P. A., Fratzl, P., et al. (2012). SMAD versus Non-SMAD Signaling Is Determined by Lateral Mobility of Bone Morphogenetic Protein (BMP) Receptors. *J. Biol. Chem.* 287 (47), 39492–39504. doi:10.1074/jbc.M112.387639

Hou, C., Yin, M., Lan, P., Wang, H., Nie, H., and Ji, X. (2021). Recent Progress in the Research of Angelica Sinensis (Oliv.) Diels Polysaccharides: Extraction, Purification, Structure and Bioactivities. *Chem. Biol. Technol. Agric.* 8, 13–26. doi:10.1186/s40538-021-00214-x

Johnson, K. A., Hessle, L., Vaingankar, S., Wennberg, C., Mauro, S., Narisawa, S., et al. (2000). Osteoblast Tissue-Nonspecific Alkaline Phosphatase Antagonizes and Regulates PC-1. *Am. J. Physiol. Regul. Integr. Comp. Physiol.* 279 (4), R1365–R1377. doi:10.1152/ajpregu.2000.279.4.R1365

Kopf, J., Paarmann, P., Hiepen, C., Horbelt, D., and Knaus, P. (2014). BMP Growth Factor Signaling in a Biomechanical Context. *Biofactors* 40 (2), 171–187. doi:10.1002/biof.1137

Lecanda, F., Avioli, L. V., and Cheng, S. L. (1997). Regulation of Bone Matrix Protein Expression and Induction of Differentiation of Human Osteoblasts and Human Bone Marrow Stromal Cells by Bone Morphogenetic Protein-2. *J. Cel Biochem* 67 (3), 386–396. doi:10.1002/(sici)1097-4644(19971201)67:3<386::aid-jcb10>3.0.co;2-b

Li, H., Zhang, D., Tan, L.-H., Yu, B., Zhao, S.-P., and Cao, W.-G. (2017). Comparison of the Antioxidant Properties of Various Solvent Extracts from Dipsacus Asperoides and Identification of Phenolic Compounds by LC-ESI-QTOF-MS-MS. *South Afr. J. Bot.* 109, 1–8. doi:10.1016/j.sajb.2016.12.018

Navarini, L., Gilli, R., Gombac, V., Abatangelo, A., Bosco, M., and Toffanin, R. (1999). Polysaccharides from Hot Water Extracts of Roasted Coffea Arabica Beans: Isolation and Characterization. *Carbohydr. Polym.* 40, 71–81. doi:10.1016/s0144-8617(99)00032-6

Needs, P. W., and Selvendran, R. R. (1993). Avoiding Oxidative Degradation during Sodium Hydroxide/methyl Iodide-Mediated Carbohydrate Methylation in Dimethyl Sulfoxide. *Carbohydr. Res.* 245, 1–10. doi:10.1016/0008-6215(93)80055-J

Park, J. Y., Park, S. D., Koh, Y. J., Kim, D. I., and Lee, J. H. (2019). Aqueous Extract of Dipsacus Asperoides Suppresses Lipopolysaccharide-Stimulated Inflammatory Responses by Inhibiting the ERK1/2 Signaling Pathway in RAW 264.7 Macrophages. *J. Ethnopharmacol* 231, 253–261. doi:10.1016/j.jep.2018.11.010

Pujari-Palmer, M., Pujari-Palmer, S., Lu, X., Lind, T., Melhus, H., Engstrand, T., et al. (2016). Pyrophosphate Stimulates Differentiation, Matrix Gene Expression and Alkaline Phosphatase Activity in Osteoblasts. *PLoS One* 11, e0163530. doi:10.1371/journal.pone.0163530

Runyan, C. E., Liu, Z., and Schnaper, H. W. (2012). Phosphatidylinositol 3-kinase and Rab5 GTPase Inversely Regulate the Smad Anchor for Receptor Activation (SARA) Protein Independently of Transforming Growth Factor-B1. *J. Biol. Chem.* 287 (43), 35815–35824. doi:10.1074/jbc.M112.380493

Ryoyama, K., Kidachi, Y., Yamaguchi, H., Kajiura, H., and Takata, H. (2014). Anti-tumor Activity of an Enzymatically Synthesized α-1, 6 Branched-1, 4-glucan Glycogen. *Biosci. Biotech. Booch* 68 (11), 2332. doi:10.1271/bbb.68.2332

Song, B., Estrada, K. D., and Lyons, K. M. (2009). Smad Signaling in Skeletal Development and Regeneration. *Cytokine Growth Factor. Rev.* 20 (5-6), 379–388. doi:10.1016/j.cytogfr.2009.10.010

Sun, X., Wei, B., Peng, Z., Fu, Q., Wang, C., Zhen, J., et al. (2019). Protective Effects of Dipsacus Asper Polysaccharide on Osteoporosis *In Vivo* by Regulating RANKL/RANK/OPG/VEGF and PI3K/Akt/eNOS Pathway. *Int. J. Biol. Macromol* 129, 579–587. doi:10.1016/j.ijbiomac.2019.02.022

Wasser, S. P. (2002). Medicinal Mushrooms as a Source of Antitumor and Immunomodulating Polysaccharides. *Appl. Microbiol. Biotechnol.* 60 (3), 258–274. doi:10.1007/s00253-002-1076-7

Xiao, K., Zhang, L., Liu, X., Wang, Z., and Yang, S. (2014). *In Vitro* anti-tumor Effects of Chemically Modified Polysaccharides from Cherokee Rose Fruit. *Int. J. Food Eng.* 10, 473. doi:10.1515/ijfe-2014-0065

Xu, D., Wang, H., Zheng, W., Gao, Y., Wang, M., Zhang, Y., et al. (2016). Charaterization and Immunomodulatory Activities of Polysaccharide Isolated from Pleurotus Eryngii. *Int. J. Biol. Macromol* 92, 30–36. doi:10.1016/j.ijbiomac.2016.07.016

Xu, F., Liao, K., Wu, Y., Pan, Q., Wu, L., Jiao, H., et al. (2016). Optimization, Characterization, Sulfation and Antitumor Activity of Neutral Polysaccharides from the Fruit of Borojoa Sorbilis Cuter. *Carbohydr. Polym.* 151, 364. doi:10.1016/j.carbpol.2016.05.091

Zhang, Y., Kiyohara, H., Matsumoto, T., and Yamada, H. (1997). Fractionation and Chemical Properties of Immunomodulating Polysaccharides from Roots of Dipsacus Asperoides. *Planta Med.* 63 (5), 393–399. doi:10.1055/s-2006-957720

Zhao, J., Deng, Y., and Li, S. P. (2017). Advanced Analysis of Polysaccharides, Novel Functional Components in Food and Medicine Dual Purposes Chinese Herbs. *Trends Analyt. Chem.* 96, 1–13. doi:10.1016/j.trac.2017.06.006

Zhao, T., Mao, G., Feng, W., Mao, R., Gu, X., Li, T., et al. (2014). Isolation, Characterization and Antioxidant Activity of Polysaccharide from Schisandra Sphenanthera. *Carbohydr. Polym.* 105, 26–33. doi:10.1016/j.carbpol.2014.01.059

Zhen, D., Chen, Y., and Tang, X. (2010). Metformin Reverses the Deleterious Effects of High Glucose on Osteoblast Function. *J. Diabetes Complications* 24 (5), 334–344. doi:10.1016/j.jdiacomp.2009.05.002

Conflict of Interest: The authors declare that this research was conducted in the absence of any commercial or financial relationships that could be construed as a potential conflict of interest.

Publisher's Note: All claims expressed in this article are solely those of the authors and do not necessarily represent those of their affiliated organizations, or those of the publisher, the editors and the reviewers. Any product that may be evaluated in this article, or claim that may be made by its manufacturer, is not guaranteed or endorsed by the publisher.

Copyright © 2022 Xu, Liu, Zheng, Gao, Gao and Leng. This is an open-access article distributed under the terms of the Creative Commons Attribution License (CC BY). The use, distribution or reproduction in other forums is permitted, provided the original author(s) and the copyright owner(s) are credited and that the original publication in this journal is cited, in accordance with accepted academic practice. No use, distribution or reproduction is permitted which does not comply with these terms.

frontiers | Frontiers in Pharmacology

ORIGINAL RESEARCH
published: 01 April 2022
doi: 10.3389/fphar.2022.855393

Ginsenoside Compound K Enhances Fracture Healing *via* Promoting Osteogenesis and Angiogenesis

Lingli Ding[1], Song Gu[2], Bingyu Zhou[1], Min Wang[1], Yage Zhang[1], Siluo Wu[1], Hong Zou[3], Guoping Zhao[4,5,6,7,8,9], Zhao Gao[10]* and Liangliang Xu[1]**

[1]Key Laboratory of Orthopaedics and Traumatology, Lingnan Medical Research Center, The First Affiliated Hospital of Guangzhou University of Chinese Medicine, Guangzhou University of Chinese Medicine, Guangzhou, China, [2]The First Affiliated Hospital, Guizhou University of Traditional Chinese Medicine, Guiyang, China, [3]Engineering Laboratory for Nutrition, Shanghai Institute of Nutrition and Health, Chinese Academy of Sciences, Shanghai, China, [4]Master Lab for Innovative Application of Nature Products, National Center of Technology Innovation for Synthetic Biology, Tianjin Institute of Industrial Biotechnology, Chinese Academy of Sciences, Tianjin, China, [5]CAS Key Laboratory of Quantitative Engineering Biology, Shenzhen Institute of Synthetic Biology, Shenzhen Institute of Advanced Technology, Chinese Academy of Sciences, Shenzhen, China, [6]CAS-Key Laboratory of Synthetic Biology, CAS Center for Excellence in Molecular Plant Sciences, Shanghai Institute of Plant Physiology and Ecology, Chinese Academy of Sciences, Shanghai, China, [7]Bio-Med Big Data Center, Shanghai Institute of Nutrition and Health, Chinese Academy of Sciences, Shanghai, China, [8]State Key Laboratory of Genetic Engineering, Department of Microbiology and Immunology, School of Life Sciences, Fudan University, Shanghai, China, [9]Department of Microbiology, The Chinese University of Hong Kong, Hong Kong, Hong Kong SAR, China, [10]Er Sha Sports Training Center of Guangdong Province, Guangzhou, China

OPEN ACCESS

Edited by:
Longhuo Wu,
Gannan Medical University, China

Reviewed by:
Xiaowei Wei,
Affiliated Zhongshan Hospital of Dalian University, China
Dong Yao,
Affiliated Hospital of Guilin Medical University, China

***Correspondence:**
Guoping Zhao
gpzhao@sibs.ac.cn
Zhao Gao
qiqin1990@163.com
Liangliang Xu
xull-2016@gzucm.edu.cn

Specialty section:
This article was submitted to Ethnopharmacology, a section of the journal Frontiers in Pharmacology

Received: *15 January 2022*
Accepted: *07 March 2022*
Published: *01 April 2022*

Citation:
Ding L, Gu S, Zhou B, Wang M, Zhang Y, Wu S, Zou H, Zhao G, Gao Z and Xu L (2022) Ginsenoside Compound K Enhances Fracture Healing via Promoting Osteogenesis and Angiogenesis. Front. Pharmacol. 13:855393. doi: 10.3389/fphar.2022.855393

Fractures have an extraordinarily negative impact on an individual's quality of life and functional status, particularly delayed or non-union fractures. Osteogenesis and angiogenesis are closely related to bone growth and regeneration, and bone modeling and remodeling. Recently Chinese medicine has been extensively studied to promote osteogenic differentiation in MSCs. Studies have found that Ginseng can be used as an alternative for tissue regeneration and engineering. Ginseng is a commonly used herbal medicine in clinical practice, and one of its components, Ginsenoside Compound K (CK), has received much attention. Evidence indicates that CK has health-promoting effects in inflammation, atherosclerosis, diabetics, aging, etc. But relatively little is known about its effect on bone regeneration and the underlying cellular and molecular mechanisms. In this study, CK was found to promote osteogenic differentiation of rat bone marrow mesenchymal stem cells (rBMSCs) by RT-PCR and Alizarin Red S staining *in vitro*. Mechanistically, we found CK could promote osteogenesis through activating Wnt/β-catenin signaling pathway by immunofluorescence staining and luciferase reporter assay. And we also showed that the tube formation capacity of human umbilical vein endothelial cells (HUVECs) was increased by CK. Furthermore, using the rat open femoral fracture model, we found that CK could improve fracture repair as demonstrated by Micro-CT, biomechanical and histology staining analysis. The formation of H type vessel in the fracture callus was also increased by CK. These findings provide a scientific basis for treating fractures with CK, which may expand its application in clinical practice.

Keywords: CK, fracture healing, Wnt/β-catenin, osteogenesis, angiogenesis

INTRODUCTION

Fractures have an extraordinarily negative influence on an individual's quality of life and functional status. Bone is one of the organs that have the capacity to regenerate. Fracture disrupts bone circulation, leading to necrosis and hypoxia of adjacent bones (Glowacki 1998). Type H vessels, with high expression of Endomucin (Emcn) and CD31, have recently been identified and have the ability to induce bone formation (Peng et al., 2020). Fracture repair usually could restore the damaged bone to its pre-injury cellular composition, structure and biomechanical function, but approximately 10% of fractures do not heal properly (Einhorn and Gerstenfeld 2015). Some alternative therapies can promote fracture healing to prevent delayed healing or non-healing, such as herbal medicine.

Ginseng is a traditional Chinese herb that has been widely used in Asia for thousands of years to keep the physical vigor, improve immunity and resistance to aging, etc. Some ginsenosides have been found to prevent osteoporosis (Liu et al., 2020) and osteoarthritis (Chen et al., 2016), and also improve fracture healing (Gu et al., 2016). Ginsenoside compound K is a metabolite produced by ginsenosides Rb1, Rb2 and Rc through the metabolism of intestinal bacteria *in vivo* (Yang et al., 2015). The metabolic pathway of protopanaxadiol type ginsenosides by human intestinal bacteria is Rb1, Rb2 or Rc→Rd→F2→CK(Zhou et al., 2008), which has also been shown to be same in hydrolytic pathway (Zhou et al., 2018). Rb2 can reduce oxidative damage and bone resorption cytokines, reflecting the ability of anti-osteoporosis (Huang et al., 2014). Treatment of 3T3-L1 cells with CK inhibited adipocyte differentiation and expression of adipocyte-specific genes (Park and Yoon 2012). Meanwhile, a variety of studies have reported that ginsenosides could regulate angiogenesis. For example, ginsenoside-Rg1 has been shown to induce angiogenesis (Kwok et al., 2015). Ginsenoside Rg1 increased the expression of VEGF through PI3K/Akt/mTOR signaling pathway and promoted cerebral angiogenesis after ischemic stroke (Chen et al., 2019a). Ginsenoside F1-induced activation of the IGF-1/IGF1R pathway to promote angiogenesis is an effective approach to alleviate cerebral ischemia (Zhang et al., 2019).

It has been reported that CK could significantly elevate the mRNA expression of genes regulating Wnt/β-catenin signaling, including Wnt10b, Wnt11, Lrp5 and β-catenin (Zhou et al., 2018). Many studies have shown that the Wnt/β-catenin signaling controls bone formation and osteoblast differentiation (Kobayashi et al., 2016; Yuan et al., 2016; Shen et al., 2020). Angiogenesis is an essentially biological process in bone regeneration and is also closely linked to the Wnt/β-catenin signaling pathway (Shi et al., 2020; Shen et al., 2021; Yu et al., 2021). However, it is unknown whether CK is effective on fracture repair, as well as the underlying mechanisms involved. In the present study, we investigated the effects of CK on rat fracture healing, including osteogenic differentiation and angiogenesis, and elucidated its potential regulation of Wnt/β-catenin signaling pathway.

TABLE 1 | Primers used for RT-PCR.

Traget gene	Sequence (5′-3′)
GAPDH	F,AGGTCGGTGTGAACGGATTTG
	R,TGTAGACCATGTAGTTGAGGTCA
OPN	F,AGCAAGAAACTCTTCCAAGCAA
	R,GTGAGATTCGTCAGATTCATCCG
OCN	F,GGTGGCTTCCGAAGGATTGTC
	R,CCCCCTGATGGGTTGTCAC
OSX	F,ATGGCGTCCTCTCTGCTTG
	R,TGAAAGGTCAGCGTATGGCTT
ALP	F,GCAAGGGTGAGGAGGGGTA
	R,CCTCTGAAGGCATTTCATAAGCC

MATERIALS AND METHODS

Reagents and Antibodies

CK was provided by Zhejiang Hongguan Bio-pharma Co., Ltd., and dissolved in DMSO, and diluted in PBS. Modified Eagle's Medium of Alpha (α-MEM), Dulbecco's Modified Eagle Medium/Nutrient Mixture F-12 (DMEM/F-12), fetal bovine serum (FBS), and penicillin/streptomycin were purchased from Gibco (United States). Beta-glycerolphosphate, dexamethasone, ascorbic acid phosphate, Safranine O, and Fast Green were purchased from Sigma (United States). Alizarin Red S was purchased from Solarbio (Beijing, China). Cell Counting Kit-8 (CCK-8) was purchased from Beyotime (Beijing, China). NucleoZOL reagent, Reverse Transcription Kit and SYBR-Green Master Mix were supplied by Takara (Japan). Hematoxylin-eosin (H&E) was purchased from biosharp (China). Primary antibodies against CD31, β-catenin, and DAPI were supplied by Santa Cruz Biotechnology (United States); Primary antibodies anti-CTSK, anti-ALP, anti-OPG, anti-RANKL, anti-Runx2, and anti-OPN were purchased from Bioss (China); Anti-GAPDH, and DAPI were obtained from Abcam (United States). Secondary antibodies HRP-conjugated Goat Anti-Rabbit IgG, Goat anti-Mouse IgG (H + L), Rabbit Anti-Rabbit IgM/Cy3 and Rabbit Anti-Mouse IgM/FITC were obtained from Bioss (China). Dual-Luciferase Reporter Assay System was supplied by Promega Company (United States). Matrigel was purchased from Becton Dickinson (United States).

RNA Extraction and qRT-PCR

After inducing differentiation for 3 days in 12-well plates with osteogenic induction medium, the total RNA was extracted using NucleoZOL, and cDNA was obtained from total RNA using a Reverse Transcription Kit. Next, qRT-PCR was performed using SYBR Green qPCR Master Mix. The relative gene expression was calculated by the $2^{-\Delta CT}$ method, and GAPDH was used as a reference for normalization. The primers were purchased from Invitrogen (United States) and primer sequences are shown in **Table 1**.

Bone Marrow Mesenchymal Stem Cells Isolation and Culture

The method of rat bone marrow mesenchymal stem cells (BMSCs) isolation and cultivation has been described

previously (Shen et al., 2018). BMSCs were isolated from Sprague-Dawley rats (male, 2 weeks old, 30–40 g) in a sterile environment. Rats were euthanized and the bone marrow of the bilateral femoral was flushed out with serum-free α-MEM to obtain a single-cell suspension. Flushed bone marrow cells was centrifuged at 1200 rpm for 6 min, the supernatant liquid was removed, and the cell pellets were resuspended in α-MEM supplemented with 10% fetal bovine serum, 1% penicillin and streptomycin. The medium was discarded after 72 h of primary culture and then changed once every 3 days. Upon 80—90% confluence, the adherent cells were further expanded with trypsin. The medium was changed several times to obtain pure BMSCs. Cells from passages 3 to 5 were used in the study.

Cell Counting Kit-8 Assay

The cell viability of CK on BMSCs was assessed using a Cell Counting Kit-8 (CCK-8) kit (C0037, Beyotime Biotechnology Co., Ltd., Shanghai, China). BMSCs or HUVECs were seeded in a 96-well plate with 5000 cells in each well and cultured without or with CK (0, 2.5,5, 10, 20, 30 and 40 μM) for 48 and 72 h. Subsequently, CCK-8 reagent was added to each well and the plates were incubated for 1 h at 37°C. The Optical density (OD) of the samples was measured at 450 nm with a spectrophotometric microplate reader (Xianke Instruments, Shanghai, China). The experiment was independently repeated 3 times.

Animal Experiments

8 week-old male Sprague Dawley (SD) rats (220 ± 10 g, $n = 18$) were purchased from the Guangzhou Medicine Laboratory Animal Center. The animals were housed in the First Affiliated Hospital of Guangzhou University of Chinese medicine animal center. All experimental methods were approved by the Animal Care and Use Committee of Guangzhou University of Traditional Chinese Medicine. All rats were fed with standard chow and free access to water with a 12 h light-dark cycle (24 ± 1°C). An open femoral fracture model with internal fixation was established. In brief, the procedure was performed under general anesthesia (pentobarbital sodium 100 mg/kg, intraperitoneally) and aseptic conditions. The right femur was exposed, and transverse osteotomy was performed with a hand saw to create a gap size of 2 mm. A K-wire (diameter: 1.2 mm, Stryker Ltd., United States) was inserted into the right femoral bone marrow cavity to fix the fracture. The rats were randomly assigned to the following two groups: fracture + PBS ($n = 9$, 100 μl/day), fracture + CK ($n = 9$, CK = 500 μM, 100 μl every other day). 5 days after the surgery, CK or PBS was locally injected at the fracture sites every other day for 4 weeks. Then the animals were sacrificed and the right femurs were collected for further analysis.

Histology

The femurs were harvested, fixed in 10% neutral formalin for 24 h, decalcified in 10% Ethylene Diamine Tetraacetic Acid (EDTA) for 21 days, dehydrated and then embedded in paraffin. After cutting into 5-μm-thick sections and dewaxing in xylene and rehydration in a decreasing alcohol gradient and distilled water, samples were processed for hematoxylin-eosin (H&E), and Safranine O-Fast Green (SO-FG) staining. For immunohistochemical staining, the sections were incubated in 0.3% hydrogen peroxide for 20 min and antigen retrieval in 0.01 M citrate buffer at 60°C for 30 min, and blocking with 5% g BSA in PBS for 1 h and then incubated overnight at 4°C with a primary antibody. The sections were then incubated with the secondary antibodies for 1 h at 37°C, counterstained with hematoxylin, and visualized using an HRP-streptavidin system. The primary antibodies used in this study included anti-OPG, anti-RANKL, anti-OPN and anti-ALP antibodies. For immunofluorescence staining, the slides were incubated in antigen retrieval in 0.01 M citrate buffer, and blocking with 5% g BSA in PBS for 1 h and then incubated overnight at 4°C with a primary antibody. The sections were then incubated with the fluorescent secondary antibodies for 1 h at 37°C. The primary antibodies used in this study included anti-Runx2, anti-Endomucin, anti-CD31 and anti-β-catenin antibodies. DAPI staining was carried out to stain the nuclei. Images were acquired with the fluorescence microscope (Olympus, IX73 L, United States).

Microcomputer Tomography

Microcomputer tomography (micro-CT) examination was applied for the fractured femurs. Samples were scanned by Skyscan 1176 micro-CT scanner (Bruker micro-CT, Kontich, Belgium), with a source voltage of 80 kV, current of 114 μA, Al 0.5 mm filter and 10.5 μm isotropic resolution. The fractured callus sites were defined as the volume of interest. The bone volume/tissue volume (BV/TV), mean volumetric bone mineral density (BMD), and Callus Volume were measured. Three dimensional images were generated using CTvol software (Bruker micro-CT, Kontich, Belgium).

Tube Formation Assay

Tube formation assay was performed as previously reported (Lin et al., 2019). The wells of the 12-well plate were coated with Matrigel and incubated for 30 min hBMSCs (5000 cells/well) were treated with or without CK (10 μM), and co-cultured with HUVECs (10^5 cells/well). DMEM/F12 basal medium containing 2% FBS (Thermo Fisher Scientific) was used. Plates were incubated at 37°C, 5% CO_2 for 8 h. Then the tube formation was observed using a microscope. Tubes were then assessed through an inverted fluorescent microscope at 10×(Olympus). Image J with the Angiogenesis Analyzer plugin were used to quantify the tube length and branch points of tube networks. Images taken at 5× magnification.

Luciferase Reporter Assays

Experiments were performed as described previously (Ren et al., 2019). Briefly, 293FT cells were seeded on 24-well plates and allowed to grow to 80% confluence. Cells were then transfected with TOPflash (500 ng) and Renilla reporter plasmid pRL-CMV (100 ng) using Lipofectamine 8000. 24 h after transfection, cells were treated with CK (10 μM) for 24 h. The luciferase activity was measured using a GloMax™ 20/20 single-tube luminometer (Promega, Madison, WI, United States).

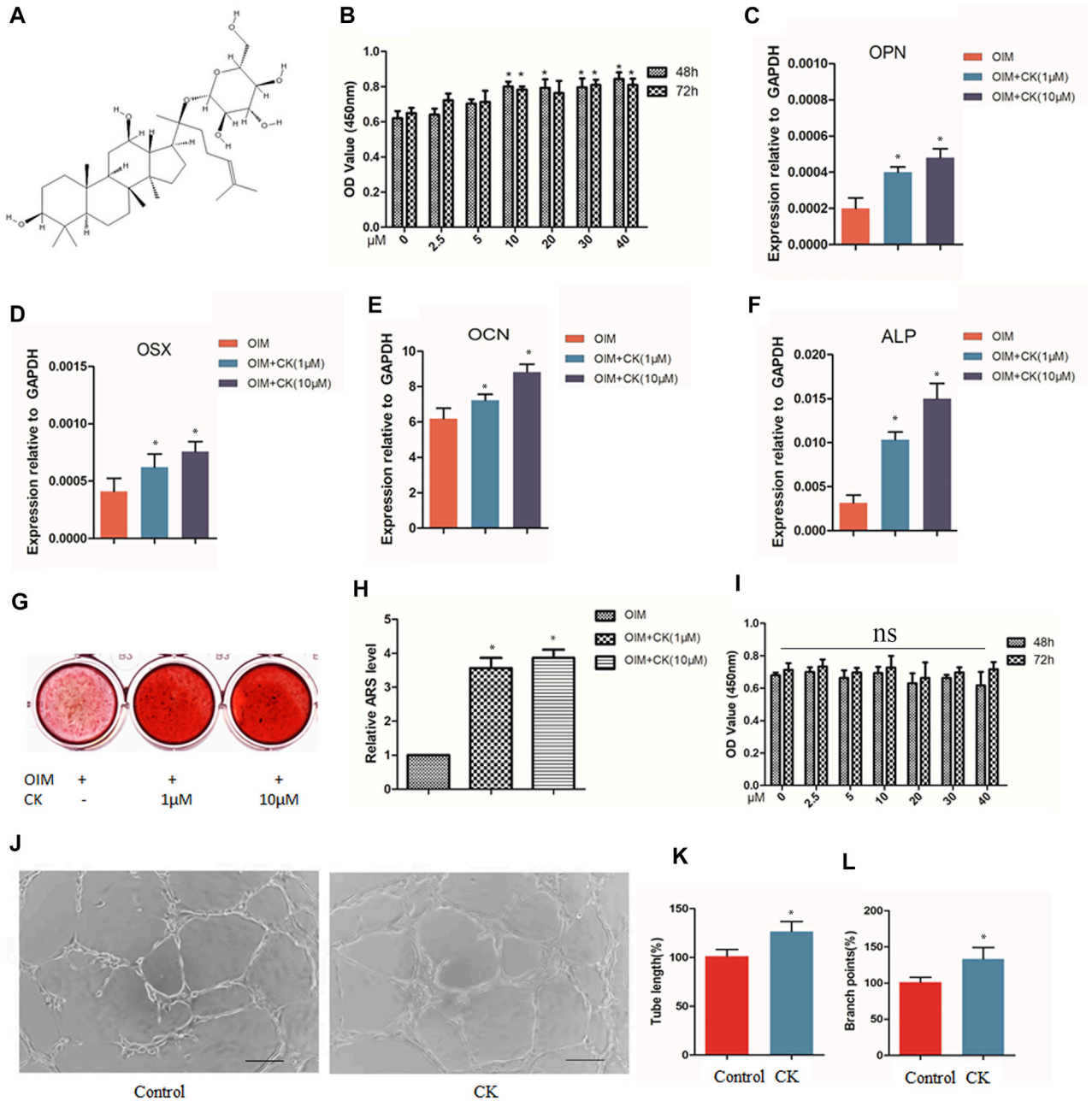

FIGURE 1 | CK enhanced cell viability, osteogenesis and angiogenesis *in vitro*. **(A)** The chemical structure depiction of CK. **(B)** Optical density (OD) values indicating the effects of CK treatment for 48 h and 72h on cell viability of BMSCs, $^*p < 0.05$, $n = 3$, compared with 0 μM CK group. **(C–F)** Real-time PCR results of osteogenesis-related genes at 3 days treated with different concentrations of CK in OIM, $^*p < 0.05$, $n = 3$, compared with OIM group. **(G)** Representative staining images and **(H)** Quantification of Alizarin Red S of BMSCs incubated with different concentrations of CK in OIM for 14 days, $^*p < 0.05$, $n = 3$, compared with OIM group. **(I)** Optical density (OD) values indicating the effects of CK treatment for 48 h and 72h on cell viability of HUVECs, $^*p < 0.05$, $n = 3$, compared with 0 μM CK group. **(J)** Representative images of tube formation assay and **(K-L)** Quantitative analysis of tube length and branch points in Matrigel MSCs and HUVEC co-culture system, Scale bars < 100 μm, $^*p < 0.05$, compared with the Control group, $n = 3$.

Three-Point Bending Biomechanical Testing

Three-point bending biomechanical testing was performed as previously reported (Lin et al., 2019). Fractured femurs were tested to failure with a constant displacement rate of 4 mm/min by a 3-point bending device (H25KS; Tinius Olsen, United Kingdom). The fractured femur was loaded in the front and back directions, and the span of the two support points was set

as 10 mm. The force loading point was set at the fracture site. After testing, ultimate load to failure and energy absorbed to failure were recorded and analyzed by the QMAT software.

Statistical Analysis

We applied GraphPad Prism 5 for comparison. Quantitative data were expressed as mean ± standard deviation (SD). Statistics were analyzed by t-test for two-group comparison, and One-way or two-way analysis of variance (ANOVA) for multi-comparison between groups. We used Tukey's post hoc multiple comparisons test as the posttest method for ANOVA. P values <0.05 were considered statistically significant.

RESULTS

CK Enhanced Osteogenic Differentiation and Angiogenesis *In Vitro*

The chemical structure depiction of CK was shown in **Figure 1A**. BMSCs were cultured without or with CK (0, 2.5,5, 10, 20, 30 and 40 μM) for 48 and 72 h. The CCK-8 assay results showed that CK exhibited no obvious cytotoxicity to BMSCs even at the high concentration of 40μM, and CK at 10–40 μM increased the cell viability of BMSCs (**Figure 1B**). To investigate the effect of CK on osteogenic differentiation of BMSCs, BMSCs were cultured in the osteogenic induction medium (OIM) with or without CK at various concentrations (0, 1, and 10 μM) for 3 and 14 days. At the third day of osteogenic induction, the expression of osteogenesis-related genes was detected and it was found that the RNA levels of osteopontin (OPN), alkaline phosphatase (ALP), osteocalcin (OCN) and osterix (OSX) were significantly up-regulated by CK (**Figures 1C–F**). Furthermore, Alizarin Red S staining showed that CK significantly increased the formation of calcium deposits after 14 days of induction (**Figures 1G,H**). As 10 μM CK showed the best effect, it was used for the following *in vitro* experiments.

HUVECs were cultured without or with CK (0, 2.5,5, 10, 20, 30 and 40 μM) for 48 and 72 h. The CCK-8 assay showed that CK exhibited no obvious cytotoxicity to HUVECs (**Figure 1I**). Some studies have reported MSCs can stimulate migration and angiogenesis of HUVECs (Chiang et al., 2018; Liu et al., 2019). To investigate the effect of CK on angiogenesis in the presence of MSCs, the HUVEC cells were co-cultured with BMSCs treated with or without CK (10 μM), and the tube length and branch points were evaluated (**Figures 1J–L**). We could observe that the tube formation capacity of HUVEC was increased by CK. The result demonstrated that CK enhanced angiogenesis *in vitro* compared with the control group.

CK Activated Wnt/β-Catenin Signaling Pathway in Bone Marrow Mesenchymal Stem Cells

It is well known that the Wnt/β-catenin signaling has been shown as an important regulatory pathway in the osteogenic differentiation of mesenchymal stem cells (Kim et al., 2013). To verify whether the Wnt/β-catenin signaling pathway is activated upon CK treatment in BMSCs, we performed immunofluorescence staining to detect the level of β-catenin and its co-location with Runx2 in rBMSCs. Immunofluorescence analysis revealed more nuclear translocation of β-catenin and an increased expression of Runx2 in the CK (10 μM) group, compared with the OIM group (**Figures 2A,B**). Additionally, the TOP flash assay was used to evaluate the effect of CK (10 μM) on the activation of the Wnt/β-catenin signaling pathway. After 24 h of stimulation, the luciferase activity was significantly increased by CK (**Figure 2C**).

CK Improved Fracture Healing

We further conducted an open femoral fracture model to evaluate whether CK could accelerate fracture healing in rats. The time points of animal modeling and sample collection were shown in **Figure 3A**. The 3-dimensional images of the femurs obtained by micro-CT analysis showed that the fracture gap was almost filled by new bone in the CK-treated rats at 4w post-fracture, compared with that of the PBS group (**Figure 3B**). The BMD, BV/TV and callus volume at femoral callus sites of CK-treated rats were significantly higher than those in the PBS group (**Figures 3C–E**). In addition, results of biomechanical testing confirmed a much stronger biomechanical property in the femoral bones of CK- treated group than those of the PBS group (**Figures 3F,G**).

Furthermore, H&E and SO-FG staining of the callus showed varying amounts of newly formed trabecular bone, cartilage tissue and fibrous-like tissue. Callus of CK-treated rats exhibited enhanced bone regeneration after 4 weeks, in comparison with the PBS group, which was evidenced by more neo-formed trabecular bone and less cartilaginous and fibrous-like tissue in the CK group (**Figures 4A,B**). Additionally, higher expression of OPG, OCN, ALP and lower expression of RANKL within the callus areas of the CK group was confirmed using immunohistochemical analysis (**Figures 4C–F**).

CK Promoted H Type Vessel Formation *In Vivo*

In addition, the H-type vessel was observed *in vivo* in sections of femur. The CD31 and Emcn double immunofluorescent staining revealed a greater population of $CD31^{hi}Emcn^{hi}$ cells within the callus of the CK group, compared with the PBS group (**Figures 5A,B**).

CK Up-Regulated the β-Catenin Expression in the Fracture Callus

To detect the expression of β-catenin in fracture callus treated with CK, we performed immunofluorescent staining to detect the level of β-catenin and Runx2 in fracture callus. Immunofluorescence analysis revealed a higher expression of β-catenin and Runx2 within the callus of the CK group, compared with PBS group (**Figures 6A,B**), which is consistent with the *in vitro* experiment.

DISCUSSION

Osteogenic differentiation of MSCs is the principal mechanism of bone regeneration and fracture repair. It has been reported that

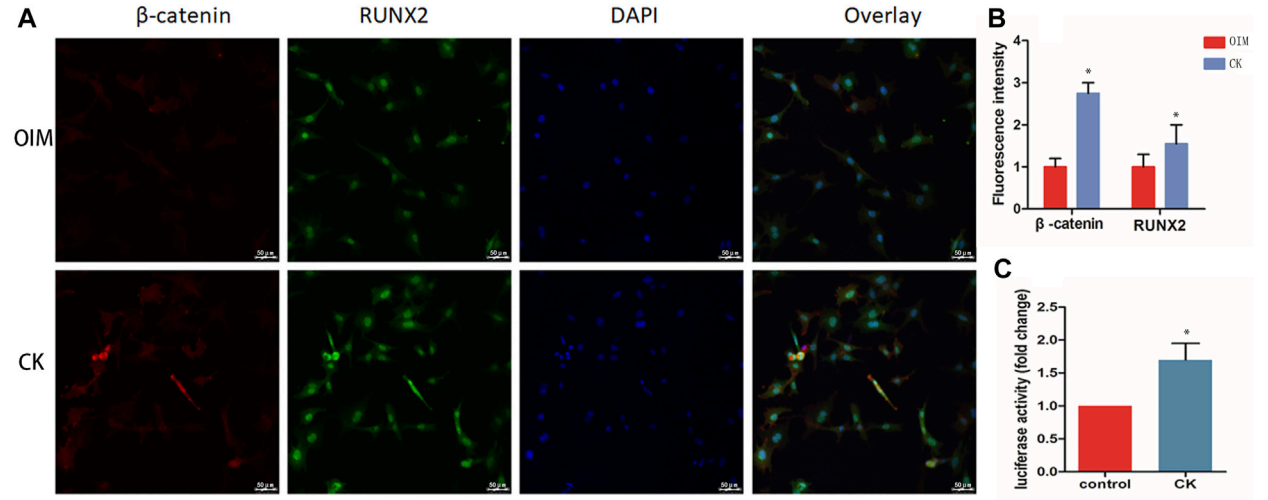

FIGURE 2 | CK increased β-catenin and Runx2 expression in BMSCs. **(A)** Representative images and **(B)** Quantification of immunofluorescence staining of β-catenin and Runx2 treated with 10 μM CK for 24 h. Scale bars = 50 μm, *$p < 0.05$, compared with the OIM group, $n = 3$ **(C)** The TOPflash luciferase activity was measured in BMSCs after treatment of CK (10 μM). *$p < 0.05$, compared with the Control group, $n = 3$.

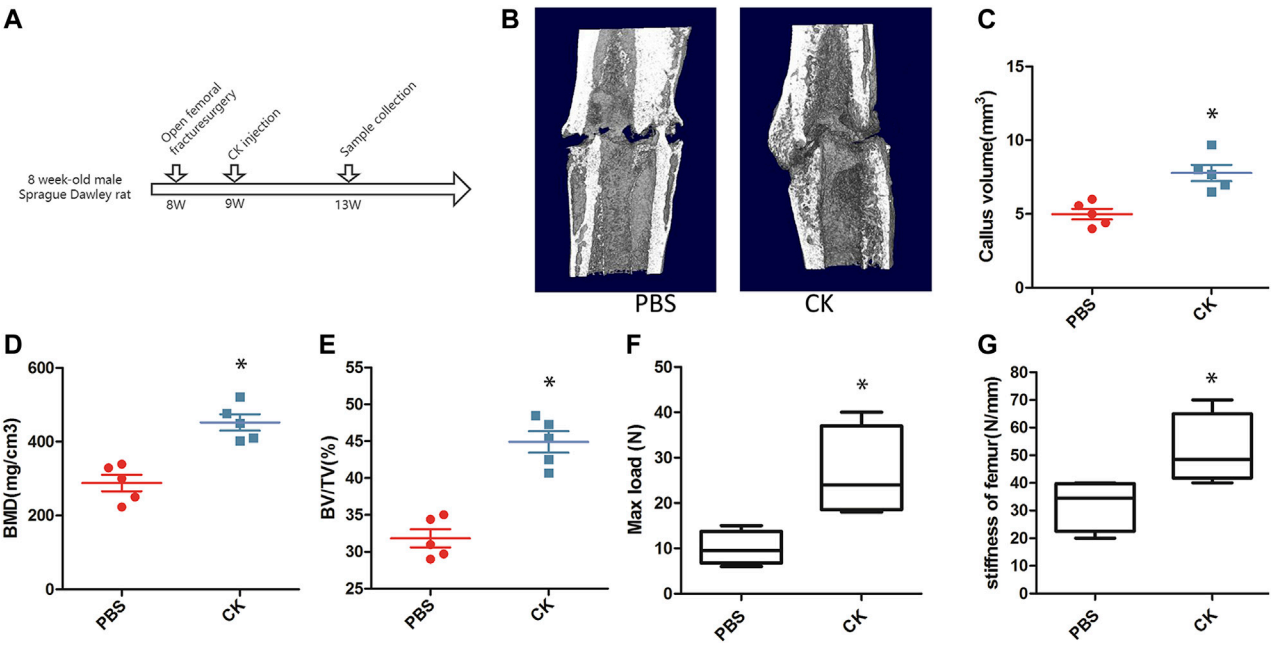

FIGURE 3 | CK accelerated the progression of fracture healing. **(A)** Schematic illustration of time points of animal modeling and sample collection. **(B)** Representative 3-dimensional micro-CT images of femurs in each group. **(C–E)** Quantitative analysis of parameters, including CV, BMD, and BV/TV, *$p < 0.05$, compared with the PBS group, $n = 3$ **(F–G)** Biomechanical properties of the fractured bones by 3-point bending test, *$p < 0.05$, compared with the PBS group, $n = 6$.

the expressions of alkaline phosphatase (ALP), type I collagen (COL-I) and mineralization were significantly increased after CK treatment in H_2O_2-stimulated MC3T3-E1 cells (Kang et al., 2016). Studies have shown that CK improved the biocompatibility and morphology of microsphere scaffolds without affecting the biocompatibility, and CK impregnated porous microsphere scaffold system may be applicable as a promising microsphere scaffold for bone regeneration (Thangavelu et al., 2020). In this study, we found that CK promoted the osteogenic differentiation of BMSCs. Our results demonstrated that CK enhanced the mineralization and mRNA expression of osteogenic markers in rat BMSCs, including ALP, Runx2, OPN and OCN. Fracture healing is closely related to the number and activity of BMSCs near the fracture site (Gu et al.,

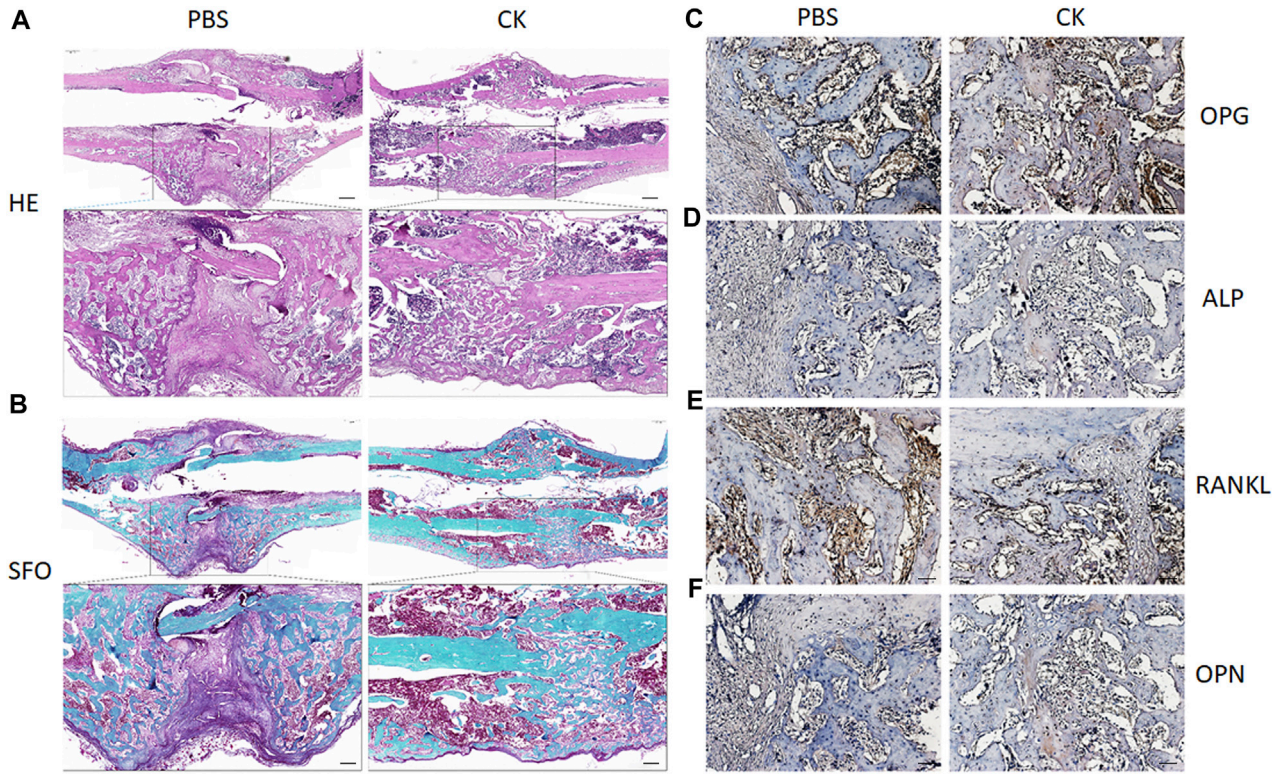

FIGURE 4 | H&E, Safranin O-Fast Green, and immunohistochemical examination of fracture callus. **(A)** Representative images of H&E staining of fracture calluses in PBS and CK groups. Insets indicate the regions shown in the enlarged images (lower). Scale bar: 500 μm. **(B)** Representative images of Safranin O-Fast Green staining of fracture calluses in PBS and CK groups. Insets indicate the regions shown in the enlarged images (lower). **(C–F)** Representative images of immunohistochemical analysis of OPG, ALP, RANKL and OPN of fracture calluses in PBS and CK groups. Scale bar = 50 μm.

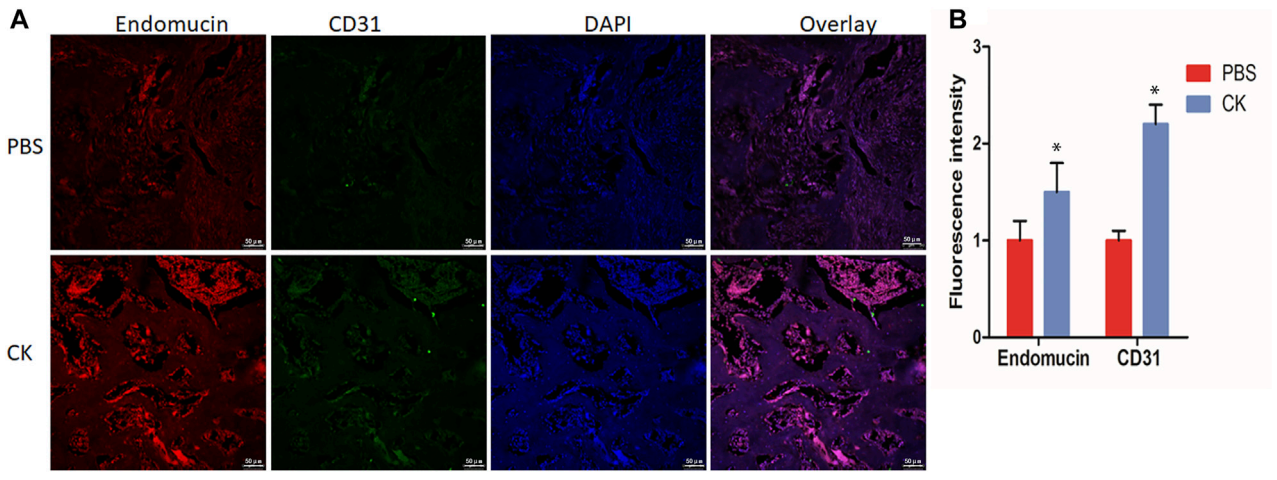

FIGURE 5 | CK regulated H-type vessel formation in fracture callus. **(A)** Representative immunofluorescence double staining and **(B)** Quantification of CD31 (green), EMCN (red) of fracture calluses in PBS and CK groups, Scale bars = 50 μm, $^{*}p < 0.05$, compared with the PBS group, $n = 3$.

2016). What's more, human umbilical vein endothelial cells (HUVECs) play an important role as a model system for studying the regulation of endothelial cell function and angiogenesis. It is well known that both osteogenesis and angiogenesis are integrated parts of bone regeneration (Huang et al., 2015). Interestingly, our results showed CK increased tube

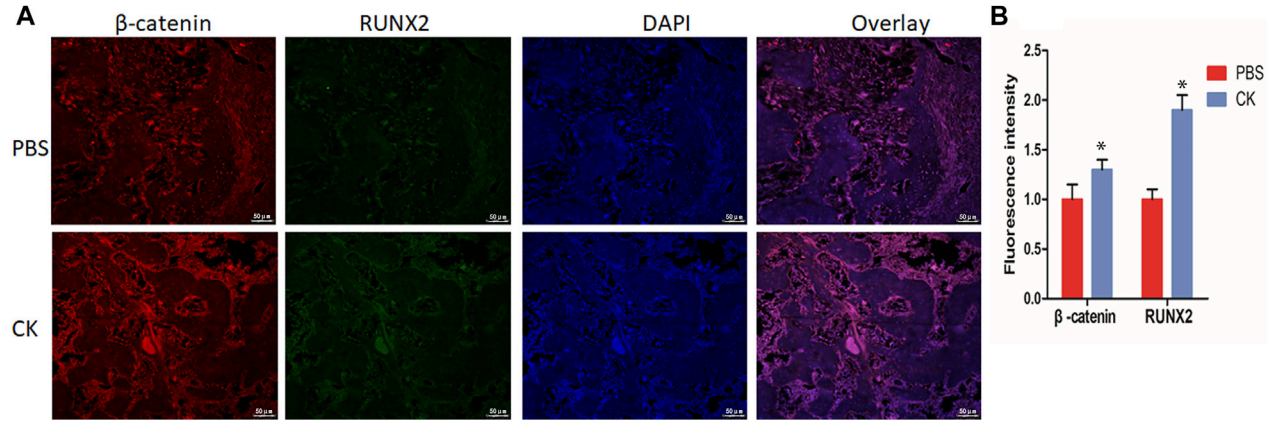

FIGURE 6 | CK up-regulated β-catenin and Runx2 in fracture callus. **(A)** Immunofluorescence staining images of β-catenin and Runx2 in PBS and CK groups and **(B)** Quantification of the immunofluorescence density of β-catenin and Runx2 of fracture calluses in PBS and CK groups, Scale bars = 50 μm, $^{*}p < 0.05$, compared with the PBS group, $n = 3$.

formation when HUVEC and BMSCs were co-cultured. Therefore, the *in vitro* experiments indicated that CK might up-regulate osteogenesis coupled with angiogenesis in bone regeneration.

CK is an initial bacterial metabolite of ginsenoside Rb1, which has many advantages of pharmacological properties, such as anti-cancer, anti-inflammatory, anti-aging, anti-allergenic, anti-diabetic, and anti-diabetic (Yoon et al., 2007; Yang et al., 2015; Wang et al., 2017; Chen et al., 2019b; Yin et al., 2021). In open femoral fracture rats, micro-CT examination showed that callus growth in rats treated with CK was substantially faster than that in control rats after fracture, and BMD, BV/TV, and callus volume were significantly increased in the CK-treated group. In addition, biomechanical testing confirmed a much stronger biomechanical property in the femoral bones of CK-treated rats than those of PBS-treated rats. The results of H&E, Safranin-O/Fast Green and IHC staining revealed that, compared with the PBS group, fracture callus in the CK treatment group had a significantly higher proportion of trabecular bone and better fracture healing but a much lower proportion of fibers and cartilage components inside the callus.

Recent studies have revealed that ginsenoside CK regulates multiple signaling pathways, such as PI3K/mTOR/p70S6K1, HIF-1α/NF-κB, Nrf2/Keap1, RhoA/ROCKs/YAP, and PI3K-Akt signaling pathway (Li et al., 2018; Yang et al., 2019; Chen et al., 2020; Tian et al., 2021; Zhang et al., 2021). Wnt/β-catenin signaling pathway is important not only in the growth and development of mineralized tissues, but also in regulating the skeletal response to load and unloading and the vitality and health of adult and aging bones (Duan and Bonewald 2016). Wnt/β-catenin signaling pathway has been widely reported in the regulation of osteogenesis and angiogenesis (Jiang et al., 2015; Shen et al., 2020). Runx2 is a master transcription factor governing osteogenesis (Vimalraj et al., 2015). In the present study, we found that the expression of Runx2 and β-catenin was significantly elevated *in vivo* by immunofluorescent staining, which is consistent with the *in vitro* result. Additionally, the luciferase activity further verified that CK activated β-catenin expression.

The vascular system is a major source of oxygen, nutrients, hormones, neurotransmitters and growth factors to bone cells and is essential for bone development, regeneration and remodeling (Filipowska et al., 2017). Bone regeneration is closely related to angiogenesis and impaired angiogenesis often leads to failure of fracture healing. H-type vessels, highly positive for CD31 and Endomucin, could mediate local growth of the vascular system, combine angiogenesis with osteogenesis by mediating the selective location of Osterix positive cells around blood vessels and the differentiation of these bone progenitor cells (Kusumbe et al., 2014; Ramasamy et al., 2014). In this study, we proved that CK could stimulate type H vessel formation, and promote bone formation in fracture rats.

CONCLUSION

Taken together, our study suggested that Wnt/β-catenin signaling contributed to the enhancement in the coupling of osteogenesis and angiogenesis induced by CK treatment during fracture healing. CK may serve as an effective component of Ginseng in bone tissue regeneration. However, many more potential mechanisms remain undiscovered. Further experiments or clinical trials are needed to be conducted to expand its clinical application.

DATA AVAILABILITY STATEMENT

The original contributions presented in the study are included in the article/Supplementary Material, further inquiries can be directed to the corresponding authors.

ETHICS STATEMENT

The animal study was reviewed and approved by Animal Care and Use Committee of Guangzhou University of Traditional

Chinese Medicine. Written informed consent was obtained from the owners for the participation of their animals in this study.

AUTHOR CONTRIBUTIONS

LX, GZ and HZ: conceptualization, methodology, and supervision. LD and SG: manuscript writing—original draft preparation, review and editing. BZ, MW, YZ and SW: investigation, data curation and formal analysis. LX and ZG: project administration and funding acquisition. All authors have read and agreed to the published version of the manuscript.

FUNDING

This work is supported by the grants from National Natural Science Foundation of China (81871778), and Key Project of the Sports Research Foundation of Guangdong Province (No. GDSS2020M006).

REFERENCES

Chen, J., Si, M., Wang, Y., Liu, L., Zhang, Y., Zhou, A., et al. (2019a). Ginsenoside Metabolite Compound K Exerts Anti-inflammatory and Analgesic Effects via Downregulating COX2. *Inflammopharmacology* 27 (1), 157–166. doi:10.1007/s10787-018-0504-y

Chen, J., Zhang, X., Liu, X., Zhang, C., Shang, W., Xue, J., et al. (2019b). Ginsenoside Rg1 Promotes Cerebral Angiogenesis via the PI3K/Akt/mTOR Signaling Pathway in Ischemic Mice. *Eur. J. Pharmacol.* 856, 172418. doi:10.1016/j.ejphar.2019.172418

Chen, K., Jiao, J., Xue, J., Chen, T., Hou, Y., Jiang, Y., et al. (2020). Ginsenoside CK Induces Apoptosis and Suppresses Proliferation and Invasion of Human Osteosarcoma Cells through the PI3K/mTOR/p70S6K1 Pathway. *Oncol. Rep.* 43 (3), 886–896. doi:10.3892/or.2020.7460

Chen, Y., Lin, S., Sun, Y., Pan, X., Xiao, L., Zou, L., et al. (2016). Translational Potential of Ginsenoside Rb1 in Managing Progression of Osteoarthritis. *J. Orthop. Translat* 6, 27–33. doi:10.1016/j.jot.2016.03.001

Chiang, Y. H., Lin, C. C., Chen, Y. C., and Lee, O. K. (2018). Treatment of Arsenite Intoxication-Induced Peripheral Vasculopathy with Mesenchymal Stem Cells. *Int. J. Mol. Sci.* 19 (4), 1026. doi:10.3390/ijms19041026

Duan, P., and Bonewald, L. F. (2016). The Role of the Wnt/β-Catenin Signaling Pathway in Formation and Maintenance of Bone and Teeth. *Int. J. Biochem. Cel Biol* 77 (Pt A), 23–29. doi:10.1016/j.biocel.2016.05.015

Einhorn, T. A., and Gerstenfeld, L. C. (2015). Fracture Healing: Mechanisms and Interventions. *Nat. Rev. Rheumatol.* 11 (1), 45–54. doi:10.1038/nrrheum.2014.164

Filipowska, J., Tomaszewski, K. A., Niedźwiedzki, Ł., Walocha, J. A., and Niedźwiedzki, T. (2017). The Role of Vasculature in Bone Development, Regeneration and Proper Systemic Functioning. *Angiogenesis* 20 (3), 291–302. doi:10.1007/s10456-017-9541-1

Glowacki, J. (1998). Angiogenesis in Fracture Repair. *Clin. Orthop. Relat. Res.* 355 (Suppl. l), S82–S89. doi:10.1097/00003086-199810001-00010

Gu, Y., Zhou, J., Wang, Q., Fan, W., and Yin, G. (2016). Ginsenoside Rg1 Promotes Osteogenic Differentiation of rBMSCs and Healing of Rat Tibial Fractures through Regulation of GR-dependent BMP-2/SMAD Signaling. *Sci. Rep.* 6, 25282. doi:10.1038/srep25282

Huang, C., Ness, V. P., Yang, X., Chen, H., Luo, J., Brown, E. B., et al. (2015). Spatiotemporal Analyses of Osteogenesis and Angiogenesis via Intravital Imaging in Cranial Bone Defect Repair. *J. Bone Miner Res.* 30 (7), 1217–1230. doi:10.1002/jbmr.2460

Huang, Q., Gao, B., Jie, Q., Wei, B. Y., Fan, J., Zhang, H. Y., et al. (2014). Ginsenoside-Rb2 Displays Anti-osteoporosis Effects through Reducing Oxidative Damage and Bone-Resorbing Cytokines during Osteogenesis. *Bone* 66, 306–314. doi:10.1016/j.bone.2014.06.010

Jiang, L., Yin, M., Wei, X., Liu, J., Wang, X., Niu, C., et al. (2015). Bach1 Represses Wnt/β-Catenin Signaling and Angiogenesis. *Circ. Res.* 117 (4), 364–375. doi:10.1161/circresaha.115.306829

Kang, S., Siddiqi, M. H., Yoon, S. J., Ahn, S., Noh, H. Y., Kumar, N. S., et al. (2016). Therapeutic Potential of Compound K as an IKK Inhibitor with Implications for Osteoarthritis Prevention: an In Silico and *In Vitro* Study. In Vitro *Cel Dev Biol Anim* 52 (9), 895–905. doi:10.1007/s11626-016-0062-9

Kim, J. H., Liu, X., Wang, J., Chen, X., Zhang, H., Kim, S. H., et al. (2013). Wnt Signaling in Bone Formation and its Therapeutic Potential for Bone Diseases. *Ther. Adv. Musculoskelet. Dis.* 5 (1), 13–31. doi:10.1177/1759720x12466608

Kobayashi, Y., Uehara, S., Udagawa, N., and Takahashi, N. (2016). Regulation of Bone Metabolism by Wnt Signals. *J. Biochem.* 159 (4), 387–392. doi:10.1093/jb/mvv124

Kusumbe, A. P., Ramasamy, S. K., and Adams, R. H. (2014). Coupling of Angiogenesis and Osteogenesis by a Specific Vessel Subtype in Bone. *Nature* 507 (7492), 323–328. doi:10.1038/nature13145

Kwok, H. H., Chan, L. S., Poon, P. Y., Yue, P. Y., and Wong, R. N. (2015). Ginsenoside-Rg1 Induces Angiogenesis by the Inverse Regulation of MET Tyrosine Kinase Receptor Expression through miR-23a. *Toxicol. Appl. Pharmacol.* 287 (3), 276–283. doi:10.1016/j.taap.2015.06.014

Li, X., Huang, Q., Wang, M., Yan, X., Song, X., Ma, R., et al. (2018). Compound K Inhibits Autophagy-Mediated Apoptosis through Activation of the PI3K-Akt Signaling Pathway Thus Protecting against Ischemia/Reperfusion Injury. *Cell Physiol Biochem* 47 (6), 2589–2601. doi:10.1159/000491655

Lin, W., Xu, L., Pan, Q., Lin, S., Feng, L., Wang, B., et al. (2019). Lgr5-overexpressing Mesenchymal Stem Cells Augment Fracture Healing through Regulation of Wnt/ERK Signaling Pathways and Mitochondrial Dynamics. *FASEB J.* 33 (7), 8565–8577. doi:10.1096/fj.201900082RR

Liu, J., Chuah, Y. J., Fu, J., Zhu, W., and Wang, D. A. (2019). Co-culture of Human Umbilical Vein Endothelial Cells and Human Bone Marrow Stromal Cells into a Micro-cavitary Gelatin-Methacrylate Hydrogel System to Enhance Angiogenesis. *Mater. Sci. Eng. C Mater. Biol. Appl.* 102, 906–916. doi:10.1016/j.msec.2019.04.089

Liu, Q., Zhou, J., Yang, Z., Xie, C., Huang, Y., Ling, L., et al. (2020). The Ginsenoside Exhibits Antiosteoporosis Effects in Ketogenic-Diet-Induced Osteoporosis via Rebalancing Bone Turnover. *Front. Pharmacol.* 11, 593820. doi:10.3389/fphar.2020.593820

Park, D., and Yoon, M. (2012). Compound K, a Novel Ginsenoside Metabolite, Inhibits Adipocyte Differentiation in 3T3-L1 Cells: Involvement of Angiogenesis and MMPs. *Biochem. Biophys. Res. Commun.* 422 (2), 263–267. doi:10.1016/j.bbrc.2012.04.142

Peng, Y., Wu, S., Li, Y., and Crane, J. L. (2020). Type H Blood Vessels in Bone Modeling and Remodeling. *Theranostics* 10 (1), 426–436. doi:10.7150/thno.34126

Ramasamy, S. K., Kusumbe, A. P., Wang, L., and Adams, R. H. (2014). Endothelial Notch Activity Promotes Angiogenesis and Osteogenesis in Bone. *Nature* 507 (7492), 376–380. doi:10.1038/nature13146

Ren, L., Chen, H., Song, J., Chen, X., Lin, C., Zhang, X., et al. (2019). MiR-454-3p-Mediated Wnt/β-Catenin Signaling Antagonists Suppression Promotes Breast Cancer Metastasis. *Theranostics* 9 (2), 449–465. doi:10.7150/thno.29055

Shen, G., Ren, H., Shang, Q., Zhao, W., Zhang, Z., Yu, X., et al. (2020). Foxf1 Knockdown Promotes BMSC Osteogenesis in Part by Activating the Wnt/β-Catenin Signalling Pathway and Prevents Ovariectomy-Induced Bone Loss. *EBioMedicine* 52, 102626. doi:10.1016/j.ebiom.2020.102626

Shen, J., Sun, Y., Liu, X., Zhu, Y., Bao, B., Gao, T., et al. (2021). EGFL6 Regulates Angiogenesis and Osteogenesis in Distraction Osteogenesis via Wnt/β-Catenin Signaling. *Stem Cel Res Ther* 12 (1), 415. doi:10.1186/s13287-021-02487-3

Shen, W., Luo, H., Xu, L., Wu, Z., Chen, H., Liu, Y., et al. (2018). Wnt5a Mediates the Effects of Bushen Huoxue Decoction on the Migration of Bone Marrow Mesenchymal Stem Cells *In Vitro*. *Chin. Med.* 13, 45. doi:10.1186/s13020-018-0200-2

Shi, L., Feng, L., Zhu, M. L., Yang, Z. M., Wu, T. Y., Xu, J., et al. (2020). Vasoactive Intestinal Peptide Stimulates Bone Marrow-Mesenchymal Stem Cells Osteogenesis Differentiation by Activating Wnt/β-Catenin Signaling

Pathway and Promotes Rat Skull Defect Repair. *Stem Cell Dev* 29 (10), 655–666. doi:10.1089/scd.2019.0148

Thangavelu, M., Adithan, A., John Peter, J. S., Hossain, M. A., Kim, N. S., Hwang, K. C., et al. (2020). Ginseng Compound K Incorporated Porous Chitosan/biphasic Calcium Phosphate Composite Microsphere for Bone Regeneration. *Int. J. Biol. Macromol* 146, 1024–1029. doi:10.1016/j.ijbiomac.2019.09.228

Tian, F., Wang, X., Ni, H., Feng, X., Yuan, X., and Huang, Q. (2021). The Ginsenoside Metabolite Compound K Stimulates Glucagon-like Peptide-1 Secretion in NCI-H716 Cells by Regulating the RhoA/ROCKs/YAP Signaling Pathway and Cytoskeleton Formation. *J. Pharmacol. Sci.* 145 (1), 88–96. doi:10.1016/j.jphs.2020.11.005

Vimalraj, S., Arumugam, B., Miranda, P. J., and Selvamurugan, N. (2015). Runx2: Structure, Function, and Phosphorylation in Osteoblast Differentiation. *Int. J. Biol. Macromol* 78, 202–208. doi:10.1016/j.ijbiomac.2015.04.008

Wang, L., Zhang, F., Cao, Z., Xiao, Y., Li, S., Yu, B., et al. (2017). Ginsenoside F2 Induces the Release of Mediators Associated with Anaphylactoid Reactions. *Fitoterapia* 121, 223–228. doi:10.1016/j.fitote.2017.07.010

Yang, Q., Lin, J., Zhang, H., Liu, Y., Kan, M., Xiu, Z., et al. (2019). Ginsenoside Compound K Regulates Amyloid β via the Nrf2/Keap1 Signaling Pathway in Mice with Scopolamine Hydrobromide-Induced Memory Impairments. *J. Mol. Neurosci.* 67 (1), 62–71. doi:10.1007/s12031-018-1210-3

Yang, X. D., Yang, Y. Y., Ouyang, D. S., and Yang, G. P. (2015). A Review of Biotransformation and Pharmacology of Ginsenoside Compound K. *Fitoterapia* 100, 208–220. doi:10.1016/j.fitote.2014.11.019

Yin, Q., Chen, H., Ma, R. H., Zhang, Y. Y., Liu, M. M., Thakur, K., et al. (2021). Ginsenoside CK Induces Apoptosis of Human Cervical Cancer HeLa Cells by Regulating Autophagy and Endoplasmic Reticulum Stress. *Food Funct.* 12 (12), 5301–5316. doi:10.1039/d1fo00348h

Yoon, S. H., Han, E. J., Sung, J. H., and Chung, S. H. (2007). Anti-diabetic Effects of Compound K versus Metformin versus Compound K-Metformin Combination Therapy in Diabetic Db/db Mice. *Biol. Pharm. Bull.* 30 (11), 2196–2200. doi:10.1248/bpb.30.2196

Yu, X., Rong, P. Z., Song, M. S., Shi, Z. W., Feng, G., Chen, X. J., et al. (2021). lncRNA SNHG1 Induced by SP1 Regulates Bone Remodeling and Angiogenesis via Sponging miR-181c-5p and Modulating SFRP1/Wnt Signaling Pathway. *Mol. Med.* 27 (1), 141. doi:10.1186/s10020-021-00392-2

Yuan, Z., Li, Q., Luo, S., Liu, Z., Luo, D., Zhang, B., et al. (2016). PPARγ and Wnt Signaling in Adipogenic and Osteogenic Differentiation of Mesenchymal Stem Cells. *Curr. Stem Cel Res Ther* 11 (3), 216–225. doi:10.2174/1574888x10666150519093429

Zhang, J., Liu, M., Huang, M., Chen, M., Zhang, D., Luo, L., et al. (2019). Ginsenoside F1 Promotes Angiogenesis by Activating the IGF-1/IGF1R Pathway. *Pharmacol. Res.* 144, 292–305. doi:10.1016/j.phrs.2019.04.021

Zhang, J., Ma, X., and Fan, D. (2021). Ginsenoside CK Inhibits Hypoxia-Induced Epithelial-Mesenchymal Transformation through the HIF-1α/nf-Kb Feedback Pathway in Hepatocellular Carcinoma. *Foods* 10 (6), 1195. doi:10.3390/foods10061195

Zhou, W., Huang, H., Zhu, H., Zhou, P., and Shi, X. (2018). New Metabolites from the Biotransformation of Ginsenoside Rb1 by Paecilomyces Bainier sp.229 and Activities in Inducing Osteogenic Differentiation by Wnt/β-Catenin Signaling Activation. *J. Ginseng Res.* 42 (2), 199–207. doi:10.1016/j.jgr.2017.03.004

Zhou, W., Li, J., Li, X., Yan, Q., and Zhou, P. (2008). Development and Validation of a Reversed-phase HPLC Method for Quantitative Determination of Ginsenosides Rb1, Rd, F2, and Compound K during the Process of Biotransformation of Ginsenoside Rb1. *J. Sep. Sci.* 31 (6-7), 921–925. doi:10.1002/jssc.200700406

Conflict of Interest: The authors declare that the research was conducted in the absence of any commercial or financial relationships that could be construed as a potential conflict of interest.

Publisher's Note: All claims expressed in this article are solely those of the authors and do not necessarily represent those of their affiliated organizations, or those of the publisher, the editors and the reviewers. Any product that may be evaluated in this article, or claim that may be made by its manufacturer, is not guaranteed or endorsed by the publisher.

Copyright © 2022 Ding, Gu, Zhou, Wang, Zhang, Wu, Zou, Zhao, Gao and Xu. This is an open-access article distributed under the terms of the Creative Commons Attribution License (CC BY). The use, distribution or reproduction in other forums is permitted, provided the original author(s) and the copyright owner(s) are credited and that the original publication in this journal is cited, in accordance with accepted academic practice. No use, distribution or reproduction is permitted which does not comply with these terms.

frontiers | Frontiers in Pharmacology

REVIEW
published: 06 April 2022
doi: 10.3389/fphar.2022.849513

The Role of Flavonoids in the Osteogenic Differentiation of Mesenchymal Stem Cells

Jinli Zhang[1], Zhihe Liu[1], Yang Luo[2], Xiaojian Li[3], Guowei Huang[1], Huan Chen[1], Aiguo Li[1] and Shengnan Qin[1]**

[1]Guangzhou Institute of Traumatic Surgery, Department of Orthopedics, Guangzhou Red Cross Hospital, Medical College, Jinan University, Guangzhou, China, [2]School of Physical Education, Southwest University, Guangzhou, China, [3]Department of Burn and Plastic Surgery, Guangzhou Red Cross Hospital, Medical College, Jinan University, Guangzhou, China

Mesenchymal stem cells (MSCs) play an important role in developing bone tissue engineered constructs due to their osteogenic and chondrogenic differentiation potential. MSC-based tissue engineered constructs are generally considered a safe procedure, however, the long-term results obtained up to now are far from satisfactory. The main causes of these therapeutic limitations are inefficient homing, engraftment, and directional differentiation. Flavonoids are a secondary metabolite, widely existed in nature and have many biological activities. For a long time, researchers have confirmed the anti-osteoporosis effect of flavonoids through *in vitro* cell experiments, animal studies. In recent years the regulatory effects of flavonoids on mesenchymal stem cells (MSCs) differentiation have been received increasingly attention. Recent studies revealed flavonoids possess the ability to modulate self-renewal and differentiation potential of MSCs. In order to facilitate further research on MSCs osteogenic differentiation of flavonoids, we surveyed the literature published on the use of flavonoids in osteogenic differentiation of MSCs, and summarized their pharmacological activities as well as the underlying mechanisms, aimed to explore their promising therapeutic application in bone disorders and bone tissue engineered constructs.

Keywords: tissue engineering, osteogenic differentiation, mesenchymal stem cells, flavonoids, osteoporosis

OPEN ACCESS

Edited by:
Daohua Xu,
Guangdong Medical University, China

Reviewed by:
Baoqing Yu,
Shanghai Pudong Hospital, China
Dejian Li,
Fudan University Pudong Medical Center, China
Baocheng Xie,
Southern Medical University Dongguan, China

****Correspondence:***
Aiguo Li
liaiguo7161@163.com
Shengnan Qin
qinqinsn@163.com

Specialty section:
This article was submitted to Ethnopharmacology, a section of the journal Frontiers in Pharmacology

Received: *06 January 2022*
Accepted: *16 March 2022*
Published: *06 April 2022*

Citation:
Zhang J, Liu Z, Luo Y, Li X, Huang G, Chen H, Li A and Qin S (2022) The Role of Flavonoids in the Osteogenic Differentiation of Mesenchymal Stem Cells. Front. Pharmacol. 13:849513. doi: 10.3389/fphar.2022.849513

INTRODUCTION

People are living longer than ever before because of medical, social and economic advances in the whole world. However, increasing life expectancy also brings tremendous challenges to the society, like chronic non-communicable diseases including osteogenesis are becoming the leading cause of death and disability (Williams et al., 2018; Garmany et al., 2021). Osteoporosis is a condition in that bones become weaker and more fragile owing to bone mass loss with ageing, diseases and drugs, so the chances are higher they'll crack or break. It is predicted that osteogenesis fractures will account for over 50% of the total fractures, and unlike bone fractures in young people, osteogenesis fractures induce a large proportion of disability and mortality in elderly people (Patel et al., 2021). Additionally, poor fracture healing can cause critical-sized bone defects (Miller, 2016; Nauth et al., 2018). Mesenchymal stem cells (MSCs)are a kind of adult stem cells with multiple differentiation potentials (Friedenstein, 1976) and exist in a variety of tissues including bone marrow, adipose tissue, umbilical cord, etc., (Baksh et al., 2004). Stand as promising candidates in the treatment of bone defects and other degenerative bone diseases, MSCs have great potential use

TABLE 1 | Structure of flavonoids subclasses.

Subclass name	Core chemical structure	Typical compounds
Flavanones	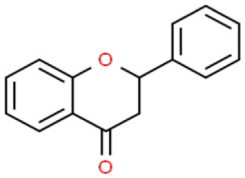	Naringin, Hesperetin
Flavonols	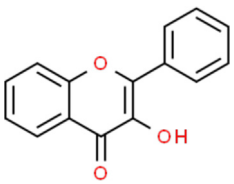	Quercetin, Kaempferol, Rutin
Flavones	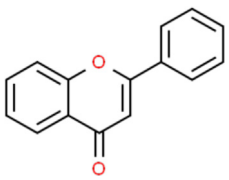	Luteolin, Apigenin
Isoflavones	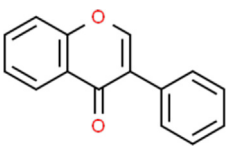	Genistein, Daidzein
Anthocyanins	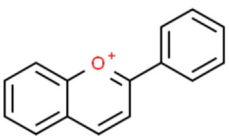	Delphinidin, Cyanidin
Chalcones	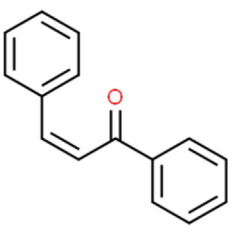	Xanthohumol

in the bone repair and regeneration owing to their osteogenic differentiation potential and extensive sources. However, the ability of MSC to differentiate into osteoblasts may become impaired under certain pathophysiological conditions including oxidative stress and inflammation (García-Sánchez et al., 2019). Hence, the strategies aimed to increase cell survival and osteogenic capacity are important for the MSCs-based bone regeneration therapies. Strategies, including promoting MSCs osteogenic differentiation through genetic modification (Armstrong and Stevens, 2019), or providing the appropriate extracellular environmental cues like scaffolds, growth factors or other bioactive molecules, are commonly used (Velasco et al., 2015; Yang et al., 2017). For example, combining β-tricalcium phosphate and BMP-2 has been proven to be effective to enhance the osteogenesis of MSCs (Dimitriou et al., 2011).

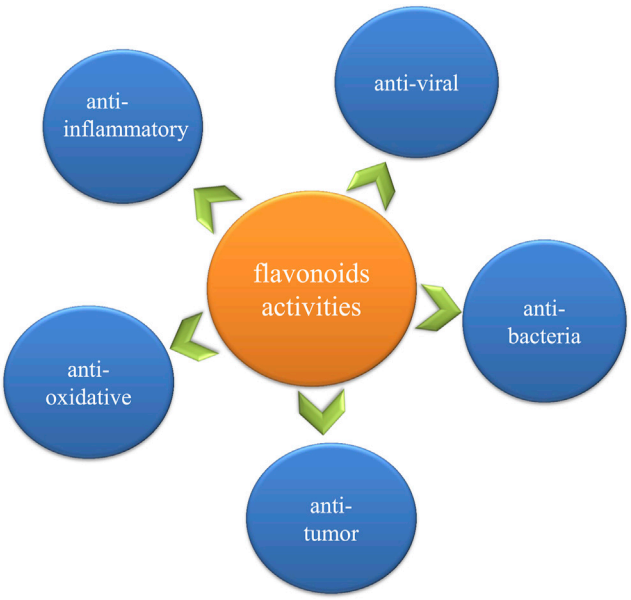

FIGURE 1 | Schematic presentation of the biological activity of flavonoids.

Some botanical drugs have been effective and safe in the treatment of fracture healing in China for a long time, and more and more evidences show many ingredients of them are beneficial to bone health. Flavonoids are commonly present in botanicals, they are synthesized in plants as secondary metabolites, and characterized with diverse pharmacological properties (Martens and Mithöfer, 2005). Natural flavonoids and their glycosides have been identified and explored for their therapeutic potentials in different fields including osteoporosis-related complication and disorders. Many flavonoids exerted promoting bone formation and anti-osteoporosis effects through stimulating osteogenic differentiation of MSCs (Huang et al., 2018; Wang et al., 2018; Casado-Díaz and Rodríguez-Ramos, 2021). Also, European nutritional studies demonstrated that daily intake of flavonoids contributed to good bone health (Zamora-Ros et al., 2016), Therefore, combining flavonoids and MSCs would be an efficient strategy to enhance bone formation and increase cell survival in the field of bone tissue engineering.

BASIC STRUCTURE AND CLASSIFICATION OF FLAVONOIDS

Flavonoids are a kind of polyphenolic compounds widely present in nature and have spectral biological activities. In terms of chemical structure, flavonoids generally refer to a series of hydroxylated phenolic molecules consisting with a C6-C3-C6 units, in which two benzene rings (A and B rings) are linked to each other through three central carbon atoms ring (ring C). These compounds can be divided into many different classes according to the oxidation degree of the central three carbons, whether the three carbons constitute a ring and the connection site of B ring, and so on. Generally,

TABLE 2 | The list of some flavonoids compounds on MSCs osteogenic differentiation.

Compound name	Dosage	*In vitro*	*In vivo*	Results and mechanism of action
Icariin	0.1–10 μM	hBMSC, hADSC	-	Enhance hBMSC and hADSC osteogenesis (Wu et al., 2017a)
	0.1 μM	rADSCs/glass scaffold	rat calvarial bone	Up-regulation VEGF expression, enhance angiogenesis, promote bone formation (Jing et al., 2018)
	5–40 μM	hBMSC	defect models	osteogenesis ↑, adipogenesis ↓; miR-23a ↓, active Wnt/β-catenin (Xu et al., 2021)
	0.01–1 μM	hBMSCs, rBMSCs	-	Osteogenesis ↑; sclerostin ↓, Wnt/β-catenin/ERα activation (Gao et al., 2021) (Wei et al., 2020)
	10–20 μM	rat mandibular MSCs	-	osteogenesis ↑, bone osteoporosis ↓; osteocalcin ↑, STAT 3 pathway activation (Xu et al., 2020)
	1 μM	rBMSCs	OVX rats	proliferation ↑, osteogenesis ↑, adipogenesis ↓; ERα pathway activation (Li et al., 2018)
	0.1–10 μM	rBMSCs	-	protect against iron overload induced dysfunction of BMSCs; active PI3K/AKT/mTOR pathway, inhibit ERK1/2 and JNK pathways (Yao et al., 2019)
	0.1 μM	rBMSCs	-	osteogenesis ↑, TAZ ↑; active ERα and Wnt/β-catenin pathway (Wei et al., 2017)
	50 mg/kg	mBMSCs	-	osteogenesis ↑, bone loss ↓; autophagy activation (Liang et al., 2019)
Quercetin	2–10 μM	hADSCs	-	proliferation ↓, osteogenesis ↑, ERK activity ↑, ER independent (Kim et al., 2006)
	1 μM	rBMSCs/nHA microspheres	OVX fracture rats	proliferation ↑, osteogenesis ↑, angiogenesis ↑; ERK, p38 and AKT activity ↑, RANKL ↓ (Zhou et al., 2017)
	10 μM	hBMSCs/scaffold	-	proliferation ↑, osteogenesis ↑, quercetin-crosslinked nHAp-modified decellularized goat-lung scaffold (Gupta et al., 2017)
	0.03 (wt%)	rabbit BMSC/SF/HAp scaffold	calvarial defect rats	osteogenesis ↑, proliferation ↑, bone regeneration ↑(Song and Tripathy, 2018)
	1–2 (wt%)	hUCMSCs/3D printing scaffold	-	cells growth and mitosis ↑, osteogenesis ↑, calcium deposit ↑(Huang et al., 2021)
	10 μM	rBMSC	-	osteogenesis ↑, adipogenesis ↓, active ERα-mediated circRNA-miR-326-5p-axis (Li et al., 2021)
Quercetin 3-O-β-D-galactopyranoside	1–25 μM	hBMSCs	-	proliferation ↑, osteogenesis ↑, adipogenesis ↓, active Wnt/BMP pathway, inhibit PPARγ pathways (Oh et al., 2020)
Isoquercitrin	0.1–1 μM	rBMSCs	maxillary expansion rats (10 mg/kg)	proliferation ↑, osteogenesis ↑, BMP2 ↑, bone formation ↑(Li et al., 2019a; Li et al., 2019b)
Hesperetin	1–10 μM	BMSCs	-	DEX-induced osteogenic inhibition ↓, active ERK signal pathway (Liu et al., 2021b)
	1 μM	hBMSCs/gelatin scaffold	rat osteotomy model	osteogenesis ↑, active ERK and Smad pathways, accelerate fracture healing (Xue et al., 2017)
	10–100 μM	PDLSCs	-	osteogenesis ↑, ROS ↓, active PI3K/Akt and β-catenin signal pathways (Kim et al., 2013)
Naringin	1–100 μg/ml	hAFSCs	-	proliferation ↑, osteogenesis ↑, BMP4 ↑, active Wnt/BMP pathway (Liu et al., 2017)
	0.03–0.1 (wt%)	hUCMSCs/SF-nHAp scaffolds	rabbit bone defect	proliferation ↑, osteogenesis ↑, angiogenesis ↑, bone regeneration ↑, active PI3K/Akt pathways (Zhao et al., 2021)
	20–100 μM	NPMSC	-	H2O2-induced cell apoptosis ↓; mitochondrial function ↑ (Nan et al., 2020)
	70 μg/ml	rabbit MSC/scaffolds	rabbit bone defect	bone formation ↑, inhibit BMPR-1A signaling (Dong and Ma, 2020)
	0.1 μM	rBMSC	-	restore TNF-α-induced osteogenesis and proliferation inhibition, p-IκBα and nuclear p65 ↓, inhibit NF-κB pathway (Cao et al., 2015)
	1–100 μg/ml	rBMSC	OVX rats	proliferation ↑, osteogenesis ↑, bone loss ↓, inhibit JAK2/STAT3 pathway (Wang et al., 2022)
Kaempferol	1 μM, 10 mg/kg	rBMSCs	OVX rats	bone density ↑, osteogenesis ↑, CXCL12 ↑, miR-10a-3p ↓(Liu et al., 2021a)
	0.1–100 μM or 25–100 mg/kg	rBMSCs	OVX rats bone defect	osteogenesis ↑, prevent OVX-induced osteoporosis, p-4E/BP1 ↓, p-S6K ↑, active mTOR pathway (Zhao et al., 2019)
	20–100 μM	rabbit BMSC	-	cells viability ↑, osteogenesis ↑, adipogenesis ↓, IL-10 ↑, IL6 ↓, inhibit NF-κB pathway (Zhu et al., 2017)
	50 μg/ml	rBMSC/TiO2 implants	rats femur bone defect	cell proliferation ↑, osteogenesis ↑, bone formation ↑, kaempferol-loaded TiO2 implants (Tsuchiya et al., 2018)
	2–10 μM	hADSCs	skull defect mice	cell proliferation ↓, osteogenesis ↑, ERK activity ↑, bone regenerating ability ↑(Kim et al., 2006)
EGCG	1–10 μM	hBMSCs	rats femoral bone defect	Osteogenesis ↑, Runx2 ↑, BMP2 ↑, bone defect healing ↑ (Lin et al., 2018b; Lin et al., 2019)
	5–40 μM	hBMSCs	-	hypoxia-induced apoptosis ↓, ameliorate hypoxia-induced osteogenesis reduction, miR-210 ↑, EFNA3 ↓(Qiu et al., 2016)
	1–10 μM	mBMSCs	-	cell proliferation ↓, osteogenesis ↑, Cbfa1 ↑, Runx2 ↑(Chen et al., 2005)

(Continued on following page)

TABLE 2 | (*Continued*) The list of some flavonoids compounds on MSCs osteogenic differentiation.

Compound name	Dosage	*In vitro*	*In vivo*	Results and mechanism of action
	1–10 μM	SCAPs	-	Proliferation ↑, osteogenesis ↑, Dspp ↑, Dmp-1 ↑, active BMP-Smad signaling pathway (Liu et al., 2021c)
	1–10 μM	rabbit BMSCs	nude mouse	EGCG/DC/HAp sponges increased cell internalization, attachment proliferation, ALP ↑ (Kook et al., 2018)
Genistein	0.01–1 μM	hBMSCs	-	Proliferation ↑, osteogenesis ↑, BMP2 ↑, SMAD5 ↑, RUNX2, ER dependent (Dai et al., 2013)
	5–20 μM	rBMSCs	-	Proliferation ↑, osteogenesis ↓, PPARγ ↑(Zhang et al., 2016a)
	1 μM	hBMSCs	-	Osteogenesis ↑, adipogenesis ↓, PPARγ ↓, ER-dependent, TGF-β ↑ (Heim et al., 2004)
Ipriflavone	0.4–0.8 μM	rBMSCs	OVX rats	osteogenesis ↑, osteoporosis ↓, BMD ↑ (Gao et al., 2018)
Malvidin	25 μM	hADSC	-	calcium deposits ↑, BMP-2 and Runx-2 ↑(Saulite et al., 2019)
Taxifolin	15 μM	hBMSC	-	Osteogenesis ↑, inhibit NF-κB pathway (Wang et al., 2017b)
Diosmin	10–100 μM	C3H10T1/2	-	Osteogenesis ↑, runx2 ↑, active FAK/ERK signaling pathway (Chandran et al., 2019)
Tricin	50–100 μM	hMSC(ATCC)	-	Proliferation ↑, osteogenesis ↑, Wnt3α- mediated (Zhang and Li, 2018)
Glabridin	5 μM	hBMSC	-	osteogenesis ↑, OCT4 gene↑(Heo and Lee, 2017)
HYSA	0.05–0.2 mg/ml	rabbit MSCs	-	prevent glucocorticoid-induced osteoporosis (Wan et al., 2014)
	0.1–0.5 mg/ml	rBMSCs/scaffold	rats bone defect	Osteogenesis ↑, HIF-1α ↑, BMP-2 ↑, new bone formation ↑(Deng et al., 2020)
Butein	1–30 μM	mBMSCs, hBMSCs	-	Osteogenesis ↑, adipogenesis ↓.activate ERK1/2 signaling pathway (Abdallah and Ali, 2020)
Baicalein	0.1–10 μM	TDSCs	tendon-bone healing rat model	Osteogenesis ↑, active Wnt/β-catenin signaling pathway (Tian et al., 2018)
Amentoflavone	0.1–5 μM	hBMSCs	-	Osteogenesis ↑, p-p38 ↑, active JNK and p38 MAPK pathway (Zha et al., 2016)
Troxerutin	25–200 μM	hBMSC	fracture rats model	Osteogenesis ↑, fracture healing ↑, active Wnt/β-catenin signaling (Yang et al., 2021)
Fisetin	200–800 μg/ml	rBMSCs/BC scaffold	-	BC scaffold loaded with fisetin promote osteogenesis (Vadaye Kheiry et al., 2018) proliferation ↓, migration ↓, YAP ↓, osteogenic differentiation ↓(Lorthongpanich and Charoenwongpaiboon, 2021)
	1–30 μM	chorion tissue hMSC	-	BC scaffold loaded with fisetin promote osteogenesis (Vadaye Kheiry et al., 2018) proliferation ↓, migration ↓, YAP ↓, osteogenic differentiation ↓(Lorthongpanich and Charoenwongpaiboon, 2021)

hUCMSCs, human umbilical cord-derived mesenchymal stem cells; hAFSCs, human amniotic fluid-derived stem cells; NPMSC, nucleus pulposus-derived mesenchymal stem cells; NG/SF/HAp, naringin-inlaid composite silk fibroin/hydroxyapatite; SCAPs, Stem cells from apical papilla; TDSCs, tendon-derived stem cells; PDLSCs, periodontal ligament stem cells; HYSA, Hydroxy Safflower Yellow A.

flavonoids are mainly classified into the following subclasses: flavanones, flavonols, flavonones, and isoflavones, anthocyanins, flavanols, (Amarowicz et al., 2009; Kumar and Pandey, 2013), and their basic chemical structure and representative compounds are shown in **Table 1**.

BIOLOGICAL ACTIVITY OF FLAVONOIDS

Flavonoids have a wide range of pharmacological activities including anti-inflammatory, anti-oxidative, anti-microbial, and anti-tumor properties (Kumar and Pandey, 2013; Wen et al., 2017) (**Figure 1**). These properties are beneficial to bone regeneration. Firstly, many flavonoids, including baicalin (Guo et al., 2019; Huang et al., 2019), Kaempferol (Hwang et al., 2019), exert their anti-inflammatory effects by inhibiting the activation of the nuclear factor NF-κB pathway which is closely associated with inflammation. Kaempferol, a bioflavonoid extracted from *Persicaria tinctoria* (*Aiton*) *Spach* (Polygonaceae), prevented bone resorption through its anti-inflammatory property on osteoclast precursor cells (Hwang et al., 2019). Flavonoids have free radical scavenging activities through inhibiting the formation of free radicals, reducing lipid peroxidation, and stimulating antioxidant enzymes (Pietta, 2000). Secondly, given their anti-oxidative roles of flavonoids, some of them have been applied in clinical treatments. For example, troxerutin, a semi-synthetic flavonoid compound prepared by hydroxymethylation of rutin, is commonly used to treat ischemic cerebrovascular diseases, thrombophlebitis, central retinitis, and so on (Ahmadi and Mohammadinejad, 2021). Finally, flavonoids have been demonstrated anti-tumor effects through inhibiting tumor cell proliferation and metastasis, inducing tumor cell autophagy or apoptosis, and preventing tumor invasion. High intake of dietary flavonols, flavones and anthocyanidins may decrease the risk of cancer (Zamora-Ros et al., 2016; Chang et al., 2018).

Botanicals containing flavonoids compounds have been extensively used in traditional medicines for centuries, and nowadays many flavonoids have been extracted or synthesized and have been applied to treat various diseases in clinics. For example, diosmin, a semi-synthetic flavonoid drug with, is used to treat chronic venous insufficiency and varicose veins (Zheng et al., 2020). However, even if there are a number of well-tried treatment experiences of botanicals that are safe for clinical use, there are still many disagreements due to their ambiguous mechanisms. Investigating the underlying mechanisms of these herbal extracts

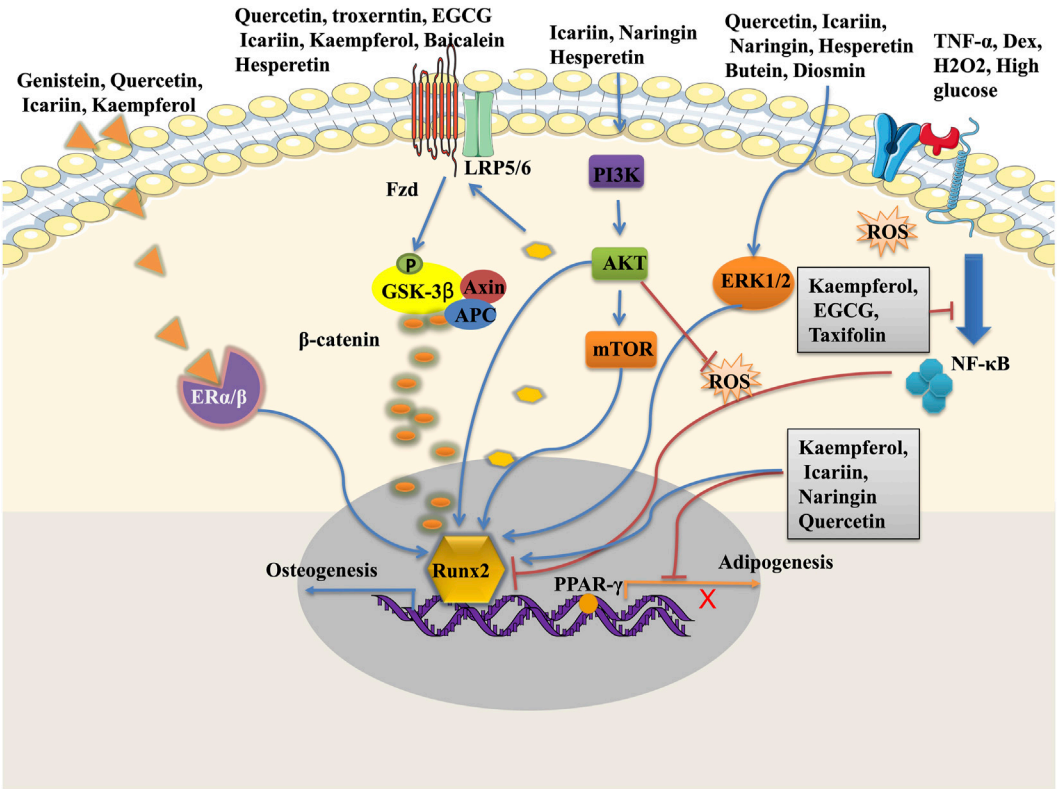

FIGURE 2 | Signalling pathways of flavonoids in MSCs osteogenic differentiation.

will help gain deeper understanding of their beneficial pharmacological activities and facilitate medicinal applications.

EFFECTS OF FLAVONOIDS ON OSTEOGENIC DIFFERENTIATION IN OF MESENCHYMAL STEM CELLS

Many herbal medicines for the treatment of fractures and other degenerative bone diseases have been used for several centuries in some countries, and modern pharmacology confirmed their major biologically active ingredients are flavonoids, such as soybean isoflavones, and flavonoids from *Drynaria roosii Nakaike* (Polypodiaceae), *Epimedium brevicornu Maxim* (Berberidaceae), *etc.* (An et al., 2016). Among them, the corresponding active monomers, including naringin, icariin, genistein, and daidzein, have been proved to be able to regulate bone tissues metabolism by enhancing osteogenic differentiation and inhibiting osteoclast-mediated bone resorption. Especially their osteogenic induction potentials make flavonoids potential candidates to interfere with the osteogenic differentiation of MSCs (**Table 2**). Studies revealed flavonoids modulated the self-renewal and osteogenic differentiation potential of MSCs by targeting multiple signal pathways such as Wnt/β-catenin pathway, ERK pathway, PI3K/Akt pathway, and regulating the bone-specific markers and transcription factors including ALP, Runx2, BMP-2, Cbfa1, Osx (An et al., 2016; Zhang et al., 2016a) (**Figure 2**). In addition to directly stimulating the osteogenesis of MSCs, flavonoids could also indirectly affect the osteogenic differentiation of MSCs by their well-known antioxidant and anti-inflammatory properties (Schilling et al., 2014; Zhang ND. et al., 2016; Zhang L. et al., 2021). Besides, flavonoids were also loaded on bioscaffolds for the promotion of MSCs self-renewal and differentiation in bone regeneration. The utilization of flavonoids in biomaterials showed to be a great prospect for bone tissue engineering.

Icariin

5Icariin (ICA) is a kind of flavonol glycoside and generally extracted from *Epimedium brevicornu Maxim* (Berberidaceae), a traditional Chinese herbal medicine for bone repair. A large number of studies have revealed that ICA had protective roles on bone loss and bone regeneration (Fu et al., 2016; Wang J. et al., 2016; Wei et al., 2017; Ye et al., 2017; Wang et al., 2018; Liang et al., 2019; Gao et al., 2021). ICA not only increased the ALP activity and mineralization of BMSCs but also reduced bone resorption mediated by overactivated osteoclasts in OVX-induced osteoporosis mice (Liang et al., 2019). In addition, ICA has been shown to promote proliferation by activating the Wnt/β-catenin signaling pathway (Wang J. et al., 2016; Gao et al., 2021), which is the most important pathway in osteogenesis. In Sprague-Dawley (SD) rats, ICA stimulated BMSCs proliferation by increasing the phosphorylation level of GSK-3β and cyclin D1 protein (Fu et al., 2016). ICA has been reported to promote proliferation and osteogenic differentiation through increasing the expression of transcriptional coactivator with PDZ-binding motif (TAZ) both in rat BMSCs and ADSCs (Wei et al., 2017; Ye et al.,

2017). Furthermore, the up-regulation of TAZ induced by ICA could be blocked by ICI 182780 or DKK1 (the Wnt/β-catenin pathway inhibitor), which indicated Wnt/β-catenin signaling pathway and ER signaling pathway were involved in the osteogenic differentiation of rBMSCs induced by ICA. The proliferation of rat BMSCs enhanced by ICA is also achieved through activating ERK and p38 MAPK signaling (Fu et al., 2016).

Similarly, Icariside II, a kind of metabolite of ICA, enhanced osteogenic differentiation of BMSCs by increasing ALP activity and calcium deposition at 10 μM (Luo et al., 2015). Icaritin, another metabolic product of ICA, significantly increased ALP activity and calcium deposition at concentrations 0.1–10 μM in human BMSCs and ADSCs through increasing the expression of BMPs, and showed better osteogenesis induction ability than rhBMP-2 (Wu T. et al., 2017).

Quercetin and Kempferol

Quercetin and kaempferol are the main representatives of flavonols, which are the 3-hydroxy derivatives of flavanones, probably the most ubiquitous subclass of flavonoids in nature. The anti-inflammatory and antioxidant effects of quercetin and kaempferol have been repeatedly reported (Babaei et al., 2018; Dabeek and Marra, 2019; Kashyap et al., 2019).

With the development of tissue engineering, the roles of quercetin on the osteogenic differentiation of MSC gradually attracted more attentions. It was reported quercetin could increase bone mineral density (BMD) and improve bone biomechanical properties in postmenopausal osteoporosis rat models (Yuan et al., 2018). The increase of BMP-2 and TGF-β1, two main osteogenic factors, was observed in rat and mouse BMSCs treated with quercetin (Li et al., 2015). Furthermore, the ability of quercetin to stimulate proliferation and osteogenic differentiation of mouse BMSCs could be blocked by estrogen receptor inhibitor ICI182780 (Pang et al., 2018). This indicates that quercetin enhances osteogenic differentiation of MSCs by an estrogen receptor-dependent mechanism. However, in another study similar effects of quercetin on human adipose tissue-derived stem cells (hADSCs) could not reversed by ICI182780, despite the fact that it up-regulated the expression of BMP2, Runx2, as well as activated ERK phosphorylation (Kim et al., 2006). Quercetin also promoted the differentiation and proliferation of BMSCs through inhibiting NF-κB activation and β-catenin degradation stimulated by TNF-α (Yuan et al., 2018). Bian et al. also observed Wnt/β-catenin pathway activation played an important role in the osteogenic differentiation of quercetin treated-BMSCs (Bian et al., 2021). Quercetin stimulated osteogenic differentiation of BMSCs by increasing connexin 43 expressions (Zhang et al., 2020) which could enhance osteogenic differentiation of BMSCs by promoting GSK-3β/β-catenin signaling pathways (Lin FX. et al., 2018).

Kaempferol, another representative flavonol, had a similar osteogenic induction potential with quercetin in periodontal ligament stem cells (PDLSCs). The treatment with 10^{-6} M kaempferol increased cell viability, ALP activity, and enhanced calcium mineralization of PDLSCs. Furthermore, these effects of kaempferol could be reversed by XAV939, a tankyrase inhibitor, indicating Wnt/β-catenin signaling pathway was involved (Nie et al., 2020). The activated Wnt/β-catenin signaling by kaempferol, to some extent, depended on estrogen receptors, as the activation of Wnt/β-catenin could be markedly blocked by the ICI 182780, the inhibitor of estrogen receptors (Sharma and Nam, 2019).

Naringin and Hesperetin

Naringin and hesperetin are two of the best-studied compounds in flavanones (Den Hartogh and Tsiani, 2019; Tutunchi et al., 2020). Naringin is rich in grapefruit and also the main active component of *Drynaria roosii Nakaike* (Polypodiaceae), a Chinese herbal medicine commonly used to treat orthopedic disorders and bone injury (Lavrador et al., 2018). Naringin dose-dependently increased ALP activity and Alizarin red S staining, and decreased PPARγ2 mRNA expression that is the marker of adipogenesis in rat BMSCs under osteogenic induction. Furthermore, this osteogenic effect of naringin could be reversed by the inhibitor of Notch signaling, indicating naringin exerted its role through activating the Notch signaling pathway (Yu G. Y. et al., 2016). In human BMSCs, wang et al. demonstrated naringin promoted proliferation and osteogenesis by activating the ERK signaling pathway (Wang H. et al., 2017). The gene expressions of bone morphogenetic protein 4 (BMP4), runt-related transcription factor 2 (Runx2), β-catenin, and Cyclin D1 were significantly up-regulated by naringin in human amniotic fluid-derived stem cells (Liu et al., 2017). In addition, Naringin alleviates the inhibitory effect of various stimulating factors on osteogenic differentiation of MSC. In a glucocorticoid-induced osteoporosis rat model, naringin not only improved bone mineral density and bone morphology parameters, but also stimulated the expression of autophagy-related factors including Beclin-1 and p62, which indicated autophagy was also involved in the bone protective effect of naringin (Ge and Zhou, 2021). Similarly, Hesperidin and its aglycone, hesperetin, two flavonoids from citrus species, also exerted protective roles in the osteogenesis of MSCs (Parhiz et al., 2015). In dexamethasone-treated BMSCs, the inhibition of MSC osteogenesis was reversed by the intervention of hesperetin through activating the ERK signal pathway (Liu L. et al., 2021). retreatment with 1–100 μM concentration hesperetin significantly increased the osteogenic activity of periodontal ligament stem cells under high glucose conditions. It was considered scavenged intracellular ROS produced and activated PI3K/Akt and β-catenin signaling pathway by hesperetin were responsible for this protective effect (Kim et al., 2013).

Epigallocatechin-3-Gallate

Tea is abundant in flavonoids, mainly including catechins, theaflavins, alkaloids, etc., (-)-epigallocatechin-3-gallate (EGCG) is the major catechin isolated from *Green Tea* (Friedman, 2007). As an antioxidant and anti-inflammatory agent, EGCG plays an important role in maintaining the balance of bone metabolism through the inhibition of bone resorption as well as the enhancement of bone formation (Nishioku et al., 2020). Although EGCG alone could not induce osteogenic differentiation of MSC, EGCG was able to enhance osteogenesis under osteogenic induction environment through upregulating BMP2 expression (Jin et al., 2021). Lin et al. showed EGCG enhanced osteogenic differentiation at the concentrations range from 1 to 10 μM both in murine and human BMSCs by increasing the expression of osteoblastic

genes including BMP2, Runx2, ALP, osteonectin, and osteocalcin, as well as promoting ALP activity and mineral deposits (Lin S. Y. et al., 2018). Furthermore, the effect of EGCG on promoting the mineralization of human MSCs is independent of its antioxidant activity (Lin S. Y. et al., 2018). In human ADSCs, 5 μM EGCG significantly enhanced cell proliferation and ALP activity, experimental data revealed that osteo-inductive effects of EGCG on human ADSCs were associated with the inhibition of adipogenesis-related gene expression (Zhang et al., 2019). For the stem cells from apical papilla (SCAPs), at low concentrations, EGCG promoted the cell proliferation and increased ALP activity as well as mineral deposition through activating the BMP-Smad Signaling Pathway (Liu Z. et al., 2021). In addition to promoting osteogenic differentiation directly, EGCG treatment significantly reversed the inhibition of MSC osteogenesis induced by hydrogen peroxide and inflammatory cytokines. EGCG could enhance osteogenic differentiation by increasing the expression of β-catenin and cyclin D1 in H2O2-induced human BMSCs (Wang D. et al., 2016). A similar protective effect of EGCG was also observed on TNF-α-induced osteogenesis inhibition of MSC, in which EGCG reversed the TNF-α-induced destructive through inhibition of NF-κB signaling (Liu et al., 2016).

Genistein

Genistein is one of the most abundant isoflavones in *Glycine max* (*L.*) *Merr* (*Fabaceae*), and it is also called a phytoestrogen owing to its similar structure to that of human estrogen. It could bind to ERα and ERβ and exert ER-mediated estrogenic effects including increasing bone formation and repressing adipose tissue (Jaiswal et al., 2019) At the same time, it possessed antiestrogenic effects as well as non-ER-mediated effects like inhibiting tyrosine kinase (Dang et al., 2003). Genistein exerted estrogenic effects mainly by binding to ER α, even with a stronger affinity to ERβ than to ERα, genistein, and 8-prenylgenistein (a prenylated derivative), all of them could inhibit GSK-3β enzymatic activities though inducing GSK-3β phosphorylation at Serine-9 in human BMSCs and murine pre-osteoblast MC3T3-E1 cells. In addition, 8-prenylgenistein showed stronger osteogenic ability than genistein in MC3T3-E1 cells by increasing ERα-dependent β-catenin protein expression (Qiu et al., 2020). It seemed that both Wnt/β-catenin and ERα-associated signaling were involved in the osteogenic activities of genistein. Owing to its well-known estrogenic ability, genistein directly or indirectly affected the osteogenic and adipogenic differentiation of MSCs. In the early stages of differentiation of human primary BMSCs osteogenic markers were strongly up-regulated by genistein, while during adipogenic differentiation, adipogenic regulators, including PPARγ and CCAAT/enhancer-binding protein-α, were down-regulated after genistein treatment (Heim et al., 2004). A lineage shift from adipogenesis to osteogenesis induced by genistein was observed in murine MSCs and pre-osteoblasts isolated from newborn mice (Li et al., 2005). However, in another study, genistein was reported to enhance adipogenesis of human MSCs and suppressed their osteogenesis through regulating the expression of PPARγ (Zhang LY. et al., 2016). These contradictory results may be caused by the dose of genistein, at low concentrations (≦1 μM), genistein acted like estrogen, stimulating osteogenesis and inhibiting adipogenesis, whereas at high concentrations (>1 μM), genistein acted as a ligand of PPARγ, leading to up-regulation of adipogenesis and down-regulation of osteogenesis (Dang et al., 2003).

Other Flavonoids

In addition to the flavonoids mentioned above, other flavonoid extracts like baicalein (Ren et al., 2021), apigenin (Pan et al., 2021), amentoflavone (Zha et al., 2016), and anthocyanins (Saulite et al., 2019) have also been found to enhance osteogenic differentiation of MSCs. In human periodontal ligament cells (hPDLCs), baicalein induced osteogenic differentiation dose-dependently (1.25–10 μM) by activating the Wnt/β-catenin signaling pathway (Chen et al., 2017). Cyanidin-3-O-glucoside (C3G), the most common type of anthocyanin in nature, was shown to increase the expression of osteoblastic markers and osteoblast proliferation rate both in mouse MC3T3-E1 cells and human osteoblasts (extracted from the hip joint of patients with osteoporosis) by regulating ERK1/2 signaling pathway (Hu et al., 2021).

Inhibitory Effects of Flavonoids on Mesenchymal Stem Cells Osteogenic Differentiation

Although most studies showed that flavonoids promoted the osteogenic differentiation of MSC, some reports showed that flavonoids sometimes had an inhibitory effect on the osteogenic differentiation of MSC, and promoted adipogenesis (Hu et al., 2011; Zhang LY. et al., 2016; Casado-Díaz et al., 2016). Some flavonoids showed that they promoted the adipogenesis and inhibited osteogenesis of MSCs (Hu et al., 2011; Casado-Díaz et al., 2016; Lorthongpanich et al., 2021). Two isoprenylated flavonoids isolated from the twigs of *Morus alba L* (*Moraceae*; *Morus alba L*) significantly promoted adipogenesis and induced up-regulation of the expression of adipocyte-specific genes, aP2 and GLUT4 in 3T3L1 cells (Hu et al., 2011). In another study showed that high concentration of quercetin inhibited osteoblastic differentiation and promoted adipogenesis through Wnt/β-catenin inhibition. Which indicate such possible adverse effects of high use concentrations should be taken into account in nutraceutical or pharmaceutical strategies using flavonoids (Casado-Díaz et al., 2016).

THE APPLICATIONS OF FLAVONOIDS IN BONE DISORDERS BY PROMOTING OSTEOGENIC DIFFERENTIATION OF MESENCHYMAL STEM CELLS

The effects of flavonoids on bone defects had been extensively established using animal models (Yu et al., 2021; Zhao et al., 2021; Zhou and Xie, 2021). Flavonoids stimulated bone formation by increasing cell viability, matrix mineralization, calcium deposition, and up-regulation of osteogenic genes (Wu Y. et al., 2017; Preethi Soundarya et al., 2018). Meanwhile, flavonoids have great importance in treating bone disorders owing to their anti-inflammatory and anti-oxidative activities

as we described above. Many flavonoids have been widely used in ovariectomized (OVX) osteoporotic, age-related osteoporotic models as well as glucocorticoid-induced osteoporosis, by regulating osteoblast-regulated bone formation and/or osteoclast-mediated bone resorption.

The impaired capability of osteogenic differentiation and senescence of MSCs are important pathogeneses of osteoporosis caused by various reasons (Jiang et al., 2021). In the aging process, as well as in glucocorticoid-induced osteoporosis, the ability of MSCs' commitment towards the osteogenic lineage is impaired, while the adipogenesis is increased. Reactivating the osteogenic differentiation ability of MSCs is considered an important way to osteoporosis treatment. Icariin was effective in preventing postmenopausal osteoporosis through stimulating osteogenic differentiation of BMSCs (Wang et al., 2018), and it also protected against glucocorticoid-induced osteonecrosis of the femoral head in rats (Huang et al., 2018). Hesperetin alleviated glucocorticoid-induced inhibition of osteogenic differentiation through ERK signal pathway in BMSCs (Liu L. et al., 2021). Flavonoids also have great potential for the treatment of diabetes-induced osteoporosis owing to their anti-oxidative and adipogenesis inhibition activities (Nelson-Dooley et al., 2005; Kawser Hossain et al., 2016). Diabetes-induced osteoporosis is caused by chronic hyperglycemia, advanced glycated end products, and oxidative stress (Mohsin et al., 2019). In a rat model of diabetic osteoporosis, icariin could prevent diabetic osteoporosis by reducing blood glucose, inhibiting bone marrow adipogenesis, as well as up-regulation the expression of Runx2 and OPG (Qi et al., 2019).

MSC-based cellular therapy is a promising novel therapeutic strategy for osteonecrosis of the femoral head (ONFH). Flavonoids can increase bone formation in femoral heads by promoting MSCs proliferation and osteogenic differentiation. In methylprednisolone-induced rat ONFH models, the lithium chloride treatment group displayed a higher vessel volume and better trabecular structures as well as more OCN expression compared with methylprednisolone group, MSCs extracted from rats treated with lithium chloride had higher proliferative and osteogenic ability (Zhang Y. L. et al., 2021). Zefeng Yu et al (2016) also demonstrated lithium could enhance angiogenesis and stabilize osteogenic/adipogenic balance in glucocorticoid-induced ONFH rat models by activating the β-catenin pathway.

COMBINATION USE OF FLAVONOIDS AND BIOMATERIALS IN BONE TISSUE ENGINEERING

Mesenchymal stem cells combined with biological scaffold materials loaded with flavonoids are an excellent option for the application of flavonoids in the field of bone tissue engineering repair, and incorporation of flavonoids into biomaterials or scaffolds has been proved as a reliable technology for bone tissue regeneration, For example, the quercetin/silk fibroin/hydroxyapatite scaffolds with BMSCs increased the formation of new collagenous tissue and tissue ingrowth in a rat calvarial defect model, quercetin was found to promote cell proliferation and osteogenic differentiation of BMSC cultured in scaffolds *in vitro* (Song and Tripathy, 2018). Flavonoids also can stabilize collagen and inhibit its degradation in biological systems (Shavandi et al., 2018). The BMSCs-laden quercetin/collagen/hydroxyapatite sponge was proved as an alternative biomaterial for bone regeneration (Song et al., 2020). Kaempferol-immobilized titanium dioxide promotes the formation of new bone and is considered an effective tool for bone regeneration around dental implants (Tsuchiya et al., 2018). Promoting the proliferation and osteogenic differentiation of MSCs on scaffolds is the main role of flavonoids in the construction of bone tissue engineering. Besides, flavonoids enhance bone regeneration by counteracting the negative effect of oxidative stress on MSCs viability and differentiation (Forte et al., 2016; Chu et al., 2018). However, recent developments in bone tissue engineering focusing on flavonoids and their potent biological properties that enhance bone health has been well-reviewed (Preethi Soundarya et al., 2018). The potential of a combination of biomaterials loaded with flavonoids and MSCs might be enormous in bone tissue engineering.

FUTURE PROSPECTIVE

Extensive evidence showed the roles of flavonoids in regenerative and therapeutic medicine. Flavonoids as stimulants significantly affect the proliferation and osteogenic differentiation of MSCs. To further effectively screen and evaluate the application potential of flavonoids in bone tissue engineering and repair, it is very necessary to establish a standard and effective osteogenic differentiation protocol of MSC induced by flavonoids. Furthermore, the dose-effect relationship between MSCs and flavonoids should also be well established to achieve desired effects and reduce side effects. Given most flavonoids compounds are not having good solubility and low hydrophilicity, delivery systems, such as nanocarriers, with flavonoids are promising strategies for the improvement of cell uptake efficiency. In addition, MSCs combined with biological scaffold materials loaded with flavonoids are an excellent option for the application of flavonoids in the field of bone tissue engineering.

CONCLUSION

Flavonoids have a wide range of pharmacological activities and widely exist in nature. Flavonoids play a crucial role in the bone repair process not only through direct induction of osteoblastic differentiation, but also through their anti-inflammatory and anti-oxidant effects. MSCs combined with flavonoids are a promising alternative in stem cell therapy and bone tissue engineering construction. Flavonoids can help to increase proliferation and osteogenic differentiation of MSCs as well as modulate the microenvironment in the injured bone. To promote their clinical use, more works need to be done to improve their safety, efficacy, and quality, and to explore the mechanisms underlying their roles.

AUTHOR CONTRIBUTIONS

JZ, YL, GH, and HC did literature retrieval and prepared the draft. JZ, ZL, and XL wrote the first revision of the manuscript. SQ and AL revised the manuscript.

FUNDING

This work was supported by grants from Guangzhou Municipal Science and Technology Project (No. 202002030049, 202102010058, 202102010060).

REFERENCES

Abdallah, B. M., and Ali, E. M. (2020). Butein Promotes Lineage Commitment of Bone Marrow-Derived Stem Cells into Osteoblasts via Modulating ERK1/2 Signaling Pathways. *Molecules* 25. doi:10.3390/molecules25081885

Ahmadi, Z., Mohammadinejad, R., Roomiani, S., Afshar, E. G., and Ashrafizadeh, M. (2021). Biological and Therapeutic Effects of Troxerutin: Molecular Signaling Pathways Come into View. *J. Pharmacopuncture* 24, 1–13. doi:10.3831/kpi.2021.24.1.1

Amarowicz, R., Carle, R., Dongowski, G., Durazzo, A., Galensa, R., Kammerer, D., et al. (2009). Influence of Postharvest Processing and Storage on the Content of Phenolic Acids and Flavonoids in Foods. *Mol. Nutr. Food Res.* 53 (Suppl. 2), S151–S183. doi:10.1002/mnfr.200700486

An, J., Yang, H., Zhang, Q., Liu, C., Zhao, J., Zhang, L., et al. (2016). Natural Products for Treatment of Osteoporosis: The Effects and Mechanisms on Promoting Osteoblast-Mediated Bone Formation. *Life Sci.* 147, 46–58. doi:10.1016/j.lfs.2016.01.024

Armstrong, J. P. K., and Stevens, M. M. (2019). Emerging Technologies for Tissue Engineering: From Gene Editing to Personalized Medicine. *Tissue Eng. Part. A.* 25, 688–692. doi:10.1089/ten.TEA.2019.0026

Babaei, F., Mirzababaei, M., and Nassiri-Asl, M. (2018). Quercetin in Food: Possible Mechanisms of its Effect on Memory. *J. Food Sci.* 83, 2280–2287. doi:10.1111/1750-3841.14317

Baksh, D., Song, L., and Tuan, R. S. (2004). Adult Mesenchymal Stem Cells: Characterization, Differentiation, and Application in Cell and Gene Therapy. *J. Cel Mol Med* 8, 301–316. doi:10.1111/j.1582-4934.2004.tb00320.x

Bian, W., Xiao, S., Yang, L., Chen, J., and Deng, S. (2021). Quercetin Promotes Bone Marrow Mesenchymal Stem Cell Proliferation and Osteogenic Differentiation through the H19/miR-625-5p axis to Activate the Wnt/β-Catenin Pathway. *BMC Complement. Med. Ther.* 21, 243. doi:10.1186/s12906-021-03418-8

Cao, X., Lin, W., Liang, C., Zhang, D., Yang, F., Zhang, Y., et al. (2015). Naringin Rescued the TNF-α-Induced Inhibition of Osteogenesis of Bone Marrow-Derived Mesenchymal Stem Cells by Depressing the Activation of NF-Kb Signaling Pathway. *Immunol. Res.* 62, 357–367. doi:10.1007/s12026-015-8665-x

Casado-Díaz, A., and Rodríguez-Ramos, Á. (2021). Flavonoid Phloretin Inhibits Adipogenesis and Increases OPG Expression in Adipocytes Derived from Human Bone-Marrow Mesenchymal Stromal-Cells. *Nutrients* 13, 4185. doi:10.3390/nu13114185

Casado-Díaz, A., Anter, J., Dorado, G., and Quesada-Gómez, J. M. (2016). Effects of Quercetin, a Natural Phenolic Compound, in the Differentiation of Human Mesenchymal Stem Cells (MSC) into Adipocytes and Osteoblasts. *J. Nutr. Biochem.* 32, 151–162. doi:10.1016/j.jnutbio.2016.03.005

Chandran, S. V., Vairamani, M., and Selvamurugan, N. (2019). Osteostimulatory Effect of Biocomposite Scaffold Containing Phytomolecule Diosmin by Integrin/FAK/ERK Signaling Pathway in Mouse Mesenchymal Stem Cells. *Sci. Rep.* 9, 11900. doi:10.1038/s41598-019-48429-1

Chang, H., Lei, L., Zhou, Y., Ye, F., and Zhao, G. (2018). Dietary Flavonoids and the Risk of Colorectal Cancer: An Updated Meta-Analysis of Epidemiological Studies. *Nutrients* 10, 950. doi:10.3390/nu10070950

Chen, C. H., Ho, M. L., Chang, J. K., Hung, S. H., and Wang, G. J. (2005). Green tea Catechin Enhances Osteogenesis in a Bone Marrow Mesenchymal Stem Cell Line. *Osteoporos. Int.* 16, 2039–2045. doi:10.1007/s00198-005-1995-0

Chen, L. J., Hu, B. B., Shi, X. L., Ren, M. M., Yu, W. B., Cen, S. D., et al. (2017). Baicalein Enhances the Osteogenic Differentiation of Human Periodontal Ligament Cells by Activating the Wnt/β-Catenin Signaling Pathway. *Arch. Oral Biol.* 78, 100–108. doi:10.1016/j.archoralbio.2017.01.019

Chu, J., Shi, P., Yan, W., Fu, J., Yang, Z., He, C., et al. (2018). PEGylated Graphene Oxide-Mediated Quercetin-Modified Collagen Hybrid Scaffold for Enhancement of MSCs Differentiation Potential and Diabetic Wound Healing. *Nanoscale* 10, 9547–9560. doi:10.1039/c8nr02538j

Dabeek, W. M., and Marra, M. V. (2019). Dietary Quercetin and Kaempferol: Bioavailability and Potential Cardiovascular-Related Bioactivity in Humans. *Nutrients* 11, 2288. doi:10.3390/nu11102288

Dai, J., Li, Y., Zhou, H., Chen, J., Chen, M., and Xiao, Z. (2013). Genistein Promotion of Osteogenic Differentiation through BMP2/SMAD5/RUNX2 Signaling. *Int. J. Biol. Sci.* 9, 1089–1098. doi:10.7150/ijbs.7367

Dang, Z. C., Audinot, V., Papapoulos, S. E., Boutin, J. A., and Löwik, C. W. (2003). Peroxisome Proliferator-Activated Receptor Gamma (PPARgamma) as a Molecular Target for the Soy Phytoestrogen Genistein. *J. Biol. Chem.* 278, 962–967. doi:10.1074/jbc.M209483200

Den Hartogh, D. J., and Tsiani, E. (2019). Antidiabetic Properties of Naringenin: A Citrus Fruit Polyphenol. *Biomolecules* 9, 99. doi:10.3390/biom9030099

Deng, Z., Chen, J., Lin, B., Li, J., Wang, H., Wang, D., et al. (2020). A Novel 3D Printed Bioactive Scaffolds with Enhanced Osteogenic Inspired by Ancient Chinese Medicine HYSA for Bone Repair. *Exp. Cel Res* 394, 112139. doi:10.1016/j.yexcr.2020.112139

Dimitriou, R., Jones, E., Mcgonagle, D., and Giannoudis, P. V. (2011). Bone Regeneration: Current Concepts and Future Directions. *BMC Med.* 9, 66. doi:10.1186/1741-7015-9-66

Dong, G. C., Ma, T. Y., Li, C. H., Chi, C. Y., Su, C. M., Huang, C. L., et al. (2020). A Study of Drynaria Fortunei in Modulation of BMP–2 Signalling by Bone Tissue Engineering. *Turk J. Med. Sci.* 50, 1444–1453. doi:10.3906/sag-2001-148

Forte, L., Torricelli, P., Boanini, E., Gazzano, M., Rubini, K., Fini, M., et al. (2016). Antioxidant and Bone Repair Properties of Quercetin-Functionalized Hydroxyapatite: An *In Vitro* Osteoblast-Osteoclast-Endothelial Cell Co-culture Study. *Acta Biomater.* 32, 298–308. doi:10.1016/j.actbio.2015.12.013

Friedenstein, A. J. (1976). Precursor Cells of Mechanocytes. *Int. Rev. Cytol.* 47, 327–359. doi:10.1016/s0074-7696(08)60092-3

Friedman, M. (2007). Overview of Antibacterial, Antitoxin, Antiviral, and Antifungal Activities of tea Flavonoids and Teas. *Mol. Nutr. Food Res.* 51, 116–134. doi:10.1002/mnfr.200600173

Fu, S., Yang, L., Hong, H., and Zhang, R. (2016). [Wnt/β-catenin Signaling Is Involved in the Icariin Induced Proliferation of Bone Marrow Mesenchymal Stem Cells]. *J. Tradit Chin. Med.* 36, 360–368. doi:10.1016/s0254-6272(16)30050-4

Gao, A. G., Zhou, Y. C., Hu, Z. J., and Lu, B. B. (2018). Ipriflavone Promotes Osteogenesis of MSCs Derived from Osteoporotic Rats. *Eur. Rev. Med. Pharmacol. Sci.* 22, 4669–4676. doi:10.26355/eurrev_201807_15527

Gao, J., Xiang, S., Wei, X., Yadav, R. I., Han, M., Zheng, W., et al. (2021). Icariin Promotes the Osteogenesis of Bone Marrow Mesenchymal Stem Cells through Regulating Sclerostin and Activating the Wnt/β-Catenin Signaling Pathway. *Biomed. Res. Int.* 2021, 6666836. doi:10.1155/2021/6666836

García-Sánchez, D., Fernández, D., Rodríguez-Rey, J. C., and Pérez-Campo, F. M. (2019). Enhancing Survival, Engraftment, and Osteogenic Potential of Mesenchymal Stem Cells. *World J. Stem Cell* 11, 748–763. doi:10.4252/wjsc.v11.i10.748

Garmany, A., Yamada, S., and Terzic, A. (2021). Longevity Leap: Mind the Healthspan gap. *Npj Regen. Med.* 6, 57. doi:10.1038/s41536-021-00169-5

Ge, X., and Zhou, G. (2021). Protective Effects of Naringin on Glucocorticoid-Induced Osteoporosis through Regulating the PI3K/Akt/mTOR Signaling Pathway. *Am. J. Transl Res.* 13, 6330–6341.

Guo, L. T., Wang, S. Q., Su, J., Xu, L. X., Ji, Z. Y., Zhang, R. Y., et al. (2019). Baicalin Ameliorates Neuroinflammation-Induced Depressive-like Behavior through Inhibition of Toll-like Receptor 4 Expression via the PI3K/AKT/FoxO1 Pathway. *J. Neuroinflammation* 16, 95. doi:10.1186/s12974-019-1474-8

Gupta, S. K., Kumar, R., and Mishra, N. C. (2017). Influence of Quercetin and Nanohydroxyapatite Modifications of Decellularized Goat-Lung Scaffold for

Bone Regeneration. *Mater. Sci. Eng. C Mater. Biol. Appl.* 71, 919–928. doi:10.1016/j.msec.2016.10.085

Heim, M., Frank, O., Kampmann, G., Sochocky, N., Pennimpede, T., Fuchs, P., et al. (2004). The Phytoestrogen Genistein Enhances Osteogenesis and Represses Adipogenic Differentiation of Human Primary Bone Marrow Stromal Cells. *Endocrinology* 145, 848–859. doi:10.1210/en.2003-1014

Heo, J. S., and Lee, S. G. (2017). The Flavonoid Glabridin Induces OCT4 to Enhance Osteogenetic Potential in Mesenchymal Stem Cells. *Stem Cell Int.* 2017, 6921703. doi:10.1155/2017/6921703

Hu, B., Chen, L., Chen, Y., Zhang, Z., Wang, X., and Zhou, B. (2021). Cyanidin-3-glucoside Regulates Osteoblast Differentiation via the ERK1/2 Signaling Pathway. *ACS Omega* 6, 4759–4766. doi:10.1021/acsomega.0c05603

Hu, X., Ji, J., Wang, M., Wu, J. W., Zhao, Q. S., Wang, H. Y., et al. (2011). New Isoprenylated Flavonoids and Adipogenesis-Promoting Constituents from Morus Notabilis. *Bioorg. Med. Chem. Lett.* 21, 4441–4446. doi:10.1016/j.bmcl.2011.06.020

Huang, K. H., Chen, C. Y., Chang, C. Y., Chen, Y. W., and Lin, C. P. (2021). The Synergistic Effects of Quercetin-Containing 3D-Printed Mesoporous Calcium Silicate/calcium Sulfate/poly-ε-Caprolactone Scaffolds for the Promotion of Osteogenesis in Mesenchymal Stem Cells. *J. Formos. Med. Assoc.* 120, 1627–1634. doi:10.1016/j.jfma.2021.01.024

Huang, T., Liu, Y., and Zhang, C. (2019). Pharmacokinetics and Bioavailability Enhancement of Baicalin: A Review. *Eur. J. Drug Metab. Pharmacokinet.* 44, 159–168. doi:10.1007/s13318-018-0509-3

Huang, Z., Cheng, C., Cao, B., Wang, J., Wei, H., Liu, X., et al. (2018). Icariin Protects against Glucocorticoid-Induced Osteonecrosis of the Femoral Head in Rats. *Cell Physiol Biochem* 47, 694–706. doi:10.1159/000490023

Hwang, D., Kang, M. J., Kang, C. W., and Kim, G. D. (2019). Kaempferol-3-O-β-rutinoside Suppresses the Inflammatory Responses in Lipopolysaccharide-Stimulated RAW264.7 Cells via the NF-Kb and MAPK Pathways. *Int. J. Mol. Med.* 44, 2321–2328.doi:10.3892/ijmm.2019.4381

Jaiswal, N., Akhtar, J., Singh, S. P., Ahsan, F., and Ahsan, F. (2019). An Overview on Genistein and its Various Formulations. *Drug Res. (Stuttg)* 69, 305–313. doi:10.1055/a-0797-3657

Jiang, Y., Zhang, P., Zhang, X., and Lv, L. (2021). Advances in Mesenchymal Stem Cell Transplantation for the Treatment of Osteoporosis. *Cel Prolif.* 54, e12956. doi:10.1111/cpr.12956

Jin, P., Li, M., Xu, G., Zhang, K., Zheng, L., and Zhao, J. (2021). Erratum: Role of (-)-Epigallocatechin-3-Gallate in the Osteogenic Differentiation of Human Bone Marrow Mesenchymal Stem Cells: An Enhancer or an Inducer? *Exp. Ther. Med.* 21, 294. doi:10.3892/etm.2021.9725

Jing, X., Yin, W., Tian, H., Chen, M., Yao, X., Zhu, W., et al. (2018). Icariin Doped Bioactive Glasses Seeded with Rat Adipose-Derived Stem Cells to Promote Bone Repair via Enhanced Osteogenic and Angiogenic Activities. *Life Sci.* 202, 52–60. doi:10.1016/j.lfs.2018.02.026

Kashyap, D., Garg, V. K., Tuli, H. S., and Yerer, M. B. (2019). Fisetin and Quercetin: Promising Flavonoids with Chemopreventive Potential. *Biomolecules* 9, 174. doi:10.3390/biom9050174

Kawser Hossain, M., Abdal Dayem, A., Han, J., Yin, Y., Kim, K., Kumar Saha, S., et al. (2016). Molecular Mechanisms of the Anti-obesity and Anti-diabetic Properties of Flavonoids. *Int. J. Mol. Sci.* 17, 569. doi:10.3390/ijms17040569

Kim, S. Y., Lee, J. Y., Park, Y. D., Kang, K. L., Lee, J. C., and Heo, J. S. (2013). Hesperetin Alleviates the Inhibitory Effects of High Glucose on the Osteoblastic Differentiation of Periodontal Ligament Stem Cells. *PLoS One* 8, e67504. doi:10.1371/journal.pone.0067504

Kim, Y. J., Bae, Y. C., Suh, K. T., and Jung, J. S. (2006). Quercetin, a Flavonoid, Inhibits Proliferation and Increases Osteogenic Differentiation in Human Adipose Stromal Cells. *Biochem. Pharmacol.* 72, 1268–1278. doi:10.1016/j.bcp.2006.08.021

Kook, Y. J., Tian, J., Jeon, Y. S., Choi, M. J., Song, J. E., Park, C. H., et al. (2018). Nature-derived Epigallocatechin Gallate/duck's Feet Collagen/hydroxyapatite Composite Sponges for Enhanced Bone Tissue Regeneration. *J. Biomater. Sci. Polym. Ed.* 29, 984–996. doi:10.1080/09205063.2017.1414480

Kumar, S., and Pandey, A. K. (2013). Chemistry and Biological Activities of Flavonoids: an Overview. *ScientificWorldJournal* 2013, 162750. doi:10.1155/2013/162750

Lavrador, P., Gaspar, V. M., and Mano, J. F. (2018). Bioinspired Bone Therapies Using Naringin: Applications and Advances. *Drug Discov. Today* 23, 1293–1304. doi:10.1016/j.drudis.2018.05.012

Li, J., Wang, X., Wang, Y., Lu, C., Zheng, D., and Zhang, J. (2019). Isoquercitrin, a Flavonoid Glucoside, Exerts a Positive Effect on Osteogenesis *In Vitro* and *In Vivo*. *Chem. Biol. Interact* 297, 85–94. doi:10.1016/j.cbi.2018.10.018

Li, M., Zhang, C., Li, X., Lv, Z., Chen, Y., and Zhao, J. (2019). Isoquercitrin Promotes the Osteogenic Differentiation of Osteoblasts and BMSCs via the RUNX2 or BMP Pathway. *Connect. Tissue Res.* 60, 189–199. doi:10.1080/03008207.2018.1483358

Li, X., Chen, R., Lei, X., Wang, P., Zhu, X., Zhang, R., et al. (2021). Quercetin Regulates ERα Mediated Differentiation of BMSCs through Circular RNA. *Gene* 769, 145172. doi:10.1016/j.gene.2020.145172

Li, X., Peng, B., Pan, Y., Wang, P., Sun, K., Lei, X., et al. (2018). Icariin Stimulates Osteogenic Differentiation and Suppresses Adipogenic Differentiation of rBMSCs via Estrogen Receptor Signaling. *Mol. Med. Rep.* 18, 3483–3489. doi:10.3892/mmr.2018.9325

Li, X. H., Zhang, J. C., Sui, S. F., and Yang, M. S. (2005). Effect of Daidzin, Genistin, and Glycitin on Osteogenic and Adipogenic Differentiation of Bone Marrow Stromal Cells and Adipocytic Transdifferentiation of Osteoblasts. *Acta Pharmacol. Sin* 26, 1081–1086. doi:10.1111/j.1745-7254.2005.00161.x

Li, Y., Wang, J., Chen, G., Feng, S., Wang, P., Zhu, X., et al. (2015). Quercetin Promotes the Osteogenic Differentiation of Rat Mesenchymal Stem Cells via Mitogen-Activated Protein Kinase Signaling. *Exp. Ther. Med.* 9, 2072–2080. doi:10.3892/etm.2015.2388

Liang, X., Hou, Z., Xie, Y., Yan, F., Li, S., Zhu, X., et al. (2019). Icariin Promotes Osteogenic Differentiation of Bone Marrow Stromal Cells and Prevents Bone Loss in OVX Mice via Activating Autophagy. *J. Cel Biochem* 120, 13121–13132. doi:10.1002/jcb.28585

Lin, F. X., Zheng, G. Z., Chang, B., Chen, R. C., Zhang, Q. H., Xie, P., et al. (2018). Connexin 43 Modulates Osteogenic Differentiation of Bone Marrow Stromal Cells through GSK-3beta/Beta-Catenin Signaling Pathways. *Cel Physiol Biochem* 47, 161–175. doi:10.1159/000489763

Lin, S. Y., Kang, L., Chen, J. C., Wang, C. Z., Huang, H. H., Lee, M. J., et al. (2019). (-)-Epigallocatechin-3-gallate (EGCG) Enhances Healing of Femoral Bone Defect. *Phytomedicine* 55, 165–171. doi:10.1016/j.phymed.2018.07.012

Lin, S. Y., Kang, L., Wang, C. Z., Huang, H. H., and Cheng, T. L. (2018). Epigallocatechin-3-Gallate (EGCG) Enhances Osteogenic Differentiation of Human Bone Marrow Mesenchymal Stem Cells. *Molecules* 23, 3221. doi:10.3390/molecules23123221

Liu, H., Yi, X., Tu, S., Cheng, C., and Luo, J. (2021). Kaempferol Promotes BMSC Osteogenic Differentiation and Improves Osteoporosis by Downregulating miR-10a-3p and Upregulating CXCL12. *Mol. Cel Endocrinol* 520, 111074. doi:10.1016/j.mce.2020.111074

Liu, L., Zheng, J., Yang, Y., Ni, L., Chen, H., and Yu, D. (2021). Hesperetin Alleviated Glucocorticoid-Induced Inhibition of Osteogenic Differentiation of BMSCs through Regulating the ERK Signaling Pathway. *Med. Mol. Morphol.* 54, 1–7. doi:10.1007/s00795-020-00251-9

Liu, M., Li, Y., and Yang, S. T. (2017). Effects of Naringin on the Proliferation and Osteogenic Differentiation of Human Amniotic Fluid-Derived Stem Cells. *J. Tissue Eng. Regen. Med.* 11, 276–284. doi:10.1002/term.1911

Liu, W., Fan, J. B., Xu, D. W., Zhang, J., and Cui, Z. M. (2016). Epigallocatechin-3-gallate Protects against Tumor Necrosis Factor Alpha Induced Inhibition of Osteogenesis of Mesenchymal Stem Cells. *Exp. Biol. Med. (Maywood)* 241, 658–666. doi:10.1177/1535370215624020

Liu, Z., Lin, Y., Fang, X., Yang, J., and Chen, Z. (2021c). Epigallocatechin-3-Gallate Promotes Osteo-/Odontogenic Differentiation of Stem Cells from the Apical Papilla through Activating the BMP-Smad Signaling Pathway. *Molecules* 26, 1580. doi:10.3390/molecules26061580

Lorthongpanich, C., and Charoenwongpaiboon, T. (2021). Fisetin Inhibits Osteogenic Differentiation of Mesenchymal Stem Cells via the Inhibition of YAP. *Antioxidants* 10, 879. doi:10.3390/antiox10060879

Lorthongpanich, C., Charoenwongpaiboon, T., Supakun, P., Klaewkla, M., Kheolamai, P., and Issaragrisil, S. (2021). Fisetin Inhibits Osteogenic Differentiation of Mesenchymal Stem Cells via the Inhibition of YAP. *Antioxidants* 10, 879. doi:10.3390/antiox10060879

Luo, G., Gu, F., Zhang, Y., Liu, T., Guo, P., and Huang, Y. (2015). Icariside II Promotes Osteogenic Differentiation of Bone Marrow Stromal Cells in Beagle Canine. *Int. J. Clin. Exp. Pathol.* 8, 4367–4377.

Martens, S., and Mithöfer, A. (2005). Flavones and Flavone Synthases. *Phytochemistry* 66, 2399–2407. doi:10.1016/j.phytochem.2005.07.013

Miller, P. D. (2016). Management of Severe Osteoporosis. *Expert Opin. Pharmacother.* 17, 473–488. doi:10.1517/14656566.2016.1124856

Mohsin, S., Baniyas, M. M., Aldarmaki, R. S., Tekes, K., Kalász, H., and Adeghate, E. A. (2019). An Update on Therapies for the Treatment of Diabetes-Induced Osteoporosis. *Expert Opin. Biol. Ther.* 19, 937–948. doi:10.1080/14712598.2019.1618266

Nan, L. P., Wang, F., Ran, D., Zhou, S. F., Liu, Y., Zhang, Z., et al. (2020). Naringin Alleviates H2O2-Induced Apoptosis via the PI3K/Akt Pathway in Rat Nucleus Pulposus-Derived Mesenchymal Stem Cells. *Connect. Tissue Res.* 61, 554–567. doi:10.1080/03008207.2019.1631299

Nauth, A., Schemitsch, E., Norris, B., Nollin, Z., and Watson, J. T. (2018). Critical-Size Bone Defects: Is There a Consensus for Diagnosis and Treatment? *J. Orthop. Trauma* 32 (Suppl. 1), S7–s11. doi:10.1097/BOT.0000000000001115

Nelson-Dooley, C., Della-Fera, M. A., Hamrick, M., and Baile, C. A. (2005). Novel Treatments for Obesity and Osteoporosis: Targeting Apoptotic Pathways in Adipocytes. *Curr. Med. Chem.* 12, 2215–2225. doi:10.2174/0929867054864886

Nie, F., Zhang, W., Cui, Q., Fu, Y., Li, H., and Zhang, J. (2020). Kaempferol Promotes Proliferation and Osteogenic Differentiation of Periodontal Ligament Stem Cells via Wnt/β-Catenin Signaling Pathway. *Life Sci.* 258, 118143. doi:10.1016/j.lfs.2020.118143

Nishioku, T., Kubo, T., Kamada, T., Okamoto, K., Tsukuba, T., Uto, T., et al. (2020). (−)-Epigallocatechin-3-gallate Inhibits RANKL-Induced Osteoclastogenesis via Downregulation of NFATc1 and Suppression of HO-1-HMGB1-RAGE pathwayEpigallocatechin-3-Gallate Inhibits RANKL-Induced Osteoclastogenesis via Downregulation of NFATc1 and Suppression of HO-1-HMGB1-RAGE Pathway. *Biomed. Res.* 41, 269–277. doi:10.2220/biomedres.41.269

Oh, J. H., Karadeniz, F., Seo, Y., and Kong, C. S. (2020). Effect of Quercetin 3-O-β-D-Galactopyranoside on the Adipogenic and Osteoblastogenic Differentiation of Human Bone Marrow-Derived Mesenchymal Stromal Cells. *Int. J. Mol. Sci.* 21, 8044. doi:10.3390/ijms21218044

Pan, F. F., Shao, J., Shi, C. J., Li, Z. P., Fu, W. M., and Zhang, J. F. (2021). Apigenin Promotes Osteogenic Differentiation of Mesenchymal Stem Cells and Accelerates Bone Fracture Healing via Activating Wnt/β-Catenin Signaling. *Am. J. Physiol. Endocrinol. Metab.* 320, E760–e771. doi:10.1152/ajpendo.00543.2019

Pang, X. G., Cong, Y., and Bao, N. R. (2018). Quercetin Stimulates Bone Marrow Mesenchymal Stem Cell Differentiation through an Estrogen Receptor-Mediated Pathway. *Biomed. Res. Int.* 2018, 4178021. doi:10.1155/2018/4178021

Patel, H. B., Lyerly, L. J., and Horlen, C. K. (2021). The Role of Novel Bone Forming Agents in the Treatment of Osteoporosis. *J. Pharm. Pract.* 34, 952–961. doi:10.1177/0897190020961227

Pietta, P. G. (2000). Flavonoids as Antioxidants. *J. Nat. Prod.* 63, 1035–1042. doi:10.1021/np9904509

Preethi Soundarya, S., Sanjay, V., Haritha Menon, A., Dhivya, S., and Selvamurugan, N. (2018). Effects of Flavonoids Incorporated Biological Macromolecules Based Scaffolds in Bone Tissue Engineering. *Int. J. Biol. Macromol* 110, 74–87. doi:10.1016/j.ijbiomac.2017.09.014

Qi, S., He, J., Zheng, H., Chen, C., and Lan, S. (2019). Icariin Prevents Diabetes-Induced Bone Loss in Rats by Reducing Blood Glucose and Suppressing Bone Turnover. *Molecules* 24, 1871. doi:10.3390/molecules24101871

Qiu, Y., Chen, Y., Zeng, T., Guo, W., Zhou, W., and Yang, X. (2016). EGCG Ameliorates the Hypoxia-Induced Apoptosis and Osteogenic Differentiation Reduction of Mesenchymal Stem Cells via Upregulating miR-210. *Mol. Biol. Rep.* 43, 183–193. doi:10.1007/s11033-015-3936-0

Qiu, Z. C., Zhang, Y., Xiao, H. H., Chui-Wa Poon, C., Li, X. L., Cui, J. F., et al. (2020). 8-prenylgenistein Exerts Osteogenic Effects via ER α and Wnt-dependent Signaling Pathway. *Exp. Cel Res* 395, 112186. doi:10.1016/j.yexcr.2020.112186

Ren, M., Zhao, Y., He, Z., Lin, J., Xu, C., Liu, F., et al. (2021). Baicalein Inhibits Inflammatory Response and Promotes Osteogenic Activity in Periodontal Ligament Cells Challenged with Lipopolysaccharides. *BMC Complement. Med. Ther.* 21, 43. doi:10.1186/s12906-021-03213-5

Saulite, L., Jekabsons, K., Klavins, M., Muceniece, R., and Riekstina, U. (2019). Effects of Malvidin, Cyanidin and Delphinidin on Human Adipose Mesenchymal Stem Cell Differentiation into Adipocytes, Chondrocytes and Osteocytes. *Phytomedicine* 53, 86–95. doi:10.1016/j.phymed.2018.09.029

Schilling, T., Ebert, R., Raaijmakers, N., Schütze, N., and Jakob, F. (2014). Effects of Phytoestrogens and Other Plant-Derived Compounds on Mesenchymal Stem Cells, Bone Maintenance and Regeneration. *J. Steroid Biochem. Mol. Biol.* 139, 252–261. doi:10.1016/j.jsbmb.2012.12.006

Sharma, A. R., and Nam, J. S. (2019). Kaempferol Stimulates WNT/β-catenin Signaling Pathway to Induce Differentiation of Osteoblasts. *J. Nutr. Biochem.* 74, 108228. doi:10.1016/j.jnutbio.2019.108228

Shavandi, A., Bekhit, A. E. A., Saeedi, P., Izadifar, Z., Bekhit, A. A., and Khademhosseini, A. (2018). Polyphenol Uses in Biomaterials Engineering. *Biomaterials* 167, 91–106. doi:10.1016/j.biomaterials.2018.03.018

Song, J. E., Tian, J., Kook, Y. J., Thangavelu, M., Choi, J. H., and Khang, G. (2020). A BMSCs-Laden Quercetin/duck's Feet Collagen/hydroxyapatite Sponge for Enhanced Bone Regeneration. *J. Biomed. Mater. Res. A.* 108, 784–794. doi:10.1002/jbm.a.36857

Song, J. E., Tripathy, N., Lee, D. H., Park, J. H., and Khang, G. (2018). Quercetin Inlaid Silk Fibroin/Hydroxyapatite Scaffold Promotes Enhanced Osteogenesis. *ACS Appl. Mater. Inter.* 10, 32955–32964. doi:10.1021/acsami.8b08119

Tian, X., Jiang, H., Chen, Y., Ao, X., Chen, C., Zhang, W., et al. (2018). Baicalein Accelerates Tendon-Bone Healing via Activation of Wnt/β-Catenin Signaling Pathway in Rats. *Biomed. Res. Int.*, 2018, 3849760. doi:10.1155/2018/3849760

Tsuchiya, S., Sugimoto, K., Kamio, H., Okabe, K., Kuroda, K., Okido, M., et al. (2018). Kaempferol-immobilized Titanium Dioxide Promotes Formation of New Bone: Effects of Loading Methods on Bone Marrow Stromal Cell Differentiation *In Vivo* and *In Vitro*. *Int. J. Nanomedicine* 13, 1665–1676. doi:10.2147/IJN.S150786

Tutunchi, H., Naeini, F., Ostadrahimi, A., and Hosseinzadeh-Attar, M. J. (2020). Naringenin, a Flavanone with Antiviral and Anti-inflammatory Effects: A Promising Treatment Strategy against COVID-19. *Phytother Res.* 34, 3137–3147. doi:10.1002/ptr.6781

Vadaye Kheiry, E., Parivar, K., Baharara, J., Fazly Bazzaz, B. S., and Iranbakhsh, A. (2018). The Osteogenesis of Bacterial Cellulose Scaffold Loaded with Fisetin. *Iran J. Basic Med. Sci.* 21, 965–971. doi:10.22038/IJBMS.2018.25465.6296

Velasco, M. A., Narváez-Tovar, C. A., and Garzón-Alvarado, D. A. (2015). Design, Materials, and Mechanobiology of Biodegradable Scaffolds for Bone Tissue Engineering. *Biomed. Res. Int.* 2015, 729076. doi:10.1155/2015/729076

Wan, T., Wu, M. R., and Qi, Z. X. (2014). [Effect of Hydroxy Safflower Yellow A on Glucocorticoid-Induced Bone Marrow Mesenchymal Stem Cells Osteogenic Differentiation]. *Zhongguo Gu Shang* 27, 224–228.

Wang, D., Wang, Y., Xu, S., Wang, F., Wang, B., Han, K., et al. (2016). Epigallocatechin-3-gallate Protects against Hydrogen Peroxide-Induced Inhibition of Osteogenic Differentiation of Human Bone Marrow-Derived Mesenchymal Stem Cells. *Stem Cell Int* 2016, 7532798. doi:10.1155/2016/7532798

Wang, H., Li, C., Li, J., Zhu, Y., Jia, Y., Zhang, Y., et al. (2017). Naringin Enhances Osteogenic Differentiation through the Activation of ERK Signaling in Human Bone Marrow Mesenchymal Stem Cells. *Iran J. Basic Med. Sci.* 20, 408–414. doi:10.22038/IJBMS.2017.8582

Wang, J., Tao, Y., Ping, Z., Zhang, W., Hu, X., Wang, Y., et al. (2016). Icariin Attenuates Titanium-Particle Inhibition of Bone Formation by Activating the Wnt/β-Catenin Signaling Pathway *In Vivo* and *In Vitro*. *Sci. Rep.* 6, 23827. doi:10.1038/srep23827

Wang, W., Mao, J., Chen, Y., Zuo, J., Chen, L., Li, Y., et al. (2022). Naringin Promotes Osteogenesis and Ameliorates Osteoporosis Development by Targeting JAK2/STAT3 Signalling. *Clin. Exp. Pharmacol. Physiol.* 49, 113–121. doi:10.1111/1440-1681.13591

Wang, Y. J., Zhang, H. Q., Han, H. L., Zou, Y. Y., Gao, Q. L., and Yang, G. T. (2017). Taxifolin Enhances Osteogenic Differentiation of Human Bone Marrow Mesenchymal Stem Cells Partially via NF-Kb Pathway. *Biochem. Biophys. Res. Commun.* 490, 36–43. doi:10.1016/j.bbrc.2017.06.002

Wang, Z., Wang, D., Yang, D., Zhen, W., Zhang, J., and Peng, S. (2018). The Effect of Icariin on Bone Metabolism and its Potential Clinical Application. *Osteoporos. Int.* 29, 535–544. doi:10.1007/s00198-017-4255-1

Wei, Q., He, M., Chen, M., Chen, Z., Yang, F., Wang, H., et al. (2017). Icariin Stimulates Osteogenic Differentiation of Rat Bone Marrow Stromal Stem Cells by Increasing TAZ Expression. *Biomed. Pharmacother.* 91, 581–589. doi:10.1016/j.biopha.2017.04.019

Wei, Q., Wang, B., Hu, H., Xie, C., Ling, L., Gao, J., et al. (2020). Icaritin Promotes the Osteogenesis of Bone Marrow Mesenchymal Stem Cells via the Regulation

of Sclerostin Expression. *Int. J. Mol. Med.* 45, 816–824. doi:10.3892/ijmm.2020.4470

Wen, L., Jiang, Y., Yang, J., Zhao, Y., Tian, M., and Yang, B. (2017). Structure, Bioactivity, and Synthesis of Methylated Flavonoids. *Ann. N. Y Acad. Sci.* 1398, 120–129. doi:10.1111/nyas.13350

Williams, J., Allen, L., Wickramasinghe, K., Mikkelsen, B., Roberts, N., and Townsend, N. (2018). A Systematic Review of Associations between Non-communicable Diseases and Socioeconomic Status within Low- and Lower-Middle-Income Countries. *J. Glob. Health* 8, 020409. doi:10.7189/jogh.08.020409

Wu, T., Shu, T., Kang, L., Wu, J., Xing, J., Lu, Z., et al. (2017a). Icaritin, a Novel Plant-Derived Osteoinductive Agent, Enhances the Osteogenic Differentiation of Human Bone Marrow- and Human Adipose Tissue-Derived Mesenchymal Stem Cells. *Int. J. Mol. Med.* 39, 984–992. doi:10.3892/ijmm.2017.2906

Wu, Y., Cao, L., Xia, L., Wu, Q., Wang, J., Wang, X., et al. (2017b). Evaluation of Osteogenesis and Angiogenesis of Icariin in Local Controlled Release and Systemic Delivery for Calvarial Defect in Ovariectomized Rats. *Sci. Rep.* 7, 5077. doi:10.1038/s41598-017-05392-z

Xu, H., Zhou, S., Qu, R., Yang, Y., Gong, X., Hong, Y., et al. (2020). Icariin Prevents Oestrogen Deficiency-Induced Alveolar Bone Loss through Promoting Osteogenesis via STAT3. *Cell Prolif* 53, e12743. doi:10.1111/cpr.12743

Xu, Y., Jiang, Y., Jia, B., Wang, Y., and Li, T. (2021). Icariin Stimulates Osteogenesis and Suppresses Adipogenesis of Human Bone Mesenchymal Stem Cells via miR-23a-Mediated Activation of the Wnt/β-Catenin Signaling Pathway. *Phytomedicine* 85, 153485. doi:10.1016/j.phymed.2021.153485

Xue, D., Chen, E., Zhang, W., Gao, X., Wang, S., Zheng, Q., et al. (2017). The Role of Hesperetin on Osteogenesis of Human Mesenchymal Stem Cells and its Function in Bone Regeneration. *Oncotarget* 8, 21031–21043. doi:10.18632/oncotarget.15473

Yang, J., Zhang, Y. S., Yue, K., and Khademhosseini, A. (2017). Cell-laden Hydrogels for Osteochondral and Cartilage Tissue Engineering. *Acta Biomater.* 57, 1–25. doi:10.1016/j.actbio.2017.01.036

Yang, X., Shao, J., Wu, X. M., Pan, F. F., Yang, S. A., Pan, X. H., et al. (2021). Troxerutin Stimulates Osteoblast Differentiation of Mesenchymal Stem Cell and Facilitates Bone Fracture Healing. *Front. Pharmacol.* 12, 723145. doi:10.3389/fphar.2021.723145

Yao, X., Jing, X., Guo, J., Sun, K., Deng, Y., Zhang, Y., et al. (2019). Icariin Protects Bone Marrow Mesenchymal Stem Cells against Iron Overload Induced Dysfunction through Mitochondrial Fusion and Fission, PI3K/AKT/mTOR and MAPK Pathways. *Front. Pharmacol.* 10, 163. doi:10.3389/fphar.2019.00163

Ye, Y., Jing, X., Li, N., Wu, Y., Li, B., and Xu, T. (2017). Icariin Promotes Proliferation and Osteogenic Differentiation of Rat Adipose-Derived Stem Cells by Activating the RhoA-TAZ Signaling Pathway. *Biomed. Pharmacother.* 88, 384–394. doi:10.1016/j.biopha.2017.01.075

Yu, G. Y., Zheng, G. Z., Chang, B., Hu, Q. X., Lin, F. X., Liu, D. Z., et al. (2016). Naringin Stimulates Osteogenic Differentiation of Rat Bone Marrow Stromal Cells via Activation of the Notch Signaling Pathway. *Stem Cell Int.* 2016, 7130653. doi:10.1155/2016/7130653

Yu, X., Shen, G., Shang, Q., Zhang, Z., Zhao, W., Zhang, P., et al. (2021). A Naringin-Loaded Gelatin-Microsphere/nano-Hydroxyapatite/silk Fibroin Composite Scaffold Promoted Healing of Critical-Size vertebral Defects in Ovariectomised Rat. *Int. J. Biol. Macromol* 193, 510–518. doi:10.1016/j.ijbiomac.2021.10.036

Yu, Z., Fan, L., Li, J., Ge, Z., Dang, X., and Wang, K. (2016). Lithium Prevents Rat Steroid-Related Osteonecrosis of the Femoral Head by β-catenin Activation. *Endocrine* 52, 380–390. doi:10.1007/s12020-015-0747-y

Yuan, Z., Min, J., Zhao, Y., Cheng, Q., Wang, K., Lin, S., et al. (2018). Quercetin Rescued TNF-Alpha-Induced Impairments in Bone Marrow-Derived Mesenchymal Stem Cell Osteogenesis and Improved Osteoporosis in Rats. *Am. J. Transl Res.* 10, 4313–4321.

Zamora-Ros, R., Knaze, V., Rothwell, J. A., Hémon, B., Moskal, A., Overvad, K., et al. (2016). Dietary Polyphenol Intake in Europe: the European Prospective Investigation into Cancer and Nutrition (EPIC) Study. *Eur. J. Nutr.* 55, 1359–1375. doi:10.1007/s00394-015-0950-x

Zha, X., Xu, Z., Liu, Y., Xu, L., Huang, H., Zhang, J., et al. (2016). Amentoflavone Enhances Osteogenesis of Human Mesenchymal Stem Cells through JNK and P38 MAPK Pathways. *J. Nat. Med.* 70, 634–644. doi:10.1007/s11418-016-0993-1

Zhang, H., and Li, H. (2018). Tricin Enhances Osteoblastogenesis through the Regulation of Wnt/β-Catenin Signaling in Human Mesenchymal Stem Cells. *Mech. Dev.* 152, 38–43. doi:10.1016/j.mod.2018.07.001

Zhang, J., Wu, K., Xu, T., Wu, J., Li, P., Wang, H., et al. (2019). Epigallocatechin-3-gallate Enhances the Osteoblastogenic Differentiation of Human Adipose-Derived Stem Cells. *Drug Des. Devel Ther.* 13, 1311–1321. doi:10.2147/DDDT.S192683

Zhang, L., Li, X., Ying, T., Wang, T., and Fu, F. (2021). The Use of Herbal Medicines for the Prevention of Glucocorticoid-Induced Osteoporosis. *Front. Endocrinol. (Lausanne)* 12, 744647. doi:10.3389/fendo.2021.744647

Zhang, L. Y., Xue, H. G., Chen, J. Y., Chai, W., and Ni, M. (2016). Genistein Induces Adipogenic Differentiation in Human Bone Marrow Mesenchymal Stem Cells and Suppresses Their Osteogenic Potential by Upregulating PPARγ. *Exp. Ther. Med.* 11, 1853–1858. doi:10.3892/etm.2016.3120

Zhang, N. D., Han, T., Huang, B. K., Rahman, K., Jiang, Y. P., Xu, H. T., et al. (2016). Traditional Chinese Medicine Formulas for the Treatment of Osteoporosis: Implication for Antiosteoporotic Drug Discovery. *J. Ethnopharmacol* 189, 61–80. doi:10.1016/j.jep.2016.05.025

Zhang, Q., Chang, B., Zheng, G., Du, S., and Li, X. (2020). Quercetin Stimulates Osteogenic Differentiation of Bone Marrow Stromal Cells through miRNA-206/connexin 43 Pathway. *Am. J. Transl Res.* 12, 2062–2070.

Zhang, Y. L., Zhu, Z. Z., Zhang, L. C., and Wang, G. (2021). Lithium Chloride Prevents Glucocorticoid-Induced Osteonecrosis of Femoral Heads and Strengthens Mesenchymal Stem Cell Activity in Rats. *Chin. Med. J. (Engl)* 134, 2214–2222. doi:10.1097/CM9.0000000000001530

Zhao, J., Wu, J., Xu, B., Yuan, Z., Leng, Y., Min, J., et al. (2019). Kaempferol Promotes Bone Formation in Part via the mTOR Signaling Pathway. *Mol. Med. Rep.* 20, 5197–5207. doi:10.3892/mmr.2019.10747

Zhao, Z. H., Ma, X. L., Zhao, B., Tian, P., Ma, J. X., Kang, J. Y., et al. (2021). Naringin-inlaid Silk Fibroin/hydroxyapatite Scaffold Enhances Human Umbilical Cord-Derived Mesenchymal Stem Cell-Based Bone Regeneration. *Cell Prolife* 54, e13043. doi:10.1111/cpr.13043

Zheng, Y., Zhang, R., Shi, W., Li, L., Liu, H., Chen, Z., et al. (2020). Metabolism and Pharmacological Activities of the Natural Health-Benefiting Compound Diosmin. *Food Funct.* 11, 8472–8492. doi:10.1039/d0fo01598a

Zhou, Y., Wu, Y., Ma, W., Jiang, X., Takemra, A., Uemura, M., et al. (2017). The Effect of Quercetin Delivery System on Osteogenesis and Angiogenesis under Osteoporotic Conditions. *J. Mater. Chem. B* 5, 612–625. doi:10.1039/c6tb02312f

Zhou, Y. H., and Xie, Q. (2021). Total Glycosides from Eucommia Ulmoides Seed Promoted Osteogenic Differentiation of Adipose-Derived Mesenchymal Stem Cells and Bone Formation in Ovariectomized Rats through Regulating Notch Signaling Pathway. *J. Orthop. Surg. Res.* 16, 660. doi:10.1186/s13018-021-02797-5

Zhu, J., Tang, H., Zhang, Z., Zhang, Y., Qiu, C., Zhang, L., et al. (2017). Kaempferol Slows Intervertebral Disc Degeneration by Modifying LPS-Induced Osteogenesis/adipogenesis Imbalance and Inflammation Response in BMSCs. *Int. Immunopharmacol* 43, 236–242. doi:10.1016/j.intimp.2016.12.020

Conflict of Interest: The authors declare that the research was conducted in the absence of any commercial or financial relationships that could be construed as a potential conflict of interest.

Publisher's Note: All claims expressed in this article are solely those of the authors and do not necessarily represent those of their affiliated organizations, or those of the publisher, the editors and the reviewers. Any product that may be evaluated in this article, or claim that may be made by its manufacturer, is not guaranteed or endorsed by the publisher.

Copyright © 2022 Zhang, Liu, Luo, Li, Huang, Chen, Li and Qin. This is an open-access article distributed under the terms of the Creative Commons Attribution License (CC BY). The use, distribution or reproduction in other forums is permitted, provided the original author(s) and the copyright owner(s) are credited and that the original publication in this journal is cited, in accordance with accepted academic practice. No use, distribution or reproduction is permitted which does not comply with these terms.

frontiers | Frontiers in Pharmacology

REVIEW
published: 01 June 2022
doi: 10.3389/fphar.2022.842101

Traditional Chinese Medicine as a Promising Strategy for the Treatment of Alzheimer's Disease Complicated With Osteoporosis

Weifan Xu[1,2†], Yiping Jiang[1†], Nani Wang[3], Huanhuan Bai[1‡], Shengyan Xu[1‡], Tianshuang Xia[1‡] and Hailiang Xin[1*]*

[1]Department of Pharmacognosy, School of Pharmacy, Naval Medical University, Shanghai, China, [2]Department of Pharmacy, Fujian University of Traditional Chinese Medicine, Fuzhou, China, [3]Department of Medicine, Zhejiang Academy of Traditional Chinese Medicine, Hangzhou, China

Alzheimer's disease (AD) and osteoporosis (OP) are progressive degenerative diseases caused by multiple factors, placing a huge burden on the world. Much evidence indicates that OP is a common complication in AD patients. In addition, there is also evidence to show that patients with OP have a higher risk of AD than those without OP. This suggests that the association between the two diseases may be due to a pathophysiological link rather than one disease causing the other. Several *in vitro* and *in vivo* studies have also proved their common pathogenesis. Based on the theory of traditional Chinese medicine, some classic and specific natural Chinese medicines are widely used to effectively treat AD and OP. Current evidence also shows that these treatments can ameliorate both brain damage and bone metabolism disorder and further alleviate AD complicated with OP. These valuable therapies might provide effective and safe alternatives to major pharmacological strategies.

Keywords: Alzheimer's disease, osteoporosis, pathophysiological link, action mechanism, traditional Chinese medicine

OPEN ACCESS

Edited by:
Longhuo Wu,
Gannan Medical University, China

Reviewed by:
Young-Ji Shiao,
National Research Institute of Chinese Medicine, Taiwan
Minyi Chen,
Universitätsklinikum Heidelberg, Germany
Rui Li,
Shaanxi Provincial People's Hospital, China

***Correspondence:**
Tianshuang Xia
18305183911@163.com
Hailiang Xin
hailiangxin@163.com

†*These authors have contributed equally to this work and share first authorship*

‡***ORCID:***
Huanhuan Bai
orcid.org/0000-0002-9943-804X
Shengyan Xu
orcid.org/0000-0002-1694-6699
Tianshuang Xia
orcid.org/0000-0001-8396-307X

Specialty section:
This article was submitted to Ethnopharmacology, a section of the journal Frontiers in Pharmacology

Received: *23 December 2021*
Accepted: *21 March 2022*
Published: *01 June 2022*

Citation:
Xu W, Jiang Y, Wang N, Bai H, Xu S, Xia T and Xin H (2022) Traditional Chinese Medicine as a Promising Strategy for the Treatment of Alzheimer's Disease Complicated With Osteoporosis. Front. Pharmacol. 13:842101. doi: 10.3389/fphar.2022.842101

INTRODUCTION

With the advent of an aging society, aging-related diseases have occupied the forefront of the disease spectrum in China. Alzheimer's disease (AD) and osteoporosis (OP) are two common aging-related diseases in clinic, which have seriously threatened the health of middle-aged and elderly people. AD is a disease dominated by a series of central neurodegenerative conditions with hidden pathogenesis and unknown etiology (Hogh, 2017). It is clinically characterized by memory impairment, aphasia,

Abbreviations: Aβ, β-amyloid; AD, Alzheimer's disease; AGEs, advance glycosylation end products; APP, amyloid precursor protein; AR, aldose reductase; BACE1, β-site amyloid precursor protein cleavage enzyme 1; BMD, bone mineral density; BMI, body mass index; BMP2, bone morphogenetic proteins 2; BMSCs, bone marrow stromal cells; CAT, catalase; Cbfα1, core-banding factor α-1; ChE, cholinesterase; DKK1, Dickkopf1; ERK, extracellular signal-regulated kinase; GSH-Px, glutathione peroxidase; IL-6, interleukin-6; JNK, c-Jun N-terminal kinase; MAO, monoamine oxidase; MDA, malondialdehyde; MSCs, mesenchymal stem cells; NFATc1, nuclear factor of activated T cells cytoplasmic 1; NF-κB, nuclear factor-κB; NFTs, neurofibrillary tangles; NMDAR, N-methyl-D-aspartate receptor; OB, osteoblasts; OC, osteoclasts; OCN, osteocalcin; OP, osteoporosis; OPG, osteoprotegerin; OPN, osteopontin; PPARγ, activate receptor-γ; RAGEs, receptor for advanced glycosylation end products; RANK, receptor activator of nuclear factor; RANKL, receptor for activator nuclear factor-κB ligand; ROS, reactive oxygen species; Runx2, runt-related transcription factor 2; STAT3, signal transducer and activator of transcription 3; TCM, traditional Chinese medicine; TL, total lignans; TNF-α, tumor necrosis factor-α; TRAF6, tumor necrosis factor associated factor 6.

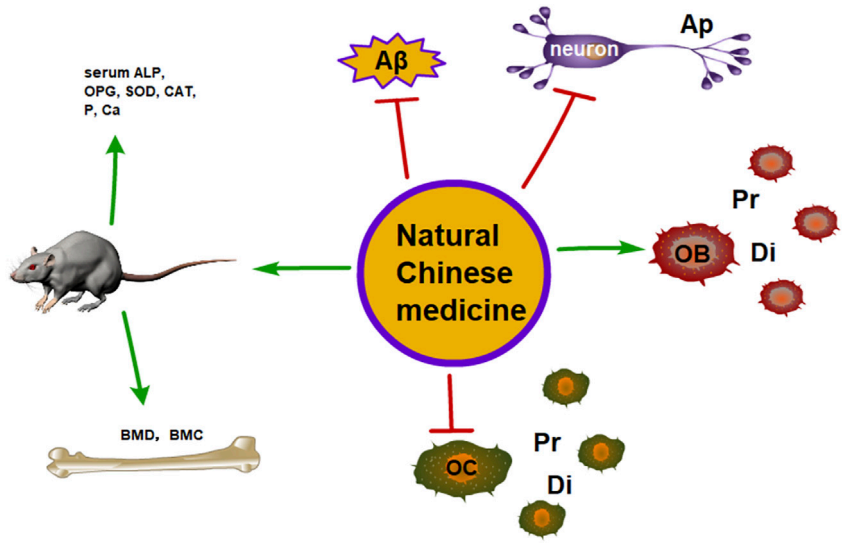

FIGURE 1 | The therapeutic potential of the natural Chinese medicine for the treatment of AD and OP (Ap, apoptosis; Pr, proliferation; Di, differentiation).

impairment of visuospatial skills, executive dysfunction, and personality and behavior changes (Zhang and Zheng, 2019), which badly affect patients' life. The pathologic hallmarks of AD are cerebral extracellular amyloid plaques and intracellular neurofibrillary tangles, but not all people with amyloid plaques or neurofibrillary tangles develop AD (Weller and Budson, 2018). However, the underlying pathophysiological mechanism is still elusive, especially for older adults. OP is a degenerative bone disease, which leads to a decrease in bone mineral density (BMD) and bone mass due to various reasons, and the degeneration of bone micro-structure increases bone brittleness, thus increasing the risk of fracture (Aspray and Hill, 2019). The pathogenesis of OP is considered to include the defect in bone micro-architecture, poor intrinsic material properties of bone, defective repair of micro-damage to the bone, and excessive bone remodeling (Armas and Recker, 2012). These points provide different treatment strategies for OP, as well as expanding the possibilities of new drug screening. In addition, clinical studies have found that patients diagnosed with AD are often accompanied by OP and hip fracture, and the BMD of patients with AD is often lower than that of the non-AD population (Chen and Lo, 2017), indicating that there is a correlation between the pathogenesis of AD and OP, and patients are prone to the symptoms of these two diseases.

Traditional Chinese medicine (TCM) has become increasingly popular thanks to its fewer side effects and high effectiveness in treating diseases. TCM formula is usually composed of more than one kind of herb, and the purpose of the herbal formula is to improve the therapeutic effects or decrease the possible side effects of a single herb through the complex interactions among herbs. Meanwhile, TCM is rich in natural components, which can provide promising ideas for the screening and research of new drugs. The TCM formula has been widely used in effectively treating a variety of aging-related diseases, including AD and OP. Some are the most classical and specific drugs, such as *Morinda officinalis* How., *Eucommia ulmoides* Oliv., *Lycium barbarum* L., *Atractylodes macrocephala* Koidz., *Salvia miltiorrhiza* Bge., *Rehmannia glutinosa* Libosch., and *Glycyrrhiza uralensis* Fisch., *Cistanche deserticola* Ma., when applied to the treatment of dementia and bone loss, with beneficial effects on the growth and development of the nervous system and skeleton tissues (**Figure 1**) (Howes et al., 2017; Pei et al., 2020; Zhang ND et al., 2016; Wang T et al., 2017). Therefore, we review the link between AD and OP from the epidemiological perspective and the underlying molecular mechanism and introduce some natural Chinese medicines for treating AD complicated with OP to provide a reference for future clinical treatment.

CORRELATION BETWEEN ALZHEIMER'S DISEASE AND OSTEOPOROSIS

The Epidemiology of AD and OP

AD is one of the most common diseases in elderly people. The World Health Organization (WHO) estimated that there was a strong link between age and the prevalence of AD, and the global prevalence of AD in the elderly (over 60) was as high as 5%–7% (Prince et al., 2013). In addition, AD is also related to sex, and recent studies have found that nearly two-thirds of AD patients are women (Kim et al., 2018). According to the Alzheimer's Disease International (ADI) statistics, over 55 million people suffer from AD worldwide. This staggering figure grew rapidly and was predicted to reach 78 million by 2030 (Alzheimer's Disease International, McGill University, 2021). In addition, as the number of AD patients continues to rise, the cost of AD treatment also rises. A report shows that the total cost of global AD treatment in 2020 was 305 billion US dollars (Wong, 2020). In China, the total cost of AD treatment in 2015 was 167.74 billion US dollars, and the total cost was expected to reach 507.49

billion US dollars in 2030 (Jia et al., 2018). These numbers reveal that AD has imposed a huge burden on the world economy. More precariously, according to a recent AD report in the United States, the number of AD patients and their cost have been increasing rapidly, despite an important breakthrough made in the prevention, mitigation, and treatment of AD, especially after the outbreak of COVID-19 (Alzheimer's Disease International, McGill University, 2021).

As for osteoporosis, it was found in a survey that the incidence of fragility fractures associated with OP in 2017 was as many as 2.7 million people in European countries (Eric, 2020), and the incidence of osteoporosis in women is generally higher than that in men, especially in postmenopausal women (Lorentzon et al., 2021), who are consistent with AD. However, although bone mass loss in women is faster, the life expectancy of women is generally longer than that of men. A cohort study in Denmark found that the remaining life expectancy was 18.2 years for men with OP at the age of 50 and 7.5 years for men at the age of 75, while for women, the figure was 26.4 and 13.5 years, respectively (Abrahamsen et al., 2015). The prevalence rate of OP in China rose from 14.94% in 2008 to 27.96% in 2012–2015, and the prevalence rate increased with age (28.09% in 25–35 years old and 34.65% in people over 50 years old) (Chen et al., 2016). According to the results of China's OP epidemiological survey in 2018, the prevalence rate of OP in people over 50 years old was 19.2%, as well as 32.0% in people over 65 years, suggesting its widespread features in middle-aged and elderly people in China (Osteoporosis and Bone Mineral Disease Branch of Chinese Medical Association, 2019). In addition, the lack of physical exercise, low vitamin D levels, smoking, drinking, and high caffeine intake can also reduce BMD, leading to OP. According to a report, the human BMD peaks at 35 years old, then begins to decline, and accelerates significantly after menopause. Hence, to prevent OP, young women, as well as men, should quit smoking, avoid excessive drinking, exercise regularly, and take in the right amount of calcium and vitamin D (Lamichhane, 2005).

In addition, the risk of OP in AD and the risk of AD in OP are two different aspects when considering the relationship between these two situations. A prospective, observational study found that lower BMD was associated with an increased risk of increasing AD (Tan et al., 2005). Dual-energy X-ray absorptiometry of the femoral neck was measured for BMD analysis in the study and the results indicated that the lowest quartile of femoral neck BMD was associated with a twice risk of AD in women but not in men, suggesting the possibility of a protective role of cumulative estrogen exposure. Compared with the general population, postmenopausal women with severe OP were found to have higher risks of AD and other dementia (Amouzougan et al., 2017). Estrogen has the potential to influence both brain aging and bone metabolism. The prevalence of AD is slightly higher in women than men, and postmenopausal women are predisposed to develop OP (Henderson, 2006; Depypere et al., 2016). AD is also considered a risk factor for OP. A population-based cohort study indicated that individuals with AD were at a higher risk of hip fracture (Wang et al., 2014). Another meta-analysis study also found that the AD population had a decreased level of hip BMD and approximately twice risk of hip fracture compared with healthy controls (Zhao et al., 2012). The circadian rhythm is usually poorly regulated, and daytime sleepiness is common in the AD population. This situation worsens as cognitive function exacerbates (Lee et al., 2007). The condition limits outdoor physical activities, which may, in turn, decrease sunlight exposure and subsequently cause vitamin D deficiency. Lack of physical activities and vitamin D deficiency may explain the higher risk of OP in the AD population (Nanes and Kallen, 2014). The relationship between AD and OP is further illustrated by the association between BMD values measured by dual-energy X-ray absorptiometry and cerebral volume measured by magnetic resonance imaging. BMD is decreased in the earliest clinical stages of AD and is connected with brain atrophy and memory loss (Loskutova et al., 2009). What is more, BMD and hypothalamic volume were demonstrated to have a positive relationship in the early AD group after controlling for age and gender (Loskutova et al., 2010).

In light of the above epidemiological statistics, it was clear that AD and OP have similarities in high morbidity and disability, strong correlation with age and gender, and high cost for treatment. Therefore, the common pathological mechanism is of great interest as it may direct the future study design for AD and OP prevention.

The Common Pathological Mechanism of AD and OP

Modern pharmacological studies indicate that there are many common pathological mechanisms between AD and OP, such as estrogen deficiency, Wnt signaling pathway inhibition, OPG/RANK/RANKL axis disorder, NF-κB signaling pathway activation, amyloid precursor protein cleavage, vitamin D deficiency, inflammation, parathyroid hormone (PTH) deficiency, calcitonin gene-related peptide (CGRP) expression, and autonomic nervous system (ANS) dysfunction (**Figure 2**).

Estrogen

Estrogen is a substance that promotes the maturation of the secondary sexual characteristics and sexual organs of the female. Estrogen receptors are distributed throughout the body, including the bones and brain. Therefore, estrogen has a wide range of important physiological effects. Estrogen can maintain the secondary sexual characteristics of women and have obvious effects on the growth and maturation of bones and the development of the brain (Patel et al., 2018). A cross-sectional study examined the BMD in women with varying degrees of cognitive impairment. It was found that cognitive impairment was related to low BMD, and cognitive impairment in postmenopausal women was significantly related to the decrease in BMD (Lee et al., 2012). This finding suggested that cognitive aging was multifactorial, and estrogen deficiency might be one of the crucial causes of cognitive impairment. By measuring the trabecular and cortical BMD of elderly women, Alice et al. found that reduced BMD showed a higher risk of cognitive decline (Laudisio et al., 2016). Similar to ovariectomized

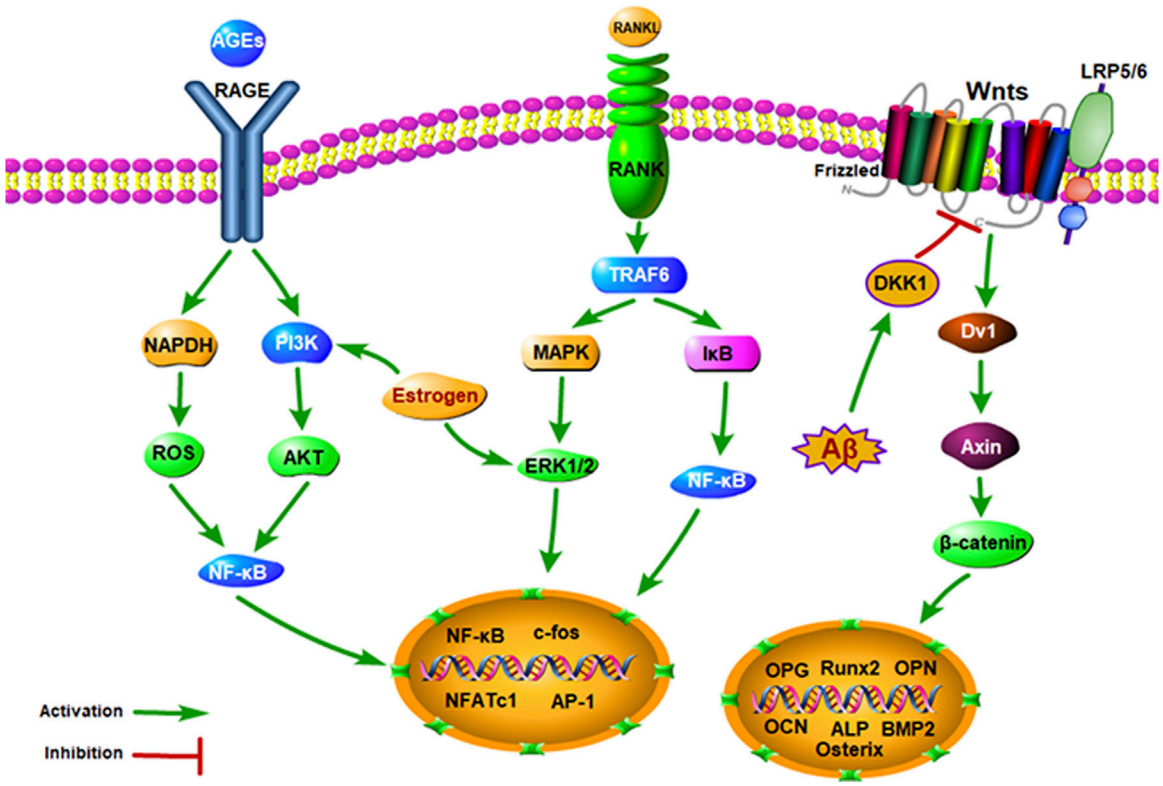

FIGURE 2 | Signaling pathways involved in the common pathogenesis of AD and OP.

(OVX) rodents, it was found that low estrogen levels could also accelerate bone mass loss and lead to memory impairment (Eiken et al., 2014). In addition, estrogen therapy with continuous dependence can improve BMD and prevent osteoporotic fractures. Estrogen has a bone protective effect, which can promote bone formation by increasing osteoblasts (OB) and inhibiting high bone turnover so as to prevent bone loss (Stevenson, 2006). β-Amyloid (Aβ) deposition is the most important pathological feature of AD (Arbor et al., 2016). Estrogen has a negative regulatory effect on Aβ in the brain by activating Aβ degrading enzymes through estrogen receptors and finally promotes the degradation of Aβ (Liang et al., 2010). In OVX rats, Li et al. discovered that the expression levels of Aβ and its substrate synthetic amyloid precursor protein (APP) were significantly increased, and Aβ was mainly located in osteocyte membrane, plasma cells, and extracellular matrix, while APP was mainly located in the bone cell membrane (Li et al., 2014). Therefore, it is suggested that cognitive degradation and BMD reduction are both closely related to the lack of estrogen.

Wnt Signaling Pathway

Wnt protein is a secretory morphogen needed for the basic development of many different tissues, which participates in axonal guidance, neuroblastoma migration, and neuronal differentiation in the brain (Steinhart and Angers, 2018). The classical Wnt pathway activates transcriptional cofactor β-catenin, which is the main driving factor of bone formation and the mediator of synaptogenesis and neurogenesis in the brain (Ross et al., 2018). Studies have shown that the cellular signal cascade of the Wnt signal pathway is closely related to bone loss and neuropathology. Christine et al. found that the expression of osteogenic genes in female and male htau mice was significantly lower than that in normal mice, indicating that their bone remodeling was impaired. Furthermore, genes in the Wnt/β-catenin signal were changed in the bone and brain of the htau mice, suggesting that Wnt pathway was inhibited (Dengler-Crish et al., 2018). Dickkopf1 (DKK1) is an antagonist of the Wnt signaling pathway, which can bind to the Wnt co-receptor of the low-density lipoprotein-associated receptor protein (LRP5/6). DKK1 inhibits bone formation by competing with Wnt to bind with LRP5/6 and block Wnt/β-catenin (Macdonald et al., 2009). By studying the relationship between serum DKK1 and BMD, Joseph et al. found that the concentration of serum DKK1 in the osteoporosis mice was significantly higher than that in normal mice, suggesting a negative correlation between DKK1 and bone mass (Butler et al., 2011). As for the mechanism, on the one hand, blocking of DKK1 can promote the differentiation of osteoblasts (OB) and bone formation (Yaccoby et al., 2007), and on the other hand, DKK1 can also promote the maturation and differentiation of osteoclasts (OC) *via* upregulating osteoprotegerin (OPG)/receptor activator of nuclear factor-κB ligand (RANKL) pathway (Fujita and Janz, 2007). What is more, the inhibitory effect of DKK1 is related to the neurotoxicity of Aβ and tau protein hyperphosphorylation. In the brain of transgenic

AD mice, it was found that Aβ deposition could increase the expression and secretion of DKK1 and indirectly lead to neuronal apoptosis. Activation of the Wnt pathway can reduce Aβ precursor protein lyase, while overexpression of DKK1 can inhibit tau protein hyperphosphorylation caused by the Wnt signaling pathway (Scali et al., 2006). These results suggest that overexpression of DKK1 will antagonize the Wnt signaling pathway, which thereby becomes a common risk factor for AD and OP.

OPG/RANK/RANKL and NF-κB Signaling Pathway

OB cell lineage secretes OPG, which is the only negative regulator of OC. *In vitro*, OPG can inhibit the differentiation of OC precursor cells and the formation of mature OC cells and induce OC apoptosis. The receptor activator of nuclear factor (RANK) is the only target receptor for RANKL to stimulate OC secretion and maturation (Li et al., 2016). It specifically binds with RANKL to activate the differentiation of osteoclast precursor cells and mediate bone resorption. Moreover, RANKL is a cytokine synthesized by OB and stromal cells, which can stimulate the formation of OB cells (Hsu et al., 1999). In *in vitro* experiments, it was shown that RANKL could make osteoclast precursor cells differentiate into OC, activate mature OC in a dose-dependent manner, finally prolong its survival time, and improve bone resorption capacity. OPG and RANK have competitive binding with RANKL, and OPG has a stronger competitive binding ability to RANKL than soluble RANK. On the one hand, OPG can promote OC apoptosis and terminate bone resorption by inhibiting the differentiation and maturation of OC. On the other hand, OPG can promote bone formation by nearly contacting OB. *In vivo* experiments have confirmed that OPG knockout mice had severe osteoporosis, while overexpression of OPG led to severe osteopetrosis (Bucay et al., 1998). Meanwhile, RANK is a signal complex with multiple downstream pathways. The binding of RANK and RANKL leads to the recruitment of tumor necrosis factor associated factor 6 (TRAF6) and rapidly activates the nuclear factor-κB (NF-κB) signaling pathway, thus initiating OC-specific gene transcription (van Dam et al., 2019). Long-term exposure to an inflammatory environment can significantly activate NF-κB and inhibit the function of OB. The activation of the NF-κB pathway is also related to neurofibrillary tangles (NFTs) and extracellular Aβ deposition. The increase in inflammatory factors in the AD brain will promote the degradation of APP to produce Aβ. Then, Aβ activates NF-κB that mediates the expression of inflammatory factors, which act on APP again to produce Aβ. This cascade reaction is critical in the pathogenesis of AD (June 2011). It was indicated that the inhibition of NF-κB could significantly decrease the inflammatory response caused by Aβ and reduce the damage of inflammatory factors to neuronal cells, as well as the deposition of NFTs and Aβ. Li et al. found that Aβ had no effect on RANKL-mediated OC production in rat bone marrow mononuclear cells, but it could promote bone resorption. At the molecular level, Aβ can improve the activity of NF-κB, activate the phosphorylation of extracellular signal-regulated kinase (ERK), and stimulate calcium ion oscillations, thus causing the upregulation of nuclear factor expression in OC-activated T cells (Li et al., 2016). All the above studies suggest that NF-κB can not only regulate the proliferation, differentiation, and apoptosis of OB and OC through OPG/RANK/RANKL axis system but also mediate inflammatory factors on APP to produce Aβ. This indicates that the activation of the NF-κB and OPG/RANK/RANKL signaling pathway can lead to AD and OP.

Amyloid Precursor Protein

Amyloid precursor protein (APP) is a membrane intrinsic protein expressed in various tissues and concentrated in the synapse of neurons. *In vivo*, APP is cleaved by β-site amyloid precursor protein cleavage enzyme (BACE1) to produce soluble APP (sAPP)β, which can bind to death receptor 6 to initiate apoptosis, and further trigger axonal pruning and neuronal death. After being cleaved by the BACE1 enzyme, γ secretase can cleave the remaining fragments of APP to produce the Aβ peptide (Corbett and Hooper, 2018; Guo et al., 2021). When Aβ transport disorders occur through the blood–brain barrier, Aβ oligomers are formed and deposited, resulting in neurotoxicity and neurological dysfunction (Magzoub, 2020). As for *in vitro* experiment, it was found that APP and Aβ could activate OC and promote osteoclastic bone resorption. In the biopsy of bone tissues, Li et al. (2014) found that Aβ42 and APP in OP patients and OVX rats were significantly higher in mRNA and protein expression, compared with the control group, and were negatively correlated with BMD. Tg257 mice are medical Swedish APP gene mutant mice with a two-way regulatory effect on the activation of OC. Cui et al. (2011) found that Aβ oligomers and receptors for advanced glycation end products (RAGE) promote OC production in Tg257 mouse models under 4 months of age. In addition, extracellular Aβ deposition is closely related to the NF-κB signal pathway. Aβ could promote the activity of NF-κB and activate ERK phosphorylation, then upregulate the expression of nuclear factor of activated T cells cytoplasmic 1 (NFATc1) and promote the OC activity (Li et al., 2016). For AD patients, the increase in inflammatory factors in the brain promotes the degradation of APP to form Aβ. Subsequently, Aβ activates the NF-κB pathway, mediates the expression of inflammatory factors, and interacts with APP degradation to produce Aβ. This cascade reaction is crucial in the pathogenesis of AD (Li et al., 2016). Therefore, it is suggested that APP/Aβ is a common characteristic of AD and OP in the regulation of bone remodeling in AD patients.

Vitamin D

Vitamin D deficiency is one of the risk factors inducing OP (Nanes and Kallen, 2014). Besides, although less well recognized, vitamin D deficiency is attracting more attention as a risk factor for AD. Observational studies have found that lower levels of plasma 25-hydroxy vitamin D are significantly related to increased risks of developing all-cause dementia and AD (Littlejohns et al., 2014). A current meta-analysis found a significant positive relationship between vitamin D deficiency and the risk of AD. It is especially noteworthy that moderate

vitamin D deficiency was more strongly connected with the risk of AD compared with severe deficiency (Chai et al., 2019). Moreover, the connection was also investigated between AD and four previously identified single nucleotide polymorphisms related to vitamin D deficiency (Wang et al., 2010). It was found that an encoded vitamin D binding protein (DBP) played an important role in ameliorating AD (Mokry et al., 2016) *via* directly inhibiting Aβ aggregation and oligomerization, as well as improving Aβ-related neuronal injury and protecting against memory impairment in mice (Moon et al., 2013). On the other hand, vitamin D plays a critical role in regulating skeletal homeostasis both indirectly and directly. It was reported that vitamin D deficiency could lead to rickets in infants or children and induce OP in adults (Goltzman, 2018). As for the mechanism, the major effect of vitamin D is to regulate Ca^{2+} and Pi metabolism, promote intestinal Ca^{2+} and Pi absorption, induce bone calcification, and further protect against OP. These results provide converging evidence that vitamin D is a promising therapeutic agent for the treatment of AD and OP.

Inflammation

Recent studies found that inflammatory bone diseases were a potential risk factor for AD. A reduced prevalence of AD was described in rheumatoid arthritis patients who were long-term users of nonsteroidal anti-inflammatory agents (NSAIDs). The epidemiological studies also demonstrated that NSAIDs use is a protective factor for AD onset (Mcgeer et al., 1990). Furthermore, an increased risk of cognitive impairment in the population with midlife rheumatoid arthritis was confirmed based on 21 years of follow-up concerning the connection between rheumatoid arthritis and AD in several case-control, hospitals, and register-based studies (Wallin et al., 2012). Besides, Kamer et al. (2008) has discovered that periodontitis induces systemic inflammation, which stimulates the production of Aβ and tau protein in the brain, leading to AD neuropathology. Interleukin-1β (IL-1β) is a key inducer of the pathogenesis and tissues damage observed in cases of inflammatory bone diseases, including periodontitis and rheumatoid arthritis (Zwerina et al., 2007). IL-1β impairs the migration of OB (Hengartner et al., 2013) and upregulates the RANKL expression induced by osteocytes (Kulkarni et al., 2012). The result of the systematic review and meta-analysis indicated that the peripheral levels of IL-1β were significantly elevated in AD patients compared with controls (Ng et al., 2018). Lipopolysaccharide-induced chronic systemic inflammation in mice resulted in prolonged IL-1β production and microglial activation in the brain (Puntener et al., 2012). Additionally, chronic elevation of IL-1β also appeared in these mice, and a rising expression of hippocampal APP and its proteolytic fragments were discovered, resulting in significant memory impairment in old age (Krstic et al., 2012). These results further suggest that inflammation is a vital risk factor for the development of AD and OP.

Others

In addition to the above factors, there are some other common risk factors associated with AD and OP, such as PTH deficiency, CGRP, and ANS dysfunction. PTH is a key regulator of calcium homeostasis that has the potential to enhance bone regeneration in large bone defects, and its mechanism lies in its anabolic effect on bone. Daily injections of PTH are an effective treatment for OP approved by the US Food and Drug Administration (FDA) that results in increases in both BMD and bone volume (Wojda and Donahue, 2018). The connections between PTH and AD have been reported in a few prospective and case-control studies. In a prospective cohort study, high PTH concentrations were significantly and positively associated with risks of vascular dementia (Hagstrom et al., 2014). Another prospective study discovered that elevated PTH concentrations were connected with a significantly increasing risk of all-cause dementia during the 1-year and 5-year follow-up (Bjorkman et al., 2010). CGRP is a 37 amino acid regulatory neuropeptide resulting from the different merging of the CGRP gene, which has various physiological effects. However, this peptide affects inducing neuroinflammation in neurologic disorders (Malhotra, 2016). CGRP inhibition was also involved in the infiltration of macrophages and the expression of inflammatory mediators such as IL-1β and TNF-α (Singh et al., 2017). As for *in vivo* study, it was discovered that genetic depletion of calcitonin receptors in AD mice could ameliorate mice spatial memory and hippocampal synaptic plasticity, which was connected with a significant reduction in certain characteristic brain markers that were indicative of AD pathology (Patel et al., 2021). Peripheral release of CGRP contributed to the relief of arthritic pain; nevertheless, CGRP would transform the normal to persistent joint synovitis, and the expression of CGRP receptors would upregulate the following arthritic induction (Walsh et al., 2015). Besides, ANS dysfunction is also a key pathogenic factor of AD and OP. In summary, the CGRP antagonists, PTH, and agents for regulating ANS might be a potential therapeutic target to prevent persistent inflammation and attenuate the pathological cascade of AD and OP.

NATURAL CHINESE MEDICINE

Morindae Officinalis Radix (*Morinda officinalis* How., Ba-Ji-Tian, MO)

Morinda officinalis How. is a traditional natural herb in China and northeast Asia, which contains many bioactive ingredients, such as iridoid glycosides, anthraquinones, and oligosaccharides. MO is known to be beneficial to the liver, kidney, and heart channels and has the action of tonifying kidney-yang, enhancing muscles and bones, and improving blood circulation. MO is widely used in TCM to treat different diseases associated with kidney-yang deficiency, such as male impotence, spermatorrhea and premature ejaculation, female infertility, and skeletal atrophy (Cai et al., 2017). Recent studies have found that MO can strengthen sexual and reproductive functions and ameliorate AD *via* regulating the microbiota-gut-brain axis, in evidence of improving memory and learning abilities (Chen et al., 2017).

According to traditional theories of Chinese medicine, cerebral diseases can be prevented by invigorating the kidneys. Therefore, MO is widely used to treat cerebral diseases, such as AD. A recent study revealed that oligosaccharides isolated from

MO could significantly enhance the learning and memory abilities of rats with dementia and alleviate dementia symptoms in behavioral experiments. Subsequent *in vivo* experiments found that the oligosaccharides of MO could also increase the superoxide dismutase (SOD), glutathione peroxidase (GSH-Px), catalase (CAT), and acetylcholine (Ach) activities; decrease the malondialdehyde (MDA), acetylcholinesterase (AChE), neuronal apoptosis; and inhibit the expression of tau and $A\beta_{1\text{-}42}$ (Chen et al., 2017). Specifically, oligosaccharide monomers, such as Bajijiasu and nystose, exhibit various biological activities, including neuroprotective, antidementia, antiosteoporosis, and antidepressant effects (Zhang et al., 2018). MO aqueous extracts could also ameliorate learning and memory impairment in AD mice. After the administration of MO aqueous extracts for 4 weeks, it was observed that MO significantly improved the learning and memory ability in a water maze test, significantly reduced the activity of aldose reductase, decreased the serum advanced glycosylation end products (AGEs) and receptor for advanced glycosylation end products (RAGEs), and then decreased the damage to brain cells (Ye et al., 2015). In D-galactose and $A\beta_{25\text{-}35}$-induced AD rats, different doses of MO also significantly increased the antioxidant enzyme activities (SOD, GSH-Px, and CAT), neurotransmitter levels (acetylcholine, gamma-aminobutyric, and dopamine), energy metabolism (Na^+/K^+-ATPsae), and relative synaptophysin expression levels (Deng et al., 2020). Furthermore, there was a significant decrease in MDA levels and relative expression levels of APP, tau, and caspase-3 in AD rats after treatment with MO.

In TCM, it is considered that kidney essence deficiency plays a vital role in the development of OP, and MO is commonly used to treat bone atrophy and OP. The aqueous extract of MO has been confirmed to be effective in the treatment of postmenopausal OP, as evidenced by a clinical trial involving 50 patients (Long et al., 2013). In modern pharmacology research, it was also discovered that MO ethanol extract had protective effects on ovariectomy-induced bone loss, as evidenced by the increased tibia bone mineral content (BMC) and BMD, improved phosphorus (Pi), calcium (Ca^{2+}), and OPG levels (Li et al., 2009). As for *in vitro* studies, the aqueous extracts of MO root could increase the expression of core-banding factorα 1 (Cbfα1) in bone marrow stromal cells (BMSCs) and promote the differentiation from BMSCs to OB (Wang et al., 2004). MO polysaccharide is also shown to have antiosteoporosis activities. It was discovered that MO polysaccharides could increase the BMD and BMC and decrease the cytokine levels in the serum interleukin-6 (IL-6) and tumor necrosis factor-α (TNF-α) of OVX rats after 30 days of oral administration (Mengyong et al., 2008). MO anthraquinone could also increase the mRNA expression of RANKL, alkaline phosphatase (ALP), and OPG, thereby promoting osteoblastic bone formation (Bao et al., 2011).

Taken together, these findings suggest that MO and its bioactive compounds may play an important role in the treatment and prevention of AD and OP. MO appears to provide a potentially effective treatment for AD and OP by the alleviation of learning and memory impairment and the attenuation of bone loss and trabecular microstructural degradation. Therefore, MO is a good choice for screening potential drugs to treat AD and OP.

Eucommiae Cortex (*Eucommia ulmoides* Oliv., Du Zhong, EU)

Eucommia ulmoides Oliv. is an important economic plant, and its dried bark, leaves, stem, and even staminate flower are widely used in TCM. EU enjoys extensive pharmacological properties as an antioxidant, anti-inflammatory, antimicrobial, anticancer, cardioprotective, and neuroprotective agent that has been applied for the treatment of cardiovascular disease, sexual dysfunction cancer, neurological disease, rheumatoid arthritis, and osteoarthritis (He et al., 2014). The bioactive compounds of EU include lignans, iridoids, phenolics, steroids, and flavonoids, most of which have been proved to possess the ability to protect against AD and OP.

The aqueous extract of EU exhibits significant neuroprotective effects in several experimental models, thus proving to be a potential therapeutic drug in the treatment of neurodegenerative diseases, such as AD. *In vivo* studies showed that the aqueous extract of EU bark exerted a neuroprotective effect on $A\beta_{25-35}$-induced mice and ameliorated learning and memory impairment (Kwon et al., 2011). The aqueous extract of EU significantly improved $A\beta_{25-35}$-induced memory deficits in the Y-maze test and increased step-through latency time with $A\beta_{25-35}$-induced learning and memory deficits in the passive avoidance test. In addition, the aqueous extract of EU also significantly inhibited AChE activity in the hippocampus and frontal cortex at 20 mg/kg concentrations and suppressed AChE activity in a dose-dependent manner, with the degrees of inhibition being 27.3% and 25.3%, respectively (Kwon et al., 2011). Moreover, aucubin in the EU appeared to ameliorate damage induced by lithium-pilocarpine in the hippocampus with status epileptics (SE), as well as reducing the number of apoptotic neurons and increasing the number of survival neurons by inducing autophagy and inhibiting necroptosis (Wang J et al., 2017). Additionally, the macranthoin G from EU effectively enhanced PC12 cells viability and increased the antioxidant enzymes, such as CAT, SOD, GSH, and GSH-Px. It also reduced intracellular reactive oxygen species (ROS), MDA content, caspase-3 activation, and PC12 cell apoptosis in *in vitro* experiments (Hu et al., 2014). These findings all revealed that EU had potential therapeutic effects on neurodegenerative diseases, such as AD.

In a rodent model of acetate-induced bone loss, EU cortex extract (EUCE) attenuated the loss of BMD of the rat's lumbar spine and femur and restored serum Ca^{2+}, Pi, ALP, osteocalcin, and RANKL to normal levels (Xiong and Zhao, 2016). Furthermore, anti-osteoclastic activity was indicated by the effect of EUCE on regulating the serum OPG/RANKL ratio to normal and significantly increased the serum Ca^{2+}, Pi, ALP, and osteocalcin (Qi et al., 2019). Total lignans (TL) extracted from EU-cortex could increase BMD, biomechanical properties, and microarchitecture and inhibit the bone loss and bone turnover rate due to estrogen deficiency-induced osteoporosis in a rodent model. *In vitro* experiments also showed

that TL not only increased the proliferation and differentiation of OB but also improved the formation of bone nodules (Zhang et al., 2014). The leaves and seeds of EU may also be of potential benefit for the treatment of osteoporosis. In a combined estrogen deficiency-induced osteoporosis and obesity rodent model, EU leaf extract decreased rats' body weight and body mass index (BMI) and increased the BMD and bone strength, which appeared to be beneficial for improving bone metabolism and restoring bone loss (Zhao et al., 2020).

Taken together, it is demonstrated that EU is good medicine to treat neurodegenerative diseases and prevent bone loss for many parts of EU, including the cortex, leaf, and seed and possesses potential therapeutic benefits for the treatment of AD and OP as depicted above.

Lycii Fructus (*Lycium barbarum* L., Gou Qi Zi, LR)

Lycium barbarum L., as a traditional Chinese medicinal herb and food supplement, has been used in China and other Asian countries for more than 2000 years. These berries have also become increasingly popular in western countries as an anti-aging and antioxidant product (Jin et al., 2013). The TCM theory thinks that LR can tonify the kidney, benefit essence, and strengthen the activity of the waist and knee by balancing the "yin" and "yang" in the body. LR has pharmacological properties as an anti-aging, antioxidant, anticancer, antifatigue, anti-osteoporosis, and neuroprotective agent exhibiting a wide array of therapeutic effects on aging, fatigue, cancer, stroke, AD, and OP.

Aβ is the major component of senile plaques and is considered the main biomarker of AD. Studies have found that Aβ develops its toxicity to neurons and other brain tissues by increasing the N-methyl-D-aspartate receptor- (NMDAR-) mediated Ca^{2+} influx and subsequently generating ROS (Pinheiro and Faustino, 2019). LR can protect against neuronal injury induced by Aβ peptides and promote neurogenesis. The LR polysaccharide (LRP) also shows a beneficial effect on Aβ-induced caspase-3 activation and neuronal cell death (Ho et al., 2007). The alkaline extract of LR (containing LRP) could also protect neurons *via* elevating the pro-survival AKT pathway (Ho et al., 2007). The water extract of LR played its neuronal beneficial effects by inhibiting the apoptotic pathway and associated c-Jun N-terminal kinase (JNK)/double-stranded RNA-dependent protein kinase (PKP) pathway (Yu et al., 2007). Much evidence indicated that the over-activation of the glutamatergic NMDARs leads to postsynaptic Ca^{2+} overload and excitotoxicity, resulting in disturbed neuroplasticity and neuronal cell death. Ho et al. (2009) found that LRP could antagonize glutamate-induced toxicity in primary cultures of cortical neurons, with a similar function as memantine (this non-competitive NMDAR antagonist was approved by US and European Food and Drug Administrations to be widely used in clinical trials to treat AD). LRP can also inhibit caspase-3 activation, decrease the generation of ROS, and exert an antioxidant effect. In an amyloid precursor protein/presenilin 1 (APP/PS1) double-transgenic mice model, LR water extracts strongly ameliorated the learning and memory impairments of mice after 2-week administration, which was demonstrated by the Morris water maze test (Zhang et al., 2013). These findings confirmed the protective effects of LR on AD, and the mechanism might be related to the clearance of Aβ.

LR has also shown a potent anti-OP effect in *in vivo* and *in vitro* experiments. After oral administration with 1 and 100 mg/kg LR extracts for 6 weeks, OVX rats exhibited an enhancement of BMD and BMC, decreased serum osteocalcin levels, and a recovery of the calcium levels (Kim et al., 2017). In addition, LRP could reverse palmitate-induced apoptosis in MC3T3-E1 cells by inhibiting the activation of caspase-12 and the phosphorylation level of JNK (Jing and Jia, 2018). In addition, the extract of LR cortex could also prevent BMD loss in OVX mice, improve cellular proliferation and differentiation, and increase ALP activity and mRNA expression of OB marker runt-related transcription factor 2 (Runx2) in *in vitro* experiment (Park et al., 2014). Taken together, the role of LR in promoting OB proliferation and differentiation is beyond doubt.

Collectively, as a common dual-purpose product for medicine and food, LR has the potential to develop into a drug for the prevention and treatment of AD complicated with OP for its effects on clearing Aβ and promoting OB bone formation.

Atractylodis Macrocephalae Rhizoma (*Atractylodes macrocephala* Koidz., Bai Zhu, AM)

Atractylodes macrocephala Koidz., a traditional medicinal plant, is widely used as a tonic agent in China and other Asian countries. In the TCM theory, AM is considered to enter the stomach and spleen channels that can tonify "Qi" and clear damp and diuresis. AM enjoys diverse pharmacological activities, including improving gastrointestinal function, exerting anti-inflammatory, anti-oxidative, anti-aging, anti-osteoporotic, and neuroprotective activities (Zhu et al., 2018).

AM extract was found to have protective activity against AD. In the experiment of the rat passive avoidance test model, it was found to significantly prolong the step-through latency, reduce the error frequency, and decrease the AChE content after the administration of AM ethanol extract (0.5–2 mg/kg) for 15 days (Hong and Yu, 2015). This demonstrated that AM might improve memory impairment and prevent AD in aging rats, and the underlying mechanism might be associated with decreased AChE activity in the hippocampus. In a water maze experiment of AD rats induced by $Aβ_{1-40}$, a supplement with AM biatractylolide (0.1–1.0 mg/kg) for 10 days led to a remarkably reduced swimming time and error frequency and reduced cholinesterase (ChE) content in rats, indicating that AM biatractylolide could improve the memory and learning ability of AD rats (Feng et al., 2009). In addition, AM atractylenolide also has a significant neuroprotective activity. It was discovered that the administration of AM atractylenolide could significantly enhance the cell viability in PC12 cells induced by hypoxia, calcium overloading, and excitatory amino acids (Luo and Sun, 2012). Likewise, in PC12 cells, it was found that the

supplement with atractylenolide III (30 μg/ml) significantly enhanced the cell activity and suppressed apoptosis (Wang, 2012). These findings indicate that AM has a potent neuroprotective activity, especially in protecting against AD.

It was discovered that intraperitoneal injection of RANKL could rapidly reduce trabecular bone loss by stimulating OC function and differentiation rather than affecting OB formation. As for the *in vitro* experiment, AM ethanol extracts could attenuate RANKL-induced activation of the NF-κB signaling pathway and then inhibit the differentiation of OC in RANKL-induced osteoclastogenesis from OC precursors. Similar to *in vitro* results, AM also has protective effects on RANKL-induced bone loss in mice. AM inhibits RANKL-induced c-Fos and NFATc1 expression in OC precursors, thereby inhibiting OC differentiation (Ha et al., 2013). Moreover, in the mesenchymal stem cells (MSCs), the treatment with atractylenolides I and III (both are 1–300 μg/ml) can significantly improve the expression of specific chondrogenic markers and promote chondrogenic differentiation (Li X et al., 2012). Nevertheless, the anti-OP effect of other active components in AM needs to be evaluated.

Therefore, evidence suggests that AM can be used as an effective therapeutic agent for the treatment of AD and OP. Further research is needed to isolate and characterize the bioactive constituents of AM and determine the molecular mechanisms and signaling pathways that produce therapeutic effects.

Salviae Miltiorrhizae Radix Et Rhizoma (*Salvia miltiorrhiza* Bge., Dan Shen, SM)

Salvia miltiorrhiza Bge. is one of the most famous TCM herbs, which has been used to treat various diseases for centuries. Its traditional efficacy is HuoXue QuYu (activate blood circulation and remove stasis), Tongjing ZhiTong (regulate menstruation and relieve pain), QingXin ChuFan (tranquilize the mind and eliminate annoyance), LiangXue XiaoYong (reduce blood flow and eliminate carbuncle). Modern pharmacological studies demonstrate that SM has diverse pharmacological activities, such as anti-oxidation, anti-inflammation, neuroprotection, anti-apoptosis, and antiosteoporosis (Sreenivasmurthy et al., 2017; Chen et al., 2019; He et al., 2019).

Accumulated evidence indicates that many ingredients of SM, such as salvianolic acids A, salvianolic acids B, cryptotanshinone tanshinone I, and tanshinone IIA, have effects on reducing cell apoptosis, inhibiting Aβ aggregation, enhancing cholinergic, and further exerting neuroprotective effects. Studies have suggested that SM extracts could significantly improve the learning and memory abilities of AD rats after being supplemented with SM for 23 consecutive days. It protected against $A\beta_{25\text{-}35}$ induced apoptosis by downregulating APP and PS1 levels (Liu M et al., 2015). Other studies showed that AM root extracts could enhance the neurogenesis of neural stem cells and progenitor cells (Zhang XZ et al., 2016). Several reports also showed that the chemical components in SM had anti-AD effects. It was discovered that salvianolic acids A and salvianolic acids B could prevent Aβ aggregation, delay AD paralysis in *C. elegans*, and reduce ROS production to protect against Aβ induced neurotoxicity (Yuen et al., 2021). Moreover, salvianolic acid B could also improve the cholinergic damage and ameliorate Aβ-induced cognitive impairment in the AD mice model (Lee YW et al., 2013). Other research suggested that tanshinone IIA could prevent spatial learning and memory deficits in APP/PS1 mice and attenuate Aβ accumulation and neuronal loss (Ding et al., 2020).

In TCM, OP is called "bone atrophy," and its pathogenesis is related to the liver and kidney. Furthermore, SM plays an effective role in nourishing the liver and kidney. *In vivo* studies showed that SM could attenuate the unbalanced levels of serum ALP, OPG, and RANKL in OVX rats after 14 weeks of treatment. The decreased bone strength and BMD were inhibited, and the impaired bone micro-structures were improved (Liu H et al., 2018). Similarly, SM extracts could prevent trabecular bone loss and improve the serum level of OPG in OVX mice (Park et al., 2017). These results indicate that SM has an excellent anti-bone loss effect. In addition, other active components of SM, such as salvianolic acid, also have strong bone anabolism activities. It was discovered that salvianolic acid B could enhance cancellous bone formation, improve cancellous thickness, and prevent bone loss in glucocorticoid-induced OP rats. *In vitro* experiment showed that salvianolic acid B could stimulate BMSCs differentiation to OB and increase OB activity *via* increasing the secretion of ALP and osteocalcin, improving Runx2 mRNA expression, and decreasing DKK1 mRNA expression (Cui et al., 2012). Moreover, it was found that salvianolic acid A could improve fracture callus formation and micro-architecture with an accelerated mineralization rate in callus on a prednisone-induced delayed fracture union mouse model (Liu Y et al., 2018).

In conclusion, these results indicate that both AM extracts and AM active components have significant anti-AD and anti-OP potentials by attenuating Aβ accumulation and regulating OPG and Wnt pathways. However, the underlying mechanism and clinical application are not very clear, so more research is needed.

Rehmanniae Radix (*Rehmannia glutinosa* Libosch., Di Huang, RR)

Rehmannia glutinosa Libosch. has been widely used in the form of decoction pieces containing dry Radix Rehmanniae and Prepared Radix Rehmanniae in clinic. RR has various pharmacological actions, such as lowering blood pressure, anti-hyperglycemia anti-inflammation, neuroprotection, improving renal function, and antiosteoporosis (Zhang ND et al., 2016). Therefore, the clinical application of RR is to treat different diseases such as renal failure, hypertension, AD, and OP.

Although RR is not indicated in the current pharmacopeia for symptoms associated with AD, it is one of the most frequently reported ingredients of multiple TCM formulas indicated for memory impairment associated with aging (May et al., 2016). In *in vivo* screening system using the *Drosophila* model of AD, the RR extract was found to have neuroprotective activities against Aβ neurotoxicity (Liu QF et al., 2015). Catalpol is one of the most active compositions of RR and has a great potential for treating AD. In AD mice, catalpol could significantly increase the activity of SOD, GSH-Px, and CAT and reduce the levels of soluble $A\beta_{40}$ and $A\beta_{42}$ in the cerebral cortex of the hippocampus, thus

inhibiting the formation of senile plaques. Morris water maze test revealed that the time spent in the target quadrant and average number of hidden platforms could be increased after the administration of catalpol, indicating its effects on improving the learning and memory impairment of AD mice (Huang et al., 2016). Liu et al. (Liu C et al. 2018) found that the treatment of endothelial (bEND.3) cells with catalpol could prevent endothelial damage, reduce blood–brain barrier hyperpermeability induced by fibrillar $A\beta_{1\text{-}42}$, and enhance soluble Aβ clearance, indicating that catalpol had a protective effect on $A\beta_{1\text{-}42}$-induced blood–brain barrier leakage. In aged rats with Aβ induced nerve injury, catalpol promoted nerve recovery and improved the expression of synaptic proteins, which was important in synaptic plasticity and neuronal development (Xia et al., 2017). Wang et al. (2018) also discovered that catalpol could upregulate α-secretase expression, promote α-cleavage of APP processing, and decrease Aβ formation *via* ERK/cAMP response element-binding protein (CREB) signaling pathway in Swedish mutant APP overexpressed N2a (SweAPP N2a) cells.

In TCM, RR has the effects on promoting blood circulation, tonifying the kidney, and regulating the liver, which are closely related to the pathogenesis of OP. Studies have discovered that water extracts of RR (300 mg/kg) could significantly improve BMD in the lumbar and femurs and markedly reduce the serum ALP level in OVX rats after an 8-week treatment (Lim and Kim, 2013). Some active components in RR, such as acteoside and catalpol, also showed a potent anti-osteoporosis effect. Acteoside could reduce ROS production and inhibit OC formation and bone resorption by macrophages *via* downregulating early RANKL signaling pathways and inhibiting the expression of TNF-α, NFATc1, and c-Fos (Lee SY et al., 2013). In addition, oral administration with acteoside could also inhibit the alteration of OP biochemical markers and bone loss in OVX rats (Lee SY et al., 2013). Similarly, Gong et al. (2019) found that acteoside, echinacoside, and catalpol could improve the proliferation and differentiation of osteoblastic MC3T3-E1 cells and increase bone morphogenetic proteins 2 (BMP2), Runx2, and osterix to prompt bone formation. As for *in vivo* study, RR extract could increase ALP activity, decrease osteocalcin (OCN) levels, and improve BMD and bone microarchitecture in diabetic rats. In addition, RR water extract could increase the serum OPG level; reduce the serum of ALP, RANKL, and tartrate-resistant acid phosphatase (TRAP) in OVX rats; and increase cortical bone and epiphyseal thickness to preserve BMD and mechanical strength by regulating Wnt/β-catenin signaling pathway (Liu et al., 2019).

Altogether, RR is considered a well-tolerated herbal medicine for AD and OP with potential neurogenic and bone-protective activities *in vivo* and *in vitro*. Its mechanism is mainly related to Aβ clearance, ERK/CREB pathway regulation, and Wnt/β-catenin activation.

Glycyrrhizae Radix Et Rhizoma (*Glycyrrhiza uralensis* Fisch., Gan Cao, GR)

Glycyrrhiza uralensis Fisch. is the dried root and rhizomes of *Glycyrrhiza uralensis* Fisch., *Glycyrrhiza inflata* Bat., or *Glycyrrhiza glabra* L. and has traditionally been used in the treatment of cough, influenza, and detoxification all over the world for hundreds of years. Its clinical application has attracted extensive attention worldwide (Ji et al., 2016). Recent studies have shown that GR has antioxidant, anti-AD, anti-inflammatory, and bone protective activities.

Licochalcone B is an active compound in GR and has neuroprotective activity through inhibiting $A\beta_{42}$ self-aggregation, reducing ROS generation, and preventing H_2O_2-induced SH-SY5Y cell death (Cao et al., 2020). In lipopolysaccharide-treated C57BL/6 mice, oral intake of GR extract (150 mg/kg) led to a significant reduction in spatial cognitive and memory impairment, as evidenced by the T-maze novel object recognition test (Cho et al., 2018). In another study, it was discovered that GR extract and its bio-activated compound semilicoisoflavone B could decrease the secretion of Aβ through regulating BACE1 transcription factors, as well as activating receptor-γ (PPARγ) expression and inhibiting the phosphorylation of signal transducer and activator of transcription 3 (STAT3) (Gu et al., 2018). Glycyrrhizic acid, another main bioactive compound of GR, has a neuroprotective effect on scopolamine-induced cognitive impairment. The Y-maze test found that glycyrrhizic acid could significantly improve the mice cognitive impairment induced by scopolamine, decrease AChE activity, and increase SOD and CAT activity. The mechanism was *via* increasing phosphorylation of JNK and ERK protein and improving the mitogen-activated protein kinase (MAPK) pathway (Ban et al., 2020). Additionally, some active components in GR also showed potent anti-AD effects. The coumarin glycyrol in GR could significantly suppress the butyrylcholinesterase (BChE) and AChE, and another compound, liquiritigenin, effectively inhibited monoamine oxidase B (MAO-B) and monoamine oxidase A (MAO-A). These results indicate that GR can be considered a promising herb for the treatment of AD with multi-targeting activities (Jeong et al., 2020).

In the theory of TCM, GR has a strong nutritious function and is usually used as a life enhancer. Previous studies have found that the extract of GR and its active ingredients have estrogenic-like activities (Tamir et al., 2001). Di et al. confirmed that the GR extracts notably protected BMD loss in OVX rats by measuring the BMD of the total tibia and proximal tibia. This protective effect did not affect changes in histology and weight of the uterine, indicating the absence of a uterus-focused effect of GR extract (Galanis et al., 2019). Liquiritigenin is an active flavonoid extracted from GR. It was discovered that liquiritigenin could inhibit the formation of OP phenotype in glucocorticoid-induced adult zebrafish model *via* inhibiting OC activation in scales (Carnovali et al., 2020). Another active ingredient, 18β-glycyrrhetinic acid (18β-GA), could also inhibit osteoclastogenesis and RANKL-mediated OC differentiation at an early stage *in vitro* by suppressing RANK expression in preosteoclasts and blocking the binding of TNF receptor-associated factor 6 (TRAF6) and RANK, thereby leading to the inhibition of MAPK and NF-κB signaling pathways. Furthermore, 18β-GA could reduce the serum tartrate-resistant acid

phosphatase 5b (TRAP5b), TNF-α, and interleukin-6 (IL-6) and increase bone matrix mineralization, which indicated that 18β-GA decreased bone loss in OVX mice *via* suppressing osteoclastogenesis (Chen et al., 2018). In addition, studies have found that ethyl acetate extract from GR could also play a similar role as estrogen and promote the proliferation of human BMSCs (Azizsoltani et al., 2018). These results indicate that GR may be a potential candidate for the prevention of OP.

These findings indicate that GR appears to provide beneficial therapeutic effects for AD and OP, including attenuating cognitive impairment and bone loss. Hence, as a potent life enhancer, GR has the potential to be developed into a drug for the prevention and treatment of AD complicated with OP.

Cistanches Herba (*Cistanche deserticola* Ma., Rou Cong Rong, CH)

Cistanche deserticola Ma., a desert living plant known as desert ginseng, is of a high medicinal value. It is characterized as the major material of tonifying kidney "yang" in the TCM theory and has been widely used to ameliorate forgetfulness, improve the strength of reproduction, and develop fertility function. Modern pharmacological studies reveal that CH has neuroprotective, immunomodulatory, anti-viral, anti-inflammatory, anti-tumor, anti-bacterial, anti-oxidative, and bone-formation activities. Therefore, CH is widely used in Chinese medicine prescriptions for treating various diseases, such as dementia, aging, and OP (Jiang et al., 2016; Fu et al., 2018; Fan et al., 2019).

Previous studies confirmed that CH extracts or its components exerted a potential neuroprotective effect against AD. Zhou et al. (2019) found that the CH extract had antiapoptotic and antioxidant stress effects *via* inhibiting Aβ deposition and tau protein hyperphosphorylation and promoting synapse protection. Chao et al. (2019) also discovered that the CH extract protected against AD by inhibiting Aβ peptide aggregation and deposition. In a clinical trial, AD patients were treated with CH capsules for 48 weeks. The results showed that the levels of TNF-α, total-tau, and IL-1β were significantly reduced, and volume changes of the hippocampus slowed down, indicating that CH could ameliorate cognitive and independent living ability through inhibiting the expression of TNF-α, total-tau, and IL-1β in the cerebrospinal fluid of AD patients (Li et al., 2015). Acteoside is one of the active phenylethanoid glycosides in CH and is known to have neuroprotective and antioxidant effects. In the AD mice model of senescence induced by a combination of $AlCl_3$ and D-galactose, it was discovered that acteoside could shorten the latency of step down, reduce the number of errors, and decrease the activity of nitric oxide synthase and caspase-3 (Peng et al., 2015). Similarly, CH decoction could also improve the mice's spatial learning and memory in the Morris water maze test by decreasing monoamine oxidase and increasing dopamine in the brain (Wang D et al., 2017).

In OVX rats, it was found that the BMD and BMC were significantly improved after treatment with CH extracts, and serum ALP and SOD CAT GSH-Px were also markedly reduced (Liang et al., 2011), suggesting that CH could reverse the bone loss and prevent postmenopausal osteoporosis. Further investigation indicated that the molecular mechanism that CH reduced bone degeneration and regulated involved bone metabolism genes, including Smad1, Smad5, TGF-β-inducible early gene 1 (TIEG1), and transforming growth factor-β1 (TGF-β1) (Liang et al., 2013). *In vitro* experiments also demonstrated that CH extracts could enhance the BMP2, osteopontin (OPN), and ALP expression and induce the OB differentiation, maturation, and bone mineralization by regulating ERK, JNK, NF-κB, and p38 (MAPK) pathways (Li TM et al., 2012). Additionally, CH polysaccharide enhanced the expression of antioxidant enzymes and reduced the RANKL-induced ROS overproduction to decrease the OC differentiation and inhibit bone resorption (Song et al., 2018).

All of these studies demonstrate the efficacy and therapeutic potential of CH in the treatment of neurodegenerative damage and bone loss. Further study is necessary to extensively characterize the bioactive effects of CH that may render better therapeutic strategies for the treatment of AD and OP.

DISCUSSION

In summary, with the increasingly aging population worldwide, dementia and osteoporotic fracture have become a major health and social issues. The side effects of existing clinical drugs have prompted researchers to study natural therapeutic compounds for their effectiveness and safety in the treatment of AD and OP, with fewer adverse side effects.

OP and hip fracture are commonly observed complications seen in patients with AD. Although the mechanisms underlying this association remain poorly understood, emerging evidence supports the view that AD risk genes may also be a risk factor for osteoporosis and that AD and OP may share conserved oxidative stress-driven pathogenic mechanisms (Weller and Schatzker, 2004). In addition, the pathogenesis of AD and OP is complicated in terms of occurrence, development, and progression, including estrogen deficiency; Aβ deposition; and the dysregulation of Wnt, RANKL, and NF-κB signaling pathways. Thus, the combination of multi-component and multi-target targeted therapy may be of great significance.

TCM herbs may contain effective components for the treatment of AD and OP, and this review summarizes current evidence of their potential bio-pharmacological effects and possible mechanisms. A summary of natural herbs against AD and OP *in vivo* and *in vitro* is shown in **Table 1** and **Table 2**, summarizing the change in related indicators of each drug in *in vivo* and *in vitro* experiments.

According to the clinical experience and the TCM theory, Chinese herbs are divided into different categories with special functions. Because of their effects on tonifying the kidney, some of them are classic and specific drugs for improving the impairment of the brain and bone. In addition, these herbs can not only treat diseases but also have a certain preventive effect. However, the development of AD and OP remains very complex in elderly people and postmenopausal women. The

TABLE 1 | Summary of *in vivo* studies for the anti-Alzheimer's disease and antiosteoporotic effects of natural Chinese medicine.

TCM	Animal model	Drug	Beneficial effects	Ref.
Morindae Officinalis Radix	AD rats	Fructo-oligosaccharides	(+) Learning and memory abilities, serum SOD, GSH-Px, CAT, and Ach (–) Serum MDA, AChE, neuronal apoptosis, the expression of Tau and Aβ1-42	Chen et al. (2017)
	AD mice	Extract	(+) Learning and memory ability (–) AR, AGEs, and RAGEs	Ye et al. (2015)
	AD rats	Extract	(+) Level of SOD, GSH-Px, and CAT (–) Level of APP, tau, and caspase-3	Deng et al. (2020)
	OVX rats	Ethanol extract	(+) BMD and BMC, the level of P, Ca, and OPG (–) Level of serum DPD/Cr, TRAcP, and ACTH	Li et al. (2009)
	OVX rats	Polysaccharides	(+) BMD and BMC (–) Serum IL-6 and TNF-α	Mengyong et al. (2008)
Eucommiae Cortex	AD mice	Water extract	(+) Learning and memory (–) AChE	Kwon et al. (2011)
	SE rats	Aucubin	(–) Neuronal apoptosis	Wang J et al. (2017)
	SOP rats	Extract	(+) BMD, serum Ca2+, P, ALP, osteocalcin, and RANKL	Xiong and Zhao (2016)
	OP rats	Polysaccharides	(+) Lumbar spine and femur BMD, serum Ca, P, ALP, osteocalcin, and RANKL	Qi et al. (2019)
	OVX rats	Total lignans	(+) BMD, bone biomechanical properties, microarchitecture (–) Bone loss, bone turnover rate	Zhang et al. (2014)
	SAMP6	Extract	(+) BMD, bone strength (–) Weight, BMI, bone loss	Zhao et al. (2020)
Lycii Fructus	APP/PS1	Extract	(–) Learning and memory impairment	Zhang et al. (2013)
	OVX mice	Extract	(+) BMD, BMC, serum Ca2+ (–) Serum osteocalcin	Kim et al. (2017)
	OVX mice	Extract	(–) BMD loss	Park et al. (2014)
Atractylodis Macrocephalae Rhizoma	Aging mice	Extract	(–) Memory impairment, AChE	Hong and Yu (2015)
	AD rats	Biatractylolide	(+) Memory and learning ability	Feng et al. (2009)
	Heathy mice	Extract	(–) Bone loss	Ha et al. (2013)
Salviae Miltiorrhizae Radix Et Rhizoma	AD rats	Extract	(+) Learning and memory ability (–) APP, PS1	Liu M et al. (2015)
	AD *C. elegans*	Salvianolic acids A, salvianolic acids B	(–) Aβ aggregating, ROS (+) AD paralysis	Yuen et al. (2021)
	AD mice	Salvianolic acids B	(–) Cholinergic damage, cognitive impairment	Lee YW et al. (2013)
	APP/PS1 mice	Tanshinone IIA	(–) Spatial learning and memory deficit, Aβ accumulation, neuronal loss	Ding et al. (2020)
	OVX rats	Extract	(+) Serum ALP, OPG, RANKL, BMD, bone strength (–) Bone microstructures impairment	Liu H et al. (2018)
	OVX mice	Extract	(+) Serum OPG (–) Trabecular bone loss	Park et al. (2017)
	OP rats	Salvianolic acid B	(+) Cancellous bone formation, cancellous thickness (–) Bone loss	Cui et al. (2012)
	Heathy mice	Salvianolic acid A	(+) Fracture callus formation and micro-architecture, mineralization rate	Liu Y et al. (2018)
Rehmanniae Radix	AD mice	Catalpol	(+) SOD, GSH-Px, and CAT activity (–) Learning and memory impairment, senile plaques formation	Huang et al. (2016)
	Aged rats	Catalpol	(+) Synaptic proteins expression, nerve recovery	Liu QF et al. (2018)
	OVX rats	Extract	(+) Lumbar and femur BMD (–) ALP	Lim and Kim (2013)
	OVX rats	Acteoside	(–) OP biochemical markers, bone loss	Lee SY et al. (2013)
	Diabetic rats	Extract	(+) ALP, OCN, BMD, bone microarchitecture	Gong et al. (2019)
	OVX rats	Extract	(+) OPG, mechanical strength, cortical bone, and epiphyseal thickness (–) ALP, RANKL, TRAP	Liu et al. (2019)
Glycyrrhizae Radix Et Rhizoma	C57BL/6 mice	Extract	(–) Spatial cognitive and memory impairment	Cho et al. (2018)
	Heathy mice	Glycyrrhizic acid	(+) CAT, SOD activity (–) AChE activity, cognitive impairment	Ban et al. (2020)
	OVX rats	Extract	(+) BMD	Galanis et al. (2019)
	Zebrafish	Liquiritigenin	(–) OC activation	Carnovali et al. (2020)
	OVX mice	18β-GA	(+) Bone matrix mineralization	Chen et al. (2018)

(Continued on following page)

TABLE 1 | (*Continued*) Summary of *in vivo* studies for the anti-Alzheimer's disease and antiosteoporotic effects of natural Chinese medicine.

TCM	Animal model	Drug	Beneficial effects	Ref.
			(–) Serum TRAP5b, TNF-α and IL-6, bone loss	
Cistanches Herba	AD rats	Extract	(–) Aβ peptide aggregation and deposition	Chao et al. (2019)
	AD patients	Decoction	(+) cognitive and independent living ability	Li et al. (2015)
			(–) TNF-α, total-tau and IL-1β expression	
	AD mice	Extract	(–) Nitric oxide content, nitric oxide synthase activity	Peng et al. (2015)
	Heathy mice	Decoction	(+) Spatial learning and memory dopamine	Wang D et al. (2017)
			(–) Monoamine oxidase	
	OVX rats	Extract	(+) BMD and BMC, serum ALP, SOD, CAT, GSH-Px	Liang et al. (2011)
			(–) MDA	
	OVX rats	Extract	(–) Bone degeneration, Smad1, Smad5, TIEG1, and TGF-β1 expression	Liang et al. (2013)

TABLE 2 | Summary of *in vitro* studies for the anti-Alzheimer's disease and antiosteoporotic effects of natural Chinese medicine.

TCM	Cells	Drug	Beneficial effects	Ref.
Morindae Officinalis Radix	BMSCs	Extract	(+) The expression of Cbfα1, differentiation	Wang et al. (2004)
	OBs	Anthraquinone	(+) RANKL, ALP, OPG, formation	Bao et al. (2011)
Eucommiae Cortex	PC12	Macranthoin G	(+) Cell viability, CAT, SOD, GSH, GSH-Px	Hu et al. (2014)
			(–) MDA, ROS	
	OBs	Total lignans	(+) ALP, proliferation and differentiation, bone nodules	Zhang et al. (2014)
Lycii Fructus	Neuronal	Extract	(+) Neurogenesis, AKT phosphorylation	Ho et al. (2007)
			(–) Lactate dehydrogenase, caspase-3	
	Neuronal	Polysaccharides	(–) Caspase-3, caspase-2, apoptosis, PKR phosphorylation	Yu et al. (2007)
	Cortical neuronal	Extract	(–) Caspase-3, ROS, apoptosis	Ho et al. (2009)
	MC3T3-E1	Polysaccharides	(–) Apoptosis, caspase-12, JNK phosphorylation	Jing and Jia (2018)
	OBs, MC3T3-E1	Extract	(+) Proliferation and differentiation, ALP, Runx2	Park et al. (2014)
Atractylodis Macrocephalae Rhizoma	PC12	Atractylenolide III	(+) Cell viability	Luo and Sun, (2012)
	PC12	Atractylenolide III	(+) Cell viability	Wang, (2012)
			(–) Cell apoptosis	
	Bone marrow cell, OBs, OCs	Extract	(–) Differentiation of OC, NF-κB activation, c-Fos, and NFATc1 expression	Ha et al. (2013)
	MSCs	Atractylenolide I, atractylenolide III	(+) Specific chondrogenic markers expression, chondrogenic differentiation	Li X et al. (2012)
Salviae Miltiorrhizae Radix Et Rhizoma	MSCs	Salvianolic acid B	(+) Differentiation, activity, secretion of ALP and osteocalcin, Runx2 mRNA expression	Cui et al. (2012)
			(–) DKK1 mRNA expression	
Rehmanniae Radix	bEND.3	Catalpol	(+) Soluble Aβ clearance	Liu C et al. (2018)
			(–) Endothelial damage, blood–brain barrier leakage	
	SweAPP N2a	Catalpol	(+) α-Secretase expression, APP processing α-cleavage	Wang et al. (2018)
			(–) Aβ formation	
	BMMs	Acteoside	(–) ROS, OC formation, bone resorption, TNF-α, NFATc1, and c-Fos expression	Lee SY et al. (2013)
	MC3T3-E1	Extract	(+) proliferation and differentiation, BMP2, Runx2, osterix	Gong et al. (2019)
Glycyrrhizae Radix Et Rhizoma	SH-SY5Y	Licochalcone B	(–) Aβ42 self-aggregation, ROS, cell death	Cao et al. (2020)
	SweAPP	Extract and semilicoisoflavone B	(+) PPARγ expression	Gu et al. (2018)
			(–) Aβ secretion, STAT3 phosphorylation	
	BMSCs	18β-GA	(–) Differentiation, RANK expression	Chen et al. (2018)
	BMSCs	Extract	(+) Proliferation	Azizsoltani et al. (2018)
Cistanches Herba	OBs	Extract	(+) BMP-2, OPN and ALP expression, differentiation, maturation, bone mineralization	Li TM et al. (2012)
	OCs	Polysaccharide	(+) Antioxidant enzymes expression	Song et al. (2018)
			(–) Differentiation, bone resorption	

mechanism of natural Chinese herbs for the treatment of AD and OP has not been fully clarified. Therefore, further study on the isolation and characterization of bioactive components against AD and OP from classic and specific drugs is necessary to widely profile components for pharmacological uses, especially their efficacy, safety, and potential interaction with other

medications. The research to determine the special and targeted cellular and molecular mechanisms of natural Chinese medicine components should develop their potential application in the treatment of AD and OP as an effective and safe alternative to the major treatment strategy or in combination with current pharmacological therapy. Besides, few high-quality clinical research studies have presented against the AD and OP effects of components with known structures. Because there maybe unknown chemical interactions between various drugs and non-specific components in traditional formulas, the clinical drug research results still have deficiencies and limitations. Therefore, more high-quality clinical research studies of TCM are required in the future to explore the anabolic and anti-metabolic effects.

CONCLUSION

As common age-related diseases, AD and OP have similarities in pathological characteristics and pathogenesis. Recent *in vivo* and *in vitro* findings indicate that TCM herbs may well be effective for the treatment of AD complicated with OP. Further study is required to assure the efficacy, safety, and specificity of the components in TCM in order to tap its therapeutic potential. Therefore, more high-quality clinical studies of these natural drugs are required to provide more powerful evidence for candidate drugs so that they can be used as beneficial and safer against AD and OP applications.

AUTHOR CONTRIBUTIONS

All authors contributed to the article and approved the submitted version.

FUNDING

This work was supported by the National Natural Science Foundation of China (82004015, 82174079) and the Project of Science and Technology Commission of Shanghai Municipality (21S21902600).

REFERENCES

Abrahamsen, B., Osmond, C., and Cooper, C. (2015). Life Expectancy in Patients Treated for Osteoporosis: Observational Cohort Study Using National Danish Prescription Data. *J. Bone Miner. Res.* 30 (9), 1553–1559. doi:10.1002/jbmr.2478

Amouzougan, A., Lafaie, L., Marotte, H., Dėnarié, D., Collet, P., Pallot-Prades, B., et al. (2017). High Prevalence of Dementia in Women with Osteoporosis. *Jt. Bone Spine* 84 (5), 611–614. doi:10.1016/j.jbspin.2016.08.002

Arbor, S. C., Lafontaine, M., and Cumbay, M. (2016). Amyloid-beta Alzheimer Targets - Protein Processing, Lipid Rafts, and Amyloid-Beta Pores. *Yale J. Biol. Med.* 89 (1), 5–21.

Armas, L. A., and Recker, R. R. (2012). Pathophysiology of Osteoporosis: New Mechanistic Insights. *Endocrinol. Metab. Clin. North. Am.* 41 (3), 475–486. doi:10.1016/j.ecl.2012.04.006

Aspray, T. J., and Hill, T. R. (2019). Osteoporosis and the Ageing Skeleton. *Subcell Biochem.* 91, 453–476. doi:10.1007/978-981-13-3681-2_16

Alzheimer's Disease International, McGill University (2021). Available at: https://www.alzint.org/resource/world-alzheimer-report-2021/ (Accessed September 21, 2021).

Osteoporosis and Bone Mineral Disease Branch of Chinese Medical Association (2019). Epidemiological Survey of Osteoporosis in China and "Healthy Bones" Special Action Results Released. *Chin. J. Osteoporos. Bone Mineral Res.* 12 (04), 317–318.

Azizsoltani, A., Piri, K., Behzad, S., Soleimani, M., Nekouei, M., Mahmoudi, Z., et al. (2018). Ethyl Acetate Extract of Licorice Root (Glycyrrhiza Glabra) Enhances Proliferation and Osteogenic Differentiation of Human Bone Marrow Mesenchymal Stem Cells. *Iran. J. Pharm. Res.* 17 (3), 1057–1067.

Ban, J. Y., Park, H. K., and Kim, S. K. (2020). Effect of Glycyrrhizic Acid on Scopolamine-Induced Cognitive Impairment in Mice. *Int. Neurourol J.* 24 (Suppl. 1), S48–S55. doi:10.5213/inj.2040154.077

Bao, L., Qin, L., Liu, L., Wu, Y., Han, T., Xue, L., et al. (2011). Anthraquinone Compounds from Morinda Officinalis Inhibit Osteoclastic Bone Resorption In Vitro. *Chem. Biol. Interact* 194 (2-3), 97–105. doi:10.1016/j.cbi.2011.08.013

Björkman, M. P., Sorva, A. J., and Tilvis, R. S. (2010). Does Elevated Parathyroid Hormone Concentration Predict Cognitive Decline in Older People? *Aging Clin. Exp. Res.* 22 (2), 164–169. doi:10.1007/BF03324791

Bucay, N., Sarosi, I., Dunstan, C. R., Morony, S., Tarpley, J., Capparelli, C., et al. (1998). Osteoprotegerin-Deficient Mice Develop Early Onset Osteoporosis and Arterial Calcification. *Genes Dev.* 12 (9), 1260–1268. doi:10.1101/gad.12.9.1260

Butler, J. S., Murray, D. W., Hurson, C. J., O'Brien, J., Doran, P. P., and O'Byrne, J. M. (2011). The Role of Dkk1 in Bone Mass Regulation: Correlating Serum Dkk1 Expression with Bone mineral Density. *J. Orthop. Res.* 29 (3), 414–418. doi:10.1002/jor.21260

Cai, H., Wang, Y., He, J., Cai, T., Wu, J., Fang, J., et al. (2017). Neuroprotective Effects of Bajijiasu against Cognitive Impairment Induced by Amyloid-β in APP/PS1 Mice. *Oncotarget* 8 (54), 92621–92634. doi:10.18632/oncotarget.21515

Cao, Y., Xu, W., Huang, Y., and Zeng, X. (2020). Licochalcone B, a Chalcone Derivative from Glycyrrhiza Inflata, as a Multifunctional Agent for the Treatment of Alzheimer's Disease. *Nat. Prod. Res.* 34 (5), 736–739. doi:10.1080/14786419.2018.1496429

Carnovali, M., Banfi, G., and Mariotti, M. (2020). Liquiritigenin Reduces Osteoclast Activity in Zebrafish Model of Glucocorticoid-Induced Osteoporosis. *J. Pharmacol. Sci.* 143 (4), 300–306. doi:10.1016/j.jphs.2020.06.001

Chai, B., Gao, F., Wu, R., Dong, T., Gu, C., Lin, Q., et al. (2019). Vitamin D Deficiency as a Risk Factor for Dementia and Alzheimer's Disease: an Updated Meta-Analysis. *BMC Neurol.* 19 (1), 284. doi:10.1186/s12883-019-1500-6

Chao, C. L., Huang, H. W., Huang, H. C., Chao, H. F., Yu, S. W., Su, M. H., et al. (2019). Inhibition of Amyloid Beta Aggregation and Deposition of Cistanche Tubulosa Aqueous Extract. *Molecules* 24 (4). doi:10.3390/molecules24040687

Chen, D., Yang, X., Yang, J., Lai, G., Yong, T., Tang, X., et al. (2017). Prebiotic Effect of Fructooligosaccharides from Morinda Officinalis on Alzheimer's Disease in Rodent Models by Targeting the Microbiota-Gut-Brain Axis. *Front. Aging Neurosci.* 9, 403. doi:10.3389/fnagi.2017.00403

Chen, P., Li, Z., and Hu, Y. (2016). Prevalence of Osteoporosis in China: a Meta-Analysis and Systematic Review. *BMC Public Health* 16 (1), 1039. doi:10.1186/s12889-016-3712-7

Chen, X., Yu, J., Zhong, B., Lu, J., Lu, J. J., Li, S., et al. (2019). Pharmacological Activities of Dihydrotanshinone I, a Natural Product from Salvia Miltiorrhiza Bunge. *Pharmacol. Res.* 145, 104254. doi:10.1016/j.phrs.2019.104254

Chen, X., Zhi, X., Yin, Z., Li, X., Qin, L., Qiu, Z., et al. (2018). 18β-Glycyrrhetinic Acid Inhibits Osteoclastogenesis In Vivo and In Vitro by Blocking RANKL-Mediated RANK-TRAF6 Interactions and NF-Kb and MAPK Signaling Pathways. *Front. Pharmacol.* 9, 647. doi:10.3389/fphar.2018.00647

Chen, Y. H., and Lo, R. Y. (2017). Alzheimer's Disease and Osteoporosis. *Ci Ji Yi Xue Za Zhi* 29 (3), 138–142. doi:10.4103/tcmj.tcmj_54_17

Cho, M. J., Kim, J. H., Park, C. H., Lee, A. Y., Shin, Y. S., Lee, J. H., et al. (2018). Comparison of the Effect of Three Licorice Varieties on Cognitive Improvement via an Amelioration of Neuroinflammation in

Lipopolysaccharide-Induced Mice. *Nutr. Res. Pract.* 12 (3), 191–198. doi:10.4162/nrp.2018.12.3.191

Corbett, N. J., and Hooper, N. M. (2018). Soluble Amyloid Precursor Protein α: Friend or Foe? *Adv. Exp. Med. Biol.* 1112, 177–183. doi:10.1007/978-981-13-3065-0_13

Cui, L., Li, T., Liu, Y., Zhou, L., Li, P., Xu, B., et al. (2012). Salvianolic Acid B Prevents Bone Loss in Prednisone-Treated Rats through Stimulation of Osteogenesis and Bone Marrow Angiogenesis. *PLoS One* 7 (4), e34647. doi:10.1371/journal.pone.0034647

Cui, S., Xiong, F., Hong, Y., Jung, J. U., Li, X. S., Liu, J. Z., et al. (2011). APPswe/Aβ Regulation of Osteoclast Activation and RAGE Expression in an Age-dependent Manner. *J. Bone Miner. Res.* 26 (5), 1084–1098. doi:10.1002/jbmr.299

Deng, S., Lu, H., Chi, H., Wang, Y., Li, X., and Ye, H. (2020). Neuroprotective Effects of OMO within the Hippocampus and Cortex in a D-Galactose and Aβ 25-35-Induced Rat Model of Alzheimer's Disease. *Evid. Based Complement. Alternat Med.* 2020, 1067541. doi:10.1155/2020/1067541

Dengler-Crish, C. M., Ball, H. C., Lin, L., Novak, K. M., and Cooper, L. N. (2018). Evidence of Wnt/β-Catenin Alterations in Brain and Bone of A tauopathy Mouse Model of Alzheimer's Disease. *Neurobiol. Aging* 67, 148–158. doi:10.1016/j.neurobiolaging.2018.03.021

Depypere, H., Vierin, A., Weyers, S., and Sieben, A. (2016). Alzheimer's Disease, Apolipoprotein E and Hormone Replacement Therapy. *Maturitas* 94, 98–105. doi:10.1016/j.maturitas.2016.09.009

Ding, B., Lin, C., Liu, Q., He, Y., Ruganzu, J. B., Jin, H., et al. (2020). Tanshinone IIA Attenuates Neuroinflammation via Inhibiting RAGE/NF-κB Signaling Pathway In Vivo and In Vitro. *J. Neuroinflammation* 17 (1), 302. doi:10.1186/s12974-020-01981-4

Eiken, P., Vestergaard, P., and Jensen, J. E. (2014). Hormone Replacement Therapy as Primary Prevention? *Ugeskr Laeger* 176 (6).

Éric, L. (2020). Epidemiology of Osteoporosis. *Rev. Prat* 70 (9), 1018–1022.

Fan, X., Chen, Y., Li, L., Wang, Y., Zhang, Y., Lu, S., et al. (2019). Efficacy of Chinese Herb Cistanche Yishen Granules in Treatment of Tinnitus for Patients with Chronic Nephritis. *J. Cel. Biochem.* 120 (4), 5505–5509. doi:10.1002/jcb.27833

Feng, X., Wang, Z., Lin, Y., Zhou, Y., Liu, Y., and Yang, H. (2009). Effects of Biatractylolide on the AD Rats Induced by Aβ_(1-40). *Chin. Pharmacol. Bull.* 25, 949–951. doi:10.3321/j.issn:1001-1978.2009.07.029

Fu, Z., Fan, X., Wang, X., and Gao, X. (2018). Cistanches Herba: An Overview of its Chemistry, Pharmacology, and Pharmacokinetics Property. *J. Ethnopharmacol.* 219, 233–247. doi:10.1016/j.jep.2017.10.015

Fujita, K., and Janz, S. (2007). Attenuation of WNT Signaling by DKK-1 and -2 Regulates BMP2-Induced Osteoblast Differentiation and Expression of OPG, RANKL and M-CSF. *Mol. Cancer* 6, 71. doi:10.1186/1476-4598-6-71

Galanis, D., Soultanis, K., Lelovas, P., Zervas, A., Papadopoulos, P., Galanos, A., et al. (2019). Protective Effect of Glycyrrhiza Glabra Roots Extract on Bone mineral Density of Ovariectomized Rats. *Biomedicine (Taipei)* 9 (2), 8. doi:10.1051/bmdcn/2019090208

Goltzman, D. (2018). Functions of Vitamin D in Bone. *Histochem. Cel Biol.* 149 (4), 305–312. doi:10.1007/s00418-018-1648-y

Gong, W., Zhang, N., Cheng, G., Zhang, Q., He, Y., Shen, Y., et al. (2019). Rehmannia Glutinosa Libosch Extracts Prevent Bone Loss and Architectural Deterioration and Enhance Osteoblastic Bone Formation by Regulating the IGF-1/PI3K/mTOR Pathway in Streptozotocin-Induced Diabetic Rats. *Int. J. Mol. Sci.* 20 (16). doi:10.3390/ijms20163964

Gu, M. Y., Chun, Y. S., Zhao, D., Ryu, S. Y., and Yang, H. O. (2018). Glycyrrhiza Uralensis and Semilicoisoflavone B Reduce Aβ Secretion by Increasing PPARγ Expression and Inhibiting STAT3 Phosphorylation to Inhibit BACE1 Expression. *Mol. Nutr. Food Res.* 62 (6), e1700633. doi:10.1002/mnfr.201700633

Guo, Y., Wang, Q., Chen, S., and Xu, C. (2021). Functions of Amyloid Precursor Protein in Metabolic Diseases. *Metabolism* 115, 154454. doi:10.1016/j.metabol.2020.154454

Ha, H., An, H., Shim, K. S., Kim, T., Lee, K. J., Hwang, Y. H., et al. (2013). Ethanol Extract of Atractylodes Macrocephala Protects Bone Loss by Inhibiting Osteoclast Differentiation. *Molecules* 18 (7), 7376–7388. doi:10.3390/molecules18077376

Hagström, E., Kilander, L., Nylander, R., Larsson, E. M., Michaëlsson, K., Melhus, H., et al. (2014). Plasma Parathyroid Hormone Is Associated with Vascular Dementia and Cerebral Hyperintensities in Two Community-Based Cohorts. *J. Clin. Endocrinol. Metab.* 99 (11), 4181–4189. doi:10.1210/jc.2014-1736

He, J., Li, X., Wang, Z., Bennett, S., Chen, K., Xiao, Z., et al. (2019). Therapeutic Anabolic and Anticatabolic Benefits of Natural Chinese Medicines for the Treatment of Osteoporosis. *Front. Pharmacol.* 10, 1344. doi:10.3389/fphar.2019.01344

He, X., Wang, J., Li, M., Hao, D., Yang, Y., Zhang, C., et al. (2014). Eucommia Ulmoides Oliv.: Ethnopharmacology, Phytochemistry and Pharmacology of an Important Traditional Chinese Medicine. *J. Ethnopharmacol.* 151 (1), 78–92. doi:10.1016/j.jep.2013.11.023

Henderson, V. W. (2006). Estrogen-containing Hormone Therapy and Alzheimer's Disease Risk: Understanding Discrepant Inferences from Observational and Experimental Research. *Neuroscience* 138 (3), 1031–1039. doi:10.1016/j.neuroscience.2005.06.017

Hengartner, N. E., Fiedler, J., Ignatius, A., and Brenner, R. E. (2013). IL-1β Inhibits Human Osteoblast Migration. *Mol. Med.* 19, 36–42. doi:10.2119/molmed.2012.00058

Ho, Y. S., Yu, M. S., Lai, C. S., So, K. F., Yuen, W. H., and Chang, R. C. (2007). Characterizing the Neuroprotective Effects of Alkaline Extract of Lycium Barbarum on Beta-Amyloid Peptide Neurotoxicity. *Brain Res.* 1158, 123–134. doi:10.1016/j.brainres.2007.04.075

Ho, Y. S., Yu, M. S., Yik, S. Y., So, K. F., Yuen, W. H., and Chang, R. C. (2009). Polysaccharides from Wolfberry Antagonizes Glutamate Excitotoxicity in Rat Cortical Neurons. *Cell. Mol. Neurobiol.* 29 (8), 1233–1244. doi:10.1007/s10571-009-9419-x

Høgh, P. (2017). Alzheimer's Disease. *Ugeskr Laeger* 179 (12), 1.

Hong, J. Z., and Yu, Y. X. (2015). *Effect of Ethanol Extracts of Atractylodis Macrocephalae on Memeory Impairment in Aging Mice*. Dalian, China: Dalian University.

Howes, M. R., Fang, R., and Houghton, P. J. (2017). Effect of Chinese Herbal Medicine on Alzheimer's Disease. *Int. Rev. Neurobiol.* 135, 29–56. doi:10.1016/bs.irn.2017.02.003

Hsu, H., Lacey, D. L., Dunstan, C. R., Solovyev, I., Colombero, A., Timms, E., et al. (1999). Tumor Necrosis Factor Receptor Family Member RANK Mediates Osteoclast Differentiation and Activation Induced by Osteoprotegerin Ligand. *Proc. Natl. Acad. Sci. U S A.* 96 (7), 3540–3545. doi:10.1073/pnas.96.7.3540

Hu, W., Wang, G., Li, P., Wang, Y., Si, C. L., He, J., et al. (2014). Neuroprotective Effects of Macranthoin G from Eucommia Ulmoides against Hydrogen Peroxide-Induced Apoptosis in PC12 Cells via Inhibiting NF-Kb Activation. *Chem. Biol. Interact* 224, 108–116. doi:10.1016/j.cbi.2014.10.011

Huang, J. Z., Wu, J., Xiang, S., Sheng, S., Jiang, Y., Yang, Z., et al. (2016). Catalpol Preserves Neural Function and Attenuates the Pathology of Alzheimer's Disease in Mice. *Mol. Med. Rep.* 13 (1), 491–496. doi:10.3892/mmr.2015.4496

Jeong, G. S., Kang, M. G., Lee, J. Y., Lee, S. R., Park, D., Cho, M., et al. (2020). Inhibition of Butyrylcholinesterase and Human Monoamine Oxidase-B by the Coumarin Glycyrol and Liquiritigenin Isolated from Glycyrrhiza Uralensis. *Molecules* 25 (17). doi:10.3390/molecules25173896

Ji, S., Li, Z., Song, W., Wang, Y., Liang, W., Li, K., et al. (2016). Bioactive Constituents of Glycyrrhiza Uralensis (Licorice): Discovery of the Effective Components of a Traditional Herbal Medicine. *J. Nat. Prod.* 79 (2), 281–292. doi:10.1021/acs.jnatprod.5b00877

Jia, J., Wei, C., Chen, S., Li, F., Tang, Y., Qin, W., et al. (2018). The Cost of Alzheimer's Disease in China and Re-estimation of Costs Worldwide. *Alzheimers Dement* 14 (4), 483–491. doi:10.1016/j.jalz.2017.12.006

Jiang, Z., Wang, J., Li, X., and Zhang, X. (2016). Echinacoside and Cistanche Tubulosa (Schenk) R. Wight Ameliorate Bisphenol A-Induced Testicular and Sperm Damage in Rats through Gonad axis Regulated Steroidogenic Enzymes. *J. Ethnopharmacol.* 193, 321–328. doi:10.1016/j.jep.2016.07.033

Jin, M., Huang, Q., Zhao, K., and Shang, P. (2013). Biological Activities and Potential Health Benefit Effects of Polysaccharides Isolated from Lycium Barbarum L. *Int. J. Biol. Macromol.* 54, 16–23. doi:10.1016/j.ijbiomac.2012.11.023

Jing, L., and Jia, X. W. (2018). Lycium Barbarum Polysaccharide Arbitrates Palmitate-Induced Apoptosis in MC3T3-E1 C-ells through D-ecreasing the A-ctivation of ERS-mediated A-poptosis P-athway. *Mol. Med. Rep.* 17 (2), 2415–2421. doi:10.3892/mmr.2017.8128

Jun, W. (2011). *Experimental Study on the Pathogenesis, Diagnosis and Treatment of Alzheimer's Disease*. Wuhan, China: Huazhong University of Science and Technology.

Kamer, A. R., Craig, R. G., Dasanayake, A. P., Brys, M., Glodzik-Sobanska, L., and de Leon, M. J. (2008). Inflammation and Alzheimer's Disease: Possible Role of Periodontal Diseases. *Alzheimers Dement* 4 (4), 242–250. doi:10.1016/j.jalz.2007.08.004

Kim, M. H., Lee, J. E., Lee, J. S., and Yang, W. M. (2017). Improvement of Osteoporosis by Lycium Chinense Administration in Ovariectomized Mice. *J. Chin. Med. Assoc.* 80 (4), 222–226. doi:10.1016/j.jcma.2016.11.006

Kim, M. Y., Kim, K., Hong, C. H., Lee, S. Y., and Jung, Y. S. (2018). Sex Differences in Cardiovascular Risk Factors for Dementia. *Biomol. Ther. (Seoul)* 26 (6), 521–532. doi:10.4062/biomolther.2018.159

Krstic, D., Madhusudan, A., Doehner, J., Vogel, P., Notter, T., Imhof, C., et al. (2012). Systemic Immune Challenges Trigger and Drive Alzheimer-like Neuropathology in Mice. *J. Neuroinflammation* 9, 151. doi:10.1186/1742-2094-9-151

Kulkarni, R. N., Bakker, A. D., Everts, V., and Klein-Nulend, J. (2012). Mechanical Loading Prevents the Stimulating Effect of IL-1β on Osteocyte-Modulated Osteoclastogenesis. *Biochem. Biophys. Res. Commun.* 420 (1), 11–16. doi:10.1016/j.bbrc.2012.02.099

Kwon, S. H., Lee, H. K., Kim, J. A., Hong, S. I., Kim, S. Y., Jo, T. H., et al. (2011). Neuroprotective Effects of Eucommia Ulmoides Oliv. Bark on Amyloid Beta(25-35)-Induced Learning and Memory Impairments in Mice. *Neurosci. Lett.* 487 (1), 123–127. doi:10.1016/j.neulet.2010.10.042

Lamichhane, A. P. (2005). Osteoporosis-an Update. *JNMA J. Nepal Med. Assoc.* 44 (158), 60–66. doi:10.31729/jnma.404

Laudisio, A., Fontana, D. O., Rivera, C., Ruggiero, C., Bandinelli, S., Gemma, A., et al. (2016). Bone Mineral Density and Cognitive Decline in Elderly Women: Results from the InCHIANTI Study. *Calcif Tissue Int.* 98 (5), 479–488. doi:10.1007/s00223-015-0102-6

Lee, D. Y., Na, D. L., Seo, S. W., Chin, J., Lim, S. J., Choi, D., et al. (2012). Association between Cognitive Impairment and Bone mineral Density in Postmenopausal Women. *Menopause* 19 (6), 636–641. doi:10.1097/gme.0b013e31823dbec7

Lee, J. H., Bliwise, D. L., Ansari, F. P., Goldstein, F. C., Cellar, J. S., Lah, J. J., et al. (2007). Daytime Sleepiness and Functional Impairment in Alzheimer Disease. *Am. J. Geriatr. Psychiatry* 15 (7), 620–626. doi:10.1097/JGP.0b013e3180381521

Lee, S. Y., Lee, K. S., Yi, S. H., Kook, S. H., and Lee, J. C. (2013). Acteoside Suppresses RANKL-Mediated Osteoclastogenesis by Inhibiting C-Fos Induction and NF-Kb Pathway and Attenuating ROS Production. *PLoS One* 8 (12), e80873. doi:10.1371/journal.pone.0080873

Lee, Y. W., Kim, D. H., Jeon, S. J., Park, S. J., Kim, J. M., Jung, J. M., et al. (2013). Neuroprotective Effects of Salvianolic Acid B on an Aβ25-35 Peptide-Induced Mouse Model of Alzheimer's Disease. *Eur. J. Pharmacol.* 704 (1-3), 70–77. doi:10.1016/j.ejphar.2013.02.015

Li J, J., Wang, G. B., Feng, X., Zhang, J., and Fu, Q. (2016). Effect of Gallium Nitrate on the Expression of Osteoprotegerin and Receptor Activator of Nuclear factor-κB L-igand in O-steoblasts In V-ivo and In V-itro. *Mol. Med. Rep.* 13 (1), 769–777. doi:10.3892/mmr.2015.4588

Li, N., Qin, L. P., Han, T., Wu, Y. B., Zhang, Q. Y., and Zhang, H. (2009). Inhibitory Effects of morinda Officinalis Extract on Bone Loss in Ovariectomized Rats. *Molecules* 14 (6), 2049–2061. doi:10.3390/molecules14062049

Li, N., Wang, J., Ma, J., Gu, Z., Jiang, C., Yu, L., et al. (2015). Neuroprotective Effects of Cistanches Herba Therapy on Patients with Moderate Alzheimer's Disease. *Evid. Based Complement. Alternat Med.* 2015, 103985. doi:10.1155/2015/103985

Li, S., Liu, B., Zhang, L., and Rong, L. (2014). Amyloid Beta Peptide Is Elevated in Osteoporotic Bone Tissues and Enhances Osteoclast Function. *Bone* 61, 164–175. doi:10.1016/j.bone.2014.01.010

Li S, S., Yang, B., Teguh, D., Zhou, L., Xu, J., and Rong, L. (2016). Amyloid β Peptide Enhances RANKL-Induced Osteoclast Activation through NF-Kb, ERK, and Calcium Oscillation Signaling. *Int. J. Mol. Sci.* 17 (10). doi:10.3390/ijms17101683

Li, T. M., Huang, H. C., Su, C. M., Ho, T. Y., Wu, C. M., Chen, W. C., et al. (2012). Cistanche Deserticola Extract Increases Bone Formation in Osteoblasts. *J. Pharm. Pharmacol.* 64 (6), 897–907. doi:10.1111/j.2042-7158.2012.01483.x

Li, X., Wei, G., Wang, X., Liu, D. H., Deng, R. D., Li, H., et al. (2012). Targeting of the Sonic Hedgehog Pathway by Atractylenolides Promotes Chondrogenic Differentiation of Mesenchymal Stem Cells. *Biol. Pharm. Bull.* 35 (8), 1328–1335. doi:10.1248/bpb.b12-00265

Liang, H., Yu, F., Tong, Z., and Huang, Z. (2011). Effect of Cistanches Herba Aqueous Extract on Bone Loss in Ovariectomized Rat. *Int. J. Mol. Sci.* 12 (8), 5060–5069. doi:10.3390/ijms12085060

Liang, H. D., Yu, F., Tong, Z. H., Zhang, H. Q., and Liang, W. (2013). Cistanches Herba Aqueous Extract Affecting Serum BGP and TRAP and Bone Marrow Smad1 mRNA, Smad5 mRNA, TGF-B1 mRNA and TIEG1 mRNA Expression Levels in Osteoporosis Disease. *Mol. Biol. Rep.* 40 (2), 757–763. doi:10.1007/s11033-012-2065-2

Liang, K., Yang, L., Yin, C., Xiao, Z., Zhang, J., Liu, Y., et al. (2010). Estrogen Stimulates Degradation of Beta-Amyloid Peptide by Up-Regulating Neprilysin. *J. Biol. Chem.* 285 (2), 935–942. doi:10.1074/jbc.M109.051664

Lim, D. W., and Kim, Y. T. (2013). Dried Root of Rehmannia Glutinosa Prevents Bone Loss in Ovariectomized Rats. *Molecules* 18 (5), 5804–5813. doi:10.3390/molecules18055804

Littlejohns, T. J., Henley, W. E., Lang, I. A., Annweiler, C., Beauchet, O., Chaves, P. H., et al. (2014). Vitamin D and the Risk of Dementia and Alzheimer Disease. *Neurology* 83 (10), 920–928. doi:10.1212/WNL.0000000000000755

Liu, C., Chen, K., Lu, Y., Fang, Z., and Yu, G. (2018). Catalpol Provides a Protective Effect on Fibrillary Aβ1-42 -induced Barrier Disruption in an In Vitro Model of the Blood-Brain Barrier. *Phytother. Res.* 32 (6), 1047–1055. doi:10.1002/ptr.6043

Liu, C., Wang, L., Zhu, R., Liu, H., Ma, R., Chen, B., et al. (2019). Correction to: Rehmanniae Radix Preparata Suppresses Bone Loss and Increases Bone Strength through Interfering with Canonical Wnt/β-Catenin Signaling Pathway in OVX Rats. *Osteoporos. Int.* 30 (7), 1537–1540. doi:10.1007/s00198-019-05028-0

Liu, H., Zhu, R., Wang, L., Liu, C., Ma, R., Qi, B., et al. (2018). Radix Salviae Miltiorrhizae Improves Bone Microstructure and Strength through Wnt/β-Catenin and Osteoprotegerin/receptor Activator for Nuclear Factor-Kb Ligand/cathepsin K Signaling in Ovariectomized Rats. *Phytother. Res.* 32 (12), 2487–2500. doi:10.1002/ptr.6188

Liu, M., Guo, H., Li, C., Wang, D., Wu, J., Wang, C., et al. (2015). Cognitive Improvement of Compound Danshen in an Aβ25-35 Peptide-Induced Rat Model of Alzheimer's Disease. *BMC Complement. Altern. Med.* 15, 382. doi:10.1186/s12906-015-0906-y

Liu, Q. F., Lee, J. H., Kim, Y. M., Lee, S., Hong, Y. K., Hwang, S., et al. (2015). In Vivo Screening of Traditional Medicinal Plants for Neuroprotective Activity against Aβ42 Cytotoxicity by Using Drosophila Models of Alzheimer's Disease. *Biol. Pharm. Bull.* 38 (12), 1891–1901. doi:10.1248/bpb.b15-00459

Liu, Y., Jia, Z., Akhter, M. P., Gao, X., Wang, X., Wang, X., et al. (2018). Bone-targeting Liposome Formulation of Salvianic Acid A Accelerates the Healing of Delayed Fracture Union in Mice. *Nanomedicine* 14 (7), 2271–2282. doi:10.1016/j.nano.2018.07.011

Long, H., Ye, W. M., and Mai, W. (2013). Effect of Medicinal Indianmulberry Root in the Treatment of Postmenopausal Osteoporosis. *China Med. Pharm.* 3 (14), 80–81.

Lorentzon, M., Johansson, H., Harvey, N. C., Liu, E., Vandenput, L., Mccloskey, E. V., et al. (2021). Osteoporosis and Fractures in Women: the burden of Disease. *Climacteric* 25, 4–10. doi:10.1080/13697137.2021.1951206

Loskutova, N., Honea, R. A., Brooks, W. M., and Burns, J. M. (2010). Reduced Limbic and Hypothalamic Volumes Correlate with Bone Density in Early Alzheimer's Disease. *J. Alzheimers Dis.* 20 (1), 313–322. doi:10.3233/JAD-2010-1364

Loskutova, N., Honea, R. A., Vidoni, E. D., Brooks, W. M., and Burns, J. M. (2009). Bone Density and Brain Atrophy in Early Alzheimer's Disease. *J. Alzheimers Dis.* 18 (4), 777–785. doi:10.3233/JAD-2009-1185

Luo, L., and Sun, Y. (2012). *Effect of Atractylenolide* III *on Neuronal Cell Injury*. Guangzhou, China: Guangdong Pharmaceutical University.

Macdonald, B. T., Tamai, K., and He, X. (2009). Wnt/beta-catenin Signaling: Components, Mechanisms, and Diseases. *Dev. Cel.* 17 (1), 9–26. doi:10.1016/j.devcel.2009.06.016

Magzoub, M. (2020). Combating Proteins with Proteins: Engineering Cell-Penetrating Peptide Antagonists of Amyloid-β Aggregation and Associated Neurotoxicity. *DNA Cel Biol* 39 (6), 920–925. doi:10.1089/dna.2020.5604

Malhotra, R. (2016). Understanding Migraine: Potential Role of Neurogenic Inflammation. *Ann. Indian Acad. Neurol.* 19 (2), 175–182. doi:10.4103/0972-2327.182302

May, B. H., Feng, M., Zhou, I. W., Chang, S. Y., Lu, S. C., Zhang, A. L., et al. (2016). Memory Impairment, Dementia, and Alzheimer's Disease in Classical and Contemporary Traditional Chinese Medicine. *J. Altern. Complement. Med.* 22 (9), 695–705. doi:10.1089/acm.2016.0070

Mcgeer, P. L., Mcgeer, E., Rogers, J., and Sibley, J. (1990). Anti-inflammatory Drugs and Alzheimer Disease. *Lancet* 335 (8696), 1037. doi:10.1016/0140-6736(90)91101-f

Mengyong, Z., Caijiao, W., Husheng, Z., Xianwu, P., and Jianmin, F. (2008). Protective Effect of Polysaccharides from morinda Officinalis on Bone Loss in Ovariectomized Rats. *Int. J. Biol. Macromol.* 43 (3), 276–278. doi:10.1016/j.ijbiomac.2008.06.008

Mokry, L. E., Ross, S., Morris, J. A., Manousaki, D., Forgetta, V., and Richards, J. B. (2016). Genetically Decreased Vitamin D and Risk of Alzheimer Disease. *Neurology* 87 (24), 2567–2574. doi:10.1212/WNL.0000000000003430

Moon, M., Song, H., Hong, H. J., Nam, D. W., Cha, M.-Y., Oh, M. S., et al. (2013). Vitamin D-Binding Protein Interacts with Aβ and Suppresses Aβ-Mediated Pathology. *Cell Death Differ* 20 (4), 630–638. doi:10.1038/cdd.2012.161

Nanes, M. S., and Kallen, C. B. (2014). Osteoporosis. *Semin. Nucl. Med.* 44 (6), 439–450. doi:10.1053/j.semnuclmed.2014.06.006

Ng, A., Tam, W. W., Zhang, M. W., Ho, C. S., Husain, S. F., Mcintyre, R. S., et al. (2018). IL-1β, IL-6, TNF- α and CRP in Elderly Patients with Depression or Alzheimer's Disease: Systematic Review and Meta-Analysis. *Sci. Rep.* 8 (1), 12050. doi:10.1038/s41598-018-30487-6

Park, B., Song, H. S., Kwon, J. E., Cho, S. M., Jang, S. A., Kim, M. Y., et al. (2017). Effects of Salvia Miltiorrhiza Extract with Supplemental Liquefied Calcium on Osteoporosis in Calcium-Deficient Ovariectomized Mice. *BMC Complement. Altern. Med.* 17 (1), 545. doi:10.1186/s12906-017-2047-y

Park, E., Jin, H. S., Cho, D. Y., Kim, J., Kim, M. C., Choi, C. W., et al. (2014). The Effect of Lycii Radicis Cortex Extract on Bone Formation In Vitro and In Vivo. *Molecules* 19 (12), 19594–19609. doi:10.3390/molecules191219594

Patel, A., Kimura, R., Fu, W., Soudy, R., Mactavish, D., Westaway, D., et al. (2021). Genetic Depletion of Amylin/Calcitonin Receptors Improves Memory and Learning in Transgenic Alzheimer's Disease Mouse Models. *Mol. Neurobiol.* 58 (10), 5369–5382. doi:10.1007/s12035-021-02490-y

Patel, S., Homaei, A., Raju, A. B., and Meher, B. R. (2018). Estrogen: The Necessary Evil for Human Health, and Ways to Tame it. *Biomed. Pharmacother.* 102, 403–411. doi:10.1016/j.biopha.2018.03.078

Pei, H., Ma, L., Cao, Y., Wang, F., Li, Z., Liu, N., et al. (2020). Traditional Chinese Medicine for Alzheimer's Disease and Other Cognitive Impairment: A Review. *Am. J. Chin. Med.* 48 (3), 487–511. doi:10.1142/S0192415X20500251

Peng, X. M., Gao, L., Huo, S. X., Liu, X. M., and Yan, M. (2015). The Mechanism of Memory Enhancement of Acteoside (Verbascoside) in the Senescent Mouse Model Induced by a Combination of D-Gal and AlCl3. *Phytother. Res.* 29 (8), 1137–1144. doi:10.1002/ptr.5358

Pinheiro, L., and Faustino, C. (2019). Therapeutic Strategies Targeting Amyloid-β in Alzheimer's Disease. *Curr. Alzheimer Res.* 16 (5), 418–452. doi:10.2174/1567205016666190321163438

Prince, M., Bryce, R., Albanese, E., Wimo, A., Ribeiro, W., and Ferri, C. P. (2013). The Global Prevalence of Dementia: a Systematic Review and Metaanalysis. *Alzheimers Dement* 9 (1), 63–e2. e2. doi:10.1016/j.jalz.2012.11.007

Püntener, U., Booth, S. G., Perry, V. H., and Teeling, J. L. (2012). Long-term Impact of Systemic Bacterial Infection on the Cerebral Vasculature and Microglia. *J. Neuroinflammation* 9, 146. doi:10.1186/1742-2094-9-146

Qi, S., Zheng, H., Chen, C., and Jiang, H. (2019). Du-Zhong (Eucommia Ulmoides Oliv.) Cortex Extract Alleviates Lead Acetate-Induced Bone Loss in Rats. *Biol. Trace Elem. Res.* 187 (1), 172–180. doi:10.1007/s12011-018-1362-6

Ross, R. D., Shah, R. C., Leurgans, S., Bottiglieri, T., Wilson, R. S., and Sumner, D. R. (2018). Circulating Dkk1 and TRAIL Are Associated with Cognitive Decline in Community-Dwelling, Older Adults with Cognitive Concerns. *J. Gerontol. A. Biol. Sci. Med. Sci.* 73 (12), 1688–1694. doi:10.1093/gerona/glx252

Scali, C., Caraci, F., Gianfriddo, M., Diodato, E., Roncarati, R., Pollio, G., et al. (2006). Inhibition of Wnt Signaling, Modulation of Tau Phosphorylation and Induction of Neuronal Cell Death by DKK1. *Neurobiol. Dis.* 24 (2), 254–265. doi:10.1016/j.nbd.2006.06.016

Singh, Y., Gupta, G., Shrivastava, B., Dahiya, R., Tiwari, J., Ashwathanarayana, M., et al. (2017). Calcitonin Gene-Related Peptide (CGRP): A Novel Target for Alzheimer's Disease. *CNS Neurosci. Ther.* 23 (6), 457–461. doi:10.1111/cns.12696

Song, D., Cao, Z., Liu, Z., Tickner, J., Qiu, H., Wang, C., et al. (2018). Cistanche Deserticola Polysaccharide Attenuates Osteoclastogenesis and Bone Resorption via Inhibiting RANKL Signaling and Reactive Oxygen Species Production. *J. Cel. Physiol.* 233 (12), 9674–9684. doi:10.1002/jcp.26882

Sreenivasmurthy, S. G., Liu, J. Y., Song, J. X., Yang, C. B., Malampati, S., Wang, Z. Y., et al. (2017). Neurogenic Traditional Chinese Medicine as a Promising Strategy for the Treatment of Alzheimer's Disease. *Int. J. Mol. Sci.* 18 (2). doi:10.3390/ijms18020272

Steinhart, Z., and Angers, S. (2018). Wnt Signaling in Development and Tissue Homeostasis. *Development* 145 (11). doi:10.1242/dev.146589

Stevenson, J. C. (2006). HRT, Osteoporosis and Regulatory Authorities Quis Custodiet Ipsos Custodes? *Hum. Reprod.* 21 (7), 1668–1671. doi:10.1093/humrep/del043

Tamir, S., Eizenberg, M., Somjen, D., Izrael, S., and Vaya, J. (2001). Estrogen-like Activity of Glabrene and Other Constituents Isolated from Licorice Root. *J. Steroid Biochem. Mol. Biol.* 78 (3), 291–298. doi:10.1016/s0960-0760(01)00093-0

Tan, Z. S., Seshadri, S., Beiser, A., Zhang, Y., Felson, D., Hannan, M. T., et al. (2005). Bone mineral Density and the Risk of Alzheimer Disease. *Arch. Neurol.* 62 (1), 107–111. doi:10.1001/archneur.62.1.107

van Dam, P. A., Verhoeven, Y., Trinh, X. B., Wouters, A., Lardon, F., Prenen, H., et al. (2019). RANK/RANKL Signaling Inhibition May Improve the Effectiveness of Checkpoint Blockade in Cancer Treatment. *Crit. Rev. Oncol. Hematol.* 133, 85–91. doi:10.1016/j.critrevonc.2018.10.011

Wallin, K., Solomon, A., Kåreholt, I., Tuomilehto, J., Soininen, H., and Kivipelto, M. (2012). Midlife Rheumatoid Arthritis Increases the Risk of Cognitive Impairment Two Decades Later: a Population-Based Study. *J. Alzheimers Dis.* 31 (3), 669–676. doi:10.3233/JAD-2012-111736

Walsh, D. A., Mapp, P. I., and Kelly, S. (2015). Calcitonin Gene-Related Peptide in the Joint: Contributions to Pain and Inflammation. *Br. J. Clin. Pharmacol.* 80 (5), 965–978. doi:10.1111/bcp.12669

Wang D, D., Wang, H., and Gu, L. (2017). The Antidepressant and Cognitive Improvement Activities of the Traditional Chinese Herb Cistanche. *Evid. Based Complement. Alternat Med.* 2017, 3925903. doi:10.1155/2017/3925903

Wang, H. K., Hung, C. M., Lin, S. H., Tai, Y. C., Lu, K., Liliang, P. C., et al. (2014). Increased Risk of Hip Fractures in Patients with Dementia: a Nationwide Population-Based Study. *BMC Neurol.* 14, 175. doi:10.1186/s12883-014-0175-2

Wang, H. M., Wang, L., and Li, N. (2004). Study the Influence of Morinda Officinalis How on the Differentiation From Marrow Stroma Cell to Osteoblast. *Rehabil. Med.* 14, 16–20.

Wang J, J., Li, Y., Huang, W. H., Zeng, X. C., Li, X. H., Li, J., et al. (2017). The Protective Effect of Aucubin from Eucommia Ulmoides against Status Epilepticus by Inducing Autophagy and Inhibiting Necroptosis. *Am. J. Chin. Med.* 45 (3), 557–573. doi:10.1142/S0192415X17500331

Wang T, T., Liu, Q., Tjhioe, W., Zhao, J., Lu, A., Zhang, G., et al. (2017). Therapeutic Potential and Outlook of Alternative Medicine for Osteoporosis. *Curr. Drug Targets* 18 (9), 1051–1068. doi:10.2174/1389450118666170321105425

Wang, T. J., Zhang, F., Richards, J. B., Kestenbaum, B., van Meurs, J. B., Berry, D., et al. (2010). Common Genetic Determinants of Vitamin D Insufficiency: a Genome-wide Association Study. *Lancet* 376 (9736), 180–188. doi:10.1016/S0140-6736(10)60588-0

Wang, X. Z. (2012). *Extraction, the Structure Modification of Atractylenolide and Protective Effect on PC12 Cells*. [Master Thesis]. Guangzhou, China: Guangzhou University of Chinese Medicine.

Wang, Z., Huang, X., Zhao, P., Zhao, L., and Wang, Z. Y. (2018). Catalpol Inhibits Amyloid-β Generation through Promoting α-Cleavage of APP in Swedish Mutant APP Overexpressed N2a Cells. *Front. Aging Neurosci.* 10, 66. doi:10.3389/fnagi.2018.00066

Weller, I., and Schatzker, J. (2004). Hip Fractures and Alzheimer's Disease in Elderly Institutionalized Canadians. *Ann. Epidemiol.* 14 (5), 319–324. doi:10.1016/j.annepidem.2003.08.005

Weller, J., and Budson, A. (2018). Current Understanding of Alzheimer's Disease Diagnosis and Treatment. *F1000Res* 7, 1. doi:10.12688/f1000research.14506.1

Wojda, S. J., and Donahue, S. W. (2018). Parathyroid Hormone for Bone Regeneration. *J. Orthop. Res.* 36 (10), 2586–2594. doi:10.1002/jor.24075

Wong, W. (2020). Economic burden of Alzheimer Disease and Managed Care Considerations. *Am. J. Manag. Care* 26 (8 Suppl. l), S177–S183. doi:10.37765/ajmc.2020.88482

Xia, Z., Wang, F., Zhou, S., Zhang, R., Wang, F., Huang, J. H., et al. (2017). Catalpol Protects Synaptic Proteins from Beta-Amyloid Induced Neuron Injury and Improves Cognitive Functions in Aged Rats. *Oncotarget* 8 (41), 69303–69315. doi:10.18632/oncotarget.17951

Xiong, W., and Zhao, L. (2016). Effect of Eucommia Ulmoides with Salt Water on Blood Biochemical Indexes in Senile Osteoporosis Rats. *Lishizhen Med. Materia Med. Res.*

Yaccoby, S., Ling, W., Zhan, F., Walker, R., Barlogie, B., and Shaughnessy, J. D. (2007). Antibody-based Inhibition of DKK1 Suppresses Tumor-Induced Bone Resorption and Multiple Myeloma Growth In Vivo. *Blood* 109 (5), 2106–2111. doi:10.1182/blood-2006-09-047712

Ye, Z. X., Xiao, L. Y., and Pan, J. Q. (2015). *Effect of morinda Officinalis Extraction Learning and Memory Impairment in Mice*. Guangzhou, China: Guangzhou Panyu sanatorium.

Yu, M. S., Lai, C. S., Ho, Y. S., Zee, S. Y., So, K. F., Yuen, W. H., et al. (2007). Characterization of the Effects of Anti-aging Medicine Fructus Lycii on Beta-Amyloid Peptide Neurotoxicity. *Int. J. Mol. Med.* 20 (2), 261–268. doi:10.3892/ijmm.20.2.261

Yuen, C. W., Murugaiyah, V., Najimudin, N., and Azzam, G. (2021). Danshen (Salvia Miltiorrhiza) Water Extract Shows Potential Neuroprotective Effects in *Caenorhabditis elegans*. *J. Ethnopharmacol.* 266, 113418. doi:10.1016/j.jep.2020.113418

Zhang, H., and Zheng, Y. (2019). β Amyloid Hypothesis in Alzheimer's Disease: Pathogenesis,Prevention,and Management. *Zhongguo Yi Xue Ke Xue Yuan Xue Bao* 41 (5), 702–708. doi:10.3881/j.issn.1000-503X.10875

Zhang, J. H., Xin, H. L., Xu, Y. M., Shen, Y., He, Y. Q., Hsien-Yeh, H., et al. (2018). Morinda Officinalis How. - A Comprehensive Review of Traditional Uses, Phytochemistry and Pharmacology. *J. Ethnopharmacol.* 213, 230–255. doi:10.1016/j.jep.2017.10.028

Zhang Nd, N. D., Han, T., Huang, B. K., Rahman, K., Jiang, Y. P., Xu, H. T., et al. (2016). Traditional Chinese Medicine Formulas for the Treatment of Osteoporosis: Implication for Antiosteoporotic Drug Discovery. *J. Ethnopharmacol.* 189, 61–80. doi:10.1016/j.jep.2016.05.025

Zhang, Q., Du, X., Xu, Y., Dang, L., Xiang, L., and Zhang, J. (2013). The Effects of Gouqi Extracts on Morris Maze Learning in the APP/PS1 Double Transgenic Mouse Model of Alzheimer's Disease. *Exp. Ther. Med.* 5 (5), 1528–1530. doi:10.3892/etm.2013.1006

Zhang, R., Pan, Y. L., Hu, S. J., Kong, X. H., Juan, W., and Mei, Q. B. (2014). Effects of Total Lignans from Eucommia Ulmoides Barks Prevent Bone Loss In Vivo and In Vitro. *J. Ethnopharmacol.* 155 (1), 104–112. doi:10.1016/j.jep.2014.04.031

Zhang Xz, X. Z., Qian, S. S., Zhang, Y. J., and Wang, R. Q. (2016). Salvia Miltiorrhiza: A Source for Anti-alzheimer's Disease Drugs. *Pharm. Biol.* 54 (1), 18–24. doi:10.3109/13880209.2015.1027408

Zhao, X., Wang, Y., Nie, Z., Han, L., Zhong, X., Yan, X., et al. (2020). Eucommia Ulmoides Leaf Extract Alters Gut Microbiota Composition, Enhances Short-Chain Fatty Acids Production, and Ameliorates Osteoporosis in the Senescence-Accelerated Mouse P6 (SAMP6) Model. *Food Sci. Nutr.* 8 (9), 4897–4906. doi:10.1002/fsn3.1779

Zhao, Y., Shen, L., and Ji, H. F. (2012). Alzheimer's Disease and Risk of Hip Fracture: a Meta-Analysis Study. *ScientificWorldJournal* 2012, 872173. doi:10.1100/2012/872173

Zhou, X. L., Xu, M. B., Jin, T. Y., Rong, P. Q., Zheng, G. Q., and Lin, Y. (2019). Preclinical Evidence and Possible Mechanisms of Extracts or Compounds from Cistanches for Alzheimer's Disease. *Aging Dis.* 10 (5), 1075–1093. doi:10.14336/AD.2018.0815-1

Zhu, B., Zhang, Q. L., Hua, J. W., Cheng, W. L., and Qin, L. P. (2018). The Traditional Uses, Phytochemistry, and Pharmacology of Atractylodes Macrocephala Koidz.: A Review. *J. Ethnopharmacol* 226, 143–167. doi:10.1016/j.jep.2018.08.023

Zwerina, J., Redlich, K., Polzer, K., Joosten, L., Krönke, G., Distler, J., et al. (2007). TNF-induced Structural Joint Damage Is Mediated by IL-1. *Proc. Natl. Acad. Sci. U S A.* 104 (28), 11742–11747. doi:10.1073/pnas.0610812104

Conflict of Interest: The authors declare that the research was conducted in the absence of any commercial or financial relationships that could be construed as a potential conflict of interest.

Publisher's Note: All claims expressed in this article are solely those of the authors and do not necessarily represent those of their affiliated organizations or those of the publisher, the editors, and the reviewers. Any product that may be evaluated in this article, or claim that may be made by its manufacturer, is not guaranteed or endorsed by the publisher.

Copyright © 2022 Xu, Jiang, Wang, Bai, Xu, Xia and Xin. This is an open-access article distributed under the terms of the Creative Commons Attribution License (CC BY). The use, distribution or reproduction in other forums is permitted, provided the original author(s) and the copyright owner(s) are credited and that the original publication in this journal is cited, in accordance with accepted academic practice. No use, distribution or reproduction is permitted which does not comply with these terms.

Advantages of publishing in Frontiers

OPEN ACCESS
Articles are free to read for greatest visibility and readership

FAST PUBLICATION
Around 90 days from submission to decision

HIGH QUALITY PEER-REVIEW
Rigorous, collaborative, and constructive peer-review

TRANSPARENT PEER-REVIEW
Editors and reviewers acknowledged by name on published articles

Frontiers
Avenue du Tribunal-Fédéral 34
1005 Lausanne | Switzerland

Visit us: www.frontiersin.org
Contact us: frontiersin.org/about/contact

REPRODUCIBILITY OF RESEARCH
Support open data and methods to enhance research reproducibility

DIGITAL PUBLISHING
Articles designed for optimal readership across devices

FOLLOW US
@frontiersin

IMPACT METRICS
Advanced article metrics track visibility across digital media

EXTENSIVE PROMOTION
Marketing and promotion of impactful research

LOOP RESEARCH NETWORK
Our network increases your article's readership